Transactions of the ASME

Gas-Turbine Progress Report—1952

Gas Turbines in Our Century . . . . . *Claude Seippel* 121

Introduction . . . . . *R. Tom Sawyer* 123

Materials, Cooling, and Fuels . . . . . *A. A. Hafer* 127

Cycle Components . . . . . *P. F. Martinuzzi* 137

Automotive . . . . . *F. L. Schwartz* 153

Railroad . . . . . *K. A. Browne, J. I. Yellott, and P. R. Broadley* 161

Marine . . . . . *W. A. Dolan, Jr., and A. A. Hafer* 169

Merchant Vessels . . . . . *W. A. Dolan, Jr., and A. A. Hafer* 177

Naval Vessels . . . . . *W. A. Dolan, Jr., and A. A. Hafer* 185

Stationary Electric Generation . . . . . *Lee Schneitter* 201

Industrial . . . . . *L. N. Rowley, Jr., and B. G. A. Skrotzki* 211

Aviation . . . . . *I. H. Driggs and O. E. Lancaster* 217

Local Heat-Transfer Coefficients on the Surface of an Elliptical Cylinder in a High-Speed Air Stream . . . . . *R. A. Seban and R. M. Drake* 235

Torsional Vibration Notes With Solutions for an Untuned Viscous Damper and Flexible Coupling With Nonlinear Elasticity . . . . . *F. P. Porter* 241

On the Solution of the Reynolds Equation for Slider-Bearing Lubrication—II . . . . . *A. Charnes and E. Saibel* 269

The Shear-Angle Relationship in Metal Cutting *M. C. Shaw, N. H. Cook, and I. Finnie* 273

Comparisons at Elevated Temperatures of Some Commercial Grades of Ferritic Cast Steels . . . . . *H. W. Wyatt, J. W. Bolton, and M. L. Steinbuch* 289

TRANSACTIONS OF THE AMERICAN SOCIETY OF MECHANICAL ENGINEERS

VOLUME 75 FEBRUARY 1953 NUMBER 2

Transactions

of The American Society of Mechanical Engineers

Published on the tenth of every month, except March, June, September, and December

OFFICERS OF THE SOCIETY:

FREDERICK S. BLACKALL, JR., *President*

JOSEPH L. KOPF, *Treasurer* — C. E. DAVIES, *Secretary*
EDGAR J. KATES, *Ass't Treasurer*

COMMITTEE ON PUBLICATIONS:

GEORGE R. RICH, *Chairman*

PAUL T. NORTON, JR. — COLIN CARMICHAEL
OTTO DE LORENZI — W. E. RAASCH
MORRIS GERR, JOSEPH SCHMERLER, *Junior Advisory Members*
GEORGE A. STETSON, *Editor* — K. W. CLENDINNING, *Managing Editor*

REGIONAL ADVISORY BOARD OF THE PUBLICATIONS COMMITTEE:

KERR ATKINSON—I
JOHN DE S. COUTINHO—II
WILLIAM N. RICHARDS—III
FRANCIS C. SMITH—IV
HENDLEY BLACKMON—V
CHESTER R. EARLE—VI
RAYMOND G. ROSHONG—VII
VENTON L. DOUGHTIE—VIII

Published monthly by The American Society of Mechanical Engineers. Publication office at 20th and Northampton Streets, Easton, Pa. The editorial department is located at the headquarters of the Society, 29 West Thirty-Ninth Street, New York 18, N. Y. Cable address, "Dynamic," New York. Price $1.50 a copy, $12.00 a year for Transactions and the *Journal of Applied Mechanics;* to members and affiliates, $1.00 a copy, $6.00 a year. Changes of address must be received at Society headquarters four weeks before they are to be effective on the mailing list. Please send old as well as new address....By-Law: The Society shall not be responsible for statements or opinions advanced in papers or ... printed in its publications (B13, Par. 4).... Entered as second-class matter March 2, 1928, at the Post Office at Easton, Pa., under the Act of August 24, 1912....Copyrighted, 1953, by The American Society of Mechanical Engineers. Reprints from this publication may be made on condition that full credit be given the Transactions of the ASME and the author, and that date of publication be stated.

Gas Turbines in Our Century

By CLAUDE SEIPPEL,[1] BADEN, SWITZERLAND

FEW of the attempts to develop a workable gas turbine prior to 1900 are of lasting interest, although it must be remembered that great physicists like Carnot, Gibbs, and Maxwell had established the fundamental laws of thermodynamics in a way which has not been surpassed. Some early inventors conceived machines which, like Stolze's, in many ways anticipated future developments but never got to the point where they would deliver appreciable power, or even run. Stolze's design of 1872 consisted of an axial compressor and an axial turbine on the same shaft, a heat exchanger, a gas producer, and a combustion chamber—an absolutely modern combination. His design shows many more stages in the turbine than in the compressor, due, as he probably thought necessary, to the higher-energy head acting on the turbine. He apparently did not know that in a compression stage, air must be treated gently as compared with the turbine. The axial compressor is not simply a reversed turbine and it requires many more stages. Its success, which was so essential to the birth of gas turbines, came relatively late. Even Sir Charles Parsons abandoned the axial compressor after having built a number of them shortly after 1900. It was not until 1932 that Brown Boveri, after some years of research and the manufacture of some single- and two-stage axial blowers, produced the first multistage axial compressors which were applied to Velox boilers and to supersonic wind tunnels.

At the core of gas-turbine history of the first decades of our century we find Stodola. Born in 1859, of Slovakian origin, Aurel Stodola was professor of thermodynamics and thermal machines at the Swiss Federal Institute of Technology, Zurich, from 1892 to 1930. He died ten years ago. Although he was not an inventor or an industrialist himself, his influence opened the way to the success of the gas turbine. Through his universal knowledge of fundamental science, through his personal contact with students, inventors, and industrialists, and through his enthusiasm, he was able, in his teaching and in his writings, to give a turn to science which was essential to progress.

The first successful attempt to build a gas turbine was made by the two Armangaud brothers in Paris around 1905. Their machine consisted of two centrifugal compressors working with a pressure ratio of four, a combustion chamber, and a Curtis-turbine wheel 3 ft in diameter and turning at 4250 rpm. Gas entered at a measured temperature of 1040 F, although Stodola estimates that it must have been higher; for it is well known that difficulties in measuring high temperatures at the turbine were encountered at the start. The set supplied not mechanical power but compressed air. The efficiency, however, did not exceed 3 per cent.

A general distinction in thermal engines should be made which, next to the obvious one of reciprocating and rotating machines, is most essential—engines with *discontinuous combustion* and engines with *continuous combustion*. This distinction is essential because it fundamentally affects problems of combustion and fuels. To the first category belong, of course, internal-combustion reciprocating engines of all descriptions; the Humphrey pump, that strange creation in which the explosion of a gas mixture chases a liquid column like a piston (and whose slow humph . . . . humph . . . . resounded through the plains of northern Italy around 1915). To the category of discontinuous-combustion engines belong also a Stauber turbine, derived from the Humphrey pump, in which the explosion chambers rotate and the water column is delivered to a turbine (a system that actually worked, although it did not survive); and the free-piston system of the brilliant inventor Pescara, a successful and promising combination of reciprocating and revolving elements which, under the tenacious efforts of a French group, has been developed to a technical and apparently a commercial success.

The principal representative of a purely rotating machine with intermittent combustion is the Holzwarth gas turbine. Stodola devoted most of his gas-turbine studies to the Holzwarth explosion turbine. Some of those studies are to be found in Stodola's voluminous book, "Steam and Gas Turbines." The remainder exist only in his unpublished notes. His work covers practically all problems—thermodynamic, mechanical, heat resistance, and cooling of the turbine—and its significance reaches far beyond the Holzwarth machine. What strikes the reader is the scarcity of fundamental experimental data which were at Stodola's disposal and the stupendous mathematical skill which he developed to find such things, for instance, as the local heat transmission in the curved channels of a blade. The more fortunate modern engineer would doubtlessly turn to the laboratory for such information and get quicker and probably more reliable results.

In 1927 Stodola was called upon, together with the German professor Schüle, to test a 500-kw oil-fired Holzwarth turbine built in the Thyssen shops in Muhlheim (Ruhr). The turbine was jacketed by evaporators and internally cooled; it was found that an unexpected amount of heat was transmitted to the water. Only 8 per cent of the calorific value of the fuel was transformed into mechanical energy at the turbine shaft, but another 10 per cent was available in the power-producing capacity of the steam generated in the jackets, giving a total of 18 per cent. Stodola predicted that, turning all experience of the 500-kw set to profit, a machine could be built that would exceed 30 per cent efficiency. Though not sharing these expectations, Brown Boveri designed and manufactured a 2000-kw turbine which was shipped to Germany in 1933, to be operated in a steel plant. No performance data are available.

Noack of Brown Boveri drew unexpected conclusions from Stodola's reports: "If heat transmission is so disturbingly high at high velocity," he said, "let this be turned to advantage in a steam boiler of extremely reduced heating surface," and hence he built his first "Velox" boiler which, like the Holzwarth turbine, worked on an explosion cycle. The reason for selecting the explosion cycle for a supercharged boiler as well as for the Holzwarth turbine is the advantage it has of producing pressure rise without the expenditure of mechanical work during combustion. This made it possible to overcome the deficiency of compressors and turbines of that period and to achieve a balance between compression work, draft losses at high velocities, and expansion work and thus to avoid the failures encountered by Stolze and Armangaud. However, there was a great desire to get away from intermittent combustion with its delicate problems of scavenging, of forming an explosive mixture, and of ignition. Hence the important decision was taken to shift to continuous combustion, a principle which has been followed by practically all designers; and a multistage axial compressor, which existed on paper

[1] Director of Research, Brown Boveri Company.

Based on an address delivered at the Gas Turbine Power Luncheon at the Fall Meeting, Chicago, Ill., Sept. 7–11, 1952, of THE AMERICAN SOCIETY OF MECHANICAL ENGINEERS.

only, and a multistage axial turbine of the reaction type were chosen.

Exhaust-gas-driven supercharging sets are predecessors to the gas turbines of today; many problems of high-temperature operation have been investigated and solved on them. Stodola, in referring to early superchargers built for aero engines, during the first world war, mentions three names, Rateau and Moss, who are well known, and Sherbondy, a distinguished American engineer with whom the author was associated in 1925, who had an extraordinary vision of the technical future and was doubtlessly the first to introduce results of wind-tunnel tests for airfoils in the study of axial compressors.

The superchargers of the Sherbondy type with single-stage compressor and turbine, which are still undisputed in the internal-combustion-engine field, were at first not considered good enough for gas turbines or even for the Velox boiler. Later, when much higher temperatures became possible, they were adopted for the great aviation development in Great Britain and the United States, and immense progress was achieved in their performance.

The multistage charging sets of the first Velox units needed some auxiliary power because the requirements of the compressor exceeded the output of the turbine. Later, the balance was reversed, and the charging set was able to deliver excess power to the station bus bars. This principle of gaining excess power from the combustion cycle in a steam plant may have a considerable future in large steam stations.

In 1936 a new application of the charging sets appeared when the Sun Oil Co. of Philadelphia called for superchargers to burn carbon residues in their Houdry-process cracking stills under pressure with the production of whatever power the cycle would be able to supply. Henry Thomas of the Sun Oil Co., having judged the idea sound, ordered the machines and built the plant. He was rewarded with full success, and more than 30 Houdry sets built by Brown Boveri and Allis Chalmers have shown remarkable reliability. The operating conditions are not too severe, it is true, because the temperature is moderate and the gases are relatively clean.

For shop tests, the charging sets for the Sun Oil Co. were fitted with an oil-burning combustion chamber, and not until the entire equipment was actually running was it realized that a regular combustion turbine had been born, and was in fact standing there showing what it could do.

Adolf Meyer was now keen to push the combustion turbine proper to success. He secured an order for a unit to deliver stand-by power to the town of Neuchâtel in Switzerland. This machine was shown in running condition at the Swiss National Exhibition in Zurich in 1939. It differed from the Houdry sets in several respects. The temperature was higher, the turbine blading had been redesigned for better efficiency, and air jackets had been provided to avoid distortion through uneven temperature distribution of the gases leaving the combustion chamber.

Brown Boveri thought it would be fitting to invite Stodola, the father of the gas turbine, to conduct official tests on this first machine. He greatly appreciated this gesture. Aged 80, he appeared with a crew of engineers and a wagonload of instruments to carry out tests of a thoroughness and accuracy that could set a standard for all time.

The Neuchâtel type of machine was very successful except for the combustion-chamber lining which was redesigned two or three times before it gave satisfaction. It has remained to the present day as the type of machine most frequently built by Brown Boveri. A unit was installed on a locomotive of the Swiss Railways in 1942.

At this time several groups in different countries started the development of some modern combustion turbines. The British Air Ministry ordered a gas turbine from Brown Boveri "to play with" and perhaps to run to the temperature of destruction. They admitted their hope of flying with turbines but carefully kept secret the fact that Whittle had a set with which he had taken to the air. Nobody can appreciate better than an engineer actively engaged in gas-turbine problems himself the immensity of the work, the skill, and the efficiency that were developed, under the menace of death and destruction, by the British and American air industries during and since the war. Much is to be learned by the designer of industrial machinery, though constructing machines to last several hundred thousand hours is obviously a different matter. But aviation history is not to be included in this review of gas turbines.

An early pioneer of the modern industrial gas turbine is George Jendrassik of Budapest. In 1939 he published the description, pictures, and test results of a 100-hp unit for which he claimed a thermal efficiency in excess of 21 per cent at a gas temperature of only about 900 F. He had a very large heat exchanger in relation to the power and the air temperature was around freezing, which favored the results.

Among the Swiss firms, which, of course, are closest to the author's sphere, Escher-Wyss launched the original idea of the closed air cycle, promoted by Ackeret, a successor to Stodola at the Institute of Technology, and by Keller. Sulzer Brothers, with no tradition in the engineering of large turbines, produced a gas turbine of a mixed open and closed cycle. A machine, installed in Weinfelden, has developed an output of about 20,000 kw. Oerlikon has built a gas turbine of conventional design with an excellent centrifugal compressor. Brown Boveri has delivered a number of machines with a record of several years of successful operation.

Admirable results have also been obtained in the United States, outside the field of aviation, as a result of years of effort, particularly by the General Electric Company which has the greatest number of machines in operation, and also by Westinghouse, Allis Chalmers, and others. In great Britain, Parsons, the British Thompson Houston Co., Metropolitan Vickers, Ruston and Hornsby, English Electric, and Allan and Sons have turned out units. One is on a ship and another on rails where it competes with a Brown Boveri gas-turbine locomotive. In France, the Compagnie Electro-Mecanique, Alsthom, Turbomeca, and Rateau have designs of their own. Gas turbines have been produced in Sweden, Holland, and Denmark. As a curiosity the reciprocating unit developed by the Phillips Co. of Holland may be mentioned. Air is compressed in multicylinder compressors, passed on to an air heater, heated by a continuous flame, and expanded again through pistons. This machine is therefore of the continuous-combustion class.

In closing, I would like to make a general remark on our subject. It seems to me that we can distinguish three typical epochs in the history of gas-turbine engineering and in engineering more generally. The first, around 1900, was the epoch of great inventors, of men acting by intuition more than by reasoning and computation. They created an almost perfect Diesel engine and a fair steam turbine, but no gas turbine worthy of the name. The second is the epoch of more precise theoretical thinking to assist intuition. It saw the growth of steam turbines to 100,000 kw and more and produced the first working gas turbines. Stodola, it is only fair to recognize, promoted this evolution, though, of course, he was not the only one. The third epoch, the present, is a period of systematic experimentation to support theoretical thinking which in turn guides intuitive action. It is the epoch of wind tunnels, of metallurgical laboratories, of research on combustion, of physicists and chemists assisting the engineer. We have learned to observe nature and to interpret her teachings and translate them into practical constructions. The gas turbine is a very pretentious machine which, unlike the combustion engine and the steam turbine, had to await the advent of the third epoch before it could be made a success

Gas-Turbine Progress Report—Introduction

By R. TOM SAWYER,[1] NEW YORK, N. Y.

THIS year (1952) we are celebrating the 161st anniversary of the granting of the first patent covering a gas turbine. In 1791 an English patent was issued to John Barber for the combination of an air compressor, a gas-fired combustion chamber, and a turbine adapted both to drive the compressor and to perform useful work. The fuel was to be drawn from a pressurized gas producer, thus enabling the plant to use solid fuel. There is no evidence that this patent was ever reduced to practice.

The first gas turbine which was actually operated was that designed and built in France by Stolze. Testing of this unit began in 1900, but the results were discouraging because of the low component efficiencies. Although the unit was not successful, it represented a major step forward in design since it employed an axial compressor and turbine as well as a regenerator.

The first United States patent covering a complete gas turbine was issued on June 24, 1895, to Charles G. Curtis. The design shown in his patent drawing is quite similar to that used in aircraft gas turbines today. For this achievement the Gas Turbine Power Division presented its first award to Mr. Curtis in 1948.

In the early part of the twentieth century many efforts to reduce the gas turbine to practice failed, largely because of lack of suitable materials to permit the high temperatures needed and of a high-efficiency compressor.

The modern era of the gas turbine begins in the 1930's. Brown Boveri had developed suitable axial-flow compressors and had gained invaluable experience with gas turbines used as auxiliaries to Diesel engines, Velox boilers, and Houdry-process charging sets. The first practical central-station gas-turbine power plant was built by Brown Boveri and tested in 1939. It is still in successful operation where it was originally placed in the city of Neuchâtel. The net output is 4000 kw with a thermal efficiency of 18 per cent. The first gas-turbine locomotive also was produced by Brown Boveri and was placed in operation on the Swiss Federal Railways, in 1941, and is still in service.

In this country credit is given to Sir Frank Whittle for instigating and promoting, as well as patenting, the jet-propelled plane used today. In 1930 Sir Frank Whittle applied for his first gas-turbine patent, consisting of a combination axial and centrifugal compressor and two-stage axial turbine. However, credit for first reducing the turbojet to practice goes to a young German physicist, Pabst von Ohain, who, while in the employ of Ernest Heinkel of Germany, designed and built the first turbojet engine (He S 3b) which flew in the Heinkel He 176 plane on August 27, 1939. The first British unit flew in May, 1941, and this was the second gas-turbine jet-propelled plane. The German design was unique in using a centrifugal compressor back to back with a radial inflow turbine.

The first boat to operate exclusively with a gas turbine was built for the United States Navy and powered with a 175-hp Boeing turbine. This first entered service on May 30, 1950. It is of interest to note that the British put a launch in the water on May 6, 1950, which was powered by two Rover gas turbines. However, this craft did have a small auxiliary Diesel engine for harbor use. In this connection it is of interest to note that the Metropolitan Vickers 3000-hp gas-turbine locomotive first placed in service early in 1952, was the first locomotive to be exclusively powered by a gas turbine. All other locomotives had a small Diesel engine on board for hostling purposes.

The Rover Company equipped the first gas-turbine-propelled automobile which entered service in 1950, and in the same year the Boeing turbine was the first to be used to operate a heavy-duty truck. It also should be pointed out that, to the author's

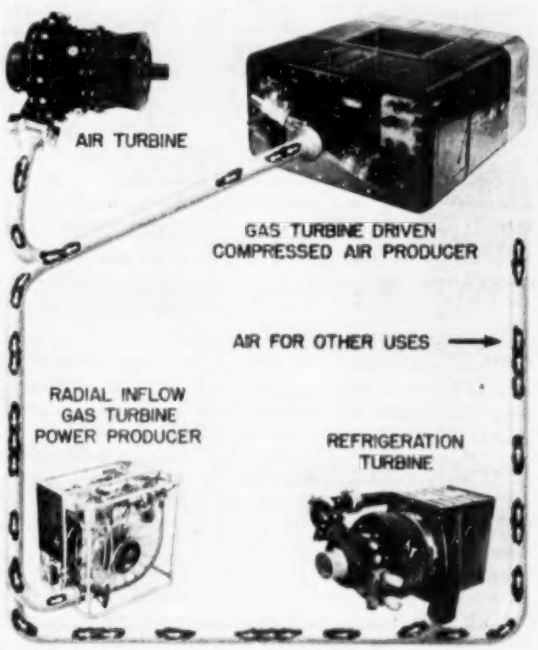

FIG. 1 AIRESEARCH TURBINES ARE EXTREMELY LIGHTWEIGHT AND SMALL FOR AIRCRAFT AUXILIARY USE

[1] Manager, Research Department, American Locomotive Company. Mem. ASME.

Contributed by the Gas Turbine Power Division and presented at the Fall Meeting, Chicago, Ill., September 8–11, 1952, of THE AMERICAN SOCIETY OF MECHANICAL ENGINEERS.

NOTES: This is paper No. 52—F-1A of a Progress Report which the Executive Committee of the Gas Turbine Power Division authorized at its 1951 Annual Committee Meeting. It is expected that similar Progress Reports will be issued at appropriate times in the future. The series includes the following: "Materials, Cooling, and Fuels," by A. A. Hafer, paper No. 52—F-1B; "Cycle Components," by P. F. Martinuzzi, paper No. 52—F-1C; "Automotive," by Frank L. Schwartz, paper No. 52—F-2; "Railroads," by K. A. Browne, J. I. Yellott, and P. R. Broadley, paper No. 52—F-3; "Marine," by W. A. Dolan, Jr., and A. A. Hafer, paper No. 52—F-4A; "Merchant Vessels," by W. A. Dolan, Jr., and A. A. Hafer, paper No. 52—F-4B; "Naval Vessels," by W. A. Dolan, Jr., and A. A. Hafer, paper No. 52—F-4C; "Stationary Electric Generation," by Lee Schneitter, paper No. 52—F-5; "Industrial," by L. N. Rowley and B. G. A. Skrotzki, paper No. 52—F-6; "Aviation," by I. H. Driggs and O. E. Lancaster, paper No. 52—F-7.

Statements and opinions advanced in papers are to be understood as individual expressions of their authors and not those of the Society.

TABLE 1 LIST OF WORLD-WIDE GAS-TURBINE UNITS

(Aircraft gas-turbine units not listed except those built by AiResearch, Boeing, B.T.H., Continental, Fairchild, Solar, Turbomeca)

Ratings

lb t = pounds thrust
hp = horsepower
ehp = equivalent horsepower = hp + (lb t/2.6)
kw = kilowatt
cfm = cu ft per min

Company and Model No.	Rating	Service built for	Remarks[a]
Denmark			
Elsinore Ship-building Co.	3000 hp	Exp. marine	(4B) High-press. part plant on test developing 500 net hp
England			
W.H. Allen & Sons	1000 kw	Gen. unit	(4C) British Navy-testing for emergency use
	300 hp	Gen. unit	(4C) British Navy
British Thompson Houston	1200 hp	Marine	(4B) In tanker Auris
	2500 kw	Stationary	(2,5) For East Africa
Sir Frank Whittle's first unit		Jet	(9) Built in 1936
W1	2000 lb t	Jet	(9) First British unit to fly, 1941
John Brown	300		(10) First operated on open cycle, then closed
	500 hp	Experimental	
Closed cycle	1000 hp	Experimental	(10,11) Testing all types of fuels in company shops
Closed cycle	700 kw	Stationary	(6) Coventry Gas works
Closed cycle	12500 kw	Stationary	(5) Dundee, Scotland
Brush Elec. Eng. Co.	2500 kw	Stationary	(5) For Metro. Water Board
Centrax	160 hp	Automotive	(2)
English Electric	150 hp		
	150 hp	Experimental	(14) In 1944
	2000 kw	Experimental	(5) One coal, one methane for Ministry of Fuel & Power
	1875 kw	Stationary	(5) Stand-by - Ashford
	20000 kw	Stationary	(5) Two on order for Ministry of Supply
	6000 hp	British Navy	(4C) HMS Nothman (on test)
Metropolitan Vickers Ltd.	2000 kw	Stationary	(5) One on shop power supply one on producer gas
	1750 kw	Stationary	(5) For Shell Petroleum, Venezuela
	2500 kw	Stationary	(5) Metro. Water Board-Ashford
	15000 kw	Stationary	(5) At Manchester
Metric - G1 (model no.)	2500 hp	British Navy	(4C) 1st in Science Museum 2nd in MTB 5559 3rd in Admy Expt Estab't
	4800 hp	British Navy	(4C) 2 units per boat 2 gun boats in operation
	3000 hp	Locomotive	(3) 1st British built
Pametrada	2000 hp	Experimental	(10) For combustion tests
	3500 hp	Marine	(4B) In Wallsend Research Station
	15000 hp	British Navy	(4C) Only combustor on test
C.A. Parsons	500 hp	Experimental	(8,11) Pulverized coal
	1800 hp	Locomotive	(3) Coal burning-mech. drive Ordered by Ministry of Fuels
	2000 kw	Only air bleed	(6) At Fyestock
	2500 kw	Stationary	(5) Shop test unit
	10000 kw	Stationary	(5) For Fyestock
	15000 kw	Stationary	(5) For Dunston
Rolls-Royce	6000 hp	British Navy	(4C) For HMS Gray Goose
Rover	200 hp	Automotive	(2) First gas turbine to operate in auto
T.B	150 - 185 hp	British Navy	(2,4C) 4 units built
Ruston & Hornsby	1070 - 1200 hp	Locomotive	(3) Proposal
T.A.	750 kw	Stationary	(5) 1 experimental burning peat 3 for Air Ministry
FRANCE			
Alsthom	5000 kw	Stationary	(8) At company plant-Belfort
Cie Electro-Mecanique	10000 hp	Experimental	(14)
Leffly	190 hp	Automotive	(2) In bus chassis, 230 lb
Rateau	2000 kw	Stationary	(5) Test unit at St. Denis
	3900 hp	Marine	(4B) Built by LACM with Rateau for Liberty Ship
Turbomeca	1600 hp	Experimental	(14) At St. Denis Lab.
	3500 hp	French Navy	(4C) Under construction for
Pimedon	1.3 lb/sec	Air bleed	(2) 160 lb
Palouste	2.3 lb/sec	Air bleed	(2) 170 lb
Oredon	170 hp	Gen. set	(2)
Artouste I	250 - 280 hp	Acc. drive	(2) 185 lb
Artouste II	330- 400 hp	Acc. drive	(2) 200 lb
Turbine Motrice	275 - 300 hp	Automotive	(2) 225 lb Artouste IB modified with free turbine
		Automotive study	(12) Palouste delivers air to another combustor and turbine
Company and Model No.	Rating	Service built for	Remarks
Pimene TR-011	175 - 242 lb t	Jet	(2) 120 lb
Palais	270 - 330 lb t	Jet	(2) 137 lb
Marbore I	530 - 650 lb t	Jet	(2)
Marbore II	710 - 880 lb t	Jet	(2) 275 lb
Aspin I	160 - 450 lb t	Jet-ducted fan	(2) 275 lb
Aspin II	660 - 790 lb t	Jet-ducted fan	(2) 300 lb
HOLLAND			
Gasturbine Maatschappij-N.V.	2000 kw	Stationary	(8) For Shell at Venezuela
ITALY			
Stablimento Ernesto Breda	350 hp	Experimental	(2) at Milan
JAPAN			
Tokyo Shibaura Electric Co.	2000 hp	Experimental	(8) For Ry. Tech. Res. Inst.
	1500 hp	Experimental	(8) For Ry. Tech. Res. Inst.
SPAIN			
C.E.T.A.	170 hp	Automotive	(12) A project
SWEDEN			
DeLaval	2400 hp	Swedish Navy	(4C) For torpedo boat
Stal Factory	2400 kw	Stationary	(5) Under test
SWISS			
Brown Boveri & Co.	23000 cfm	Boudry Unit	(6) 1 unit - Magnolia Pet.
	40000 cfm	Boudry Unit	(6) 2 units - Sun Oil Co.
	26500 cfm	Blast Furnace	(6) At Baracaldo, Spain
	2200 hp	Locomotive	(3) First gas turbine loco. Swiss Federal Rys.
	2500 hp	Locomotive	(3) British Rys.
	4000 hp	Experimental	(15) Compres at Co. Shops
	1500 kw	Experimental	(16) at Co. Shops
	2000 kw	Blower Drive	(6) In steel mill, Spain
	4000 kw	Stationary	(5) 1st plant at Neuchatel 1 for Peru, 3 Iran
	1200 kw	Stationary	(5) at Alexandria, Egypt
	1650 kw	Stationary	(5) 2 for Caracas
	5000 kw	Stationary	(5) 1 for Caracas 4 Arabian oil fields
	5400 kw	Stationary	(5) at Luxembourg
	10000 kw	Stationary	(5) 1 at Roumania 1 at Peru
	13000 kw	Stationary	(5) 1 at Reznau Station
	27000 kw	Stationary	(5) 1 at Reznau Station
Escher Wyss	2000 kw	Experimental	(5) 1st closed-cycle plant started in company shops 1939
Oerlikon	12500 kw	Experimental	(5) At Paris, France
	1000 kw	Experimental	(5) At company shops
	730 kw	Stationary	(5) For "Bone" Algeria
Saurer	250 hp	Experimental	(1C) Automotive
Sulzer Bros.	7500 hp	Marine	(4B) Rebuilt for experimental use
	20000 kw	Stationary	(5) At Winterthur Station
UNITED STATES			
AiResearch			
GTC 41/44	65 air hp	Air Bleed	(2)
GTC 85	100 air hp	Air Bleed	(2)
GTP 70	100 hp	Power Shaft	(2) 100 lb
GTM 125	125 - 150 hp	Gas Turbine Motor	(2) 80 lb (variable missile)
Allis Chalmers	16000 cfm	Boudry Unit	(6) 1 at Marcus Hook
	23000 cfm	Boudry Unit	(6) 7 units plus 1 at L.D.C. (Locomotive Development Committee)
	40000 cfm	Boudry Unit	(6) 11 Units
	60000 cfm	Boudry Unit	(6) 1 Unit
Navy No. X30LV50AC-1	3000 hp	Experimental	(4C) Tested at Annapolis at 1500 F
	4250 hp	Experimental	(3) Owned by L.D.C., on test
Boeing			
Navy No. 2MV27B-2	160 hp	Navy	(4C,2) 1st boat powered by gas turbine only 1st gas turbine truck
Navy No. 2MV27B-4	320 hp	Auxiliary	(4C,5) Minesweeper gen. unit
500	180 lb t	Jet	(2) 1st Boeing unit built 120 lb
502	220 ehp	Prop	(2) First unit in Helicopter
Clark Bros.	5500 hp	Pipe line	(6) At Moorehead, Ky.
Continental Motors (2) Have license from French Turbomeca for all units except "Oredon"			
DeLaval	3000 hp	Locomotive	(8) Only designed
Navy No. X7MV36D-1	750 hp	Experimental	(4C) Dismantled
Elliott	3000 hp	Marine	(4B) For Maritime Commission, held up
Navy No. X25LV30E-1	2500 hp	Experimental	(4C) Completed and dismantled

TABLE 1 (*Continued*)

Company and Model No.	Rating	Service built for	Remarks
Navy No. 30LV7E-2	2379 hp	U.S. Navy (4C)	1 Completed and dismantled 1 Stopped construction
	3750 hp	Experimental(8,13)	Stopped construction, cancelled. For L.D.C.
	3900 hp	Locomotive (8,14)	For Santa Fe Ry. Completed, tested and cancelled
	3500 hp	Experimental (17)	On test at company shops
	5000 hp	Experimental (17)	Under development
Fairchild (Stratos) Oredon J 44	140 hp 1000 lb t	Gen. drive (2) Jet (18)	Licensed from Turbomeca 300 lb
General Electric	4500 hp	Locomotives (3)	Demonstrator in service 11/14/48 1st unit sold U.P.-Delivered Jan. 1952
	5000 hp) 3500 kw)	Stationary (5)	1st U.S.A. central station 7/29/48 Others sold and built
	5000 kw	Stationary (5)	2 shafts, 2 comp. Many sold and built
	4000 kw	Stationary (5)	Split turbine At Gainesville, Tex.
	5000 hp	Pipe line (6)	Split turbine, variable nozzles Large number on order
General Motors			
Allison Div - Navy No. 20MV20A-1	2000 hp	Navy (4C)	Split turbine
G.M. Research Laboratory Div.	300 hp	Automotive (2)	Small split turbine
Solar - M80	140 hp	Experimental (2)	Twin turbines geared to 1 gen.
Mars - T41	25 kw	Gen. unit (2)	
Mars - T45 - Navy No. 1MC4,5S-2	47 hp	Fire pump (4C,2)	Hand started
Mars - T55	47 hp	Fire pump (2)	Improved T45 165 lb
Jupiter - T400 Navy No. 3MV80S-1	200 kw	Gen. unit (4C,2,5)	One built
Jupiter - T520	280 -		
Navy No. 5MC20S-5	340 kw	Gen. unit (4C,2)	Improved T400
Jupiter - T522	420 -		
Navy No. 5MV20S-4	520 hp	Propulsion (4C,2)	Split turbine
Westinghouse Electric	1800 hp	Pipe line (6)	1st unit in pipe-line service
	2000 hp	Loco otive (3)	Two units in experimental locomotive
	1250 kw	Stationary (5)	Shop test unit
	5000 kw	Stationary (5)	West Texas utilities
	15000 kw	Stationary (5)	2-shaft unit, Oklahoma Public Service
	3500 kw) 5000 hp)	Pipe line (5,6)	(Split turbine and regenerator (Shop test unit

[a] Numbers in parentheses apply to the references accompanying the table.

knowledge, the Boeing turbine was the first gas turbine to propel a helicopter through the usual means of transmission, actually replacing a reciprocating engine. The first flight was made on December 10, 1951, at Bradley Field, Conn. The British Thomson-Houston Company was the first to place a gas turbine in a commercial ship, the *Auris*, and operate it at sea for some period of time, making a run in 1951, from England to the Gulf Coast and return. This 1200-hp turbine replaced one of the four Diesel-engine generator sets.

England is taking the lead in the development of the marine gas turbine with many builders actually in this field, including Allen, B. T. H., English Electric, Metropolitan Vickers, Pametrada, Rolls Royce, and Rover.

The Escher Wyss factory is the birthplace of the closed-cycle system which is noted for its high efficiencies and capability of burning any fuel.

The Locomotive Development Committee of Bituminous Coal Research, Inc., adhering to the simple open cycle, is currently running high-load tests on a 4250-hp coal-fired plant. In England the Parsons Company has a contract for an 1800-hp locomotive which will use the exhaust-heated cycle. The power turbine will drive the locomotive through a two-speed transmission. The John Brown Company is conducting extensive experiments with the closed cycle using a stoker-fired air heater. A number of projects are under way in England and elsewhere directed toward the development of successful methods for using peat, lignite, mine gas, and other materials, as gas-turbine fuel.

Table 1 lists all gas-turbine plants on which details have been made public. These range from the small units produced by AiResearch, of which thousands have been produced, Fig. 1, to the largest unit in service today, Brown Boveri's 27,000-kw gas turbine in the Beznau, Switzerland plant, Fig. 2.

Details of the units listed in Table 1 can be found in the companion papers of this symposium.

Conclusions

The following conclusions may be drawn from the papers constituting this Progress Report:

1 Statements are made as to the tremendous future role the gas turbine will play in the power field. As we are all human, it is hard for us to realize fully what this means until we actually see with our own eyes the turbine applied to some of these many uses. For example, most of us are automotive-minded. We know about what a jeep engine looks like and it is hard for us to think that an engine that size could power a 30-ton truck. However, that is just what the Boeing turbine is doing—powering a huge truck and it isn't as big as a jeep engine.

2 Practical "by-products" have resulted from many development programs. In more than one case considerable money has been spent to develop a turbine for a certain use, and after being put to that use it was found to be better in an entirely different application, and with only a few modifications. In other words, we learn a great deal by actually doing rather than just theorizing.

3 Fuel flexibility is the subject of the most important develop-

References

1A "Gas-Turbine Progress Report—Introduction," by R. Tom Sawyer, Paper No. 52—F-1A.

1B "Gas-Turbine Progress Report—Materials-Cooling-Fuels," by A. A. Hafer, Paper No. 52—F-1B.

1C "Gas-Turbine Progress Report—Cycle Components," by P. F. Martinuzzi, Paper No. 52—F-1C.

2 "Gas-Turbine Progress Report—Automotive," by Frank Schwartz, Paper No. 52—F-2.

3 "Gas-Turbine Progress Report—Railroad," by K. A. Browne, J. I. Yellott, and P. R. Broadley, Paper No. 52—F-3.

4A "Gas-Turbine Progress Report—Marine," by W. A. Dolan, Jr., and A. A. Hafer, Paper No. 52—F-4A.

4B "Gas-Turbine Progress Report—Merchant Vessels," by W. A. Dolan, Jr., and A. A. Hafer, Paper No. 52—F-4B.

4C "Gas-Turbine Progress Report—Naval Vessels," by W. A. Dolan, Jr., and A. A. Hafer, Paper No. 52—F-4C.

5 "Gas-Turbine Progress Report—Stationary Electric Generation," by Lee Schneitter, Paper No. 52—F-5.

6 "Gas-Turbine Progress Report—Industrial," by L. N. Rowley and B. G. A. Skrotzki, Paper No. 52—F-6.

7 "Gas-Turbine Progress Report—Aviation," by I. H. Driggs and O. E. Lancaster, Paper No. 52—F-7.

8 "Gas-Turbine Manual," by R. J. Welsh and Geoffrey Waller Temple Press Ltd., London, England, 1951, pp. 214–225.

9 "The Story of the British Gas Turbine," Sidney-Barton, Ltd., London, England, 1951, p. 22.

10 "What's Going on in England?" by Hamish Ferguson, *Diesel Progress*, Diesel Engines, Inc., Los Angeles, Calif., April, 1952, p. 66.

11 "The Oil Engine and Gas Turbine," Temple Press Ltd., London, England, August, 1951, pp. 152–164.

12 "The Oil Engine and Gas Turbine," Temple Press Ltd., London, England, November, 1951, p. 287.

13 "The Oil Engine and Gas Turbine," Temple Press Ltd., London, England, March, 1951, p. 350.

14 "Power," by L. N. Rowley, McGraw-Hill Book Company, Inc., New York, N. Y., 1949, pp. 95–97.

15 "Gas Turbine Construction," by R. Tom Sawyer, Prentice Hall, Inc., New York, N. Y., Copyright 1947, p. 82.

16 "The Modern Gas Turbine," by R. Tom Sawyer, Prentice Hall, Inc., New York, N. Y., Copyright 1947, second edition, p. 107.

17 Letter to R. Tom Sawyer dated March 27, 1952, from The Elliott Company, Jeannette, Pa.

18 "Ordnance," American Ordnance Association, Washington, D. C.; advertisement by company, May-June, 1952, p 977.

ments which are currently under way. Splendid records have been made in this country with plants which burn natural gas and high-grade distillate fuels. Problems begin to be encountered as soon as less expensive fuels are used which contain solid residues. Most of the plants now in service can burn Diesel oil satisfactorily but only a few can burn residual fuel without encountering vanadium difficulties. After seven years of work, the Locomotive Development Committee is now operating its large turbine at high loads with bituminous coal as its only fuel. Tests have been made at the Dunkirk laboratory using Australian lignite, which burns with a short hot flame like jet fuel and leaves a minimum of ash to be removed from the heated air. Other ways of using coal in the gas turbine are being tried by at least seven separate organizations throughout the world, and more than one method should be perfected within the next few years.

The burning of heavy oil, once thought to be a simple assignment when compared with the problem of burning coal, has been found to be difficult because of deposits and corrosion at high temperatures. The immediate solution to burning heavy oil is to find a suitable additive, but even this is being difficult and a satisfactory one has not yet been found for general use. It is, therefore, possible that a satisfactory method of burning coal may be found as soon as we economically can burn heavy oil in high-temperature turbines.

4 With the use of the gas turbine definite progress has been made in safety. This is a factor which will come to the front more and more. "Jet fuel" is safe compared to gasoline. Years ago the railroads discarded practically all large gasoline-burning power plants for safety reasons. In time the air lines no doubt will follow suit. The trucking industry has largely made this change and it is possible with the use of the gas turbine that even private automobiles may get away from an explosive fuel.

5 The authors of the Progress Reports have tried to give objective statements of the present and future position of the gas turbine in various fields. As stated previously, these papers do not cover power plants of which only a portion of the plant is a gas turbine, and here lies a great expanding field, not only for the gas turbine but other types of power plants that have reached their limit and can be expanded only by the use of the gas turbine.

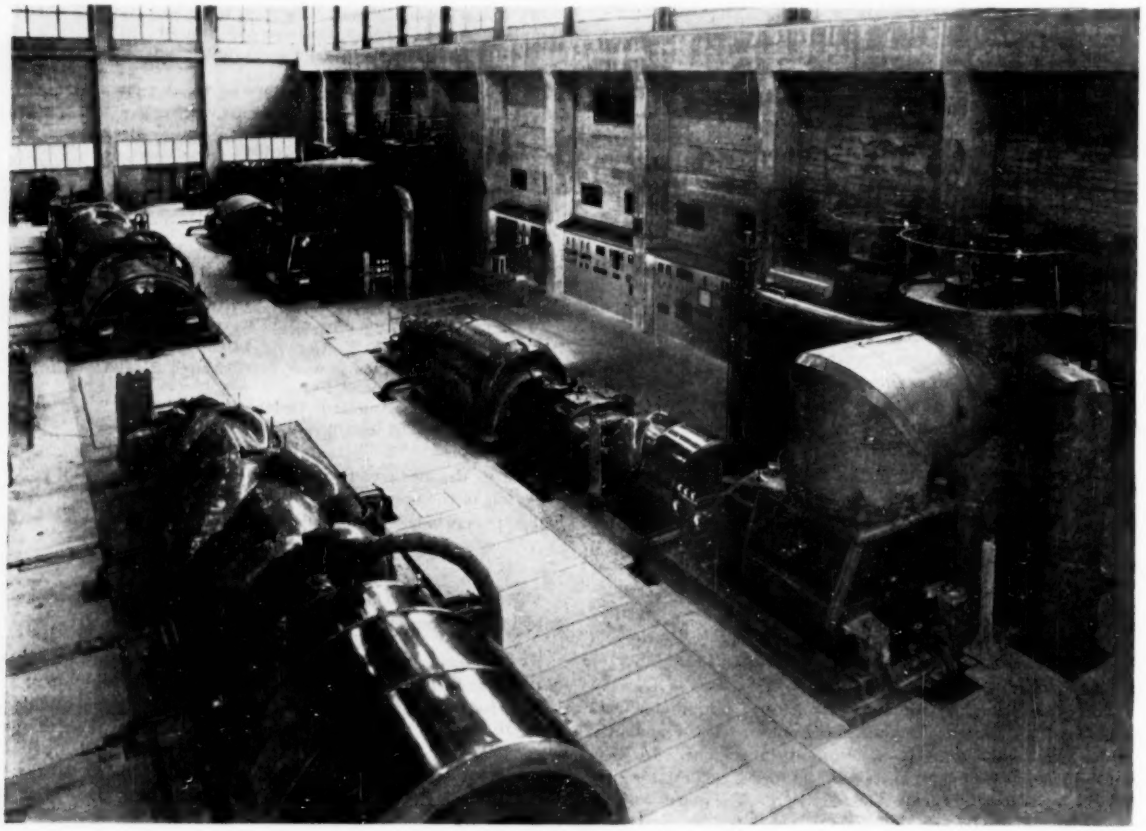

FIG. 2 BROWN BOVERI TURBINES IN THE BEZNAU PLANT

(The unit in the foreground is rated 13,000 kw; rear unit is rated 27,000 kw. The latter is the largest unit and the plant is the largest gas-turbine plant in the world.)

Gas-Turbine Progress Report—Materials, Cooling, and Fuels

By A. A. HAFER,[1] WASHINGTON, D. C.

1 MATERIALS

Improved Alloys

THE obvious way of raising the gas-turbine cycle efficiency would be by using superior high-temperature alloys to permit higher inlet temperatures. The trend toward developing materials with good high-temperature properties has been going on for many years. Since 1930 there has been a sharp upswing in research to perfect high-temperature materials and this high level of research is still continuing (1).[2] Since 1940 the tremendous amount of time and effort devoted to high-temperature alloys has certainly been influenced strongly by the desirability of obtaining higher operating temperatures in the gas-turbine engine.

It is difficult to produce an alloy which will satisfy the stringent requirements imposed by such gas-turbine-engine components as the turbine blades and disks. Such components demand materials having the following characteristics (2):

1 Good high-temperature properties.
2 Desirable characteristics at room temperature.
3 Consistency of quality.
4 Good oxidation and corrosion resistance.
5 Good load-carrying ability.
6 Good structural stability.
7 Rentention of ductility.
8 Good fatigue strength.
9 Good damping capacity.
10 Good machinability.
11 Good weldability.

The exact value or relation of these various characteristics will vary, depending on the temperature, pressure, speed, and application to which the gas-turbine engine will be subjected.

A tremendous amount of literature has been published in the past several years furnishing data on high-temperature alloys (3, 4, 5, 6, 7, 8, 9, 10, 11). The Bureau of Ships has recently compiled data on 39 gas-turbine alloys as given in Table 1.

There have been some differences of opinion in the past as to the type of laboratory tests which should be used to evaluate the suitability of an alloy for highly stressed high-temperature parts. Where only a short life is desired, this can be determined easily. If the engine is to have a life of 10,000 to 50,000 hr or more, the problem is much more difficult. Even if it were feasible to run tests lasting 50,000 to 100,000 hr, it can be seen that a number of years would elapse before a final answer were known. Creep tests have been commonly employed to determine life at given conditions (12). Sulzer Brothers, Ltd., also supplements creep tests with observation of structural changes occurring during such tests (13). Other work has indicated that the effect of creep predominates above a certain temperature and fatigue is more important below this temperature. A combined stress test, in which both fluctuating and steady stresses are involved, is proposed to evaluate both conditions (14). In a series of wheel bursting tests carried out by General Electric it was concluded that the most important factor contributing to high and consistent bursting speed is ductility (15).

A possible explanation concerning the relative importance of tensile strength and ductility may be due to differences between ferritic and austenitic steels. Ferritic steels have good plastic properties so that maximum tensile strength is an adequate criterion. In austenitic steels, however, presence of brittle networks might prevent the full plasticity from being available, so that perhaps only 80 per cent of the test tensile strength should be used for design (16). It has been proposed that for selecting blade materials the laboratory tests should include evaluations of fatigue, stress rupture, impact, creep, and thermal shock (17).

As would be suspected, the development of new high-temperature alloys has resulted in new or more complex production procedures. This, coupled with the necessity of obtaining precise airfoil shapes in certain components for maximum efficiencies, have resulted in the following problems (18):

1 Machining of materials having considerably worse machining properties.
2 Production of components requiring high degree of finish and closer tolerances than usual.
3 Inspection of these components.

The foregoing problems have been solved to varying degrees. For example, such inspection methods as "ultrasonic" and "zyglo" inspection partially resulted from the stringent requirements of the jet engine.

Heat-treatment required new ingenuity. Heat-treating large forgings at temperatures in the order of 2200 F resulted in new advances in this field (19). In addition, a stimulus was provided for research on new metals. One of the most promising metals for gas-turbine components is titanium. It is now commercially feasible to cast titanium ingots weighing up to 650 lb (20). Gas-turbine-engine requirements also have resulted in new advancements in the precision-casting field. The adaptation of the precision investment-casting method or "lost-wax" process now permits cast turbine blades (21). It now seems feasible also to cast small axial-turbine disks (22). In addition, the small radial-turbine rotor may be cast with integral blades. The Solar Navy Model No. IMC458-2 gas-turbine engine is being produced with

[1] Lieutenant, USNR, Gas Turbine Project Officer, Turbine and Gear Branch, Bureau of Ships, Department of the Navy. Jun. ASME.

[2] Numbers in parentheses refer to the Bibliography at the end of the paper.

Contributed by the Gas Turbine Power Division and presented at the Fall Meeting, Chicago, Ill., September 8–11, 1952, of The American Society of Mechanical Engineers.

Notes: This is paper No. 52—F-1B of a Progress Report which the Executive Committee of the Gas Turbine Power Division authorized at its 1951 Annual Committee Meeting. The series includes the following: "Introduction," by R. Tom Sawyer, paper No. 52—F-1A; "Cycle Components," by P. F. Martinuzzi, paper No. 52—F-1C; "Automotive," by Frank L. Schwartz, paper No. 52—F-2; "Railroads," by K. A. Browne, J. I. Yellott, and P. R. Broadley, paper No. 52—F-3; "Marine," by W. A. Doian, Jr., and A. A. Hafer, paper No. 52—F-4A; "Merchant Vessels," by W. A. Dolan, Jr., and A. A. Hafer, paper No. 52—F-4B; "Naval Vessels," by W. A. Dolan, Jr., and A. A. Hafer, paper No. 52—F-4C; "Stationary Electric Generation," by Lee Schneitter, paper No. 52—F-5; "Industrial," by L. N. Rowley and B. G. A. Skrotzki, paper No. 52—F-6; "Aviation," by I. H. Driggs and O. E. Lancaster, paper No. 52—F-7.

Statements and opinions advanced in this paper are to be understood as the individual expressions of the author and not to be construed as official or reflecting the views of the Navy Department, of the Naval Service, or of the Society. Paper No. 52—F-1B.

TABLE 1 GAS-TURBINE ALLOY DATA SHEET

ALLOY	CONDITION	NOMINAL COMPOSITION										STRESS RUPTURE (X 10^3 p.s.i.)											
												1200°F		1350°F		1500°F		1600°F		1700°F		1800°F	
		C	Cr	Ni	Co	Mo	W	Cb	Ti	Fe	Other	100 Hr	1000 Hr	100 Hr	1000 Hr	100 Hr	1000 Hr	100 Hr	1000 Hr	100 Hr	1000 Hr	100 Hr	1000 Hr
AISI 302	F*	.14	18.	9.						Bal		23.	16.5		7.5		3.5						
AISI 310	F	.25	25.	21.						Bal			17.		8.7		4.5		3.		2.4		1.95
AISI 316	F	.10	17.	12.		2.5				Bal			25.		14.0		7.		4.		2.3		1.3
AISI 321	F	.08	18.	9.5					5xC	Bal		29.5	17.5		7.6		3.7		2.75				
AISI 347	F	.08	18.	10.5				10xC		Bal			17.0		9.0		4.4						
Inconel	F	.05	14.	78.						7.		22.	14.5	10.5	6.8	5.7	3.7	4.2	2.7			2.5	1.55
Inconel X	F	.05	15.	73.				.70	2.5	7.	Al .9	80.	68.	50.	40.	28.	18.	17.					
Inconel W	F	.05	15.	73.					2.5	7.	Al .9	63.	49.	45.	32.	22.5	11.						
Nimonic 80A	F	.04	20.	75.					2.4	.5	Al1.2	63.	49.	45.	32.	22.5	11.						
Nimonic 90	F	.04	20.	55.	20.				2.4	.5	Al1.2	76.	64.	50.	38.	28.	18.	17.					
Waspaloy	F	.07	20.	Bal	14.	3.			2.5	2.0	Al1.2			52.5	40.	28.	20.	16.					
Hastelloy B	E	.05		65.		29.				5.0		58.	33.2	34.	25.	17.	11.3	11.7	8.3				
Hastelloy C	E	.1	14.5	57.		17.	4.5			5.5						14.1	10.7						
Refractalloy 26	F	.03	18.	37.	20.	3.			3.	Bal	Al .3	74.		48.		29.	18.						
Refractalloy 70	C	.1	20.	20.	30.	8.	4.			Bal						19.	15.	12.5	9.6				
Vitallium (H.S. 21)	C	.2	28.	2.	62	6.				2.		54.	43.	36.5	28.0	22.	16.	18.4	14.5	13.1	10.5	8.8	6.4
422-19 (H.S. 30)	C	.4	25.	16.	52.	6.				2.				47.	36.3	30.4	23.5	19.0	14.7	14.7	11.5	10.1	7.1
M.I.T. "J" Alloy	C	.7	23.	6.	60.	6.				2.3	Ta 2.			52.5	40.5	34.8	28.2	26.4	21.	17.2	12.3	12.8	9.3
M.I.T. 100 NT-2	C	1.	20.	30.	20.	3.	2.2			Bal	Ta 2.					30.5	22.8	26.1	19.3	18.2	13.1	13.6	9.9
X-63 (G.E.)	C	.4	25.	10.	55.	6.				3.6						26.8	20.2						
X-40 (H.S. 31)	C	.5	25.	10.	55.		7.			2.		55.	46.	44.8	34.	28.	23.2	21.3	18.5	17.3	14.4	11.3	9.8
61 (H.S. 23)	C	.4	24.		68.		6.			2.		58.	47.	35.2	27.	26.7	20.5	17.1	11.8	13.5	9.4	8.7	5.6
6059 (H.S. 27)	C	.5	26.	33.	34.	6.				2.		55.	46.	36.4	30.	24.	18.8	16.	12.	12.	8.6	9.2	7.
19-9 DL	F	.3	19.	9.		1.3	1.2	.4	.2	Bal		60.	50.	35.	20.5	13.3	10.						
19-9 W-Mo	F	.12	19.	8.5		.35	1.25	.5	.35	Bal		54.5	42.	28.5		13.5							
S-590	F	.5	20.	20.	20.	4.	4.	4.		Bal		52.	40.	31.5	23.5	20.	15.5	14.0	10.5	9.2	6.5	5.5	3.4
S-816	F	.4	20.	20.	44.	3.5	4.	4.		4.		64.	49.2	40.	29.5	27.	21.1	14.8	10.	9.8	6.4	5.3	3.1
L-251	C	.4	18.5	10.	53.		14.5			2.	B .06	72.	59.5			28.1	22.8						
L-605	F	.15	20.	10.	Bal		15.			2.		45.				24.	19.					7.2	4.5
HE 2048	C	.4	26.	30.	15.	4.	2.			Bal	B .15			36.	28.	22.	16.	17.5	13.			9.5	
N-155 (Med. C)	E	.35	20.	20.	20.	3.	2.5	1.		Bal	N .1	60.	45.5	36.	26.	24.5	18.6	15.5	11.4	7.6	4.7	4.9	2.75
I-1360 (G.E.)	C	.1	10.	Bal		5.		2.		6.4	Al 6. B .5					45.	32.5						
GT-45	F	.08	17.	14.		3.		.5	.3	Bal	Cu 3.	46.1	39.	27.	22.4	15.	12.						
H.S. 88	F	.15	12.	15.		2.	.5		.6	Bal	B .1	43.	36.	25.	19.3	12.1	9.2						
Timken (16-25-6)	F	.1	16.	25.		6.				Bal	N .15	57.	42.	28.	19.	13.3	9.						
Discaloy 24	F	.03	13.	26.		3.			2.3	Bal	Al .6	56.	46.	30.5	17.								
Tinidur (A-286)	F	.08	15.	26.		1.3			1.9	Bal	V .3 Al.35	65.5	45.	34.5	21.3	13.	8.						
K-42-B	F	.06	18.	42.	22.				2.6	Bal	Al .6	62.	39.5	36.5	26.5	22.5	15.						
G-18-B	F	.4	13.	13.	10.	2.	2.5	3.		Bal		52.	37.	28.5	20.5	16.	11.						

NOTES: The stress-rupture data tabulated and compiled by Bureau of Ships Code 343 have been taken from typical test values reported by one or more accredited sources known to the Bureau of Ships. The test specimens were subjected to the usual fabrication procedure and optimum heat-treatment prior to testing. These values are not intended for use as design data (December 19, 1951). C, cast; F, forged; E, either cast or forged.

the radial-turbine rotor cast by the lost-wax process. Each of these metallurgical advances makes the gas-turbine engine much more competitive with the other forms of prime movers.

Many of the new high-temperature alloys which have been developed unfortunately have contained large percentages of strategic elements. In the past several years much effort has been expended to reduce the use of critical elements in high-temperature alloys. Some of the new less-critical compositions which have been developed appear to have better properties than the alloys which were replaced (23). At least abroad there appears to be some sentiment in favor of ferritic steels for gas-turbine-engine rotors. If a ferritic steel can be obtained having comparable high-temperature properties to the austenitic-type steel, then it has the following advantages (25):

1 Cheaper.
2 Less strategic material.
3 More easily welded.
4 Responds to heat-treatment.
5 Lower coefficient of expansion.
6 Higher heat conductivity.
7 Easier to produce, especially in large sound forgings.
8 Less prone to vanadium attack.

The future prospects of obtaining much higher turbine temperatures by advances in improved alloys seem somewhat limited. It has been suggested that the probable practical limits for alloys is from 1500 to 1600 F (26). The perfection of new alloys using such elements as molybdenum, or chromium for the base element offers some hope of raising this limit ultimately to 1700 F (27).

Ceramics

Ceramics are materials which contain as primary constituents one or more of the refractory oxides, carbides, nitrides, borides, silicides, silicates, carbon, and graphite (17, 28, 29). This group of materials is characterized by brittleness, a high melting point, and a low density. The properties of a high melting point, low density, and potentially low cost make ceramics attractive for gas-turbine-engine hot parts (30). Brittleness and inability to withstand thermal shock have prevented the extensive use of ceramics to date.

A comparison of melting points for carbon steels (about 2700 F) stainless steels (2550 to 2650 F) and ceramics (2300 to 7500 F) indicates the potential advantage enjoyed by ceramics. Even though the tensile strength of ceramics may seem low at certain temperatures when compared with the best "superalloys" now used, it should be noted that the primary stress in a rotor blade is due to centrifugal force, and as the ceramic has a low density, the strength-to-density ratio of the blade material is more important than its absolute strength (30).

A number of ceramic rotor blades have been test-evaluated by the NACA. A turbine with sillimanite ($Al_2O_3SiO_2$) blades was run for 38 hr up to speeds of 8700 rpm and temperatures of 1725 F. After operating for this period, and while running at 8300 rpm with an inlet temperature of 1500 F, the blades failed (30). Another turbine using the National Bureau of Standards ceramic, (No. C-4811) which is high in beryllia, ran 50 hr at a temperature of 1800 F and a final speed of 14,000 rpm (tip speed 737 fps) before the blades failed. Failure in this case was caused by a very severe thermal shock resulting from a stoppage in the air supply. It was found that the carbide materials, with the exception of boron carbide, were greatly superior to the oxides in their ability to withstand thermal shock but had very poor oxidation resistance (17).

An investigation of seven hot-pressed ceramics disclosed that titanium carbide was the most promising of the ceramics tested, having good resistance to thermal shock, and a strength of 15,850 psi at 1800 F and 9400 psi at 2200 F. Zirconium carbide had a strength of 15,850 psi at 2200 F, but had very poor oxidation resistance (31).

Although ceramic rotor blades do not look promising at this time, stator blades or metal-supported combustion-chamber liners offer possibilities (28). The real value of ceramics now, however, appears to be in the form of an extremely thin coating applied to metals for corrosion and oxidation resistance. In tests conducted on two different alloys in a corrosive atmosphere (hydrogen sulphide) at 1350 F, an uncoated S-816 blade disintegrated in 471 hr while a ceramic-coated (alumina type) S-816 blade had an average tensile strength of 69,000 psi (measured at room temperature) after being exposed to the same test conditions. The same test applied for 101 hr showed a S-590 blade to have a tensile strength of 33,000 psi, while a ceramic-coated S-590 (cobalt-oxide type) blade had a strength of 76,000 psi (32).

The use of ceramic coatings to protect metal from oxidizing was practiced during World War II. Such a coating developed by the National Bureau of Standards was used extensively on aircraft and vehicle exhaust systems with excellent results (33). A newer ceramic coating was applied to both sides of an engine exhaust header and prevented any corrosion from occurring during 1234 hr of operation (34). A number of companies are engaged in applying ceramic coatings.

Ceramals

Ceramals or cermets are a combination of ceramics and metals that are pressed and sintered or hot-pressed (29). By such a combination it is attempted to combine the good high-temperature strength properties and low density of the ceramic with the good thermal-shock resistance and ductility of the metal. The metal serves as a binder in combination with the ceramic and there is a certain optimum ratio for the two (29, 35). The substitution of ceramals for the presently used superalloys in gas-turbine components would reduce greatly the amount of critical materials required.

The NACA has tested a number of ceramals. Boron carbide used with iron as the binder and titanium carbide separately using cobalt, tungsten, and molybdenum as binders indicated that titanium carbide was more promising than boron carbide owing to the extremely poor oxidation resistance of the latter above 1600 F (36). A ceramal containing 80 per cent titanium carbide and 20 per cent cobalt had a strength of 57,800 to 100,800 psi at 1600 F and 29,400 to 71,900 psi at 2000 F. Another ceramal composed of 90 per cent titanium carbide and 10 per cent molybdenum had a strength of 16,100 to 20,900 psi at 2400 F (37). The oxidation characteristics of these titanium-carbide ceramals was found to limit the service life to 10 hr at 2400 F, necessitating an oxidation-resistant ceramic coating for longer life (17). It has since been found that nickel is nearly as effective as cobalt as a binder for titanium carbide (38). A ceramal containing 86.7 per cent titanium carbide and 13.3 per cent nickel had a tensile strength of 16,150 psi at 2000 F and survived 100 cycles of a thermal-shock test. Iron was found to be less effective as a base metal for titanium carbide than nickel (39). NACA has conducted tests with an 80 per cent titanium carbide and 20 per cent cobalt ceramal blades in a turbine. A total of 12 hr running time with a blade-tip speed up to 716 fps and inlet-gas temperature of 2200 F was obtained before the turbine disk failed. Subsequent runs for as long as 110 hr have been made. These tests indicated that present turbine-disk and blade-root design practices will have to be modified to utilize ceramals (17).

As many of the ceramals have very high heat conductivity, it will be necessary to provide better cooling of the turbine wheel where ceramal rotor blades are used, or the stator case, when

ceramal stator blades are used. It would appear that turbine stator blades made from ceramals are now feasible (26, 40).

2 COOLING

Cooling of the gas-turbine-engine components exposed to the hot gas is the only means by which marked increases in turbine-inlet temperatures are likely to be achieved in the near future. Such components as the turbine blades and disk, stationary nozzles or fixed blades, connecting ducting, turbine-stator case, and combustion-chamber liner will require new or improved cooling methods. The most difficult component to cool from a mechanical and thermal standpoint will be the turbine blades, and therefore this discussion, in general, will be limited to the blades. Cooling also may be utilized to reduce critical materials in the gas-turbine engine while maintaining present operating temperatures. The concept of cooling gas-turbine-engine hot parts is certainly not new. Parsons referred to water-cooling of gas-turbine blades in his patent of 1884 (41). It also may be recalled that the internal-combustion engine had a very limited application until fluid cooling was utilized. The two main substances which have been employed as the cooling medium to date have been air and water. Liquid metal and oil also may be used at some future date. It should be noted here that the increase in over-all thermal efficiency resulting from the higher temperatures made permissible by cooling will be somewhat less than an uncooled gas-turbine engine operating at the same temperature. Cooling introduces losses which may include the following to varying degrees, depending upon the type of cooling employed:

1 Cooling employed in the early stages results in a heat loss which reduces the available energy in the later stages of the turbine (42).

2 It appears that in a cooled turbine it is desirable to have a high ratio of axial velocity to peripheral velocity, which will result in increased volute losses (43).

3 Air cooling requires the extraction of air from the compressor with a consequent increase in the compressor-turbine work.

4 Reduction in turbine-exhaust temperature resulting in reduced thermal effectiveness in the regenerator, where used (43).

5 Larger aerodynamic losses caused by thicker blades, thick trailing edges, disturbance of the gas flow with air-cooled blades, and possibly larger blade-tip clearances (43).

There is one other factor which must be considered when analyzing extremely high turbine-inlet temperatures. When the temperature increases, the optimum pressure ratio also increases. The difficulty in assessing realistically the effect of cooling on thermal efficiency is the incertitude concerning the magnitude of the losses introduced by such cooling. Calculations have been made using cooling losses of 12 per cent and 25 per cent which indicate very high efficiences (40). In this case consideration also was given to utilizing steam generated from the turbine cooling water to drive a steam turbine or to cool the compressor-inlet air by a steam-refrigeration system. The introduction of such complexities into many gas-turbine plants may be questionable. On the other hand, it was found on the Schmidt turbine having water-cooled blades that the heat loss of the steam was about 40 per cent (44). The losses vary widely according to the type of cooling used; simple water cooling gives the highest losses, sweat and boundary-layer cooling the lowest. Water-cooling losses can be decreased notably if the blades are coated with a low-conductivity material, providing the mechanical problems associated with such a coating can be solved. In general, reliable data on cycle losses due to cooling are not available, but a comprehensive study of various cooling methods is given in reference (43).

Even if the high temperatures permissible in a cooled turbine do not result in as high a thermal efficiency as might be anticipated, it will result in two other important benefits. The first benefit is a reduction in strategic materials and the other is an increase in specific power. Both of these improvements will enhance greatly the gas-turbine engine. It has been shown that an increase of turbine-inlet temperature from 1540 F to 2500 F for a simple-cycle engine would result in an increase in power of about 140 per cent for a given plant volume and weight (45).

A number of methods have been investigated or used to accomplish cooling in the gas-turbine engine. Each method is discussed briefly in the following.

Internal Air Cooling

The turbine rotor and stator blades may be cooled by circulating compressor extraction air through such blades fabricated with a hollow interior or provided with cooling passages. The Germans used hollow rotor blades in the BMW 003 and Jumo 004 Jet engines and hence this is one of the first cooling methods to be employed in the gas-turbine engine. The Jumo 004 was equipped with nozzles containing 18 per cent manganese and 9 per cent chromium, and the rotor blades were of 30 per cent nickel and 15 per cent chromium. Cooling air amounting to about 4 per cent of the engine air throughput permitted this engine to operate at 1400 F (43). The use of these hollow sheet-metal blades resulted in a large conservation of material also, as they required only $^1/_8$ as much material as a forged blade (46). It has been estimated that with a turbine-inlet temperature of 1650 F and a blade circumferential velocity of 984 fps, 5 per cent cooling air would be required. The power to furnish this cooling air is 2.9 to 4.5 per cent of the turbine power (47).

Tests conducted by NACA have shown that the temperature of an uncooled blade dropped from 1400 to 1100 F when 1 per cent of the compressor air was bled for cooling. Increasing the cooling air to 3 per cent resulted in a blade temperature of 875 F, and 5 per cent air reduced the temperature to 775 F (48).

The General Electric Company has used this type of cooling in two different models of gas-turbine engines which it produces. The first-stage nozzle partitions in the GE 5000-hp regenerative engine and 5000-kw complex-cycle engine both utilize internal air cooling (49, 50). A number of these engines are now in regular commercial service. It has been reported that GE extracts about 1 per cent of the compressor air at intermediate pressures for cooling purposes, and that under these conditions the extraction loss does not exceed $^1/_2$ per cent in equivalent compressor efficiency (51).

The most advanced internally air-cooled blades use a small number of relatively large holes provided with finned inserts to increase the effective cooling area (43). Internal air cooling furnishes the advantage of providing effective cooling at the blade root where it is most needed (44).

Boundary-Layer Cooling

The simplest and most extensively used cooling method now employed in gas-turbine engines employs the circulation of air over the surface to be cooled. The majority of gas-turbine engines utilize this boundary-layer cooling for the combustion-chamber liners. In one instance better combustion-chamber cooling increased the life of this component by 5 times (51). In addition, this method is used extensively to cool the faces of the turbine disks. Many of the jet engines and commercial gas-turbine engines now in service use this method of disk cooling (49, 52, 53).

It is also interesting to note that the first gas-turbine engine

designed for marine service, by Compagnie Electro-Mecanique, made extensive use of boundary-layer cooling. The four-stage turbine had hollow stator and rotor blades with slits near the leading edges. Compressed air was fed into the blades and escaped through the slits to form a cool envelope around each blade. This same arrangement was used in nozzle blades of a French aircraft gas-turbine engine with the result that the blade temperature at the trailing edge was only 1020 F in a gas stream having a temperature of 1470 F with a 1 per cent cooling air flow (43). The turbine disk also was air-cooled in this plant (54). The first marine gas-turbine plant to go to sea, the Metropolitan-Vickers G-1, also used boundary-layer cooling for each side of the turbine disk (55). This cooling arrangement can be surprisingly effective as found in one engine where the maximum temperature of a rotor operating in a gas stream of 1340 F was only 650 F (52).

Transpiration Cooling

This method is also known as effusion cooling. It consists essentially of introducing compressor air inside blades made of porous or permeable material with the result that the air passes out into the gas stream, thereby effectively cooling and insulating the blade (56). When a liquid is substituted for the air, this method is known as "evaporative transpiration" or "sweat cooling" (57). This method has important advantages. The cooling air will be brought up to the blade-surface temperature as a result of the intimate contact between the cooling air and the blade wall, and the effusion of the cooling air into the boundary layer may produce about a 30 per cent reduction in the heat-transfer coefficient (43).

As might be suspected, the main problem in developing transpiration cooling is the production of materials with uniform porosity and the required mechanical strength. Such materials likely will be produced by the powder-metallurgy method (58). Needless to say, the cooling air will have to be perfectly clean to prevent plugging the small pores in the material. A great deal of research is now going on in this country and in England to perfect methods of producing, fabricating, and machining porous materials (43, 59, 60, 61). It must be noted that both boundary-layer and transpiration cooling, if carried out effectively, also provide protection from blade corrosion due to combustion of bad fuels, which is discussed later, because they prevent contact of the combustion gases with the blade.

Internal Liquid Cooling

This type of cooling depends upon the circulation of water or other suitable liquids inside the component to be cooled. The early work on the water-cooled gas-turbine engine was done by Schmidt in Germany during World War II (62). He ran a single-stage turbine with internal water-cooled blades for 50 hr at 2000 F, and for 2 hr at 2300 F. Later a four-stage turbine was manufactured in Germany and tested in England after the war at the National Gas Turbine Establishment. This unit was designed to operate at 2190 F but was run only up to 1380 F due to poorly cooled substitute stator blades (43). The NACA also has conducted experiments on a single-stage turbine with water-cooled blades. These units had blades with drilled holes fed with water through the hollow turbine shaft. Unless it is feasible to use the steam generated during the cooling process, the losses incident to the internal liquid-cooled system may be very high.

This type of cooling will necessitate an air-free closed circuit utilizing distilled water (40). In addition, a pump, heat exchanger, plumbing system, and elaborate control will be required.

General Electric has two types of gas-turbine engines now in commercial operation which have the turbine stator case cooled by water circulation. Brown Boveri recently has taken out a patent on a centrifugal separator for the removal of impurities from cooling water employed in a gas turbine having hollow blades and shaft (63).

Spray Cooling

Spray cooling prevents excessive blade temperature by spraying water directly on the blades from suitably located nozzles. Although there are no gas-turbine engines in service with this type of cooling, experimental work on this system has been done here and abroad. The National Gas Turbine Establishment has investigated spray cooling in a Whittle W2/700 jet engine. Tap water was used and a deposition was obtained on the blades after 12 hr running (43). This would indicate the need to use distilled water which would tend to rule this type of cooling out for many applications.

Water-Pad Cooling

This type of cooling circulates water through pads adjacent to the turbine disk. Heat is transferred from the disk to the cooling water by means of radiation and convection. This in turn results in lower blade-root temperatures. This type of cooling will not permit as high gas temperatures as the types discussed previously. This method of cooling is used in the GE 5000-kw complex-cycle gas-turbine plant (50, 64).

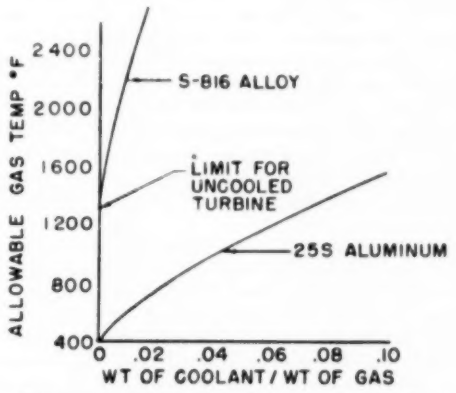

Fig. 1 Cooling Effectiveness of Water-Cooled Blades for Two Different Materials
(Courtesy reference 97.)

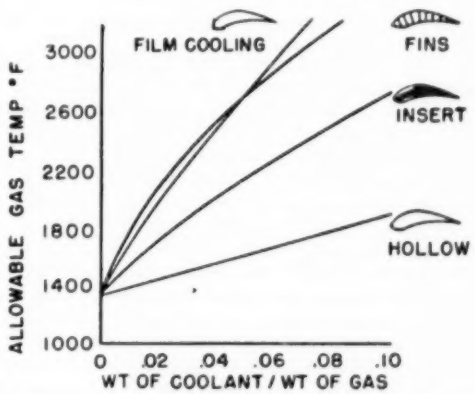

Fig. 2 Cooling Effectiveness of Various Blade Configurations for Air Cooling of S-816
(Courtesy reference 97.)

Cooling Summary

Figs. 1 and 2 indicate the effectiveness of the various types of blade-cooling methods with relation to the coolant flow. Also it is an indication of the top temperatures obtainable with the various cooling methods. There are advantages and disadvantages to both the air and water-cooling methods. Air cooling is inherently simpler, as it requires no complicated plumbing, heat exchanger, or distilled make-up water. Water cooling is a very effective method as shown in Fig. 1. The magnitude of the cooling losses in water cooling will determine the maximum permissible temperatures. If the cooling losses are 25 per cent the highest temperature feasible for maximum cycle efficiency will be 2300 F (40). The Brown Boveri Holzwarth gas-turbine engine had internal water-cooled blades but impurities and rust in the water circuit plugged the blade passages with a resultant stoppage in circulation and blade failures. Suitable inhibitors may prevent or reduce corrosion in the cooling-water circuit (65). Whether the inherent simplicity and reliability of the air-cooling methods will dictate their choice over the water-cooling methods, remains to be seen. Certainly the former type will be preferable in small gas-turbine engines. It appears that transpiration cooling will permit the highest maximum turbine-inlet temperatures.

3 FUELS

It is generally agreed that the gas-turbine engine can expect no widespread application in the merchant marine, industrial, or locomotive fields until it is able to burn residual fuel oil. Gas-turbine engines will and are being used extensively in the industrial field where natural gas is an economic fuel. The ability of the gas-turbine engine to burn coal will further enhance its position in the industrial and locomotive fields if and when it is feasible. Inasmuch as this prime mover can now operate on gasoline, kerosene, distillate fuel, and natural gas, and as the problems yet to be solved in burning coal are well known, this discussion is limited to residual fuels.

The actual design or fabrication of suitable combustion equipment for burning residual fuel oil is, in general, similar to that for distillate fuel (66, 67). The heavier fuel may result in a greater tendency for temperature stratification at the outlet of some types of combustion chambers. The real problem is caused by burning an ash-bearing fuel which introduces the hazard of deposition in the combustion system, on turbine blades, and all other surfaces exposed to the exhaust gas.

Numerous land gas-turbine engines have been run on residual fuel but they have either had relatively low turbine-inlet temperatures (below 1200 F) or have had selected grades of such fuel. Even these units, in general, have experienced some difficulty.

The Oerlikon Company's gas-turbine engine has been running on residual fuel for a long period, with some blade deposits (about 0.04 in.). Every two weeks these are easily washed off and no traces of corrosion remain. NGTE ran residual fuels in a jet engine with not only blade fouling but also a significant degree of blade-alloy corrosion (66). The Metropolitan Vickers' Gatric gas-turbine engine was run at idling speed for 20 min on residual fuel and then compressor stalling occurred. A heavy carbon deposit was found in the combustion chamber and on the high-pressure-turbine blading. Compressor stalling had been caused by partial blocking of the high-pressure-turbine blade passages (68). The experimental C. A. Parsons and Company 500-hp gas-turbine engine experienced compressor surge after 8 hr of operation on residual fuel which caused ash deposition, resulting in turbine blockage (69). Other companies such as General Electric, Elliott, Westinghouse, and Brown Boveri have had considerable experience in burning residual fuels.

As serious as the ash-deposition problem is, it is secondary to corrosion resulting from such deposition. The deposits may be cleaned off but the corrosion process is irreversible (66).

Corrosion results from the presence of vanadium (in various forms, including vanadium pentoxide), (V_2O_5), certain sodium salts (especially Na_2SO_4) and sulphur (S) being present in the fuel ash (1, 41, 52, 66, 69, 70, 71, 72, 73). High-temperature boilers and Diesel engines also suffer from these same impurities. It has been suggested that the residual fuels used in Diesel engines be limited to a low-ash and sulphur (2 per cent or less) content (74).

Generally, sodium is in the fuel as a natural constituent but it may be introduced in the refinery process, or by salt-water contamination (75). This latter contaminating process will make it more difficult to burn residual fuel in the marine gas-turbine plant than in its land counterpart. The disastrous effects resulting from salt water in boiler fuels are well known (76).

Most residual fuel oil has a considerable ash content. A large percentage of this ash may be composed of V_2O_5 and alkali compounds which combine to form low-melting slags (72).

Not only is vanadium present in almost every crude, but it is often the predominant impurity. A study also indicates that vanadium concentrations do not seem to occur in the absence of sulphur. Sodium is also a likely constituent, and, as has been mentioned in the case of marine service, may additionally be introduced by sea water. The relative percentages of these deleterious elements will vary according to the source of the fuel oil (66). It can be seen that this problem is complicated in marine plants because a vessel may receive fuel from every part of the world and, therefore, must be able to burn any fuel likely to be encountered. Certain land gas-turbine plants are in a position to obtain residual fuels containing a specified maximum amount of such impurities as vanadium, sodium, and sulphur.

The exact melting point of V_2O_5 seems to be in some dispute. It has been variously reported as being 1202 F, 1247 F, 1270 F, and 1274 F (66, 72, 73, 77, 78). This conflict probably results from the different methods of preparation (66).

The corrosion or oxidation attack of the fuel ash affects primarily the gas-turbine blades and combustion-chamber liner, or, in other words, the high-temperature parts in the gas stream. "The mechanism of this attack seems to consist in the fact that the vanadium compounds prevent the formation of, or destroy, the protective scaling on heat-resistant steels. Layers permeable to oxygen and of little resistance to scaling are carriers, with vanadates as an intermediary stage. The existence of such vanadates has been proved roentgenographically" (72). The V_2O_5 must be either in the liquid or gaseous state and, therefore, no great difficulty from this source is to be expected below its melting point. Certain elements seem susceptible to an "accelerated" or "catastrophic" type of oxidation. The rate of reaction is so rapid that the liberated heat of the reaction raises the temperature of the metal and results in a further acceleration of oxidation (79).

The sulphate content of the ashes does not depend upon the sulphur content of the fuel but upon the elements, particularly sodium, which enter into combination with the sulphur (74). If vanadates of sodium or sodium pyrosulphate are present, a sticky ash is likely. The melting point of sodium pyrosulphate is 754 F, sodium sulphate 1623 F, and of metavanadate ($NaVO_3$) and pyrovanadata ($Na_4V_2O_7$) about 1165 F (66). Therefore, below 1200 to 1275 F, the main troubles from burning residual fuels will result from sodium or sodium vanadates, and above this temperature from V_2O_5, Na_2SO_4, or other vanadates. Below about 1200 F blade fouling will be the main problem, whereas above the melting point of V_2O_5, corrosion will be the limiting factor.

Ash deposition and rate of attack appear to increase with increasing turbine-inlet temperatures (66, 72). Accelerated oxidation rises sharply with temperature to a certain point and then

seems to remain about constant (79). It can be seen that with the present state of the art from a practical application it will be impractical to burn unselected residual fuels in high-temperature gas-turbine engines.

No alloy has yet been found that will resist the V_2O_5 or vanadate attacks. Certain alloys seem to be more resistant than others to such attacks but not necessarily for all temperatures, length of time, or percentages of deleterious impurities in the fuel oil. This may account for some of the conflicting reports which have been received concerning the resistance or susceptibility of various alloys to attack. The most controversial of the various elements is nickel. It has been reported that chromium-nickel steels, without other alloying elements, appear to have the best resistance to attack (72). A study with 16 Cr, 25 Ni, and 6 Mo steel found that only when the Ni was increased above 30 per cent was there satisfactory resistance to oxidation (79). Residual fuel tests conducted for 300 hr on the 500-hp John Brown & Company Ltd., open-cycle gas-turbine engine indicated that all of the rotor blades except those with high nickel content showed signs of scaling (69). Inasmuch as this unit has an inlet temperature of only 1200 F, the corrosion evidently was due to something other than V_2O_5—perhaps a sodium vanadate. Tests run by Elliott for 168 hr at 1350 F found that the superalloys had the worst corrosion resistance, and that nickel-free alloys had the best. Tests of 50-hr duration on the Gatric gas-turbine engine, using a distillate fuel with 2.78 per cent sulphur, resulted in the combustion-chamber fuel-jet shields being badly oxidized. These shields had a high nickel content (68). It would be interesting to know whether the sulphur content of the fuel proved particularly injurious to nickel. In the reported cases where nickel was found to resist corrosion, the sulphur content of the fuel was low or absent, whereas in the tests which found nickel to be particularly susceptible to corrosion the sulphur content was about 3 per cent.

There seems to be little doubt that alloys containing relatively large percentages of molybdenum and vanadium are prone to accelerated oxidation (72, 74, 79, 80). A 4800-hp General Electric gas-turbine engine with 16 Cr, 25 Ni, and 6 Mo turbine-nozzle partitions, was run for 492 hr on residual fuel. At the end of this time one of the nozzle partitions had oxidized completely through and many of the others had been attacked excessively (80).

It has been reported that Cb, Ti, Ta, Mn, and W when used as alloying elements have no appreciable influence on the attack (72). Ordinary 18-8 stainless steel was found to have the best resistance of the austenitic alloys to attack. Ceramics show varying behavior in their resistance to the ash attack and appear sensitive to small differences in method of manufacture and purity. Some ceramals, including titanium carbide combined with cobalt, columbium, and tantalum are heavily attacked (70).

It has been found generally that the higher the vanadium content of the ash the more rapid the oxidation, providing the temperature is above the melting point of the vanadium constituent. In addition, it has been found that the sodium content of the ash affects the oxidation rate. As the ratio of alkali to V_2O_5 is increased, the rate of attack increases up to a ratio of 1 to 1. Further increases of alkali in relation to V_2O_5 reduce the rate of attack, as the alkali content dilutes the V_2O_5 with a resultant weakening of the corrosion-dissolving components (72). Also, it has been found that the rate of attack increases with the mass of attacking material (70, 72).

As would be expected, time plays an important part on total oxidation of a material. The attack seems to be proportional to time (72, 79). In the Elliott experiments it was found that alloys which appeared satisfactory after 168 hr of exposure at 1350 F, showed heavy corrosion after 504 hr of exposure (70).

It also has been found that accelerated oxidation is favored in stagnant atmospheres (70, 79). Fortunately, proper design and operation will prevent stagnant atmospheres at high-temperature levels.

A number of methods exist by which the adverse effects of vanadium, sodium, and sulphur may be minimized, and it is hoped eventually eliminated. Several of these methods are as follows:

(*a*) *Distillation.* There is presently no distillation process which will remove vanadium from residual petroleum economically. This is a possibility, however, and some investigators believe this will be more economical than the addition of additives to the oil (81).

(*b*) *Additives.* It is possible that the addition of certain metallic oxides to the fuel will minimize the vanadium attack by forming vanadates having very high melting points (82). Equal parts of lime (CaO) and V_2O_5 form calcium orthovanadate ($3CaO.V_2O_5$), which is a stable compound with a melting point of 2500 F (83). Tests have shown that oxides of calcium, zinc, magnesium, aluminum, and iron reduce the corrosion at 1290 F (84). However, additives may increase the total ash and hence deposition troubles (73). Care also must be taken to introduce the proper proportion of additive—it has been shown that the addition of less than 23.5 per cent of CaO to V_2O_5 results in a eutectic with a melting point of only 1150 F (70). The optimum additive would be one which would alter the nature of the ash in such a way as to prevent it from adhering to the blades (75).

(*c*) *Coating.* Coating the parts subjected to the high-temperature attack with a material which will reduce the adhesion of the material or be impervious to the vanadium attack is another promising method (66, 70, 85, 86). The Elliott tests indicated that "ihrigizing" was best for carbon steel with "chromizing" also effective, while "siliconizing" reduced the amount of attack on some of the superalloys. Aluminum metallizing held promise in protecting 18-8 steel (70). Even a chalk coating considerably reduced the attack (85).

(*d*) *Alloys.* Alloys should be selected which show a minimum susceptibility to corrosive attack, providing they have the other necessary properties. Alloys containing very large percentages of Mo or V, of course, will not be used. It is unlikely, however, that any alloy will be found which will resist the attack of all possible residual fuels at all temperatures.

(*e*) *Cooling.* Cooling the turbine-blade surface below 1200 F should reduce the rate of attack on these components (87). Vanadium eutectics could cause corrosion below 1200 F, however, and, therefore, to be completely effective it would be necessary to cool the blade surface to a temperature lower than the melting point of the lowest eutectic (88). With most cooling methods this is very difficult to do as only the blade core and root, but not the surface, are cooled; with internal water or air cooling it seems difficult to bring the blade-surface temperature low enough particularly near the trailing edge. On the other hand, boundary-layer and transpiration cooling, if effectively done, prevent corrosion because they insulate the blade surface from contact with the combustion gases, and also cool the surface itself.

(*f*) *Incomplete Combustion.* It has been reported that incomplete combustion resulting in soot will reduce the rate of attack (73). It appears that the ash passes through the turbine embedded in a matrix of carbon which renders the ash relatively innocuous (66). It remains to be seen whether this will occur for all turbine-inlet temperatures. Therefore poor combustion may be promoted deliberately except when a regenerator is incorporated in the gas-turbine plant. This method would be normally undesirable.

(*g*) *Temperature Stratification.* The elimination of temperature stratification at the turbine inlet of one engine reduced the corrosion rate (80). This would be expected, as if an engine had a

wide spread of temperature at the turbine inlet, for a given average temperature, portions of the blades would be subjected to much higher temperatures.

(*h*) *Thermal Shock.* The deposits may be cracked off the turbine blades by a sudden thermal shock (75, 89). This will result inherently in a shorter engine life, however, so the extent of the thermal shock would require careful consideration.

(*i*) *Aerodynamic Design.* Distribution of deposits on turbine blades suggests that aerodynamic forces play a part in ash deposition (75). Therefore, if turbines can be designed to minimize ash deposition (without affecting the component efficiency appreciably) corrosion attack will also be reduced.

(*j*) *Fly-Ash Separator.* The location of a mechanical fly-ash separator between the combustion chamber and turbine inlet has been suggested to eliminate the deposit trouble. Such a separator would be independent of the kind of ash and origin of the fuel. There appears to be no single mechanical system which would separate all of the ash but it is possible that a combination of two or more systems would work (75). Unfortunately, it is the smallest and least separable of the particles which are most likely to deposit, and these small particles are most likely to have a higher concentration of inorganic matter (66). Certainly the extra weight, space, first cost, and maintenance of such a system would be undesirable. A somewhat similar method would be to trap the ash before it reached the turbine by interposing an artificially cooled passage between the combustion chamber and turbine, or introducing a number of rows of fixed blades, widely pitched so as to cause no pressure drop (90, 91).

(*k*) *Fuel-Oil Centrifuge.* It might be possible to eliminate the sodium introduced into the fuel oil in the form of salt water by centrifuging the fuel oil before use.

(*l*) *Cleaning.* It has been suggested that the turbine should be designed to allow for ready cleaning (92). Tests actually have been made on the 500-hp C.A. Parsons and Company Ltd., gas-turbine engine to determine the effectiveness of removing ash deposits by spraying water on the turbine blades while running. This method will be effective only when the ash is water-soluble. The success of this method is to use a large quantity of water (25 per cent of the air flow) in a short time so that solution occurs before evaporation. Best results were obtained when the spray was not too fine. For this engine about 32.4 gal were sprayed into the turbine during a 15-min period every 4 to 6 hr (75). This would amount to about 130 to 195 gal per day. Assuming that the water required increased proportionately to power, a 5000-hp gas-turbine engine would require 1300 to 1950 gal per day. Use of distilled water likely would be required for long periods of operation. Cleaning, of course, will only reduce the corrosive attack and not prevent it.

(*m*) *Alternate Burning of Residual and Distillate Fuels.* The Gatric tests indicated that the ash deposition from residual fuels could be burned off by running at high speed on distillate for 10 min (68). Another source has indicated that the success of this method is dependent upon the nature of the ash (75). Inasmuch as residual-burning gas-turbine engines will require a supply of distillate oil for starting and stopping, all facilities for such a procedure will be readily available.

Residual Fuel-Oil Summary

The perfection of one or a combination of the foregoing methods should reduce the adverse effects of burning residual fuel in the gas-turbine engine. Whether any of these methods will find general application is primarily an economic question. If a refinery process or additive increases the cost of the treated residual fuel oil above that of distillate oil, it is apparent that it would be preferable to burn the distillate fuel. Other of the methods will result in increased weight, volume, maintenance, first cost, reduced life, and lower the power and thermal efficiency of the residual-burning gas-turbine engine in relation to the distillate-burning engine.

A tremendous amount of work is now being done on this problem by both industry and government agencies in England and in the United States, and by industry in Switzerland. The problem is so complex and so many variables exist that a great deal of work must still be done before a satisfactory solution is likely to be obtained. The British Admiralty and NGTE are carrying out a six-point program of investigation which includes (93, 94, 95) the following:

1 Fuel characteristics.
2 Atomization.
3 Combustion.
4 Heat transfer.
5 Blade and heat-exchanger fouling.
6 Materials.

The residual-fuel-burning experience of the British Thomson-Houston gas-turbine plant in the *Auris* should furnish much useful information for marine gas-turbine plants, but inasmuch as this engine has a turbine-inlet temperature of only 1200 F, no difficulty from V_2O_5 is likely.

The high-temperature closed-cycle gas-turbine plant also may suffer from corrosion, but only the air-heater tubes and supports will be affected. This is the same type of corrosion as occurs in high-temperature steam boilers, although the top temperatures now found in the closed-cycle air heater exceed that of the steam boiler. The turbine and regenerator of the closed-cycle plant handle only pure, dustless air and not the products of combustion as in the open-cycle plant. Therefore the closed-cycle turbine has an important advantage because air-heater corrosion becomes serious only when the life of the tubes is threatened while even slight deposits on the turbine blades immediately decrease power and efficiency. The residual fuel-oil test experience on the John Brown & Company Ltd., 500-hp closed-cycle plant resulted in severe corrosion of the air-heater tubes in 200 hr of running. This was attributed to the breakdown of carbon tetrachloride which had been added to the fuel for the purpose of preventing vanadium attack (96). Owing to the immunity of closed-cycle turbines from corrosion, Escher Wyss is experimenting with pulverized-coal-fired air heaters and no great difficulties have been encountered.

The residual fuel-burning high temperature boilers and Diesel engines experience some of the same difficulties from sodium and vanadium that are found in the gas-turbine engine. Any solution to this problem, therefore, will benefit the three main prime movers.

BIBLIOGRAPHY

1 "The Gas Turbine in Perspective," by Hayne Constant, Proceedings of The Institution of Mechanical Engineers, vol. 163, 1950, pp. 185–192.

2 "High Temperature Materials for Gas Turbines," by R. H. Smith, *The Iron Age*, vol. 161, January 22, 1948.

3 "Symposium on Materials for Gas Turbines," Forty-ninth annual meeting, American Society for Testing Materials.

4 "Haynes Alloys for High-Temperature Service," by W. O. Sweeny, Trans. ASME, vol. 69, 1947, pp. 569–581.

5 "Precipitation-Hardened Alloys for Gas-Turbine Service, Parts I and II," by H. Scott, and R. B. Gordon, Trans. ASME, vol. 69, 1947, pp. 583–599.

6 "Materials for Power Gas Turbines," by C. T. Evans, Jr., Trans. ASME, vol. 69, 1947, pp. 601–608.

7 "Nickel-Chromium Alloys for Gas-Turbine Service," by C. A. Crawford, Trans. ASME, vol. 69, 1947, pp. 609–612.

8 "Heat-Resistant Alloys for Use in Jet Propulsion Engines," by J. W. Freeman, E. E. Reynolds, and A. E. White, *Journal of the Aeronautical Sciences*, vol. 14, December, 1947, pp. 693–702.

9 "The Rupture-Test Characteristics of Heat-Resistant Sheet

Alloys at 1700° and 1800° F," by J. W. Freeman, E. E. Reynolds, and A. E. White, NACA Technical Note No. 1465, February, 1948.

10 "Turbo-Supercharger and Aircraft Gas Turbine Metallurgical Development," by W. L. Badger, General Electric Company Publication No. GET-1716, pp. 1–20.

11 "Technical Data on Allegheny Ludlum Alloy A-286, Allegheny Ludlum Steel Corporation, Watervliet, N. Y., pp. 1–21.

12 "The Problem of High Temperature Alloys for Gas Turbines," by Sir W. T. Griffiths, *Journal of the Royal Aeronautical Society*, vol. 52, 1948, pp. 1–26.

13 "Creep Tests and Their Application to Gas-Turbine Design," by Dr. W. Siegfried, *Sulzer Technical Review*, No. 4, 1948.

14 "High Temperature Steels and Alloys for Gas Turbines—No. III," discussion of papers Group IV, presented at the Iron and Steel Institute, February 21 and 22, 1951, London, England, by E. R. Gadd. Reprinted in *The Engineer*, vol. 191, March 23, 1951, pp. 373–374.

15 "High-Temperature Disk-Forging Developments for Aircraft Gas Turbines," by L. B. Fonda, Trans. ASME, vol. 70, 1948, pp. 1–12.

16 "Stresses in Gas-Turbine Discs and Rotors," by Dr. R. W. Bailey, paper presented at the Iron and Steel Institute, February 21 and 22, 1951, London, England. Abstract reprinted under "High-Temperature Materials for Gas Turbines," in *Engineering*, vol. 171, March 30, 1951.

17 "Review of NACA Research on Materials for Gas Turbine Blades," by G. M. Ault and G. C. Deutsch, SAE Quarterly Transactions, vol. 4, July, 1950, pp. 398–409.

18 "Gas-Turbine Steels," by K. J. B. Wolfe and P. Spear, *Aircraft Production*, vol. 13, March 1951, pp. 80–83.

19 "Heat Treatment of Steel Forgings for Gas Turbines," by H. W. Kirkby, *Metallurgia*, vol. 41, April, 1950, pp. 317–320.

20 "Casting and Forging of Titanium," by J. B. Sutton, E. A. Gee, and W. B. DeLong, *Metal Progress*, vol. 58, November, 1950, pp. 716–720.

21 "Precision Investment Casting for Gas Turbine Blades," by N. F. Silsbee, *Aero Digest*, vol. 58, February, 1949, pp. 62–65.

22 "The Development and Evaluation of Cast Turbine Rotors," by N. J. Grant, L. W. Kates, and N. E. Hamilton, BuShips Research Memorandum No. 1–49. NavShips 250-330-13 of September 1, 1949, pp. 1–47.

23 "Trends in Gas Turbine Engine Materials," by R. H. Thielmann, J. C. Mertz, and W. P. Eddy, Jr., paper No. 701 presented at SAE annual meeting, January 14–18, 1952.

24 "How Critical Metals Problems Are Licked," *Aviation Week*, vol. 54, May 28, 1951, pp. 36–38.

25 "A Review of Gas Turbine Progress—1951," *The Engineer*, vol. 193, January 18, 1952.

26 "High-Temperature Materials," by G. J. Christenson, *Naval Propulsive Power*, vol. 3, May, 1950, pp. 26–29.

27 "Gas Turbine Alloys, 10 Years Later," by H. Scott, *Metal Progress*, vol. 58, October, 1950, pp. 503–511.

28 "The Outlook for Ceramics in Gas Turbines," by W. H. Duckworth and I. E. Campbell, *Mechanical Engineering*, vol. 72, 1950, pp. 128–130.

29 "The Applicability of Ceramics and Ceramals as Turbine-Blade Materials for the Newer Aircraft Power Plants," by A. R. Bobrowsky, Trans. ASME, vol. 71, 1949, pp. 621–629.

30 "Preliminary Investigation of a Gas Turbine With Sillimanite Ceramic Rotor Blades," by F. J. Hartwig, B. W. Sheffin, and R. J. Jones, NACA Technical Note No. 1399 dated July, 1947.

31 "Physical Properties at Elevated Temperature of Seven Hot-Pressed Ceramics," by J. J. Gangler, C. F. Robands, and J. E. McNutt, NACA Technical Note 1911, dated July, 1949.

32 "Ceramic Materials Show Promise for High Temperature Mechanical Parts," by J. R. Bressman, *Materials and Methods*, vol. 27, January, 1948, pp. 65–70.

33 "Ceramic Coatings for High Temperature Protection of Steel," by W. N. Harrison, D. G. Moore, and J. C. Richmond, Research Paper RP 1773, *Journal of Research*, Bureau of Standards, vol. 38, March, 1947, pp. 293–307.

34 "Ceramics: Exhaust Protection," *Aviation Week*, vol. 54, May 21, 1951, p. 30.

35 "Investigation of Bonding Between Metals and Ceramics, I—Nickel, Cobalt, Iron or Chromium With Boron Carbide," by H. J. Hamjian and W. G. Lidman, NACA Technical Note 1948, dated September, 1949.

36 "NACA Studies Ceramals for Turbine Blades," by G. M. Ault and G. C. Deutsch, *SAE Journal*, vol. 58, May, 1950, pp. 40–42.

37 "Elevated Temperature Properties of Several Titanium Carbide Base Ceramals," by G. C. Deutsch, A. J. Repko, and W. L. Lidman, NACA Technical Note 1915 dated July, 1949.

38 "High Temperature Steels and Alloys for Gas Turbines—No. III," discussion of paper Group VII, presented at the Iron and Steel Institute, London, England, February 22, 1952, by Dr. W. Woodward. Reprinted in *The Engineer*, vol. 191, March 23, 1951, pp. 373-374.

39 "Elevated Temperature Properties of Titanium Carbide Base Ceramals Containing Nickel or Iron," by A. L. Cooper and L. E. Colteryahn, NACA Research Memorandum RM E 51I10 dated December 3, 1951.

40 "Some Factors in the Use of High Temperatures in Gas Turbines," by Dr. T. W. F. Brown, paper presented to The Institution of Mechanical Engineers, January 27, 1950. Proceedings of The Institution of Mechanical Engineers, vol. 162, 1950, pp. 167–181.

41 "British Marine Gas Turbines," by Dr. T. W. F. Brown, Transactions, North East Coast Institution of Engineers and Shipbuilders, vol. 65, 1949, pp. 117–192.

42 "The Effect of Blade Cooling on Efficiency of a Simple Gas Turbine Cycle," by W. M. Rohsenow and A. B. Walker, Technical Report No. 1, pp. 1–17, "A Theoretical Study of the Thermodynamic Conditions in Gas Turbines Due to Blade Cooling by the Use of Liquid," dated July, 1951, Office of Naval Research Contract N5ori-7862, NR-091-158.

43 "The Cooled Gas Turbine," by A. G. Smith and R. D. Pearson, Proceedings of The Institution of Mechanical Engineers, vol. 163, 1950, pp. 221–234.

44 Discussion on reference (40), by Dr. A. T. Bowden, Proceedings of The Institution of Mechanical Engineers, vol. 162, 1950, pp. 179-180.

45 "High Temperature Gas Turbines With Cooled Blades," by W. R. Hawthorne, Technical Report No. 4, "A Theoretical Study of the Thermodynamic Conditions in Gas Turbines Due to Blade Cooling by the Use of Liquid," dated May, 1949. Office of Naval Research Contract N5ori-78, Task Order 21, NR-220-101, pp. 1–10.

46 "Hollow Turbine Blades," *Shipbuilding and Shipping Record*, vol. 68, December 26, 1946.

47 "Temperatures and Stresses on Hollow Blades for Gas Turbines," by E. Pollmann, NACA Technical Memorandum No. 1183, dated September, 1947.

48 "NACA Shows Cooler Blades for Hot Jets," by A. McSurely, *Aviation Week*, vol. 55, October 22, 1951.

49 "Design Features of a 5000-Hp Gas Turbine," by B. O. Buckland and D. C. Berkey, Trans. ASME, vol. 74, July, 1952, pp. 655–661.

50 "5000-Kw Gas Turbine for Power Generation," by A. Howard and C. J. Walker, paper No. 48—A-83 presented at the 1948 Annual Meeting of the ASME.

51 "An Evaluation of Engine Design Compromises," by N. Burgess, Preprint No. 140, Institute of the Aeronautical Sciences, pp. 1–7.

52 "The Gas Turbine Manual," by R. J. Welsh and G. Waller, Copyright 1951, Temple Press Ltd., London, England.

53 "Design Features of a 4800-Hp Locomotive Gas-Turbine Power Plant," by A. Howard, *Mechanical Engineering*, vol. 70, 1948, pp. 301–306.

54 "Gas Turbine Progress in France," *The Oil Engine and Gas Turbine*, vol. 18, August, 1950, pp. 139–144.

55 "Gas Turbine Propelled MGB 2009-No. I," *The Engineer*, vol. 184, September 5, 1947, pp. 218–220.

56 "Experimental Study of Cooling by Injection of a Fluid Through a Porous Material," by P. Duwez and H. L. Wheeler, Jr., Preprint No. 137, Institute of the Aeronautical Sciences.

57 "Some NACA Investigations of Heat-Transfer Characteristics of Cooled Gas Turbine Blades," by H. H. Ellerbrock, Jr., paper presented at a General Discussion on Heat Transmission, London, England, September, 1951, pp. 1–41.

58 "Sweat-Cooling," by P. Grootenhuis and N. P. W. Moore, paper presented at the Iron and Steel Institute, London, England, on February 22, 1951.

59 "Production of Porous Metal Compacts," by R. L. Reddy, O. W. Reen, and F. V. Lenel, Rensselaer Polytechnic Institute, Bimonthly Progress Report No. 9, October 6, 1951, BuAer Navy Research Contract Noa(s) 11022, pp. 1–19.

60 "Process for Fabrication of Materials for Porous Turbine Blades," by G. M. Thomas and G. J. Comstock, Stevens Institute of Technology, Progress Report No. 19, April 1, 1950, BuAer Navy Research Contract Noa(s) 10607.

61 "A Method for Machining Porous Metals," by H. L. Wheeler, Jr., California Institute of Technology, Progress Report No. 4–97, April 15, 1949, Ordnance Department Contract No. W-04-200-ORD-455, pp. 1–8.

62 "Water-Cooled Blade Research," *The Oil Engine and Gas Turbine*, vol. 15, October, 1947, p. 195.

63 "Recent Inventions—Brown Boveri Cooled Gas Turbine Rotor," *The Oil Engine and Gas Turbine*, vol. 19, January, 1952.

64 "Standard American 5,000 Kw Plants," *The Oil Engine and Gas Turbine*, vol. 18, May 6, 1950.

65 "Discussion on Marine Gas Turbine," by Dr. A. Meyer, Transactions, North East Coast Institution of Engineers and Shipbuilders, vol. 63, 1947, pp. D-111-D-122.

66 "The Problem of Burning Residual Oils in Gas Turbines," by P. Lloyd and R. P. Probert, Proceedings of The Institution of Mechanical Engineers, vol. 163, 1950, pp. 206–224.

67 "Combustion System for Burning Bunker C Oil in a Gas Turbine," by B. O. Buckland and D. C. Berkey, paper No. 48—A-109, presented at the 1948 Annual ASME Meeting, pp. 1–11.

68 "Heavy Fuel Tests on a Gatric Gas Turbine," Metropolitan Vickers Electrical Company, Ltd. Report on April 9, 1951, pp. 1–25.

69 "Experimental Running of Open-and-Closed-Cycle Gas Turbines," by J. B. Bucher, paper No. 1125, Transactions, Institution of Engineers and Shipbuilders in Scotland, vol. 93, 1949–1950, pp. 275–310.

70 "Oil Ash Corrosion of Materials at Elevated Temperatures," by C. T. Evans, Jr., ASTM Special Technical Publication No. 108, 1950, pp. 1–47.

71 "Ship Research—No. III," by S. L. Smith, *The Engineer*, vol. 193, February 8, 1952.

72 "The Attack of Vanadium-Bearing Oil Ash on Heat-Resistant Steels," by P. Schlapfer, P. Amgwerd, and H. Pries, *Schweizer Archiv. Annales Suisses*, vol. 15, October, 1949, pp. 292–299.

73 "A Review of Gas Turbine Progress, 1951," *The Engineer*, vol. 193, January 18, 1952.

74 "Characteristics and Development of Naval Fuel Oils," by M. Blancher, paper No. 5, presented at the 1951 International Conference of Naval Architects and Marine Engineers, London, England.

75 "Some Considerations Dealing With the Formation of Deposits in Gas-Turbine Plant," by D. F. Hughes and R. G. Voysey, *Journal of the Institute of Fuel*, April, 1949, pp. 197–203.

76 "Sea Water Contamination of Boiler Fuel Oil and Its Effects," by Engineer Rear Admiral C. J. Gray, RN, and W. Killner, Transactions of The Institute of Marine Engineers, vol. 60, February, 1948.

77 Discussion of Mr. T. F. Eden on reference (69).

78 "Mechanism of the Rapid Oxidation of High Temperature, High Strength Alloys Containing Molybdenum," by W. C. Leslie and M. G. Fontana, Trans. ASM, vol. 49, 1949.

79 "Accelerated Oxidation of Metals at High Temperatures," by A. des. Brasunas and N. J. Grant, thesis for Doctor of Science degree, Massachusetts Institute of Technology, Cambridge, Mass.

80 "Test of a 4800-Hp Gas Turbine Power Plant," by A. Howard and B. O. Buckland, paper No. 48-A-98, presented to the 1948 Annual ASME Meeting.

81 Discussion of Dr. A. T. Bowden on "Materials and Performance," by Dr. A. T. Bowden and W. Hryniszak, paper presented to the Iron and Steel Institute, London, England, February 22, 1951. Abstract of discussion printed in *Engineering*, vol. 171, March 30, 1951 pp. 380-381.

82 Discussion by D. G. Sopwith on papers in Group IV, presented to the Iron and Steel Institute, London, England, February 22, 1951. Abstract of discussion printed in *The Engineer* vol. 191, March 23, 1951, pp. 373-374.

83 "Investigation of CaO-V_2O_5 Systems," by A. Morozov, *Metallurgie*, vol. 13, 1938.

84 Discussion by Dr. N. Stephenson on papers in Group II, presented to the Iron and Steel Institute, London, England, February 22, 1951. Abstract of discussion printed in *Engineering*, vol. 171, March 30, 1951, pp. 380-381.

85 Discussion by Dr. W. Siegfried on papers in Group IV, presented to the Iron and Steel Institute, London, England, February 22, 1951. Abstract of discussion printed in *The Engineer*, vol. 191, March 23, 1951, pp. 373-374.

86 Discussion by Dr. H. R. Cox on papers in Group II, presented to the Iron and Steel Institute, London, England, February 22, 1951. Abstract of discussion printed in *Engineering*, vol. 171, March 30, 1951, pp. 380-381.

87 Discussion by H. J. J. Redwood on papers in Group IV, presented to the Iron and Steel Institute, London, England, February 22, 1951. Abstract of discussion printed in *The Engineer*, vol. 191, March 23, 1951, pp. 373-374.

88 Discussion by C. T. Evans, Jr., on papers in Group IV, presented to the Iron and Steel Institute, London, England, February 22, 1951. Abstract of discussion printed in *The Engineer*, vol. 191, March 23, 1951, pp. 373–374.

89 "Marine Gas Turbine Progress," by John Lamb, *Lloyd's List Annual Review*, 1951, pp. 1–6.

90 Discussion by Dr. A. T. Bowden on reference (75); *Journal of the Institute of Fuel*, April, 1949.

91 Discussion by J. R. Rylands on reference (75); *Journal of the Institute of Fuel*, April, 1949.

92 Discussion by Dr. N. P. Allen on papers in Group II, presented to the Iron and Steel Institute, London, England, February 22, 1951. Abstract of discussion printed in *Engineering*, vol. 171, March 30, 1951, pp. 380-381.

93 "Gas Turbines Planned for Battleships," *Marine Journal*, vol. 77, April, 1950.

94 "Admiralty Work on Heavy Fuels," *The Oil Engine and Gas Turbine*, vol. 18, May, 1950, p. 14.

95 "The Story of the British Gas Turbine," Power Jets (Research and Development, Ltd.), A Festival of Britain Survey, published by Sidney-Barton, Ltd., London, England, pp. 1–40.

96 Discussion by J. B. Bucher of reference (69).

97 "The Advantages of High Inlet Temperature for Gas Turbines and Effectiveness of Various Methods of Cooling the Blades," by O. W. Schey, paper No. 48—A-105, presented to the 1948 Annual Meeting of the ASME.

Gas-Turbine Progress Report—Cycle Components

By P. F. MARTINUZZI,[1] HOBOKEN, N. J.

Introduction

THE gas turbine is not a single machine which delivers power, as is, for instance, the internal-combustion engine; it is a power plant consisting of several components, some essential (compressor, combustor, turbine), some very important to the cycle performance (regenerator, intercoolers, and so on), and so it resembles the steam plant. The gas-turbine cycle is extremely sensitive to variations of component arrangement and efficiency, even more than the steam cycle. This is an advantage from the customer's point of view; it can be tailor-made to suit his needs. If a simple, light power plant is wanted, it can be obtained by sacrificing efficiency; if very high efficiency is needed, it can be had at the cost of added weight and complication. The gas turbine is also the only type of power generator in which specific power output (hp/lb air/sec) and thermal efficiency can be independent of each other. In internal-combustion engines and steam plants, the same means are used to increase both specific power and efficiency. In gas turbines, this applies only to cycle-temperature increases; other means (such as regeneration) affect the thermal efficiency but not the specific output.

This paper deals with the effect of components, as regards design, arrangement, and efficiency, on the performance of the modern gas-turbine plant. For reasons of space, only a few characteristic modern developments of main component design can be discussed. The effect of component improvement on cycle performance also will be covered, except for high-temperature turbine cooling, which is dealt with in a companion paper, "Gas-Turbine Progress Report—Materials, Cooling, and Fuels," by A. A. Hafer, paper No. 52—F-1B.

Aircraft Gas-Turbine Components

A sharp distinction must be made between aircraft gas turbines and all other types. To reduce weight and frontal area, all aircraft machines follow the simplest possible pattern; only the essential components, compressor, combustors, and turbine are used. Notwithstanding the crying need for lower fuel consumption, no serious attempt to use a regenerator has been made since this feature was discarded in the Bristol *Theseus* turboprop. The jet-engine afterburner is a crude form of reheat; but it is used for such short periods and its effect is so radically different from that of ordinary reheat that it must be considered as a special military aircraft accessory.

Most of the characteristics which make of the aircraft gas turbine an almost distinct species are imposed by the need for the lowest possible drag, that is, for the smallest frontal area. This condition, much more than considerations of weight, forces the design of aircraft turbines into a uniform mold. Whenever a small frontal area is not required, as in auxiliary power plants, the design develops freely according to requirements and to the designer's ingenuity, as can be seen in the AiResearch and Turbomeca units. However, a small frontal area is required only in relatively small aircraft (fighters) or whenever the engine is carried in outside engine pods. It is, however, quite possible that in the future these conditions will not always prevail; for instance, in very large land aircraft and even better, in very large flying boats, the turboprop power plant can be located accessibly inside the fuselage or hull, only the multiple power turbines, with reduction gear and propellers, being placed on the wings. When this development matures, the aircraft gas turbine will evolve unfettered; then, intercooling, regeneration, and reheat will probably find their place also in the aircraft machine, as will the large-diameter radial compressor and turbine. Until then, however, and as long as aircraft-engine design is dictated and financed by the military, the classical small-frontal-area engine will continue to prevail.

Component Design. The only departures from normal aircraft practice are the combined axial and centrifugal compressor in the Bristol *Proteus* turboprop, shown in Fig. 1, which will be used in a large series of Bristol Britannia airliners, and the two-stage centrifugal compressor in the Rolls Royce *Dart* turboprop, Fig. 2, a relatively old but very reliable machine, the first aircraft gas turbine ever to have carried paying passengers. The old contest between centrifugal and axial compressor appears to turn in favor of the axial, which equips all known new prototypes. It must be noted, however, that there are many more jet engines in operation with radial compressors than with axials; the jet used on the Russian MIG 15 has a radial compressor, as have other types derived from the Rolls Royce *Nene*, such as the Pratt and Whitney. The centrifugal compressor is more reliable, sturdier, lighter, and much easier to manufacture than the axial. These advantages are outweighed by two defects which are particularly bad for very fast military aircraft—a large frontal area and the inability to give a high pressure ratio. That is why the axial compressor prevails.

Aircraft axial compressors must give first of all a large flow per unit frontal area; this is necessary not only to obtain high specific thrust but also because, at high altitudes, the air density is very low. This leads to very long blades and very high axial velocities. The ratio between hub and tip diameter in the low-pressure stages of aircraft compressors can be as low as 0.4, as against about 0.7 for other types. These very long blades require not only special design to resist stress due to centrifugal force and vibrations, but also special blading diagrams. Free-vortex variation of the tangential absolute-velocity components along the radius becomes impractical for radius ratios smaller than 0.66; the modern large jet compressor bladings are of the solid

---

[1] Professor of Mechanical Engineering Stevens Institue of Technology. Life Mem. ASME.

Contributed by the Gas Turbine Power Division, and presented at the Fall Meeting, Chicago, Ill., September 8–11, 1952, of The American Society of Mechanical Engineers.

Notes: This is paper No. 52—F-1C of a Progress Report which the Executive Committee of the Gas Turbine Power Division authorized at its 1951 Annual Committee Meeting. The series includes the following: "Introduction," by R. Tom Sawyer, paper No. 52—F-1A; "Materials, Cooling, and Fuels," by A. A. Hafer, paper No. 52—F-1B; "Automotive," by Frank L. Schwartz, paper No. 52—F-2; "Railroads," by K. A. Browne, J. I. Yellott, and P. R. Broadley, paper No. 52—F-3; "Marine," by W. A. Dolan, Jr., and A. A. Hafer, paper No. 52—F-4A; "Merchant Vessels," by W. A. Dolan, Jr., and A. A. Hafer, paper No. 52—F-4B; "Naval Vessels," by W. A. Dolan, Jr., and A. A. Hafer, paper No. 52—F-4C; "Stationary Electric Generation," by Lee Schneitter, paper No. 52—F-5; "Industrial," by L. N. Rowley, Jr., and B. G. A. Skrotzki, paper No. 52—F-6; "Aviation," by I. H. Driggs and O. E. Lancaster, paper No. 52—F-7.

Statements and opinions advanced in this paper are to be understood as the individual expression of the author and not those of the Society.

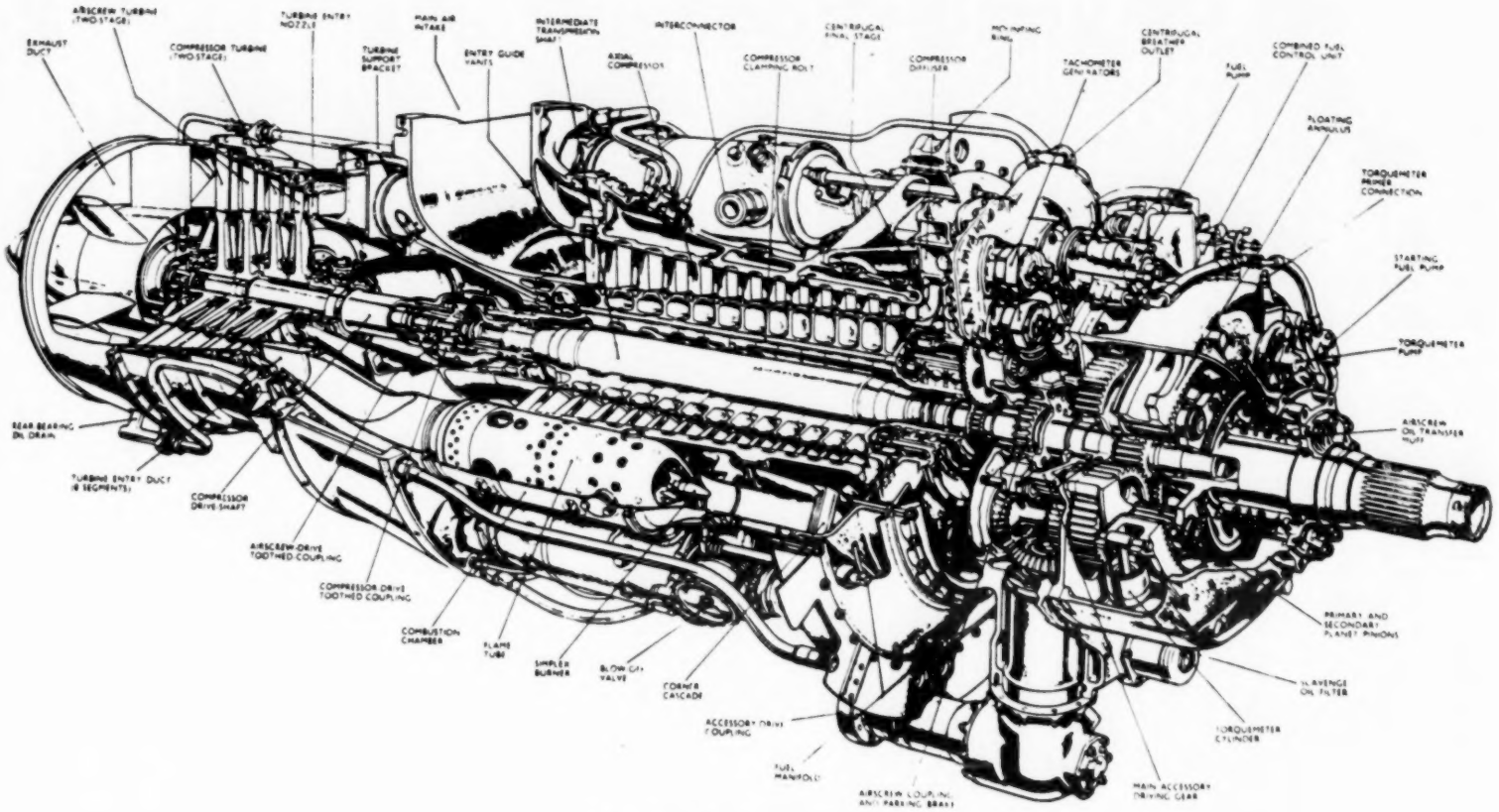

FIG. 1 BRISTOL PROTEUS TURBOPROP
(Courtesy of *Flight*)

Data		Data	
Length, airscrew cone to jet pipe	8 ft–4.5 m.	Max. s.l. power, shp	4100
Diameter	3 ft–3.5 m.	Max. compressor, rpm	12000
Weight, bare, dry, lb	2650	Airscrew turbine, rpm	10700
Reduction-gear ratio	0.09:1	Minimum idling speed (compressor), rpm	7200
Airscrew rotation	L.H. tractor	Minimum idling fuel consumption, lb per hr	400

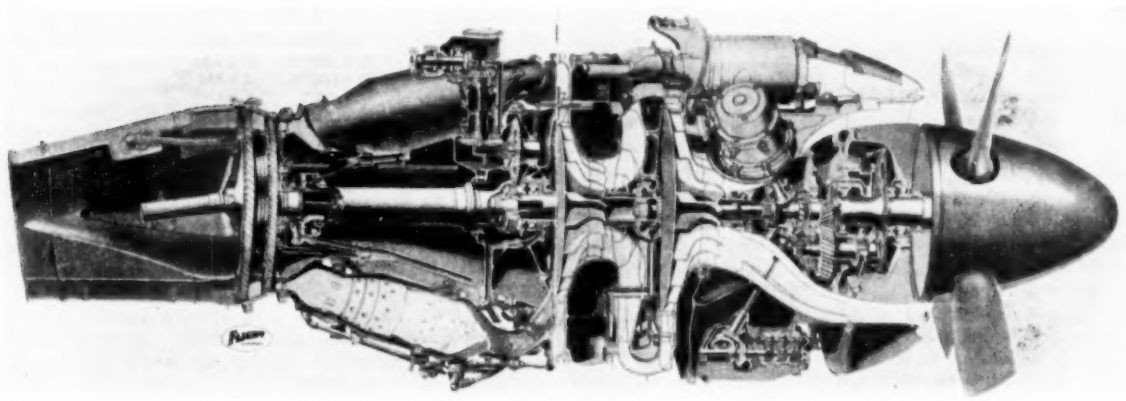

FIG. 2 ROLLS-ROYCE DART TURBOPROP (Courtesy of *Flight*)

rotation or similar types, in which the tangential components of the absolute velocities are proportional to a positive power of the radius, instead of being inversely proportional to it, as in the free-vortex type. To obtain radial equilibrium, this requires variable axial velocity along the radius.

Compressor blading is discussed in references (1, 2, 3).[2] The mean axial velocity goes up to 700 fps, as against 450 fps for other compressors, and so efficiency is reduced. To decrease the number of stages, very high peripheral velocities are used; consequently, the first stages work at very high Mach numbers, near or above 1. This is not as bad as it might seem because, if the compressor is designed for operational altitude conditions, then at any lower altitude the warm air gives a higher velocity of sound and a lower Mach number. Special thin transonic blade profiles are used to reduce the efficiency loss. Solid rotation or similar blades are generally not tapered; the chord is as wide at the tip as at the hub; this, combined with the great blade length and the high Mach number, enhances the danger of self-induced blade vibration, which has caused lots of trouble in the development of very large compressors (4, 5). The blade-vibration problem is particularly serious in turboprop engines, where propeller and reduction gear are a source of externally induced vibration. Blade vibration has been the main cause of the slow or arrested development of several large turboprops; small turboprops are much less sensitive to vibration, hence the trend toward double turboprops (two coupled small turbines), such as the double Allison and the double Armstrong-Siddeley *Mamba*.

To reduce the number of compressor stages, very high aerodynamic lift coefficients are used in axial jet compressors; the profiles and the polars used are secret, but it can be safely assumed that values of c_L of 0.9 and perhaps even higher are permissible, as against 0.7 which many of the manufacturers still consider maximum for good efficiency. These high aerodynamic loads cause the pressure-flow characteristic curve to fall sharply. This is particularly unfortunate in aircraft compressors, where the usual difficulties in matching compressor and turbine are enhanced by the variation of density and temperature with altitude. As maximum power is required both for take-off (low altitude) and for combat (high altitude), in practice the engine is run in both cases at the maximum safe turbine-inlet temperature, so that compression, temperature, and air-fuel ratios are quite different in the two cases.

Axial compressors now in operational use have pressure ratios varying from about 4 for centrifugal types to about 6 for axial types. The urgent need for improved fuel consumption makes the use of much higher pressure ratios imperative for jet engines. From this point of view, a clear distinction must be made between turbojets and turboprops. As regards thermodynamic cycle, the turboprop behaves like any other gas turbine; the best way to increase efficiency and power output is to raise the turbine-inlet temperature. Contrary to a very widespread opinion, the pressure ratio for some turboprops and for nonaviation gas turbines is chosen not at the point of maximum efficiency but at, or near, the point of maximum work, that is, of minimum air-rate. The reasons for this will be discussed later.

The thermodynamics of the turbojet engine are completely different. As was first shown by Professor Ackeret (6), the thermal efficiency of a jet engine, for a given aircraft speed and other conditions, does not increase with the turbine-inlet temperature; it

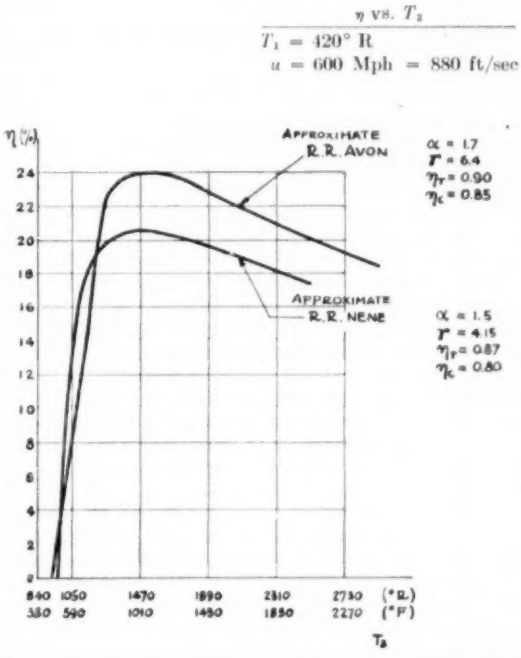

FIG. 3 EFFICIENCY—TURBINE INLET TEMPERATURE IN TURBOJETS

[2] Numbers in parentheses refer to the Bibliography at the end of the paper.

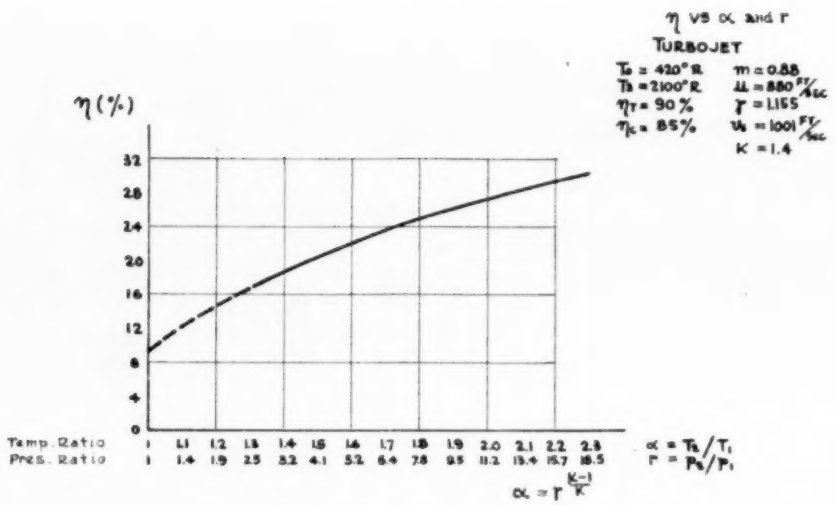

FIG. 4 EFFICIENCY—PRESSURE RATIO IN TURBOJETS

reaches a maximum at a relatively very low inlet temperature and then falls gradually, as shown in Fig. 3. Owing to the fact that the specific thrust does increase rapidly with temperature, modern jets operate at temperatures considerably above the maximum efficiency value. While temperature increases do not improve the efficiency and fuel consumption of jets, pressure ratio increases do, to a much greater extent than in turboprops or other gas turbines. The variation of efficiency versus pressure ratio for equal conditions is shown in Fig. 4. This is not the place to discuss more fully jet-cycle properties; reference (7) gives briefly but clearly the influence of temperature and other factors on turbojet and turboprop performance. The recent trend toward very high pressure ratios becomes understandable because lower fuel consumption is essential both in military and commercial jet engines to increase the aircraft range. Modern axial-compressor jets nearly ready for wide operational use have ratios between 6 and 8; but the newest models under design study have much higher ratios, reputedly up to 24.

Design and development of an axial compressor for such high ratios under aviation conditions (that is, a single machine with no intercooling) is a difficult problem indeed. The great density difference gives very long blades in the first stages, very short ones in the last. To avoid this, the stage diameter can be tapered down, but then the peripheral velocity in the last stages decreases, increasing the already excessive number of stages. Too many stages render flow conditions at the high-pressure end very bad, causing loss of efficiency and making the characteristic curves very steep. The temperature in the last stages exceeds the safe limits for aluminum. All this makes the development of a single compressor for very high ratios an almost impossible task. In industrial turbines, the problem can be solved easily by using two or three separate compressors in series, with intercooling; but this is ruled out under aircraft conditions by reasons of space and weight.

Two ways can be followed to solve the problem. One is to use a supersonic compressor, in which the pressure ratio per stage is very high (up to 6 in theory, perhaps up to 4 in practice). Much classified work is being done on this subject both in the United States and in Europe. In the United States the trend is toward getting as high a ratio per stage as possible; the difficulty is that a shock-wave diffuser works only at the exact design conditions, so that these compressors function only at a definite point and not along a characteristic curve; they are very far from practical use. In Europe the supersonic compressor is evolved from another angle; slightly supersonic stages are used, giving relatively low ratios per stage, about 1.5. This type is much less sensitive to changes in conditions, and some satisfactory results apparently have been obtained, both as regards efficiency and shape of the characteristic curve. Their development is not easy, because at Mach number 1 there is always trouble. Special blading diagrams and profiles must be studied, to give constant Mach number along the radius, while in ordinary compressors the Mach number decreases from tip to hub.

The other way of solving the problem of the high-compression axial is to use the so-called "spool" arrangement; two coaxial compressors turn at different speeds driven by two turbines, the high-pressure compressor being driven by the high-pressure turbine through a hollow shaft, the low-pressure compressor by the low-pressure turbine by means of a thin shaft running inside the hollow shaft. In this way the high-pressure compressor can have a small diameter and, consequently, longer blades, and yet run at very high peripheral speed. No Mach-number trouble need be feared there as the air is hot. Also, owing to the fact that the two sets can run at variable-speed ratio, a much flatter characteristic curve and much easier matching are obtained. This is a very useful virtue which actually prompted the spool development. It was first used very successfully, but in a slightly different form, in the now abandoned Rolls Royce *Clyde* turboprop.

Many jet manufacturers are now experimenting with the spool arrangement, which is the coming thing in jets; one accepted British type, built under license in the United States, already has it. The spool type works satisfactorily for moderately high ratios, up to 12 and higher; much work is still needed to obtain higher ratios. The reduction in number of stages, compared with an ordinary compressor, is considerable; it becomes even greater if the blading diagram of each compressor half is changed from stage to stage, increasing the degree of reaction toward the high pressure end (3). The two units can be made counter-rotating, to counterbalance the gyroscopic effect.

Turbine Design. In aircraft power plants, the turbine problem is less acute than that of the compressor, and the departures from standard practice are few. The typical jet turbine is used, with a very low degree of reaction at the hub (about 0.1) and free-

vortex distribution along the radius. The mean degree of reaction varies with the radius ratio and is often about 0.4. The fact that there is some reaction along the whole blade and, consequently, an accelerated flow, insures high efficiency. This arrangement gives a very high power per stage. New engines with very high compression ratios inevitably must use several stages, with or without the spool arrangement. The new high-powered engines have very long blades and vibration trouble can be expected. In jets, the trend is toward lower temperatures, to improve fuel consumption; in turboprops, toward very high temperatures, up to 3000 F. As already mentioned, however, the high-temperature aspect is covered in a companion paper (paper No. 52—F-1B).

Other military aircraft components, such as combustors, variable jet nozzles, supersonic intakes, afterburning, and water injection are special subjects and cannot be discussed here.

Nonaviation Gas Turbines—Cycle Properties

Figs. 5 and 6 show how various factors influence gas-turbine performance. These curves are only correct for the conditions given on each curve. Performance is influenced by many factors in different ways, so these curves should be considered as showing general trends only.

Ambient Temperature. Thermal efficiency and air rate are extremely sensitive to variations in ambient temperature, as shown in Fig. 6. If in a given installation a minimum power output is guaranteed, the engine must be rated at the highest ambient temperature likely to be met. For instance, the 1000-kw marine gas turbogenerator set built by W. H. Allen and Sons is rated for tropical temperatures. In the United States the general industrial and marine practice is to use a standard temperature of 80 F. In Europe the usual temperatures are 15 C or 20 C. In

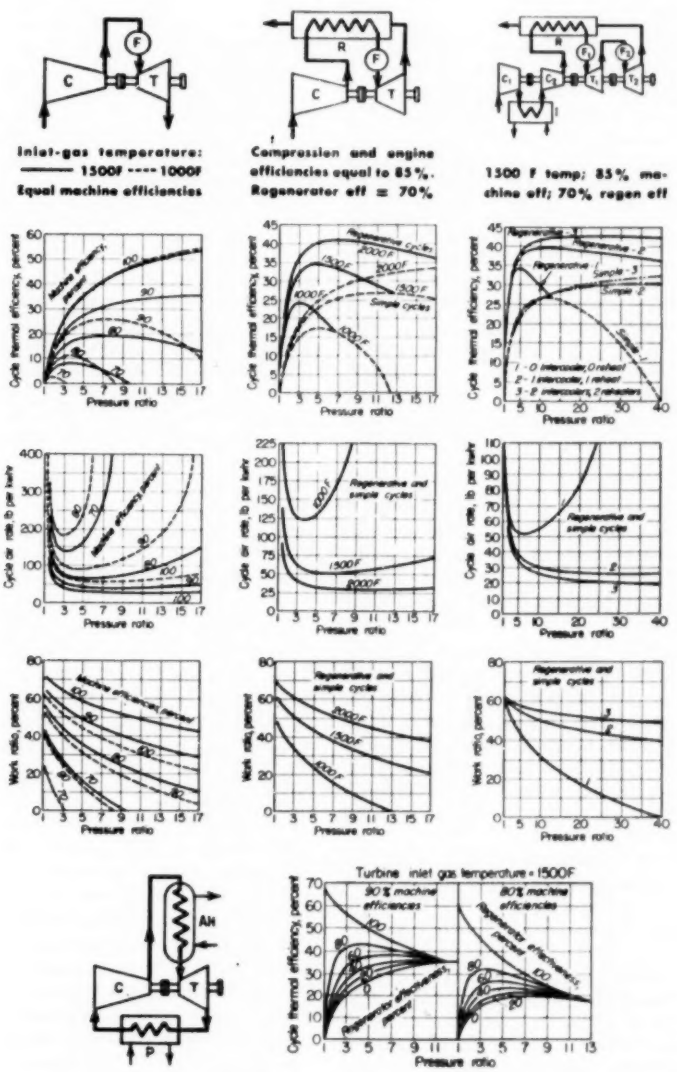
Inlet-gas temperature:
1500F ---- 1000F
Equal machine efficiencies
Compression and engine efficiencies equal to 85%. Regenerator eff = 70%
1500 F temp; 85% machine eff; 70% regen eff
Cycle thermal efficiency, percent
Pressure ratio
Regenerative and simple cycles
Simple cycles
Cycle air rate, lb per kwhr
Work ratio, percent
Turbine inlet gas temperature = 1500F
90% machine efficiencies
80% machine efficiencies

Fig. 5 Gas-Turbine Performance Curves (Courtesy of *Power*)
(Assumptions: Ambient temperature 60 F; no secondary losses; industrial turbine conditions.

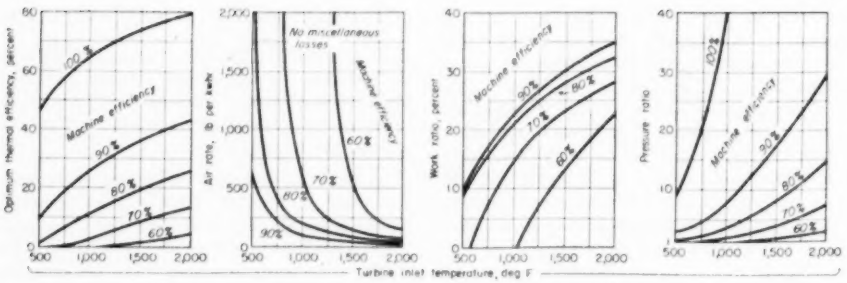

FIG. 6(*a*) SIMPLE-CYCLE PERFORMANCE VARIATION WITH TURBINE-INLET TEMPERATURE AND MACHINE EFFICIENCIES
(Assumptions: Inlet-air temperature 60 F; equal compressor and turbine efficiencies; values of air rate, work ratio, and pressure ratio correspond to optimum thermal efficiencies as given in Fig. 5.)

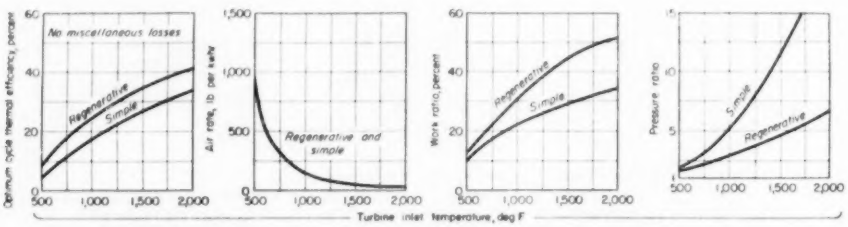

FIG. 6(*b*) COMPARISON OF SIMPLE AND REGENERATIVE CYCLE PERFORMANCE
(Assumption: Inlet-air temperature 60 F; 85 per cent compressor and turbine efficiency; 70 per cent regenerator effectiveness.)

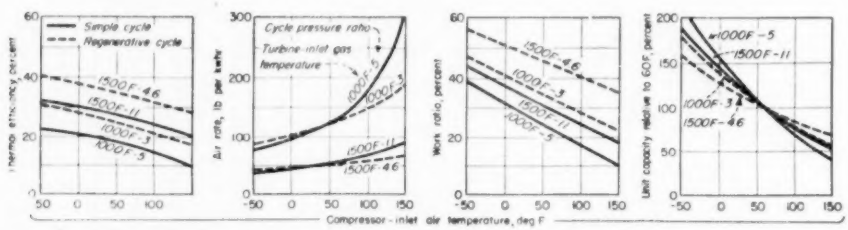

FIG. 6(*c*) PERFORMANCE VARIATION WITH COMPRESSOR INLET-AIR TEMPERATURE (Courtesy of *Power*)
(Assumption: Constant compressor efficiency. The cycle pressure ratios are optimum for each case; they are shown on the curves after the temperature.)

making comparisons between different plants, corrections must be made for inlet temperature.

It is possible to get extra power from gas turbines by reducing the inlet-air temperature. This is done in a 3500-kw General Electric unit, installed at the Belle Isle Station of the Oklahoma Gas and Electric Company, in which precooling is used; up to May 1, 1952, the average load has been about 4500 kw, that is, nearly 28 per cent above rated power, in about 21,000 hr of operation. The unit cost of power and the specific weight of the power plant both decrease for lower ambient temperature, provided the plant is designed to carry the excess power.

The extra power at low inlet temperature is obtained with no increase in turbine-inlet temperature. Conversely, if no increase in load is desired at low inlet conditions, the turbine inlet temperature can be reduced and the life of the plant is increased. Consequently, the gas turbine is ideal for applications which require more power during cold weather, such as gas pipe-line pumping units, and for base-load power stations designed to supplement hydroelectric plants during the winter months, such as Beznau, Weinfelden, and Dundee. The Brown Boveri locomotive provides the considerable amount of current required for electrically heating the train without decrease of power or increase in fuel consumption over summer conditions.

Component Efficiency. The best way to increase gas-turbine efficiency is to improve the efficiency of the three major components, turbine, compressor, and combustor. This is the only means of increasing efficiency without affecting the life and simplicity of the unit. The axial-flow compressor efficiency has risen by about 10 percentage points since 1937, and is now increasing at the rate of half a percentage point per year. Progress will slow down before reaching the maximum feasible value of about 93 per cent (8).

Turbine efficiencies have advanced about 4 percentage points since 1943 (8). They reach now 90 per cent, and 86 per cent is not unusual. Higher values can be expected as a result of future developments. In any case, turbine efficiencies should be from 1 to 3 percentage points higher than axial-compressor efficiencies, because boundary-layer conditions are better in an accelerated flow (turbine) than in a decelerated flow (compressor). Turbine efficiency is lower when, for reasons of economy or compactness a low number of turbine stages is used. European industrial units generally use more turbine stages than comparable American machines, and are more efficient but more expensive. Aircraft turbines can be quite efficient with few stages (generally one or two in jets, two to four in turboprops) because the high

exit velocity, which would cause a considerable leaving loss in other types, is integrally utilized for jet propulsion.

The open-cycle gas turbine now normally has a combustion efficiency of 98 per cent or higher, at least in large plants where there is room for well-proportioned combustors. Where space is at a premium and the combustors are too compact, such as in aircraft and small gas turbines, combustion efficiency is lower, down to 95 per cent. In closed-cycle gas turbines, the air-heater efficiency, which corresponds in cycle calculations to the open-cycle combustor efficiency, is about 92 per cent (9, 10, 11); there is not much room for improvement. However, if a gas turbine uses heat through a primary heat exchanger, such as in the British waste-heat unit or in atomic plants, then the primary heat-exchanger efficiency takes the place of combustor or air-heater efficiency. In this case the closed cycle is better; the primary heat exchanger is smaller and more efficient owing to better heat transmission due to high air pressure.

Component efficiencies are also influenced by the type of compressor or turbine chosen. The advantages and limitations of axial and radial turbomachines are well known. At present, the axial compressor is more efficient than the centrifugal for large plants, though the best centrifugals are nearly as good as the best axials; there is every reason to believe that the future top limit will be the same for both types. As regards turbines, there are at present no experimental data on large radials; small radials have proved more efficient than small axials. Radial turbomachines give a flatter characteristic curve, very useful in plants working at variable speed or altitude so that the components tend to be mismatched. They are more rugged, cheaper, and easier to produce. On the other hand, they cannot deal with the flow of very large volumes of gas, so that they are unsuitable for the lower stages of large machines. Radials have a large diameter and a short length; axials a considerable length and small diameter. Axial compressors are expensive and difficult to manufacture owing to the large number of blades, which must be twisted for high efficiency; axial-compressor blade production constitutes a serious bottleneck in jet-engine production. For large machines, an interesting combination is the use of axial compressors for the low-pressure side and centrifugals for the high-pressure side, either in the form of separate machines, as in the Escher-Wyss St. Denis plant, Fig. 12, or as the last stage of a single machine, as in the English Electric locomotive unit, Fig. 8.

Axial compressors present two special difficulties. One is dust and dirt deposits on the blades, which can be cured by suitable air cleaners, as has been done in the Brown Boveri plant. The other, much more serious, is vibration in the long blades of large compressors. This has already been discussed as regards aircraft machines (4, 5); it has recently caused serious trouble in industrial compressors too; experimental and theoretical proof has been given that this type of vibration is self-induced. When this trouble arises, and it is very capricious, the only cure is to lash the blades with wire, with a bad drop in efficiency. The long-range cure, on which much work is being done, will probably consist in changes in blade profile to take into account rigidity as well as aerodynamic properties.

Pressure Ratio. The choice of a suitable pressure ratio is of paramount importance for the success of a gas turbine and is governed by many factors. Ambient temperature, turbine-inlet temperature, component efficiency and design, type and arrangement of cycle all affect the best pressure ratio, which consequently varies from case to case. Fig. 5 shows clearly that for a simple cycle, thermal efficiency reaches a maximum at a relatively high pressure ratio, for usual temperatures and component efficiencies. However, as already stated, and contrary to a widespread opinion, the pressure ratios used in practice are much lower than the maximum efficiency values; they are generally at or near the minimum air-rate point, that is, the maximum specific work point. This choice is due to two reasons:

(*a*) For ordinary conditions, the air-rate curve rises sharply for compression ratios higher than the minimum air-rate point, while the efficiency curve is very flat between points of minimum air rate and of maximum efficiency; consequently, choosing the minimum air-rate value implies a small loss in efficiency but a considerable gain in size, weight, and cost. (*b*) Compressor losses, size, and weight increase with increasing compression ratios. A large pressure-ratio increase to gain a few per cent in efficiency is largely self-defeating, because the pressure increase brings about a lower component efficiency and consequently a lower thermal efficiency. This can be seen clearly in Fig. 5.

In the regenerative cycle, efficiency actually increases with a decrease of pressure ratio, reaching a maximum at very low values, while the air-rate minimum is about at the same point as in the simple cycle, Figs. 5 and 6. With the development of the compact lightweight rotary regenerator (see later) which is suited only to low pressure ratios, new possibilities open to the transport and automotive turbine. As the work ratio (useful power/gross power) increases sharply with a decrease of pressure ratio, the combination of a low-pressure cycle, with single-stage centrifugal, and a rotary regenerator gives a very light, compact, and simple machine with fuel consumption comparable to that of automotive Diesel engines. The properties of the complex cycle, with regeneration, reheat, and intercooling, are similar to those of the regenerative cycle, Figs. 5 and 6.

In conclusion, very high pressure ratios are not necessary except when high turbine-inlet temperatures are used. The only type of gas turbine where really high ratios would be really useful if they could be obtained is the turbojet engine, as already seen, Fig. 4.

Regeneration. The use of a regenerator allows considerable gain in thermal efficiency; this depends on the pressure ratio, the regenerator effectiveness, and the pressure losses. A very effective regenerator with too high a ratio gives smaller gains than a less effective one with the right ratio. Using the same basic machine with or without regenerator, as is done in some United States industrial turbines, does not lead to best results; the pressure ratio should be adapted carefully to the regenerator employed. Intercooling and reheat combined with regeneration add their advantages and cancel out their defects, allowing the best performance. A regenerator has the sole effect of reducing fuel consumption, that is, of increasing thermal efficiency; it does not improve specific output; on the contrary, due to pressure losses, it decreases it, sometimes considerably. Regenerators are discussed in references (9, 10, 12, 13, 14, 15, 16, 17, 18). Regenerators are essential to the closed-cycle gas turbines; the fluid must start the cycle again at the same inlet temperature and the only reasonable means of subtracting heat from it is a regenerator.

The main types of regenerator are (*a*) tubular, (*b*) extended surface, (*c*) rotary; they are listed in order of decreasing weight and bulk. The first two types are well-known in the United States. The development of the rotary regenerator has taken place primarily in England. Developed originally in Sweden for boilers, its use in gas turbines was proposed by Professor Ritz of Göttingen about 10 years ago. After the war, the National Gas Turbine Establishment and some private British firms (Shell, Pametrada) took up the development; NGTE built three units (18). The rotary regenerator, which has a very high effectiveness and very small size and weight, present serious problems as regards leakage. If there is considerable leakage of high-pressure air into the exhaust, any advantage resulting from regeneration will be lost owing to the increase

in compression work. Some leakage is inevitable, as high-density air and low-density exhaust alternate in the same regenerator cells. This loss increases with the pressure ratio and renders the prospects of the rotary regenerator for high pressure cycles rather dim.

The seal between rotary and stationary parts is another source of leakage, which also increases with the pressure ratio, but can be reduced by ingenuity in design and improvements in materials. A very complete study of the problem is given in (18). The rotary regenerator probably will find its earliest applications in small turbines with low compression ratios, lower than 4; even within these limits, it might greatly improve the chances of the gas turbine in the transport field. It has already been pointed out that a low compression ratio increases the cycle efficiency if an effective regenerator of suitable size is used. Work on rotary regenerators is actively pursued in England and the United States.

Intercooling. Intercooling, when used alone, improves considerably the specific work but gives little or no increase in efficiency. When used with regeneration, it gives excellent results, as the virtues are enhanced and the defects cancel out. The use of intercoolers, when water and space are available, has considerable indirect advantages. When high pressure ratios are obtained with axial compressors, intercooling has the unexpected effect of increasing the component efficiency of the compressor. This is due to the fact that if an axial compressor has too many stages, flow and boundary-layer conditions become very bad and efficiency drops. Intercooling, which requires the use of several units, each with few stages and with the flow slowed down and reaccelerated, allows a considerable gain in compressor efficiency.

Another indirect advantage of intercooling is that excess humidity in the air condenses in the intercoolers and can be trapped and separated, sometimes with marked effect on turbine-blade deposits and corrosion. Precooling is, in general, desirable only for higher ambient temperatures, unless the excess power made available by precooling can be exploited effectively. Precooling requires a supply of water well below the ambient temperature—the wider the difference, the more attractive precooling becomes. The General Electric precooled plant in Oklahoma has already been discussed; the investment of about $75,000 in a precooling system has paid handsome dividends.

Precooling is an essential part of the closed cycle. The fluid, exhausting from the turbine at high temperature, must be brought back to the compressor inlet at the original temperature; most of the heat is extracted by the regenerator, but the rest must be eliminated in the precooler. Precooling, and also intercooling, could be effected by an absorption refrigeration system utilizing the gas turbine-exhaust heat. Long-range development work is being done in the United States on this problem.

Reheat. Reheat is never used without intercooling, and generally regeneration is also added. The three features as already pointed out, have complementary advantages. Intercooling and reheat substantially increase the temperature differential between turbine exhaust and compressor outlet that can be utilized in the regenerator. For a given regenerator size, the efficiency gain obtained becomes very considerable if either or both are used. Reheat, and to a lesser degree, intercooling, considerably decrease the air rate, and thus more than compensate the air-rate increase due to pressure drop in the regenerator, and reduce the size of the regenerator and of the whole unit.

Reheat is costly, because it normally requires expensive high-temperature blades, rotors, pipes, and volutes in each of the turbines. Consequently, reheat is interesting in low-temperature gas turbines, working at no more than 1000 F, such as atomic turbines or those utilizing waste heat. In this case no expensive metals are needed, while the increase in efficiency and reduction in air rate is particularly valuable in a low-temperature cycle. In turbines of this type, which are often of the closed-cycle type, and in closed-cycle units in general, reheat becomes simple, as only one air heater or primary heat exchanger is needed, with separate tube circuits for the different reheat pressures. Experience has recently shown, however, that the correct proportion between high-pressure and low-pressure tubes is not easily found by calculation, and so there are difficulties in reaching the right temperatures. Provision must be made in new designs to allow for easily adjustable changes in tube distribution.

Although only one stage of reheat has been used up to now, theoretical studies show that multiple reheat stages are advantageous for large high-efficiency atomic turbines (19). As a matter of expediency, the first atomic submarine apparently will be powered by a steam plant; but the atomic gas turbine seems to present advantages over steam, and is, of course, for aircraft applications. The British already have studied, and perhaps built, an atomic gas turbine for power generation at Harwell.

Regulation. The curves in Figs. 5 and 6 are drawn for full load conditions, but they can be used to study what happens at part load. In constant-speed single-shaft open-cycle units, the only practical way to decrease load is to reduce the turbine-inlet temperature, which entails a considerable drop in efficiency. If a separate power turbine is used, there is greater latitude, as the pressure ratio can be varied by changing the compressor-driving turbine speed. Even better flexibility and part-load efficiency is obtained in multiple-shaft reheat cycles. The gain given by a regenerator at part load must be examined for each single case; it is often greater than at full load. From the point of view of part-load performance, the closed cycle is unsurpassed, as it gives in theory a constant efficiency at all loads. The actual efficiency decrease with falling load is very small (from 30.5 per cent at full load to 29.5 per cent at half load in the Escher-Wyss 2000-kw experimental turbine) as shown in reference (11), and is due to the increased importance of mechanical losses with decreasing load.

The problem of gas-turbine regulation is quite complex and will become very serious when large gas-turbine power stations come into general use. In open-cycle gas turbines, particularly if a heat exchanger is used, the thermal inertia of the system is tremendous. If a sudden change of load occurs, the machine needs time to follow it. If the load decreases, it is possible to blowout or by-pass some of the fluid, but no such simple solution exists for a load increase. Reheat improves the situation, and an answer to the problem will be found, even at the cost of added complication. Some of the large gas turbines now used for power generation are not able to follow the sudden load changes required by the net. They work on a time table, leaving peak-load changes to other stations. Closed-cycle turbines are regulated by changing the density of the fluid in the system and leaving the temperatures constant. If there are reserve pressure tanks, such as are used in the 12,500-kw St. Denis and in the 2000-kw experimental Escher-Wyss plant, but not in Dundee, any load variation in either direction can be followed immediately, as energy is stored in the reserve tanks. But, if wide-amplitude load variations are frequent, the closed cycle is not suitable, because filling the reserve tanks represents a pure loss, prohibitive if too frequent; also, the reserve tanks and piston compressors become very bulky and costly.

One of the advantages of well-designed open-cycle units is the very short time required to obtain full power from a cold start. Aircraft gas turbines can get to take-off overload almost instantly. Even large industrial sets, such as the Brown Boveri Beznau and Filaret units, can reach full load in an extremely short time, less

than 20 min. In many applications, this represents a great advantage over steam.

Turbine-Inlet Temperature. Beside increasing component efficiencies, there is another way to raise the full-load plant efficiency while reducing weight and bulk; it consists in raising the turbine-inlet temperature, with a corresponding increase in pressure ratio. The effect is very marked, as can be seen from Figs. 5 and 6. If blade and rotor cooling is not used, metallurgical considerations set a limit to the maximum allowable temperature. As a result of fatigue and creep, this temperature depends on the life expected of the machine. Short-life units, such as aircraft engines, or those which run at full power and temperature only occasionally, can run at higher temperatures than industrial plants designed for continuous full-power use. There has been no significant increase in maximum temperature in machines built in the last few years. For nonaviation machines, these temperatures vary from 1100 to 1550 F; United States turbines run at considerably higher temperatures than European machines, and the highest values are used on small units.

Higher temperatures than those now in use depend on turbine cooling, on which much work goes on everywhere, but which is not yet quite ready for practical use. Unfortunately, most turbine-cooling work is done for aircraft engines, where the problem is simpler because pure expensive fuels are used and no corrosion is to be feared. The use of high temperatures in those industrial or marine units which must rely on cheap fuels is much more difficult. Even at 1300 F, deposits and blade corrosion present very serious problems. Although considerable work has been done on additives and fuel purification, the integral solution probably will be given by blade-cooling systems in which the blade surface is insulated from the stream of combustion gases—for instance, boundary-layer cooling and especially sweat cooling. Further details on high temperature and fuels can be found in a companion paper (No. 52—F-F1B).[2]

Nonaviation Gas Turbines—Design

General Arrangement. Industrial turbine layout has not changed much in recent years; it varies from country to country. The two largest United States firms, General Electric and Westinghouse, retain their simple arrangement, clearly inspired by their aviation experience. The latest 5000-hp GE type is shown in Fig. 7 and described in reference (20). A single axial compressor, without intercooling, is followed by multiple can-type combustors; then comes the first turbine stage, which drives the compressor through a long shaft, and the second, independent but coaxial, power-turbine stage. Although the compressor has 14 stages and the pressure ratio is 5.5, only two turbine stages are used. Component efficiency is relatively low and the turbine-inlet temperature high, 1450 F; the thermal efficiency is modest.

The new Westinghouse industrial turbine, of similar power, follows the same pattern. Both machines use a regenerator; consequently, the multiple-can combustors, although placed directly after the compressor, are not fed from it but from the regenerator. This layout, which gives a longer machine and shorter combustors than necessary, is justified if the machines are meant to be used also without regeneration, in which case the arrangement becomes very simple and pressure losses are reduced to a minimum. However, for best results, the pressure ratio should be varied when the regenerator is dropped, and this cannot be done in the GE and Westinghouse machines. These are simple and light, and the high turbine-inlet temperature makes them particularly suitable for gas-pumping stations. The GE industrial turbines have been amazingly successful; very many units have been sold in the last year.

Swiss gas turbines follow their usual practice. Single well-proportioned separate combustors are used and, when particularly high efficiency is required, intercooling, regeneration, and often, reheat are used in multishaft arrangement. The component efficiency is high, the turbine-inlet temperature low, 1200 to 1300 F, the thermal efficiency very high; weight and bulk are correspondingly higher. British practice is intermediate between that of the United States and of Switzerland. Many interesting British industrial gas turbines are being tested or near completion. A very interesting layout is used in the English Electric locomotive unit shown in Fig. 8. The high-pressure part of the 20,000-kw English Electric machine follows a similar design. Turbine and compressor main casings are not split horizontally, as is usual in industrial machines, but are composed of a series of cylindrical or axisymmetrical pieces, joined together axially by means of spigoted flanges; each piece is relatively short and, of course, not split horizontally. Assembly and inspection become less easy, but the layout is justified in a machine subjected to high temperature and temperature variations. Axisymmetrical pieces expand evenly, while horizontally split casings can give rise to unequal expansion and high thermal stresses. The English Electric arrangement is also lighter and provides for turbine-rotor cooling by means of compressor air. Other British firms apparently are working along similar lines.

Small turbines, when a centrifugal compressor and an axial turbine are used, follow the aircraft layout with either a single can combustor or an annular combustion chamber, as in the

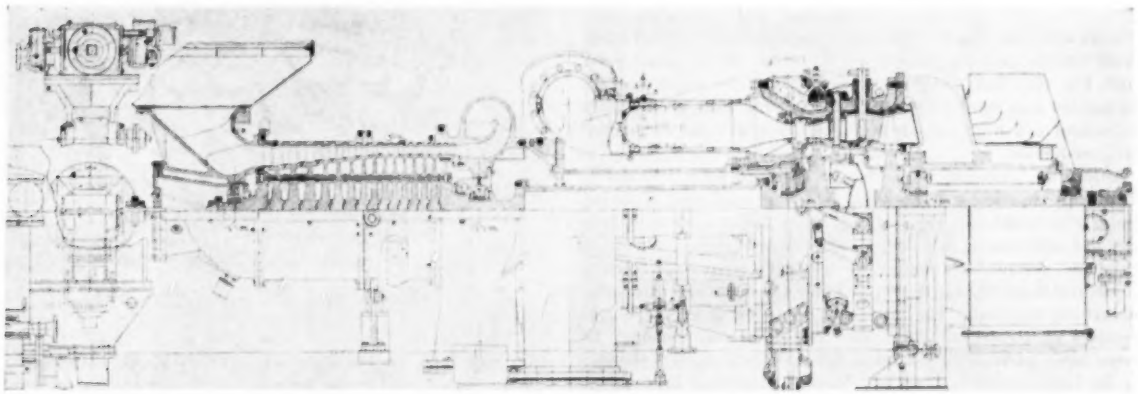

Fig. 7 General Electric 5000-Hp Gas Turbine

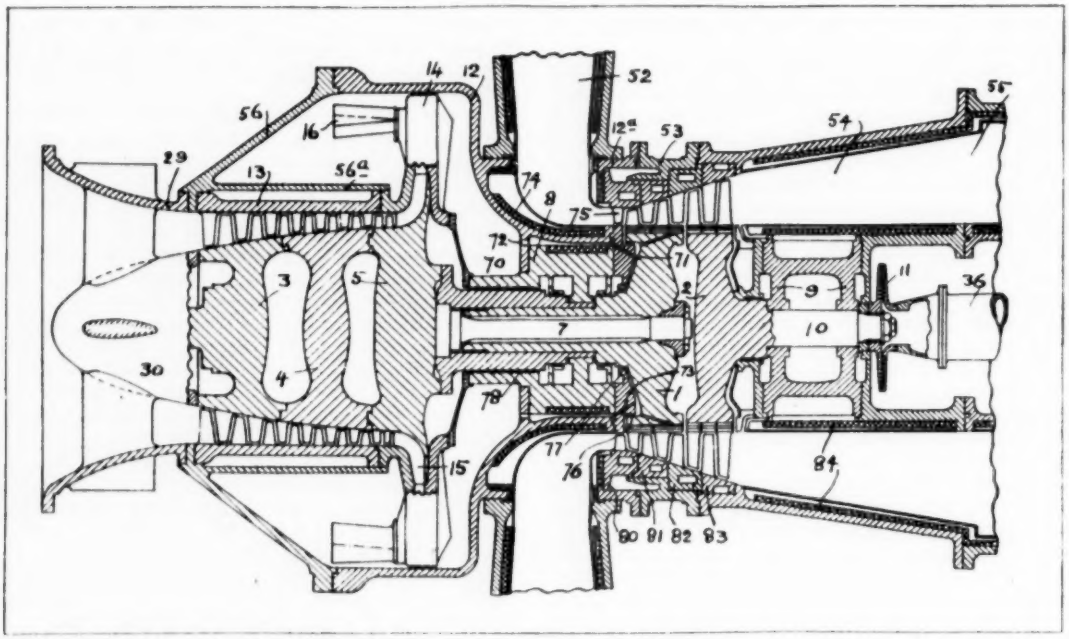

FIG. 8 ENGLISH ELECTRIC LOCOMOTIVE GAS TURBINE

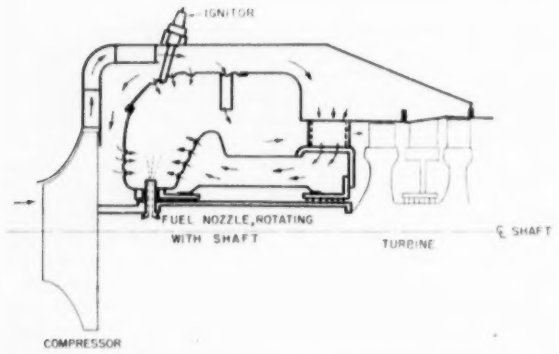

FIG. 9 SCHEMATIC ARRANGEMENT OF TURBOMECA COMBUSTOR

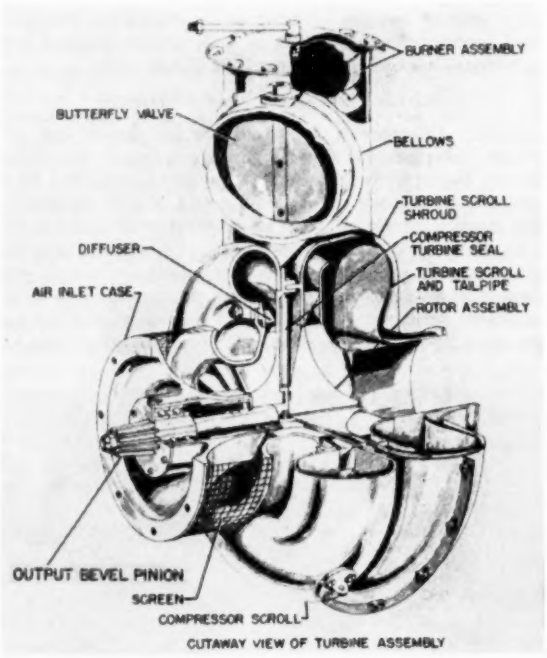

FIG. 10 CUTAWAY VIEW OF SOLAR 45-HP GAS TURBINE

Turbomeca unit, Fig. 9. The utmost simplicity is reached when both turbine and compressor are radial, as in the small Solar unit, Fig. 10. This 45-hp gas turbine drives a fire pump and can be carried and started by hand (21). It has proved extremely successful and arrangements are being made to build it in quantity production.

Silencing. Some of the early gas turbines were very noisy. However, experience has proved that if proper care is taken, noise is no problem in gas turbines. The major sources of noise are the compressor, combustion chambers, reduction gear, and exhaust. Usually the compressor gives the most objectionable noise, but it can be suppressed by lining the inlet duct with some absorbent material. The air casing discussed in reference (22) reduces effectively all noise from the other components. In some cases, particularly for automotive or marine units, a silencer is the best solution. The U. S. Naval Engineering Experiment Station at Annapolis has designed and tested a light and compact muffler which causes no loss in engine power or efficiency; the noise reduction for the operating crew is about 40 per cent. The gas turbine, unlike the internal-combustion engine, produces no noise due to engine vibration.

In existing gas-turbine installations, the noise problem is

not serious. The author can personally testify to the quietness of operation of the British MTB 5559 and also of the Rover turbine-powered motor launch. In large central-station plants, the noise level is substantially the same as in a steam plant. If a reduction gear is fitted between power turbine and generator, as in the 13,000-kw Brown Boveri set in Beznau, the predominant noise is caused by the gear. However, axial compressors give a very high-pitched hum or whistle which travels through the air intake. At Beznau, this compressor whistle, while completely inaudible inside the engine room, originally was quite noticeable outside the building, though the noise level was not disturbing. The installation of an air-cleaning chamber, made to prevent dust deposits on the compressor blades, reduced this whistle to the vanishing point. The General Electric 5000-hp unit in Fig. 7 will be fitted with a compressor-inlet silencer which is expected to reduce the compressor noise level from 100 to about 85 decibels (20).

Compressors. Large axial compressors show no particular new design features. Aerodynamic loadings, peripheral speeds, and Mach numbers are relatively low. In this way, high efficiency is obtained at the price of a greater number of stages. In large machines, self-induced vibration, already discussed (5), have caused a lot of trouble. At least one European firm is changing its compressor-blade design not in order to improve efficiency but to obtain a blade shape inherently less prone to vibration. Although small axial compressors are considered inefficient, good results have been obtained, as in the Solar 250-kw auxiliary power-generation set (23).

Centrifugal compressors are more than holding their own in industrial use, even for large machines. The most efficient type remains the well-known Oerlikon multiple-spiral compressor, applied to Oerlikon gas turbines and also to two B.T.H. units installed in Nairobi. This installation is experimental; ordinary B.T.H. gas turbines have axial compressors. An Oerlikon compressor is shown in Fig. 11. In its latest form, on the Bône turbine, this compressor has three stages in a single housing without intercooling; the pressure ratio is 3.45 the efficiency 85 per cent. A very interesting solution is the combination of a last centrifugal stage and several axial stages, as in the English Electric locomotive unit in Fig. 8. This design is similar to that of the Bristol *Proteus* turboprop, Fig. 1. Centrifugal compressors are particularly suitable for the high-pressure end of multiple compressors, because the air density is high and the flow areas better adapted. A very interesting example is given by the 12,500-kw Escher-Wyss closed cycle unit in St. Denis. The low- and medium-pressure compressors are axial, while the high pressure is given by four centrifugal stages in a single housing (9). Fig. 12 shows the medium- and high-pressure compressors open. They run on the same shaft. Other recent Escher-Wyss designs for smaller machines employ centrifugal compressors only.

A remarkable type of centrifugal compressor is the rotating-diffuser compressor, the theory of which is given in reference (24). In this type of machine, the diffuser rotates in the same direction as the rotor, either as a power turbine or freely. For a given peripheral speed of the compressor rotor, the more power is

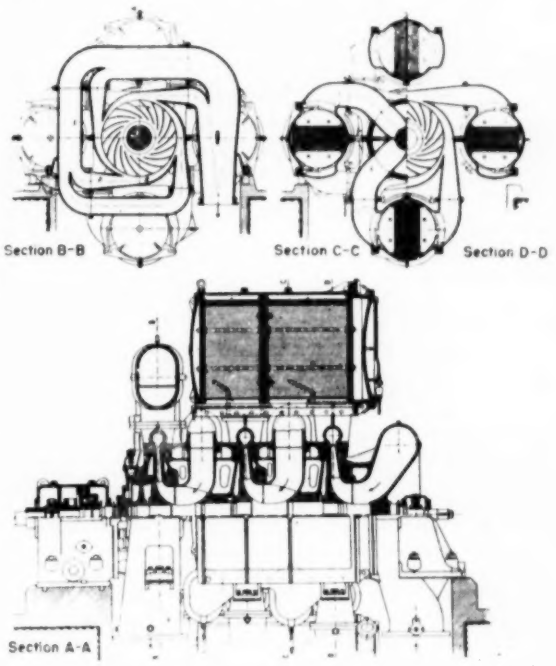

FIG. 11 OERLIKON RADIAL COMPRESSOR

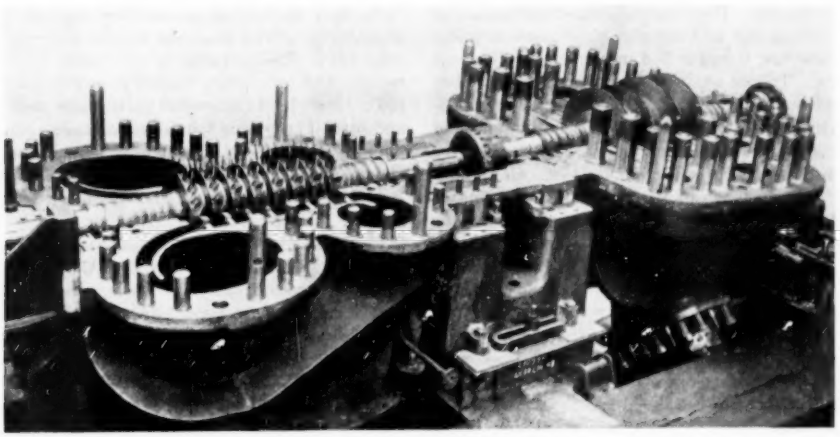

FIG. 12 ESCHER-WYSS 12,500-KW GAS TURBINE
(Middle and high-pressure compressors.)

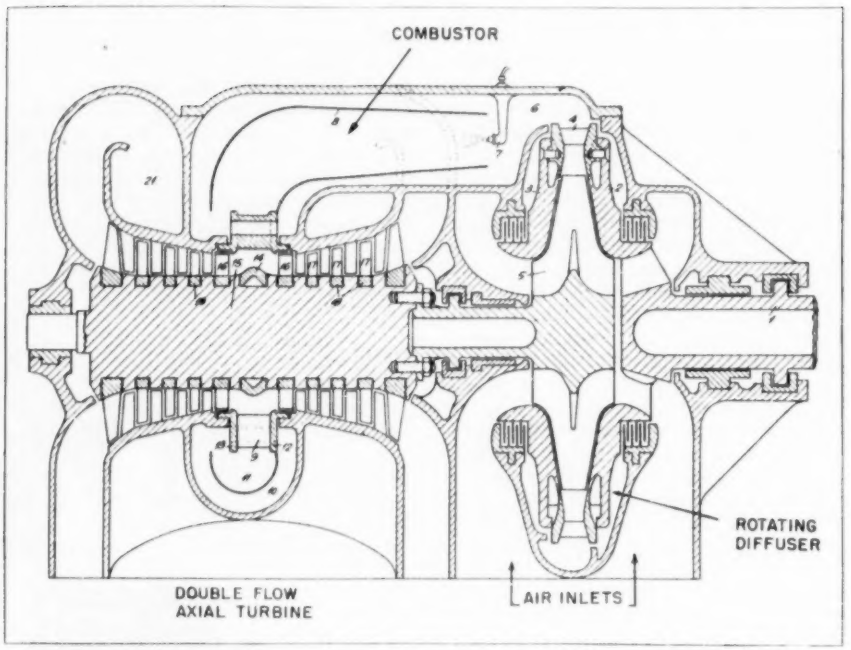

FIG. 13 HEPPNER GAS TURBINE WITH ROTARY-DIFFUSER COMPRESSOR, 1939 PATENT

taken out of the diffuser, the smaller the pressure ratio. Even if the air leaving the rotor has a supersonic speed, it strikes the diffuser blades with a subsonic relative velocity, thus reducing shock losses considerably; also, the air in the diffuser spends its kinetic energy producing mechanical work at high efficiency, instead of being decelerated into pressure at low efficiency. Consequently, even small machines give efficiencies of 85 per cent and over. This type of compressor, originally patented by Heppner (25), was reinvented and developed independently by the Swiss firm Saurer of Arbon several years later. A number of United States firms are working on this type of compressor with either free or power-developing diffusers.

Fig. 13 shows a gas turbine with rotating-diffuser compressor as described by Heppner in his original 1939 patent (25). Saurer has under test a small unit. The rotating-diffuser gas turbine is tricky to calculate and design and can give unpleasant surprises to the unwary. However, it might find interesting applications for traction engines. Torque characteristics are good as, when power shaft and diffuser slow down, the pressure ratio automatically increases. This type of gas turbine is naturally suited to the rotary regenerator, because the low pressure ratio given by the compressor reduces the regenerator leakage loss. Considerable improvements and changes can be expected in the rotary-diffuser machine as a consequence of the work now being done.

Turbines. There are few novelties in axial turbines, except the 5000-hp GE unit (20) in which the second (power) turbine-stage stator nozzles are mounted on pivots and can be swiveled, thus giving a variable-nozzle area; the arrangement can be clearly seen in Fig. 7. This device is complicated, the nozzle pivots are disposed radially, their actuation is not easy, and they must be water-cooled. However, there are considerable advantages, especially as regards regulation at variable speeds and loads. The part-load efficiency and flexibility are considerably improved.

Radial turbines recently have obtained wide diffusion in small units; they are simple and cheap to make, and remarkably efficient. For instance, the small 45-hp Solar radial turbine shown in Fig. 10 (21), gives 78 per cent efficiency, while the much larger 250-kw Solar axial turbine (23) gives 79 per cent. These small radial turbines have either the form of inverted centrifugal compressors, as in the Solar unit, or they have real turbine blades cast integrally with the rotor, as in the AiResearch turbine in Fig. 14 (26). In radial turbines, the gas flow is almost truly two-dimensional. There are only tangential and radial components and, even in high-efficiency machines, there is no need to twist the blades. Rotor and blades can be cast in one piece without using the lost-wax method. Turbines of this type have run at 1400 F and 1400 fps peripheral speed for several hundred hours (24).

Although no large radial turbines are known to have been built, they have great possibilities, even in the form of multi-stage turbines with rotor and several stages of blades cast integrally (24). Radial turbines can easily be fitted with pivoted swiveling stator nozzles, to give improved part-load performance (26). They lend themselves particularly well to turbine cooling, and several promising solutions have been proposed. Considerable project and development work is under way in several countries. The results should become apparent in the next few years. Radial turbines are thoroughly discussed in references (21, 24, 26, 27).

Combustors. Nothing new has occurred in large turbine combustors. As already seen, most American and some British turbines use can-type combustors, other British and all Swiss the single separate type. This is bulkier and requires more complicated pipe work, with corresponding pressure losses, but it gives very high combustion efficiency, up to 98 per cent. The Oerlikon turbine has a remarkably efficient single-type combustion chamber. The fuel is injected by a very small pressure differential (that between compressor exit and combustor) acting on a constant-level chamber. Pressure is varied under control of the governor, giving a particularly simple regulation. A very strong

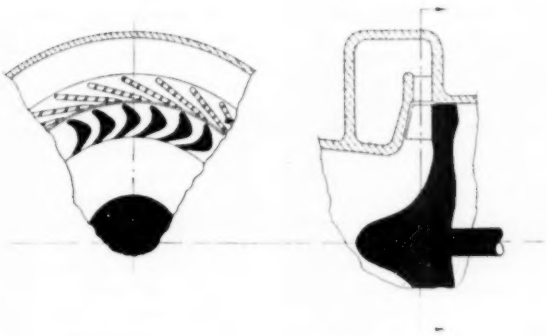

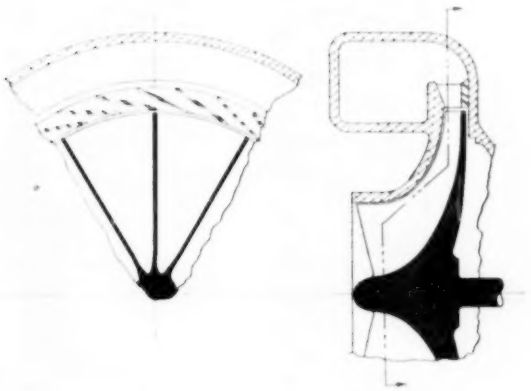

FIG. 14 RADIAL-INFLOW TURBINES

vortex action is employed in the flame tube and the heaviest fuel oils have been burned successfully.

In small turbines the most successful and original combustion chamber is the annular type employed on the Turbomeca units and shown in Fig. 9 (28). The fuel is introduced through the hollow compressor shaft so that the injectors rotate at very high speed and centrifugal force gives a powerful spray action. The air from the compressor is divided into three parts: one cools the turbine stator nozzles, being warmed in the process, then enters the flame chamber from the back with a strong swirl in the opposite direction to that of the fuel spray; the second part enters the flame chamber, also with an inverse swirl; the third part constitutes the secondary air and cools the outside of the combustion chamber, mixing afterward with the hot flame. Combustion efficiency is over 96 per cent, very high indeed for such a small machine, and remains remarkably constant under all load and density conditions. The great success of the Turbomeca machine is due undoubtedly to this remarkable combus-

tion chamber. Two United States firms, Continental and Fairchild, have acquired Turbomeca licenses.

Remarkable advances have been made recently in air heaters for closed-cycle gas turbines; the radiant-heat type, with combustion air at atmospheric pressure appears to prevail over the supercharged convection type, either crossflow or counterflow, previously used. Fig. 15 shows the latest Escher-Wyss radiant-heat air heater and Fig. 16 the supercharged crossflow type, both for the same size of plant, 12,500 kw (9). Tests of the St. Denis and Dundee plants will show if the air heater is a really practical device. On this depends, to a considerable extent, the future of the closed cycle. St. Denis has been running on and off for nearly a year; conclusive evidence is not expected before another year.

Other Components. The greatest improvement has taken place in regenerators. The rotary type discussed in references (12) and (18) shows great promise for traction engines where small weight and bulk are essential. The problem of a satisfactory seal is not yet quite solved, even for low pressure ratios under 4; there is little prospect of success for high pressure ratios. Figs. 17 and 18 show the latest NGTE experimental types (18).

The tubular heat exchanger also has made considerable progress, especially because of the introduction of extended-surface tubes (16). Some of the very large heat exchangers fitted to high-efficiency European plants have given rather disappointing results; the many bends in the pipes, due to the plant layout, caused unexpectedly high pressure losses, and thermal efficiency and power output were below the contract values. In the latest designs, smaller regenerator surfaces and a simpler pipe layout are used. In practice the difference in efficiency is not great. The tubular heat exchanger is at its best in closed-cycle machines. The high pressures give excellent transmission coefficients; the clean air inside and outside allows very small-diameter tubes to be used; the saving in weight and in bulk is considerable. In its latest designs, Escher-Wyss considers using extended-surface tubes of 2 mm (about $^1/_{12}$ in.) inner diameter, while the smallest practical tube diameter in open-cycle turbines is $^1/_2$ in.

Much should be said about governing devices and turbine regulation; there is little published material on this subject, except for the closed cycle, and many problems remain to be solved. With the increasing diffusion of gas turbines for power generation and with the need for automatic gas pipe-line pumping stations, regulation problems will come ever more to the fore. But this is a very specialized subject which cannot be discussed here.

Acknowledgment

The author is grateful to the editors of *Power* and especially to Mr. L. N. Rowley, for permission to publish the curves in Figs. 5 and 6, and for their unfailing help and advice.

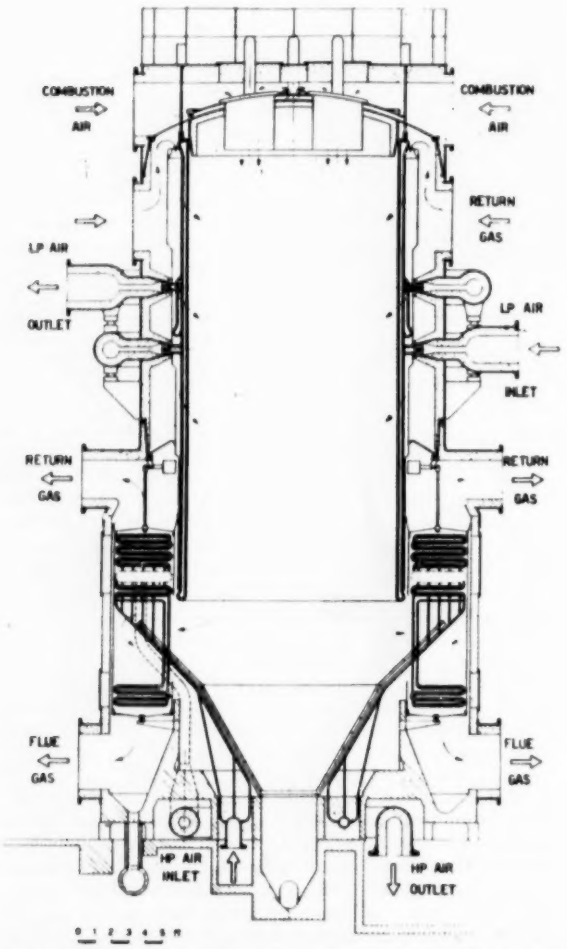

Fig. 15 Escher-Wyss Unsupercharged Radiant-Heat Air Heater

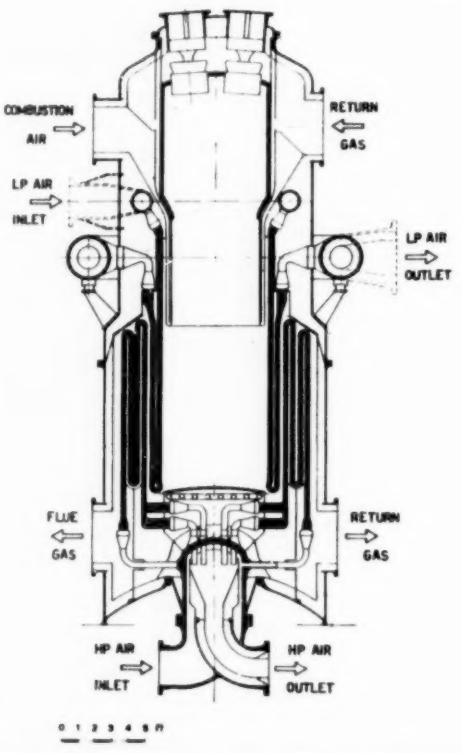

Fig. 16 Escher-Wyss Supercharged Crossflow Convection Air Heater

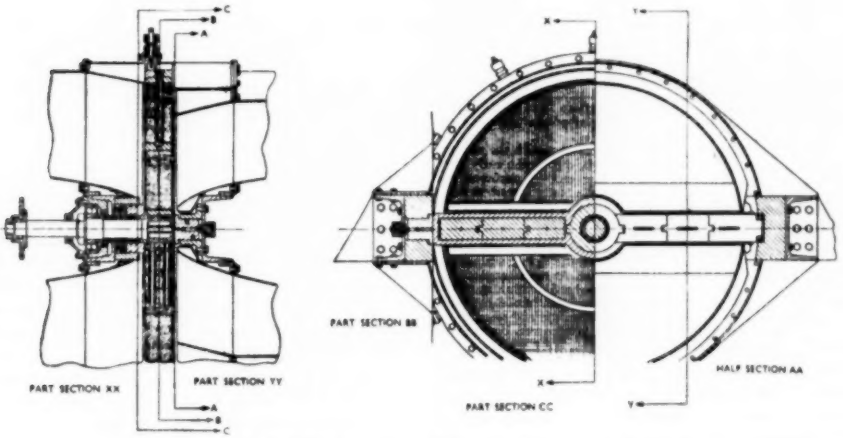

FIG. 17 NGTE EXPERIMENTAL ROTARY REGENERATOR NO. 3

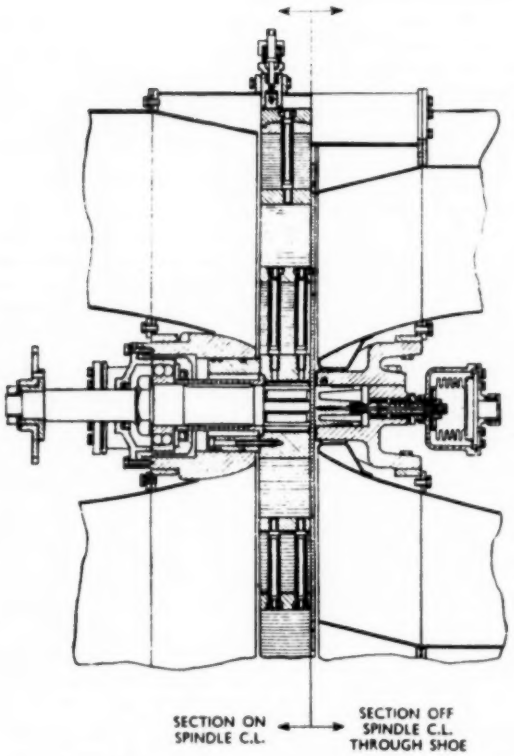

FIG. 18 NGTE EXPERIMENTAL ROTARY REGENERATOR NO. 3 AFTER MODIFICATION

BIBLIOGRAPHY

1 "The Theoretical Possibilities for Balanced Flow in Compressor and Turbine Design," by R. W. Pinnes, ASME Paper No. 50—A-66.

2 "Aerodynamic Problems in Axial Compressors for Aircraft Jet Engines," by R. S. Hall, Preprint 216 Institute of Aeronautical Sciences.

3 "Continental and American Axial Compressor Calculation Methods Compared," by P. F. Martinuzzi, ASME Trans., May, 1949.

4 "Aus Unserer Strömungsforschung," by J. Lalive d'Epinay, *Brown Boveri Mitteilungen*, October, 1949.

5 "Selbsterregte Schaufelschwingungen in Turbomaschinen," by Ch. Bellenot and J. Lalive d'Epinay, *Brown Boveri Mitteilungen*, October, 1950.

6 "Bemerkungen über den Rueckstossantrieb der Flugzeugen," by J. Ackeret, *Schweizerische Bauzeitung*, May 13, 1944.

7 Paper by O. A. Saunders, *Engineering*, October 6, 1950, p. 293.

8 "The Gas Turbine in Perspective," by Hayne Constant, Proceedings, of The Institution of Mechanical Engineers, London, England, vol. 163, 1950.

9 "Closed-Cycle Gas Turbines," by C. Keller, Trans. ASME, August, 1950.

10 "The Escher-Wyss Closed-Cycle Gas Turbine," by C. Keller, Trans. ASME, vol. 68, 1946, p. 791.

11 "Compte-Rendu des Essais de la Turbine Aérodynamique Escher-Wyss A-K," by H. Quiby, *Revue Polytechnique Suisse*, June 9 and 16, 1945.

12 "The Gas Turbine Manual," by R. J. Welsh and G. Waller, Temple Press, Ltd., London, England, 1951.

13 "Heat-Exchange Equipment for a 5000-Kw Gas Turbine-Generator," by G. R. Fusner, ASME Paper No. 49—A-84.

14 "Gas Turbine Regenerator Design Studies," by A. L. London and W. M. Kays, Technical Report No. 8, Navy Contract NG-ONR-251, Department of Mechanical Engineering, Stanford University.

15 "Optimum Design of Gas-Turbine Regenerators," by W. M. Rohsenow, T. R. Yoos, and J. F. Brady, ASME Paper No. 50-A-103.

16 "Design and Performance of an Extended Surface Regenerator for a Gas-Turbine Plant," by S. Holm and R. L. Lyerby, ASME Paper No. 51—A-106.

17 "Review of Optimum Design of Gas-Turbine Regenerators," by D. Aronson, ASME Paper No. 51—A-107.

18 "The Regenerative Heat-Exchanger for Gas Turbine Power Plants," by M. Cox and R. K. P. Stevens, Proceedings of The Institution of Mechanical Engineers, vol. 163, 1950.

19 "A 50,000-Kw Closed-Cycle Gas Turbine Plant Employing Helium," by E. Reshotko, Master's thesis, Cornell University, Ithaca, N. Y., June, 1950.

20 "Design Features of a 5,000-Hp Gas Turbine," by B. O. Buckland and D. C. Berkey, ASME Paper No. 51—A-113.

21 "Radial-Flow Compressors and Turbines for the Simple Small Gas Turbine," by L. R. Wosika, ASME Paper 52—S-13.

22 "Gas-Turbine Progress Report—Marine," by Capt. W. A. Dolan, Jr., USN, and Lieut. A. A. Hafer, USNR, ASME Paper No. 52—F-4A.

23 "Design Features of a 250-Kw Gas-Turbine Engine for Driving Shipboard Emergency Generator," by R. R. Peterson and P. G. Carlson, *Mechanical Engineering*, 1952.

24 "Multistage Radial Turbines," by P. F. Martinuzzi, Trans. ASME, July, 1952.

25 Patents 536,238 and 548,180 to F. A. Heppner, Britain.

26 "Single-Stage Radial Turbines for Gaseous Substances With High Rotative and Low Specific Speeds," by W. von der Nuell, Trans. ASME, May, 1952.

27 "A Contribution to the Problem of Designing Radial Turbomachines," by O. E. Balje, Trans. ASME, May, 1952.

28 "Une Turbine à Gas entièrement Française de Petite et Moyenne Puissance," by Ch. Brull, *Journal SIA*, September, 1949.

Gas-Turbine Progress Report—Automotive

By F. L. SCHWARTZ,[1] ANN ARBOR, MICH.

ALMOST any gas turbine with a separate power turbine of less than 500 hp might be classed as suitable or adaptable for propulsion of a road vehicle. Therefore this part of the report will include an account of the development of small gas turbines—those under 500 hp with special attention being given to the problem of applications to turbines for automobiles, trucks, and buses. A fairly large number of companies have developed small gas turbines to a point where they are available and competitive for specific applications or have small gas turbines on test. Only three notable applications for vehicles have appeared to date. The Rover turbine has actually been installed in an automobile; the Boeing turbine has been successfully used to propel a large truck, while the Laffly turbine-powered bus was exhibited at the 1951 Paris Motor Show. Small gas turbines also have been used to drive pumps for pipe-line service, auxiliaries in aircraft and aboard ship, for driving a fire pump, propel a small launch, propel lightweight airplanes and helicopters, and to furnish a source of compressed air for starting large turbines or compressed air for other purposes.

Are Small Gas Turbines Practicable?

Varied opinions have appeared in the literature as to the feasibility of using gas turbines in cars and trucks. The most important drawback to the use of gas turbines in automobiles is its poor specific fuel consumption, especially at part load as compared with reciprocating engines. Steady progress in improving the fuel consumption of reciprocating engines is to be expected and it is this progress which must be met by continued progress in developing small gas turbines. One fact appears certain, that any real competition offered by present gas turbines will spur development of reciprocating engines much as the advent of jet propulsion for aircraft gave an added incentive to develop propellers which could handle larger powers more efficiently at higher flight speeds. Gas turbines in aircraft have been able to compete with reciprocating engines largely because of superior performance at high-altitude, high-flight speed, and because they could be built in larger power output. These advantages disappear in propulsion of road vehicles. The large aircraft gas turbine has been improved to a point where its specific fuel consumption is comparable to that of large reciprocating engines. The scaling down of a gas turbine to a small size does not carry with it similar performance. In general, the smaller the size the more difficult it is to provide high efficiency.

It should be noted that the trend in automobile and truck engines is toward larger engines. In 1952 there are nine models of automotive engines having 150–190 hp. With the trend toward larger engines it becomes easier for the gas turbine to match performance. This is particularly true in using gas turbines in trucks and buses and especially in those applications where near full power can be used almost continuously. Several small gas turbines using the simple cycle are available having a specific fuel consumption of 0.9 lb per hphr and, with continued development and the use of regeneration, this consumption may be reduced to 0.7 lb per hphr. When coupled with the outstanding advantages inherent in gas turbines, this expected fuel consumption begins to be competitive.

The major reason for a decreased efficiency accompanying the scaled-down sizes of gas turbines is the Reynolds number. The thermodynamic cycle efficiency depends on factors such as pressure ratio, temperature, and regenerator effectiveness, not size. For an efficient cycle the density, gas velocity, and viscosity are about the same in a small turbine as in a large turbine so that the Reynolds number decreases with diameter, making it more difficult to control boundary layers, and the size of the boundary layer becomes a higher percentage of the flow area. This effect reduces the component efficiency of compressors and turbines. It appears that the component efficiencies of small turbines is about 5 percentage points less than those of large turbines, those over 1000 hp. For example, peak compressor efficiencies of 86 per cent are now common in the larger sizes whereas several small compressors have been designed and used having efficiencies above 80 per cent. Turbine efficiencies of several per cent higher than compressor efficiencies are to be expected.

Advantages and Disadvantages of the Automotive-Type Gas Turbine

The advantages offered by small gas turbines of the automotive type with the free turbine are as follows:

1 Smooth operation, free of vibration.

2 Operation over a wide range of fuels without requiring especially refined fuels such as high-octane or high-cetane fuels.

3 Lubrication system may be simplified and lubrication consumption as low as 1 per cent of that of a Diesel engine.

4 Electric ignition required only for starting.

5 The turbine produces its maximum torque at standstill.

6 The gas turbine inherently incorporates a torque converter and a gas fluid drive in the driving member.

7 A transmission with possibly as low as only one or two speed changes and a reverse is needed and used only occasionally.

8 Elimination of a clutch.

9 Light weight; as much as 3000 lb can be saved on weight of engine and transmission over a large truck Diesel.

10 Small installation space required, especially if regeneration is not resorted to.

[1] Professor of Mechanical Engineering, University of Michigan. Mem. ASME.

Contributed by the Gas Turbine Power Division and presented at the Fall Meeting, Chicago, Ill., September 8–11, 1952, of The American Society of Mechanical Engineers.

Notes: This is paper No. 52—F-2 of a Progress Report which the Executive Committee of the Gas Turbine Power Division authorized at its 1951 Annual Committee Meeting. The series includes the following: "Introduction," by R. Tom Sawyer, paper No. 52—F-1A; "Materials, Cooling, and Fuels," by A. A. Hafer, paper No. 52—F-1B; "Cycle Components," by P. F. Martinuzzi, paper No. 52—F-1C; "Railroads," by K. A. Browne, J. I. Yellott, and P. R. Broadley, paper No. 52—F-3; "Marine," by W. A. Dolan, Jr., and A. A. Hafer, paper No. 52—F-4A; "Merchant Vessels," by W. A. Dolan, Jr., and A. A. Hafer, paper No. 52—F-4B; "Naval Vessels," by W. A. Dolan, Jr., and A. A. Hafer, paper No. 52—F-4C; "Stationary Electric Generation," by Lee Schneitter, paper No. 52—F-5; "Industrial," by L. N. Rowley and B. G. A. Skrotzki, paper No. 52—F-6; "Aviation," by I. H. Driggs and O. E. Lancaster, paper No. 52—F-7.

Statements and opinions advanced in papers are to be understood as individual expressions of their authors and not those of the Society.

11 Few parts; only 10 per cent as many as the average reciprocating engine.
12 Easily and quickly maintained.
13 Good cold-weather starting characteristics.
14 Maximum fuel economy occurs at maximum output.
15 No external cooling system required.
16 Clean exhaust.

The following disadvantages are inherent in the gas turbine as applied to vehicle propulsion:

1 Large ducts required.
2 High specific fuel consumption, especially at part load.
3 High rotative speeds requiring high-quality bearings and a high gear reduction.
4 Certain parts are made of high-cost alloys, costs depending upon temperatures and ratings.
5 Service life is limited if maximum temperature and therefore high thermodynamic cycle efficiency is used for a high percentage of the time the turbine is in operation, unless the turbine is especially built for long life and controlled within definite limits.

Cost, noise, and exhaust are questions which remain to be answered in many cases. Cost figures of turbines now being built are high but they include development costs and involve small production. With further development of materials and high productions, the cost eventually may be reduced to that of a reciprocating engine. This is possibly to be expected especially when the number of parts required in the two prime movers are compared. Many of the parts of a reciprocating engine use high-cost alloys too and are heavier. The noise of a compressor always has been feared to be excessive but actual applications installed do not appear to present this as a serious problem. During acceleration the Rover turbine exhibited excessive noise but at constant speed the sound was reported to be not more severe than that of large city traffic. No special effort was made to reduce the noise. The noise produced by the Boeing turbine in a Kenworth truck is less than that of the Diesel engine it replaces. The sound is of a character which reduces in intensity very rapidly a few feet from the turbine. The temperature of exhaust gases is high as in a reciprocating engine without the benefit of long exhaust pipes and mufflers which effectively reduce the temperature of the expelled gas. When the Rover turbine was operated on its first official run it was reported that one could hold his hand over the exhaust at idle with no detrimental results, but at speed the procedure would be comparable to the hot exhaust of a racing car.

Some Characteristics of Small Gas Turbines

Small gas turbines such as might be used for driving an electric generator have a specific weight as low as 0.6 lb per hp. Those with a separate power turbine as used in vehicles have a specific weight between 1 and 2 lb per hp not allowing for extended duct work. The space required is also small unless long large ducts on the inlet and outlet are added. A gas turbine requires about five times as much air through the machine as a comparable reciprocating engine. This requires large ducts where used. Also, the gas-turbine efficiency is susceptible to pressure losses in ducts and passages between elements so that large ducts are desirable if used at all. However, if one considers the air required for cooling a piston engine along with that aspirated, the two types of engines use somewhere near the same air consumption. By placing a turbine in the rear or judiciously choosing its location in a vehicle, little duct work would be required.

The gas turbine saves additional weight and space by not needing an external coolant, extended fins and fan, or a radiator with its pump and plumbing. If a regenerator is added to improve fuel consumption, much of the advantage of small size and weight vanishes. Regenerators are bulky, expensive, heavy, and it is anticipated would add to maintenance difficulties. The number of moving parts is small but the materials are either stainless steel or other alloys which are high in cost and at present not easy to fabricate. There is practically no cast iron in a gas turbine. With continued improvement in fabrication and materials it may be possible to produce turbine and compressor wheels in large numbers at a very low cost. Bearings of small turbines are nearly always ball or roller bearings running at speeds as high as 40,000 rpm. Some very small turbines have used speeds as high as 60,000 rpm.

Gas-turbine efficiencies and power output are susceptible to inlet-air conditions as shown in Fig. 1. At low temperatures the

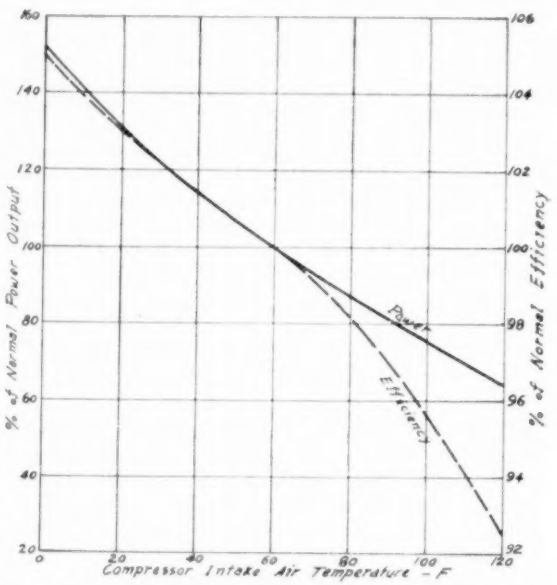

Fig. 1 Power and Efficiency Varied With Compressor Intake Air Temperature

gain in power and efficiency is greater than that in reciprocating engines whereas at above normal ambient conditions the deleterious effect of high ambient temperature is greater than for piston engines. This is due largely to the fact that the percentage of the turbine work required to drive the compressor is as much as twice the percentage of expansion work used to supply compression work of a piston engine. Cold-starting of a gas turbine is relatively easy so long as the low temperature does not affect the fuel properties or fuel-injection system seriously.

A gas turbine for vehicles requires two controls in addition to a fuel throttle, one to protect against overspeed and one to prevent excessive temperature in the turbine. The overspeed control is relatively simple but the measurement of either combustion temperature or exhaust temperature requires more than a simple thermocouple.

Types of Compressors

Compressors which may be used are of three types, each with a distinct advantage over the others. Centrifugal compressors are capable of developing high pressure ratio per stage, as much as 4.6 with good efficiency. They can be cast or machined from an aluminum forging at low cost. When cast they can be double-

shrouded. Double-shrouding adds a small increase to the efficiency. Axial compressors require many stages but are well adapted to multistaging whereas compounding of centrifugal compressors adds numerous turns and passages. Axial compressors are usually several per cent more efficient than centrifugal compressors. Rotary compressors of the Roots or Lysholm type have the advantage of maintaining good efficiency over a large range of air flows. The principal disadvantage is the difficulty in manufacturing the lobes accurately. The rotary type has not been used in small turbines. The axial type has appeared in only a few installations.

Nearly all small turbines use a single centrifugal compressor. Thus the cycle efficiency is limited by pressure ratios between 2.5 and 4.4. To obtain better fuel consumption while retaining the simple cycle, higher pressure ratios and temperatures must be resorted to. Higher pressure ratios require either a compound centrifugal compressor or an axial compressor, either of which adds to the size and cost, and compounding a centrifugal compressor will lower somewhat the compressor efficiency. When high pressure ratios are used in an axial compressor for small air flow, the last stages require very short blades with increased flow losses.

The maximum temperature used in small gas turbines has been 1600 F. Most of the small turbines use gas temperatures 1350 to 1600 F. Increasing the temperature as might be expected to be possible with the development of cooled blades or the use of new alloys, does not improve the specific fuel consumption very fast when the pressure ratio is low and the component efficiencies are high.

Fig. 2 shows the relationship between efficiency, pressure ratio, and temperature for component efficiencies of 80 per cent. As

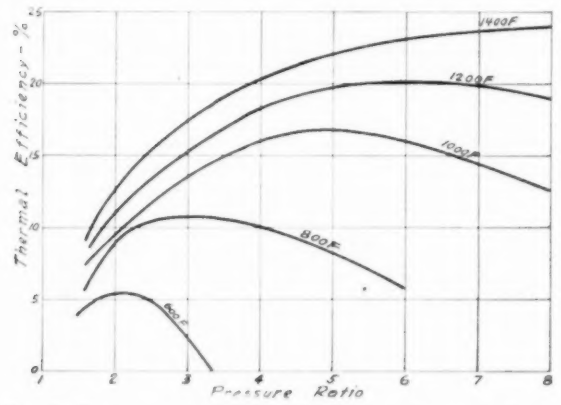

Fig. 2 Relationship Between Efficiency, Pressure Ratio, and Temperature

the pressure ratio is increased, higher gas temperatures become more effective in increasing efficiency. Several of the small gas turbines which have been built allow for incorporating a heat exchanger at a later date. At higher pressures and temperatures a heat exchanger is not as desirable as at low pressure ratio. If heat exchangers should be used generally the low-pressure-ratio range of a single-stage centrifugal compressor probably will remain common practice.

The piston engine has one inherent advantage which cannot be matched by a gas turbine. At idle or low power requirements the engine uses air at a very low rate, even less than an amount proportional to the speed because of the throttling. The speed can be reduced to a very low value expressed as a percentage of maximum speed. Under these conditions, although the specific fuel consumption may be high, the fuel consumption per hour is very low. The gas-producer unit of the gas turbine must remain at relatively high speed at all times except idle, for if the speed is reduced excessively, the component efficiencies and pressure ratio become prohibitively low and the turbine ceases to function. The compressor turbine runs at 50 to 80 per cent of maximum during normal operation of a vehicle. Thus the fuel consumption at low power is not proportionately less than at full power.

Torque Characteristic

The most inviting feature of a gas turbine for propelling vehicles is its excellent torque characteristic. The arrangement of components with a split turbine using a simple cycle without regeneration is shown in Fig. 4. The first turbine stage drives the compressor through a direct drive with the compressor and turbine turning at the same speed. The second turbine stage is connec-

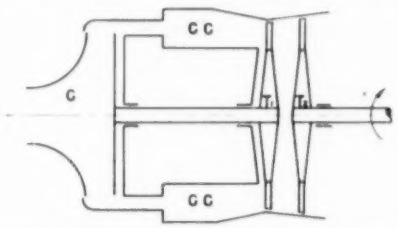

C = compressor
CC = combustor
T_1 = compressor turbine
T_2 = power turbine exchanger

Fig. 3 Arrangement of Simple-Cycle Components With a Split Turbine

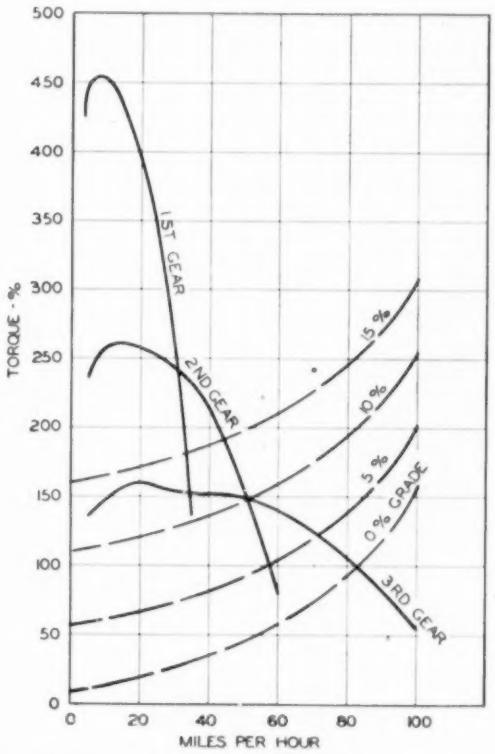

Fig. 4 Typical Curve of Torque, Speed, and Grade for a Passenger Car With a Conventional Three-Speed Transmission

ted directly to the rear axle through a gearbox which has a high reduction ratio and may or may not incorporate one change in gear ratio and a reverse gear.

Fig. 5 shows a typical curve of torque, speed, and grade for a passenger car with a conventional three-speed transmission. A study of Fig. 6 will indicate the suitability of the gas turbine to vehicle propulsion. Turbines have characteristically parabolic horsepower curves. Efficiency curves are approximately the same shape. With control of load by gas-producer speed variation, the grade curves fall near the loci of maximum efficiency and horsepower. If the design point is selected at the peak of a given horsepower curve, say, one corresponding to 1500 F, the torque multiplication is 2:1.

By designing the turbine for a blade-speed/jet velocity ratio somewhat above the ratio of maximum efficiency, the grade curves will fall reasonably close to the peaks of the horsepower curves over a range of grade curves, and the torque multiplication becomes greater than 2:1. Shifting the design point beyond the peak of the horsepower curve causes a small increase in fuel consumption on steep grades and at moderate speeds. Also, a slightly larger turbine is required. An extra gear may be needed only for moving the vehicle when stalled in mud or snow or exceptionally steep grades. Calculated fuel consumption is shown in Fig. 6 for a turbine having a compressor of 3.5:1 pressure ratio and an isentropic efficiency of 80 per cent with a turbine having an isentropic efficiency of 85 per cent. On the first official run of the Rover car its fuel consumption was 7 miles per Imperial gallon at 85 mph.

Table 1 presents data of small gas turbines built to date.

Automotive Production Models

The AiResearch Manufacturing Company has three models of gas turbines in production and several others under development. The GTC43/44 is a bleed-off type of machine used to supply compressed air for auxiliary power. The GTP70 is a shaft-power version of the GTC43/44. These turbines have a compressor flow of 1.9 lb per sec and a pressure ratio of 3:1. Maximum gas temperature ranges between 1500 and 1600 F. The shaft machine develops better than 100 hp and weighs 100 lb without an enclosure. The compressors of the two machines are identical and have two centrifugal stages with impellers of the backward-curved type. Two stages with low pressure ratio per stage were used to develop high efficiency and permit a wide range of air flow without promoting surge. This latter factor is important in air-bleed turbines. Maximum bleed is about 35 per cent of total compressor flow. The air may be bled directly after the compressor or after the combustor if hot gas is required, or air may be bled from both points and mixed to give an intermediate temperature. Two can-type combustors are utilized and their output is fed into a single-stage radial-flow turbine.

The model GTC20 having a single-stage compressor and about one half the air-bleed rating of the GTC43/44 has been developed and tested but is not in production.

The GTM 125 is a gas-turbine motor without a compressor. Compressed air must be furnished from an outside source for its operation, as when used with a bleed turbine. This machine utilizes a radial-flow turbine having variable-area nozzles and a single combustor. It has a power output rating of 124 to 150 hp and weighs 80 lb.

AiResearch gas-turbine designs have been characterized by the use of centrifugal compressors with backward-curved blades, radial inflow turbines, and completely enclosed power packages. Although the radial-flow turbine has some advantages with respect to broad operating ranges, the primary justification for its existence is in respect to manufacturing costs. The efficiencies

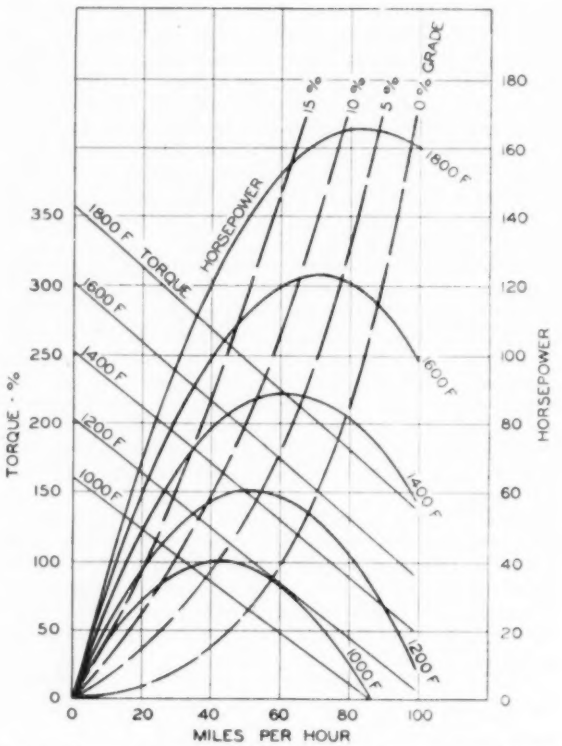

Fig. 5 Typical Curve of Torque, Speed, Power, and Grade (in Relation to Hp) for a Gas-Turbine Vehicle

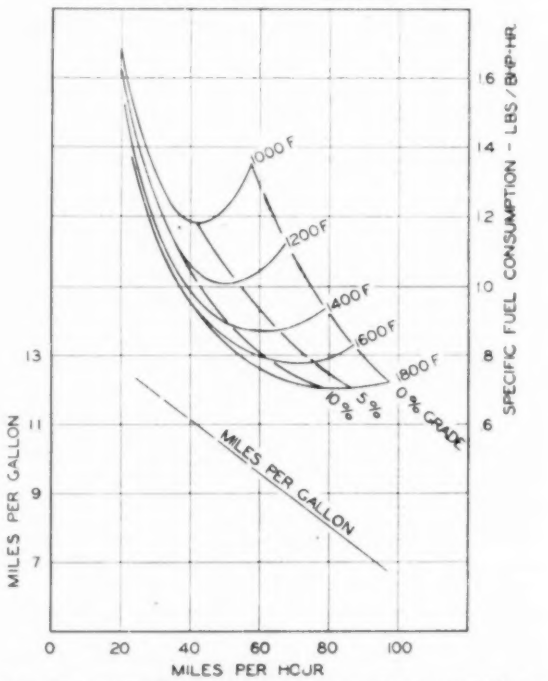

Fig. 6 Calculated Fuel Consumption for a Compressor, With 3.5 to 1 Ratio and 80 Per Cent Isentropic Efficiency
(Turbine isentropic efficiency is 85 per cent. No heat exchanger used.)

TABLE 1 SMALL GAS-TURBINE DATA

Country	Manufacturer	Model	Type	Rating, hp	Continuous SFC	PR	Weight	Application	State of development	Maximum temp, deg F
U. S.	AiResearch Mfg. Company	GTC43/44	One-shaft bleed	65 air hp		3.0	88	Compressed air	In production	1600
		GTC 85	One-shaft bleed	100 air hp		3.4	100	Compressed air	In development	1600
		GTP 70	One-shaft	100 hp		3.0	109	Shaft power	In production	1600
		GTM 125	Gas-turbine motor	125–150			80	Accessory drive	In production	1600
U. S.	Boeing Airplane Company	500	Jet	180 lb thrust	1.2 lb/lbh/hr	3.2	120	Aircraft	In production	1550
	Boeing Airplane Company	502	Free turbine	175	1.2 lb/hp hr	3.6	230	Truck (marine, etc.)	In production	1550
U. S.	Continental		All Turbomeca units except the Oredon below							
U. S.	Fairchild (Stratos)	Oredon	Experimental	300				Vehicle	In development	1500
U. S.	General Motors Corp.	M 80	Free turbine	140				Vehicle	Completed	1500
U. S.	Solar Aircraft Company	Jupiter T 400	Twin shaft, geared	200 kw	1.00 lb/hp hr	4.2		Generator aux.	Superseded by T520	1500
		Jupiter T520-J1	One shaft	280–340 kw		4.8		Generator drive (USN)	In development	1520
		Jupiter T522-J1	Free turbine	420–520 hp (80 F)		4.8		Generator (USN)	In development	1520
		Mars T 41	One shaft	25 kw (17 DC & 8AC)	2.09	4.8		Marine, etc. (USN)	In development	1520
		Mars T 45	One shaft	47 hp (80 F)	2.22 lb/hp hr	2.24	165	Generator drive (USAF	In production	1150
		Mars T 55	Improved T 45			2.44		Water pump (USN)	In production	1200
England	Centrax Power Units		Open cycle	160 (2.15 lb/sec)	.7 lb/hp hr	5.8		Vehicle		
England	Rover Company	Old	Free turbine	200				Vehicle	Tested in car	
England	Rover Company	New	Free turbine	150–185			300	Auto & marine	Developed	1600
Scotland	Cowal Engineering Co.	New	Free turbine	33				Vehicle		
France	Turbomeca	Oredon	Shaft turbine	140	1.02 lb/hp hr			Shaft power	In production	1425
		Pimedon	Air generator	1.3 lb/sec at 50 psia		3.5	160	Aircraft acc. drive	In production	1425
		Palouste	Air generator	2.3 lb/sec at 50 psia		4.0	170	Helicopter acc. drive	In production	1425
		Turbine Motrice (Auto)	Free turbine	275–300 (4.4 lb/sec)	0.98 lb/hp hr	4.0	225		In development	1508
		Artouste I	Shaft turbine	250–280	1.02 lb/hp hr	4.0	285	Helicopter acc. drive	In production	1425
		Artouste II	Shaft turbine	330–400	1.0 lb/hp hr	4.0	300	Helicopter acc. drive	In development	1425
		Pimene	Jet	175–242 lb thrust	1.06 lb/lb	4.0	118	Jet propulsion	In production	1425
		Palas	Jet	270–330 lb thrust	1.15 lb/lb	4.0	137	Guided missiles-Target plane	In production	1425
		Marbore I	Jet	530–650 lb						
		Marbore II	Jet	710–880 lb	1.12 lb/lb	4.0	275	Training plane	In production	1425
		Aspin I	Ducted fan	360–450 lb thrust			275	Light airplanes		1425
		Aspin II	Ducted fan	660–790 lb thrust	0.566 lb/lb	4.1	300	Light airplanes	In production	1425
France	Laffly		Free turbine	180–200	0.80 lb/hp hr		230	Truck and bus	In production	1472
Italy	Breda		Free turbine	350		3.35		Experimental	In construction	1256

FIG. 7 AIRESEARCH RADIAL-INFLOW TURBINE AND COMBUSTOR USED AS AN INDEPENDENT MOTOR AS ITS AIR SUPPLY COMES FROM ANOTHER TURBINE UNIT

achieved are at least as good as those for axial-flow turbines of similar capacity and the quality-control problems consistent with high efficiency are minimized. There are twelve blades per wheel, bent only slightly at the exit end.

Variable nozzle area always has been intriguing to gas-turbine designers. The radial turbine lends itself more readily to variable-area turbine nozzles than does the axial type. Only the GTM 125 model has variable-area nozzles. The radial turbine is capable of utilizing efficiently a large pressure ratio. A pressure ratio across the turbine larger than the centrifugal compressor ratio is possible. It is equivalent of $1^1/_2$ to 2 axial stages. The 90-deg inward-flow radial turbine as used in the AiResearch turbines has been found to be superior to cantilever-blade types from the stress and manufacturing standpoints.

The Boeing Airplane Company gas turbine Model 502 has a free turbine wheel beyond a gas-producing section. It has been used experimentally to drive a 70,000-lb truck more than 15,000 miles in 550 hr. Other applications include units for driving a small launch, a helicopter, an electric generator, and one for pipeline pumping. The fuel consumption in the truck application is about three times that for an equivalent Diesel engine. The fuel used is kerosene or Diesel fuel.

Model 502 consists of a single-stage centrifugal compressor with two outlets, two straight-through can-type burners, a primary turbine which drives the compressor and accessories, and a second-stage power turbine driving the output shaft through a 9:1 reduction gear. The turbine develops 175 hp at 60 F or 160 hp at 80 F ambient temperature and weighs 230 lb with accessories and reduction gear. The primary turbine and compressor have a speed of 36,000 rpm, the power turbine a maximum speed of 26,000 rpm, and the output shaft a maximum speed of 3000 rpm. The centrifugal compressor has a diameter of 8.5 in. and an isentropic efficiency of 76 per cent maximum.

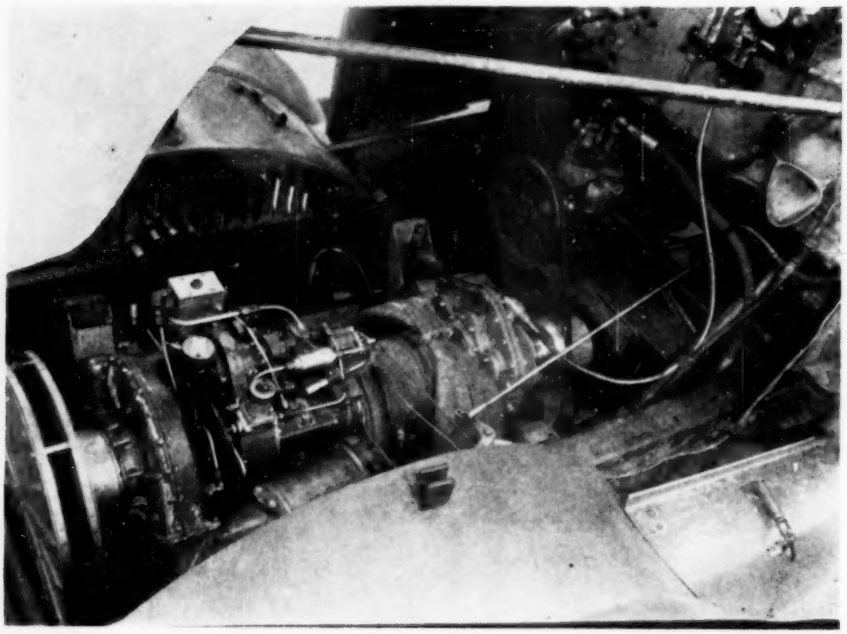

FIG. 8 BOEING GAS-TURBINE UNIT IN TRUCK

The turbine blades designed for free vortex are impulse at the root and 50 per cent reaction at the tip. The isentropic efficiency of the turbine wheels is 85 per cent total to total pressure. The primary turbine is 7 in. diam and the secondary turbine 9 in. The air flow at rated power is 3.6 lb per sec, the temperature 1550 F, and the specific fuel consumption about 1 lb per hphr.

Rated power is developed in 15 sec from a cold start. It can accelerate from idle speed of 14,000 rpm to full speed in 5 sec.

VARIED APPLICATIONS

The General Motors Corporation has a 300-hp gas turbine under development. It will have a free-power turbine and be of conventional design. It is hoped that valuable experience in analyzing production methods, evaluating materials and costs will be obtained in the development, rather than outstanding performance.

The Solar Model 80 gas turbine comprises two separate gas-turbine power sections mounted in a single assembly with a common reduction gear connecting them and driving an alternator. One turbine developing 105 hp at sea level is sufficient to drive the alternator at sea level but the two units with a combined output of 90 hp at 40,000 ft are used at altitude. Only one of these was built, this for experimental purposes.

The Solar Model T45 turbine was designed to replace a piston engine driving a centrifugal water pump for fire fighting aboard ship. Simplicity, size, weight, and ease of starting were primary considerations. Fuel consumption was of secondary consideration. The unique feature of the unit is a centrifugal compressor developing a pressure ratio of 2.44 set back to back with a radial-inflow turbine wheel. Both units are overhung at one end of a single shaft mounted in two bearings beyond the compressor. To conserve space an elbow-type combustion chamber joins the compressor and turbine casings. Only 0.5 in. separates the compressor and turbine at the hub. At rated power of 47 hp the air flow is 2.35 lb per sec, the compressor efficiency is 74.5 per cent, the turbine efficiency 78 per cent, the turbine-inlet temperature is 1142 F, and the specific fuel consumption 2.22 lb per hphr. The compressor is 6.97 in. diam, the turbine rotor 7.42 in., and the speed 40,300 rpm. Speed reduction between turbine and pump is accomplished through a single-reduction spiral bevel gear and pinion providing a right-angle drive.

A means is provided for cooling the exhaust gas with water supplied by the pump sprayed into the gas. The Model T45 turbine is the first turbine to be started by hand. Starting is accomplished through a hand crank and a chain and sprocket connecting to the pump shaft which has a maximum speed of 4428 rpm. An over-all speed ratio of 81 to 1 is accomplished between the hand-crank shaft and the turbine shaft. When the turbine speed after starting exceeds the speed derived from the hand crank an overrunning clutch disconnects the starting device. The turbine is self-sustaining after the pump speed reaches 1200 rpm.

The T55 is the production version of the T45. Only two T45 units have been built while several T55 are now building, with more to come.

The T-400 was one experimental generator auxiliary unit actually placed on board a ship. The T-520 is similar to the T-400, being somewhat larger and a production model. The T-522 also has a 3-stage turbine the same as the T-520 except the last stage is a free-running power turbine which makes it suitable for use in the automotive field—the only Solar unit actually suitable for this purpose.

DEVELOPMENTS IN ENGLAND

The Centrax Power Units of Acton, England, exhibited the first gas turbine intended for vehicle propulsion. In 1948 a Centrax gas turbine was exhibited at the British Industries Fair. The turbine was designed to develop 160 hp. It had eight stages of axial compression followed by a centrifugal stage developing an over-all pressure ratio of 5.8:1. A three-stage turbine drives the compressor at 40,000 rpm. A single-stage free turbine delivers power at 35,000 rpm maximum speed. The drive shaft was

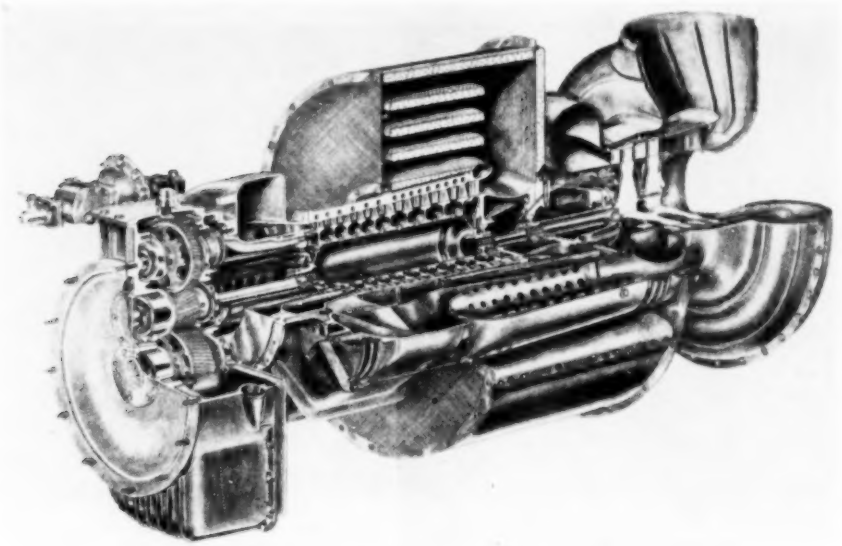

FIG. 9 CUTAWAY VIEW OF SOLAR JUPITER T-400 GAS-TURBINE UNIT

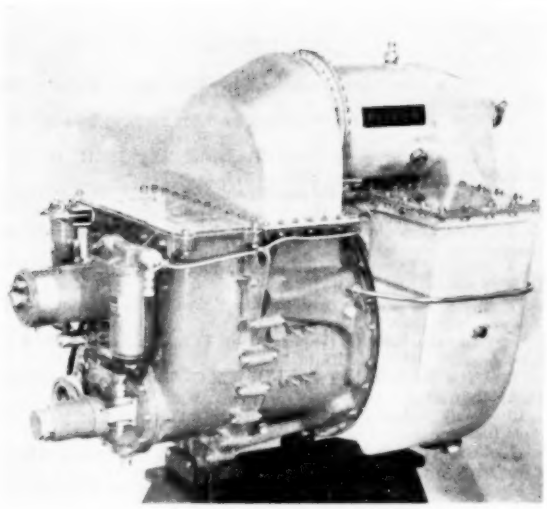

FIG. 10 ROVER 150-HP GAS TURBINE

designed for 5000 rpm. The unit weighed 300–350 lb, had a maximum diameter of 17 in., and was expected to have a specific fuel consumption of 0.7 lb per hr. The maximum gas temperature was 1525 F. No further announcement of the progress of this turbine has been published.

On March 8, 1950, the Royal Automobile Club conducted the first official tests of a gas turbine in an automobile. The Rover Company of Birmingham installed a turbine of its own design in a standard Rover car adapted for rear-end installation.

Almost no technical details of the turbine are available other than that the turbine was mounted ahead of the rear axle and consisted of a centrifugal compressor, dual combustion chambers, a single-stage compressor turbine, and a free-power turbine coupled through a reduction gear having a reverse to the rear axle. Kerosene fuel was used. The turbine was started with an electric starter with a push button. The time taken to start the turbine and accelerate it to idling speed was 13.2 sec. The car moved forward in another 3.4 sec. The only control used by the operator was a throttle pedal and brake pedal. The maximum speed in the test was 85 mph but this was not the maximum possible. At 85 mph the compressor-turbine speed was 35,000 rpm. From standstill the car accelerated to 60 mph in 40 sec. The specific fuel consumption was twice that of a comparable piston engine. Seven miles per gallon was observed. The turbine idles at 7000 rpm and ignites at 4000 rpm. The maximum speed was 40,000 rpm and the turbine was capable of developing 200 hp. A new design under development is a smaller turbine intended to be installed in the front end of a car.

FRENCH CONTRIBUTIONS

The Turbomeca Company of Bordes, France, has developed a wide line of gas turbines with some unique features. Many of the components in the various units are interchangeable. A novel high-swirl annular combustor of very short axial length which permits close coupling of the turbine and compressor elements, resulting in design simplifications, is used in these turbines. The only fuel nozzle is a rotating disk of about 4 in. diam with several radial holes of small diameter mounted on the turbine shaft. The only fuel pump required is a small transfer pump. The compressors have high efficiency for such a small size, approximately 10 in. OD, and are machined from solid aluminum forgings. Likewise, the turbine wheels and blades are machined from a single piece of Nimonic 80, achieving high efficiency and capable of withstanding high stress.

The Oredon is a single-shaft turbine developing 140 hp. The Pimedon is an air-bleed generator producing 1.3 lb per sec of bleed air at 50 psia. The compressor pressure ratio is 3.5/1. The weight of the unit is 160 lb. The Palouste is a larger air-bleed generator capable of supplying 2.3 lb per sec of bleed air at 50 psia. It has a compressor pressure ratio of 4.0:1 and the unit weighs 170 lb. This unit has been considered for supplying air through the rotors of a helicopter to ram-type combustors at the wing tip for helicopter propulsion. The Artouste is a larger shaft-power turbine than the Oredon. It

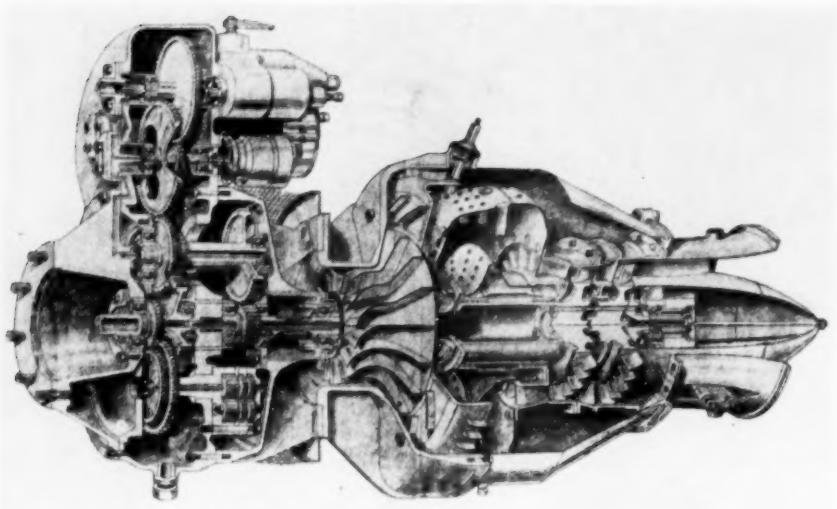

FIG. 11 TURBOMECA'S ARTOUSTE I SHOWING REDUCTION GEAR AND COMPLETE TURBINE UNIT

develops 250 hp under continuous conditions with a specific fuel consumption of 1 lb hphr. The Artouste weighs 200 lb and uses the same compressor as the Palouste. The Pimene, Palas, and Marbore are jet units developed for small airplanes, target planes, guided missiles, and so on. They have a compressor pressure ratio of 4.0/1 and produce a thrust of 200 to 880 lb with specific fuel consumptions of about 1.1 lb/lb thrust. The Aspin is a gas turbine driving a ducted fan of low pressure ratio. Two sizes have been developed for airplanes to fly at 250 to 350 mph. The static specific fuel consumption is about 0.6 lb/lb thrust. The Stratos Division of Fairchild Aviation and Engine Company has been licensed to sell and manufacture the Oredon whereas the Continental Aviation and Engineering Company has been licensed to manufacture and sell all models except the Oredon.

Turbomeca is now developing the turbine Motrice, an automotive turbine using the Artouste unit, plus a power turbine which has a maximum speed of 27,000 rpm and a gear reduction of 8 to 1. The compressor speed is 35,000 rpm. As the power turbine is located some distance in back of the gas producer, the entire unit is 3 ft 4 in. long × 1 ft 4 in. wide and high. A second model has been studied consisting of the Palouste feeding air into an automotive power turbine. This is known as the air-generator system.

The 1951 Paris Motor Show exhibited a Laffly gas-turbine-driven bus and truck chassis. Another is on road test which has one two-stage centrifugal compressor delivering air into two combustors located crosswise, making a compact unit. The combustors lead into a dual-stage split turbine, one stage driving the compressor, the other the gearbox. The compressor speed is 30,000 rpm while the maximum speed of the power turbine is 24,000 rpm with a gear reduction of 12 to 1.

The Stabilimento Ernesto Breda, Sesto S. Giovanni (Milan, Italy) has a 350-hp gas turbine with maximum temperature of 680 C (1256 F), 10,000 rpm for 6-stage axial compressor, 1-stage centrifugal, compression ratio 3.35; two-stage compressor driving turbine, one-stage power turbine, free and coaxial. This is in construction and component test and is purely an experimental turbine.

Small gas turbines have been successful in an area of applications where small size, lightweight, and superior performance have been more important than specific fuel consumption. As improvements continue to develop and first costs decrease, a wider field of application will follow.

REFERENCES

1 "More About Gas Turbines," by G. G. Smith, *Autocar*, May 14, 1948, p. 456.

2 "Gas Turbines for Automobiles," by F. L. Schwartz, *Auto Industry*, June 1, 1948, p. 30.

3 "Gas Turbines for Road Transport," by R. H. H. Barr, *G. & O. Power*, November, 1948, p. 371.

4 "The Gas Turbine for Road Transport," by J. Hodge, *G. & O. Power*, February, 1949, p. 48.

5 "Gas Turbines for Road Vehicles," by H. H. Barr, *Product Engineering*, March, 1949.

6 "Boeing Develops Small Gas Turbine Power Plant," by S. D. Hage, *SAE Journal*, April, 1949, p. 40.

7 "Gas Turbines in Automobiles," by W. A. Turunen, *SAE Journal*, July, 1949, pp. 18–23.

8 "Gas Turbines for Vehicles," by F. L. Schwartz, *Auto Engineer*, January, 1950, pp. 13–18.

9 "The Rover Gas Turbine Motor Car," *Engineering*, March 17, 1950, p. 305.

10 "Will the Low-Priced Car Be Turbine Powered?" by H. C. Hill, *Auto Industry*, July, 1950, p. 41.

11 "Gas Turbine Auxiliary Power Plants," by P. H. Wilkinson, *Aero Digest*, March, 1950, p. 30.

12 "Facts About the Rover Gas Turbine Car," by W. F. Bradley, *Auto Industry*, April 1, 1950, p. 40.

13 "Road Trials of First Gas Turbine Car," *Oil Engine*, April, 1950, p. 426.

14 "Rover's Turbocar, Operation and Design," by G. G. Smith, *SAE Journal*, July, 1950.

15 "More Payload for Same GVW Possible With Truck Turbines," by W. M. Brown, *SAE Journal*, November, 1950, p. 52.

16 "Gas Turbine Propulsion for Ground Vehicles," by W. M. Brown, Transactions of the SAE, January, 1951, p. 81.

17 "Progress Review 15—Gas Turbines," by D. H. Mallinson, *Journal of the Institute of Fuel*, March, 1951, p. 67.

18 "The Gas Turbine," Auto Corp., March, 1951, p. 103.

19 "Brenngasturbinen für Kraftfahrzenge," by W. Neuschaefer, *Zeitschrift des Vereines deutscher Ingenieure*, May 11, 1951, p. 400.

20 "Latest Facts About Turbine Driven Trucks," by R. C. Norris, *SAE Journal*, October, 1951, p. 24.

21 "AiResearch Extends Gas Turbine Field," by G. L. Christian, *Aviation Week*, January 21, 1952, p. 48.

22 "Gas Turbine Truck Part I," by H. C. Hill, *SAE Journal*, January, 1952, p. 29.

23 "Gas Turbine Truck Part II," by H. C. Hill, *SAE Journal*, February, 1952, p. 39.

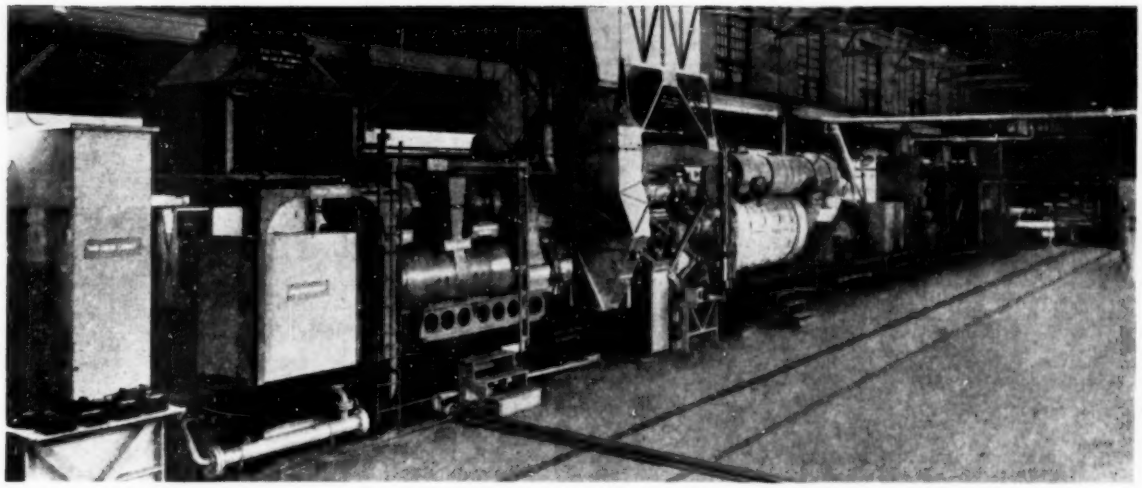

FIG. 1 LOCOMOTIVE DEVELOPMENT COMMITTEE'S TURBINE TEST INSTALLATION AT DUNKIRK

Gas-Turbine Progress Report—Railroad

BY K. A. BROWNE,[1] J. I. YELLOTT,[2] AND P. R. BROADLEY[3]

INTRODUCTION

BROWN Boveri brought out the first gas-turbine locomotive in 1941. This experimental unit has been in service since that time burning heavy oil, whenever and wherever circumstances permitted. The first gas-turbine locomotive which should be called a commercial product also was delivered by Brown Boveri to the Great Western Railway in England on March 10, 1950.

The second gas-turbine locomotive was that built by General Electric Company and first operated on November 14, 1948. This was definitely an experimental type but it proved to be so successful in extensive tests on western lines that an order was placed in December, 1950, by the Union Pacific Railroad for ten similar locomotives. The first unit was double-ended but all of its operation was in single-ended service and so the subsequent locomotives used the second cab space for oil storage and other purposes. The first of these locomotives was delivered in January, 1952, and is thus the first commercially built gas-turbine locomotive in the United States.

The Westinghouse Electric Company has built a 4000-hp, twin-turbine locomotive which first entered service in May, 1950. Since that time it has seen extensive operation on eastern and western lines.

The Metropolitan Vickers 3000-hp locomotive No. 18,100 was the first British-built gas-turbine locomotive, and went into service in 1951, also on the Great Western Railway.

The Ministry of Fuel and Power in England has been active in developing the coal-burning gas turbine for locomotive service. In 1951 this agency placed an order for a 1600-hp exhaust-heated coal-burning gas turbine for locomotive service, with C. A. Parsons and Company, Limited. In this country the Locomotive Development Committee has been at work since 1945, and is currently testing a 4250 Allis-Chalmers open-cycle turbine, direct-fired with pulverized coal, Fig. 1.

This report does not cover various designs or examples of turbines which are not expected to be placed in locomotive service, neither does it cover the thousands of Diesel locomotives now in service which depend upon gas-turbine superchargers. Table 1 shows the relative features of each of the locomotives listed in the foregoing with particular emphasis on the turbine unit. Several salient points are of interest.

1 All of these locomotives use the open cycle, with no water required for the gas turbine.

2 Only the Parsons, and Ruston and Hornsby units use free-power turbines.

[1] Research Consultant, The President's Office, The Chesapeake & Ohio Railway Company, Cleveland, Ohio. Mem. ASME.

[2] Director of Research, Locomotive Development Committee, Dunkirk, N. Y. Mem. ASME.

[3] Assistant Director of Research, Locomotive Development Committee, Dunkirk, N. Y. Mem. ASME.

Contributed by the Gas Turbine Power Division and presented at the Fall Meeting, Chicago, Ill., September 8–11, 1952, of THE AMERICAN SOCIETY OF MECHANICAL ENGINEERS.

NOTES: This is paper No. 52—F-3 of a Progress Report which the Executive Committee of the Gas Turbine Power Division authorized at its 1951 Annual Committee Meeting. The series includes the following: "Introduction," by R. Tom Sawyer, paper No. 52—F-1A "Materials, Cooling, and Fuels," by A. A. Hafer, paper No. 52—F-1B; "Cycle Components," by P. F. Martinuzzi, paper No. 52—F-1C; "Automotive," by Frank L. Schwartz, paper No. 52—F-2; "Marine," by W. A. Dolan, Jr., and A. A. Hafer, paper No. 52—F-4A; "Merchant Vessels," by W. A. Dolan, Jr., and A. A. Hafer, paper No. 52—F-4B; "Naval Vessels," by W. A. Dolan, Jr., and A. A. Hafer, paper No. 52—F-4C; "Stationary Electric Generation," by Lee Schneitter, paper No. 52—F-5; "Industrial," by L. N. Rowley and B. G. A. Skrotzki, paper No. 52—F-6; "Aviation," by I. H. Driggs and O. E. Lancaster, paper No. 52—F-7.

Statements and opinions advanced in this paper are to be understood as the individual expressions of the authors and not those of the Society.

TABLE 1 GAS-TURBINE LOCOMOTIVE DATA

Turbine builder	Brown Boveri	Brown Boveri	Met. Vickers	Ruston & Hornsby
Locomotive builder	Swiss Loco. Works	Swiss Loco. Works	Met. Vickers	Loco proposed
Electrical builder	Brown Boveri	Brown Boveri	Met. Vickets	
Customer	Swiss Federal Rys.	British Rys.	British Rys.	
Order placed	March, 1939	Oct., 1946	July 1947	
Date first operated	August, 1941	Oct., 1949	Feb. 1952	
Mf'r. rating-loco., hp	2200	2500	3000	2140
No. turbines per loco	1	1	1	2
No. gen. per turbine	1	1	3	1
Generator, rpm	750	800	1600	
Hp per 2000 lb wt loco	21.7	18.8	20.7	
Wheel arrangement	1A-B-A1	A1A-A1A	C - C	
Total weight, lb	203,000	266,890	290,000	
Weight on drivers, lb	142,000	177,920	290,000	
Length over-all, ft-in	53 - 10	63	67	
Wheel base, total, ft - in	41 - 10	50 - 1	53	
Wheel Base, rigid, ft - in	11 - 1	11 - 10	15	
Width, ft - in	9 - 6	9 - 3	9	
Height, ft - in	13 - 11	13 - 4	12 - 10	
Service	Mixed	Passenger	Pass & freight	
Max. mph	70	90	90	
Cont. tractive effort, lb	14,000	12,400	30,000	
Mph at cont. tractive effort, lb.	47.5	64	30	
Unit Data				
Rating to main gen. for traction, hp	2150	2500	2850	1070
Max. total rating, hp	2200	2500	3000	1070
Cycle	Open	Open	Open	Open
Cycle arrangement	One shaft	One shaft	One shaft	Split turbine
Top cycle temp, deg F	1110	1110	1300	1340
Pressure ratio	4.0 to 1	4.0 to 1	5.25 to 1	4.15 to 1
Weight turbine unit			9400 net 17,600 gross	22,250
Weight lb per hp (no. gen)	18.0 about	18.0 about	3.15 net 9.0 gross	20.8
Length,[c] ft - in	31[c]	33 - 3[c]	16	15 - 3
width, ft - in	6 - 4	6 - 3	4 - 9	8 - 7
Height, ft - in	9 - 2	9 - 6	6 - 3-	10
Starting method	Diesel gen	Diesel gen	Battery, 96 v	Battery
Air flow, lb/sec			50	22.46
Spec. power, hp/lb/sec			60	50.5
SFC, lb/hp/hr (full load)	0.83	0.84	0.725	0.598
η percent (HHV) (full load)	16	15.8	18	21.5
HHV (of fuel used), Btu/lb	18,900	18,900	19,500	19,760
Combustors				
Type	Large	Large	Flame tube	Metal walled
Number	1	1	6	1
Fuel	800 Redwood sec.	800 Redwood sec	Gas oil	Distillate or residual
Regenerator				
Type	Cross flow	Cross flow	None	Plate
Number	1	1		2 Sections
Effectiveness, per cent	50	42		78
Compressor				
Type	Axial	Axial	Axial	Axial, 50 per cent reac.
Number stages	21	20	15	13
Rpm	5200	5300	7000	11,400
Adiabatic efficiency, per cent	86	86	-	82.5
Discharge psia	57	57	77	61
Main Turbine				
Type	Reaction	Reaction	Axial flow	Axial
No. stages	6	7	5	2
Rpm	5200	5300	7000	11,400
Adiabatic efficiency, per cent	86	86		
Type cooling			Natural	Air on disk faces
Power Turbine (if separate)				
Type				Axial, free
No. stages				2
Rpm				6000
Adiabatic efficiency, per cent				85
Type cooling				Air on disk faces

[a] With exhaust heater.
[b] 23.3 per cent maximum at 3120 hp. All above data are test results burning coal based on 80 F inlet air.
[c] With generator.

TABLE 1 (*Continued*)

C.A. Parsons & Co.	Allis-Chalmers	General Electric	General Electric	Westinghouse Elec.
N. British Loco Co.	Proposed-Alco	General Electric	General Electric	Westinghouse Elec.
None	A-C and GE	General Electric	General Electric	Westinghouse Elec.
Ministry Fuel & Power	Loco. Dev. Com.	General Electric	Union Pacific	Westinghouse Elec.
1951	Turbine Unit now	Pilot model	Dec. 1950	1948
-	Under test	Nov. 14, 1948	Jan. 1952, 1st. of 4	1949
1600	4250	4500	4500	4000
1	1	1	1	2
Mech drive	4	4	4	2
2-speed gear box	2000	1650	1650	1150
13.8	12.1	18	17.3	15.68
C - C	C - C + B - 2	B-B-B-B	B-B-B-B	B-B-B-B
262,000	644,000	500,000	520,000	510,000
262,000	514,000	500,000	520,000	510,000
68 - 6	132 - 4	83 - 8	83 - 7	77 - 10
about 53 - 9	118 - 8	68 - 3	68 - 1	62 - 9
about 13 - 0	15 - 6	9 - 4	9 - 4	9
8 - 8	10 - 0	10 - 7	10 - 7	10 - 1
13	14 - 8	15 - 4	15 - 5	15 - 1
Mixed	Freight	Freight	Freight	Passenger
50 - 1st; 75 - 2nd	69.0	69.3	65	100
45,000; 30,000	100,000	77,800	105,000	52,800
at 0	13.6	18.2	12.9	23
	3900	4500	4500	2000
1800	4250	4870	4870	2200
Open[a]	Open	Open	Open	Open
Split turbine	One shaft	One shaft	One shaft	One shaft
1300 to turbine	1300	1290	1290	1350
	5.9 to 1	5.83 to 1	5.83 to 1	4.5 to 1
		26,000	26,000	9,760
		5.35	5.35	4.4
about 30	39 - 10	18 - 8	18 - 8	28 - 11[c]
about 8	6 - 9	7 - 1	7 - 1	3 - 6
about 12	9 - 10	7 - 2	7 - 2	5 - 10
Diesel eng.	Diesel gen.	Diesel gen.	Diesel gen.	Battery
	79.6 (4121 hp)	90.7	90.7	33.0
	52.0 (4121 hp)	53.7	53.7	60.6
	0.93 (4121 hp)	0.84	0.84	0.78
	21[b] (4121 hp)	16	16	16.9
	13,300	18,500	18,500	18,500
Very large	Metal-film cooled	Metallic	Metallic	Can
1	2	8	6	12
Coal	Coal	Bunker C	Bunker C	Distillate or residual
(Heater)				
Cross flow	Cross flow	None	None	None
1 , 1560 F max.	1			
	52.65			
eac. Axial	Axial	Axial	Axial	Axial
	21	15	15	23
	5700	6900	6900	8750
	82.8	-	-	82.5
	86.7	82.8	82.8	86.1
Axial	Axial-reaction	Vortex	Vortex	Reaction
	6	2	2	8
	5700	6900	6900	8750
	87.7			84
	-	Air wheel space	Air wheel space	Air
Axial				
8000				

3 All but the Parsons unit use electric transmission.

4 All have axial-flow turbines and compressors.

5 All of these locomotive turbines follow closely designs which are currently in use as stationary power plants.

Owing to the part-load characteristics of the gas turbine, all of these locomotives are designed for road service, to handle trains in through service. In the early days of the Diesel locomotive the first dozen units were put into switching service because of their economy when operating at light loads, as well as at full load. It is noted that, in each case, the new type of power is first placed in that class of service which utilizes its most economical range.

The emphasis on the coal-burning gas turbine for locomotive service should be noted. One experimental project is under way in Canada at McGill University, and at least five projects of various kinds are in progress in England, including Parsons, English Electric, Metropolitan Vickers, John Brown, and Ruston and Hornsby. These developments are applicable to stationary as well as to locomotive installations. There is also intensive development work now going on to solve the problems involved in the burning of residual oils. The Brown Boveri locomotives appear to be the only units which can handle this type of fuel without difficulty at this time because of their relatively low turbine-inlet temperature, 1110 F. These units obtain satisfactory thermal efficiency through the use of regenerators and high-efficiency turbines and compressors.

Brown Boveri Units

Today, after eleven years, the first gas-turbine locomotive is still in service on European railways. The design of this locomotive was so fundamentally correct that no major changes were made when Brown Boveri built the second unit which is now operating in England, Fig. 2. Both locomotives have a single-shaft turbine with one axial compressor supplying an axial turbine through a regenerator and a single large combustor. This combustor is especially designed for burning a selected heavy fuel oil and the regenerator aids in improving the plant efficiency despite the relatively low turbine-inlet temperature. This temperature was kept low in the first unit because high-temperature alloys were not available. In the second unit a similarly low temperature was used in order to prevent the severe attack of vanadium upon the turbine blades which is encountered at high temperatures.

Space limitations must be considered in adapting a conventional regenerator to a locomotive gas turbine. With British clearances, 2500 hp is close to the upper limit for the use of such a regenerator. In the United States, the Allis-Chalmers 4250-hp locomotive turbine, now under tests by the Locomotive Development Committee, uses a 52 per cent effective regenerator, and can fit within most United States railway clearances. The usefulness of the regenerator in locomotive service is questioned by some designers, and actual operating experiences will tell whether or not they will be used in the future.

Metropolitan Vickers Electric Company, Limited

This is the first British-built gas-turbine locomotive and it possesses a number of unique features. As shown in Fig. 3, it is the only gas-turbine locomotive which uses six traction motors on two six-wheel trucks. It is the most powerful locomotive now in use in England and it has the lowest weight ratio in pounds per horsepower of any self-propelled locomotive in main-line service today. This demonstrates in practical fashion one of the points which has been emphasized by advocates of the gas turbine—this type of power plant allows more horsepower to be put into a single cab than does the Diesel-electric system. This is also the first locomotive to be powered 100 per cent by a gas turbine. All others now in use or under construction use a small Diesel auxiliary set for hostling and starting.

The Metropolitan-Vickers locomotive was designed to handle 18 passenger cars with a total trailing load of 730 tons, and a maximum grade $^1/_{36}$ on the line between London and Plymouth. The locomotive also is capable of handling the lightweight freight trains normally found in England. It should be pointed out that two of these 2500-hp locomotives placed in multiple would have plenty of power to handle either fast freights or high-speed passenger trains in the United States.

C. A. Parsons and Company, Limited

In December, 1945, C. A. Parsons and Company, Ltd., put into operation at its Heaton Works the first British industrial gas turbine. This 500-hp unit subsequently has been in experimental operation burning many kinds of fuel, including heavy oil and pulverized coal. The locomotive now being designed by Parsons, Fig. 4, proposes to use the exhaust-heated cycle in which the compressed air is heated in a large heat exchanger, and the fuel is burned in the turbine exhaust. It has the advantage of giving clean air to the turbine, but it puts a heavy load upon the heat exchanger. Parsons proposes to use pulverized coal in its combustion chamber, and to use an air cleaner before the hot side of the heat exchanger. The temperature at the inlet to the heat exchanger will be 1560 F, and the heater itself will be built to withstand at least 1600 F, to take care of possible temperature fluctuations.

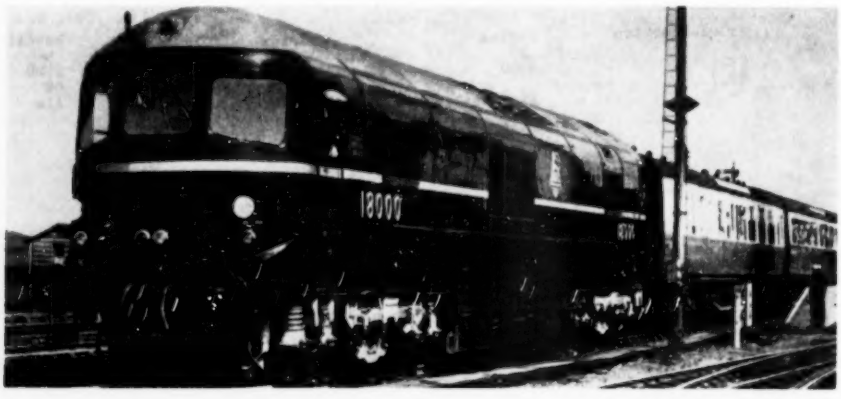

Fig. 2 Brown Boveri 2500-Hp Locomotive in Service in England

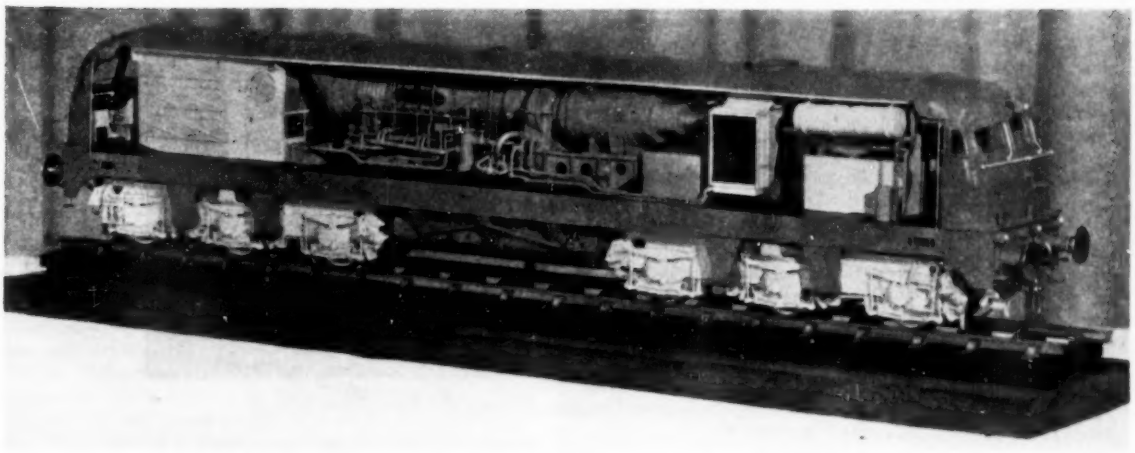

FIG. 3 METROPOLITAN VICKERS 3000-HP LOCOMOTIVE—THE FIRST BRITISH-BUILT UNIT

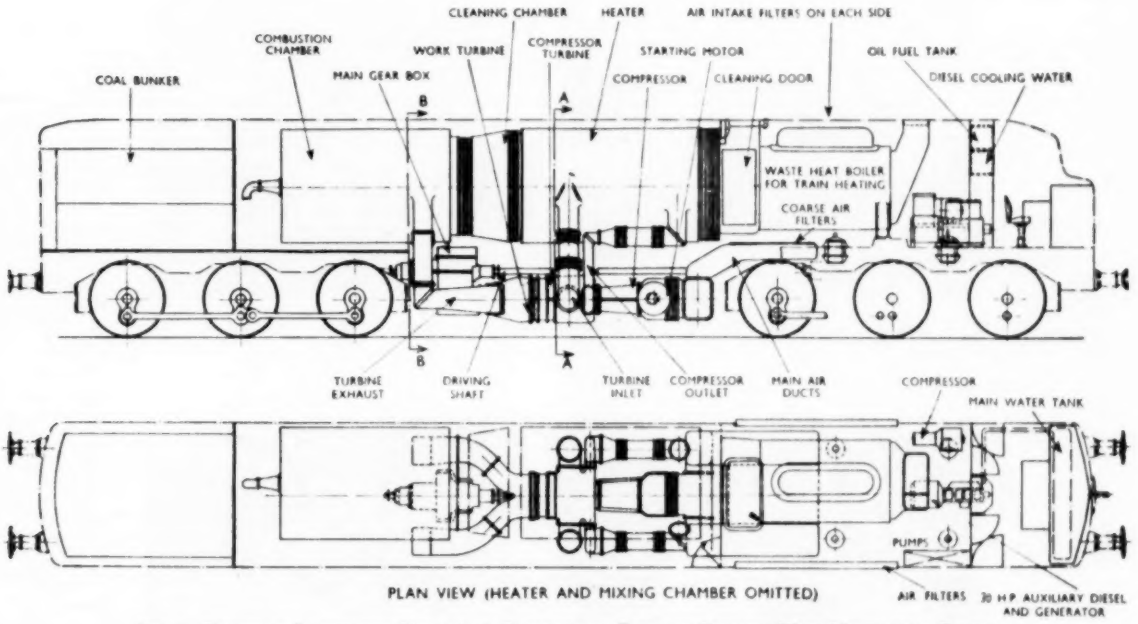

FIG. 4 DESIGN OF LOCOMOTIVE USING C. A. PARSONS AND COMPANY TURBINE WITH MECHANICAL DRIVE

The turbine will be of the two-shaft type with one turbine driving the axial compressor and a second turbine driving the locomotive through a mechanical transmission.

Experimental work on a similar cycle also is being carried out at the Ste. Anne de Bellevue Laboratory of McGill University, under the direction of Prof. Donald Mordell. This installation uses a Rolls-Royce Dart propeller-drive turbine which has been fitted with a reduction gear and a loading device. An external cyclone combustion chamber is contemplated, which will use crushed coal, and will heat the turbine-exhaust air to such a temperature that, in passing through the tubes of the heat exchanger, this low-pressure air can raise the compressed air to 1300 F. Work on the combustion aspects of this problem has been under way for some time in the Ottawa laboratory of the Canadian Bureau of Mines.

RUSTON AND HORNSBY, LIMITED

This company has made extensive tests with a 1070-hp gas-turbine plant coupled to a 750-kw generator, Fig. 5. As consideration is being given to using this turbine in locomotive service, pertinent data are given herewith. The unit is similar to the Brown Boveri design in that it has a regenerator and a single combustor designed for burning residual fuel, but it is unique in that it has a free-power turbine. Owing to the rapid acceleration of the gas-turbine unit, not more than 5 minutes from starting to full power, this company does not propose to use a Diesel generator set for starting but, instead, will start by motorizing the generator from a storage battery. The manufacturer believes that the free-power turbine eventually can be used to advantage in a direct mechanical-drive locomotive.

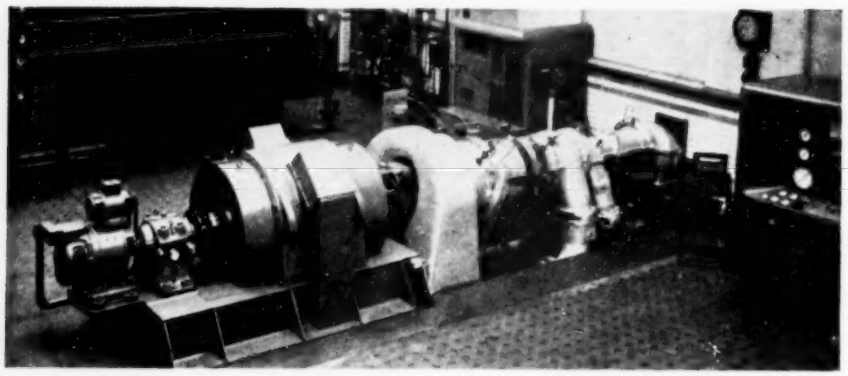

FIG. 5 RUSTON AND HORNSBY TURBINE SUITABLE FOR LOCOMOTIVE SERVICE

FIG. 6 GENERAL ELECTRIC 4500-HP LOCOMOTIVE ON THE UNION PACIFIC—FIRST OF AN ORDER OF TEN

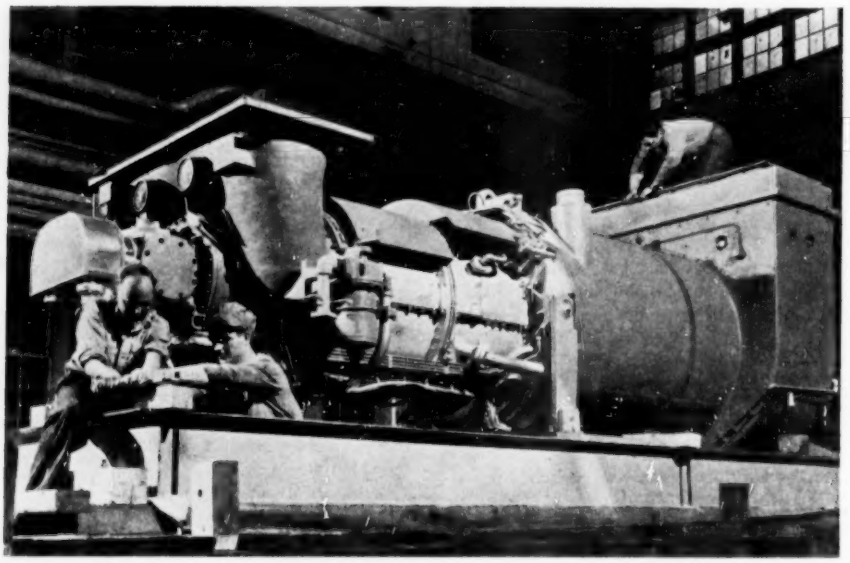

FIG. 7 GENERAL ELECTRIC LOCOMOTIVE TURBINE
(Note, one of these units can be replaced with another in the locomotive in only about 10 hr.)

Locomotive Development Committee of Bituminous Coal Research, Inc.

The work of this committee has been widely publicized since its inauguration in June, 1945. The objective was the development of a road-locomotive power plant which would use pulverized coal in the open-cycle gas turbine, and achieve an economy which would be superior to that of the Diesel. The experimental work has covered the burning of coal in many sizes and types of combustors. In addition, various types of pulverizers, coal pumps, fly-ash separators, and so forth, have been designed and tested. Much knowledge has been gained, consisting, in part, of learning what not to do. It is hoped that those in other parts of the world who are interested in burning pulverized coal in the open-cycle gas turbine will benefit from the Locomotive Development Committee's experiences.

All experimental work has been done by having the pulverizing equipment adjacent to and coupled with the coal-burning equipment. It is probable, however, that when coal-fired gas turbines are operated in large numbers, they will carry prepared coal on board. This should enable such locomotives to be built at first costs comparable with that of the oil-burning gas-turbine locomotive and the Diesel-electric. The most recent activities of the Locomotive Development Committee have been concentrated on coal-burning tests of its 4250-hp Allis-Chalmers turbine. This unit was installed at the Dunkirk laboratory late in 1950, and the initial operating problems consumed a number of months. The official acceptance test was run on September 28, 1951, during which the unit exceeded its rated output of 3750 hp, based upon 80 F ambient-air temperature, by 13.5 per cent when burning Diesel fuel. The turbine was immediately put into coal-burning operation, and a preliminary run totaling 178 hr was carried out. The unit was then inspected carefully, and a number of minor but persistent difficulties were overcome. The unit has been reassembled and is now on high-load high-temperature test; 260 hours of a projected 750-hour test period have been completed at this writing, with more than 75 per cent of the operating time at power outputs above 3000 hp. Fig. 1 shows the equipment used during this test.

It should be noted that wide publicity has been given to the activities of the Locomotive Development Committee in many magazines for the past six years. A complete record, of course, has not only been kept by the committee, but each year Mr. John I. Yellott, Director, together with his associates, has delivered a Progress Report before the Midwest Power Conference.[4]

General Electric Company

The General Electric experimental gas-turbine locomotive mentioned previously went into service on Western lines early in 1949. It was operated under all kinds of conditions for 110,000 miles before it was returned to its home plant at Erie, Pa., for special tests. This locomotive has been an extremely useful "guinea pig," and it has proved beyond doubt that the gas-turbine locomotive has a place on American railroads, just as the first Brown Boveri unit proved that European railroads could use this type of motive power effectively.

The General Electric design shown in Figs. 6 and 7 utilizes a single 4500-hp aircraft-type open-cycle gas turbine. Air is taken in through filters in the side panels of the locomotive, as shown in Fig. 6, and a silencer is fitted around the compressor intake within the cab. The turbine exhausts up through the roof of the locomotive and deflectors were installed during the early tests to direct the exhaust stream toward the rear of the train. No difficulty was experienced in operating through long tunnels, and it proved that it could handle longer and heavier trains than those normally drawn by Diesel-electric locomotives rated at the same power. The running gear of this locomotive consists of four 4-wheel trucks.

The General Electric unit has made an excellent showing when it is supplied with vanadium-free oil. When oils of high vanadium content were used, difficulties were experienced owing to the corrosion of the high-temperature parts of the turbine by the vanadium compounds released during combustion. No overall solution to this problem has yet been found, although it is being attacked in a number of different ways.

Because of its relatively moderate inlet temperature, 1280 F, at full load, the thermal efficiency of the plant at full load is held to approximately 17 per cent. The relatively high speed which is required by the single-shaft design at partial loads results in high fuel consumption at idling. The locomotive is thereby restricted in economic applications to those lines which have large quantities of residual oil available at low cost. The first large-scale application of this locomotive is now being made on the Union Pacific Railway and the results will be watched with great interest.

Westinghouse Electric Corporation

The 4000-hp Westinghouse locomotive, shown in Fig. 8, was first in operation on the Pennsylvania Railroad. Since then it

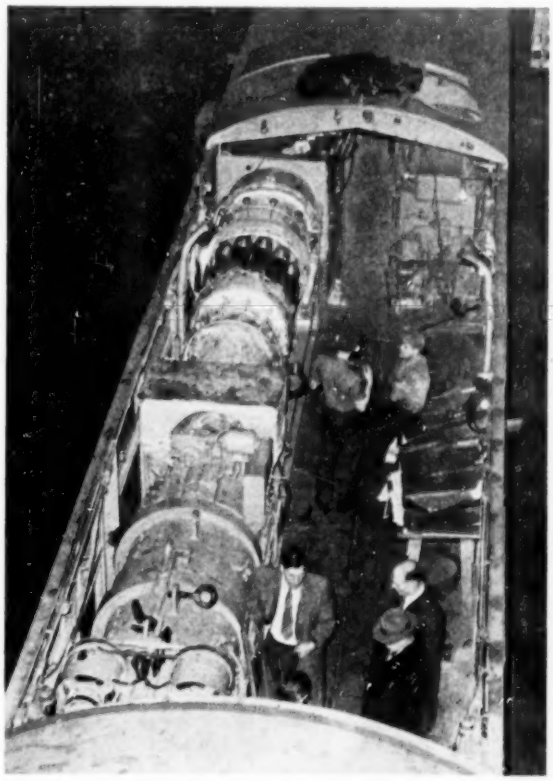

Fig. 8 Inside View of Westinghouse Locomotive Under Construction Showing One Turbine in Place

[4] Refer to Proceedings of the Midwest Power Conference; vol. IX, 1947, pp. 319–327; vol XI, 1949, pp. 360–375; vol. XII, 1950, pp. 419–433; vol. XIII, 1951, pp. 97–120. The 1952 Proceedings have not yet been published. However, the name of the organization has been changed to the American Power Conference. Headquarters of the Midwest Power Conference are at the Illinois Institute of Technology Chicago Ill

has been on the Missouri Kansas & Texas and possibly other western railways. This locomotive is notable because of its use of twin turbines in a side-by-side arrangement. One of the turbines exhausts through a waste-heat boiler, which is the first application of this idea in railway circles. The other turbine exhausts directly through the roof. Both turbines are of the aircraft type using an axial-flow compressor with can-type combustors. This arrangement has the benefit of simplicity and flexibility but it eliminates the possibility of using a regenerator, and thus restricts the obtainable cycle efficiency.

Various types of heavy fuel oil have been tried in this locomotive and it is being used to some extent as a fuel laboratory to help determine and establish the necessary specifications for heavy gas-turbine fuel oil. A Westinghouse representative has stated that the only fuel specification has been a low-sulphur residual with a maximum of 0.5 per cent ash, with the vanadium-pentoxide content of the ash not to exceed 15 per cent. Various combustion tests are being carried out to determine the effect of additives but, at the time of writing this paper, Westinghouse had not officially adopted their use.

FIG. 1 MGB 2009, FIRST VESSEL INCORPORATING A GAS-TURBINE ENGINE
(Photo by *The New York Times.*)

Gas-Turbine Progress Report—Marine

BY W. A. DOLAN, JR.,[1] AND A. A. HAFER,[2] WASHINGTON, D. C.

INTRODUCTION

IT seems appropriate after approximately the first 10 years of work in the marine gas-turbine-engine field to review the present status of this prime mover as applied to ship application. As might be expected, the evolution during a decade of anything with as many possible variables as the gas-turbine engine results in an involved and extensive paper. This is especially true when all aspects influencing this development are considered. It is felt, however, that the lessons learned to date are so significant as to warrant this detailed analysis.

The first entry into the marine gas-turbine-engine field was made by the Compagnie Electro-Mecanique of France in 1938 (1).[3] The engine designed by this company was rated at 10,000 shp and was quite advanced in design even by today's standards. It was a complex-cycle engine with high-pressure, intermediate- and low-pressure turbines having an over-all pressure ratio of 11.5 and an inlet temperature of 1562 F to the high-pressure turbine. Plans were made to install this gas-turbine engine in a vessel of the Marine Nationale. Work had commenced on the plant when France fell in 1940.

The Bureau of Ships of the U. S. Navy next entered the field by placing an order with the Allis-Chalmers Company for a 3500-bhp experimental gas-turbine engine in 1940.

It was learned after World War II that the German Navy also had been interested in the gas-turbine engine for ship propulsion. The firm of Bruckner and Kanis had designed two marine gas-turbine plants rated at 5000 and 10,000 hp, respectively. The latter was intended to power a high-speed torpedo boat (2). The choice of application for this engine would appear to have been a good one inasmuch as all large marine gas-turbine engines which have performed afloat to date in naval service, have been for this type of duty.

A milestone was reached when on July 14, 1947, the British Navy's MGB 2009 (later the MTB 5559) put to sea with a gas-turbine engine providing part of the propulsive power (3). Fig. 1 shows this boat under way. Actually, the British Admiralty actively entered the gas-turbine field at a relatively late date. The contract for the *Gatric* gas-turbine engine used in the MGB 2009 was not placed until August, 1943 (4). The fact that this gas-turbine engine was the first to be installed afloat may be attributed to the adaptation of a simple-cycle aircraft turbojet engine to marine service.

Fig. 2 shows the second vessel embodying gas-turbine engines. This is the English launch *Torquil* which commenced trials on May 6, 1950. The first vessel to be propelled solely by a gas-turbine engine was a 24-ft plane-personnel boat powered by a Boeing engine which was developed for the Navy's Bureau of

[1] Captain, U. S. N., Director, Ship Technical Division, Bureau of Ships, Department of the Navy.

[2] Lieutenant, U. S. N. R., Gas Turbine Project Officer, Bureau of Ships, Department of the Navy. Jun. ASME.

Contributed by the Gas Turbine Power Division and presented at the Fall Meeting, Chicago, Ill., September 8 – 11, 1952, of THE AMERICAN SOCIETY OF MECHANICAL ENGINEERS.

NOTES: This is paper No. 52—F-4A of a Progress Report which the Executive Committee of the Gas Turbine Power Division authorized at its 1951 Annual Committee Meeting. The series includes the following: "Introduction," by R. Tom Sawyer, paper No. 52—F-1A; "Materials, Cooling, and Fuels," by A. A. Hafer, paper No. 52—F-1B; "Cycle Components," by P. F. Martinuzzi, paper No. 52—F-1C; "Automotive," by Frank L. Schwartz, paper No. 52—F-2; "Railroads," by K. A. Browne, J. I. Yellott, and P. R. Broadley, paper No. 52—F-3; "Merchant Vessels," by W. A. Dolan, Jr., and A. A. Hafer, paper No. 52—F-4B; "Naval Vessels," by W. A. Dolan, Jr., and A. A. Hafer, paper No. 52—F-4C; "Stationary Electric Generation," by Lee Schneitter, paper No. 52—F-5; "Industrial," by L. N. Rowley and B. G. A. Skrotzki, paper No. 52—F-6; "Aviation," by I. H. Driggs and O. E. Lancaster, paper No. 52—F-7.

The present paper, 52—F-4A, and paper Nos. 52—F-4B, 52—F-4C, dealing with the subject of "Marine Progress," all by the same authors, are to be treated as a group; hence the Bibliography, figure numbers, and numbers of tables run consecutively through the three sections.

Statements and opinions advanced in this paper are to be understood as the individual expressions of the authors and not to be construed as official or reflecting the views of the Navy Department, of the Naval Service, or of the Society.

[3] Numbers in parentheses refer to the Bibliography at the end of the third paper, No. 52—F-4C.

FIG. 2 GAS-TURBINE-PROPELLED BRITISH LAUNCH "TORQUIL"
(Courtesy of *The Oil Engine Gas Turbine.*)

FIG. 4 GAS-TURBINE-PROPELLED LAUNCH HL 3964
(Photo by Keystone Pictures, Incorporated, New York, N. Y.)

FIG. 3 BOEING GAS-TURBINE-PROPELLED PLANE-PERSONNEL BOAT

FIG. 5 U. S. NAVY GAS-TURBINE-PROPELLED LCVP
(Official U. S. Navy photograph.)

Ships. This boat, shown in Fig. 3, started trials on May 30, 1950. The fourth gas-turbine-engine-propelled vessel was the British Admiralty launch HL 3964 shown in Fig. 4. The engine in this launch is similar to that used in the *Torquil*. The HL 3964 commenced operating on June 18, 1951. The fifth water-borne gas-turbine-engine installation was in a U. S. Navy LCVP, powered by the same type engine as that used in the earlier plane-personnel boat (5). Fig. 5 shows this boat in operation.

The first vessel ever to be designed and built specifically to exploit the advantages of the gas-turbine engine for propulsion, was launched by the British Admiralty on August 18, 1951. This vessel is the *Bold Pioneer* (MTB 5701). A somewhat similar boat, the *Bold Pathfinder* (MTB 5720), was launched on September 17, 1951 (6). Both of these boats will be powered by two gas turbine and two Diesel engines. The gas-turbine engines are similar to those used in the earlier MTB 5559 except they have about double the horsepower (7).

The first gas-turbine engine installed aboard a naval ship, as opposed to the smaller vessels previously mentioned, was developed by Solar Aircraft Company for the Navy's Bureau of Ships. This is also the first gas-turbine engine to go afloat for auxiliary service. It provides power for an emergency generator set. This engine was delivered to the Bath Iron Works Corporation in February, 1951, for installation in a ship which was under construction at that shipyard (8).

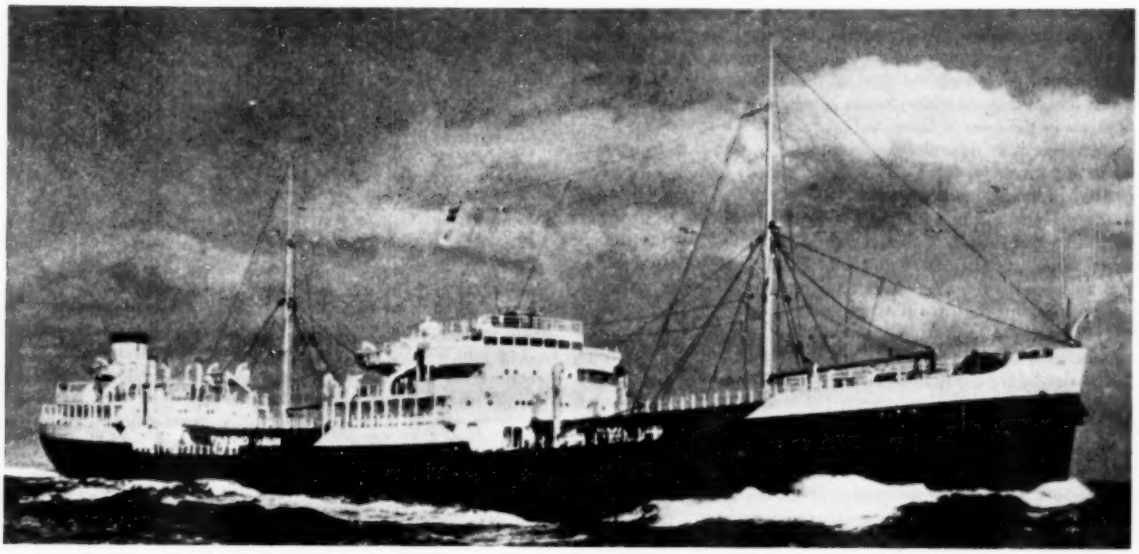

FIG. 6 THE ANGLO-SAXON PETROLEUM COMPANY'S TANKER "AURIS" WITH GAS-TURBINE PROPULSION
(A Shell photograph.)

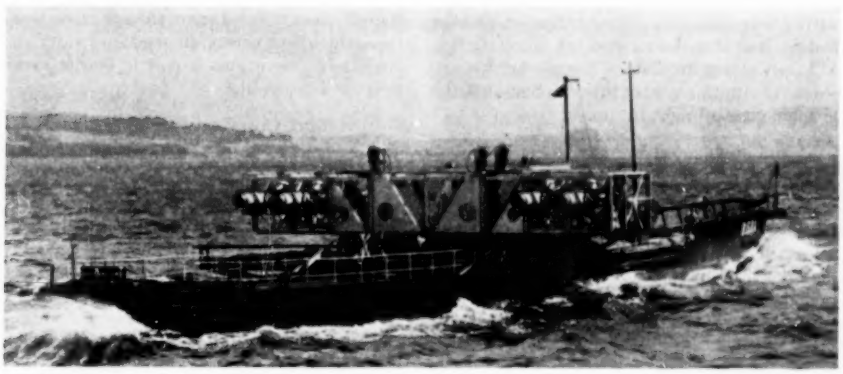

FIG. 7 JET-ENGINE-PROPELLED "LUCY ASHTON"
(Photo by European Picture Service.)

On October 28, 1951, the first ocean-going merchant ship powered by a gas-turbine engine completed her sea trials off the coast of England. This ship, the tanker *Auris* (12,250 tons deadweight) is owned by the Anglo-Saxon Petroleum Company Ltd., of England (9). The *Auris* is shown in Fig. 6.

It will be noted that all nine of the water-borne gas-turbine plants installed to date are of the open-cycle type. Perhaps even more significant is the fact that all but one of these installations consist of simple-cycle engines.

The extreme versatility of the gas-turbine engine is demonstrated by a very unusual sea-going installation. In the autumn of 1950, four Rolls Royce Derwent V turbojet engines were installed topside on the *Lucy Ashton* for main propulsion, as shown in Fig. 7. Each of these engines is rated to deliver a thrust of 3600 lb. This application of turbojet engines to marine propulsion was dictated in the interests of full-scale hull-resistance tests conducted by the British Shipbuilding Research Association. The advantage of using this type of engine over any other type is the ability of a turbojet engine to provide a steady thrust, capable of being easily and rapidly changed by simple controls. When the engines are mounted beyond the vessel's beam, so as to prevent the impingement of the exhaust gases on any part of the hull or water, the recorded thrust gives an accurate assessment of the hull resistance. It is rather interesting to note that the *Lucy Ashton* was first put into service in 1888, as a paddle-wheel steamer (10).

CONCLUSIONS

The gas-turbine engine has now progressed to the point where its use is advantageous in a number of naval applications. These include small short-range boats, landing craft, PT boats, emergency power generation, and portable power equipment. Booster gas-turbine engines combined with base-load Diesel, steam, or gas-turbine plants are also attractive. In general, all of these applications but the base-load plant will utilize a simple-cycle engine.

For merchant-marine propulsion the gas-turbine plant is not now economically superior to either the Diesel or steam plant

except in special applications. The choice of a prime mover is basically a question of economics. After analyzing such factors as engine first cost, maintenance, life, fuel consumption, and cost of operating personnel, the type of prime mover most advantageous for a particular installation is usually apparent. Such an analysis in the case of the naval prime mover is somewhat more involved as it is difficult to give an economic value to certain engine features.

Any progress made toward higher turbine temperatures, ability to burn residual fuel, or a radical reduction in regenerator size will make the use of the marine gas-turbine plant that much more advantageous. It should not be anticipated that the gas-turbine engine will replace both the Diesel and steam plants in the near future, but that it will supplement them.

It is safe to say that the number of marine gas-turbine engines in service in several years will number in the hundreds. A large proportion of these will be small naval units.

There is every reason to believe that progress will continue at a high rate during the next decade. We are all aware of the tremendous activity being carried on by the Department of Defense, NACA, and industry in this country. Advances in one gas-turbine field will directly or indirectly benefit the other fields. Some may be less familiar with the gas-turbine work now going on in England. In addition to private English concerns, the Ministry of Supply, Admiralty, National Gas Turbine Establishment, National Physical Laboratory, British Electric Authority, British Railways, Power Jets (Research and Development) Ltd., Ministry of Fuel and Power, National Coal Board, Department of Scientific and Industrial Research, Fuel Research Station, and the British Coal Utilization Research Association are administering or actively engaged in advancing the state of the gas-turbine art. There can be little doubt, with this type of interest, but what the marine gas-turbine engine has a bright future.

Acknowledgment

The contribution of essential data by all of the companies mentioned in this report is gratefully acknowledged. The direct and indirect assistance of many personnel in the Bureau of Ships has been of real assistance. In particular, the interest, encouragement, and constructive criticisms of Commander Ivan Monk, USN, have been invaluable.

Special Considerations For Marine Gas-Turbine Engines

There are certain peculiarities of the gas-turbine engine which require careful consideration for its most effective utilization in marine service. Many of these considerations, of course, apply in varying degrees to the other fields which utilize this engine.

Thermal Efficiency

One of the heaviest burdens the marine gas-turbine-engine designer must bear is the extremely wide range of ambient temperatures which may be encountered. A ship may operate from the tropics to the arctic during its lifetime. The power and thermal efficiency of a gas-turbine engine are extremely sensitive to variation in ambient temperature and the plant initially should be designed with this in mind.

The gas-turbine engine must compete with the Diesel engine and steam-turbine plant for general marine application. It is therefore desirable to compare the typical efficiencies of these three types of prime movers, as shown in Table 1. This table is based on typical existing plants. It does not represent either the best or worst plant of its type. The figure given is for the design load condition and includes gear loss where applicable. The higher heating value is used for each fuel—18,500 Btu per lb for residual fuel and 19,690 Btu per lb for Diesel oil. The ship's "hotel load" is not included for any of the three types of plants.

TABLE 1 TYPICAL EFFICIENCIES OF EXISTING MARINE PRIME MOVERS

Kind of heat engine	Service	Fuel	Thermal efficiency, per cent	Specific fuel consumption, lb/hp-hr
Diesel engine	Merchant	Diesel oil	37	0.35
Diesel engine	Naval	Diesel oil	34	0.38
Steam turbine (World War II)	Merchant	Residual	23	0.60
Steam turbine (Postwar)	Merchant	Residual	25	0.55
Steam turbine (Supertanker)	Merchant	Residual	27.6	0.50
Steam turbine	Naval	Residual	24	0.57
Simple gas turbine[a]	Naval	Diesel oil	17.2	0.80
Complex gas turbine	Naval	Diesel oil	24	0.55
Complex gas turbine	Merchant	Diesel oil	28	0.47

[a] Large units only.

There was no attempt to compare the three heat engines at the same power rating.

The addition of regeneration, intercooling, and reheat to the simple-cycle engine, singly or in combination, will of course alter the thermal efficiency and/or the air rate. The only gas-turbine engine to date in marine service with a regenerator is the British Thomson-Houston unit installed in the *Auris*. This engine has a tubular regenerator mounted vertically to form part of the stack uptake (12). This is certainly a desirable arrangement from the standpoint of space utilization.

The addition of either intercooling or reheat to the simple cycle has little effect on thermal efficiency until a high pressure ratio is used. They both reduce the plant air rate, especially at high pressure ratios. Reheat would not be used alone in a marine plant, as intercooling is almost as effective and introduces less complication (13). Intercooling is attractive for marine use because there is an ocean full of cooling water always available (14). No gas-turbine engine is now in marine service using either reheat or intercooling.

Engine Compartment Ventilation Requirements

Temperatures existing in the gas-turbine engine may be as high as 3500 F in the central zone of the combustion chamber, 1500 F to the turbine inlet, and from 800 to 1250 F at the turbine exhaust. In addition, in marine gas-turbine engines, where reduction in weight and volume are generally important, large quantities of thin sheet metal may be used in the engine. Use of lagging methods now commonly employed in steam-turbine practice will not be feasible for many gas-turbine-engine hot parts. Fortunately, the solution to the lagging and compartment ventilation problem is contained within the gas-turbine plant itself.

The velocity of the exhaust gas in the stack of this type of engine may be from 200 to 300 fps. By utilizing the energy in this exhaust gas it is possible not only to solve the heat-rejection problem from the gas-turbine engine, but also to ventilate the compartment. This eliminates bulky and costly ventilating fans. This dual function is performed by fitting an air casing around the engine joined to an outer stack surrounding and extending above the gas-turbine engine stack. Air is drawn into the engine air casing from the compartment by the ejector effect of the exhaust gases, and is passed on out the stack. This ejector effect places the engine compartment under a slight vacuum so that if there are air openings to the compartment, a constant circulation of air into and out of the compartment results. The immediate removal of heat rejected from the engine by the air passing through the air casing has the additional advantage of reducing the total compartment ventilation requirements. This, of course, is due to the fact that the heat does not have the opportunity to circulate around the compartment with a resultant compartment temperature rise.

This system of heat rejection is actually an air-flow-insulation system. Information is available which permits accurate predictions in designing such a system (15). It has the same ad-

vantages as the air-flow-insulation system, namely, reduction in weight and volume of insulation, provision of a definite path for discarded heat, and the avoidance of high metal temperatures and high rates of radiation in the engine room. When applied to a gas-turbine engine using an ejector, it has the additional advantage of utilizing waste exhaust energy to circulate the required air.

There are several approaches to the best method of obtaining this ejector effect. By restricting the flow of the engine exhaust gas as it leaves the inner stack we can obtain a good ejector. This has the undesirable effect of reducing engine power and thermal efficiency. Therefore this method ordinarily will not be used. It is interesting to note, however, that this system has been investigated in relation to cooling turbojet installations (16, 17).

The type of stack-ejector system which seems best suited for use with a gas-turbine engine was surprisingly enough used on the first marine installation, the MTB 5559, some five years ago. The intent of this original system was not for the purpose of ventilating the compartment, however. The MTB 5559 had two gasoline engines in addition to the gas-turbine engine. To prevent any gasoline vapors from coming into contact with the hot parts of the gas-turbine engine, an air casing was fitted around the latter (5). Outdoor air was supplied to this casing by a $12^1/_2$-in. fan and exhausted up the annulus between the inner and center stack. It was anticipated that the ejector effect from the exhaust gas would encourage this air flow (4). It was desired to keep the air case under pressure in this case so as to prevent the entry of any gasoline vapors, and it was thought that the supply fan would perform this function. The ejector effect from the exhaust gas proved to be so high, however, that the case originally was under a vacuum. This was remedied by fitting two additional cowls leading into the air casing (18).

This system is well illustrated in Fig. 8. It will be noted from this figure that there is a total of three stacks. The annulus between the center and outer stack was provided for circulation of topside air. The ejector effect drew air in through openings at the base of the stack and exhausted it from the top. This provided for a very low metal temperature of the outer stack. The third stack may be dispensed with by installing a thin layer (in the order of $^1/_2$ in.) of aircraft-type jet-engine lagging on the outside of the inner stack and a very thin layer of sprayed insulation on the outside of the outer stack.

A study made by London and McIntosh of Stanford University for the Bureau of Ships indicated that, in a particular installation using Boeing gas-turbine engines, it would be possible to ventilate the engine compartment solely by the ejector effect. An investigation and tests run concurrently at the U. S. Naval Engineering Experiment Station at Annapolis also established this. These tests also indicated that by such a system the ventilating requirements of the compartment were reduced by some 17 per cent over what would have been necessary with a forced-draft system exhausting at a location other than around the stack. The ejector system also lowered the engine exhaust pressure with a slight increase in power and thermal efficiency. This ventilation method eliminated several blowers with a consequent reduction in weight, and a saving of several kilowatts of power.

London and McIntosh also reported that the ejector effect could be improved, if desired, over that of the straight stack, with the addition of a diffuser. There is, of course, information available for guidance in designing such a diffuser (19).

Noise Requirements

Noise considerations of machinery should be given more careful attention in marine gas-turbine engines than perhaps in any other application. The crew, and passengers if carried, must live, eat, and sleep within close proximity to the machinery plant. Fortunately, the gas-turbine engine will be acceptable from a noise standpoint if proper consideration is given to the design of the installation. The air casing, discussed previously from the standpoint of ventilation, will lend itself effectively to the reduction of noise passing through the engine casing.

Elimination of Salt From Compressor Inlet Air

Numerous test reports have indicated the serious effects on plant performance caused by compressor fouling. For land gas-turbine engines this fouling is caused by impurities, such as dirt, smoke, and oil in the atmosphere. In a series of tests on a 500-hp gas-turbine engine made by John Brown & Company, Ltd., it was found that compressor fouling lowered the compressor efficiency from 77 to 73.5 per cent in a 20-hr run (20). This would cause an increase in specific fuel consumption of about 10 per cent.

Fortunately, with proper design the marine gas-turbine engine will not be subject to the large number of impurities to which its land counterpart is exposed. Care must be taken to prevent recirculation of the exhaust gas into the compressor inlet of course. In addition, no lube-oil vents should be located in the vicinity of the intake. The marine engine is exposed to one impurity which is not normally experienced in other types of service. This is the salt-laden air. Salt deposition on the compressor blades will reduce compressor efficiency in the same manner as any other type of foreign matter. In addition, it might be detrimental in the combustion process at some future date.

The first consideration to this problem is to prevent the entry of salt spray into the compressor. Fig. 8 illustrates how this was

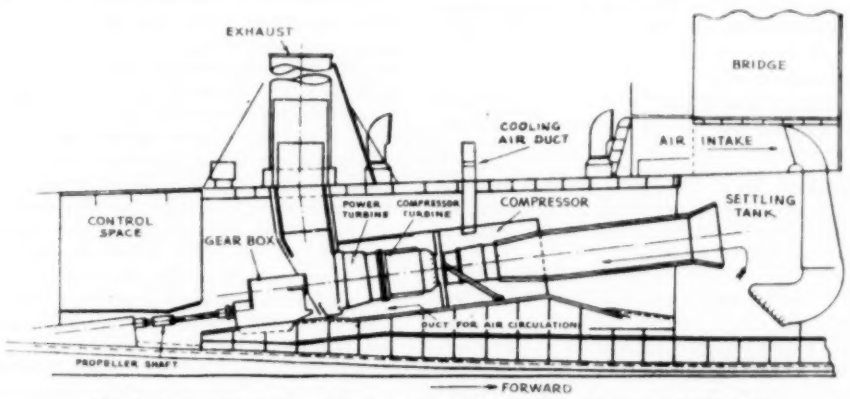

Fig. 8 Installation Diagram of "Gatric" Gas-Turbine Engine in MTB 5559

very effectively done in the case of the MTB 5559. By taking air suction from a sheltered location topside and passing the air through a settling tank it was anticipated that the air would drop most of the globules of water in suspension with the air (4). It is unlikely that this will remove all of the salt, however. Therefore some additional expedient must be provided to prevent salt build-up in the compressor. The larger the ship the less probability of fouling by sea air, as the air intakes will be at a greater height above the sea surface.

In the tests run by John Brown & Company, Ltd., it was found that by spraying about 2 gal of a liquid (paraffin), into the compressor inlet, while running, the compressor performance was almost completely restored to the design value (20). A similar procedure seems desirable for marine service. During the trials of the MTB 5559 some 3000 tons of salt air were passed through the gas-turbine engine. "The company's (Metropolitan-Vickers) previous experience is that washing with fresh water easily removes the salt and restores the performance (21)." The compressor inlet of the gas-turbine engine in the MTB 5559 is fitted with five equally spaced nozzles contained in a sprayer ring assembly. Ten gallons of water are injected through these nozzles in from $2^1/_2$ to $5^1/_2$ min every 3 to 12 hr, depending upon drop in engine performance. Distilled water is used when obtainable, but very often fresh water is used. "This frequent water injection maintained the horsepower and specific fuel consumption at a fairly steady level (22)." The sprayer nozzle holes were plugged with rust during one period of operation and a sharp drop in power was caused by running in fog for several hours (22).

The only method actually of preventing the entry of any salt into the engine is by some such device as an electrostatic precipitator. Such a device has the disadvantage of increasing the weight and volume of the installation and also requires power to operate.

Operating experience of the *Auris* and MTB 5701 and 5720 undoubtedly will furnish additional information as to the best method of preventing or minimizing salt deposition.

Reversing Methods

When the gas-turbine engine was first considered for marine propulsion there were serious misgivings as to how the reversing requirements of the ship could be handled. As often happens, time has shown that these misgivings were largely unfounded. There appears to be little likelihood that reversing for a gas-turbine-engine-propelled ship will be handled in the same manner as for a steam plant, that is, by a separate astern turbine. There have been several "trick" cycles proposed which, by means of suitable clutches, would provide reversing power without a separate astern turbine (1, 23). The four reversing methods which seem best suited for use with the gas-turbine plant are as follows:

1 Direct-current electric drive.
2 Alternating-current electric drive.
3 Mechanical reversing gear.
4 Controllable-pitch propeller.

Direct-Current Electric Drive. Because of the high first cost, low efficiency, and large weight and space requirements, the direct-current electric drive will rarely be used with the gas-turbine plant in marine service (24, 25, 26).

Alternating-Current Electric Drive. The cost and weight of this system compares favorably with mechanical drive unless it also requires a reduction gear. However, the lower efficiency of this system, which may reduce the cycle efficiency by approximately 3 per cent, will dictate its choice only for special classes of vessels such as tankers or dredges, where a large deck-machinery load is required. When this requirement occurs simultaneously with propulsion, it is even more advantageous. A reduction gear will have to be employed with this system unless much higher electrical frequencies are used than is now general practice (26, 27, 28, 29).

Mechanical Reversing Gear. This method offers a very satisfactory solution to the reversing problem, especially at the lower powers. Reversing is accomplished with a mechanical reversing gear in the two marine gas-turbine installations made to date in this country, that is, the Boeing powered LCVP and PPB. A promising development in the reversing-gear field is the adaptation of the epicyclic gear for this service. It can be operated with simple foolproof clutching mechanisms and has the same efficiency as a conventional double-reduction gear (29). Many companies throughout the world now build this type of gear. Approximately 3000 reverse reduction gears were used during World War II by the U. S. Navy, ranging in rating from 750 to 1600 shp per unit. There is no lower limit to this type of gear and the upper limit has never been determined, although one manufacturer has studied the application of a 6000-shp reversing gear (24).

Controllable-Pitch Propeller. Perhaps the most controversial of the reversing methods is the controllable-pitch propeller. Fortunately, a number of authoritative papers have been presented on this system which allow a good assessment of the merits of this device (26, 30, 31, 32). The controllable-pitch propeller is not a new device—one was installed on the 450-hp motor tanker *Poseidon* in Holland in 1915 (29). Today, companies in the United States, Switzerland, Sweden, England, Denmark, Norway, and Holland are producing this type of propeller.

The U. S. Navy became interested in the controllable-pitch propeller in 1940 and installed one on a 250-hp Diesel tug. The highest-powered controllable-pitch propellers ever designed were installed on the USS *Dahlgren* (DD187) in 1941. These propellers were to absorb 14,000 shp each, but owing to lack of time and insufficient design data available at that time, would only absorb 11,000 shp. Even so the preliminary test results were encouraging for such an ambitious undertaking, but were cut short by the urgent military need for the vessel at that time. The U. S. Navy also installed controllable-pitch propellers on 1100 L.C.I.'s and 100 P.C.'s (both twin-screw vessels) during World War II.

About 150 merchant ships have been fitted with Swedish-made controllable-pitch propellers. The highest-rated controllable-pitch propellers now in use are on the *Los Angeles*, a 7200-ton ship with 7000 shp per shaft. It is interesting to note that while operating at the same power, the trial speed of the *Los Angeles* was about $^1/_2$ knot faster than her two sister ships, the *Seattle* and *Golden Gate*, which were equipped with fixed propellers (33).

The reliability of the controllable-pitch propeller would seem to be satisfactory. Over 100 Kamewa propellers covering all powers up to the 7000-shp previously mentioned, have been in operation for about 15 years without any breakdown to the hub mechanism (33). Rear Admiral W. D. Leggett, Jr., USN, has reported that the controllable-pitch propellers used on the L.C.I.'s during World War II often suffered damage to the blades when making landings around coral reefs (as did the fixed-blade propellers in the same service), but rarely harmed the hub or operating mechanism (34). The U. S. Navy also has been operating three tugs fitted with controllable-pitch propellers for about 5 years without difficulty. The twin-screw 3200-shp towboat *Delta Cipies*, equipped with controllable-pitch propellers, is now operating on the Mississippi River. The small lake vessel *Etzel*, equipped with an Escher-Wyss controllable-pitch propeller, has been in constant service for over 14 years with continued dependable operation (32). The *Succia* (3500 hp per shaft), also equipped with controllable-pitch propellers, has given dependable service for about eight years.

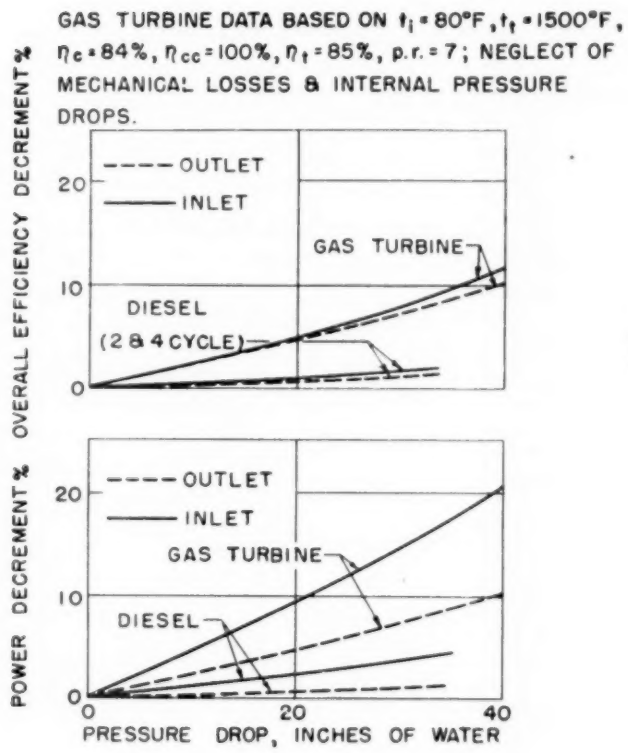
GAS TURBINE DATA BASED ON t_1 = 80°F, t_t = 1500°F, η_c = 84%, η_{cc} = 100%, η_t = 85%, p.r. = 7; NEGLECT OF MECHANICAL LOSSES & INTERNAL PRESSURE DROPS.
POWER DECREMENT % OVERALL EFFICIENCY DECREMENT %
OUTLET
INLET
GAS TURBINE
DIESEL (2 & 4 CYCLE)
DIESEL
0
10
20
40
PRESSURE DROP, INCHES OF WATER

FIG. 9 EFFECT OF INLET AND EXHAUST PRESSURE DROPS ON PERFORMANCE OF A SIMPLE OPEN-CYCLE GAS-TURBINE ENGINE AND OF TYPICAL DIESEL ENGINES

(Courtesy reference 5.)

There is little doubt but that this type of propeller does give excellent backing characteristics. Vice Admiral E. W. Mills, USN (ret.) has related his experience with the backing characteristics of a small boat fitted with a controllable-pitch propeller made by S. Morgan Smith Company. He was standing in the stern sheets of the under-way boat when the operator changed the pitch of the propeller without slowing the engine down. In Admiral Mills' own words, "I took a header right from the back of that boat clean over the bulkhead and the engine!" (35).

Under certain operating conditions the efficiency of the controllable-pitch propeller is superior to the fixed propeller, but this is not generally true. The reduction in propulsive efficiency introduced by the controllable-pitch propeller is approximately of the same value as the losses caused by the astern stages of a steam turbine (36).

The reversing feature of the Elliott gas-turbine plant which was to have been installed in the *Liberty Collier* EC2-G-AW2 was to have been a controllable-pitch propeller. Other United States vessels operating with this type of propeller include the *Single Hitch*, *Albatross III*, *Commercial Clipper*, USS *Apohola*, and USS *Chononaga*.

Most gas-turbine authors have expressed a preference for either the controllable-pitch propeller or mechanical reversing gear, to provide reversing (13, 26, 31, 32, 37, 38, 39). The final choice between these two methods will probably depend upon economic factors. One such study indicates that the mechanical reversing gear is preferable up to 3000 shp and the controllable-pitch propeller above 6000 shp. Between these two ratings either method is acceptable (26). Other factors such as employment of the ship and type of cargo carried also will influence the final choice for each particular vessel.

DUCT CONSIDERATIONS

The adverse effect on output and efficiency of extensive ducting with numerous bends in a complex-cycle gas-turbine plant is well known. Pressure losses in either the compressor inlet ducting or exhaust ducting is also serious as shown in Fig. 9. If it is desired to maintain the same power reduction resulting from duct losses, the gas-turbine plant ducting must be about six times as voluminous as that of the Diesel engine (5). It has been suggested that the compressor-inlet velocity might be 60 fps and the exhaust velocity 120 fps (13). The higher the inlet and exhaust-duct velocities the smaller these ducts may be, but with a resultant increase in power loss and noise level. The foregoing figures can hardly be termed limits, however, as the exhaust volute velocity of the gases in the MTB 5559 were given as 340 fps, with a somewhat lower velocity at the top of the stack (4). An inlet-duct area of 2¼ sq ft per 1000 hp also has been suggested which, although slightly in excess of 60 fps, seems reasonable (37).

The exhaust-stack diameter for a 15,000 shp single-stack gas-turbine plant would be acceptable for cargo vessels with present beam dimensions (38). Naval ships are likely to require more than one stack if all or a large percentage of their installed horsepower is in the form of gas-turbine engines. Most large naval vessels now have more than one stack. It will be desirable to integrate provisions for the compressor inlet air opening into the design of the vessel. It also will be desirable, from the standpoint of minimizing duct losses, to have the gas-turbine engine located as high in the vessel as possible. Thought should be given in locating the engine room to enable both the compressor inlet and the exhaust ducting to be as free of bends as is feasible.

Gas-Turbine Progress Report—Merchant Vessels

By W. A. DOLAN, JR.,[1] and A. A. HAFER,[2] WASHINGTON, D. C.

Requirements

SEVERAL studies have indicated that the gas-turbine engine is most effective in the 5000 to 10,000-hp power range. Therefore, to evaluate the prospects of the gas-turbine engine as a prime mover in merchant vessels it should be determined what powers are generally required. Table 2 lists powers found in a number of United States cargo ships, and Table 3 shows recently ordered or built passenger ships.

TABLE 2 CARGO SHIPS

Type	Hp per shaft	No. screws
Liberty ship	2500	1
T2-SE-A1 tankers	6000	1
C2, AP2 Victory	6000	1
C3, AP3 Victory	8500	1
T2-SE-A2 tankers	10000	1

TABLE 3 PASSENGER SHIPS

Name	Hp per shaft	No. screws
P2 transports	10000	2
Oslofjord	8150	2
Cote d'Azur	11000	2
Stockholm	7300	2
Rijndam	4250	1
Pretoria Castle	15000	2
USS *Barrett* (AP196)	12500	1
Rhodesia Castle	7500	2
Himalaya	17000	2
Ruahine	7100	2
Aureol	4700	2
Normannia	8000	2
Kenya	5600	2

It can be seen from Table 2 that the power requirements for a number of cargo ships fall within the optimum power range of the gas-turbine engine. All of the listed vessels are single-screw drive. Table 3 indicates that many of the recent passenger liners also have powers within the optimum range for a gas-turbine plant.

During 1951, 70 per cent of the merchant ships built in England had Diesel engines for main propulsion. For the same period 68 per cent of the new gross tonnage built throughout the world was Diesel-powered. Perhaps more surprising is the fact that the power of 22 of these Diesel-powered ships exceeds 10,000 hp and the largest, the *Giulio Cesare*, has a main propulsion plant of 32,000 hp. The majority of merchant ships built during 1951 had main propulsion plants in the 6000 8000-hp range (40).[3] This trend toward Diesel-powered ships is not new; during the first nine months of 1948, 68.5 per cent of the vessels between 6000 and 8000 tons were Diesel-powered, and 74.5 per cent of the vessels between 8000 and 10,000 tons were so propelled (41). Therefore the prime competitor of the gas-turbine engine in the merchant-marine field is the Diesel engine.

Fortunately for the gas-turbine engine the merchant ship operates for the majority of its life near full power, and therefore high part-load efficiency is not important (38, 42).

Life requirements of a marine engine for mercantile purposes is usually considered as a minimum of 10 years (43). For a merchant ship averaging 200 days at sea each year this would equal about 50,000 hr. At least one marine gas-turbine engine, the Allen 1000-kw turbogenerator set has been designed for a total life of 100,000 hr (44). It has been proposed recently that the life of the merchant vessel gas-turbine engine be 10,000 hr or 2 years, with replacement at that time (30). Since the gas-turbine plant in this case would have only one fifth the life of the steam or Diesel plants, it is seriously questioned if it would be economically competitive.

The requirements of the marine propulsion plant in order of importance have been listed by Sawyer (5) as follows:

1 Maximum reliability.
2 Minimum operating fuel cost.
3 Minimum first cost.
4 Minimum maintenance and operating personnel cost.
5 Maximum maneuverability.
6 Minimum weight.
7 Minimum volume.

The reliability of any prime mover can be proved only by service. Fortunately enough, service experience has and is being accumulated to make an assessment of the reliability of the marine gas-turbine engine. The British MTB 5559 obtained dependable service from the gas-turbine engine while visiting a number of Scandinavian and British ports in 1949 (45). The first merchant gas-turbine-propelled ship, the *Auris*, covered 13,211 nautical miles with the gas-turbine engine operating 1391 hr on its first voyage. "On no occasion was it necessary to stop the turbine at sea, nor had repairs to be effected at any of the ports visited." (46). Perhaps even more significant is the operating record of the Oklahoma Gas and Electric Company's first gas-turbine engine which, so far as is known, has operated longer than any other gas-turbine plant in the world (in excess of 20,000 hr since 1949).

A survey made early in 1950, of the first 4 months of operation of the four prime movers most recently acquired by that company showed that this gas-turbine engine had no hours of forced outage, a steam topping turbine had 145 hr or 5 per cent forced

[1] Captain, U. S. N., Director, Ship Technical Division, Bureau of Ships, Department of the Navy.

[2] Lieutenant, U.S.N.R., Gas Turbine Project Officer, Bureau of Ships, Department of the Navy. Jun. ASME.

Contributed by the Gas Turbine Power Division and presented at the Fall Meeting, Chicago, Ill., September 8 – 11, 1952, of The American Society of Mechanical Engineers.

Notes: This is paper No. 52—F-4B of a Progress Report which the Executive Committee of the Gas Turbine Power Division authorized at its 1951 Annual Committee Meeting. The series includes the following: "Introduction," by R. Tom Sawyer, paper No. 52—F-1A; "Materials, Cooling, and Fuels," by A. A. Hafer, paper No. 52—F-1B; "Cycle Components," by P. F. Martinuzzi, paper No. 52—F-1C; "Automotive," by Frank L. Schwartz, paper No. 52—F-2; "Railroads," by K. A. Browne, J. I. Yellott, and P. R. Broadley, paper No. 52—F-3; "Marine," by W. A. Dolan, Jr., and A. A. Hafer, paper No. 52—F-4A; "Naval Vessels," by W. A. Dolan, Jr., and A. A. Hafer, paper No. 52—F-4C; "Stationary Electric Generation," by Lee Schneitter, paper No. 52—F-5; "Industrial," by L. N. Rowley and B. G. A. Skrotzki, paper No. 52—F-6; "Aviation," by I. H. Driggs and O. E. Lancaster, paper No. 52—F-7.

The present paper, 52—F-4B, and papers 52—F-4A; 52—F-4C, dealing with the subject of "Marine Progress," all by the same authors, are to be treated as a group; hence the Bibliography, figure numbers, and numbers of tables run consecutively through the three sections.

Statements and opinions advanced in this paper are to be understood as the individual expressions of the authors and not to be construed as official or reflecting the views of the Navy Department, of the Naval Service, or of the Society.

[3] Numbers in parentheses refer to the Bibliography at the end of the third paper, No. 52—F-4C.

outage, a gas Diesel-engine unit 286 hr or 10 per cent, and a condensing steam turbine 592 hr or 20 per cent (47). In the first 4200 hr of operation this gas-turbine engine had no forced outage (48). It has been reported that the initial start-up of this gas-turbine engine "was much smoother all round than for a boiler and steam turbine" (49). During the first 20,000 hr of operation of this gas-turbine engine only two forced outages have been reported, and both of these were caused by auxiliaries. One outage was for less than 1 hr and the other for a few hours' duration.

The engines of both the MTB 5559 and the Oklahoma Gas and Electric Company's first unit (a second unit has been installed recently) were simple-cycle engines. The gas-turbine engine installed in the *Auris* had the additional complexity of a regenerator. More complex cycles inherently will have less reliability, but it is not now known how various forms of complex-cycle gas-turbine engines will compare with the steam plant and Diesel engine.

Table 1[4] indicates relative efficiencies of the three types of prime movers. Whereas the steam and complex gas-turbine plants have roughly the same thermal efficiency, the ability of the steam plant to burn residual fuel gives it a fuel-cost advantage over the gas-turbine plant in the ratio of 3 to 2 (50). The specific fuel consumption of the Diesel is about 25 per cent less than the gas-turbine engine. It also has been demonstrated that the low-speed large Diesel engine can burn residual fuel satisfactorily with some provisions (51, 52, 53, 56). There were 100 Diesel-powered ships running exclusively on residual fuel in 1951, with 600 more under contract (54). Inasmuch as the gas-turbine engine cannot now burn residual fuel, unrestricted as to source at turbine-inlet temperatures above about 1200 F, it suffers a serious fuels-cost disadvantage in relation to the Diesel engine (5, 11).

The marine gas-turbine plant is so new that it is difficult to compare first costs with the steam and Diesel plants. It may be stated safely that the installed cost of the simple-cycle gas-turbine engine will be less than either the steam or Diesel plant. The complex-cycle gas-turbine plant probably will fall between the steam and Diesel plant, depending upon the amount of complexity of the gas-turbine engine.

In maintenance the gas-turbine engine should be superior to both the steam and Diesel plants. Turning again to the Oklahoma Gas and Electric Company's unit it has been reported: "Little maintenance has been necessary on the unit and all work has been done by regular plant forces." (55). The owners of the *Auris* gas-turbine plant also have indicated that the gas-turbine engine will be superior to both the steam and Diesel plant in respect to maintenance (46). As the gas-turbine engine lends itself admirably to automatic control it should require less operating personnel than the other two types of prime movers.

The maneuverability of the gas-turbine engine has been demonstrated thoroughly in locomotive service, central station, industrial applications, and in the nine existing water-borne plants. The gas-turbine engine is far superior to the steam plant in regard to total starting time and is also superior to the large slow-speed Diesel. The Boeing 2MV27B-2 marine gas-turbine engine supplied to the Bureau of Ships requires about 20 sec to go from dead cold plant to full power (5).

Unfortunately, the merchant-marine tonnage laws are such as to discourage any attempt to reduce radically the volume and hence weight of the main propulsion plant (5, 38). This is reflected in the size and weight of the *Auris* gas-turbine plant as shown in Table 4. The gas-turbine engine is inherently suited to extremely small specific volumes and weights. Fig. 10 indicates that the open simple-cycle gas-turbine engine may have $^1/_{10}$ the weight and $^1/_5$ the volume of the Diesel engine. Even the more complex open-cycle gas-turbine engines will show weight and volume advantages over the Diesel and steam plants.

[4] See paper No. 52—F-4A.

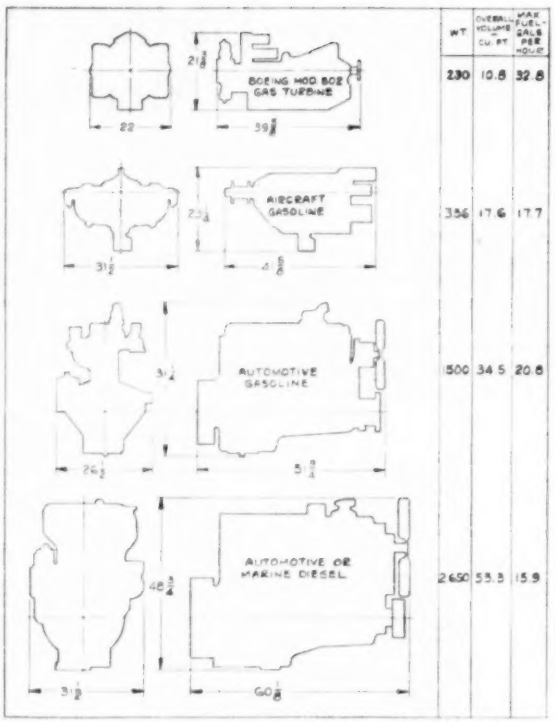

FIG. 10 WEIGHT AND VOLUME COMPARISON OF GAS-TURBINE AND PISTON ENGINES OF EQUAL RATING

The early Elliott gas-turbine plant which embodied reheat, regeneration, and intercooling had a specific weight of only 30 lb per shp (5). The weight of the typical merchant-marine steam plant is something like 75 lb per shp.

A recently proposed 4000-hp merchant-marine gas-turbine plant embodying intercooling and regeneration has a specific weight, without gear, of from 3 to 5 lb per shp (39). This can hardly be termed a typical plant however, as will be noted from the values shown in Table 4.

By adding components such as intercoolers and regenerators to the simple gas-turbine plant its fuel cost becomes more competitive with the steam and Diesel plants. However, the complex gas-turbine plant will have greater first cost, maintenance, weight, and volume with possibly less reliability than the simple-cycle gas-turbine engine.

CHOICE OF CYCLE

It will have been noted that the paper thus far has been limited to the open-cycle-type gas-turbine plant. This has been done because the open-cycle engine seems to be more desirable and competitive for marine propulsion in certain ships in comparison to the Diesel and steam plants than either the semiclosed or closed-cycle gas-turbine plants. Both the semiclosed and closed-cycle (also known as hot-air or aerodynamic) engines are generally more complicated than even the complex open-cycle gas-turbine engine. They also are inherently more efficient at part load. However, whenever this equipment is used the over-all size and weight are increased. In some respects the closed-cycle gas-turbine plant is a steam plant using air instead of vapor as the

TABLE 4 MERCHANT MARINE PROPULSION GAS-TURBINE PLANTS

1. Builder	British Thompson Houston Co.	Elliott Co.	Elsinore Co.	Fiastreda	Rateau	Sulzer Bros. Ltd.
2. Shaft hp continuous	1,200	2,500 *	3,000	3,500	3,200	7,500
3. Shaft hp max.	1,200	2,500 *	3,000	3,600 *	3,900	7,500
4. Cycle - See Ref.23	1-0-51	2-1-72	2-1-90	2-1-75	2-1-84	2-2-?
5. Compressor Inlet Temp. °F	68	80	68	-	-	-
6. Turbine Inlet Temp.°F	1,200	1,400	1,202	1,153 *	1,400	1,200
7. Turbine Inlet Temp.after reheat °F	None	1,400	1,202	1,172 *	1,292	
8. Pressure Ratio	4.24	5.75	5	5.5	9	19
9. Total plant wght.lbs	118,000 (1)	126,300 (1)	156,800	320,000	192,000	-
10. Specific plant weight lbs/hp	98.4	50.5	52.2	91.5	49.4	-
11. Length	24' 2" (1)	21-3/4'	30'	-	24' 7"	-
12. Width	6' 5"	16-1/2'	24'	-	22' 2"	-
13. Height	12' 5"	15-1/2'	11'	-	28' 7"	-
14. Starting Method	Electric Motor 50 hp	Electric Motor 150 hp	Electric Motor	Steam Turbine (Compressed Air)	Steam Turbine	Electric Motor
15. Air Mass Flow lbs/sec	29.9	28.8	41.5	50	40	103
16. Specific Power hp/lbs/sec	40.1	95.5	72.5	70	92.5	72.8
17. Specific Fuel Consumption lbs/hp hr	0.685	0.55	0.45	0.497 *	-	0.46
18. Plant thermal eff. %	20.1	23.6	30.6	26 *	28.2	30
19. Higher Heating value	18,500	19,690	18,500	19,690	-	18,500
20. No. Primary Combustion Chambers	2	1	1	1	1	1
21. Type Primary Combustion Chambers	Refractory Lined	Cylindrical	Counter Flow	Cylindrical	-	Tubular
22. Fuel	Residual Fuel 1500 secs red.No. 1 at 100° F	Diesel Oil	Residual Fuel 370 secs red. at 100° F	Diesel Oil	Residual Fuel	Residual Fuel
23. No. Reheat Combustion Chambers	None	1	1	2	1	1
24. No. Intercoolers	None	1	1	1	1	2
25. Type	-	Extended Surface	Tubular	Tubular	Multicellular	Tubular
26. Intercooler Thermal Ratio %	-	90	83	-	85	-
27. Type Regenerator	Tubular	Extended Surface	Rotary	Tubular	Tubular	Tubular
28. Regenerator Effectiveness %	51	72 *	90	75 - 80	84	?
29. Components cooled	None	Turbine casing, bearing casing	Turbine Shaft	-	-	-
30. Type Cooling	-	Internal Air Boundary Layer Air	Internal Air	-	-	-
31. Ship Reversing Method	Electric Drive	Controllable Pitch Propeller	Controllable Pitch Propeller	Reverse Gear	Controllable Pitch Propeller	Electric Drive
32. Compressor Drive turbine	High Pressure turbine	Low Pressure / High Pressure	High Pressure	High Pressure	Low Pressure / High Pressure	Air Turb. / High Pressure
33. No. Turbines	1	1 / 1	1	1	1 / 1	1 / 1
34. Turbine rpm	5,996	3,600 / 3,800	6,300	4,518*	5,680 / 9,100	7,300 / -
35. Type Turbine	Axial	Axial / Axial	Axial	Axial	Axial / Axial	Axial / Axial
36. No. Turbine Stages	7	10 / 10	4	13 Double Flow	5 / 3	- / -
37. Adiabatic Turbine Eff. %	84.3	91 / 89	86	-	86 / 85	- / -
38. Power Turbine	Low Pressure	Low Pressure	Low Pressure	Low Pressure	Low Pressure	Low Pressure
39. Power Turbine rpm	3,000	Same Turbine as Low Pressure Unit	5,400	3,080	Same Turbine as Low Pressure Unit	-
40. Type Turbine	Axial		Axial	Axial		Axial
41. No. Turbine Stages	6		4	8 Double Flow		5
42. Adiabatic Turbine Eff. %	85.2		86	-		- / -
43. Compressor	-	Low Pressure / High Press.	Low Press. / High Pressure	Low Press. / High Press.	Low Press. / High Pressure	Low Press. / High Press.
44. No. Compressors	1	1 / 1	1 / 1	1 / 1	1 / 1	2 / 2
45. Compressor rpm	5,996	3,800 / 3,600	6,300 / 6,300	4,518* / 4,518*	5,680 / 9,100	- / 7,300
46. Type Compressor	Axial	Lysholm / Lysholm	Axial / Axial	Axial / Axial	Axial / Axial	Axial / Axial
47. No. Compressor Stages	24	1 / 1	11 / 13	10 / 17	15 / 15	- / 16
48. Adiabatic Comp. Eff. %	86.3	78 * / 78 *	83 / 83	- / -	86 / 86	- / -
49. Compressure Pressure Ratio	4.24	2.75 / 2.1	2.18 / 2.3	2.04 / 2.77	3 / 3	4.75 / 4.01
50. Compressor Discharge (psia)	58.24	40.5 / 84.5	32.0 / 71.0	30 / 81	42.5	70 / 280
51. No. Recoolers	-	-	-	-	-	1

[1] Includes generator.
* Actual test data

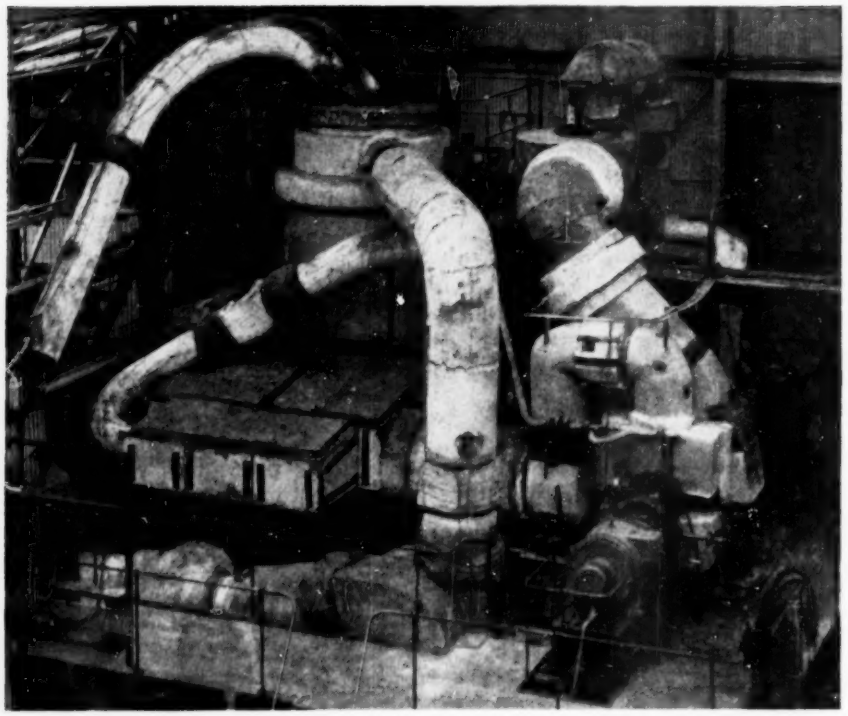

FIG. 11 CLOSED-CYCLE GAS-TURBINE PLANT
(Air heater shown in left background. Photo by John Brown & Company, Ltd., and *The Engineer*.)

working substance, having an air heater instead of a boiler, a precooler in place of the condenser, and an air-heater charging group, in place of the feedwater system. It does of course have the advantages of eliminating the need for distilled water, and better efficiency under certain operating conditions.

Fig. 11 shows a closed-cycle land gas-turbine plant. There has been no great need to try and save weight and space for this application of course, but it can be seen that the air heater represents a large proportion of the plant weight, space, cost, and materials. In addition, the efficiency of the air heater for the closed-cycle plant is 86 to 91 per cent as compared to 98 per cent or higher for the combustion chambers of the open-cycle engine. The warm-up time for the closed-cycle plant generally will be much longer than the open-cycle plant owing to the large thermal capacity of the air heater (38).

The air heater also will necessitate large quantities of strategic materials both for the tubes and the ducting interconnecting the air heater with the high-pressure turbine. All of the heat supplied at the high-temperature part of the cycle must pass through the air-heater tubes so that these tubes are simultaneously under a high pressure and a temperature even higher than the highest cycle temperature, in order to provide the heat transmission to the cycle air from the furnace (56). The conductance between the gas and air in the air heater is of course many times less than between gas and water in a steam boiler (13). It is the practice in some marine gas-turbine engines to group the combustion chambers around the engine between the compressor and turbine with a resultant short distance for the hot gas to travel between the combustion chamber and high-pressure turbine. This will not be possible with the closed-cycle plant.

Another disadvantage of the closed-cycle gas-turbine plant is the present limited prospects of much higher top-cycle temperatures (13, 56, 57, 58). Higher top-cycle temperatures will benefit the gas-turbine engine greatly and there are many ways in which this can be accomplished in the open-cycle engine. The air heater limits the closed-cycle plant to near present levels. It appears that the closed-cycle plant is nearing the upper limit of its thermal efficiency.

The main advantages of the closed-cycle gas-turbine plant include the following (20, 38, 59, 60): 1, Clean operating air; 2, better part-load efficiency; 3, use of residual fuel and coal; and 4, future prospects of atomic power.

For marine service the only substance in the air which will be troublesome is the salt. As was shown in paper 52—F-4A the under-way injection of fresh water into the compressor will prevent build-up of salt deposits. This process might be compared to "blowing tubes" in a steam boiler. Part-load efficiency is not important in merchant-marine service, as previously explained. The use of residual fuel in the marine engine is very desirable. It has been shown in reference (11) that the open-cycle gas-turbine engine can use residual fuel if the inlet temperature is limited to less than 1200 F. There are some eight such low-temperature open-cycle residual-fuel-burning land gas-turbine engines now in operation in various parts of the world (61). Neither the open nor the closed-cycle gas-turbine plant can presently use residual fuels, unrestricted as to source, above about 1200 F, as shown in reference (11).

There is no doubt that one of the means of utilizing nuclear power in ship propulsion will be a closed-cycle gas-turbine engine using perhaps helium as the working substance (62, 63). This form of power is not likely to be available for merchant ships for a few years anyway, and the experience gained in the open-cycle marine gas-turbine engine and the closed-cycle land gas-turbine engine will insure that the technical knowledge is available to build such a plant when the time comes.

It can be seen that of the seven requirements previously listed for a marine engine the closed-cycle gas-turbine plant is inferior to the open cycle in six, and is likely to soon be poorer in the

seventh also. The same applies to the semiclosed cycle in varying degrees. Whereas no closed-cycle marine gas-turbine plant is now building, a semiclosed-cycle engine has been built as discussed under Present Propulsion Plants. There is now no indication that this semiclosed-cycle engine will ever be installed aboard a ship.

Booster or Combined Cycle

Numerous methods have been proposed for combining the gas-turbine engine with other components, usually for the purpose of increasing the thermal efficiency. Most of these schemes utilize the waste-heat energy from the engine exhaust. Some of these methods are as follows:

1 Utilizing steam generated in a liquid-cooled gas-turbine in a steam turbine (2).

2 Utilizing engine waste heat to form steam in a recuperator for the following purposes:

(*a*) Precooling of compressor inlet air.

(*b*) Ship's heating.

(*c*) To heat boiler feedwater such as is done at the Belle Isle Station of the Oklahoma Gas and Electric Company (55, 64, 65, 66).

(*d*) Introduction of the hot engine exhaust gas into a steam boiler either before or after passing through a regenerator, as combustion air. (67, 68, 69, 70).

3 Use of a steam turbine to drive the air compressor and the gas turbine to drive the load (69).

4 Producing distilled water in a vapor-compression distilling plant obtaining energy from the engine exhaust gas (70).

5 The Velox or Sural systems where a turbine is driven by boiler exhaust gases, thereby providing power to drive the compressor, which supplies compressed air to the boiler. Any excess turbine power can be utilized for other purposes (13, 66, 71, 72).

6 Use of the exhaust of a supercharged reciprocating internal-combustion engine to drive a turbine. The turbine may supply only part of the useful work, such as in the Buchi system, or all of the useful work, as in the Götaverken system (72).

All of the foregoing systems may increase the plant thermal efficiency, but at the expense of some or all of the other requirements, that is, reliability, first cost, maintenance, maneuverability, weight, and volume. Therefore, in general, the foregoing systems will find marine application only in special cases. The Götaverken, Buchi, and Sural systems already have seen limited marine service. The turbine in the case of these three systems is not a true combustion-gas-turbine engine, but an exhaust-gas turbine.

Present Propulsion Plants

It would appear from a fuel-cost standpoint that the marine gas-turbine engine burning distillate fuel, is not now competitive with the best steam plants burning residual fuel. It is certainly not competitive with a Diesel engine which burns residual fuel. Therefore, until it can be proved that the marine gas-turbine engine is superior to the steam or Diesel plants in such factors as maintenance, first cost, reliability, weight, and volume to an extent necessary to offset the increased fuel costs, there is little likelihood that it will widely supplant both the steam and the Diesel plants. However, if and when the gas-turbine plant can either burn residual fuel unrestricted as to turbine-inlet temperature and source, operate at appreciably higher temperatures, or incorporate a successful rotary regenerator, the entire situation may change.

Regeneration probably will be used in the great majority of merchant-marine plants. The use of intercooling and/or reheat will depend upon the requirements of the particular vessel. Certainly intercooling is desirable where the plant pressure ratio necessitates the compression process to be done in two compressors. The merchant marine gas-turbine plant would now seem to be limited to special applications. Small passenger vessels which spend a majority of their time in port, such as a cross-channel boat, might be one such application (73).

There is perhaps another interesting special application of the marine gas-turbine plant. It is well known that most cargo ships are too slow for ideal use in wartime service. The high-speed submarine will make such ships even more vulnerable to torpedo attack in any future war. Unfortunately, because of the hull form and "propeller law," there are practical limitations on increasing a vessel's speed by installing additional horsepower. For example it would require the power of a C2 cargo vessel to be increased by about 140 per cent to increase the ship's speed by 3 knots. On the other hand, the hull form is such that an increase of about 83 per cent in power would raise the speed of a C3 cargo vessel 3 knots.

If it could be shown that a vessel with a speed of 21 knots, had a 25 per cent better chance of not being torpedoed than one of 18 knots, there might be justification for raising the horsepower of suitably designed vessels in time of war. This could be done by designing the steam plant originally so that the turbine rotor could operate at the higher speed, and the reduction gear, shafting, and bearings to absorb the extra "wartime" power. Simple compact open-cycle gas-turbine engines, stored during peacetime, could be installed quickly at the outbreak of the war.

Shipowners cannot economically carry excess power around in normal peacetime operation, as it results in increased maintenance, and additional operating personnel and higher wages due to union regulations. This method would therefore seem to offer an economical and quick way of boosting the speed of suitable cargo vessels in time of war.

The merchant marine and gas-turbine industries both owe a tremendous debt of gratitude to the foresight and faith of Mr. John Lamb, and the Anglo-Saxon Petroleum Company, Ltd., for the pioneering effort in installing a gas-turbine plant in the *Auris*.

There are at present six merchant-marine propulsion plants under construction or in operation. These are discussed in alphabetical order.[5] It will be noted that all of these gas-turbine plants, with the exception of the B.T.H. unit, incorporate the three complexities, intercooling, regeneration, and reheat. This perhaps explains why the B.T.H. plant is now the only one at sea, even though construction on all six plants started at about the same time.

1 *British Thomson-Houston Company.* This is a 1200-shp open-cycle gas-turbine plant with a regenerator. Fig. 12 shows the relative arrangement of the plant components. It is now providing part of the propulsive power for the *Auris* and is the only marine gas-turbine plant in commercial service. The vessel *Auris*, a tanker owned by The Anglo-Saxon Petroleum Company, Ltd., was designed originally as an experimental ship. When the *Auris* was commissioned in April, 1948, it was powered by four 1105-bhp Hawthorn-Sulzer Diesel engines each coupled to a generator. In 1951 the starboard inner Diesel alternator was removed and the gas turboalternator substituted in its place. The gas-turbine plant has operated several thousand hours since October 28, 1951. For the second voyage of the *Auris*, from England to Curaçao, the ship was driven solely by the gas-turbine generator set. The vessel's speed was slightly in excess of 7 knots so the passage required 23 days. The gas-turbine plant ran continuously for 543 hr on a residual fuel of 1300 sec Redwood No. 1 at 100 F (1483 SSU) (74). Inasmuch as t_1

[5] Detailed design data on these plants are given in Table 4.

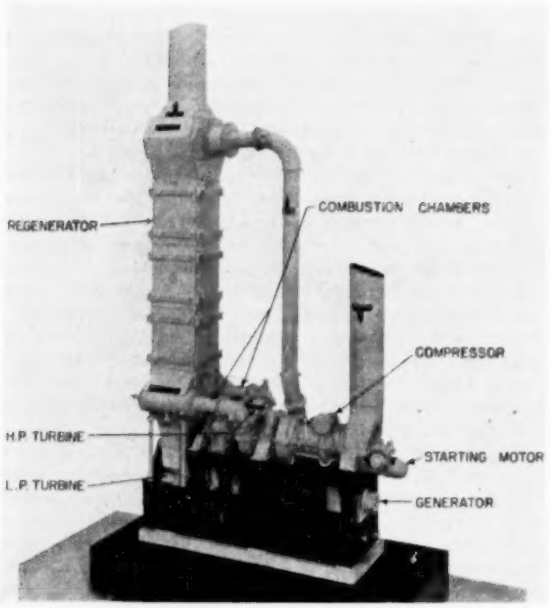

FIG. 12 ASSEMBLY OF BTH GAS-TURBINE PLANT PRIOR TO INSTALLATION IN THE "AURIS"

equals 1200 F[a] for this plant, no great difficulty is likely to result from burning residual fuel (11).

During the shakedown trials of the *Auris*, while fully loaded, the vessel was run for 6 hr on the gas-turbine engine alone. "The absence of vibration during this period was a marked feature of the trial" (75). During the first 1391 hr of operation the gas-turbine engine used only 30 gal of lube oil.

The maximum load obtained on test with this plant was 1022 kw or a 19 per cent overload (76). There is evidently no heat rejection or noise problem in this installation as an observer has reported: "On the demonstration run, apart from the sight glasses of the combustion chambers which indicate that fuel is being burned within, we found it difficult to tell if the gas turbine was in operation" (77).

This plant has an interesting constructional feature. A by-pass valve is provided so that the gas may pass directly from the high-pressure turbine (compressor turbine) to the atmosphere via the heat exchanger, thereby by-passing the power turbine. If either turbine overspeeds this valve automatically opens. It also reduces the starting power and time by being open during the starting cycle, thereby reducing the back pressure on the compressor turbine (78).

It is reported that when this engine was on the test stand the SFC was about 10 per cent lower than the design value at full load, with t_1 50 F below its design value. It requires less than 10 min for this plant to go from rest to full load. The compressor-inlet duct incorporates a silencer. The regenerator is a counterflow tubular type with the air inside the tubes (78). The tubes are 22 ft long and have 1/16 in. OD. Photoelectric cells mounted to "see" the flame in the combustion chambers through ports, cut off the fuel supply if the flame goes out. If one of the burners in the two combustion chambers fails it is possible to remove it without shutting the engine down (79).

It should be noted that this gas-turbine engine was installed in the *Auris* for the purpose of testing a gas turbine under service conditions and obtaining experience in its operation, maintenance, and reliability (80). Future designs will incorporate the lessons learned from this plant (79).

2 *Elliott Company.* The United States Maritime Administration ordered a 3000-shp complex-cycle gas-turbine engine which is a duplicate of two units ordered by the U. S. Navy. For a detailed description of this engine see paper No. 52—F-4C. This engine was to replace the standard reciprocating-engine installation of the Liberty ship collier EC2-G-AW2. Reversing for this vessel was to be performed by a four-bladed controllable-pitch propeller. The present emergency necessitated the services of this vessel elsewhere and therefore the installation of this plant is held in abeyance. Reference (81) gives a description of the originally planned installation features of the plant.

3 *Elsinore Shipbuilding and Engineering Company (Denmark).* In collaboration with Burmeister and Wain and Denmark's Technical University the Elsinore Shipbuilding and Engineering Company commenced work on a 3000-shp open-cycle experimental gas-turbine plant in 1945. The cycle diagram of this unit is shown in Fig. 13. This plant is designed to have a low and high-pressure axial compressor, reheat, intercooling, a rotary regenerator, an axial high-pressure turbine driving both compressors, and an axial low-pressure turbine driving an a-c generator. Reversing is therefore performed by the generator which operates at 3500 rpm directly connected to the low-pressure turbine. The plant is designed for a life of 100,000 hr, but it is expected that the turbine blades may require replacement every 4 years and the combustion-chamber liner yearly. The compressor blades are die-forged from manganese bronze. The high-pressure compressor has 14 stages and the high-pressure turbine 4 stages. The combustion chambers are of the contraflow type. An unusual feature of the turbine casing is that it can be adjusted axially, thereby altering the blade clearances.

Owing to financial considerations only the high-pressure portion of the plant has been built. It went on test in July, 1949, developing 500 hp. The power produced is being used as electrical energy. As the rotary regenerator, with a design effectiveness of 90 per cent, has not yet been perfected, the high-pressure section is using a tubular regenerator with an effectiveness of about 60 per cent.

A layout of this plant in the passenger ship *Hans Broge* indicates that it requires less height, and the length is reduced by one frame space and the whole recess below the third deck in compari-

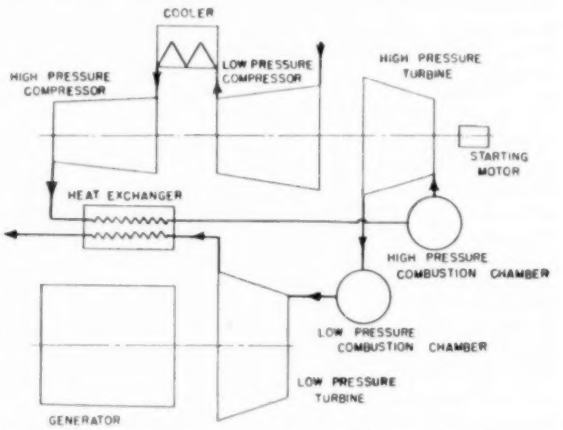

FIG. 13 CYCLE DIAGRAM OF ELSINORE MARINE GAS-TURBINE PLANT
(From *The Motor Ship.*)

[a] Turbine-inlet temperature.

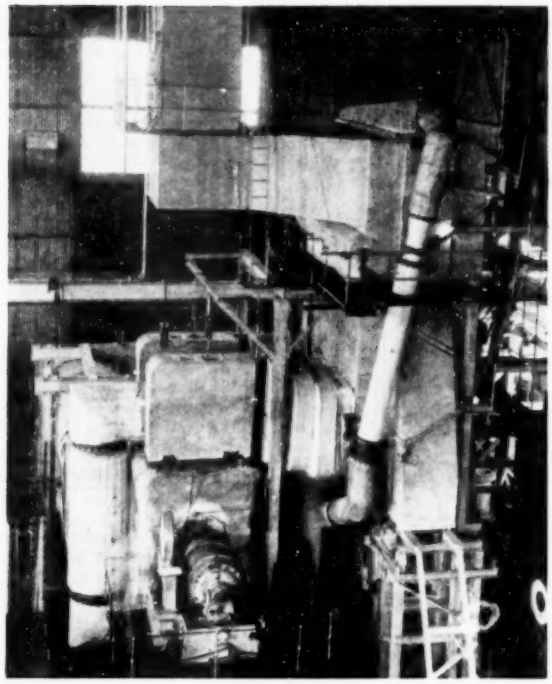

FIG. 14 PAMETRADA 3500-HP MARINE GAS-TURBINE PLANT ON TEST

son with the presently installed Diesel plant. The gas-turbine plant weighs 190 tons including auxiliaries and outfit in the engine room, as compared to the Diesel plant of 325 tons (56, 82, 83, 84).

4 *Parsons and Marine Engineering Turbine Research and Development Association*—(*Pametrada*). This organization was formed in 1944 with the backing of 20 companies from the British shipbuilding industry. Pametrada began gas-turbine design work in 1945, and completed drawings for a 3500-shp open-cycle marine unit in 1946 (85). This plant, shown on test in Fig. 14, includes maneuvering couplings for astern operation, and a speed-reduction gear to provide a main shaft speed of 85 rpm (13).

The cycle diagram for this plant is shown in Fig. 15. This plant incorporates intercooling, reheat, and regeneration. The low-pressure compressor is 10-stage axial flow and the high-pressure compressor 17-stage axial flow, both driven by the high-pressure turbine. The compressor rotor blades are precision-forged from aluminum-bronze and the stator blades are milled from the same material. An unusual feature of this plant is that both turbines are double flow. The low-pressure turbine has 8 stages on each side and the high-pressure turbine 13 stages on each side.

The regenerator is a tubular crossflow unit with the gas making four passes across the tubes. It contains 52 miles of $^3/_8$-in-OD Yorcalnic tubes. The plant is designed for a life of 100,000 hr with a life of 10,000 hr for some of the minor components. Starting power is provided by an auxiliary turbine supplied with either compressed air or steam. A gas by-pass valve is fitted in the entry to the low-pressure (power) turbine so that it may be removed from the gas circuit during starting. A valve is also fitted on the air side of the intercooler to enable blow-off if the low-pressure compressor stalls at low speeds. It is interesting to note that eleven member concerns of Pametrada built components for this plant.

Testing of this gas-turbine engine commenced in 1950. Initially unsatisfactory air-inlet ducting encouraged blade stalling in the compressors. This difficulty has now been corrected and the plant ran about 150 hr during 1951. The maximum load attained during 1951 was 3600 shp at a SFC of 0.497 lb per hphr. As this run was made in December, it is assumed that a lower-than-standard ambient temperature existed. It has been reported that during 1952 the thermal efficiency of this engine has been improved further. The test bed on which this unit is installed is the same as that for a tanker, and it is hoped to install this plant in a merchant ship when the test-stand operation indicates it is ready for sea trials (61, 77, 86, 88, 89).

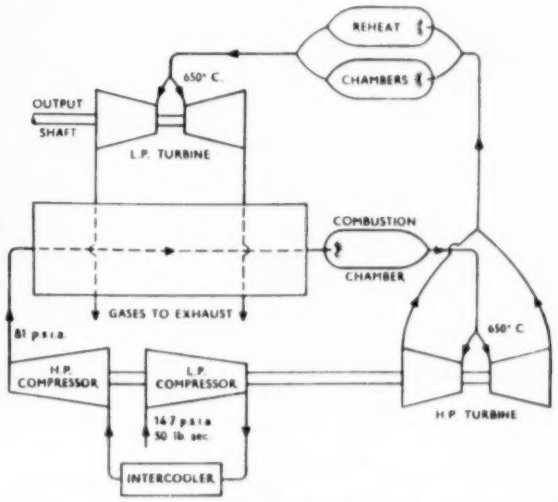

FIG. 15 CYCLE DIAGRAM OF PAMETRADA MARINE GAS-TURBINE PLANT
(From *The Oil Engine and Gas Turbine.*)

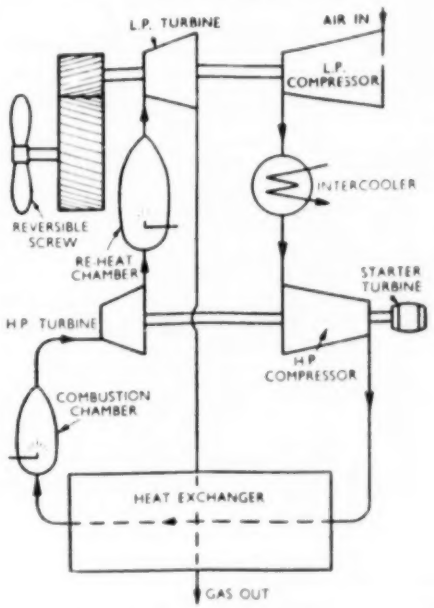

FIG. 16 CYCLE DIAGRAM OF SOCIÉTÉ DES ATELIERS ET CHANTIERS DE BRETAGNE MARINE GAS-TURBINE PLANT
(From *The Oil Engine and Gas Turbine.*)

5 *Rateau—Société des Ateliers et Chantiers de Bretagne.* This is a 3900 maximum shp open-cycle gas-turbine plant incorporating intercooling, regeneration, and reheat. Fig. 16 shows the cycle arrangement. The 5-stage low-pressure turbine drives both the 15-stage axial-flow low-pressure compressor and the ship's propeller. The 3-stage high-pressure turbine drives the 15-stage axial-flow high-pressure compressor. A steam turbine is connected to the high-pressure compressor to provide starting power.

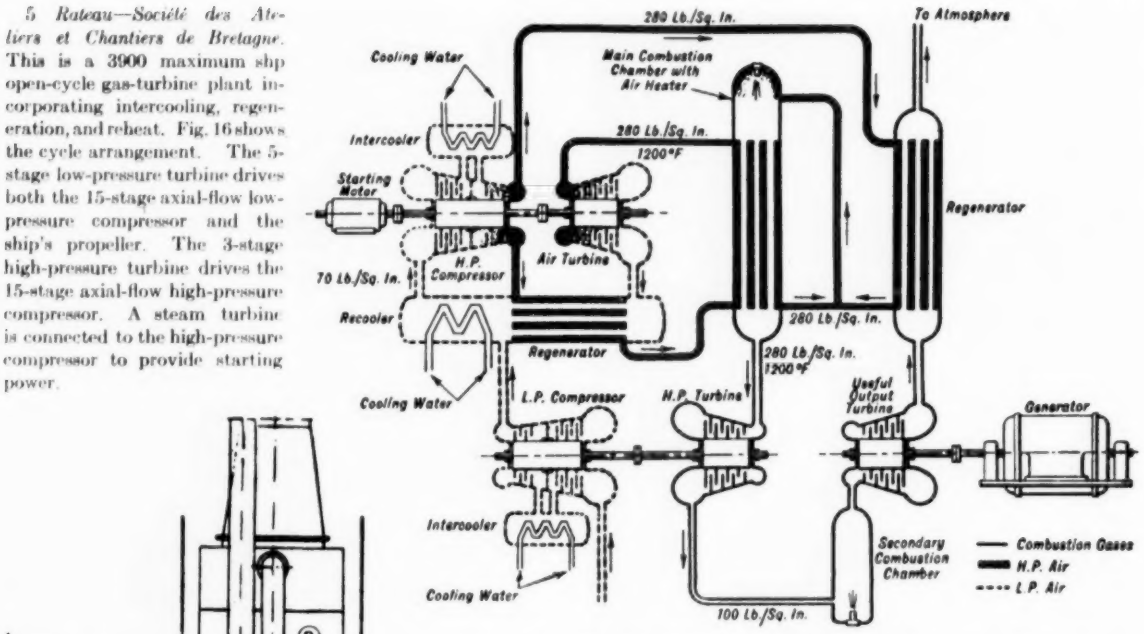

FIG. 18 CYCLE DIAGRAM OF SULZER SEMICLOSED-CYCLE MARINE GAS-TURBINE PLANT
(From *The Engineer.*)

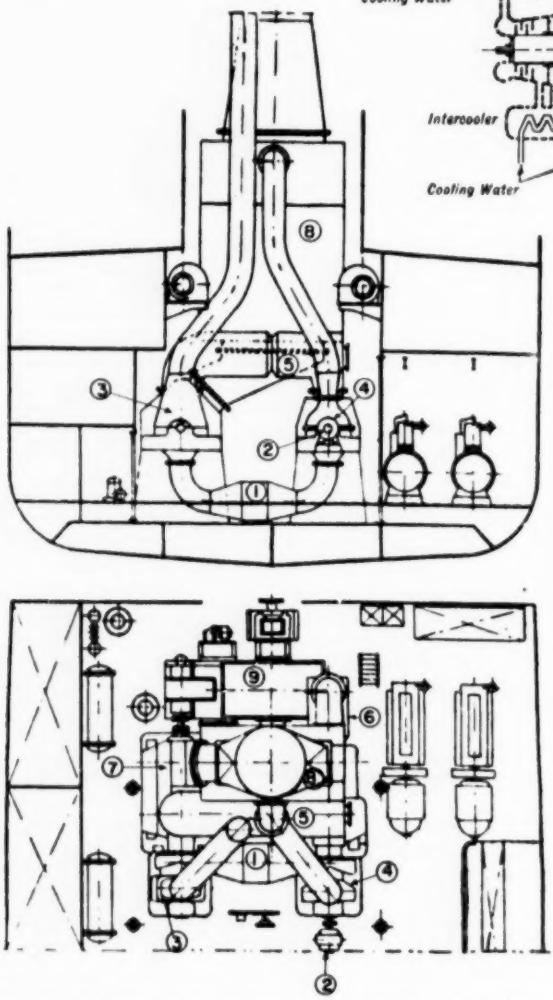

FIG. 17 PROPOSED INSTALLATION ARRANGEMENT OF SOCIÉTÉ DES ATELIERS ET CHANTIERS DE BRETAGNE MARINE PLANT IN LIBERTY SHIP
(1, Intercooler, 2, starting motor, 3, low-pressure compressor, 4, high-pressure compressor, 5, combustion chamber, 6, high-pressure turbine, 7, low-pressure turbine, 8, regenerator, 9, gear. Photo from *The Oil Engine and Gas Turbine.*)

The manufacture of this plant is now complete and it is being assembled on the test stand. The installation of this engine aboard a Liberty ship is being planned for early 1953. Fig. 17 shows the layout of the plant in this ship. Reversing will be handled by a controllable-pitch propeller (1, 9, 56).

6 *Sulzer Brothers, Ltd.* This company has built the only semiclosed-cycle marine gas-turbine plant to date. It is a 7500-bhp engine incorporating intercooling, reheat, and regeneration. The cycle diagram for this plant is shown in Fig. 18. Two axial-flow intercooled low-pressure compressors in series are driven by an axial-flow high-pressure turbine. Two 16-stage axial-flow intercooled high-pressure compressors are driven by an axial-flow air turbine. The useful power is produced by the 5-stage axial-flow low-pressure turbine. The regenerators are tubular counterflow heat exchangers. A starting motor is connected to the high-pressure-compressor shaft. The plant includes four compressors, three turbines, two intercoolers, two regenerators, two combustion chambers, and a recooler.

This engine was operated on test in 1948 but has been so de-emphasized by the builder that little running has taken place since that time. Sulzer has announced no plans concerning the possible installation of this gas-turbine plant aboard a vessel (5, 56, 90, 91).

COMMENT ON AUXILIARY PLANTS

So far as is known, no gas-turbine engine is being built specifically for auxiliary service in a merchant vessel. Such features of the gas-turbine engine as quick-starting, self-contained operation, low weight, and volume will make this engine attractive for many applications requiring intermittent load. Emergency generators or portable fire pumps are two such applications. Cargo vessels or tankers requiring large electrical loads for short periods also offer a good application for a gas turbogenerator set.

Gas-Turbine Progress Report—Naval Vessels

By W. A. DOLAN, JR.,[1] and A. A. HAFER,[2] WASHINGTON, D. C.

Introduction

MANY of the considerations for a propulsion plant discussed in a companion paper[3] apply equally well to naval service. Therefore this paper will be limited to items where the requirements for naval propulsion differ from those for merchant-marine propulsion.

The life of a naval gas-turbine plant may vary from 500 hr, for a small boat engine, to 10,000 hr at full power for a large base-load plant. No hard and fast rule can be laid down for life; the operating characteristics for naval vessels vary widely and hence the life requirements of a propulsion plant.

Powers for the naval propulsion plant also vary tremendously. A small ship's boat may require less than 50 shp while an aircraft carrier would require in excess of 50,000 shp per shaft. A base-load gas-turbine engine of 50,000 shp seems out of the question at this time.

The operating characteristics of the naval vessel are also radically different from the merchant ship. Whereas the latter operates the majority of its life near full power, a destroyer uses the upper 60 per cent of its installed power for less than 0.3 per cent of its operating life (92).[4] Since most combatant vessels cruise between 8 and 30 per cent full power, this low use factor tends to place the gas-turbine engine at a serious disadvantage for a base-load plant, as both the Diesel and complex steam plants have much better part-load efficiency (5).

The requirements of the naval propulsion plant in order of importance have been listed by Sawyer (5) as follows:

1 Maximum reliability.

2 Optimum cruising or light-load fuel economy, plus good fuel economy at higher loads as well.

3 Minimum weight.

4 Minimum volume.

5 Maximum maneuverability, including rapid starting.

6 Minimum maintenance and operating personnel requirements.

7 Resistance to shock or other battle damage.

8 Economy of strategic materials and production effort.

In general, the gas-turbine engine is now superior to the Diesel or steam plants in weight, volume, maneuverability, starting time, maintenance, and operating personnel requirements. As more experience is gained the gas-turbine engine also should be superior in reliability. The gas-turbine engine is now superior to the steam plant in shock and battle damage, but inferior to the Diesel engine. All three types of prime movers require comparable amounts of strategic materials (5). The only requirement where the gas-turbine engine is at a serious disadvantage is in the part-load fuel economy. A companion paper effectively demonstrates how rapidly the SFC of the gas-turbine engine increases at very light[45] loads. It is, therefore, apparent that the gas-turbine plant is suitable for a base-load plant only when the normal cruising power of the vessel is in excess of 50 per cent of the base-load plant rating.

Since the reduction of the propulsion-plant weight and volume is so important in a naval vessel, emphasis will be placed on compact combustion chambers (similar to those used in jet engines), lightweight, highly loaded reduction gears and the rotary regenerator or other compact regenerators. Every pound of weight or space that can be removed from the engine room can be used to enhance the military characteristics of the ship by the addition of supplies, ordnance, or electronic equipment. In this case engine-room weight and volume must include feedwater and fuel storage space. The gas-turbine plant will eliminate the need for the majority of feedwater, but the plant thermal efficiency must be such that the gas-turbine plant plus fuel does not weigh more than the steam or Diesel plants plus fuel for the desired cruising range. Therefore indiscriminate application of the gas-turbine engine to combatant ships actually may result in an increase of plant plus fuel weight. This indicates the need for the naval engineer to understand the limitations as well as the possibilities of the gas-turbine engine. Fortunately there are numerous propulsion-plant applications where the gas-turbine engine is now superior to both the Diesel and steam plants. The wise naval engineer will limit the use of the gas-turbine engine at this time to these applications.

Booster Gas-Turbine Engines

All of the naval gas-turbine engines in excess of 1000 hp that have gone to sea to date have been for booster or peak-load service. The British MTB 5559 has two gasoline engines for cruising power and one gas turbine for use at full power. The MTB's 5701 and 5720 have Diesel engines for cruising power and gas-turbine engines for obtaining high speeds (6, 93). This type of service is analogous to the use of jet engines on the B-36 bombers to provide high bursts of speed during active combat.

The power requirements of large combatant ships are such as

[1] Captain U.S.N., Director, Ship Technical Division, Bureau of Ships, Department of the Navy.

[2] Lieutenant, USNR, Gas Turbine Project Officer, Bureau of Ships, Department of the Navy.

[3] "Gas-Turbine Progress Report—Merchant Vessels," paper No. 52—F-4B.

[4] Numbers in parentheses refer to the Bibliography at the end of the paper.

Contributed by the Gas Turbine Power Division and presented at the Fall Meeting, Chicago, Ill., September 8–11, 1952, of The American Society of Mechanical Engineers.

Notes: This is paper No. 52—F-4C of a Progress Report which the Executive Committee of the Gas Turbine Power Division authorized at its 1951 Annual Committee Meeting. The series includes the following: "Introduction," by R. Tom Sawyer, paper No. 52—F-1A; "Materials, Cooling, and Fuels," by A. A. Hafer, paper No. 52—F-1B; "Cycle Components," by P. F. Martinuzzi, paper No. 52—F-1C; "Automotive," by Frank L. Schwartz, paper No. 52—F-2; "Railroads," by K. A. Browne, J. I. Yellott, and P. R. Broadley, paper No. 52—F-3; "Marine," by W. A. Dolan, Jr., and A. A. Hafer, paper No. 52—F-4A; "Merchant Vessels," by W. A. Dolan, Jr., and A. A. Hafer, paper No. 52—F-4B; "Stationary Electric Generation," by Lee Schneitter, paper No. 52—F-5; "Industrial," by L. N. Rowley and B.G.A. Skrotzki, paper No. 52—F-6; "Aviation," by I. H. Driggs and O. E. Lancaster, paper No. 52—F-7.

The present paper, 52—F-4C, and papers 52—F-4A, 52—F-4B, dealing with the subject of "Marine Progress," all by the same authors, are to be treated as a group; hence the Bibliography, figure numbers, and numbers of tables run consecutively through the three sections.

Statements and opinions advanced in this paper are to be understood as the individual expressions of the authors and not to be construed as official or reflecting the views of the Navy Department, of the Naval Service, or of the Society.

to necessitate the substitution of the steam plant in place of the Diesel engine as the cruising plant. A study made by Captain R. T. Simpson, U.S.N., and Commander W. T. Sawyer, U.S.N., indicates that a combustion steam-gas-turbine plant would reduce the weight of the propulsion equipment of a destroyer by 28 per cent and reduce the length of the machinery space required by the plant by more than 10 ft (92). A steam plant of 9000 shp per shaft would provide sufficient power up to a ship's speed of 20 knots after which the gas-turbine engines would be cut in. Conversely, it would be possible to concentrate higher powers in the same space and weight as the existing steam plant by the substitution of a combustion steam-gas-turbine plant.

Fuels

For large naval gas-turbine engines it would be desirable to burn a fuel heavier than Diesel oil. The residual fuel used by the U. S. Navy, called "Navy Grade Special," is about a grade 4 residual fuel having an upper limit on viscosity of 225 SSU at 122 F. There is at present no incentive for gas-turbine engines used by the U.S. Navy to burn grade 6 or "Bunker C" residual fuel due to the resultant complication of the logistics problem.

Unfortunately, the Navy Grade Special fuel may have as high an ash content and contain as high percentages of vanadium and sodium as Bunker C residual fuel. In addition, the possibility of the fuel being contaminated by salt water in marine service will make it more difficult to use residual fuel in the marine gas-turbine engine than in its land counterpart (11).

There are many applications of the naval gas-turbine engine where it is desirable to burn Diesel oil. These include propulsion for small craft, portable units, generators on Diesel-powered vessels, emergency generators, and booster gas-turbine engines on high-speed craft which have Diesel engines for cruising power. In these applications Diesel oil would probably be used even if the gas-turbine engine could burn residual fuel unrestricted as to source, as the equipment required to heat the residual fuel would be unwarranted.

It would be extremely desirable for the base-load, or booster gas-turbine engine combined with a steam plant to burn residual fuel. The need for large quantities of two fuels required by the combined steam-gas-turbine plant presents many problems. It would be difficult to proportion the tankage between the two fuels, as various employments of the ship would require various ratios of fuel needed by the steam to the gas-turbine plant. The residual-burning steam plant can burn Diesel oil with certain modifications, but the gas-turbine plant is now limited to Diesel oil. Therefore it would probably require carrying a higher percentage of Diesel oil than otherwise might be desirable and hence result in the steam plant burning Diesel oil for appreciable periods with resultant increased fuel costs. A combined steam-gas-turbine plant is, therefore, only justified where the improvements in the ship's military characteristics are such as to override the increased fuel costs.

Even after the marine gas-turbine engine can burn residual fuel unrestricted as to source, it will be necessary to carry a small amount of Diesel fuel for use during starting and stopping (94, 95). This will present no problem on larger naval vessels, since most of them now carry some Diesel fuel for emergency generators and their Diesel-powered boats.

Wet Compression

Wet compression consists of injecting a liquid into the compressor inlet in order to approach an isothermal compression process. The liquid usually used is water, but mixtures of water and alcohol are frequently used in aircraft jet engines. The cooling effect of the evaporating water results in an increase in compressor pressure ratio and air flow (96). The total mass flow also is increased by the amount of injected liquid.

An increase in ambient relative humidity decreases the benefits of wet compression (97). This, of course, indicates that wet compression will be somewhat less effective in marine service than in land service.

The usual aim of wet compression is to inject just enough water to insure saturation of the compressor discharge air. The NACA standard for the amount of water necessary to produce this condition is 0.048 lb of water per lb of air at 59 F. Higher ambient temperatures will require a higher water-air ratio (96). It is generally agreed that if wet compression is to be used for any length of time, distilled water is necessary (70, 98, 99). Wet-compression tests conducted at the U. S. Naval Engineering Experiment Station verified the necessity for distilled water. After running for 15 hr with the injection of tap water, compressor-blade deposits became so serious that the compressor surged and the turbine-inlet temperature was 350 F higher than normal during starting (100). The need for distilled water in wet compression makes its continued use in a base-load naval gas-turbine engine infeasible, especially since intercooling gives the same general advantages as wet compression and is admirably suited to marine service.

A comparison of the water requirements of a typical naval steam plant and a gas-turbine plant indicates that about six times as much distilled water is necessary for wet compression as for make-up feed in the steam plant. A typical 5000-hp gas-turbine engine would require about 39,000 gals of water per day when operating at full power (100). As has been discussed previously, the weight of the gas-turbine plant also must include the fuel required. In case wet compression were used it also would be necessary to include the weight and volume of the additional water tankage and distilling plants required. One test has shown that the total fuel plus water required in the case of a gas-turbine engine using wet compression is about 3.88 times as much as the same engine without wet compression (97).

Wet compression is used extensively in military jet aircraft to produce short bursts of high power (101). There are several naval applications where this same type application appears desirable. PT boats or other naval vessels which require extremely high powers for short periods could obtain bursts of high speed by water injection into the compressor inlet. For this type of service the disadvantages of wet compression would be acceptable. A destroyer having half of its power produced by gas-turbine engines could operate, using water injection, for about 3 hr assuming the same capacity of feed and potable water tanks as now installed (100). Inasmuch as these engines probably will have to incorporate water-spray equipment in the compressor inlet, as discussed in a companion paper,[5] no additional equipment will be required for this type of wet compression.

Advantages of the Naval Gas-Turbine Engine

It is apparent that if the gas-turbine engine is to see extensive use in naval service it will be only because it is superior in some way to all other types of heat engines available. A study of the potential advantages of the gas-turbine engine is therefore in order. Most of these advantages apply more to the simple-cycle gas-turbine engine than the complex cycle, but the latter also embodies the same advantages to varying degrees. These advantages are not necessarily listed in their order of importance, as in various vessels, and applications characteristics desired from the propulsion plant may vary somewhat.

Weight. The gas-turbine engine can be lighter than any other form of existing prime mover (5, 13, 23, 38, 42, 102, 103, 104, 105, 106).

[5] Paper No. 52—F-4A.

Volume. The gas-turbine engine can be installed in less space than any other form of heat engine (5, 45, 102, 103, 104, 105, 106).

Simplicity. This engine is inherently the simplest type now known (23, 37, 102, 103, 104). Rear Admiral W. D. Leggett, Jr., U.S.N., in describing the Solar 1 MC45S-2 gas-turbine engine, produced for the Bureau of Ships, said, "The simplest fuel-burning prime mover yet constructed" (5).

Maintenance. Owing to the small number of moving parts the gas-turbine engine will require less maintenance than other types of power plants (5, 37, 45, 102).

Power. Because the gas-turbine engine is lighter and requires less volume than any other heat engine it is possible to install more power in a given engine space than by any other means (45). This is extremely important in high-speed craft such as PT boats.

Quick Starting and Rapid Acceleration. With the advent of the high-speed submarine and jet airplane this is an extremely important feature. The Boeing 2MV27B-2 gas-turbine engine develops full power from dead cold start in about 20 sec. The 2500-hp Gatric gas-turbine engine in the MTB 5559 requires 90 sec to go from cold start to full power. This is less than one tenth of the time required for the gasoline engines in the same vessel (5). A 15,000-hp Brown Boveri unit has repeatedly gone from cold start to full power in 6 min (37). When this is compared with starting times in the order of 1 to 2 hr for steam plants, the tremendous advantage of the gas-turbine engine is evident.

Rapid Maneuvering. Not only can the simple open-cycle gas-turbine engine be started quickly but it can vary its load at the will of the operator giving excellent maneuverability.

Reliability. Because of the small number of moving parts in the gas-turbine engine it is inherently more reliable than other prime movers. Even at this very early stage of its development operating experience has tended to confirm this.

Minimum Operating and Maintenance Personnel. As the power of the gas-turbine engine is varied ordinarily by changing the fuel flow, only one operator is needed. Most engines can even be started by one person. Also, because of the reduced maintenance of the gas-turbine engine, fewer maintenance personnel will be required. This will enable combatant ships to operate with considerably less engineering personnel.

Reduced Operating-Personnel Training. Because of the simplicity of the operating controls of the gas-turbine engine and the automatic safety devices employed, less time will be required to train competent operating personnel. Three naval enlisted men who had never heard of a gas-turbine engine, and who had no previous engineering training, were given 10 min instruction in operating an LCVP powered by the Boeing 2MV27B-2 engine. With no difficulty, this crew then took the LCVP out by themselves and maneuvered the boat extensively, including beaching operations. The No. 1 3500-kw Okalahoma Gas and Electric Company's gas-turbine plant has been started and brought up to speed by one operator who had no previous instruction on the operation of the unit but merely followed a single-page printed instruction sheet.

Low First Cost. The larger simple-cycle gas-turbine engines even while handmade, are now less expensive than either the Diesel or steam plants. The more complex cycles also should be cheaper once they are on a mass-production basis. It probably will be some time, however, before small gas-turbine engines are cheaper than equivalent Diesel or gasoline engines.

Economy of Production Effort. Because of the smaller weight, volume, and number of parts, the gas-turbine engine should require less total raw materials and man-hours to build on a production basis.

Remote Control. The simple operating control required by the gas-turbine plant lends itself admirably to remote control. In at least one vessel, the gas-turbine plant will be controlled entirely from the bridge.

Excess Power. Power in excess of the rated power will be available whenever the ambient temperature is below the standard temperature.

The gas-turbine engine also enjoys the following additional advantages over the steam plant:

Increased Resistance to Battle Damage. The much smaller size of the gas-turbine plant and lack of extensive steam lines make the gas-turbine plant much less susceptible to damage than the steam plant.

Increased Operating-Personnel Safety. The gas-turbine engine has a much smaller amount of stored energy in it at any instant in comparison to the steam plant (103).

During the war operating personnel sometimes were killed as a result of steam lines rupturing from battle damage. As both the compressor-inlet and exhaust-duct gases are at atmospheric pressure, and the engine "fails safe," it is extremely safe for operating personnel.

Elimination of Components. The gas-turbine plant eliminates the following components required by the steam plant: Boilers, main condensers, air ejectors, main circulating pumps, main feed pumps, main feed booster pumps, emergency feed pumps, main condensate pumps, deaerating feed tanks, and feed heaters.

Elimination of Feedwater. The gas-turbine plant requires little distilled water as compared to the steam plant and, therefore, the size of the evaporating plant and feed storage tanks can be reduced radically. In addition, it will eliminate feedwater treatment.

Smokeless Combustion. Because of the large excess of air in the gas-turbine plant smokeless combustion will result (107). This will eliminate the danger of a ship's smoke being observed by enemy vessels or aircraft.

Suitability for Lower Powers. The steam plant, for main propulsion, is economically limited to a lower rating of about 5000 hp. The gas-turbine engine can be effectively used at much lower powers.

The gas-turbine plant also enjoys the following additional advantages over the Diesel engine:

Reduction of Vibration. The gas-turbine plant has much less vibration at full power than the Diesel plant.

Reduction of Lube-Oil Consumption. The Diesel engine uses about 42 times as much lube oil as the gas-turbine engine (5).

Suitability for Higher Powers. The upper horsepower limit for the naval Diesel engine is about 5000 hp. The gas-turbine plant has its best efficiency at ratings in excess of 5000 hp.

High Torque at Low Powers. The gas-turbine engine develops maximum torque at zero-power turbine speed. This gives it an important advantage over a reciprocating internal-combustion engine for amphibious vehicles.

The gas-turbine engine also has the following additional advantage over the gasoline engine:

Nonvolatile Fuel. The ability of the gas-turbine engine to burn distillate fuel gives it a significant advantage over the gasoline engine, as the use of a volatile fuel in naval service is undesirable from the standpoint of fire hazard.

Disadvantages of the Naval Gas-Turbine Engine

Residual Fuel. The inability of the high-temperature gas-turbine engine to burn residual fuel including Navy Grade Special, unrestricted as to source at this time, is a serious handicap for large base-load plant application.

Thermal Efficiency. The simple-cycle gas-turbine engine has a lower thermal efficiency than either the steam or Diesel plants. Both the simple and complex-cycle gas-turbine engines have

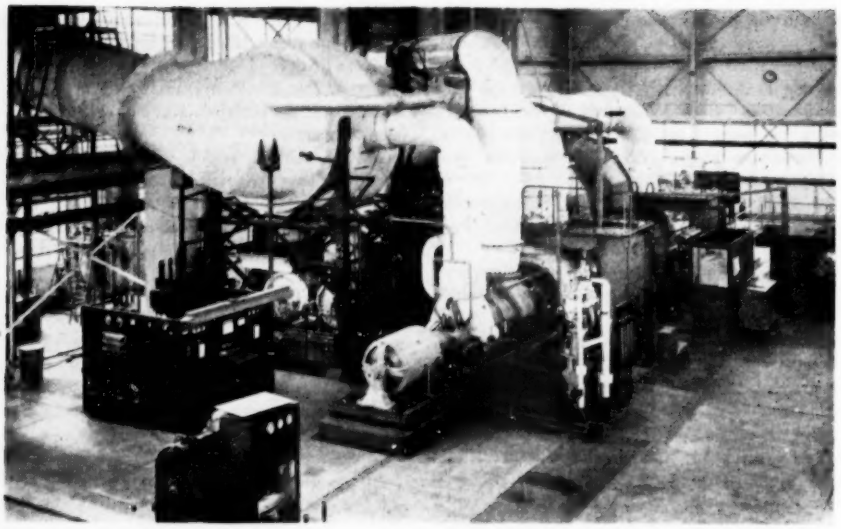

FIG. 19 U. S. NAVY'S ALLIS-CHALMERS GAS-TURBINE PLANT ON TEST AT U.S.N. ENGINEERING EXPERIMENT STATION
(Official U. S. Navy photograph.)

poorer part-load thermal efficiency than the Diesel or steam plants.

Ducting. The gas-turbine engine requires larger air-inlet and exhaust ducting than the Diesel or steam plants.

SUMMARY OF NAVAL GAS-TURBINE PLANT

It would appear that the gas-turbine engine can now be used advantageously to power small short-range vessels, landing craft, and high-speed craft such as PT and air-sea rescue boats. It is ideal for providing booster power for base-load Diesel plants. It is attractive for the same type combination with a steam plant, and when able to burn residual fuel may well see extensive application in a combined steam-gas turbine plant. A complex-cycle base-load gas-turbine plant, augmented by simple-cycle gas-turbine engines for high powers, is attractive where the cruising power requirements of the vessel are not less than about 3000 to 4000 hp per shaft. The base-load engine should operate at 50 per cent or more of its rated power at the cruising condition.

As higher pressure ratios and turbine-inlet temperatures are more important in the naval engine than in the merchant-marine plant, regeneration for base-load plants may be used only at part loads.

PRESENT PROPULSION PLANTS

A number of naval propulsive gas-turbine engines have been, or are now being built to power naval vessels in both this country and abroad. As was noted in a companion paper,[5] most of the units now at sea are for naval propulsive service. If we include experimental units, there are 15 different types of gas-turbine engines manufactured or building for this usage. The actual number of engines is much higher. Naturally, much of the data on these engines have not been released for publication. A description of these plants is given in the following by country and in chronological order.[6]

[6] Detailed design data on the following plants when available is given in Table 5 of this paper.

United States.

The United States Navy was the first to enter the naval gas-turbine field when, in 1939, the Bureau of Engineering (now the Bureau of Ships) requested the National Academy of Sciences to investigate the feasibility of the gas-turbine engine for naval service. After 2 years of study this committee recommended the establishment of a naval gas-turbine program including the construction and exhaustive laboratory testing of a gas-turbine engine capable of sustained operation at 1500 F (108). This resulted in a contract being awarded to the Allis-Chalmers Company in 1940, for the design and construction of a 3500-hp unit suitable for laboratory testing (109). As this unit incorporated an axial-flow compressor and turbines, in 1942 two other laboratory units were ordered. A 2500-hp engine utilizing Lysholm compressors was ordered from the Elliott Company, and a 750-hp unit utilizing Birmann mixed-flow compressors and turbines was ordered from the DeLaval Steam Turbine Company (92). As a result of the test experience gained on these laboratory units, a number of gas-turbine engines have been ordered from the Boeing Airplane Company, the Solar Aircraft Company, and Allison Division of General Motors for installation aboard naval vessels.

The system used in assigning model numbers to these Navy gas-turbine engines is as follows:

1 X preceding designation indicates an experimental unit.
2 First part of designation—Shp/100 to nearest hundred.
3 Second part of designation—life (normal rated load):
  (*a*) S, short (0 to 500 hrs).
  (*b*) M, medium (501 to 5000 hrs).
  (*c*) L, long (above 5000 hrs).
4 Third part of designation:
  (*a*) C, constant shaft speed.
  (*b*) V, variable shaft speed.
5 Fourth part of designation—output shaft rpm to nearest hundred/100 (after integral gear where included).
6 Fifth part of designation—manufacturer.
7 Sixth part of designation—Model No. (consecutive numbers

TABLE 5 NAVAL PROPULSION GAS-TURBINE PLANTS

| | | |

assigned for each different-type engine produced by that manufacturer).

A brief discussion in chronological order of these gas-turbine engines, including the laboratory units, follows:

Allis-Chalmers Manufacturing Company (Navy Model No. X30LV50AC-1). This was an open-cycle unit designed for 3500 hp utilizing regeneration as shown in Fig. 19 of this paper. The three primary objectives of the test program carried out at the U. S. Naval Engineering Experiment Station at Annapolis were as follows:

(*a*) To determine the feasibility of continuous operation at a turbine-inlet temperature of 1500 F.

(*b*) To gain experience in the operation of an internal cooling system.

(*c*) To gain experience in the control and operation of a parallel-shaft arrangement.

The plant consists of a 20-stage axial compressor driven by a 5-stage turbine with its own combustion chamber. The power turbine is a 5-stage turbine quite similar to the compressor turbine and has its own combustion chamber. The single regenerator, with an effectiveness of 57 per cent, is a counterflow tubular type containing 8658 $^5/_8$-in-OD tubes. The hot exhaust gas flows inside the tubes.

The first-stage turbine nozzles and both sides of the first-stage rotor disk can be air-cooled. The turbines are similar in construction to steam turbines having two impulse stages followed by three reaction stages. A throttle valve or orifice is installed in the power-turbine combustion-chamber inlet line to control the division of air flow between the two turbines. A by-pass valve is installed in the compressor turbine to allow the first stage to be by-passed during starting to prevent compressor surge.

As this unit was designed for laboratory tests, safety, flexibility of operation, and accessibility were of primary importance and, therefore, weight and efficiency were sacrificed. The unit was first fired on December 7, 1944, and operated about 3700 hr before all tests were completed. The maximum plant output, corrected to standard conditions, was 2990 hp at a turbine-inlet temperature of 1500 F. This plant was dismantled during 1951 (9, 56, 102, 110, 111).

DeLaval Steam Turbine Company (Navy Model No. X7MV36 D-1). This unit was a complex open-cycle plant incorporating regeneration, intercooling, and two stages of reheat. The unusual feature of this gas-turbine plant was that all of the compressors and turbines were of the Birmann mixed-flow type. The 2-stage low-pressure compressor was driven by a single-stage intermediate turbine and the 2-stage high-pressure compressor by a single-stage high-pressure turbine. The power turbine was a single-stage low-pressure turbine incorporating movable nozzle vanes. All three turbines were air-cooled. Plant output was to be controlled by maintaining constant temperature ahead of each turbine and changing only the flow through the plant with the movable nozzle vanes.

Initially, a plant of 4000 hp was contemplated but the difficulties in procuring the large forgings necessary for the Birmann wheel made it desirable to down-rate the development to 750 hp. "Due to mismatching of the turbine and compressor components and due to low turbine efficiency under some operating conditions, this plant did not reach its predicted design efficiency and performance" (102). After the plant tests were completed in 1950, it was dismantled (33, 56).

Elliott Company (Navy Model No. X25LV30E-1). This was a complex-cycle plant incorporating regeneration, intercooling, and reheat designed for an output of 2500 hp. The unusual feature of this plant was the use of Lysholm positive-displacement-type compressors. The low-pressure compressor was driven by a 12-stage high-pressure turbine developing 2500 hp. A 15-stage low-pressure turbine developing 5000 hp, half of which was required to drive the high-pressure compressor, produced the useful work. The compressor casings were water-cooled while the turbine casings were air-cooled. Both turbines had shrouded blades. Elbow-type combustion chambers were employed. A tubular counterflow-type regenerator, consisting of three identical units in parallel, was used with the cold air passing inside the tubes and the hot gas making three passes across the tubes. A total of 8$^1/_2$ miles of $^5/_{16}$-in-OD tubing was contained in the regenerator. The plant-design life was 100,000 hr.

Shore tests were completed on this unit in 1947 and the plant was dismantled (5, 56, 60, 72, 99, 102, 112, 113).

Elliott Company (Navy Model No. 30LV7E-2). The Navy ordered two of these plants which also had a cross-compound cycle quite similar to the first Elliott plant except that the turbine-inlet temperature was increased by 200 F, as noted in Table 5, and the design power was increased to 3000 hp. The Maritime Administration also ordered a duplicate of this plant as discussed previously. A 10-stage high-pressure turbine producing 2330 hp turned the low-pressure Lysholm compressor and a 10-stage low-pressure turbine producing 4500 hp, 1500 hp of which was required for the high-pressure Lysholm compressor, produced the useful work. The plant pressure ratio of 5.8 used in the earlier 2500-hp plant was lowered to 5.75.

The low-pressure compressor had two sets of rotors; both the upper and lower rotors had 4 lobes in the male and 6 lobes in the female rotor. The high-pressure compressor had one set of rotors. Each turbine rotor was built up of 10 disks welded together. The same type of turbine-rotor construction was used in the earlier plant. Only one extended-surface-type regenerator was used.

It would appear that the disadvantages of the Lysholm compressor, that is, low rotative speed, high noise level, increased cost, high specific weight and limited-stage pressure rise, make this type unsuitable for future marine propulsion (114). "On testing the low-pressure turbine, it was discovered that incipient cracks were prevalent in the welds between the disks. The multistage wheels necessitated by the low rpm of the Lysholm compressors and the earlier decision to avoid the complication of reduction gears (between the turbines and compressors) proved to be a misguided choice since the inspection of the earlier 2500-hp plant disclosed the same cracks" (102).

The tests on the Navy's first plant were completed in 1951 and the plant was dismantled (5, 9, 56, 115).

Boeing Airplane Company (Navy Model No. 2MV27B-2-Boeing Model No. 502-2). This is a 160-hp simple open-cycle engine with a free-power turbine. Boeing initially commenced work on gas-turbine engines in 1943, and since 1946 the work on this engine has been sponsored jointly by the Bureau of Ships and Boeing. The engine consists of a single-sided one-stage centrifugal compressor driven by the single-stage axial high-pressure turbine and has a single-stage low-pressure axial power turbine. It embodies two can-type combustion chambers.

The first engine commenced trials in a 10-ton Kenworth truck in March, 1950. The tractor and semitrailer combination gross 68,000 lb. Since that time this truck has traveled many thousands of miles during hundreds of hours of operation. The first tests were made in a truck as the Bureau of Ships was testing a new semiautomatic planetary transmission in this truck chassis and it appeared logical to combine the two tests. The second installation was in a plane-personnel boat (PPB) as shown in Fig 3. This boat underwent tests at the U. S. Naval Engineering Experiment Station (EES) at Annapolis. The third installation was in an LCVP as shown in Fig. 5. This boat is now being tested at EES. Fig. 21 shows the installed engine.

The versatility of the gas-turbine engine is demonstrated by the many different applications made of this engine. In addition to those previously discussed, this same basic engine is being test-evaluated for possible future military application by a number of the Armed Forces. Among these is the Navy's Bureau of Aeronautics for a helicopter drive, the Army's Corps of Engineers for several applications and, as discussed in the next section, it is also being used by the Bureau of Ships in minesweepers (5, 9, 56, 57, 112, 116, 117, 118, 119, 120, 121).

Solar Aircraft Company (Navy Model No. 5MV20S-4-Solar Model No. T-522). This is a 500-hp simple open-cycle gas-turbine engine with a free-power turbine. It is similar to the Solar Model No. 3MC80S-1 engine discussed in the next section. This engine will be used for propulsion of small naval craft.

Allison Division of General Motors Corporation (Navy Model No. 20MV20A-1). This is a 2000-hp simple open-cycle gas-turbine engine with a free-power turbine. It will be used for propulsion of high-speed naval craft.

England.

Metropolitan-Vickers Electrical Company, Ltd. (Model G-1 Gatric). This is a 2500-shp simple open-cycle engine with a free-power turbine which is an adaptation of the F.2 jet engine made by Metrovick (56). The MGB 2009 (later the MTB 5559) shown in Fig. 1, with one Gatric engine and two Packard gasoline engines, first went to sea in 1947. The gasoline engines were used for cruising and reversing power while the gas-turbine engine was used for high-speed operation. The compressor is a 9-stage axial-flow unit having aluminum blades and casing and is driven by the 2-stage axial-flow high-pressure turbine. The mechanically independent low-pressure power turbine is a 4-stage axial-flow unit. It has an unusual-type combustion chamber for a marine unit—an annular chamber with 20 fixed-orifice jet nozzles. Another unusual feature for a marine propulsion engine is the oil-mist type of lubrication system. Each side of the compressor turbine disk is cooled by air taken from the compressor outlet. The interior of the power-turbine drum is air-cooled by fifth-stage compressor extraction air.

The installation details of the Gatric engine are shown in Fig. 8 and the installed engine is shown in Fig. 20. Initially, the gas-turbine engine was fitted with a clutch located between the propeller and reduction gear (and integral with the gear) to prevent the power turbine from motoring when the boat was powered by only the gasoline engines. Tests indicated that this clutch was unnecessary as the power being wasted in windmilling the power turbine with both gasoline engines at rated power was only 1.3 per cent. The difference in vessel speed between having the clutch locked in the engaged position and being freed was only 0.18 knots (122).

Three Gatric engines have been built and used in the MTB 5559. The first is now in the South Kensington Science Museum and the second is undergoing turbine blade-vibration and residual-fuels tests for the Admiralty (3, 4, 5, 7, 9, 18, 21, 45, 56, 85, 102, 123, 124, 125, 126, 127, 128, 129).

Rover Company, Ltd. (Model T.8). As mentioned in a companion paper,[5] the gas-turbine engine manufactured by this company has been installed in two vessels: the *Torquil* shown in Fig. 2, and the HL 3964 shown in Fig. 4. It is a 150 to 185-hp open simple-cycle engine with a free-power turbine as shown in Fig. 22. This engine is similar to the Boeing engine and, interestingly enough, is also being used for vehicle propulsion but in an automobile instead of a truck. It consists of a single-sided one-stage centrifugal compressor driven by a single-stage axial-flow high-pressure turbine and has a single-stage low-pressure axial-flow power turbine. Only one can-type combustion chamber is used as opposed to the first Rover engines which used two combustion chambers.

Two of the Rover T.8 gas-turbine engines were installed in the triple-screw launch *Torquil*. The central screw was powered by a Dorman 4 DSM Diesel engine. The British Admiralty launch HL 3964 has a single Rover T.8 engine for main propulsion. It is the first British boat to depend solely on a gas-

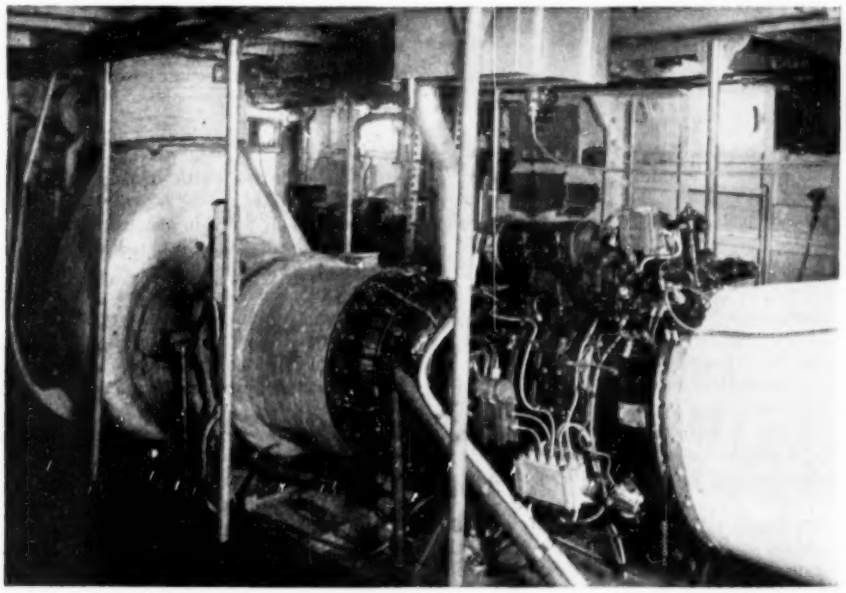

FIG. 20 "GATRIC" GAS-TURBINE ENGINE AS INSTALLED IN MTB 5559

(Official Admiralty photograph.)

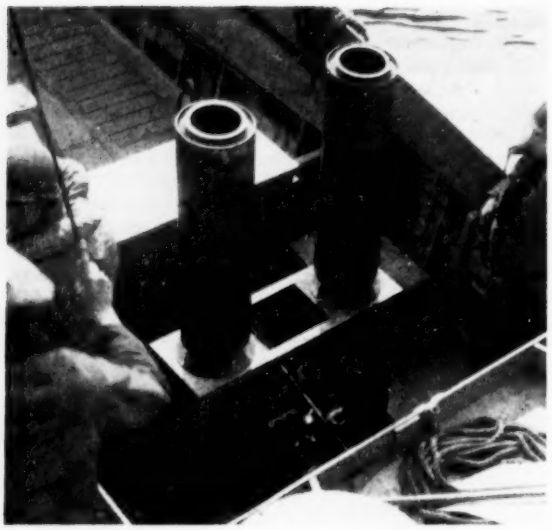

FIG. 21 INSTALLATION OF BOEING-GAS-TURBINE ENGINE IN A U. S. NAVY LCVP
(Official U. S. Navy photograph.)

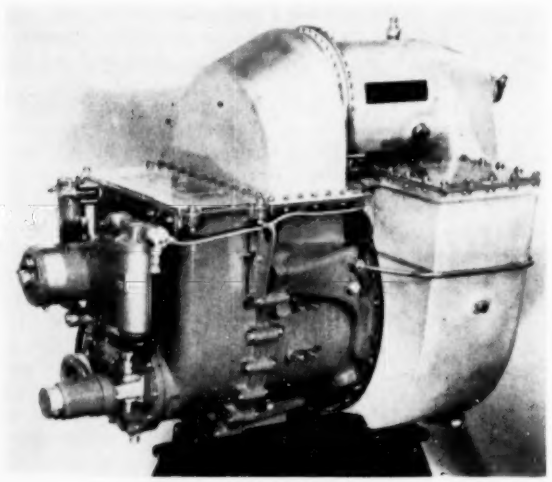

FIG. 22 ROVER 150-HP GAS-TURBINE ENGINE

turbine engine for propulsion following soon after the Boeing powered PPB in the United States. The Admiralty installed this gas-turbine engine in the HL 3964 to evaluate maintenance, as present engines in coastal craft, ship's boats, and harbor launches have always presented a major maintenance problem (130). Four of these engines have been furnished the British Admiralty (85). The Rover Company is working on a regenerator to add to this engine in order to improve the thermal efficiency (5, 9, 45, 56, 131, 132, 133).

Metropolitan-Vickers Electrical Company, Ltd. This is a 4800-shp open-cycle gas-turbine engine of the same general type as the "Beryl" turbojet engine and the earlier 2500-shp Gatric unit made by Metrovick (4, 7). It is a light, medium-life engine. Two gas-turbine engines and two Diesel engines are installed in both the MTB 5701 and 5720. The gas-turbine engines are used for boost power and the Diesel engines for cruising and reversing (7). The MTB 5701 is 120 ft long with a beam of 25 ft. The MTB 5720 is 122 ft 8 in. long with a beam of 20 ft (5, 6, 134, 135).

Pametrada. Design work has been done on a 15,000-shp gas-turbine plant for the Admiralty. A combustion chamber for this plant is reportedly on test. However, it is no longer intended to build the plant (13, 56, 85, 136).

The English Electric Company, Ltd. This company has built a 6000-shp gas-turbine plant for the Admiralty, to be installed in the 1400-ton Captain Class frigate the HMS *Hotham*. This vessel now has a steam-driven turboelectric plant of 6600 hp. The gas-turbine plant was designed with the same output speed as the steam plant so that all of the existing electrical propulsion equipment could be retained, allowing a direct-comparison performance between the steam and gas-turbine plants.

Few details on the arrangement of this plant have been released. It is reportedly a heavy long-life plant using "Yorcalnic" tubes in a regenerator, and includes a 15-stage axial-flow compressor (5, 13, 45). This plant is now on test (9, 56, 85, 102, 123, 136, 137).

Rolls-Royce, Ltd.: This concern is building a 6000-bhp medium-life gas-turbine plant for the Admiralty. It will be installed in the 250-ton gunboat HMS *Gray Goose* which is now propelled by an 8000-shp steam-turbine plant. No other details are available on this unit (5, 9, 56, 85, 102, 137).

France.

Société Turbomeca. This company has specialized in light-weight gas-turbine engines. The French Navy has ordered a 3500-shp simple open-cycle short-life unit for boost power in a naval gunboat. This engine has a centrifugal compressor and a 2-stage axial-flow free-power turbine. Fig. 23 shows the installation details of this engine in the gunboat. This engine is now under construction at Bordes (1, 5, 56).

Sweden.

DeLavals Angturbin. A 2400-hp simple open-cycle engine is being built by this company for the Swedish Navy. It will be installed in a torpedo boat in an installation similar to that of the MTB 5559. The engine has a centrifugal compressor, a single-stage axial high pressure-compressor-drive turbine, and a single-stage low-pressure axial free-power turbine.

PRESENT AUXILIARY PLANTS

The possibility of battle damage, to which naval vessels are always susceptible in time of war, creates a demand for equipment not usually found in merchant service. Two such applications found on all major combatant ships are emergency electrical generators and portable fire-fighting equipment. The gas-turbine engine is a "natural" for emergency power generation owing to its quick-starting characteristics, low weight, and volume, simplicity of control, and low maintenance. Another ideal application of this type engine is to furnish power for portable fire pumps. In addition to the foregoing advantages, for this service the ability of the gas turbine engine to use nonvolatile fuel is extremely important. Another advantageous use of the gas-turbine engine would be for portable air heaters.

It would be anticipated that the gas-turbine engine used for auxiliary purposes would be of the simple open-cycle type. The three applications just discussed have low use factors and, therefore, thermal efficiency is relatively unimportant.

The propulsion gas-turbine plants discussed in a companion paper[2] and in the preceding section of this paper had at least two turbines, mechanically independent of each other. Auxiliary gas-turbine engines usually will be constant-speed single-shaft en-

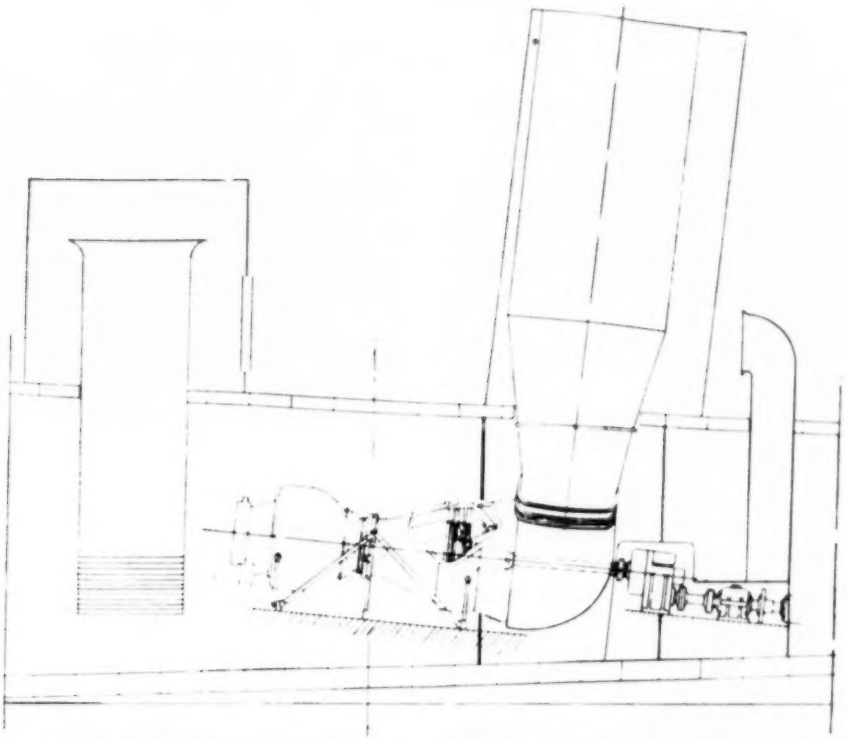

FIG. 23 DIAGRAM OF PROPOSED INSTALLATION OF TURBOMECA 3500-HP GAS-TURBINE ENGINE IN FRENCH GUNBOAT
(Photo from *The Oil Engine and Gas Turbine.*)

gines and, therefore, will be able to attain the ultimate in simplicity.

It is not surprising, considering their many advantages, that a large number of gas-turbine engines are built or building for naval auxiliary service.

Six different types of auxiliary gas-turbine engines are now in service, on test, or under construction. Four of these engines were developed for the Bureau of Ships. These gas-turbine engines are discussed in the following by country.[7]

United States.

Solar Aircraft Company (Navy Model No. 1MC45S-2, Solar Model No. T-45). This is a 45-hp open simple-cycle gas-turbine engine shown in Fig. 24. A contract was awarded Solar in June, 1948, to develop this engine to drive a centrifugal water pump of the same rating as the pump used on the Navy type P-500 portable water pump. This engine has been undergoing tests at the U. S. Naval Engineering Experiment Station since June, 1950.

The engine is extremely simple, consisting of a single-sided single-stage centrifugal compressor, an elbow-type combustion chamber, and a single-stage radial turbine. The simplicity of the compressor-turbine rotor assembly is shown in Fig. 25. It is the first gas-turbine engine in the world to utilize manual starting. The starting method employs two handcranks on a shaft turned by either one or two men. One operator can crank the unit up to sustaining speed in 45 sec.

Two men can carry the engine-pump assembly easily. After once being started, occasional checks of the fuel supply and oil pressure are the only functions necessary for the operator to perform. As this engine is presently used in portable fire-fighting equipment, Diesel fuel is used.

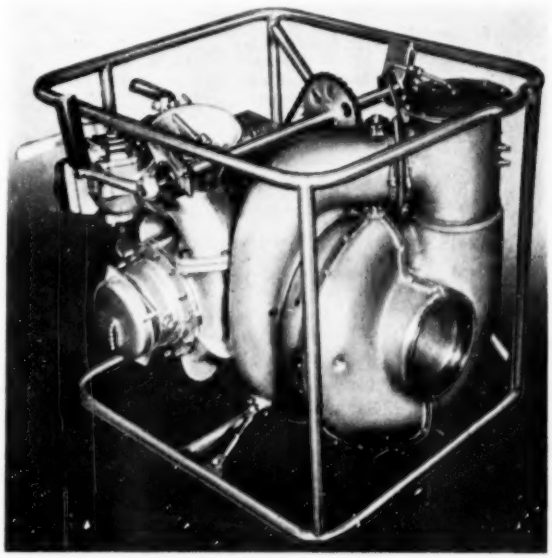

FIG. 24 U. S. NAVY'S SOLAR GAS-TURBINE-ENGINE-DRIVEN FIRE PUMP

[7] Detailed design information when available, is listed for these engines in Table 6 of this paper.

TABLE 6 NAVAL AUXILIARY GAS-TURBINE PLANTS

1. Builder	W. H. Allen Sons & Co. Ltd.	Boeing Airplane Company	Solar Aircraft Company	Solar Aircraft Company
2. Shaft hp Continuous	1,800	160	47 *	317 *
3. Shaft hp (Max.)	1,820 *	-	57	317
4. Cycle See Ref. 23	1-0-70	1-0-0	1-0-0	1-0-0
5. Compressor Inlet Temp. °F	60	80	80	80
6. Turbine Inlet Temp. °F	1,200	1,550	1,142 *	1,500
7. Pressure Ratio	4.25	3	2.44 *	4.8
8. Total Plant Weight lbs	19,000	230	104	561
9. Specific Plant Weight lbs/hp	10.5	1.44	2.21	1.77
10. Length	16' 0"	23.2"	24.5"	53.8"
11. Width	8' 6"	23"	17.5"	29"
12. Height	7' 0"	39.8"	22.3"	33"
13. Starting Method	Electric Motor	Electric Motor (1¼ hp)	Hand Crank	Compressed Air
14. Air Mass Flow lbs/sec	37	3.2	2.35 *	6.6
15. Specific Power hp/lbs/sec	48.5	50	20	48
16. Specific Fuel Consumption lbs/hp hr	0.625	1.3	2.22 *	1.07 *
17. Plant Thermal Eff. %	20.8	10	5.8	12.1
18. Higher Heating Value	19,690	19,690	19,690	19,690
19. No. Combustion Chambers	8	2	1	1
20. Type Combustion Chambers	Can Type	Can Type	Elbow	Can Type
21. Fuel Used	Diesel Oil	Diesel Oil	Diesel Oil	Diesel Oil
22. Type Regenerator	Tubular	None	None	None
23. Regenerator Effectiveness %	70	-	-	-
24. Components Cooled	Turbine Casing, Turbine Disc	None	None	Turbine Disc, Bearing Casing
25. Type Cooling	Internal Air, Boundary Layer Air	-	-	Boundary Layer Air, Boundary Layer Air
26. Compressor Drive Tur.	High Pressure	High Pressure	-	-
27. Turbine rpm	8,000	36,000	40,300	20,138
28. Turbine Type	Axial	Axial	Radial	Axial
29. No. Turbine Stages	2	1	1	2
30. Adiabatic Turbine Eff. %	85 *	79	78 *	-
31. Power Turbine	Low Pressure	Low Pressure	None	None
32. Turbine rpm	6,750	2,750	-	-
33. Turbine Type	Axial	Axial	-	-
34. No. Turbine Stages	1	1	-	-
35. Adiabatic Turbine Eff. %	85 *	79	-	-
36. Compressor No.	1	1	1	1
37. Compressor rpm	8,000	36,000	40,300	20,138
38. Compressor Type	Axial	Centrifugal	Centrifugal	Axial
39. No. Compressor Stages	13	1	1	10
40. Adiabatic Compressor Eff. %	85 *	75	74.5 *	80
41. Compressor Discharge	60	44	36	70

* Actual test data.

This engine has made about 500 starts and has operated 92 hr on tests at the U. S. Naval Engineering Experiment Station (5, 9, 138, 139, 140, 141).

Solar Aircraft Company (Navy Model No. 3MC80S-1, Solar Model No. T-400). In June, 1947, a contract was awarded Solar to construct a 250-kw gas-turbine-generator set to provide emergency power for a ship being constructed by the Bath Iron Works Corporation for the U. S. Navy. This engine consists of a 10-stage axial compressor, a 2-stage turbine, and a single can-type combustion chamber as shown in Fig. 26. It incorporates an inlet silencer and an exhaust muffler. The compressor discharge air makes a 180 deg reversal in direction before entering the combustion chamber. This shortens the power plant by more than 15 per cent. Three cooling-air fans provide cooling air for the area around the compressor thrust bearing at the inlet end, the forward side of the first-stage turbine disk, and the after side of the second-stage turbine disk. One fan is mounted integrally with the forward first-stage turbine disk and the third on the downstream side of the second-stage turbine disk.

The engine is started by high-pressure compressed air (3000 psi reduced to 400 psi) and requires 17 sec to go from dead cold plant to full speed. Inasmuch as this unit is for emergency service it has completely automatic controls. The plant can start, come up to rated speed, and apply load to the generator with no operating personnel present. It is interesting to note that this gas-turbine engine weighs only 7 per cent as much as the Diesel engine which it supplants.

This plant was initially run in September, 1949, and was de-

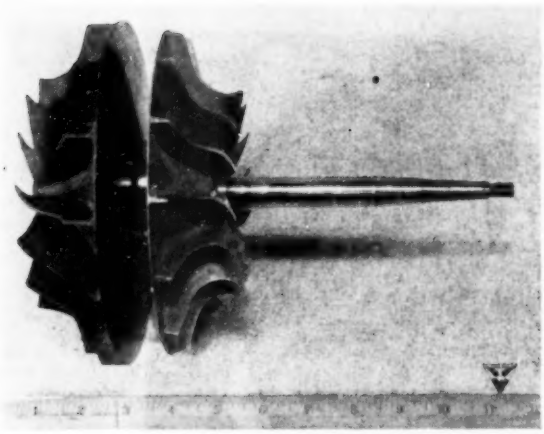

FIG. 25 TURBINE-COMPRESSOR ROTOR FROM SOLAR 45-HP GAS-TURBINE ENGINE

livered to the U. S. Naval Engineering Experiment Station in June, 1950, for further testing. It successfully completed about 90 hr of shore test operation before it was delivered to the shipyard in February, 1951, for installation (5, 8, 92).

Boeing Airplane Company (Navy Model No. 2MV27B-4, Boeing Model 502-6). In September, 1950, the Bureau of Ships awarded a contract to Boeing for the construction of a number of gas-turbine engines to furnish power for mine-sweeper generators. With the exception of the control and exhaust systems these engines are similar to the Boeing Model 2MV27B-2 discussed in the preceding section. Fig. 27 shows one of these gas-turbine-generator sets. A number of these units will shortly be in service (56, 142).

Solar Aircraft Company (Navy Model No. 5MC20S-5, Solar Model No. T-520). This gas-turbine engine is similar to the Solar Model 5MV20S-4 discussed in the preceding section.

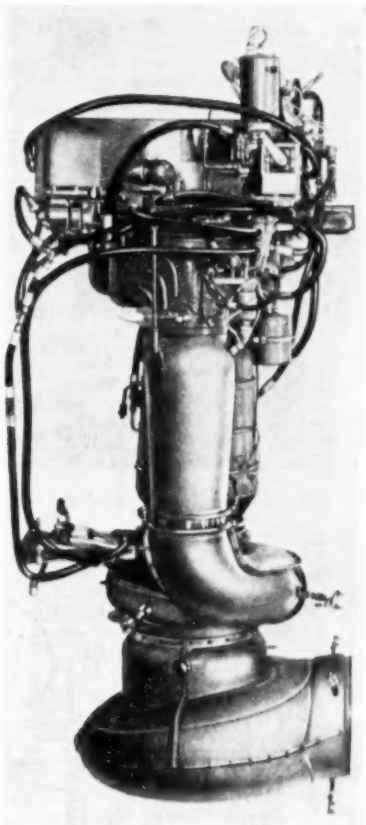

FIG. 26 U. S. NAVY'S SOLAR GAS-TURBINE ENGINE FOR EMERGENCY GENERATOR DRIVE

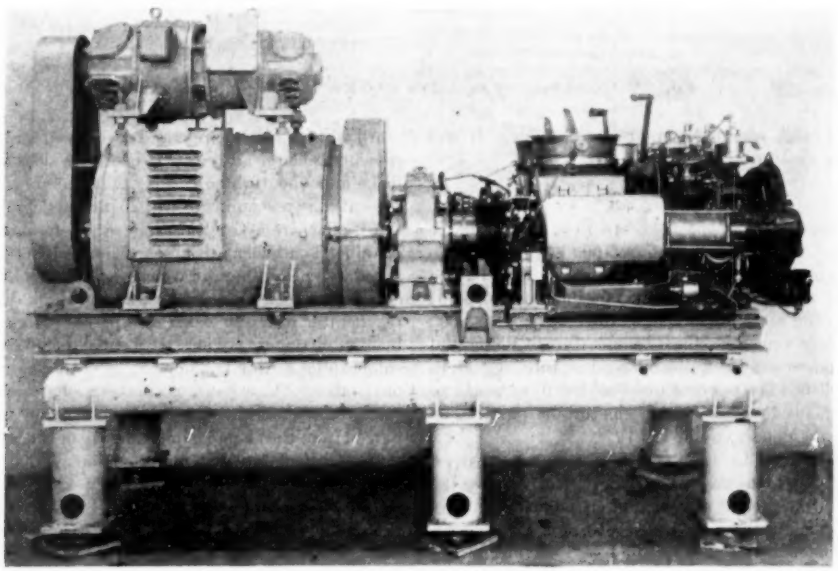

FIG. 27 U. S. NAVY'S BOEING GAS-TURBINE GENERATOR SET

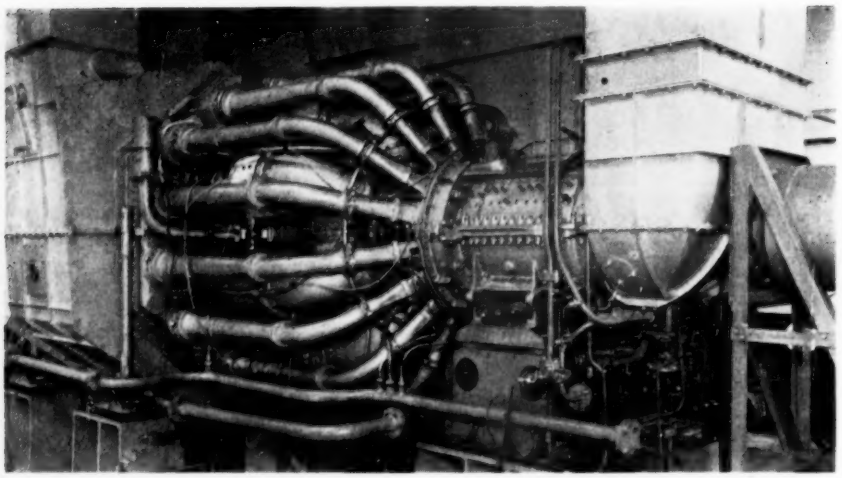

FIG. 28 ALLEN 1000-KW GAS-TURBINE ENGINE ON TEST

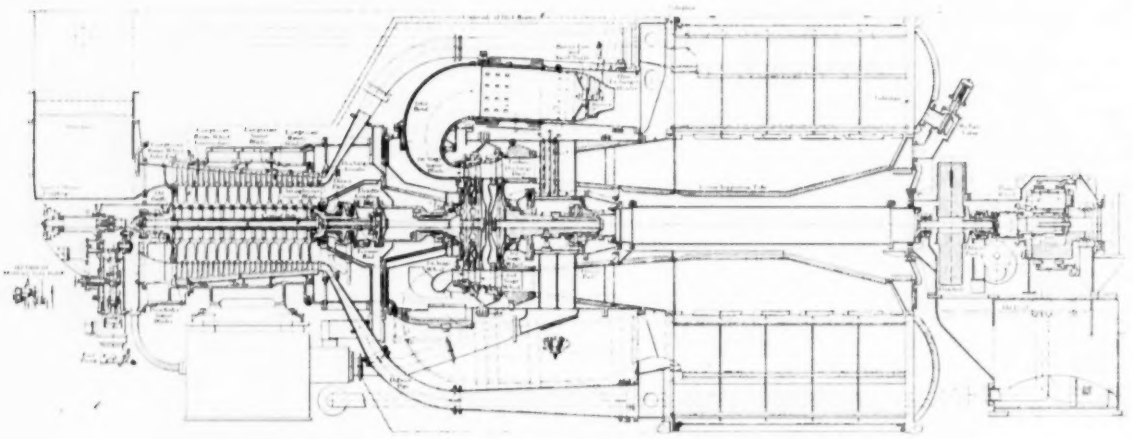

FIG. 29 CROSS SECTION OF ALLEN 1000-KW GAS-TURBINE ENGINE

with the exception that it is a constant-speed engine. It will initially be used for generator drive.

England.

W. H. Allen, Sons and Company, Ltd. In 1948 the Admiralty awarded a contract to this concern for a 1000-kw gas-turbine-generator set shown on test in Fig. 28. The unit was to have a total design life of 100,000 hr, 65,000 hr of which was to be at 80 per cent power and an ambient temperature of 60 F; 33,000 hr at 80 per cent power at an ambient temperature of 100 F; and 2000 hr at full power at an ambient temperature of 100 F. It was to be capable of a 200 per cent overload for 10 min. In so far as is known, this is the first marine gas-turbine plant to be rated at an ambient temperature of 100 F

This engine consists of a 13-stage axial-flow compressor driven by a 2-stage axial-flow high-pressure turbine, a free single-stage axial-flow power turbine, eight combustion chambers, and a regenerator with an effectiveness of 70 per cent. Fig. 29 shows a cross section of this engine, and it will be noted the hot gas reverses flow between the combustion chamber and the compressor-drive turbine.

All turbine blades are wired together in groups of ten. Compressor discharge air is used to cool both sides of the turbine rotor disks and the turbine casing. The combustion chambers are typical can-type units but with an unusual ignition system. Four spark plugs are located in every other crossfire tube so that each chamber is adjacent to a spark plug. This engine also has an annular-type regenerator which results in a compact arrangement. Sixteen diffuser pipes lead the compressor discharge air to the regenerator where it makes two passes before entering the combustion chambers. There is a total of 16,500 $^1/_{16}$-in-OD Yorcalnic tubes in this regenerator, resulting in a total tube length of 12 miles. The exhaust gas makes a single pass across the tubes. Each component of the engine is so constructed that it can be removed from the engine independently of the others.

It is anticipated that major engine overhauls will occur every 5000 hr and minor overhauls every 1000 hr. The time from cold plant to full load is given as $1^1/_2$ min, although the normal time taken is about 6 min. This gas-turbine engine, without its heat exchanger, has been on test since early 1951. Full speed, full load, and overload were achieved in the first series of tests (5, 44, 45, 85, 123, 143, 144, 145, 146).

W. H. Allen, Sons and Co., Ltd.: The Admiralty has announced that this concern is also constructing a 300-hp, simple-cycle, short-life, gas-turbine engine for emergency power generation.

BIBLIOGRAPHY

1 "Gas-Turbine Progress in France," *The Oil Engine and Gas Turbine*, vol. 18, 1950, pp. 139–144.

2 "German Gas Turbine Developments During the Period 1939–1945," by J. W. Adderley, B.I.O.S. Overall Report No. 12, and *Engineering*, vol. 167, April 1, 1949, p. 293.

3 "Prime Movers in 1947," *The Engineer*, vol. 185, January 23, 1948.

4 "Installation of Gas Turbine," by A. T. G. Coleborn, *Marine News*, vol. 35, October, 1948, pp. 36–46.

5 "The Marine Gas-Turbine Plant in 1951," by Cdr. W. T. Sawyer, USN, paper No. 3 presented at the Annual Meeting, November 15 and 16, 1951, of The Society of Naval Architects and Marine Engineers.

6 "Naval Construction in 1951, No. 1," by R. V. B. Blackman, *The Engineer*, vol. 193, January 18, 1952.

7 "Gas Turbines in 1951—No. 1," *The Engineer*, vol. 193, January 11, 1952.

8 "Design Features of a 250-Kw Gas-Turbine Engine," by R. R. Peterson and P. G. Carlson, *Mechanical Engineering*, vol. 74, March, 1952.

9 "Marine Gas Turbine Progress," by John Lamb, Lloyd's List Annual Review, 1951, pp. 1–6.

10 "Resistance Experiments on the *Lucy Ashton*," by Sir Maurice E. Denney, paper presented to the International Conference of Naval Architects and Marine Engineers, London, England, June 26, 1951. Reprinted in abridged form in *Engineering*, vol. 172, July 27, 1951, pp. 121–123.

11 "Gas Turbine Progress Report—Materials-Cooling-Fuels," by Lieut. A. A. Hafer, U.S.N.R., paper no. 52—F-1B, presented at the 1952 ASME Fall Meeting.

12 "Gas Turbine-Alternator Set for D. E. S. *Auris*," The British Thomson-Houston Company, Ltd., publication AG. 944, pp. 1–10.

13 "British Marine Gas Turbine," by Dr. T. W. F. Brown, Trans. North East Coast Institution of Engineers and Shipbuilders, vol. 65, 1949, pp. 117–192.

14 "Discussion on Marine Gas Turbine," by Dr. A. Meyer, Trans. North East Coast Institution of Engineers and Shipbuilders, vol. 63, 1947, pp. D111–D122.

15 "Air Flow Insulation," by E. P. Peregrine and G. Rowland, from advance copy of General Discussion on Heat Transfer, Section II—"Heat Transfer Between Fluids and Surfaces," The Institution of Mechanical Engineers, September 11, 1951, London, England, pp. 23–26.

16 "Ejectors for Cooling a Turbojet Installation," by H. C. Towle and F. V. H. Judd, *Aeronautical Engineering Review*, vol. 10, September, 1951, pp. 20–24.

17 "Analysis of Ejector Thrust by Integration of Calculated Surface Pressures," by J. C. Sanders and V. L. Brightwell, NACA Technical Note 1958, October, 1949, pp. 1–37.

18 "Gas Turbine Propelled M.G.B. 2009," by A. T. G. Coleborn, *The Engineer*, vol. 185, June 25, 1948, pp. 621–624.

19 "Modern Diffuser Design," by G. N. Patterson, *Aircraft Engineering*, vol. 19, September, 1938, pp. 267–273.

20 "Experimental Running of Open-and-Closed-Cycle Gas Turbines," by J. B. Bucher, Paper No. 1125, Trans. Institution of Engineers and Shipbuilders in Scotland, vol. 93, 1949–1950, pp. 275–310.

21 "Power for the Royal Navy," *The Oil Engine and Gas Turbine*, vol. 15, February, 1948.

22 "British Admiralty's Review of 'Experience Gained in M. G. B. 2009' on Compressor Fouling by Sea Air."

23 "The Modern Gas Turbine," by R. T. Sawyer, Copyright 1945, 1947, by Prentice-Hall, Inc., New York, N. Y.

24 "Partial-Load Characteristics of Marine Gas-Turbine Cycles, Part II," by E. G. Sterland, *Engineering*, vol. 166, December 31, 1948, pp. 625–627.

25 "An Introduction to the Gas Turbine," by D. G. Shepherd, D. Van Nostrand Company, Inc., 1949. Copyright Constable & Company, Ltd.

26 "Transmission Systems for Marine Propulsion Gas-Turbine Plants," by W. E. Hammond, Trans. ASME, vol. 71, 1949, pp. 43–57.

27 "Diesel Electric Propulsion of Ships," by E. L. N. Towle, Trans. of the Institution of Engineers and Shipbuilders in Scotland, vol. 93, November, 1949.

28 "Reversible Gear Unit for Uni-Directional Marine Turbines," *Mechanical World*, vol. 120, December 13, 1946.

29 "Merchant Ship Propulsion," by L. Baker, *The Engineers' Digest*, vol. 10, August, 1949.

30 "Propellers With Adjustable Blades," by H. F. Nordstrom, *Meddelande Fran Statens Skeppsprovningsanstalt*, 1945, pp. 1–34.

31 "Controllable-Pitch Propellers," by Cdr. L. A. Rupp, U.S.N. Trans. The Society of Naval Architects and Marine Engineers, vol. 56, 1948, pp. 272–358.

32 "Latest Developments in Reversible Propellers," by Prof. I. C. Burrill, Trans. The Institute of Marine Engineers, vol. 61, 1949, pp. 1–19.

33 Discussion by Major E. C. Hatcher on Reference (32).

34 Discussion by Rear Admiral W. D. Leggett, Jr., U.S.N., on Reference (31).

35 Discussion by Vice Admiral E. W. Mills, U.S.N., on Reference (31).

36 Discussion by G. A. Burkhard on Reference (32).

37 "Marine Gas Turbine," by Dr. A. Meyer, Trans. North East Coast Institution of Engineers and Shipbuilders, vol. 63, 1947, pp. 169–182.

38 "A Gas-Turbine Plant With Reference to a Cargo Vessel," by Cdr. J. J. McMullen, U.S.N., paper No. 4, presented at the 1951 annual meeting of The Society of Naval Architects and Marine Engineers, pp. 1–20.

39 "The Marine Gas Turbine From the Viewpoint of an Aeronautical Engineer," by A. H. Fletcher, paper presented to The Institution of Mechanical Engineers, London, England, January 25, 1952, pp. 1–10.

40 "Motor Shipbuilding in 1951," *The British Motor Ship*, vol. 32, January, 1952.

41 "Shipbuilding in 1948," *The Marine Engineer*, vol. 71, January, 1948.

42 Discussion on "The Gas Turbine as a Possible Marine Prime Mover," by C. R. Soderberg and R. B. Smith, by Captain Lybrand Smith, U.S.N. (Retired), Trans. The Society of Naval Architects and Marine Engineers, vol. 51, 1943, pp. 141–143.

43 "Partial-Load Characteristics of Marine Gas-Turbine Cycles," Part I, by E. G. Sterland, *Engineering*, vol. 166, December 24, 1948, pp. 601–602.

44 "Allen 1000-Kw Gas Turbo-Generator," *The British Motor Ship*, vol. 32, November, 1951, p. 311.

45 "The Story of the British Gas Turbine," Power Jets (Research and Development, Ltd.), A Festival of Britain Survey, published by Sidney-Barton, Ltd., 27 Old Bond Street, London, England, pp. 1–40.

46 "Shell Oil Tanker, *Auris*," by John Lamb, The Anglo-Saxon Petroleum Company, Ltd., release dated January 21, 1952.

47 "Huey (Belle Isle) Gas Turbine Establishes Excellent Operating Record," by J. W. Blake, *Electric Light and Power*, August, 1950.

48 "Operating Experiences With the Gas Turbine at Huey (Belle Isle) Station," by O. Howard, paper presented to the ASME District Meeting, Dallas, Texas, March 30, 1950.

49 "Huey (Belle Isle) Gas Turbine Ticks off 3400 Hours," by J. W. Blake and R. W. Tumy, *Power*, February, 1950.

50 "Post-War Passenger Ship Design," *The British Motor Ship* vol. 32, November, 1951.

51 "Boiler Fuels in Marine Diesel Engines," *The British Motor Ship*, vol. 31, May, 1950.

52 "Burning of Boiler Fuels in Marine Diesels," *The Marine Engineer*, vol. 71, January, 1948.

53 "The Burning of Boiler Fuels in Marine Diesel Engines," by John Lamb, Trans. The Institute of Marine Engineers, vol. 60, February, 1948.

54 "Boiler Oil as Standard Fuel," *The British Motor Ship*, vol. 32, January, 1952.

55 "Combination Gas Turbine—Steam Turbine Unit," by J. W. Blake, *Mechanical Engineering*, vol. 73, 1951, pp. 14–16.

56 "The Gas Turbine Manual," by R. J. Welsh and G. Waller, Copyright 1951, Temple Press, Ltd., London, England.

57 "A Comparison of Gas and Steam Turbines," by Dr. O. A. F. Munzinger, *Combustion*, vol. 20, September, 1948, pp. 39–42.

58 "Some Factors in the Use of High Temperatures in Gas Turbines," by Dr. T. W. F. Brown, Proceedings of The Institution of Mechanical Engineers, London, England, vol. 162, 1950, pp. 167–181.

59 "Closed-Cycle Gas Turbine, Escher Wyss—AK Development, 1945–1950," by Curt Keller, Trans. ASME, vol. 72, 1950, pp. 835–850.

60 "Gas Turbine Construction," by R. T. Sawyer, Copyright 1947, by Prentice-Hall, Inc., New York, N. Y.

61 "Operating Experiences With Stationary Gas Turbines," by P. R. Sidler, paper No. 51—A-104 presented to the 1951 Annual Meeting, ASME.

62 "Atomic Energy Year Book," by John Tutin, Copyright 1949, by Prentice-Hall, Inc. New York, N. Y.

63 "Brevities of Gas Turbine Interest—Utilization of Atomic Energy," *The Oil Engine and Gas Turbine*, vol. 18, July, 1950, p. 105.

64 "3500 Kw Gas Turbine Raises Station Capability by 6000 Kw," by J. W. Blake and R. W. Tumy, *Power*, September, 1948.

65 "The Huey Gas Turbine," by C. C. Willis and E. C. Goldsworth," *Mechanical Engineering*, vol. 72, 1950, pp. 881–885.

66 "Economic Place of Today's Gas Turbines," by A. G. Mellor, General Electric Company publication GER-317.

67 "The Possibilities of Combined Gas and Steam Turbine Installations," by P. Chambadal, *La Technique Moderne*, vol. 42, September 1–15, 1950; reprinted in *The Engineers' Digest*, vol. 11, November, 1950, pp. 395–400.

68 "Gas Turbine-Steam Turbine for Ship Propulsion," by D. Morosoff, *Teknisk Tidskrift*, vol. 21, May, 1949; reprinted in *Marine Engineering and Shipping Review*, vol. 55, May, 1950, pp. 40–47.

69 "Steam and Air Turbine Generating Plants," by R. F. Davis, *Engineering*, vol. 167, January 21, 1949, pp. 49–50.

70 "Values of Wet Compression in Gas-Turbine Cycles," by R. V. Kleinschmidt, *Mechanical Engineering*, vol. 69, 1947, pp. 115–116.

71 "Heat Engines," by K. Baumann, *Engineering*, vol. 167, April 22, 1949, pp. 381–384.

72 "Steam and Gas Turbines, Vol. II," by Dr. A. Stodola, translated by Dr. L. C. Loewenstein, Copyright 1947 by McGraw-Hill Book Company, Inc., New York, N. Y.; reprinted by Peter Smith, New York, N. Y., 1945.

73 "The Prospects of Land and Marine Gas Turbines," by Hayne Constant, from *Internal-Combustion Turbines*, lectures sponsored by The Institution of Mechanical Engineers and reprinted by the ASME, pp. 191–197.

74 "*Auris* Voyage to Curaçao," *The Engineer*, vol. 193, March 28, 1952.

75 "Gas-Turbine Alternator Propelling Machinery in Tanker *Auris*," *Engineering*, vol. 173, January 25, 1952.

76 "Gas Turbines in 1951—No. II," *The Engineer*, vol. 193, January 18, 1952.

77 "The Shell Tanker *Auris*," *Shipbuilding and Shipping Record*, vol. 79, January 31, 1952, pp. 136–137.

78 "*Auris* Set Completes Shore Tests," *The Oil Engine and Gas Turbine*, vol. 18, March, 1951, pp. 348–351.

79 "Gas-Turbine Alternator Propulsive Machinery for Tanker *Auris*," *Engineering*, vol. 171, February 23, 1951, pp. 209–212.

80 "Gas Turbine in the Tanker *Auris*," *The British Motor Ship*, vol. 32, October, 1951, p. 258.

81 "A Marine Gas Turbine Installation," by C. J. Johnson, *Journal of the American Society of Naval Engineers, Inc.*, vol. 59, February, 1947.

82 "Danish Open-Cycle Marine Gas Turbine," *The Oil Engine and Gas Turbine*, vol. 17, October, 1949, pp. 192–193.

83 "An Experimental Danish Marine Gas Turbine," by H. P. Christensen, *The Engineer*, vol. 188, September 9, 1949, pp. 281–283.

84 "A Danish Marine Gas Turbine," by H. P. Christensen, *The Motor Ship*, vol. 30, October, 1949, pp. 281–284.

85 "British Industrial and Marine Gas Turbines," *The Oil Engine and Gas Turbine*, vol. 19, August, 1951, pp. 159–168.

86 "Marine Unit Designed for Long Life," *The Oil Engine and Gas Turbine*, vol. 18, July, 1950, pp. 102–105.

87 "The Pametrada Research Station, Wallsend," *Engineering*, vol. 169, June 16, 1950, pp. 676–678.

88 "Pametrada Research Station," *The Engineer*, vol. 189, June 16, 1950, pp. 714–716.

89 "Marine Gas-Turbine Research," *The British Motor Ship*, vol. 31, July, 1950, p. 129.

90 "Prime Movers in 1947—No. II," *The Engineer*, vol. 185, January 16, 1948, pp. 71–72.

91 "The Sulzer High-Pressure Design," *The Oil Engine and Gas Turbine*, vol. 16, September, 1948, pp. 172–175.

92 "The Prospects of Gas Turbines in Naval Applications," by Captain R. T. Simpson, U.S.N., and Cdr. W. T. Sawyer, U.S.N., *Mechanical Engineering*, vol. 72, 1950.

93 "The Royal Navy, 1951—No. I," *The Engineer*, vol. 193, January 4, 1952.

94 "Combustion System for Burning Bunker C Oil in a Gas Turbine," by B. O. Buckland and D. C. Berkey, paper No. 48—A-109 presented to the 1948 Annual Meeting of the ASME, pp. 1–11.

95 "Heavy Fuel Tests on a Gatric Gas Turbine," Metropolitan Vickers Report dated April 9, 1951.

96 "Theoretical Analysis of Various Thrust-Augmentation Cycles for Turbojet Engines," by B. T. Lundin, NACA Report 981 of 1950.

97 "Theoretical Turbojet Thrust Augmentation by Evaporation of Water During Compression as Determined by Use of a Mollier Diagram," by A. M. Trout, NACA Technical Note 2104, dated June, 1950.

98 "Wet Compression in an Axial-Flow Compressor," by Dr. Shao-Lee Soo, Trans. ASME, vol. 74, July, 1952, pp. 879–890.

99 "The Theory and Design of Gas Turbines and Jet Engines," by E. T. Vincent, Copyright, 1950, McGraw-Hill Book Company, Inc., New York, N. Y.

100 Discussion by Lt. A. A. Hafer, USNR, on reference (98).

101 "An Evaluation of Engine Design Compromises," by N. Burgess, paper No. 140 presented at the Third National Flight Propulsion Meeting, Cleveland, Ohio, March 19, 1948; published by the Institute of the Aeronautical Sciences.

102 "Gas Turbines and Jet Propulsion—Theory and Application," by Cdr. P. W. Gill, USN., Copyright 1952, The United States Naval Institute, Annapolis, Md.

103 "Discussion by Vice Admiral E. W. Mills," USN (Retired), on reference (107).

104 "The Basic Gas-Turbine Plant and Some of Its Variants," by J. K. Salisbury, *Mechanical Engineering*, vol. 66, 1944, pp. 373–383.

105 Discussion by Cdr.(E) G. F. A. Trewby, R. N., on reference (39).

106 "Gas Turbine Performance Characteristics, Design Considerations, and Applications," by Dr. J. T. Rettaliata, *Journal of the American Society of Naval Engineers, Inc.*, vol. 59, August, 1947, pp. 306–333.

107 "The Gas Turbine as a Possible Marine Prime Mover," by C. R. Soderberg and R. B. Smith, Transactions of The Society of Naval Architects and Marine Engineers, vol. 51, 1943, pp. 115–155.

108 "An Investigation of the Possibilities of the Gas Turbine for Marine Propulsion," Bureau of Ships, Navy Department Technical Bulletin No. 2.

109 "Design and Operation of Some Experimental High-Temperature Gas-Turbine Units," by A. D. Hughes, Trans. ASME, vol. 69, 1947.

110 "Test Experience With the Annapolis 3500-Hp Experimental Gas Turbine Plant," by A. C. Skortz and F. R. Gessner, Jr., paper No. 50—S-12, presented at the 1950 ASME Spring Meeting.

111 "A Pioneer Plant in the USA," *The Oil Engine and Gas Turbine*, vol. 17, January, 1950, p. 304.

112 "Steam and Gas Turbines," by R. G. A. Skrotzki and W. A. Vopat, Copyright 1950, McGraw-Hill Book Company, Inc., New York, N. Y.

113 "A Marine Gas Turbine Plant," by C. R. Soderberg, R. B. Smith, and Lt. Cdr. A. T. Scott, U.S.N.R., paper presented to the 1945 Annual Meeting of The Society of Naval Architects and Marine Engineers, pp. 249–289.

114 "Rotary Gas Turbine Compressors," by I. E. Jackson, Jr., *Journal of the American Society of Naval Engineers, Inc.*, vol. 61, November, 1949.

115 "American Marine Gas Turbines," by E. S. Dennison, *The British Motor Ship*, vol. 30, June, 1949, pp. 94–96.

116 "Potent Power Packages—The Boeing Gas Turbines," by H. M. Jacklin, Jr., paper No. 474A presented at the 1950 SAE Summer meeting.

117 "Gas Turbine Propulsion for Ground Vehicles," by W. M. Brown, SAE Quarterly Transactions, vol. 5, January, 1951, pp. 81–93.

118 "Gas-Turbine Auxiliary Power Plants," by P. H. Wilkinson, *Aero Digest*, March, 1950, pp. 30–31.

119 "Three Units in the 50-200 B. H. P. Class," *The Oil Engine and Gas Turbine*, vol. 18, May, 1950, pp. 8–9.

120 "160-Hp Gas-Turbine Unit Will Do Many Chores," by J. C. Anderson, *Power*, vol. 94, January, 1950, pp. 98–101.

121 "Boeing Builds Automotive Gas Turbine," *Product Engineering*, vol. 21, October, 1950, pp. 122–123.

122 "Testing Report, Gatric Set No. 3," Metropolitan Vickers Report No. ET 1094 of September, 1949, pp. 1–31.

123 "A Review of Gas Turbine Progress, 1951," *The Engineer*, vol. 193, January 18, 1952.

124 "A Naval Pioneer," *The Oil Engine and Gas Turbine*, vol. 15, September, 1947, pp. 170–172.

125 "First Marine Application of Gas Turbine," by A. E. Jones, *Motorship*, vol. 32, December, 1947, pp. 33–34.

126 "Gas-Turbine Propulsion in a Naval Vessel," *The Shipbuilder and Marine Engine-Builder*, vol. 54, October, 1947, pp. 458–555.

127 "The Marine Pioneer," *The Oil Engine and Gas Turbine*, vol. 15, April, 1948, pp. 418.

128 "Gas Turbine Propulsion," *British Engineering Export Journal*, October, 1947, pp. 1–8.

129 "Gas Turbine Propelled MGB 2009," *The Engineer*, Part I, vol. 184, September 5, 1947, pp. 218–220; Part II, vol. 184, September

12, 1947, pp. 248–249, and Part III, vol. 184, September 19, 1947, pp. 261–262.

130 "Naval Construction in 1951—No. II," by R. V. B. Blackman, *The Engineer*, vol. 193, January 25, 1952.

131 "Gas Turbine Powered Boat Undergoes Tests in England," *Automotive Industries*, vol. 103, December 1, 1950, pp. 46 and 73.

132 "Two Gas Turbines in a 60-Ft Launch," *The Oil Engine and Gas Turbine*, vol. 18, September-October-November, 1950, pp. 170–171.

133 "60-Ft Gas-Turbine Launch," *Engineering*, vol. 170, October 20, 1950, pp. 308–309.

134 "The Royal Navy, 1951—No. I," *The Engineer*, vol. 193, January 4, 1952.

135 "Brevities of Gas Turbine Interest—Another Gas Turbine Powered M.T.B.," *The Oil Engine and Gas Turbine*, vol. 19, October, 1951, p. 253.

136 "Marine Gas Turbine Progress," *The Oil Engine and Gas Turbine*, vol. 17, February, 1949, p. 345.

137 "Gas Turbine Progress," *The Marine Engineer*, vol. 71, 1948.

138 "The T-45 Power Plant," by A. D. Zakarian and R. R. Peterson, *Journal of the American Society of Naval Engineers, Inc.*, vol. 63, August, 1951, pp. 555–567.

139 "Solar T-45 Portable Gas-Turbine-Driven Pump," Solar Aircraft Company pamphlet.

140 "New Gas Turbine Pump Designed for Navy," *Nickel Topics*, vol. 4, 1951, p. 96.

141 "Simple 45 B.H.P. Gas Turbine for the U. S. Navy," *The Oil Engine and Gas Turbine*, vol. 19, October, 1951, pp. 248–251.

142 "Gas Turbines in 1951—No. III," *The Engineer*, vol. 193, January 25, 1952.

143 "The Allen Gas Turbine," *Shipbuilding and Shipping Record*, vol. 78, November 15, 1951, pp. 623–628.

144 "1000 Kw Gas-Turbine Alternator Set for the Royal Navy," *Engineering*, vol. 172, November 16, 1951, pp 609–613.

145 "1000 Kw Marine Gas Turbine Set," *The Engineer*, vol. 192, November 16, 1951, pp. 612–614.

146 "1000 Kw Gas-Turbine Alternator Set for the Royal Navy," *The Allen Engineering Review*, January, 1952, pp. 7–15.

Gas-Turbine Progress Report—Stationary Electric Generation

By LEE SCHNEITTER,[1] NEW YORK, N. Y.

Domestic Progress

THE demand for jet engines during World War II provided a stimulus for broader development of gas turbines in this country. Shortly after the war, several manufacturers built and tested experimental units of modified aircraft design and on July 29, 1949, the first stationary-type gas-turbine electric-generating unit went into service in a central station in this country. To date, this unit has operated over 20,000 hr and generated about 90,000,000 kwhr.

About six manufacturers in this country are building gas-turbine units suitable for electric generation. Records show that these manufacturers have built, or have under construction, about twenty-three generating units with total capacity approximately 100,000 kw. Some operating experience has been accumulated from units in service but much more is needed. Reports indicate favorable results with units operating on natural gas but some troubles with units burning residual fuel oils. No coal-burning units have been installed but experimental work on a coal-fired locomotive unit is being followed with interest.

Table 1 shows principal specification data on gas-turbine units built or under construction in this country for electric generation. It will be noted that all gas-turbine units sold to date for central-station service in the United States are designed for open-cycle operation. Machines of the simple-cycle type develop thermal efficiencies around 15 to 18 per cent while those with one stage of regeneration show efficiencies around 21 to 23 per cent. Units of the compound type with intercooler and regenerator are offered with efficiencies around 26 per cent or better.

A review of the data shows that there is an equal distribution of units sold for operation with natural gas and with oil fuel. Designs are based on inlet-gas temperatures ranging from 1350 to 1540 F. While advantages claimed for closed and semi-closed cycles are recognized, builders in the United States apparently feel that the simple and direct solution offers the greatest immediate possibilities for success in this country. Complex designs with dual shafts, various stages of compression, intercooling, regeneration, and, in some cases, secondary reheat, have been avoided. Even where need for higher efficiency or control flexibility requires two-shaft design and complication of the cycle by intercooling and reheating, every effort has been made to retain simplicity of layout and compactness. In some designs this has led to use of the so-called split turbine, giving the advantages of two-shaft design while permitting in-line arrangement of component parts.

Further details on types and designs of gas-turbine units for electric generation are given in the paragraphs which follow.

The largest gas-turbine-generating unit under construction in this country is a 15,000-kw Westinghouse Electric Corporation set, ordered by the Public Service Company of Oklahoma for a station at McAlester, Okla. Installation will be completed by the end of 1953, for operation in 1954. This is an open cycle, compound, intercooled, regenerative unit. Its over-all thermal efficiency will be 25.7 per cent, based on high-heat value of natural gas. Unit will have a maximum continuous overload rating (at low ambient temperatures) of 25 per cent. The turbine will be direct connected to a 3600-rpm, enclosed, hydrogen-cooled generator. Approximate dimensions are 45 ft × 80 ft × 18 ft high, and total weight about 689,000 lb. The cycle diagram for this unit is shown in Fig. 1. This cycle shows a low-pressure compressor driven by a low-pressure turbine. Air from the low-pressure compressor is cooled in an intercooler and then passes to the high-pressure compressor, which is driven by the high-pressure turbine. Air from the high-pressure compressor passes through the regenerator and then to the combustors where fuel is supplied. Hot gases from the combustors pass through the high-pressure turbine and then the low-pressure turbine, and the exhaust passes through the regenerator and to the atmosphere. The electric generator is driven from shaft at the end of the high-pressure compressor.

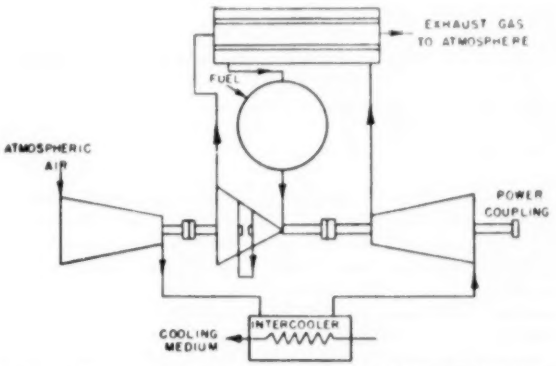

Fig. 1 Cycle Diagram for Westinghouse 15,000-Kw Gas-Turbine Generating Unit

Eleven 5000-kw, open-cycle, compound, electric-generating units are being furnished by General Electric Company. Five of the eleven already have been installed and placed in operation. The operating cycle is similar to that for the 15,000-kw Westinghouse unit just described, although the gas-inlet temperature is 1500 F instead of 1350 F. The pressure ratio is 9:1 and turbine shaft speeds are 8700 and 7200 rpm, respectively, with power

[1] Mechanical Engineer, Ebasco Services, Inc. Mem. ASME.

Contributed by the Gas Turbine Power Division, and presented at the Fall Meeting, Chicago, Ill., September 8–11, 1952, of The American Society of Mechanical Engineers.

Notes: This is paper No. 52—F-5 of a Progress Report which the Executive Committee of the Gas Turbine Power Division authorized at its 1951 Annual Committee Meeting. The series includes the following: "Introduction," by R. Tom Sawyer, paper No. 52—F-1A; "Materials, Cooling, and Fuels," by A. A. Hafer, paper No. 52—F-1B; "Cycle Components," by P. F. Martinuzzi, paper No. 52—F-1C; "Automotive," by Frank L. Schwartz, paper No. 52—F-2; "Railroads," by K. A. Browne, J. I. Yellott, and P. R. Broadley, paper No. 52—F-3; "Marine," by W. A. Dolan, Jr., and A. A. Hafer, paper No. 52—F-4A; "Merchant Vessels," by W. A. Dolan, Jr., and A. A. Hafer, paper No. 52—F-4B; "Naval Vessels," by W. A. Dolan, Jr., and A. A. Hafer, paper No. 52—F-4C; "Industrial," by L. N. Rowley and B. G. A. Skrotzki, paper No. 52—F-6; "Aviation," by I. H. Driggs and O. E. Lancaster, paper No. 52—F-7.

Statements and opinions advanced in this paper are to be understood as the individual expression of the author and not those of the Society.

TABLE 1 GAS TURBINES FOR ELECTRIC GENERATION

Number and normal rating,[a] kw	Builder[b]	User	Location	Initial operation	General Characteristics: Thermal eff, per cent	Operating cycle	Press ratio	Fuel type
15000	W	Pub Serv Co of Oklahoma	McAlester, Okla. Electric generation	1954	25.7	compound	...	Nat gas
5000	W	West Texas Utilities	Stockton, Tex. Electric generation	1952	18.3	simple	...	Nat gas
(2) 5000	GE	Bangor Hydro-Elect Co	Bangor, Me. Electric generation	1950–1952	26.4	compound	9.0	Oil
(3) 5000	GE	Central Vt Pub Service	Rutland, Vt. Electric generation	1951–1952	26.4	compound	9.0	Oil
(4) 5000	GE	Connecticut Lt & Pwr Co	Electric generation	1952–1953	26.4	compound	9.0	Oil
5000	GE	Pub Serv Co of Oklahoma	Elk City, Okla. Electric generation	1951	25.5	compound	9.0	Nat gas
5000	GE	Narragansett Elect Co	Electric generation	1953	26.4	compound	9.0	Oil
4000	GE	Texas Pwr & Lt Co	Gainesville, Tex. Electric generation	1952	21.5	regenerative	5.5	Nat gas
3500	W	Shop Test Unit	.....	1952	22.5	regenerative	...	Oil
3500	GE	Oklahoma Gas & Elect Co	Belle Isle Station Electric generation	1949	15.6	simple	6.0	Nat gas
3500	GE	Oklahoma Gas & Elect Co	Belle Isle No. 2 Electric generation	1952	15.6	simple	5.0	Nat gas
3500	GE	Central Maine Pwr Co	Augusta, Me. Electric generation	1950	16.2	simple	6.0	Oil
(2) 3500	GE	Montana-Dakota Util Co	Williston, Dak. Electric generation	1953	15.6	simple	6.0	Nat gas
1250	W	Shop Test Unit	.....	1949–1952	15.9	simple	5.0	Oil
200	S	U S Navy—Bureau of Ships	Emergency gen unit	1949–1951 (under test)	11.0	simple	4.8	D-oil
320 hp	B	U S Navy—Bureau of Ships	Mine sweepers Aux gen units	1950 (under test)	10.0	simple	2.9	D-oil

[a] Figures in parentheses indicate number of units.
[b] Builders:
B, Boeing Airplane Co.
GE, General Electric Co.
S, Solar Aircraft Co.
W, Westinghouse Electric Corp

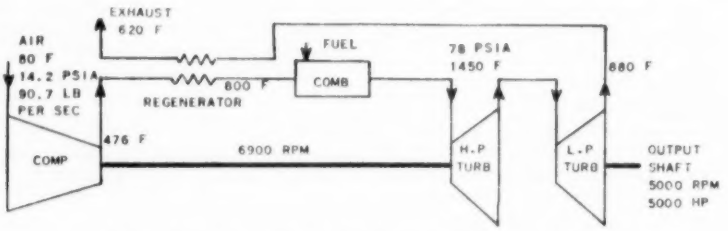

FIG. 2 GENERAL ELECTRIC GAS TURBINE WITH REGENERATOR

take-off at 3600 rpm. The dual axial-flow compressors have 9 and 11 stages, respectively. All but one of the 5000-kw General Electric gas turbines were sold to power companies in New England for operation on oil fuel. Units installed have seen very few operating hours to date. The single unit installed by a utility company in Oklahoma for operation on gas fuel has operated over 4200 hr.

Another type of gas turbine developed by General Electric consists of a simple-cycle, split-shaft machine, with regenerator. This machine is nominally rated at 5000 hp for mechanical drive with variable speed or load, or rated 3500/4000 kw for constant-speed power generation. One of these machines was recently installed by the Texas Power & Light Company at a generation station in Texas for operation on natural gas. Operating gas temperature is 1450 F, at which the thermal efficiency is expected to be 21.5 per cent. Regenerator effectiveness is 80 per cent.

The unit includes a high-pressure turbine that drives a compressor for supplying air to the combustion chambers through the regenerator, and heated by the turbine exhaust. Hot gases discharged from the high-pressure turbine pass through an independently mounted load-shaft turbine, which is in the same casing with the high-pressure turbine. A cycle diagram for the regenerative-type gas turbine is shown in Fig. 2. A similar type unit rated at 3500 kw is also under shop test by Westinghouse.

A number of simple-cycle gas-turbine generating units have been constructed. A 5000-kw Westinghouse set designed for gas temperature of 1350 F and expected efficiency of 18.3 per cent is being furnished to the West Texas Utilities Company. Five 3500-kw units have been sold by General Electric Company. The first of these units, installed at Belle Isle Station of the Oklahoma Gas & Electric Company in July, 1949, already has been referred to as operating over 20,000 hr and as generating about 90,000,000 kwhr. The General Electric units are designed for gas temperature of 1400 F and thermal efficiency of 15.6 per cent on gas. Performance of these units on gas fuel has been most satisfactory.

Another 3500-kw General Electric, simple-cycle, generating unit installed by Central Maine Power Company in August, 1950, for operation on residual fuel oil, has operated 726 hr only and has generated about 2,000,000 kwhr. This unit developed trouble from corrosion due to the presence of vanadium pentoxide in the fuel ash. While research is under way to develop metals that will resist this form of corrosion, the problem is still unsolved. Fuel oils, purchased on special specifications, are required in order to avoid vanadium-pentoxide corrosion.

Several designs of small, high-speed, gas-turbine generating sets have been developed during the past two or three years. A 200-kw emergency generating unit has been developed by Solar Aircraft Company and is under test by the United States Navy. The unit is designed for 1540 F gas temperature and for operation on light Diesel oil with thermal efficiency around 10 to 11 per cent. Units of this type are of light weight and require minimum space but are suitable only for low use factor, where fuel consumption is of secondary importance. The turbine is designated Model T-400 and operates around 20,000 rpm. After

IN THE UNITED STATES (BUILT OR UNDER CONSTRUCTION)

Turbine				Inter-coolers	Regenerators		Com-bustors	Compressors			
Inlet gas temp, deg F	Shafts No.	Shaft speeds, rpm	Blade cooling	No.	No.	Eff, per cent	Type[d]	Type[e]	No.	Stages No.	Air flow, lb per sec
1350	2	3600/3600 Power 3600	Yes	1	1	75	M	A	2	...	..
1350	1	5700/3600	Yes	0	0	..	M	A	1	16	..
1500	2	8700/7200 Power 3600	Yes	1	1	75	M	A	2	9 & 11	72
1500	2	8700/7200 Power 3600	Yes	1	1	75	M	A	2	9 & 11	72
1500	2	8700/7200 Power 3600	Yes	1	1	75	M	A	2	9 & 11	72
1500	2	8700/7200 Power 3600	Yes	1	1	75	M	A	2	9 & 11	72
1500	2	8700/7200 Power 3600	Yes	1	1	75	M	A	2	9 & 11	72
1450	2	6900/5000 Power 3600	Yes	0	1	80	M	A	1	14	91
1350	2	6500/5000 Power 3600	Yes	0	1	75	M	A	1	11	..
1400	1	6700/3600	Yes	0	0	..	M	A	1	15	94
1400	1	6700/3600	Yes	0	0	..	M	A	1	15	94
1400	1	6700/3600	Yes	0	0	..	M	A	1	15	94
1400	1	6700/3600	Yes	0	0	..	M	A	1	15	94
1350	1	8700/3600	None	0	0	..	M	A	1	20	36
1540	1	20138/3600	None	0	0	..	S	A	1	10	6 6
1500	2	36000/22500 Power 3600	Disk	0	0	..	D	C	1	1	3 3

[c] Efficiencies on basis of high-heat value of fuel.
[d] Combustors:
M, Multiple (more than two).
S, Single.
D, Double (two combustors in parallel).

[e] Compressors type:
A, Axial flow.
C, Centrifugal.

some modifications and improvements, the unit has completed rigid tests and is ready for production. The Solar unit is also being considered for propulsion of land vehicles and small Navy craft. Tests also are under way on a 45-hp Solar gas turbine that is hand-started and arranged to drive a portable emergency fire pump or generator.

The Boeing Airplane Company also has developed a high-speed, lightweight, auxiliary generating unit rated around 320 hp with twin-turbine drive. The Boeing turbine is a split-shaft machine with turbines operating at 36,000 and 22,500 rpm, respectively. Gas temperature is 1500 F when operating on Diesel fuel and thermal efficiency around 10 per cent or less. Tests have been under way since 1950, and some design changes have been made to improve reliability and operation. Although many difficulties have been encountered and fuel consumption is far from good, development work is continuing and further improvements are expected.

Allis-Chalmers, after building around twenty-five gas turbines during the past 15 years, for operation in Houdry refineries, has not as yet furnished any electric generating units for central stations. The company previously offered units up to 7500 kw, but reports a slowing down in sales activity until the present limitations on materials and manpower clear up.

Elliott Company—a builder of several gas-turbine units for the U. S. Navy and for locomotive service—has not as yet entered the central-station field.

Recent reports indicate that the United States Navy, Bureau of Yards and Docks, issued specifications for bids on a compact, mobile, gas-turbine generating plant, rated 4000 kw. The unit is designed to fit a 70-ft railway car, but will be removable for barge or ship transportation. Specifications are precise and rigid covering all kinds of service and operating conditions.

While no coal-burning gas-turbine units have been offered for central-station operation, the work of the Locomotive Development Committee on this project will be of interest to some of the central-station operators. At the same time, certain gas-turbine manufacturers are continuing their support of a coal-gasification program. This development relating to combination gas producer and gas turbine seems to offer some solution to the problems connected with burning solid fuels. Research on this project no doubt will be continued.

Corrosion of the high-temperature gas-path parts by residual fuel-oil ash has proved to be a major problem. The chemical elements of vanadium, sodium, and carbon in the ash deposit resulting from combustion of residual fuels, have been found to be active attacking agents. Investigation of the problem has developed ways of distinguishing sodium from vanadium corrosion and has led to the selection of alloys having greater resistance to corrosion. However, the problem is still not solved, and further research will be required.

It is interesting to note that practically all gas-turbine-electric generating units sold to date have been ordered by public-utility operating companies. Aside from the gas turbines placed in Houdry refinery service, there is no record of any units for electric generation having been ordered by industrial plants. Therefore it is apparent from this report that the gas turbine for electric generation is still in its infancy. The few units purchased by utility companies have been justified on the basis of some special economic advantage or on the basis of their need for seasonal, stand-by, peak-load or end-of-line service, in connection with certain power systems. The possibility of using waste-heat recovery from a gas turbine to increase the capacity or in other ways to improve the over-all heat rate of an existing plant has been applied in one case only. It can be concluded that gas turbines of larger capacity and greater efficiency must be developed before the major power companies will become interested to any extent in this type of prime mover as a base-load power unit. Until refinements in design and efficiencies are made, we may expect to see a limited number of basic types of gas turbines used for electric generation in this country.

Foreign Progress

Reports from foreign manufacturers of gas turbines show continuous development of units for central-station and industrial power generation. English, Swiss, and French builders are leading in number of stationary units built or under construction for electric generation. Builders in these three countries, plus one in Sweden, have delivered or have under construction a total of

TABLE 2 FOREIGN GAS TURBINES FOR ELECTRIC GENERATION (BUILT OR UNDER CONSTRUCTION)

Builder[a]	User	Normal rating,[b] kw	Inlet gas temp, deg F	Press ratio	Operating cycle	Fuel type	Thermal eff, per cent[c]	Remarks
	BRITAIN							
BTH	East African P & L Co Ltd	(2) 2500	1200	4.6	Simple	Oil	20	Under construction
JB	No of Scotland Hydro-Electric Board —Dundee	12500	1250	10.0	Closed compound	Oil	30.9	Being erected—Escher-Wyss Lic
BR	Metropolitan Water Board	2500	1340	4.0	Simple	D-oil	15.6	For stand-by service
EE	Metropolitan Water Board	1875	..	..	Simple	Oil	..	For stand-by service
EE	Ministry of Fuel & Power	(2) 2000	..	..	.....	Pulv coal	..	For coal and gas-burning tests
EE	Unspecified	(2) 20000	..	..	.....	Oil	..	Peak-load generation
MV	British Electricity Authority, Trafford Gen Station	15000	1200	10.0	Compound	D-oil	26.3	Being installed
MV	Metropolitan Water Board	2500	1200	5.4	Simple	D-oil	16.0	Under construction
MV	Ministry of Fuel & Power	2000	1250	3.2	Simple	Prod gas	19.4	For coal-burning tests
MV	Shell Petroleum Co Ltd—Maracaibo, Venezuela	1750	1185	5.2	Simple	Nat gas	15.0	Under construction
P	Shop test unit	2500	1200	4.0	Simple	Oil	..	Under construction
P	Nat'l Gas Turb Establishment—Pyestock Station	10000	1200	10.0	Compound	Oil	26.4	Under construction
P	British Electricity Authority—Dunston "A" Power Station	15000	1200	8.0	Compound	Oil	26.3	Under construction
RH	No of Scotland Hydro-Elect Board	750	1345	4.0	Compound	Peat	..	Under construction
	FRANCE							
RT	Test unit	2000	1292	3.8	Simple	Oil	15.0	Under test and redesign
	SWITZERLAND							
BB	Municipal Electric Supply—Neuchâtel, Switzerland	4000	1020	4.0	Simple	D-oil	16.9	In service since 1939
BB	Anglo-Iranian Oil Co Ltd	(3) 4000	1100	4.6	Simple	Nat gas	16.4	Two installed—operation delayed
BB	Corp Peruano del Santo Chimbote, Peru	4000	1100	4.6	Simple	Oil	18.3	Installed 1949
BB	Filaret Sta—Bucharest, Romania	10000	1100	12.0	Compound	Nat gas	21.4	Refinery unit
BB	Lima Lt Pwr & Tramwy Co, Santa Rosa Station, Peru	10000	1100	8.0	Compound	Oil	28.2	Base-load unit
BB	C A Venezolana de Cementos Caracas, Venezuela	(2) 1650	1100	3.0	Regenerative	Oil	20.7	Two units operating
BB	Arabian-American Oil Co	(4) 5000	1200	4.6	Simple	Nat gas	17.0	For oil-field operations
BB	C A Venezolana de Cementos Caracas, Venezuela	5000	1112	4.6	Simple	Nat gas or oil	18.0	For installation in 1952
BB	Raymond Arcache & Co, Alexandria, Egypt	1200	1100	3.0	Regenerative	Oil	21.6	Refrigeration plant
BB	Arbed Steel Works, Dudelange, Luxemburg	5400	1112	3.6	Regenerative	Gas	21.4	In operation
BB	N E Pwr Co—Beznau Station	13000	1112	8.0	Dbl compound	Oil	28.7	Stand-by to hydro
BB	N E Pwr Co—Beznau Station	27000	1112	8.0	Dbl compound	Oil	32.4	Stand-by to hydro
EW	Shop test unit	2000	1292	3.8	Closed	D-oil	29.6	Closed-cycle compound unit
EW	Electricite de France—St. Denis Station, Paris	12500	1250	11.6	Closed	Oil	32.0	Closed-cycle compound unit
O	Shop test unit	1000	1200	4.0	Compound	Oil	..	Tested extensively
O	Compagnie Electricite et Gas d'Algerie	730	1200	..	Regenerative	Oil	..	Waste-heat recovery included
S	N E Pwr Co—Weinfelden Station	20000	1200	20.0	Semiclosed	Oil	30.1	Stand-by to hydro
	SWEDEN							
SW	STAL Factory	2400	..	..	.....	....	..	Under test

[a] Builders
BB, Brown Boveri & Co., Ltd.
BTH, British Thomson-Houston Co., Ltd.
BR, Brush Elect. Engr. Co., Ltd.
EE, English Electric Co., Ltd.
EW, Escher-Wyss Engrg. Works, Ltd.
JB, John Brown & Co., Ltd.
MV, Metropolitan-Vickers Elec. Co., Ltd.
O, Ateliers de Construction Oerlikon
P, C. A. Parson Co., Ltd.
RH, Ruston and Hornsby, Ltd.
RT, Rateau Co.
S, Sulzer Bros., Ltd.
SW, Swenska Turbinsfabriks Aktiebolaget Ljungstrom.

[b] Figures in parentheses indicate number of units.

[c] Thermal efficiencies based on high-heat value of fuel

forty-five gas-turbine-generating units, totaling about 275,000 kw. Activity in England increased beyond all expectations during the past year.

Table 2 shows general specification data for the principal foreign gas-turbine generating units already built or under construction. Doubtless there are other units under test or in use for experimental purposes on which we have no report. The table includes a wide variety of types and sizes. The smallest unit listed is 750 kw, and the largest 27,000 kw. The list includes twelve units of 10,000-kw rating and above. The Swiss firm of Brown Boveri & Company reports fourteen electric generating units in service or nearing completion. Several French firms are carrying on development, but much of this work is related to the free-piston type of gasifier, which is being promoted by one large builder. The STAL company of Sweden has started construction of one unit. The majority of foreign generating units are designed to operate on the open simple-cycle principle. Where higher efficiency is required, manufacturers turn to designs with regenerators and intercoolers, and to the more complex two-shaft, reheat cycles. The table lists three units that will operate on the closed cycle, and one unit of the semiclosed type. It is interesting to note that gas-inlet temperatures for foreign-built turbines are lower than for most American units. The majority of foreign gas turbines are designed for gas temperatures of 1200 F or less. Further details on some of the more important machines ordered for electric generation follow.

The British Thomson-Houston Company, Ltd., reports progress in construction of two 2500-kw gas-turbine-generating sets for the East African Power & Lighting Company, Ltd. These are simple-cycle units that will operate on oil at a gas temperature of 1200 F and expected efficiency around 20 per cent. This company also is building gas turbines for marine applications.

The 12,500-kw closed-cycle gas turbine built by John Brown & Company, Ltd., is being erected at the Dundee plant of the North of Scotland Hydro-Electric Board. The unit will operate on oil fuel and is designed for a gas temperature of 1250 F, at which thermal efficiency should approximate 30.9 per cent. John Brown & Company built the closed-cycle unit for Dundee as a licensee of Escher-Wyss Engineering Works, and for that reason the plant consists of practically the same machinery and elements as the Escher-Wyss unit at St. Denis. More details on the closed-cycle system are included in later paragraphs dealing with the St. Denis installation. The company is also continuing work on several smaller units for closed-cycle operation in plants using coal and waste heat.

John Brown & Company further reports operation of a gas-turbine unit on peat. A cycle diagram of the peat-burning plant

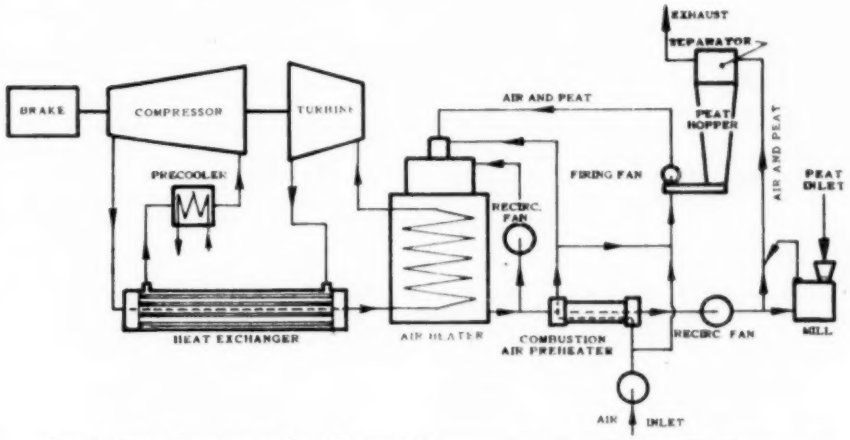

FIG. 3 CYCLE DIAGRAM OF JOHN BROWN & COMPANY, LTD., PEAT-BURNING GAS TURBINE

is shown in Fig. 3. The complete plant was operated solely on peat for the first time in November, 1951, thus being the first peat-fired gas turbine in the world. Circuit air leaves the compressor at 50 psig, being heated to 675 F in the heat exchanger, and to 1200 F in the air heater at which temperature it passes to the gas turbine. From the turbine the circuit air returns to the heat exchanger where it transfers heat to the cooler high-pressure air. It then passes to a precooler where its temperature is reduced to about 75 F before it returns to the compressor inlet and thus completes the closed cycle. The balance of the plant consists of the peat-drying, pulverizing, and combustion system, which is completely separate from the closed-turbine system. However, part of the exhaust gases from the air heater is recirculated for temperature-control purposes, and the remainder passes to an induced-draft fan through a combustion-air preheater, where the inlet air is raised to about 750 F. Some exhaust gas also passes to the pulverizing mill and the separator for drying purposes. Tests on this plant have indicated a peat consumption around 2 lb per kwhr output. It is stated that operation with peat of moisture content up to 50 per cent has been satisfactory but during the coming year, further drying equipment will be installed in order to enable the plant to take peat of a higher moisture content without loss of efficiency.

Reports indicate that English Electric Company, Ltd., has completed tests of several gas-turbine units. The company has several important developments in hand. Units of 2000-kw size are being built for the Ministry of Fuel and Power and will be used for coal- and methane-burning experiments. The pulverized coal will be burned in a cyclone slagging combustion chamber, the resulting gases passing through a dust collector before reaching the turbine. No further details of the plant are available, but it is understood that the unit will be in operation sometime this year. General arrangement of the English Electric 2000-kw coal-burning test plant is shown in Fig. 4. Reports also show that this company is building an 1875-kw generating unit for the Metropolitan Water Board. English Electric also has a contract for two 20,000-kw peak-load generating sets, the exact location of which has not as yet been announced. These will be the largest of all units so far ordered in England.

Metropolitan-Vickers Electrical Company, Ltd.—the largest gas-turbine builder in England—completed a 15,000-kw unit for the British Electricity Authority. The unit is being installed

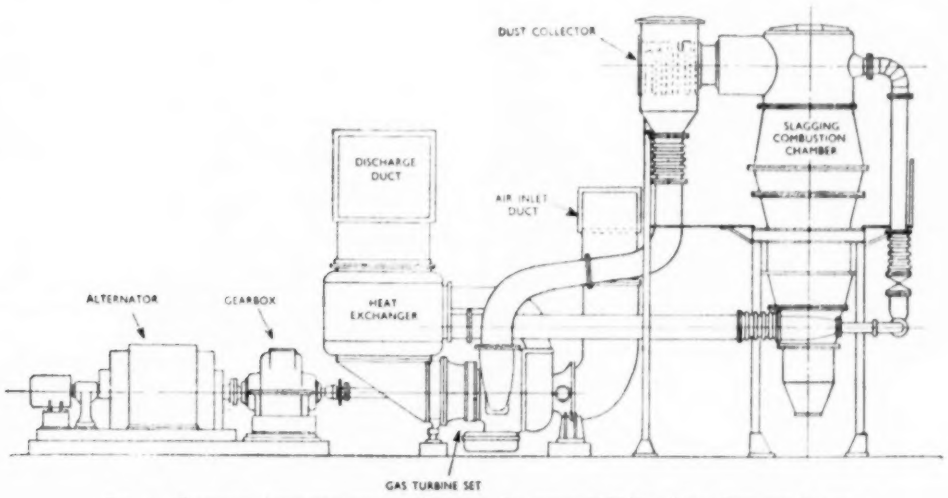

FIG 4 GENERAL ARRANGEMENT OF ENGLISH ELECTRIC 2000-KW COAL-BURNING PLANT

at the Trafford Generating Station. The turbine is a compound-cycle unit designed for 26.3 per cent thermal efficiency and will operate on light oil at a gas temperature of 1200 F. Other units nearing completion include a 2500-kw simple-cycle machine for the Metropolitan Water Board, a 2000-kw set for the Ministry of Fuel and Power, and a 1750-kw set for a refinery installation of the Shell Petroleum Company in Venezuela.

The unit for the Ministry of Fuel and Power is designed for coal burning and makes use of two stages of combustion; the first producing combustible gas, and the second completing combustion of the gas. Cleaning of the gas thus can be confined to the first or gasification stage.

C. A. Parsons & Company, Ltd., is about to complete the 15,000-kw gas-turbine generator for Dunston "A" Power Station, and a 10,000-kw unit for the National Gas Turbine Establishment. Units are similar in design and are expected to operate on heavy oil, with a gas temperature of 1200 F and thermal efficiency around 26.4 per cent. The Parsons design includes a low-pressure compressor, two parallel intercoolers, a high-pressure compressor, four regenerators in parallel pairs, four combustion chambers, and high-pressure and low-pressure turbines without reheat. The low-pressure turbine drives the low-pressure compressor while the high-pressure turbine drives the high-pressure compressor and electric generator. The 10,000-kw unit for the National Gas Turbine Establishment is also arranged for space heating by using exhaust from the low-pressure turbine in a system of heat exchangers for generation of low-pressure steam. Further, this company has under construction a 2500-kw simple-cycle unit intended for shop tests on oil fuel. The company also is carrying out tests on coal- and peat-burning gas-turbine plants, in co-operation with the Ministry of Fuel and Power.

Ruston and Hornsby, Ltd., reports continued operation of a 750-kw gas turbine started over a year ago. The Ruston prototype gas turbine has now reached the point where the plant is regularly operated for electric generation. The unit has given good results even on some special heavy-oil products selected by the Admiralty for test. Construction of a test unit for peat burning is in an advanced stage. The company continues its research on combustion and burning of heavy fuels. Considerable progress is reported in connection with preparation and combustion of peat. Problems of dewatering peat by pressing and thermal drying have been investigated, and complete equipment for the first full-size experiments is being assembled. Ruston and Hornsby also plan to increase their facilities for production of several sizes of small gas-turbine units.

The Brush Electrical Engineering Company, Ltd., reports development and construction of a 2500-kw gas-turbine-generating unit. The turbine will operate at 1340 F with an expected thermal efficiency of 15.6 per cent on light oil. The unit was ordered by the Metropolitan Water Board and will operate on the simple cycle for stand-by service.

In France as many as eight to ten companies are working on gas turbines, but nearly all of the development is for marine or automotive applications. Much of the work in France also is related to the free-piston type of gas generator, used in conjunction with the gas turbine. However, Rateau Company is reported to have a 2000-kw electric-generating set under test and redesign. This unit operates on the simple cycle at 1292 F and with oil fuel is designed for an efficiency of about 15 per cent. Tests on this unit are being continued. Other French developments are still in the construction stage.

In Switzerland, four concerns are reported as building gas turbines. Of these, Brown Boveri & Company, Ltd., reports fourteen units in service or nearing completion. The company has built gas-turbine generating units in sizes ranging from 1200 to 27,000 kw. An interesting report on performance of the units in service has been given by Paul R. Sidler,[2] president of Brown Boveri Corporation, New York, N. Y.

The first Brown Boveri gas turbine for commercial service in a generating station and rated 4000 kw was installed by the Municipal Electric Supply at Neuchâtel, Switzerland, in 1939. All gas turbines built by Brown Boveri have been for stationary generating sets, except a 2200-hp unit installed in a locomotive for the Swiss Federal Railways in 1941, and a 2500-hp locomotive unit delivered to the British Western Railways in 1950. Major units built include a 13,000-kw generating set installed in 1948, at the Beznau Station of the North East Power Company in Switzerland, and a 27,000-kw unit for the same station started in 1949.' Both units are operated on light oil and the first has given 6000 hr of service, while the second has operated 3000 hr. A variety of troubles were experienced with these machines, including turbine-blade breakage, self-induced vibration failure of axial-flow compressor blades, deposits on blades, soot deposits, and corrosion problems in heat exchangers, and short life of combustion-chamber liners. The manufacturer reports that all of these troubles have been corrected and that operation of both units has been satisfactory since the winter of 1949–1950.

A cycle diagram for the 27,000-kw Brown-Boveri unit installed at Beznau Station is shown in Fig. 5. It will be noted that the design covers an open-cycle type with two shafts. It features two low-pressure compressors in parallel, along with a double-flow low-pressure turbine and an intermediate-pressure compressor all on one shaft. Air from the intermediate-pressure compressor, after cooling, is passed to the high-pressure compressor and then through a regenerator to the high-pressure combustor and finally to the high-pressure turbine. Exhaust from the high-pressure turbine is heated in a reheat combustor and is then passed to the low-pressure turbine from which it is discharged to the regenerator and then to the atmosphere. The high-pressure turbine drives the high-pressure compressor and the electric generator. This cycle is designed for a thermal efficiency of 32 per cent or better. The design is indicative of what can be accomplished with two-shaft units, together with multicompressors, intercoolers, and a regenerator and second stage of combustion. Gas-turbine sets of this type, however, are handicapped by space requirements and extra cost of accessory equipment including interconnecting piping.

Brown Boveri also built and installed two 10,000-kw gas-turbine-generating sets; one at the Santa Rosa Station in Lima, Peru, and the other at Filaret Station in Bucharest, Rumania. The unit in Lima was installed in 1949, and has operated about 6500 hr—the unit at Bucharest was started in 1951 and has seen little service. The unit installed at Lima suffered about the same troubles as reported for the units as Beznau, but the problems encountered were corrected quickly.

Other units sold by Brown Boveri include 1200- to 5400-kw generating sets installed in Iran, Peru, Venezuela, Egypt, and Luxemburg. In Iran, three 4000-kw simple-cycle units were purchased by the Anglo-Iranian Oil Company, Ltd., but operation has been delayed. The unit in Peru consists of a 4000-kw set installed in 1949. Two 1650-kw generating sets were installed in a cement factory in Venezuela in 1949, and have operated around 7000 to 8000 hr each. Performance of these machines is reported as satisfactory, and a third unit of 5000 kw has been ordered for installation this year. A regenerative-type generating unit of

[2] "Operating Experiences With Stationary Gas Turbines," by P. R. Sidler, paper presented at the Annual Meeting, New York, N. Y., November 25–30, 1951, of THE AMERICAN SOCIETY OF MECHANICAL ENGINEERS.

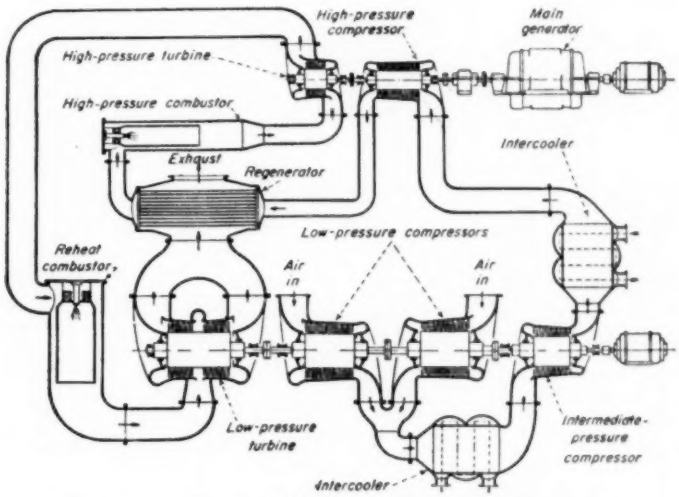

FIG. 5 BROWN BOVERI 27,000-KW GAS-TURBINE-GENERATING UNIT

1200 kw is operating in an ice plant in Egypt and another of 5400 kw is installed at a steel mill in Luxemburg.

A more recent order covers four 5000-kw natural-gas-burning units for the oil fields of the Arabian-American Oil Company (Aramco). Each will be a single-shaft, simple-cycle machine rotating at 3600 rpm and directly coupled to a 6250 kva, 13,800-volt 3-phase generator. The design rating of 5000 kw at about 17 per cent thermal efficiency is based on an ambient temperature of 120 F and a turbine-inlet temperature of 1200 F.

Brown Boveri engineers conclude that problems connected with the ash in heavy fuel oils have not been solved. They feel that difficulties experienced to date, with some of the residual fuels, are greatly intensified by operating gas turbines with high gas temperatures. In the interest of reliability and long life, the company has continued its policy of designing gas turbines with maximum operating temperatures of 1100 to 1200 F. They also feel that certain restrictions as to quality must be placed on heavy fuel oil, if good performance is to be expected.

Escher-Wyss Engineering Works has continued experiments with a 2000-kw closed-cycle gas turbine, which has been under test in its shops for almost 10 years. Although the design is complicated and consists of various stages of compression, intercooling, regeneration, and reheat, it is understood that few serious troubles have developed. Experience with the test unit led to the design of a 12,500-kw set, the first of which has been installed at a plant in St. Denis, Paris. The unit is designed for operation on oil fuel, and with 1250 F gas-inlet temperature. It is expected to deliver an efficiency around 32 per cent. Running tests on this unit were started late in the summer of 1951. In November, the set was connected to the electrical-grid system and since then, load tests have been carried out with the complete set in operation. Apart from minor preliminary troubles, mainly with auxiliary equipment, the various tests up to January, 1952, gave very satisfactory results.

Fig. 6 shows the cycle diagram for the 12,500-kw Escher-Wyss closed-cycle gas-turbine unit. The plant at St. Denis is operating under a maximum pressure of 735 psi. The inlet pressure of the compressor is 73.5 psi, and air flow is at the rate of 132 lb per sec. Item 1 in the cycle diagram represents the combustor air heater and preheater; item 2 is the compressor for combustion air; item 3, a circulating fan for combustion air, and item 4, the starting motor; item 5 is a heater for combustion air; and items 6 and 7 are, respectively, high-pressure and low-pressure gas turbines. Items 8, 9, and 10 are, respectively, low-pressure, intermediate, and high-pressure air compressors. Item 11 is the starting motor for the high-pressure group and items 12 and 13 are the generator-exciter unit. Item 14 is a regenerator; item 15 a precooler, and items 16, 17, and 18 are intercoolers. Items 19 and 20 are make-up air compressors; item 21 is a cooling-water pump, and item 22 a fuel pump; item 23 is the low-pressure turbine for combustion air and item 24 is a gas cooler for combustion air; item 25 is a cooler for by-passed gas at the low-pressure turbine, and item 26 is the control of the by-pass at the low-pressure turbine. Item 27 is a vent valve, and item 30 a compressor for accumulators. Item 31 is an accumulator for low-pressure air; items 32 and 33 are control valves, and item 34 is an accumulator for high-pressure air. Item 35 is a by-pass around the combustor.

It is understood that the design and construction of this plant resulted in experience which will lead to a higher degree of simplification of this type of power plant. One step in simplification is that the heater can be designed with atmospheric combustion. Thus the whole charging unit, consisting of the exhaust-gas turbine, flue-gas-recirculation blower, and combustion-air compressor can be eliminated. The company feels that the closed-cycle gas-turbine plant has attractive possibilities for future development and is arranging for the design of smaller units in conjunction with the co-operation of several licensees.

Oerlikon Company of Switzerland has announced the receipt of an order for a 730-kw gas-turbine-generating set from Compagnie Electricite et Gaz d'Algerie. The turbine will be an open-cycle, regenerative-type unit, operating on heavy oil with a temperature of about 1200 F. In most respects, the plant will resemble the 1000-kw experimental gas turbine in the Oerlikon Works, which has been tested for many years. Design of the unit for Algiers shows that part of the turbine exhaust will be passed to the regenerator and part to a boiler for generation of steam. Steam will be used for preheating the heavy fuel oil used at the plant. Oerlikon feels assured of the soundness of its gas-turbine designs, and is prepared to offer units in sizes up to 15,000 kw.

Several years ago, Sulzer Bros., Ltd. set out to develop a cycle which would meet the conflicting requirements of efficiency, space, and weight. The result of its work was development of

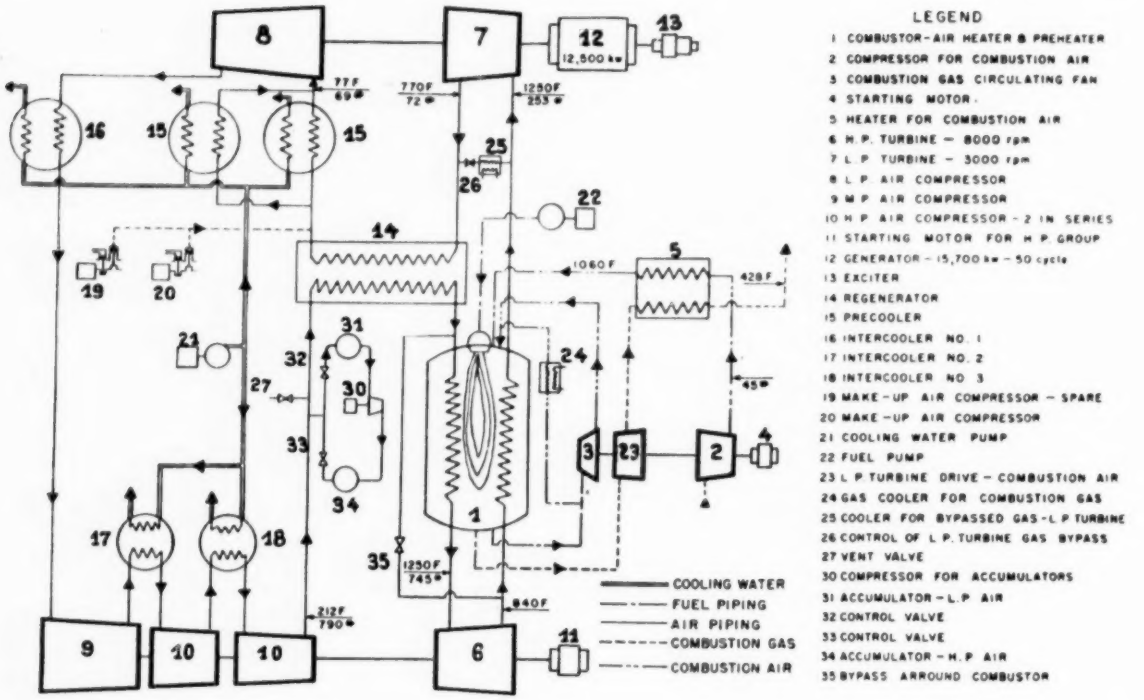

FIG. 6 CYCLE DIAGRAM OF 12,500-KW ESCHER-WYSS CLOSED-CYCLE GAS-TURBINE UNIT INSTALLED AT ST. DENIS, FRANCE

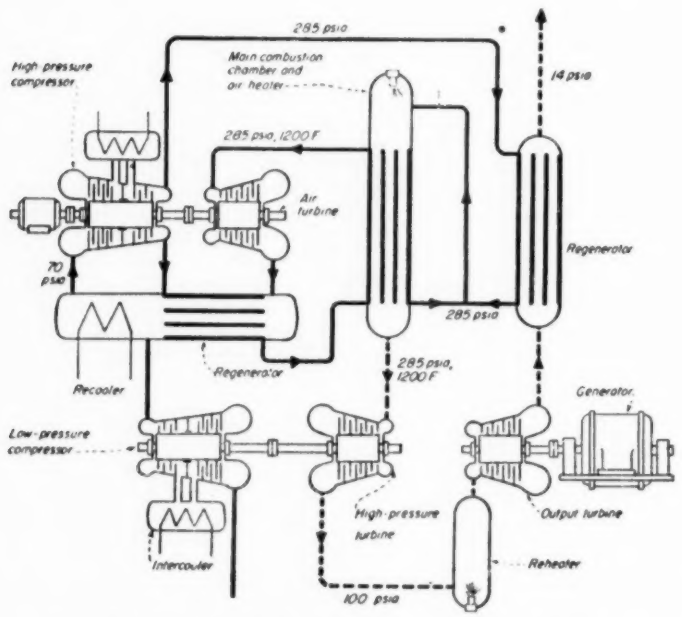

FIG. 7 CYCLE DIAGRAM OF 20,000-KW SULZER BROS. LTD., SEMI-CLOSED-CYCLE GAS TURBINE UNIT INSTALLED AT WEINFELDEN, SWITZERLAND

the so-called high-pressure or semiclosed cycle. A 7000-hp, semiclosed-cycle unit, intended for a marine installation, has been under test for some time. Also a 20,000-kw semiclosed-cycle, electric-generating unit was placed in service in 1950 at the Weinfelden Station of the North East Power Company in Switzerland. Tests at Weinfelden have been made on heavy fuel oil at a turbine temperature of 1200 F, at which the thermal efficiency of the cycle is reported to be about 30 per cent. At full load the unit requires only 1600 cf per sec of air—about half the quantity which would be required for a two-stage, open-cycle turbine. For cooling, the gas turbine requires about 3100 gpm of water.

Fig. 7 shows the cycle diagram for the 20,000-kw Sulzer semiclosed-cycle unit at Weinfelden. One part of the plant consists of a closed circuit through which air flows only under pressure. This air is drawn in at a lower pressure level, for instance, 70 psi, by the high-pressure compressor which brings the air pressure up to about 280 psi. Part of the air then flows in the usual way through a regenerator and an air heater, in which it is heated to its maximum temperature, 1200 F. Expansion to about 71 psi takes place in an air turbine which drives the high-pressure compressor referred to. After leaving this turbine, the air passes through the regenerator again and also through a recooler, where it is cooled to around 70 to 80 F, and then returns to the high-pressure compressor. While this closed circuit supplies no useful power in return for the calorific energy introduced, it justifies its use for the reason that the high-pressure compressor handles much more air than is expanded in the air turbine. The surplus of compressed air is used as combustion air in the air heater and this is, in fact, the fundamental feature distinguishing this cycle from the closed cycle. Before reaching the combustion chamber, the air is preheated by exhaust gases in another regenerator. The combustion gases produced in the chamber serve first to heat the circuit air to its maximum temperature, while passing through the tube nest, but the injection of fuel is regulated so that at the outlet of the reheater, these gases are still at a temperature practically equal to that of the heated air itself. They are then expanded to about 100 to 115 psi in the high-pressure turbine, or reheated to their initial temperature in a secondary combustion chamber or reheater and finally expanded to nearly atmospheric pressure in the output turbine. Gases escape to the atmosphere after passing through the regenerator, where they give up part of their residual heat to the combustion air.

The low-pressure compressor driven by the high-pressure turbine introduces into the circuit a quantity of air equal to that extracted at the outlet from the high-pressure compressor at the upper left. Drawing the air from the atmosphere, it passes through the recooler and thus into the circuit at the inlet to the compressor. The low-pressure turbine at the lower right serves exclusively for the generation of useful power. Although this system is also a high-pressure cycle with a closed air circuit, combustion does not take place outside the flow of the working medium.

Sulzer reports several distinct advantages of the semiclosed cycle system, as compared with other gas-turbine cycles. It is certain that Sulzer will continue its research and development of this cycle.

Announcement has been made that the Swedish company of Swenska Turbinsfabriks Aktiebolaget Ljungstrom (STAL) has a 2400-kw gas-turbine-generating set under test at the factory. No details on specifications or design of this unit are available as yet.

Foreign reports indicate that all gas-turbine developments are being pushed seriously and in a spirit of confidence. On the whole, all builders appear to be extremely conscious of gas-turbine commercial possibilities.

Gas-Turbine Progress Report—Industrial

By L. N. ROWLEY, JR.,[1] AND B. G. A. SKROTZKI,[2] NEW YORK, N. Y.

THE versatility of the gas turbine, and the ease with which it may be adapted to a wide variety of service conditions, makes it particularly attractive in the industrial field. This section of the progress report deals with three broad classes of industrial applications: (1) Gas turbines supplying shaft power to drive compressors and pumps; (2) gas turbines furnishing pressure air; (3) gas turbines utilizing waste heat *from* industrial processes or supplying heat *to* industrial processes. More than 80 such units have been built or are building, Table 1.

Gas Pipe-Line Compressor Drives

Since about 1947, centrifugal compressors, inherently high-speed high-capacity machines, have found increasing application to gas pipe-line service. Their only wearing parts are shaft journal bearings, thrust bearing, and some designs of shaft-sealing devices. High efficiency can be sustained over a long life. They are easily maintained; a complete overhaul takes less than 3 man-days. Small physical size leads to minimum foundation, housing, and crane requirements.

The high-pressure centrifugal compressors used in pipe-line service normally have pressure ratios in the range 1.06 to 1.15. Since most pipe-line systems require higher pressure ratios, the compressors are usually arranged in series. Centrifugal compressors are easily adapted to automatic operation.

In early applications, electric motors drove the compressors. The possibilities of gas turbines as drives have been recognized for some time and the excellent "matching" of gas-turbine and compressor characteristics, plus many over-all advantages, has resulted in extensive current interest.

The combination of gas turbine and centrifugal compressor needs only (1) light foundation, (2) small housing, (3) few auxiliaries, (4) little or no water, (5) simple piping connections. Such booster units do not produce gas-line pulsations and are easily adaptable to remote or automatic control.

Experience with one installation has shown that they can be restarted after a long shutdown without any trouble. Furthermore, since they draw their fuel directly from the pipe line this vital supply offers no problem. Natural gas has proved itself an ideal fuel for gas turbines.

Studies have shown that gas turbine-compressor stations can be justified economically to serve 20-in-diam lines or greater. Simple single-shaft units prove ideal as booster units taking care of peak loads when no great operating flexibility is needed. Where variable loads must be served and greater flexibility is needed, the two-shaft unit with separate load-driving turbine has advantages, unless greater flexibility is built into the compressor itself (adjustable diffusers, prerotation stage, and so on). Regenerators and intercoolers can be used when economically justified by operating conditions.

The first gas-line unit, in the form of a gas turbine driving a centrifugal gas compressor, was an 1800-hp single-shaft open-cycle plant, Fig. 1, built by the Westinghouse Electric Corporation. Originally built as a locomotive prototype, this unit underwent extensive shop testing before the generator was replaced by a centrifugal compressor for pipe-line service. This unit served on the 22-in-diam line of the Mississippi Fuel Corporation at Wilmar, Ark., from May, 1949, to the fall of 1950. Changes in the pipe line eliminated the need for the unit at this point.

The unit was then moved to Bonne Terre, Mo. Here it started service in January, 1951, to take up its present duty of packing the end of the transmission line and also an underground gas-storage field.

Based on experience with this first gas-line unit and studies of the needs of main-line service, Westinghouse has built a 5000-hp 2-shaft gas turbine with regenerator, Fig. 2 and Fig. 7. The unit has an 11-stage axial-flow compressor, six combustors, 2-stage compressor-drive turbine and single-stage power turbine. The regenerator is of the extended-surface type.

The General Electric Company is building a series of 5000-hp 2-shaft gas turbines intended primarily for gas-transmission line service, Fig. 2. A single-stage high-pressure turbine drives the 14-stage axial-flow compressor developing a 5.5 compression ratio. The single-stage load-driving turbine is in the same casing with the high-pressure wheel. Nozzle vanes for the load turbine rotate so the gas-flow area can be controlled. Variable flow area (1) limits overspeed during load loss by tripping wide open, (2) gives better part-load performance, (3) increases capability at high ambient temperatures, (4) controls amount of auxiliary power developed by the gas-generator shaft, (5) reduces starting power, (6) gives control of exhaust temperature.

Six combustors supply 1450 F gas to the turbines at maximum capability. The cylindrical regenerator mounts on end outdoors (see suggested station design, Fig. 8). Single-stage mechanical-drive turbines expanding natural gas from the lines will crank the unit for starting. Each start will waste about 35,000 cu ft of gas to the atmosphere.

The gas-generator shaft drives an auxiliary electrical generator through a gear. These 125-kw units supply power to the evaporative coolers, oil-cooling system, circulating-water pumps, and to the station lighting system.

The turbine wheels are cooled by air streams flowing from the hubs on both sides of each wheel outward to the rims. Air cooling also serves the first-stage nozzle vanes. Air flowing through them

[1] Executive Editor, *Power*, McGraw-Hill Publishing Company. Mem. ASME.

[2] Associate Editor, *Power*, McGraw-Hill Publishing Company. Mem. ASME.

Contributed by the Gas Turbine Power Division, and presented at the Fall Meeting, Chicago, Ill., September 8–11, 1952, of The American Society of Mechanical Engineers.

Notes: This is paper No. 52—F-6 of a Progress Report which the Executive Committee of the Gas Turbine Power Division authorized at its 1951 Annual Committee Meeting. The series includes the following: "Introduction," by R. Tom Sawyer, paper No. 52—F-1A; "Materials, Cooling, and Fuels," by A. A. Hafer, paper No. 52—F-1B; "Cycle Components," by P. F. Martinuzzi, paper No. 52—F-1C; "Automotive," by Frank L. Schwartz, paper No. 52-F-2; "Railroads," by K. A. Browne, J. I. Yellott, and P. R. Broadley, paper No. 52—F-3; "Marine," by W. A. Dolan, Jr., and A. A. Hafer, paper No. 52—F-4A, "Merchant Vessels," by W. A. Dolan, Jr., and A. A. Hafer, paper No. 52—F-4B; "Naval Vessels," by W. A. Dolan, Jr., and A. A. Hafer, paper No. 52—F-4C; "Stationary Electric Generation," by Lee Schneitter, paper No. 52—F-5; "Aviation," by I. H. Driggs and O. E. Lancaster, paper No. 52—F-7.

Statements and opinions advanced in this paper are to be understood as the individual expressions of the authors and not those of the Society.

TABLE 1

User	Location	Application	No. of units	Builder	Status in late initial operation	Rated capacity, hp	Turbine inlet temperature, °F	Pressure ratio	Cycle No.	Thermal efficiency, % (net)	Shaft speeds, 1000 rpm	Fuel	Combustion type	Turbine: No. stages	Turbine: Rotation, axial or radial, turning	Compressor: Type	Compressor: No. stages	Regeneration effectiveness, %	Remarks
El Paso Natural Gas Co			20	GE	51-53														
Northern Natural Gas Co			9	GE	53														
Atlantic Seaboard Corp		Gas pipe line	1	GE		3000	1450	5.1	2	22.6	6.9/5.0	NG	M	2	All	A	14	80	Variable inlet nozzles, 2 single-stage turbines
Southern Counties Gas Co			1	GE															
Texas Petroleum Co			10	GE		5000	1400	6.0	2	16.7	6.7	NG	M	2	All	A	15	None	
Tennessee Gas Transmission Co	Woodsboro, Ky	Gas pipe line	1	CF	52	5500	1360	5.0	2	28.0	6.8/6.4	NG	S	2	Disc	A	10	80	2 single-stage turbines, starting turbine expands natural gas
Mississippi Fuel Corp	Bonne Terre, Mo	Gas pipe line	1	WE	46	1800	1350	5.0	1	16.7	9.2	NG	M	3	None	A	20	None	Built as test unit, first installed Wilmar, Ark. 1949, present location 1951
		Gas pipe line		WE		5000			2		6.2/6.5	NG	M	3		A	11	75	3-stage compressor-drive turbine, 1-stage power turbine
Tidewater Associated Oil Co	Bayonne, N.J.	Heavy	1	AC		60[1]	950	4.1	3		4.32	WH	S[2]		None	A		None	Electric energy produced as byproduct
	Marcus Hook, Pa.	Heavy	2	BB		60[1]													
Sun Oil Co			4	AC		60[1]													
	Toledo, Ohio	Heavy	1	AC		60[1]													
Terminal Refinery	Corpus Christi, Tex	Heavy	1	AC		60[1]													
Magnolia Petroleum Corp	Beaumont, Tex	Heavy	2	AC		60[1]													
Standard Oil of California	El Segundo, Calif	Heavy	1	AC		60[1]	950	4.1	3		5.10	WH	S[2]	5	None	A	20	None	Drives byproduct electric generator, 1500 hp.
Gulf Oil Corp	Port Arthur, Tex	Heavy	1	AC		60[1]													
Sinclair Refining Corp	Houston, Tex	Heavy	1	AC		60[1]													
Southport Petroleum	Southport, Tex	Heavy	1	AC		60[1]													
Standard Oil of Ohio	Cleveland, Ohio	Heavy	1	AC		60[1]													
Magnolia Petroleum Corp.	Beaumont, Tex	Heavy	1	BB		25[1]													
			2	AC		25[1]													
	Trenton, Mich	Heavy	1	AC		25[1]													
	Brooklyn, N.Y.	Heavy	1	AC		25[1]													
	Buffalo, N.Y.	Heavy	1	BB		25[1]													
Socony Vacuum Oil Co	East St. Louis, Ill.	Heavy	1	BB		25[1]	950	4.1	3		6.08	WH	S[2]		None	A		None	Electric energy produced as byproduct
	Augusta, Kan.	Heavy	1	AC		25[1]													
	Paulsboro, N.J.	Heavy	1	BB		25[1]													
	East Chicago, Ind.	Heavy	1	AC		25[1]													
Standard Oil of Ohio	Cleveland, Ohio	Heavy	1	AC		25[1]													
Sun Oil Co	Marcus Hook, Pa	Heavy	1	AC		25[1,3]													
Raffineria de Berre	Berre, France	Heavy	1	BB	45	16[1]	950	4.1	3		5.10	WH	S[2]	5	None	A		None	
Raffineria di Napoli	Naples, Italy	Heavy	1	BB	37	10[1]	950	4.1	3		5.10	WH	S[2]	5	None	A		None	
Altos Hornos de Vizcaya	Baracaldo, Spain	B F Air	1	BB	51	26.5[1]	1100	3	4			BFG	S		None	A			Centrifugal gas compressor, for simplicity gas turbine uses same compression ratio as air delivery
National Gas Turb Establishment	Pyestock, Hampshire, England	Compressed air	1	P		20[2]	1125	4	4[4]		4.6	LO	S	6	None	A	14		Provides compressed air for test facilities
		Power and space heating	1	P		10[4]	1200	5.5	6		7.8/3.0	LO	M	8	None	A	24	75	Regenerator exhaust provides space heating
West Midlands Gas Board	Coventry, England	Power	1	JB	52	0.7[4]	1112	4.4	5[5]	25.0	9.5	WH		8	None	A C	10 1	86	Input from heat exchanger or waste flue of group of continuous vertical retorts in gas works

1 – 1800 cfm
2 – Starting combustor – operating combustor is catalytic cone
3 – 72,000 cfm casing, blades cut for 36,000 cfm
4 – 1000 kw
5 – – Closed cycle
a – – Without gas combustor and regenerator
7 – – ½ psi to at 4 atmospheres
A – – Axial flow
AC – Allis-Chalmers Mfg Co
BB – Brown, Boveri & Co., Ltd
BFG – Blast-furnace gas
C – Centrifugal
CF – Clark Bros and Fluidyne Flader, Inc
GE – General Electric Co
JB – John Brown & Co., Ltd
LO – Light oil
M – Multiple
NG – Natural gas
P – CA Parsons & Co., Ltd
S – Single
WE – Westinghouse Electric Corp
WH – Waste heat

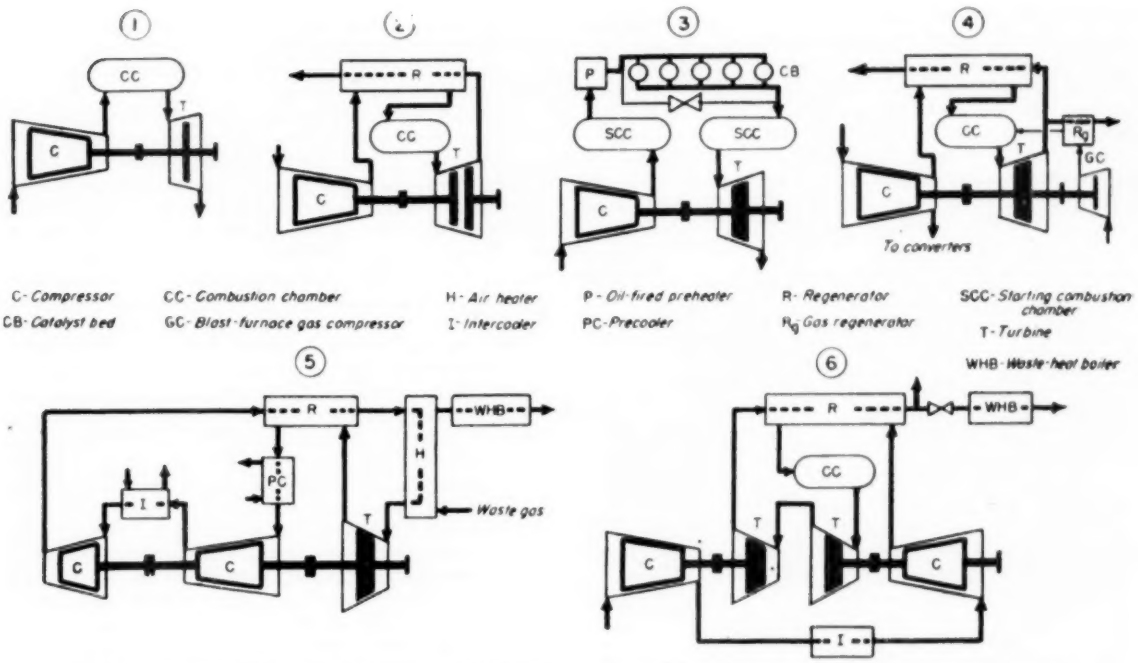

FIGS. 1 TO 6 CYCLE DIAGRAMS FOR INDUSTRIAL GAS-TURBINE APPLICATIONS DESCRIBED IN TEXT AND LISTED IN TABLE 1

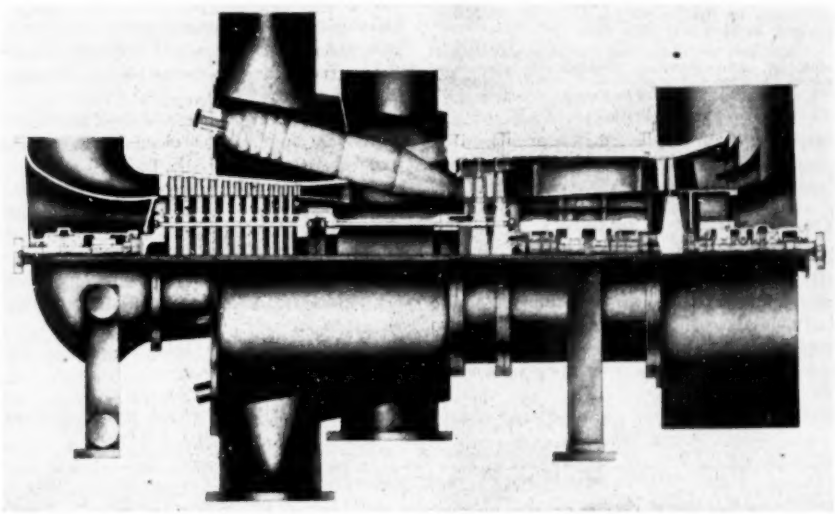

FIG. 7 TWO-SHAFT 5000-HP GAS TURBINE DESIGNED BY WESTINGHOUSE FOR GAS-LINE COMPRESSOR DRIVE
(Consists of 11-stage axial compressor driven by two-stage turbine and single-stage load-driving turbine. Compressor discharge passes through extended-surface regenerator and six combustors.)

discharges along the side wall on the inlet side of the nozzles to join the main gas stream. The turbine shell is water-cooled.

Clark Bros. Company, Inc., manufactured a pioneering industrial gas turbine designed specifically for driving centrifugal compressors. The turbine operates on a simple open cycle incorporating an advanced pin-fin-type surface regenerator for greater efficiency, Fig. 2. A two-shaft turbine is used to match rotative speeds of driver and load, while a single combustion chamber allows a close mean approach to turbine design inlet temperatures. The Clark turbine was installed in a station on a major gas-transmission line and placed in operation during the spring of 1952.

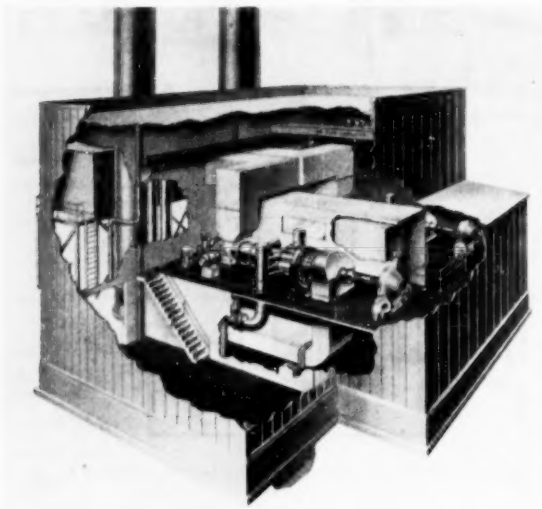

FIG. 8 SUGGESTED DESIGN OF TWO-UNIT GAS-LINE COMPRESSOR STATION BY GENERAL ELECTRIC

(These 5000-hp gas turbines drive centrifugal gas compressors at thermal efficiency of 22.5 per cent, hhv. Air compressors take in air through evaporative precoolers and washers. Turbine discharge through outdoor regenerator supporting steel stacks.)

GAS-TURBINE PLANTS FOR AIR SUPPLY

Earliest industrial uses of gas turbines had supply of pressure air as their objective—turbocharging internal-combustion engines and Velox boilers. Application of gas-turbine plants to the Houdry process of oil refining was in many respects analogous to these—the units supplied air for pressure charging and their energy source was exhaust of waste gas from the process—but they differed importantly in a number of ways. The units were relatively large, combustion chambers were required, and they produced some shaft power. Hence they served as prototypes for later gas-turbine generating sets.

A typical Houdry catalytic-cracking unit for manufacture of high-octane gasoline requires about 40,000 cfm of 45-psi air, heated to about 750 F, for regenerating the catalyst. This air is supplied by an axial compressor which raises air temperature to about 350 F. An oil-fired heater may do the remainder of the preheating, or air may be heated further in a salt-to-air heat exchanger before going to the catalyst cases. Oxidation of carbon deposits on the catalyst releases heat and the combustion products leave the catalyst cases at higher temperature and only slightly lower pressure. Gas at about 850–950 F and 40 psig is thus available for expansion in a turbine. This produces power enough to drive the axial compressor, with some excess available for generating electricity. Two oil-fired combustion chambers are provided for starting the turbine and heating the cases, Fig. 3. Burners are shut off when the plant goes on stream. Regeneration of the catalyst is controlled by a cycle timer so there is always a group of cases connected to the air system to yield a steady source of heat energy.

The first Houdry set (built by Brown Boveri & Company) was installed at the Marcus Hook refinery of the Sun Oil Company in 1936. In the years immediately following, a total of 27 units were installed in United States refineries, Table 1. Six of these were of Brown Boveri manufacture, the remainder were built by Allis-Chalmers Manufacturing Company under Brown Boveri license. During the war years, 10 units were built by Allis-Chalmers for the United States Government for lend-lease, two of which were never shipped out of the United States. One of these has been used for experiments on coal burning by the Locomotive Development Committee; another is at Gorgas, Ala., where work on underground gasification of coal is being carried out. Two Brown Boveri units were installed in European refineries, Table 1.

Sets were built in three basic sizes, for outputs of 23,000, 40,000, and 60,000 cfm. All were of similar design. A typical 40,000-cfm unit consisted of a 5-stage reaction turbine driving a 20-stage axial compressor at 5180 rpm and, through reduction gears, a 1500-hp generator. With relatively low throttle temperature, materials of construction included steels of the 18–8 class and familiar steam-turbine alloys.

In 1945 A. E. Pew[3] reported experience with six Sun Oil Company units, representing a total of more than 25 years of opera-

[3] "Operating Experience With Gas Turbines," by A. E. Pew, Jr., *Mechanical Engineering*, vol. 67, 1945, p. 594; also private communication from H.E. Melton, May 7, 1952.

TABLE 2 RECORD OF OPERATION OF SUN OIL COMPANY HOUDRY GAS-TURBINE SETS; NUMBER OF FAILURES AND DAYS LOST TO FEBRUARY 29, 1952

	Cause of failure													
	Bearings		Lubrication		Blades		Air Seals		Explosions		Misc.		Total	
Turbo	No.	Days	No.	Days	No.	Days	No.	Days	No.	Days	No.	Days	No.	Days
11-4	18	43							1	5	1	2	20	50
12-3	6	17.5			2	10	1	3	1	2	6	17.5	16	50
Toledo	3	10							1	4	2	6	6	20
12-4	7	44.7	3	14	2	26.5					4	83.3	16	168.5
10-3N	3	15	3	14	4	18			1	5	3	9.5	4	61.5
10-38					6	24.3			1	4	2	14	9	42.3
15-1					2	10.5							2	10.5
Total	37	130.2	6	28	16	89.3	1	3	5	20	18	132.3	73	402.8

	No. days to date			
	Operating days	Days off acct. turbo trouble	Total days	Per cent time turbo trouble
11-4	4853.1	50	4903.1	1.02
12-3	4287.7	50	4337.7	1.15
Toledo	4469.3	20	4489.3	.45
12-4	3085.5	168.5	3254.0	5.18
10-3N	3677.0	61.5	3738.5	1.65
10-38	3654.7	42.3	3697.0	1.15
15-1	2721.8	10.5	2732.3	.38
Total	26749.1	402.8	27142.9	Avg 1.48

tion. Availability equaled the best steam-turbine practice; forced outage averaged slightly less than 2 per cent. Principal sources of trouble were not peculiar to gas turbines—bearings and lubrication. Some blade loosening was corrected by changes in root design. Erosion of blades resulting from carry-over of fine catalyst particles occurred but did not prove serious.

Since 1945, forced outages have become more and more infrequent. There have been no bearing failures for several years, or since changing from radial thrust to Kingsbury bearings. Blade failures have been practically eliminated since dust collectors were installed to eliminate catalyst carry-over.

A complete record of seven Sun Oil Company units, representing almost 75 years of operation, appears in Table 2. It should be noted that outages tabulated are all of the "forced" variety; in addition to these days out of service, an average of 1 week per turbine per year is allowed for inspection and overhaul. At all other times the units have been ready for operation of the catalytic-cracking plants. Sometimes these latter have been operated as thermal crackers or vis breakers, so operating days tabulated refer only to catalytic-cracking operation when gas-turbine sets are required. Intervals of noncatalytic operation, plus downtime for changing catalyst and revamping some of older units account for about 10 per cent of the total life of the Houdry gas-turbine sets. As the tabulation shows, forced outages represent only 1.48 per cent of total time on catalytic operation, an outstanding record for any power-plant unit.

The development of "fluidized" catalysts, as distinguished from the static-bed type used in the Houdry process, changed the requirements and led to systems in which gas turbines did not fit. Although most of the original installations are still operating, no new ones have been made in recent years.

Aside from historical interest, the Houdry plants deserve comment here because they typify many possible uses in the chemical and process industries. Such an application has been proposed for nitric-acid production, with pressure air supplied from a compressor driven by a gas turbine utilizing the tail gases from the process. Also we must bear in mind that the Houdry units, until recently, have been our only source of long-term gas-turbine operating data.

For the steel industry, gas-turbine plants offer a compact and economical source of blast-furnace or converter air. It is possible to apply them in a variety of ways: (1) The gas-turbine set may serve merely as a source of shaft power, driving an axial or centrifugal blower supplying blast air; (2) air from the compressor of the gas-turbine set, which would be larger than normally required, may be "bled" to the blast stoves; (3) a heat exchanger may be substituted for the conventional blast stove and all combustion, both for the gas-turbine set and blast heating, may be carried out in a single combustion chamber under pressure.

For immediate application, the bled design of (2), or modifications of it, seems most attractive. It can be fitted to existing equipment and practices of the steel industry. It involves less equipment than scheme (1) and seems simpler to control. Control simplicity derives from the fact that blast-air needs form only a small fraction of total air; hence variations in them have relatively little effect on compressor operation. Installations to date have followed the general lines of scheme (2).

What would have been the first blast-furnace installation was begun during World War II in the Hermann Goering Steel Works. When Germany was occupied in 1945, two sets built by Brown Boveri AG of Mannheim (affiliate of Brown Boveri & Company of Switzerland) were nearing completion. One was dismantled and shipped to C. A. Parsons Company in England, for study.

In these units, all air passes through 13 stages of a 21-stage axial compressor. Blast air bleeds off at this point (17 psi), while air for the turbine passes through the remaining 8 stages and discharges at 30.4 psi. A separate compressor, driven from the main shaft by gearing, raises the pressure of blast-furnace-gas fuel for admission to the combustion chamber. A regenerator heats cycle air but not the blast-furnace-gas fuel, as proposed in earlier design studies.

The first unit to see actual service in a steel plant is at Baracaldo, Spain. It was built by Brown Boveri & Company and began operation in 1951. Generally similar to designs proposed for blast furnaces, it supplies air for a converter. For simplicity, air for the gas-turbine cycle is used at the same rather low pressure as the blast air, 29 psig. Thus the compressor is not bled; its discharge is merely divided between the converter and the gas-turbine cycle, Fig. 4. The compressor handles 83,000 cfm and 26,500 cfm goes to the converter, about 32 per cent of the total. Even large changes in converter-air needs affect air flow through the compressor only slightly. For sudden changes, momentary surplus may be blown off to keep the compressor from surging. A separate centrifugal compressor, gear-driven from the main shaft, boosts blast-furnace-gas fuel to 65 psi. There are two regenerators, one for cycle air, the other for preheating the blast-furnace-gas fuel.

A similar cycle is used in a turbine-compressor set built by C. A. Parsons and Company for the National Gas Turbine Establishment in Great Britain. It is oil-fired and has an equivalent rating of about 2000 kw. Net output is compressed air used for experimental purposes—20 lb per sec at 4 atm.

Industrial Waste-Heat Applications

The Houdry-process plants previously discussed as an example of pressure-air supply, also serve to illustrate the utilization of waste heat from an industrial process.

A current example of using waste heat from an industrial process is the closed-cycle plant being built by John Brown and Company under Escher Wyss license. This 700-kw unit will serve the Foleshill (Coventry) gas works of the West Midland Gas Board. The source of energy will be a heat exchanger built into the waste-gas flue of a group of continuous vertical retorts. After heating the working fluid of the gas-turbine plant, gas goes to a waste-heat boiler to generate low-pressure steam.

The gas-turbine plant is relatively simple in layout, Fig. 5, consisting of two compressors with intercooling, a single 8-stage turbine, and a regenerator. Low-pressure compressor is a 10-stage axial, the other a 3-stage centrifugal. There is, of course, the usual closed-cycle "precooler" to restore the working fluid to its original temperature before it starts around the cycle again. The water used to cool the circuit air in this precooler is raised to 115 F and then used in the various processes of the gas works.

In a recent paper,[4] J. Burns discussed application of gas turbines in gas works. A gas turbine installed to make use of waste gas from a continuous vertical retort setting, if combined with a steam turbine using the lower-grade heat, ought to generate, he said, some 50 to 70 kwhr per ton of coal carbonized. He cited figures indicating that over-all cost of electricity generated in this fashion is likely to be favorable. In a works with one vertical retort house, a gas turbine would generate current considerably in excess of works needs. He suggested that the excess (1) could be delivered into the "grid," (2) used as direct current for electrolysis of water to hydrogen and oxygen, the oxygen being used with steam for production of high-grade producer gas, or (3) used to make oxygen by liquefaction, oxygen going into producer gas as in (2) and nitrogen being used about the works for purging.

A scheme prepared by W. H. Allen Sons and Company, Ltd.,

[4] "Some Aspects of Gas Manufacturing Practice in the North Thames Gas Board," by J. Burns, Institution of Gas Engineers, Communication No. 385, June, 1951; also in *Gas World*, vol. 133, June 2, 1951, pp. 576–585.

and Woodall-Duckham Vertical Retort and Oven Construction Company for a London gas-works project uses an open-cycle gas-turbine plant combined with a mixed-pressure extraction steam turbine. Studies show this plant to have a 40 per cent greater output from the waste heat than the conventional steam plant.

To utilize waste heat from industrial processes, the "inverted" cycle has been proposed. Instead of using a heat exchanger to transfer energy from hot waste gases to the working fluid of the gas-turbine plant, the hot gases are expanded directly in a gas turbine, cooled, and compressed back to atmospheric pressure for discharge as exhaust. Simplicity is the major advantage of this scheme; it eliminates the heat exchanger, which is usually bulky and expensive. Disadvantages are the need for a cooling medium, large unit sizes resulting from subatmospheric pressures in the circuit, and the fact that it is usually not possible to use in the cycle the heat rejected in the cooler.

Undoubtedly, there are many processes where waste heat is available to supply energy to a gas-turbine plant. Practicality of such applications depends, of course, on the capital cost of utilizing apparently "free" heat.

The waste heat in the gas-turbine exhaust also offers opportunity for recovery. Although this has been discussed many times and the possibilities surveyed,[4] little has been done to realize these possibilities on a commercial basis. Two examples of waste-heat recovery are to be found in plants for central-station power generation. At Belle Isle Station of the Oklahoma Gas & Electric Company, exhaust gas heats feedwater for existing steam units. A unit to be installed by Compagnie l'Electricite et Gaz d'Algerie, will have both a regenerator and a waste-heat boiler supplying steam to preheat bunker oil for the existing main boiler plant of the station. When steam demand is low, exhaust gas does all boiler heating; when steam demand is high, the turbine exhaust forms a preheated air supply for an oil burner fitted to the boiler. Since, in both cases, recovered heat is utilized within the power plant, neither forms a true example of industrial waste-heat recovery.

Closest approach to an industrial installation is the 10,000-kw plant built for the National Gas Turbine Establishment by Parsons. This unit, Fig. 6, has a low-pressure compressor, two parallel intercoolers, a high-pressure compressor, four regenerators in parallel pairs, four combustion chambers, high-pressure and low-pressure turbines without reheat. The low-pressure turbine drives the low-pressure compressor, while the high-pressure turbine drives the high-pressure compressor and alternator.

Exhaust from the low-pressure turbine passes through the four parallel regenerators and into four gas-water heat exchangers, which produce low-pressure steam for space heating. While this is an "in the flesh" example of waste-heat recovery for a typical industrial purpose, space heating, the nature of the installation, as part of an experimental establishment, is not likely to produce any conclusive proofs of the economics of such designs.

Proposals have been made for the combination of gas-turbine and steam cycles, and studies have indicated apparently attractive heat rates. In many of these "hybrid" designs, the gas turbine is superposed on the combustion-air circuit of the steam plant. The Velox boiler is, of course, a specialized application of such a combination, without using the gas-turbine cycle to produce any net power.

The objective of most of these proposals has been to produce a plant for central-station or marine service having attractive overall economy and performance. They do not aim at utilizing industrial waste heat or supplying waste heat to an industrial process—hence are not dealt with here except for this passing reference.

[4] "Where Gas Turbines Will Fit in Future Power Fields," by Hans Pfenninger and S. A. Tucker, *Power*, vol. 90 November, 1946, p. 64; vol. 91, January, 1947, p. 86.

"The Gas Turbine as a Stationary Prime Mover," by L. N. Rowley and B. G. A. Skrotzki, Trans. ASME, vol. 61, 1949, p. 35.

Gas-Turbine Development—Aviation

By I. H. DRIGGS[1] and O. E. LANCASTER,[2] WASHINGTON, D. C.

THE first flight of an airplane propelled by a turbojet engine[3] was August 27, 1939, when the Germans flew the HE-178 powered by the He S3B. The British, completely unaware of the work of the Germans, flew the Gloucester E 28/39 aircraft powered by the W-1 turbojet engine May 15, 1941.[4]

Although it has been only 13 years (12 years, 11 months) since the first flight and the year and a half advantage of the Germans was mostly lost by World War II, the fighter airplanes which make the headlines in today's war news—the MIG-15, *Banshee*, *Panther*, *Cougar*, *Sabre Jet*, *Shooting Star*, and others, are all powered by turbojet engines. Moreover, many of the other types of military aircraft which are now in the design and experimental stages will be powered by turbojets or their companion engine, the turboprop. These engines have even begun to enter the commercial field. The British Overseas Airway Corporation has put into operation between London and Johannesburg, South Africa, the world's first turbojet transport.

All of this indicates the impact that the gas-turbine engine has had on the field of aviation. It has permitted the penetration of a speed range in excess of that previously attainable and as a result has stimulated new configuration and concepts of design.

During the 11-year period, tremendous strides also have been made in the improvement and development of the turbine engines themselves. It is the object of this paper to illustrate this progress by presenting permissible facts about existing aircraft engines. So, in a way, it is a progress report or a survey. For completeness it is well to start with the history of the early development.

Initiation of Development

Although the first flights of jet aircraft were made in late 1939 and early 1941, several years of development preceded this. A stationary gas turbine existed in France as early as 1905. But it was not until the late 1920's that serious thought was given to the use of gas turbines for flight. The first practical proposal was made by Griffith of England in 1926, when he outlined a theory for the design of axial-flow compressors. A single-stage compressor unit actually was built along these principles and tested in 1927. Then there was a lull in activities until the early 1930's when Whittle asked for a leave from the Royal Air Force to organize a company to develop turbojet units. It was difficult for him to get support on this project so the work did not really get under way until 1936, when he formed the Power Jets Company and began the development of a centrifugal-compressor unit. His labors met with success and his first compressor-turbine gas engine ran in the test bed in 1937. In 1936 a second group under the direction of Griffith and Constant at the Royal Aircraft Establishment began to construct and test axial-flow compressors. A little later in the same year, a group in Germany under the direction of von Ohain at the Heinkel Aircraft Company began development work on a centrifugal compressor. The Germans began preliminary work on the axial-flow turbojets in 1937. The English groups were completely unaware of the activities of the German groups and probably vice versa.

In March, 1938, the British Air Ministry placed a development contract with Power Jets, Ltd., and a little over a year later, in July, 1939, the first flight unit was ordered. The engine produced was the W-1 which powered the first British jet flight. This centrifugal-compressor-type turbojet unit delivered about 855 lb of static thrust and weighed 623 lb, Fig. 1.

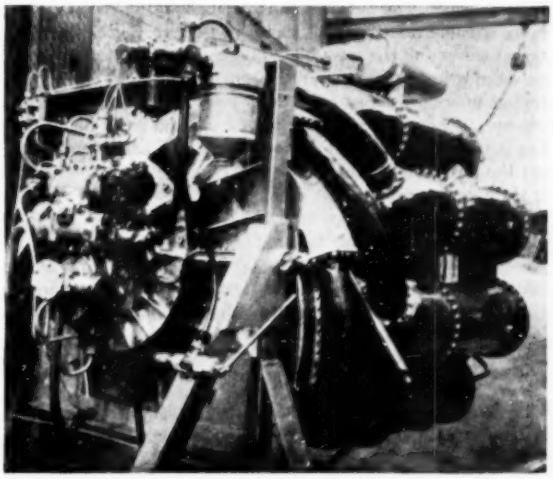

Fig. 1 W-1X Engine
(Courtesy of British Information Service.)

The development in Germany was more of a private investigation. The initial design, the He S3B, which propelled the first turbojet flight, was also a centrifugal-compressor unit. It differed from the W-1 in that it had an annular combustion chamber instead of the can type. It delivered about 1100 lb of thrust.

---

[1] Director Research Division, Bureau of Aeronautics.

[2] Head, Applied Mathematics Branch, Research Divison, Bureau of Aeronautics.

[3] A turbojet is an engine consisting of an air compressor, a burner, a turbine, and a nozzle. The compressor is powered by the gas turbine, and the exhaust gases depart in an axial direction, thereby giving a force on the engine in the opposite direction.

[4] The Caproni-Campini flight on August 27, 1940, is excluded here, since the compressor was driven by a reciprocating engine.

Contributed by the Gas Turbine Power Division and presented at the Fall Meeting, Chicago, Ill., September 8–11, 1952, of The American Society of Mechanical Engineers.

Notes: This is paper No. 52—F-7 of a Progress Report which the Executive Committee of the Gas Turbine Power Division authorized at its 1951 Annual Committee Meeting. The series includes the following: "Introduction" by A. Tom Sawyer, paper No. 52—F-1A; "Materials, Cooling, and Fuels," by A. A. Hafer, paper No. 52—F-1B; "Cycle Components," by P. F. Martinuzzi, paper No. 52—F-1C; "Automotive" by Frank L. Schwartz, paper No. 52—F-2; "Railroads," by K. A. Browne, J. I. Yellott, and P. R. Broadley, paper No. 52—F-3; "Marine," by W. A. Dolan, Jr., and A. A. Hafer, paper No. 52—F-4A; "Merchant Vessels," by W. A. Dolan, Jr., and A. A. Hafer, paper No. 52—F-4B; "Naval Vessels," by W. A. Dolan, Jr., and A. A. Hafer, paper No. 52—F-4C; "Stationary Electric Generation," by Lee Schneitter, paper No. 52—F-5; "Industrial," by L. N. Rowley, Jr., and B. G. A. Skrotzki, paper No. 52—F-6.

Statements and opinions advanced in this paper are to be understood as the individual expressions of the authors and not to be construed as official or reflecting the views of the Bureau of Aeronautics, or of the Society.

Since the numerical values presented here have been taken from a variety of unclassified and unofficial sources, including newspapers, magazines, etc., the authors are not responsible for the accuracy of the data.

Description of Compressors

In order to eliminate the possibility of confusion the main types of compressors will be described briefly. A typical centrifugal compressor consists of a rotor mounted on a shaft so that it can be rotated in a stationary casing with small axial clearance. The rotor is composed of a circular metal disk with attached radial vanes or blades. As a result of the centrifugal force imparted to the air by the rotor, a flow is established in which air enters the annular inlet of the casing near the axis and flows between the vanes and out radially into the stationary casing. The casing contains fixed guide vanes which direct and diffuse the air as it leaves the rotor. The air is diffused further in collection chambers and then discharged through one or more ducts, Fig. 2.

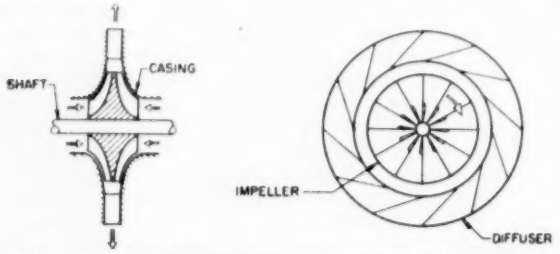

Fig. 2 Schematic Illustration of Centrifugal Compressor

An axial-flow compressor is composed of an alternating sequence of fixed and movable sets of short blades. The sets of fixed blades are spaced around the inside periphery of an outer stationary casing and together they constitute the stator. The sets of the movable blades are fixed to a spindle and the combination constitutes the rotor. The axial spacing between each consecutive set of stator blades is just wide enough to permit the sets of rotor blades to pass between them as the rotor revolves about its axis. The radius of the rotor hub and the length of the blades are determined so that there is only a very small tip clearance at the end of the rotor blades. One set of stator blades and one set of rotor blades constitute a single compressor stage. The number of stages varies from three on up depending upon the pressure. Energy is added to the air by the rotor blades and then it is redirected by the following stator blades before entry into the next stage. In order to avoid excessive velocities the air is diffused in each stage, either in the stator, in the rotor, or in both. The successive sets of blades are reduced in length to compensate for the reduction in volume resulting from the increased pressures.

A mixed-flow compressor differs from a centrifugal compressor in that the vanes are attached to a hub with increasing diameter, instead of a metal disk perpendicular to the axis.

Centrifugal-Compressor Jet Engines

The W-1 unit was so satisfactory that it stimulated a concentrated development program in both England and America. Its design was brought to America, and General Electric Company produced a duplicate called the I-A. Immediately thereafter, the General Electric engineers began to make design improvements and to increase the size of the units. They built in sequence a few I-14's, many I-16's, some I-20's, and a large number of I-40's. These units were designed to develop 1400, 1600, 2000, and 4000 lb of static thrust, respectively. Engines of the first two of this series were employed to propel the twin-engine Bell P-59A aircraft, the first American jet plane. The I-20 had the best specific fuel consumption of any of these early designs, but

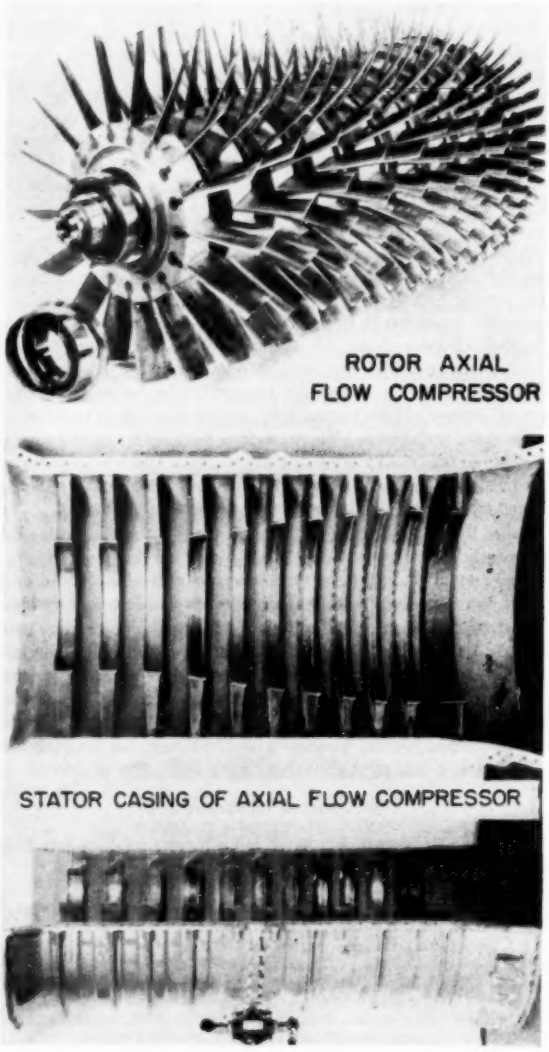

Fig. 3 Axial-Flow Compressor
(Courtesy of Westinghouse Electric Corporation.)

because of the requirement for larger units only a few were built. The I-40, on the other hand, was the initial design of the turbojet which has been built in larger quantities than any other unit. It was conceived early in 1943 and was run initially in December of the same year. It was first used in the Lockheed XF-80, the *Shooting Star*, in June, 1944. In order to secure expanding facilities the blueprints of the engine were given to Allison Division of General Motors for mass production. The initial production model, which is now designated the J33-A-21, delivered 3825 lb of static thrust with a specific fuel consumption of 1.22 lb of fuel per hr per lb of thrust. It weighed 1850 lb. Through a continual development program by Allison the engine has been improved in two successive major steps. The first increased the static thrust to 4600 lb and the second was even a greater increase. These increases, unlike the ones in the I-series, were made without increasing the diameter of the engine. The increases in

thrust were obtained by increasing the air flow and the compression ratio. Simultaneously, with the thrust increase the specific fuel consumption was reduced. The weight of the engine was only increased slightly and as a consequence the specific weight was reduced, Fig. 4.

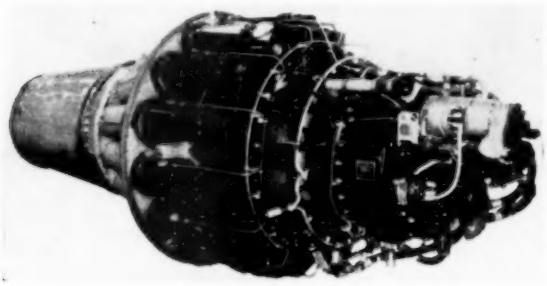

FIG. 4 J33-A-35 ENGINE
(Courtesy of Allison Division of General Motors Corporation.)

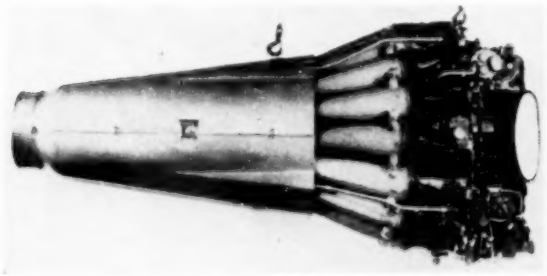

FIG. 5 THE GOBLIN
(Courtesy of De Havilland Engine Company, Ltd.)

At the same time that General Electric and Allison were developing and making improvements the British engineers were also making great strides along the same line. The DeHavilland Company produced the *Goblin* and the *Ghost*. The Rolls-Royce Company designed in order the *Welland*, the *Derwent*, and the *Nene*. The essential difference between the developments of the two companies was that the DeHavilland engines employed single-entry compressors while the Rolls-Royce concentrated on the double-entry type. The latter-type compressor has vanes on both sides of the impeller and has the advantage of increased air flow with only a small increase in weight. The former has the possible advantage of greater ram-pressure recovery. (The American engines previously mentioned are of the double-entry type.) The thrusts of these engines varied from 3000 to 3500 lb for the *Goblins*, from 4450 to 5000 lb for the *Ghosts*, from 3600 to 4000 lb for the *Derwents*, and from 5000 lb for the *Nene I* to 6250 lb for the *Nene TAY*. The development in England kept a close pace with that in America. In fact, in all phases except production, the English have maintained the leadership. The *Nene TAY* and the J33-A-16 are of about equivalent development advancement and they both sprang from the Whittle W-1 which was the grandfather of them all.

Americanized versions of both the *Nene I* and the *Nene TAY* are being produced by Pratt and Whitney. Other versions of the same engines are also in production in France, Russia, and Australia. Versions of the *Goblin* and the *Ghost* are being produced in Sweden and Italy and the *Derwent* in Belgium and Argentina. A limited number of the *Goblins*, or more precisely,

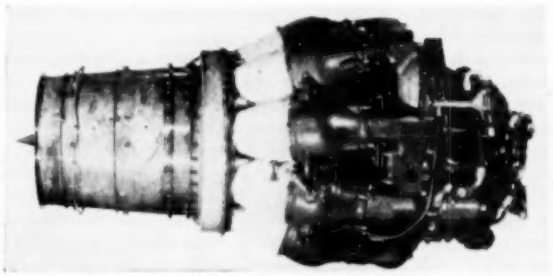

FIG. 6 J48 ENGINE
(Courtesy of Pratt & Whitney Aircraft.)

the forerunner of the *Goblins*, the *Halifford H-1* was produced in the United States by the Allis-Chalmers Company.

The Turbomeca Company in France is producing two series of small centrifugal jet engines with air flows of 4.6 to 16.5 lb per sec. They develop thrust in the range from 200 to 720 lb. The Continental Aviation and Engineering Corporation is licensed to produce these engines in America. The Boeing Aircraft Company has developed an even smaller unit with thrust of about 150 lb.

AXIAL-COMPRESSOR JET ENGINES

Although the development on axial-flow turbojet units began almost as early as the work on centrifugal and many more designs have been made, the production in America and England has lagged behind that of the centrifugal type. The reverse was true in Germany. In spite of the fact that the first German flight was with a centrifugal-type jet and they continued to make other designs, the axial-flow engines emerged the favorites and were the first to be put into production. The Jumo 004 was the only operational German turbojet. It had an eight-stage axial compressor, six combustion chambers, and a one-stage impulse turbine. It delivered a static thrust of from 2200 to 2500 lb with a specific fuel consumption of about 1.36 to 1.4 lb. It was the power plant used in the Me 262, the first operational jet bomber. The construction of the Jumo 004A was begun in early 1940, and the first unit ran in December of that year. It required a period of about 6 months to eliminate the vibration troubles; consequently the unit was not flight-tested until late in 1941. The second of this series, the 004B unit, was designed about this time and flight-tested in 1942. It was this version which went into production in 1943.

In this country the Westinghouse Electric Corporation and the General Electric Company pioneered in the field of axial-flow turbojets. Although some thought was given to the possibilities of such engines in 1941, the fabrication of units did not begin until 1942, and the first units were tested in 1943. The Westinghouse Corporation built the 19A, 19B, 9½A, 9½B, 19XB, 24C, and the J40 in sequence. The designations of the first six of these units were based upon the diameter in inches of the units, and their static thrusts delivered were 1100, 1365, 270, 275, 1600, 3000 lb, respectively, Figs. 7 and 8.

The General Electric designed and built the TG180, TG190, and is currently developing other new engines. The TG180 known as the J35 was placed into quantity production by Allison in 1947. The TG190 or J47 is being produced by General Electric. These two engines are similar; the latter has one more compressor stage, and increased air flow and thrust. The first of these engines developed 3750 and 4800 lb of static thrust, respectively. Again, both of these engines have gone through extensive development programs until now the thrusts have been increased to 5600 and over 5800 lb, respectively. In addition, both have

been redesigned completely to give even higher rated values, Figs. 9 and 10.

As was indicated earlier, the British began the development work on axial-flow units almost as soon as on centrifugal units. There was a long development program on compressors, consisting of the construction and testing of several. The first complete axial turbojet, F-1, was produced in December, 1939. It had a compression ratio of 4, a mass flow of 38 lb per sec, and delivered 2150 lb of thrust when operating at 1930 deg R. The production version, the F-2 made by Metropolitan-Vickers, first ran in December, 1941. It delivered 2200 lb of thrust, weighed 1530 lb, and gave a specific fuel consumption of 1.07 lb. This engine was superior to the German contemporary, the Jumo 004, by 25 per cent in fuel consumption and 5 per cent in specific weight. After the F-2 the Metropolitan-Vickers produced the F-2/4, *Beryl I* and the *Beryl II*. The Armstrong-Siddeley built the ASX, the *Adder I*, and the *Sapphire*. The Bristol Company has designed the

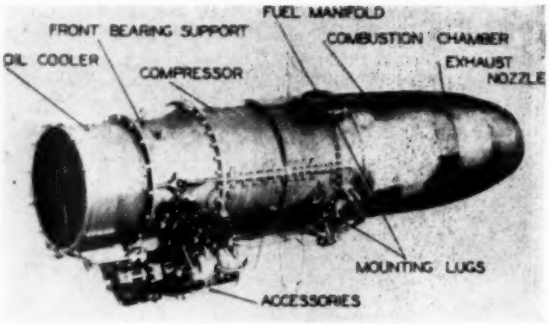

FIG. 7 19XB ENGINE
(Courtesy of Westinghouse Electric Corporation.)

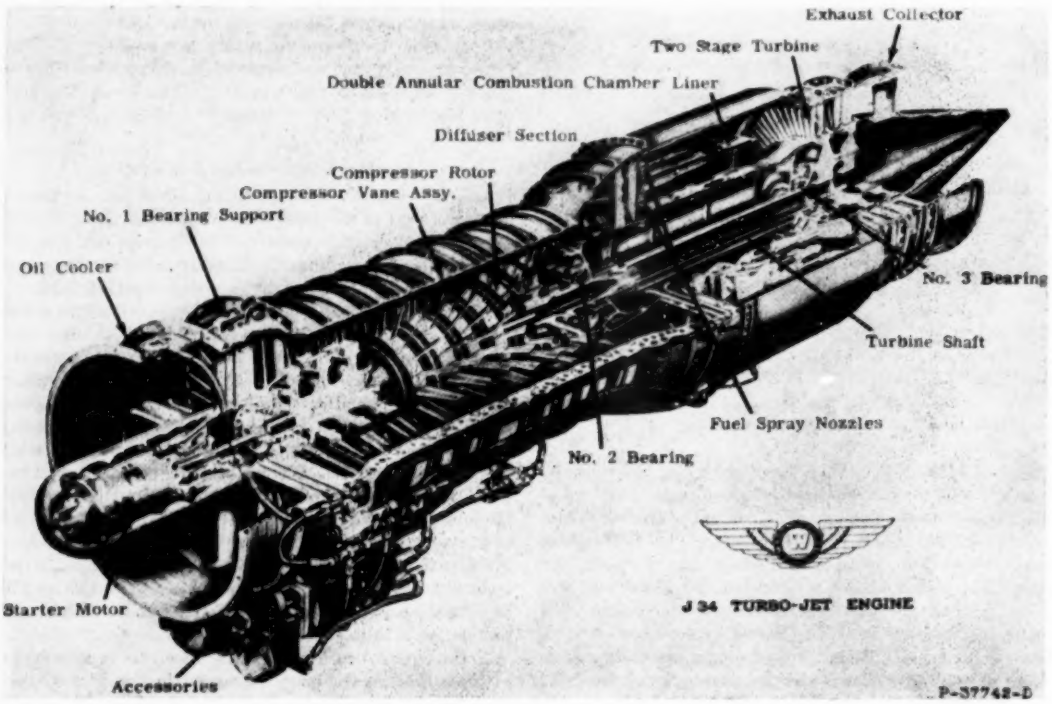

FIG. 8 J34 ENGINE
(Courtesy of Westinghouse Electric Corporation.)

Olympus. Because of their merit, American versions of the latter two are now under contract for production in the United States by Wright Aeronautical Company, Fig. 11. Simultaneously with later developments of the other companies the Rolls-Royce Company has designed and built the *Avon*.

Except for the production of the British *Nene*, the design development and production of jet engines in France has been concentrated upon the axial-flow type. Rateau has designed units with high compression ratios and large thrust values. The Ste' Nationale d'Etude et de Construction de Moteurs d'Aviation and Ste' de Construction et d'Equipments Mecaniques pour L'Aviation have also designed a series of axial-flow turbojets.

In Canada the AV Roe Canada, Ltd., has built two axial-flow turbojets, the *Chinook* and the *Orenda*. The first has a static thrust of about 2600 lb and the latter about 6500 lb, Fig. 12.

The Swenska Turbinfabriks Company in Sweden has developed the *Skuten I*, an axial-flow engine of about 3200 lb of thrust.

The Russians have produced several axial-flow turbojets which were developed from the German engines. They have improved versions of the BMW 003, the Jumo 004, the Jumo 012, and the BMW 018. These engines deliver thrusts of about 3750, 4000, 6600, and 7700 lb, respectively. The compression ratios vary in the range from 3.4 to 7.0 and specific fuel consumption of 1.2 to 1.08 lb.

AUGMENTATION

In spite of the fact that the turbojet engine, as a result of its

low weight and large thrust output at high velocities has revolutionized aviation, it has some disadvantages. One of these is its low thrusts for take-off. This deficiency has been partially corrected by augmentation of the thrust by water injection or by afterburning.

Until now, the thrust values quoted have been those for a simple open Brayton cycle with air as the fluid, namely, compression, heat addition at constant pressure, and an expansion back to initial pressure. In the expansion, the turbine extracts the exact amount of energy required for the compressor; the remainder of the energy is converted into velocity by the nozzle to form the jet stream which is directed backward. Since the total pressure

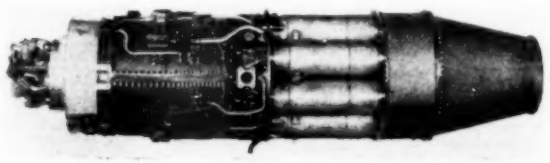

FIG. 9 J35 ENGINE
(Courtesy of Allison Division of General Motors Corporation.)

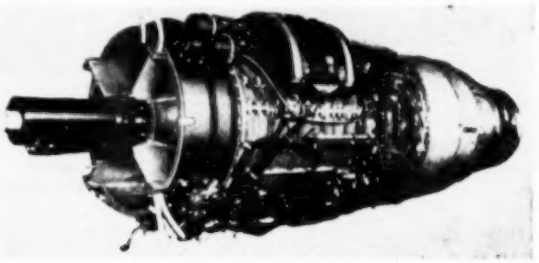

FIG. 11 J65, AMERICAN VERSION OF SAPPHIRE ENGINE
(Courtesy of Wright Aeronautical Corporation.)

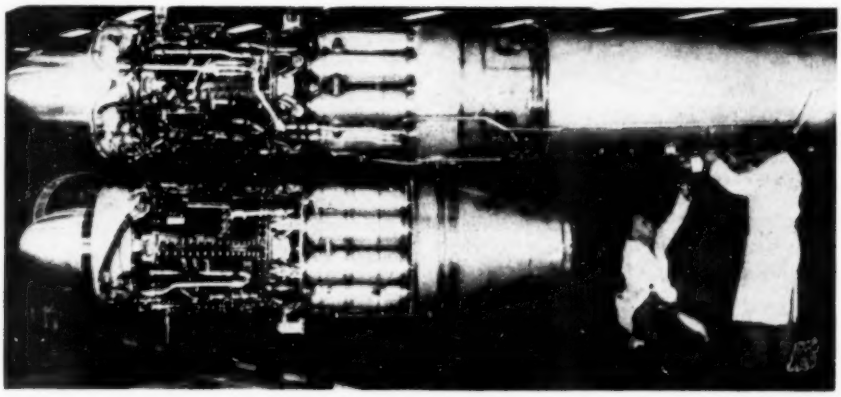

FIG. 10 J47 ENGINE WITH AND WITHOUT AFTERBURNER
(Courtesy of General Electric Company.)

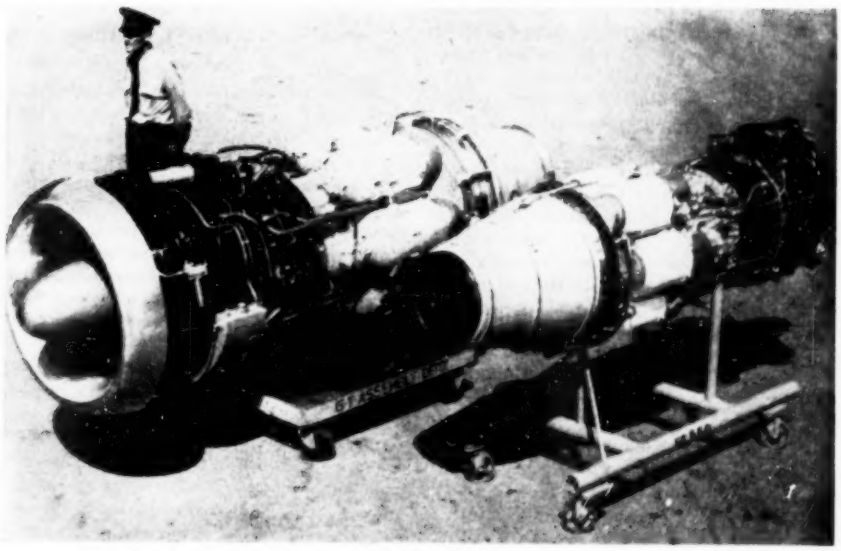

FIG. 12 *Left*, ORENDA ENGINE; *right*, CHINOOK ENGINE
(Courtesy of A. V. Roe Canada, Ltd.)

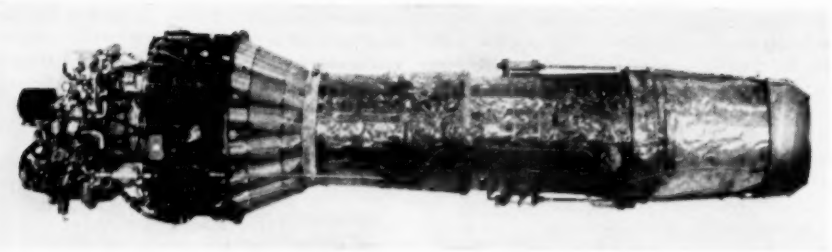

FIG. 13 J33 ENGINE WITH AFTERBURNER
(Courtesy of Allison Division of General Motors Corporation.)

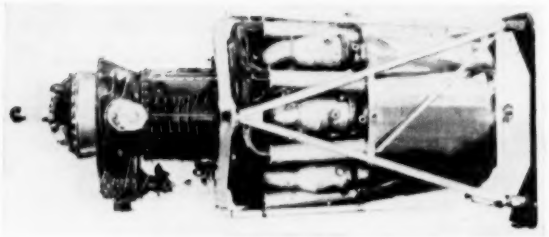

FIG. 14 THESEUS I ENGINE
(Courtesy of Bristol Aeroplane Company.)

after the turbine is greater than the atmospheric pressure, a second addition of heat before the expansion through the nozzle would yield an even higher jet velocity. Such a process is called afterburning.

The experiments of the British, early in 1944, demonstrated that the additional burning in a jet stream of a turbojet was possible. The first experiments in this country were made by Woodhull, Gibson, and Knapp. In these early tests, the problem was to get the fuel to burn. The art has progressed so that now the problem is to improve the efficiency, reduce the pressure losses, and increase the altitude of operation. (Although the introductory paragraph of this section referred only to take-off, additional thrust at other altitudes and speeds is frequently desired.) Now, nearly all production turbojets have a model equipped with an afterburner which augments the static thrust by 40 to 60 per cent and the thrust at a Mach number of 1 by as much as 100 per cent. This gain is not all velvet because there is an additional pressure loss in the elongated exhaust nozzle (the second burner) which persists even when the afterburner is not operating, thereby increasing the specific fuel consumption at all powers and decreasing the maximum attainable thrust without afterburner operation. Besides this, the specific fuel consumption for the additional thrust delivered when the afterburner is in operation is from 4 to 5 times that for the simple-cycle engine without afterburner. As a result, the specific fuel consumption on the total thrust is about $2^1/_4$ times that of the simple engine. Nevertheless, the afterburner has its place and for a short interval of operation the excessive use of fuel will not equal the additional weight required for the basic engine which could deliver the thrust without augmentation.

Another method of augmentation is the injection of water or other liquids into the airstream at or near the compressor entrance. The cooling of the air by the evaporation of the water injected at the entrance of a compressor admits three beneficial effects, namely, (*a*) an increased mass flow, (*b*) a lower power requirement for a given compression ratio, and (*c*) a higher pressure ratio. The increase in mass flow results from the density increase associated with the lower temperature. The decrease in enthalpy per pound of mass required for compression to a given pressure is evident at a glance of an h-s chart. The lower temperature makes the Mach number of flow higher for the same rate of rotation and, since the pressure ratio by the similarity law is an increasing function of the Mach number, the pressure ratio for the maximum rpm is higher. This increase in pressure ratio, on the current engines with low compression ratio, produces an increase in cycle efficiency. Additional fuel may be added since the gases may be heated to the same top temperature. Hence there will be an increased amount of useful energy per pound of gas. Thus with water injection there are two beneficial effects, increased mass flow and increased useful energy per pound. Of the two effects, the latter is the greater. Usually, the water is mixed with alcohol for two reasons: (*a*) To supply the additional energy required to evaporate the liquid and heat the additional mass, and (*b*) to avoid possible freezing of the water. An increase of from 10 to 20 per cent in the static sea-level thrust can be obtained in this manner, and a somewhat higher percentage may be obtained at high speeds. The total liquid (water, alcohol, and fuel) consumption for water injection is much higher than it is for afterburning. Hence the method would be used for even shorter periods of time.

Some current engines are equipped for both water injection and afterburning. The two effects are additive so it is possible to obtain 70 per cent increase in static thrust over the basic engine.

TURBOPROP DEVELOPMENT

Another possible method of improving the static thrust and thrust at low speeds is to activate a larger mass of air. This can be done by extracting additional power in the turbine and utilizing it to drive a propeller or fan. In spite of the additional complications and weights resulting from the extra turbine stages, the gearbox, and the propeller, the higher possible propulsive efficiencies have made the idea attractive. Soon after the success of the first turbojets, the British launched out on the project of making such engines. The Armstrong-Siddeley Company used the ASX axial-flow turbojet as a basis of the development of the *Python* turboprop. This engine first ran in March, 1945. The Rolls-Royce made an adaptation of its *Derwent* turbojet to form an experimental turboprop, the *Trent*. In September, 1945, it became the first turboprop to propel an aircraft.

The Bristol Company was the first to concentrate upon the development of a turboprop per se; their first unit was the *Theseus I*. It had a combined compressor consisting of eight axial stages followed by one centrifugal stage. The compressor was run by the first two stages of the turbine and the third turbine stage drove a propeller by means of an independent shaft which extended forward through the hollow compressor-rotor shaft. This unit was unique in that it had a heat exchanger; that is, the

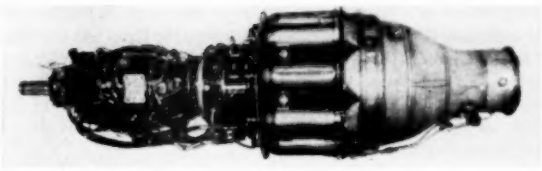

FIG. 15 T31 FORMERLY TG100 ENGINE
(Courtesy of General Electric Company.)

hot exhaust gases and the air leaving the compressor were passed through adjacent tubes in a matrix so that the hot exhaust gases transferred some heat to the compressed air, thereby reducing the amount of fuel required in the burner. At about the time of these British developments, the General Electric Company in America designed and produced the TG100. This engine made its maiden flight on December 21, 1945, when it propelled the XP-81, Fig. 15.

Actually, the first turboprop designed in the United States was the turbodyne of the Northrop Aircraft Company. The commitment for the production of this engine began in 1941, and the engine was wrecked in the test bed some 4 years later.

Subsequent to the early developments in England, the Bristol Company produced a larger unit, the *Proteus*, the Rolls-Royce produced the *Clyde* and the *Dart*, the Armstrong-Siddeley the *Python* II and the *Mamba I* and II, and the Napier Company the *NAIAD*.

After the removal of the energy to run the propeller, there is still energy in the jet stream which, from the standpoint of aviation, is still useful. It delivers a jet thrust so now the thrust horsepower or useful thrust is obtained from two sources, the shaft power and the jet power. A complete description of the engines would specify the exact division of the total energy between these two. However, for comparison purposes it is convenient to combine the two into a single approximately correct one called the equivalent shaft horsepower, denoted by ESHP. The static value is taken to be the sum of the shaft power and 0.4

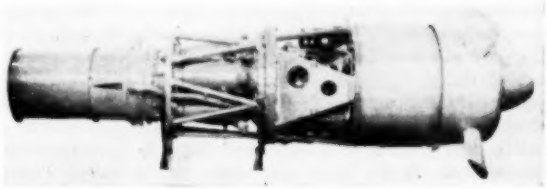

FIG. 16 THE NAIAD
(Courtesy of British Information Services.)

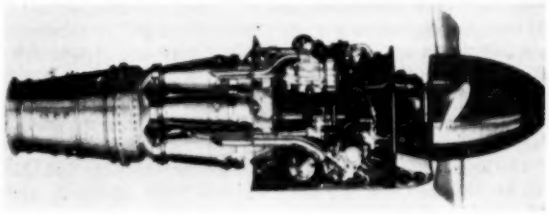

FIG. 17 MAMBA ENGINE
(Courtesy of British Information Services.)

times the jet thrust, that is, static

$$\text{ESHP} = \text{SHP} + \frac{F}{2.5}$$

while the values at flight speed are the sum of the shaft power and the thrust horsepower of the jet divided by 0.85 (assumed propeller efficiency)

$$\text{ESHP} = \text{SHP} + \frac{FU}{(550)(.85)}$$

where U is the flight speed in feet per second. Since in most cases the amount of thrust power delivered by the jet is a small per cent of the total thrust power an error in assuming an incorrect value for the propeller efficiency gives at most a small error

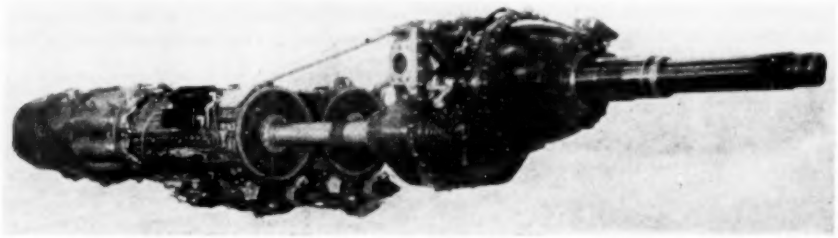

FIG. 18 T40 ENGINE
(Courtesy of Allison Division of General Motors Corporation.)

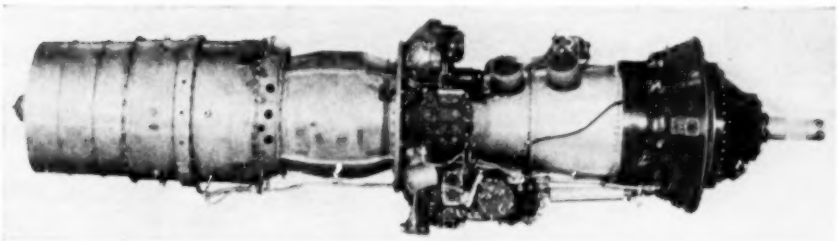

FIG. 19 T34 ENGINE
(Courtesy of Pratt & Whitney Aircraft.)

on the entire shaft power. (The percentage of error would equal the error in efficiency times the percentage of jet-thrust power.) The static power of the British engines mentioned vary from 1100 to 4600 ESHP. They also have coupled units of the principal engines: the *Python*, the *Mamba*, the *Proteus*, and the *NAIAD*, which delivers twice the power of the single units.

Although there have been several paper designs from the simplest units to the most complicated heat-exchanger cycles, there are only three companies in the United States producing large turboprop units; Allison, Pratt and Whitney, and Wright Aeronautical. Allison has a unit which will deliver over 2780 equivalent shaft horsepower and an engine consisting of two of these units coupled to a single shaft. Pratt and Whitney has one unit which will deliver about 5500 ESHP and Wright Aeronautical has one of similar size.

The Germans had thought of building turboprops and it is believed that the Russians have built one following the preliminary design of the Germans.

The French have a medium-size axial-flow turboprop and again the Turbomeca Company has a series of small turboprop units with airflow of 4.4 to 6.8 lb per sec. These latter units develop from 225 to 350 SHP.

The Boeing Aircraft Company also has a small turboprop, the Boeing 502.

In addition to the *Theseus*, the *Proteus* and the *Clyde* have a compressor composed of several axial stages followed by a centrifugal stage. The *Dart* and the T35 have two-stage centrifugal compressors. The others mentioned (except the *Trent* and Boeing 502) all have axial-flow compressors.

Ducted Fans

Many studies have been made concerning the possibilities of developing an engine intermediate between the turbojet and the turboprop. The engines have been described by the terms ducted-fan, by-pass engine, and so on. Essentially, more energy than that required for the compression of the main air stream is removed by the turbine. This energy is employed to drive a fan attached to the turbine which augments the mass in the jet stream, or to drive longer compressor blades which compress a second mass of auxiliary air that augments the jet stream either with or without heat additions in this auxiliary stream. Although there is a possible advantage of this type of engine over the other gas turbines for some applications, so far it has not been of sufficient merit to encourage the development in the United States. In England, the Metropolitan Vickers designed and produced the F3 and F5. The first has a ducted fan and the latter an open fan, Fig. 20. In addition to these the British are also developing a by-pass engine.

Once again, the Turbomeca Company in France has a small unit, the *Aspin I*, of about one tenth the size of the British units.

Designations

In 1946 the Armed Services of the United States formulated an official designation system for gas-turbine engines. The designation consists of a letter to denote the type, J for a turbojet and T for a propeller turbine. The latter is followed by a number 30 and above, which specifies the engine regardless of the manufacturer. The number is even for engines developed under Navy contract and odd for those developed under Air Force contract. A dash then precedes one or two letters which denotes the manufacturer and this (these) letter(s) is followed by a dash and another number which denotes the specific modification. Again, the last numbers are even for naval use and odd for Air Force use. This is true even when the engines are identical.

For example, the J33-GE-4 is a turbojet designed and produced under Air Force contract, manufactured by the General Electric Company and is to be used by the Navy. In the case of experimental engines, the described designation would be preceded by the letter X. For example, the XJ34-WE-22 is an experimental jet engine under Navy contract with Westinghouse Electric Corporation to develop an engine for a naval use. Although the first part of the designation appears clear the dash numbers which denote the modifications are confusing since they do not appear in any definite order.

All existing turbojets and turboprops and all of those that have been in design and development stages in the United States have been given one of these standard designations. The contracts on some of the engines were canceled even before any were built so there are some missing numbers in the present J and T series. To date, the J series extends from 30 to 48 on the even numbers and from 31 to 73 on the odd numbers. The old designations and the new ones are co-ordinated in Table 1. The T series

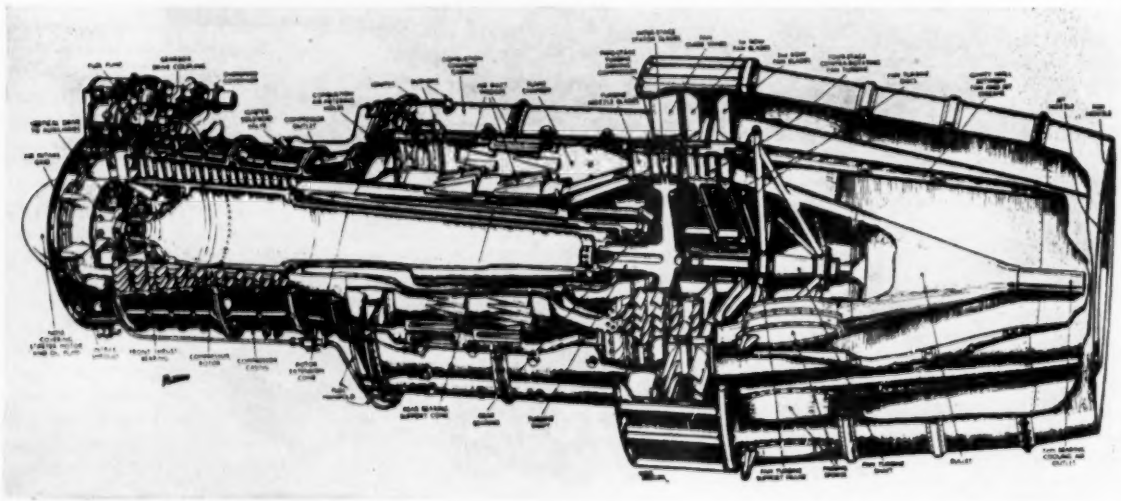

Fig. 20 F3 Engine
(Courtesy of British Information Services)

also began with 30 and currently goes up to 50. Even and odd numbers again give the same distinction as for the turbojet.

Fundamental Characteristics

So far this paper has been confined to historical facts. Many engines have been produced in this short interval of time. The question arises: Are the new engines better? Or, in other words, what is the "state of the art"?

Of the many characteristics of engines the ones most important from the standpoint of aviation are the thrust or power of the unit, the specific fuel consumption, the specific weight, the thrust per unit frontal area and per unit size. A large thrust is important for take-off and high velocity; a low specific fuel consumption is required for long range or endurance. A light engine permits smaller airplanes, or greater range, or more payload or a combination of all. A small frontal area admits the possibility of a cleaner airplane with less drag, hence one which requires less thrust for a given performance. In some designs, space considerations are important, hence, the smaller the better.

A high maximum static sea-level thrust is essential for take-off; however, the most important point for low fuel consumption is at the altitude, speed, and thrust employed for the cruise or at the high-speed condition, depending upon the type of operation. It is unfortunate that engines are sold on the basis of their static sea-level performance for the time of operation there is so short. It is quite probable that many if not most of the early designs have been designed for static sea-level performance even at the expense of better performance at current flight speeds and altitudes for application. Nevertheless, the tables and graphs given herein, which are made to show the progress of the art, will be based largely upon the static sea-level performance, since more uniformity can be obtained for the data there.

The basic characteristics of the turbojets are given in Table 1 and those for the turboprops in Table 2. The values refer to operation at maximum temperature and rpm without augmentation, except those for cruise which refer to the normal rating. The following nomenclature is employed:

F = static thrust, lb
F_c = thrust at a speed of 400 knots at 35,000 ft, lb
W_F = fuel at static sea level, lb per hr
W_{Fc} = fuel at speed of 400 knots at 35,000 ft, lb per hr
W = engine weight, lb
A = maximum frontal area, sq ft
L = length, ft
ESHP = static equivalent shaft horsepower

The year is the date of the experimental engine operation.

TABLE 1 TURBOJET ENGINES

Name	J-designation	Year	F	$\frac{W_F}{F}$	$\frac{W}{F}$	$\frac{F}{A}$	$\frac{F}{L}$	$\frac{W_{Fc}}{F_c}$
Centrifugal Compressors								
HeS3B		1939	1100	1.450	0.722	151		
W-1		1941	855		0.729			
I-14		Early 1942	1400					
I-16	J31-GE	Mid 1943	1670	1.182	0.525	178	286	
I-20	J39-GE	1944	2000		0.401	203	343	
I-40	J33-GE	1944	3750	1.185	0.475	255	440	
	J33-A-21	1945	3825	1.220	0.484	274	446	
	J33-A-14	1948	4600	1.140	0.386	316	517	1.400
	J33-A-27	1951						
Halifford H-1	J36-AC-2	1944	2700		0.519			
Goblin 2		Mid 1944	3000	1.230	0.517	219	336	
Goblin 3		1945	3350		0.470	248	400	
Ghost 2		1946	5000	1.080[a]	0.402	329	520	
Welland I		Early 1943	1600	1.120	0.530	159	310	
Derwent I		Late 1943	2000	1.170	0.490	198	286	
Derwent V		1944	4000	1.080[a]	0.312	398	577	
Nene		Late 1944	5000	1.060	0.313	376	620	
Am. ver. Nene II	J42-P-4	1947	5000	1.120	0.345	376	580	1.219
TAY		1951	6250		0.320			
Am. ver. Nene TAY	J48-P-6	1951	6250	1.120	0.325	454	702	1.29
Pimene		1950[a]	242	1.160	0.486	173	72	
Palas		1951[a]	330	1.200	0.400	237	95	
Marbore I	J69-T-1	1951[a]	640	1.075	0.825	234	141	
Marbore II	J69-T-3	1951[a]	880	1.090	0.818	321	194	
Boeing 500		1947[a]	150	1.300	0.570	56	62	
Axial-Flow Compressors								
Jumo 004B		1940	2200	1.400	0.790	450	187	1.740
BMW-003		1940	1760	1.400	0.762			1.650
Jumo-012		1943	6070	1.200	0.636			1.320
BMW-018		1943	7700	1.180	0.715			1.250
F-2		1941	2200	1.070	0.695	280	166	
F-2/4		1942	3500	1.050	0.500	478	264	
Beryl I			3850		0.464	510	286	
19A		1942	1360	1.350	0.610	691	163	
19B		1943	1365	1.280	0.620	694	157	
9½A	J32-WE	1943	250	1.900	0.580	510	54	
9½B		1943	275	1.700	0.520	560	60	
19XB	J30-WE	1944	1560	1.170	0.440	791	199	1.680
24C	J34-WE-22	1948	3000	1.080	0.395	755	300	1.290
	J34-WE-32	1949	3370	1.080	0.504	848	220	1.240
	J34-WE-38	1950	3500	1.040	0.426	883	375	1.200
	J46-WE	1951						
	J40-WE-8	1951						
	J40-WE-6	1952						
TG-180	J35-GE	1944	3750	1.115	0.655	421	267	
	J35-A-15	1947	3750	1.115	0.655	428	276	
	J35-A-17	1949	4900	1.080	0.461	560	402	1.295
	J35-A-29	1951	5600		0.411	722	460	
TG-190	J47-GE	1947	4850	1.100	0.510	586	404	1.240
	J47-GE-17	1950	5425	1.150	0.618	655	288	1.314
	J47-GE-27	1951	5810		0.441	696	480	
ASX		1944	2600	1.100[a]	0.730	271	187	
Adder 1		1950	1100		0.500	81	180	
Sapphire		1950	7200		0.347			
	J65-W	1950	7220					
Avon		1947	6500	0.890	0.292	692	630	
Rateau		1946[a]	3300	1.060	0.67	311	490	
SRA-1								
Rateau SRA-101		1948[a]	7275		0.303	860	608	
ATAR-101		1948[a]	4850	1.060[a]	0.387	731	454	
TGAR-1008		1948[a]	4850		0.570	541	379	
Chinook		1948	2600	1.050[a]	0.480	465	249	
Orenda		1949	6000	1.060[a]	0.417	626	545	
Olympus		1952	9750		0.308			
	J67-W	1952						
Viper	ASV2	1951	1590	1.170	0.360			
	J44-R-1	1950	950	1.650	0.3135	350	158	
	J53-GE-1	1953						
	J55-FF-1	1948						
	J57-P-1	1949						
	J71-A	1952						
	J73-GE-3	1952						

[a] Denotes estimated values.

Note: The J-38 is a turbosupercharged unit. The J-37, J-41, J-43, J-45, J-49, J-51, J-59, and J-61 were canceled.

TABLE 2 TURBOPROPS

Name	Designation	Year	ESHP	$\frac{W_F}{ESHP}$	$\frac{W}{ESHP}$	$\frac{ESHP}{A}$	$\frac{ESHP}{L}$
Theseus 1		1945	2075	0.940	0.980	159.0	235.0
Theseus 21		1947	2142		0.880	163.0	242.0
Theseus 11		1948	2425		0.760	185.0	352.0
Theseus 502		1950	2540		0.870	159.5	368.0
Proteus I		1947	3885				
Proteus II		1949	3510		0.830	433.0	422.0
Coupled Proteus II		1949	7040		1.020	347.0	505.0
Trent I		1945	1062		1.175		
Clyde		1946	3460	0.618	0.810		
Dart I		1948	1125	0.830	0.890	139.0	142.5
Dart 504		1951	1515		0.610	187.0	
Mamba I		1944	1136	0.765	0.660	284.0	170.0
Double Mamba II		1949	2855	0.780	0.700	183.0	338.0
Mamba II		1949	1435		0.610	312.0	224.0
Python I		1945	4130	0.765	0.720	328.0	364.0
Python II		1949	4560		0.650		
NAIAD 1		1948	1590		0.690	372.0	187.0
Coupled NAIAD		1950	3150		0.710	315.0	367.0
TR-1000		1950	1520		0.700	370.0	169.5
TG-100	T31	1945	2440		0.820	325.0	259.0
	T38-A	1948	2780	0.580	0.95	310.0	218.0
	T40-A	1948	5580	0.580	0.465	631.0	386.0
	T34-P	1950	5206	0.610	0.456	635.0	454.0
	T34-P-12	1951	5700	0.615	0.495	576.0	392.0
Turbodyne	T37-NA-4	1947	10000	0.615	0.700	1000.0	782.0
	T35-W-1	1947	5500	0.591	0.625	501.0	681.0
	T47-W	1951					
	T49	1952					
Boeing 502	T50	1948	220		0.640	100.0	630.0

DUCTED FANS

Name	F	$\frac{W_F}{F}$	$\frac{W}{F}$	$\frac{F}{A}$	$\frac{F}{L}$
F-3	4300		0.53	292	368
F-5	4850		0.47	280	398

Note: Based on area of fan

Trends for Turbojets

Tables 1 and 2 give some of the fundamental facts arranged in a somewhat logical manner, yet it is difficult to see from these tables the progress of the development. These and other values have been plotted versus the experimental engine year for the early period from 1937 to 1952. Because of the tremendous scatter of the points it is not possible to construct precise trend curves which have significant values at every point. The curves shown here are estimates of the median values for the series of years. They are included so as to give a general indication of the changes. The discrete points show the scatter.

Thrust

Although turbojet engines are being designed for a variety of thrust, from the small to the very large, there is a definite tendency to build more powerful units. Curves which give an idea of this trend for both centrifugal and axial-flow-compressor types are shown in Fig. 21. The new designs for both types show a

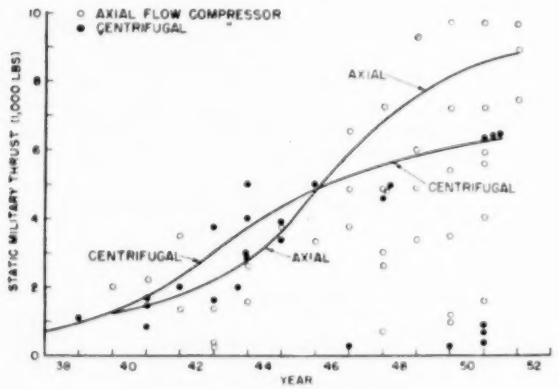

Fig. 21 Thrust of Turbojets

definite increase. These curves indicate a leveling off for size of the centrifugal compressors. The early units of both types were about the same size, but in the last few years the largest engines are all of the axial-flow type. Thus the axial-flow engines show a greater rise in the growth curve. Many of these are of a two-spool design; that is, a portion of the compressor rotor and a portion of the turbine rotor are secured to one shaft and the remainder of the compressor and turbine are secured to another concentric shaft free to move inside the first shaft. It might be possible to conclude from this that the axial-flow engines are more readily adaptable for larger sizes. On the other hand, the extremely small units have been of the centrifugal-compressor type.

Specific Fuel Consumption

The static specific fuel consumption has decreased over the years, Fig. 22. However, this decrease has been small for the centrifugal type since 1944. On the other hand, the specific fuel consumption of the axial-flow type still has a definite downward trend. The values for axial-flow engines are continually less than those for centrifugal engines. This difference is in accordance with prediction and it appeared in the early designs and has been maintained. The trend curves show from 6 to 8 per cent advantage for the axial-flow type. It is of interest to compare the curves in Fig. 22, based upon the engines of the world with similar curves on the British engines published by Constant in 1950. The curves for the centrifugal type are similar in nature

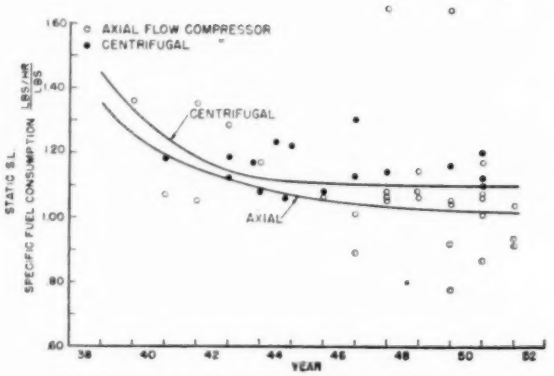

Fig. 22 Specific Fuel Consumption of Turbojets

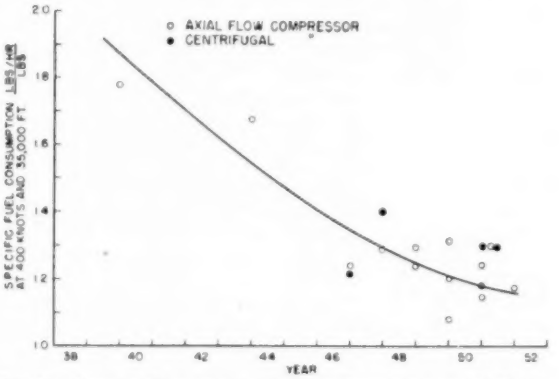

Fig. 23 Specific Fuel Consumption of Turbojets at 400 Knots and 35,000 Ft

but the British curve is from 4 to 6 per cent lower than the one in Fig. 22. Perhaps his curve represents more of an envelope curve rather than a curve of median values. The specific fuel consumption for the axial-flow engines given here does not show the abrupt increase in downward slope at the beginning of 1948. There are only a few engines with sfc less than 0.9. The projected values of Constant's curves appear to have been optimistic. At the present "state of the art," in addition to the technical knowledge, it seems necessary to have exceptionally good luck in order to achieve the lower values. This statement is not facetious, because axial-flow compressors of several stages have been designed which had an adiabatic efficiency of about 0.92 while other compressors designed and manufactured by the same company on the same principles have had much lower efficiency.

The curves, Fig. 23, for specific fuel consumption for cruising at 400 knots at 35,000 ft are based upon less accurate data and fewer points; however, it is believed that the trends are reliable. Only the curve for the axial-flow engine is shown, but the solid dots for a few centrifugal engines show that the two types have maintained their relative positions, the specific fuel consumption of the centrifugal remaining more throughout the operating range. In general, the specific fuel consumption at cruise decreases with altitude but increases with velocity.

The tremendous increase in fuel consumption required for augmentation is shown in Fig. 24. In spite of the advancement, the pounds of fuel per pound of augmented thrust at static sea level appears to be about 5 times what it is for the basic engine. For injection the situation is even worse. The total liquid consumption of alcohol plus water plus fuel per pound of augmented

thrust runs from 3½ to 4 times higher than that for afterburning as illustrated in Fig. 25.

Specific Weight

The specific weights of the turbojets are given in Fig. 26. Rapid progress has been made in this important phase for both the axial and centrifugal types. The specific weights of the axial-flow engines are distinctly higher than those for the centrifugal engines. For points on the trend curves the weight advantage of the centrifugal engines is as much as 20 per cent. The curves do not give any evidence of crossing as was predicted by the extrapolations, the dotted portions, of Constant's curves for the specific weights of British engines. The trend curves presented here indicate it will be several years before the specific weights are as low as 0.3 for axial-flow turbojets. Although a few axial-flow engines are approaching this value, the majority of the designs are above 0.4. Again, Constant's curves appear more like envelope values. The British are even talking about engines with a specific weight of 0.2 to 0.25. Although they have excelled the Americans on this question of minimum weight as is evident from the weight rise in the American versions of the British engines, the achievement of the goal of specific weights of 0.2 appears to be in the distant future. One reason for the higher weights of the American engines is high stress requirements created by the Mach number limit at sea level. A second factor is the weight of the auxiliary gear.

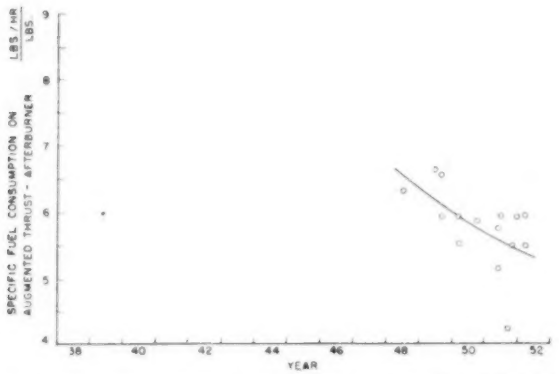

Fig. 24 Specific Fuel Consumption on Augmented-Thrust Afterburner

Size

Not only has the specific weight decreased but the specific size also has been reduced. There has been an increase in thrust per unit length as well as per unit area. As has been generally known, the centrifugal-compressor turbojets give a much higher thrust per unit length and much smaller thrust per unit frontal

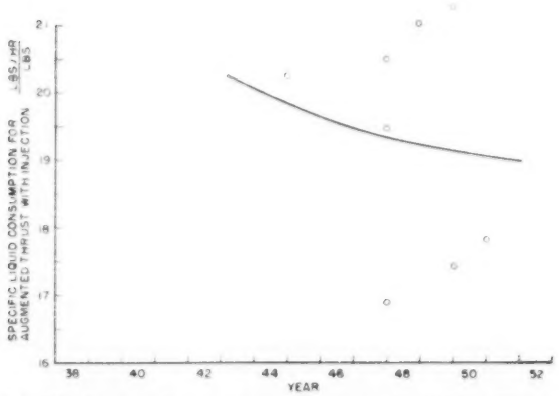

Fig. 25 Specific Liquid Consumption for Augmented Thrust With Injection

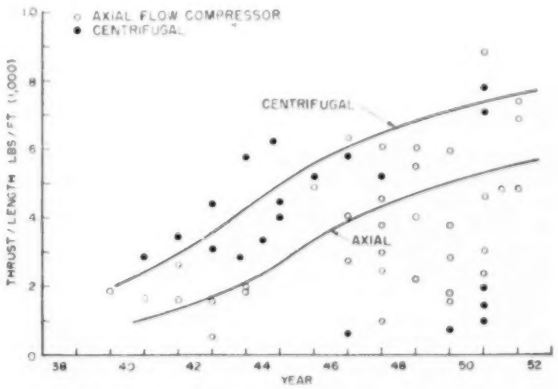

Fig. 27 Ratio of Thrust to Length Turbojets

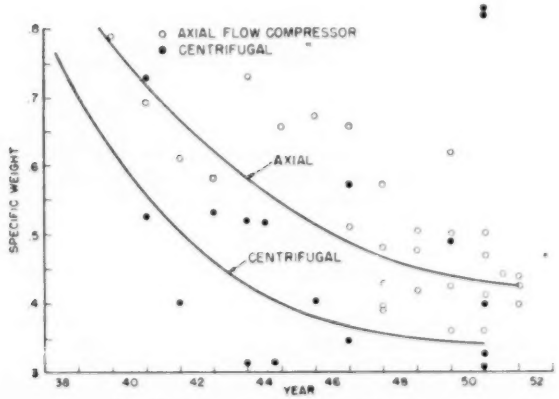

Fig. 26 Specific Weight of Turbojets

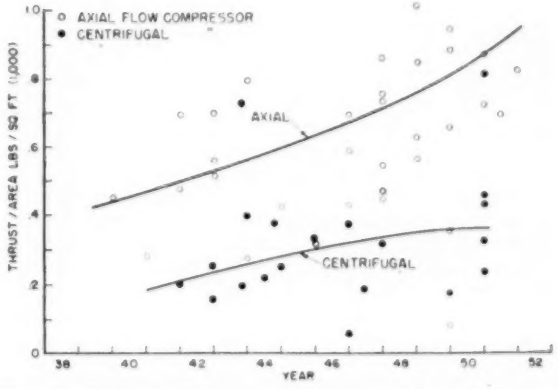

Fig. 28 Ratio of Thrust to Frontal Area for Turbojets

area. The thrust per unit frontal area of the centrifugal type appears to be reaching its maximum but that for axial type seems to be ascending more rapidly than ever. As previously mentioned in the general discussion, the thrust of many of the engines has been increased substantially without increasing the over-all dimension. This can only result from two effects, increased air flow or increased cycle efficiency.[5] Because of the limitation of the latter, most of the improvement must come from the former. This is revealed by the curve in Fig. 29. In fact, if one were to isolate the single greatest improvement which has taken place in the past 7 or 8 years, it would be the large increase in mass flow per unit area. As a result of this, it has been possible to increase the thrust without increasing the weight and length an appreciable amount. As has been mentioned previously, the magnitude

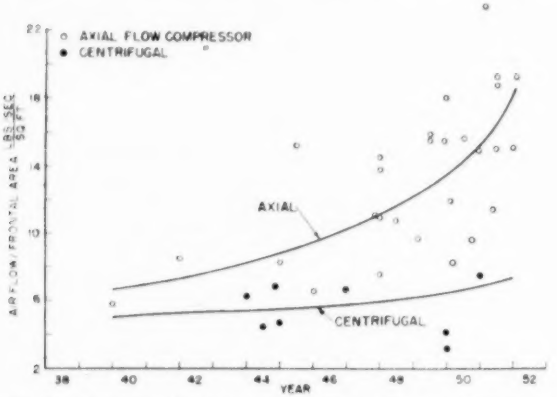

Fig. 29 Ratio of Air Flow to Frontal Area for Turbojets

of thrust per unit frontal area is of especial importance in aviation because of its effect upon the drag of the airplane. Within limits, the larger the diameter of the engine the larger the fuselage or the engine nacelles, either of which will increase the drag of the airplane. These effects become of especial importance in the compressible high-speed range. Every additional pound of drag effectively reduces the thrust by a pound.

The increased mass flow per frontal area has resulted from a reduction in hub/tip ratio, higher relative Mach numbers, and changes in the type of designs, most of which are mentioned in a companion paper.[6] An indication of the change in hub/tip ratio for axial-flow compressors is given in Fig. 30.

Cycle Changes

For the most part, the engines have remained of the simple-cycle type, consisting of compression, heat addition, and expansion. Hence the changes in the cycle efficiency depend upon the changes in these factors. The trend in compression ratio, Fig. 31, has been toward higher values. This is especially true for the axial-flow type in the past few years. In the present temperature range, higher compression ratios give more efficient cycles, provided the compressor efficiency does not decrease too rapidly when the pressure ratio is increased. This opens the discussion for the trends of the maximum operating temperatures, the compressor efficiency, the turbine efficiency, and the changes in compressor and turbine efficiencies with pressure ratio. The maximum operating temperatures, Fig. 32, have increased only slightly over the period of time. The early engines operated at a peak

[5] The cycle efficiency is the ratio of the useful energy to the fuel energy.

[6] "Gas-Turbine Progress Report—Cycle Components" by P. F. Martinuzzi, paper No. 52—F-1C.

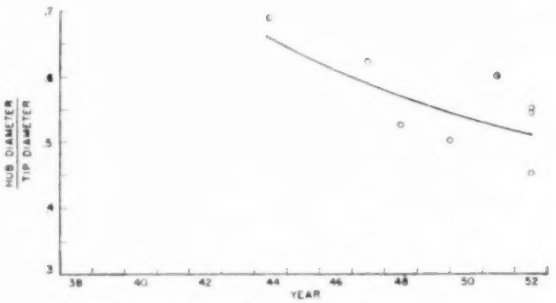

Fig. 30 Front Hub-Tip Ratio of Axial Compressors

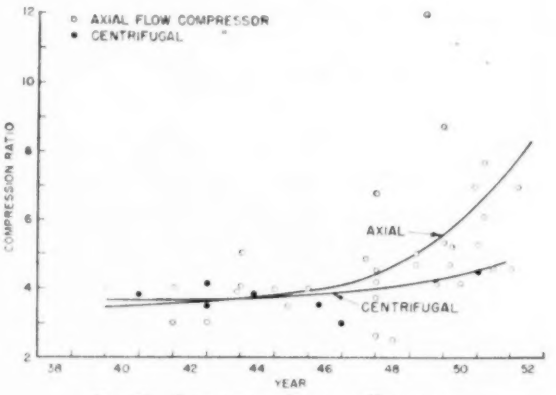

Fig. 31 Compression Ratio of Turbojets

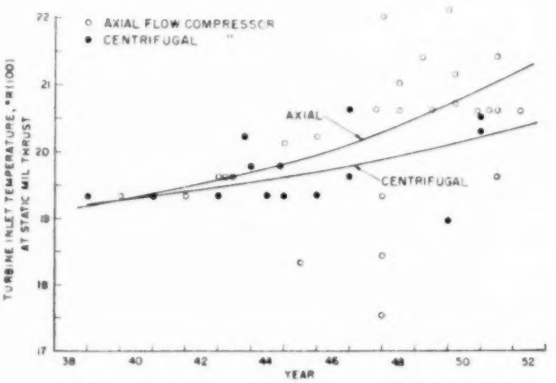

Fig. 32 Turbine-Inlet Temperature of Turbojets

temperature of about 1900 deg R and the median point for present engines is about 2060 deg R. In order to obtain the higher temperatures some companies are using a small amount of air cooling.

Efficiency

Before giving the changes in efficiencies which have been made in the few years of development, it is well to define the terms, since for the turbine at least, the definitions used in aviation are different from those employed in other gas-turbine fields.

The adiabatic efficiency is essentially the ratio of the useful energy output over the energy input. For the compressor the useful energy is measured in terms of pressure rise. In order to

convert to thermal units the useful energy is considered to be the energy required to develop the pressure if the process were isentropic. Thus the useful energy in Btu per pound of air is $h'_2 - h_1$ where h_1 is the total enthalpy per pound in front of the compressor and H'_2 is defined by the isentropic law

$$\frac{h'_2}{h_1} = \left(\frac{P_2}{P_1}\right)^{\frac{\gamma-1}{\gamma}} \quad \ldots\ldots\ldots\ldots\ldots\ldots [1]$$

where P_2/P_1 is the total pressure ratio across the compressor. Hence

$$\eta_{ac} = \frac{h'_2 - h_1}{h_2 - h_1} = \frac{\left(\frac{P_2}{P_1}\right)^{\frac{\gamma-1}{\gamma}} - 1}{\frac{h_2}{h_1} - 1} \quad \ldots\ldots\ldots\ldots [2]$$

This definition has some disadvantages. The principal one is its failure to give the same result for compression in two or more steps as would be obtained for a single step if the steps and the entire procedure were assumed to have the same adiabatic efficiency. A definition which does not have this objectionable feature is the polytropic or small-stage efficiency. It is named after a polytropic process; a process which follows a law like the isentropic law, Equation [1], except the value γ does not denote the ratio of specific heats. In other words, the polytropic efficiency of a compressor, η_{Pc} is defined by the equation

$$\frac{h_2}{h_1} = \left(\frac{P_2}{P_1}\right)^{\frac{\gamma-1}{\gamma\eta_{Pc}}} \quad \ldots\ldots\ldots\ldots\ldots\ldots [3]$$

or

$$\eta_{Pc} = \frac{\text{Log } h'_2 - \text{Log } h_1}{\text{Log } h_2 - \text{Log } h_1}$$

where h and P denote the total enthalpies and pressures and the subscripts denote as previously indicated the conditions in front and after the process. If successive stages of a compressor could be added with each state as efficient as the preceding one, then the over-all polytropic efficiency would be constant. Although this assumption is not quite true, it still appears that the polytropic efficiency is the best basis for the comparison since it does tend to eliminate the effect of compression ratio. Hence it will be employed here.

The curve in Fig. 33 shows a definite increase in polytropic efficiency for axial-flow compressors. This curve corresponds closely with the curve of Constant on the British engines. At the present state of the art it appears that one should be able to design an engine with a small-stage efficiency of 0.9 and it does not seem practical to obtain values higher than 0.95. One compressor has been tested which has this high value. The corresponding values of the adiabatic efficiency are less. The two efficiencies are related by Equations [2] and [3]

$$\eta_{ac} = \frac{\left(\frac{P_2}{P_1}\right)^{\frac{\gamma-1}{\gamma}} - 1}{\left(\frac{P_2}{P_1}\right)^{\frac{\gamma-1}{\gamma\eta_{Pc}}} - 1} \quad \ldots\ldots\ldots\ldots\ldots [4]$$

A second question which cannot be separated completely from the efficiency of the compressor is the pressure ratio developed by a given weight. A measure of this is the pressure ratio produced

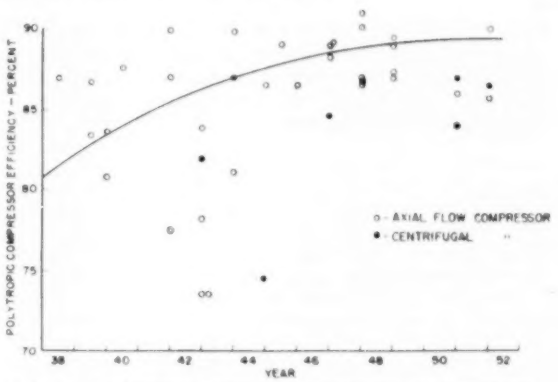

FIG. 33 POLYTROPIC COMPRESSOR EFFICIENCY FOR TURBOJETS

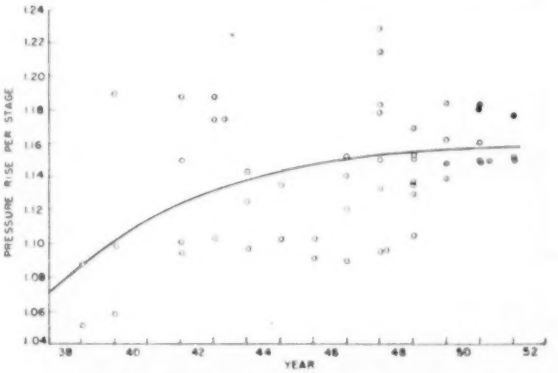

FIG. 34 PRESSURE RISE PER STAGE TURBOJETS AXIAL FLOW

per stage of the compressor. In other words, how large can the lift coefficient be without undue sacrifice in efficiency? Practically all the data are on subsonic compressors. Fig. 34 shows that there was a slight increase in the early days but more recently the values have remained rather constant at about 1.15 to 1.16. However, the most efficient compressor known by the authors had a ratio of 1.168 per stage.

In aviation the velocity of exhaust gas is not wasted; it is used to produce the jet thrust. This is essentially different from that in other gas-turbine applications; hence, in defining the efficiency of a turbine, the total pressures and enthalpies are used instead of the static pressures and temperatures. The only loss which is charged against the turbine is that energy which no longer can be recovered for use in accelerating the jet stream. This loss can be measured in terms of the loss in total pressure. The total pressure is obtained by converting the velocity to pressure by means of the isentropic law, that is

$$P = P_s\left(1 + \frac{\gamma-1}{2}\,\mathbf{M}^2\right)^{\frac{\gamma}{\gamma-1}} \quad \ldots\ldots\ldots\ldots [5]$$

where P is the total pressure, P_s is the static pressure, $\mathbf{M}$ is the Mach number of flow, and γ is the ratio of the specific heats of the gas. The adiabatic efficiency of the turbine is defined as

$$\eta_{at} = \frac{h_3 - h_4}{h_3 - h_{4'}} = \frac{1 - \frac{h_4}{h_3}}{1 - \left(\frac{P_4}{P_3}\right)^{\frac{\gamma-1}{\gamma}}} \quad \ldots\ldots\ldots [6]$$

where the values of h and P without primes are the actual total enthalpies and pressures, primed quantities denote isentropic values, and subscripts 3 and 4 denote values in front and rear of the turbine, respectively. The corresponding polytropic efficiency is defined by the equation

$$\frac{h_4}{h_3} = \left(\frac{P_4}{P_3}\right)^{\frac{\gamma-1}{\gamma}\eta_{Pt}} \quad \ldots\ldots [7]$$

Fig. 35 shows the steady increase in polytropic efficiencies over the development period. It is again important to consider the pressure drop or enthalpy drop per stage in the turbine. Because of the lack of available information, a plot of significance could not be made. The enthalpy drop per stage is largely dependent upon the number of stages. Although there is still a predominance of single-stage turbines, the present trend is toward an increase in the number of stages with the hope of improving the efficiency.

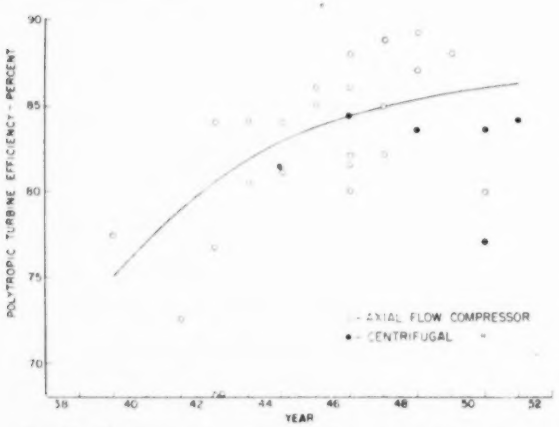

Fig. 35 Polytropic Efficiency of Turbines for Turbojets

The values plotted in the last three curves are for the static sea-level military operation. This is really only a small portion of the picture. In addition to running at this point the engines must operate at partial throttle and at many altitudes and speeds. The efficiencies are functions of all of these factors. The first effect is somewhat common for all gas-turbine operations; the efficiencies fall off as the operation deviates from the design point. The extreme changes in altitude and speed from sea level to 60,000 ft and from zero to 700 knots is encountered only in the aviation field. High speeds at any one altitude yield hotter air at an elevated pressure at the diffuser. There are two consequences, (*a*) less fuel may be added and (*b*) the turbine and nozzle have a different expansion ratio, since the expansion is still to ambient pressure. These effects change the operating point and as a consequence change the component efficiencies.

Basically, the compressor and turbine are aerodynamic devices and their performance can be explained in terms of the lift and drag coefficients of the blades. It is well known from the aerodynamic theories and tests that the lift/drag ratio which can be obtained by airfoil sections depends upon a quantity called the Reynolds number, a nondimensional number, the quotient of the product of the length times the velocity divided by the kinematic viscosity. The lift/drag ratio decreases with a decrease in Reynolds number. As a result, the efficiencies of both the compressor and the turbine are reduced when the Reynolds number is reduced. Once the engine is designed the chord lengths of the blades are fixed, the relative air velocities are nearly the same so the Reynolds number is changed appreciably only by changes in air density and temperature, the first of these two having the predominant effect. Increases in velocity at a given altitude increase the density and as a consequence, the Reynolds number, hence tend to improve the efficiency of the compressor and turbine. On the other hand, with an increase in altitude the density is decreased, producing a decrease in the Reynolds number and a corresponding decrease in compressor and turbine efficiency. The density over the range of current operation changes by a factor of 5 to 1. This change may reduce the compressor efficiency by as much as 4 or 5 per cent, depending upon the design. The turbine is usually affected much less.

As a result of the wide operating range, the designer must make certain compromises which will give the best over-all performance. As was indicated earlier, engines should be designed for peak efficiency at the point of greatest operation which is at some altitude above sea level and at a fairly high speed, say, 500 knots at 35,000 ft. There is now a definite tendency in this direction.

Combustion Problems

Of the problems which are distinctly unique to aircraft, probably the most pronounced is the combustion. Because of the extreme ranges of altitude and speed mentioned, the burner has to function over a wide deviation of air quantity per unit time. Since the top temperature is fixed this means that the fuel flow also must have extreme variations. The fuel-air ratio must be maintained within certain limits. The actual metering of the fuel as a function of the air density can be obtained, but to insure the combustion of the fuel is a more difficult problem. The lower the density, the more significant the time delays, the more space for the molecules the less likely the reaction. To make a long story short, there is an altitude blowout limit beyond which a turbojet cannot operate because the fuel will not burn. This is the altitude where the lean and the rich blowout values are equal. The problem is even more critical for afterburners. The blowout limits are lower because of the higher velocities of flow and lower pressures. Fig. 36 illustrates maximum altitudes of operation guaranteed by the manufacturers. The actual blowout limits may be somewhat higher. The operation limits of the afterburners are about 15,000 ft lower than those for the main burner.

The burner efficiency has been found to be a function of the temperature, pressure, fuel-air ratio, and air velocity at the entrance to the combustion chamber. The magnitude of the efficiency varies from one combustion chamber to another but the

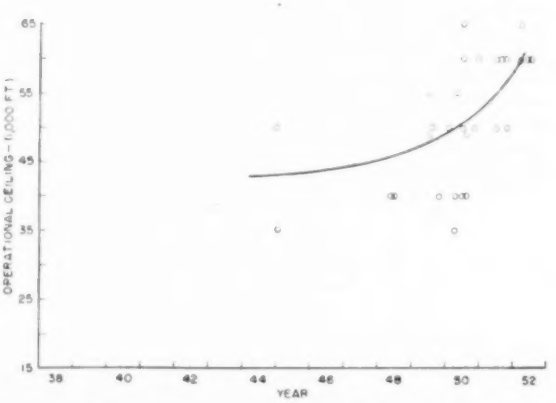

Fig. 36 Operational Ceiling of Turbojets

general nature of the curves is the same. A typical example of such curves is shown in Fig. 37. In this example the tests were not extended up to the rich mixture-blowout limit. Other tests do show that above a certain fuel-air ratio the efficiency decreases until the rich-blowout limit is reached. In order to illustrate more clearly the effect of altitude and speed on burner efficiency, the single curve in Fig. 37 for the maximum fuel-air ratio is expanded to make a plot in Fig. 38. These contours are given in terms of the maximum burner efficiency. Nearly all current engines have an efficiency of more than 97 per cent at static sea level and this efficiency decreases with altitude, as illustrated, until just before the blowout limit where the efficiency in the main burner is only about 50 per cent. Increases in velocity

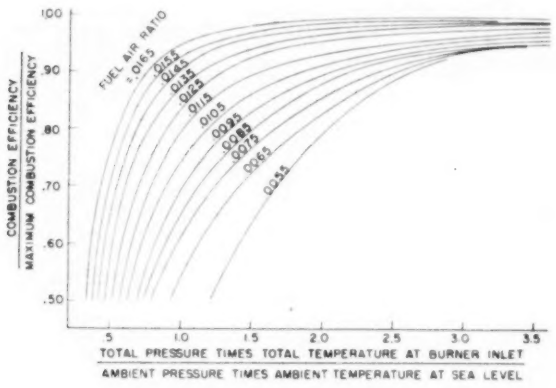

FIG. 37 BURNER EFFICIENCY

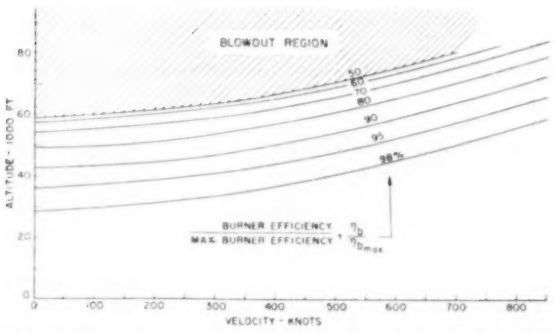

FIG. 38 VARIATION OF BURNER EFFICIENCY FOR MAXIMUM OPERATING TEMPERATURE

offset the adverse effects of altitude so, theoretically, there is some flight velocity at any altitude, within the atmosphere, at which the burner should work but because of the temperature limitations the fuel-air ratio must be reduced as the velocity is increased. Thus there is actually a limiting altitude of operation which cannot be exceeded at any speed.

Combustion efficiency alone does not give the true picture of the burner operation. Usually, a higher burner efficiency can be obtained by introducing more obstructions in the chamber which will produce more turbulence and better mixing. The obstructions, however, produce pressure losses, hence affect the cycle. The problem is to design the burner such that the combination of pressure losses and burner efficiency will give the optimum engine performance. The pressure losses in the combustion chamber vary from 4 to 6 per cent of the total pressure and the losses in afterburners are from 10 to 12 per cent of the total pressure.

Two types of primary burners are in common use today—the can and the annular. The can-type combustion chamber gets its name from the fact that the burning takes place inside a set of cans distributed around the axis of the engine. Each can is a separate burner unit in itself. It consists of an inner chamber which admits the primary air through swirl vanes near the fuel jets or nozzles, and through other perforations near the entrance. Other perforations downstream admit the secondary air. The burning occurs inside the inner chamber. It is surrounded by an outer chamber through which originally both the primary and secondary air flow. Gradually, the air between the two chambers is reduced in the downstream direction until finally all of the secondary air is forced into the inner chamber where the two streams are mixed, cooling the primary air down from flame temperature to a uniform temperature. The fundamental idea is an outer casing carrying cooling air surrounding an inner perforated flame tube. A high degree of turbulence and cooling is required. The number of cans per engine varies from 6 to 16 and they are interconnected to insure simultaneous operations of all the units. In the earlier designs, the flow was reversed so as to save length; now the flow is straight through.

The annular combustion chamber as the name implies is composed of concentric surfaces surrounding the axis of the rotor so that perpendicular planar intersections at any point give annuli. The basic idea is the same as for the can type; there is an inner annular chamber in which the fuel and the primary air enter and burn. This chamber is surrounded by another annular chamber containing secondary cooling air which passes into the flame chamber as the gases move toward the burner exit. The location of the holes for the entrance of the secondary air is quite critical in the design of both types of burners. In both types the primary air consists of about 25 per cent of the total air flow. This is necessary to insure a high fuel-air ratio in the combustion zone.

The greatest step forward in improving the combustion efficiency at high altitudes has been the development of the vaporizing combustion chamber, in which the fuel lines are passed through a heated section so that the fuel comes out of the nozzles in the form of vapor instead of in atomized droplets.

The greatest single factor in the reduction of the efficiency of gas turbines at altitude is the loss in burner efficiency. When a correction is made for the increase in fuel resulting from poor combustion, the performance of turbojets will almost generalize on the principle of similarity of flow for constant Mach number; that is, the losses in the compressor and turbine efficiency with altitude do not appear to play as prominent a role as that of combustion.

CONTROLS

Another problem which appears to be more critical in aviation than in other gas-turbine fields is the controls. The time to accelerate from idle to full power must be short. There should be only one control lever. It should schedule the operation of the engine to give the minimum fuel consumption for the required thrust at all altitudes and speeds. For rapid acceleration the operating line (steady-state points for various thrusts) must not lie too close to the compressor stall line. Yet, the points for the best economy lie close to the stall line; hence a compromise must be made.

Most of the current jets have a fixed-area nozzle, hence have only one independent degree of freedom—fuel flow, or its equivalent. Thus they cannot operate along the minimum possible fuel-consumption curve which is an envelope determined by two parameters. Engines with variable-area nozzles, however, can approximate the best fuel-consumption operation. Even then,

if the essential independent variables, nozzle area and fuel flow, are interrelated so as to have one control lever the envelope can be obtained at only one altitude and speed. Although variable-area nozzles were originally of interest from the standpoint of fuel consumption, they are of tremendous value in reducing the accelerating time for the engines. Their merit has been recognized almost from the beginning. The German Jumo 004 and the Westinghouse 19XB both had variable-area nozzles. Then there was a time when the complication of variable area was eliminated. Now, it is almost mandatory to have a variable area for engines equipped with an afterburner.

High-Temperature Metals

Nothing has been said about the development program for high-temperature metals. This is no more critical in aviation than in other fields. It might even be less critical, for studies have shown that for continuous operation of extended duration of turbojets the current temperatures are sufficiently high to give the minimum total weight of power plant plus fuel. However, with turboprops or with turbojets which are to operate for only short durations, elevated temperatures are advantageous.

Reliability

The turbojets have proved to be reliable engines. The time between overhauls has increased rapidly over this early operation period. Some current engines operate 500 hr between overhauls

Comparison of Centrifugal- and Axial-Compressor Turbojets

Ever since the advent of the turbojet the possible advantage of the axial-flow compressor for aircraft uses has been recognized. Yet, today about two thirds of the actual flight time with jet planes has been with centrifugal-type engines. The tables and charts herewith clearly point out two disadvantages—the large diameter for a given thrust, and the higher specific fuel consumption. On the other hand, they show two advantages—a shorter length and a lighter weight. These two advantages alone would not have kept the centrifugal type so prominently in the field. However, when they are coupled with the low production cost in materials and man-hours, and the rugged construction, it is not surprising that they have remained in the competitive field, and they may continue to do so for some time to come.

Turboprop Characteristics

The trends of the fundamental characteristics of the turboprop engines are presented in Figs. 39 to 43, inclusive. Although most of the first engines were intermediate in size, the more recently designed turboprops are very large units. Before the design of the larger engines there was a tendency to couple two units to one shaft so as to double the power. The multiple units have an advantage over a large single unit for cruise operation, where one unit supplies enough power for flight, for the specific fuel consumption is lower the higher the percentage of normal power output of a unit.

Fig. 40 shows that there has been an improvement in static specific fuel consumption over the few years of development. A corresponding improvement has been made at cruise conditions. The reductions in fuel consumption are analogous to those for turbojets and are derived from similar results. Because of the desirability of higher compression ratios for turboprops, improvements in the compressor and turbine efficiencies have a more significant effect. In the case of turbojets the efficiency of the turbine and compressor are of about equal importance; however, in turboprops, improvements of efficiency of the turbine are twice as effective as improvements of the efficiency of the compressor.

The reduction in specific weight of the turboprops has not been as pronounced as for the turbojet engines. On the other hand, the increase in power per unit frontal area and unit length have shown corresponding increases.

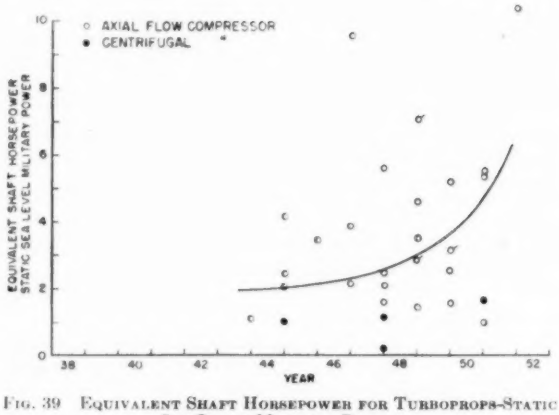

Fig. 39 Equivalent Shaft Horsepower for Turboprops-Static Sea-Level Military Power

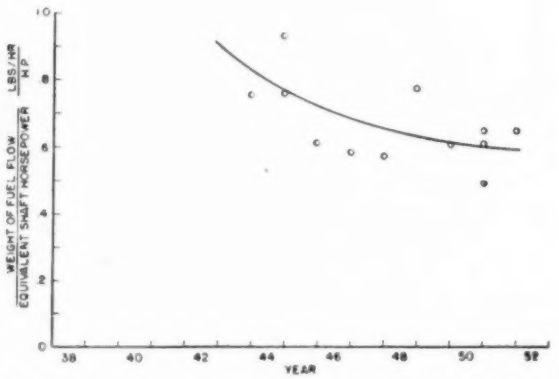

Fig. 40 Specific Fuel Consumption of Turboprops–Static Sea-Level Military Power

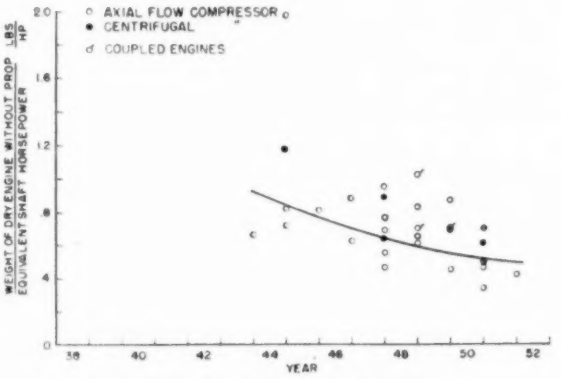

Fig. 41 Specific Weight of Turboprops

Comparison of Turbojet and Turboprop

The data in the Tables 1 and 2 and in the graphs for turbojets and turboprops are not given in the same units. In the custom-

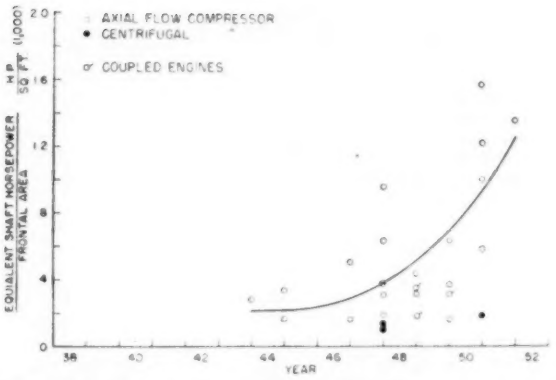

FIG. 42 RATIO OF EQUIVALENT SHAFT HORSEPOWER TO FRONTAL AREA FOR TURBOPROPS

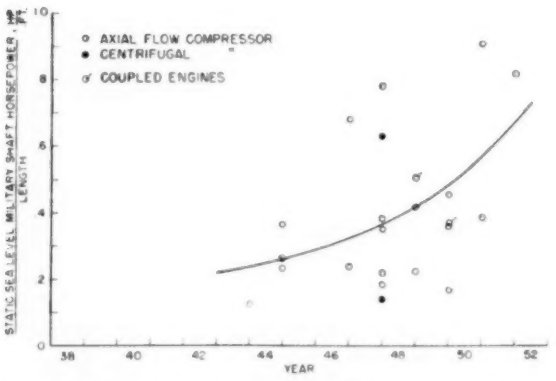

FIG. 43 RATIO OF EQUIVALENT SHAFT HORSEPOWER TO LENGTH FOR TURBOPROPS

ary manner, the ratings for the turbojet are given in terms of pounds of thrust, pounds of fuel per pound of thrust, and pounds of thrust per pound of weight; while the rating for the turboprop engines are given in terms of the equivalent shaft horsepower, pounds of fuel per equivalent shaft horsepower, and equivalent shaft horsepower per pound of engine weight. Hence the values cannot be compared directly.

The tabular values in columns four to eight, inclusive, are based upon static condition. A close approximation of the static thrust developed by a turboprop is 2.5 times the equivalent shaft horsepower. Thus, when comparing the specific fuel consumptions with those for turbojets, the values in Table 2 must be divided by 2.5. The power per unit area and length should be multiplied by 2.5. When comparing the specific weights, an additional correction term is necessary to account for the weight of the propeller which is approximately 0.18 times the shaft horsepower or about 0.16 times the equivalent shaft horsepower. Thus the specific weight of a turboprop in terms of static thrust is given approximately by the relation

$$\frac{W}{2.5\ \mathrm{ESHP}} + 0.064$$

At the flight velocity of 400 knots the specific fuel consumption for the turboprop can be converted approximately into pounds of fuel per hour per pound of thrust by multiplying by 1.40.

Naturally, all of these values could be converted the other way and the results expressed in terms of equivalent shaft horsepower. When this is done, the values may be compared directly to the more familiar values employed in describing reciprocating engines. Typical values in these terms are presented in Table 3.

TABLE 3 COMPARISON OF VARIOUS ENGINE TYPES

	Static sea level		400 knots at 35,000 ft	
Type of engine	$\frac{W_F}{\mathrm{ESHP}}$	$\frac{W + W_P}{\mathrm{ESHP}}$	$\frac{W_{Fc}}{(\mathrm{ESHP})_c}$	$\frac{W + W_P}{\mathrm{ESHP}}$
Reciprocating engine	0.73	1.360	0.42	3.30
Turboprop (current)	0.56	0.600	0.44	1.63
Turbojet, axial (current)	2.55	1.050	0.83	0.80
Turbojet, centrifugal (current)	2.75	0.825	0.90	0.65

Table 3 brings out some very interesting facts. People usually think of the jet engine as a very light power plant. It is for very high velocities and altitudes, but at static sea level it is not as light as its companion the turboprop in spite of the large propeller and gear weights. Both are much lighter than the best of the reciprocating engines which run about 1 lb per shp without the propeller. The values in the first, second, and fourth columns refer to military power. At maximum power, reciprocating engines do not give their best fuel consumptions; as a result, the turboprop is the best engine on both accounts. The values in column three refer to the best cruise power at a speed of 400 knots at 35,000 ft. Both of the propellered engines excel here with the reciprocating engine having the slight advantage. The numbers in column four refer to the maximum power which can be developed divided into the total power-plant weight. In order to operate, the reciprocating engine must have a supercharger. These figures show the decided weight advantage of the turbojets at 400 knots and the difference becomes more pronounced as the velocity is increased.

SUMMARY

The development of gas turbines for aircraft use began in the 1930's. The first jet engines were built independently by the Germans and the English, and in both cases the first engines employed for flight were of the centrifugal type. However, the development by the Germans soon shifted to the axial type and their first production models were axial. The British, on the other hand, were more successful with the centrifugal type and their early designs may be called the ancestors of all the current centrifugal turbojets which have been greatly improved in both Britain and the United States. The Americans and the British also have developed several axial-flow engines. These engines have lower specific fuel consumption and smaller frontal area than centrifugal-type engines, but have higher specific weight. Turboprop development has lagged that of turbojets but at present there are several good turboprops in operation. These engines show a decided specific-fuel-consumption advantage over the turbojets with a weight advantage over the reciprocating engines.

During the short period of development, there has been a trend toward higher rated engines, a larger mass flow per frontal area, a reduction in specific fuel consumption, lower specific weight, and to increased compression ratios with only a slight increase in operating temperature.

REFERENCES

1 "The Gas Turbine in Perspective," by Hayne Constant, Proceedings of The Institution of Mechanical Engineers, London, England, vol. 163, 1950, pp. 185–192.

2 "Overall and Stage Characteristics of Axial Flow Compressors," by A. R. Howell and R. P. Bonham, Proceedings of The Institution of Mechanical Engineers, vol. 163, 1950, pp. 235–248.

3 "The Early History of the Axial Type of Gas Turbine Engine,"

by Hayne Constant, The Institution of Mechanical Engineers, War Emergency Issue No. 12, pp. 411–426.

4 "The Design and Development of Centrifugal Compressors for Aircraft Gas Turbines," by L. J. Cheshire, The Institution of Mechanical Engineers, War Emergency Issue No. 12, pp. 426–440.

5 "Fluid Dynamics of Axial Compressors," by A. R. Howell, The Institution of Mechanical Engineers, War Emergency Issue No. 12, pp. 441–452.

6 "The Jet Engine Comes of Age," by R. P. Kroon, *Westinghouse Engineer*, September, 1950, pp. 194–200.

7 "German Turbojet Development," by R. M. Salter and G. G. Emerson, Bureau of Aeronautics, Power Plant Memorandum No. 12, June, 1945.

8 "Gas Turbines and Jet Propulsion," by G. G. Smith, third, fourth, and fifth edition, Aircraft Books, Inc., New York, N. Y.

9 "Enemy Jet History," by D. R. Maguire, *Journal of the Royal Aeronautical Society*, vol. 52, 1948, pp. 75–84.

10 "British Aircraft Gas Turbines," by H. R. Cox, *Journal of the Aeronautical Sciences*, vol. 13, February, 1946, pp. 53–87.

Local Heat-Transfer Coefficients on the Surface of an Elliptical Cylinder in a High-Speed Air Stream

By R. A. SEBAN[1] and R. M. DRAKE,[2] BERKELEY, CALIF.

Local heat-transfer coefficients and recovery factors have been determined for an elliptic cylinder of 1:4 axis ratio at zero and at a 5-deg angle of attack in an air stream. These results are presented for Reynolds numbers from 607,000 to 1,330,000, for which the onstream Mach numbers were from 0.20 to 0.53.

Nomenclature

The following nomenclature is used in the paper:

c_p = heat capacity of fluid, Btu/(lb deg F)
D = length of major axis of elliptical cylinder, ft
g = acceleration of gravity, 32.2 ft/sec^2
h = local heat-transfer coefficient Btu/hr sq ft deg F
J = conversion factor, 778 ft-lb/Btu
k = thermal conductivity of fluid, Btu/(hr sq ft deg F/ft)
p = static pressure, psf
q = heat-transfer rate, Btu/sq ft hr
s = peripheral distance from leading end of major axis, ft
T = surface temperature, deg F
T_s = air stagnation temperature, deg F
U_a = onstream velocity, fps
U_l = local velocity at edge of boundary layer, fps
ν = kinematic viscosity of the fluid, sq ft per sec
ρ = fluid density, slugs per cu ft

Dimensionless quantities:

C_p = pressure coefficient (Equation [1])
r = recovery factor (Equation [2])
$\frac{hD}{k}$ = Nusselt number
$\frac{U_a D}{\nu}$ = Reynolds number

Introduction

Experimental investigations of the manner in which the local rate of heat transfer varies over the surface of a heated body immersed in a fluid stream have been conducted for a number of body shapes. Typical results are those presented for circular cylinders (1, 2, 3),[3] inclined flat plates (4), and airfoils (5), all of which were examined in low-velocity air streams. These results are valuable in terms of a direct design objective, for characterizing the flow around the body, and for providing means for checking theoretical methods whereby the distribution of the local heat rate might be predicted.

Further results of this general type are presented in this paper for an elliptical cylinder of 1 to 4 axis ratio which was tested in an air stream. In these tests, air velocities were sufficiently high so that frictional heating was significant, and thus the correct evaluation of the temperature difference to account for the effect of frictional heating is also demonstrated. These present results are given for the major axis of the cylinder parallel to the stream and at a 5-deg angle of attack, the Reynolds-number range being from 607,000 to 1,330,000, with onstream Mach numbers from 0.20 to 0.53.

Apparatus

The elliptical cylinder, of 1:4 axis ratio, had a major axis of 5.50 in. and a width of 7 in. The cylinder was made of bakelite, to which were affixed three nichrome ribbons 1 inch wide and 0.002 inch thick. Twenty-one iron-constantan thermocouples were spot-welded to the inside surface of the nichrome ribbon to indicate the local temperature of the ribbon; under the conditions of the experiment, this temperature corresponded to the temperature of the outer ribbon surface. In the $^1/_2$-in. space between the central ribbon and one of the adjacent ribbons there were located 21 pressure taps corresponding in location to the thermocouples on the central ribbon. This instrumentation was located symmetrically about the major axis of the cylinder, extending around the nose and for about 80 per cent of the major (chord) axis. At the 80 per cent point the ribbons were attached as smoothly as possible to copper bars inlaid into the cylinder surface in such a way that the electrical heating current passed through the three ribbons in series.

All pressure-tap lines, and all thermocouple and heater leads passed through the interior of the ellipse and out through the hollow mounting bosses of the ellipse.

Heating current was supplied through a constant-voltage transformer and metered by an ammeter of a type insensitive to the current wave form. Pressures were indicated on vertical water manometers and thermocouple responses were measured with a potentiometer having a least count of 10 microvolts.

The cylinder was mounted centrally in the 7-in-square throat of a heat-transfer wind tunnel. Fig. 1 is a picture of the cylinder installed in the tunnel with the top of the tunnel removed.

In addition to the measurements associated with the model, the upstream air-state temperature and upstream and throat static pressures were determined. It was known that the velocity distribution across the tunnel throat was uniform and that the temperature of the approach air stream was uniform to $\pm^1/_2$ deg F across the flow cross section. The turbulence level of the tunnel was unknown but the present and prior test results indicate that the level was not high.

Procedure

A test at one air speed and one angle of attack involved the measurement of all local static pressures and of ribbon tempera-

---

[1] Associate Professor of Mechanical Engineering, University of California. Mem. ASME.

[2] Assistant Professor of Mechanical Engineering, University of California.

[3] Numbers in parentheses refer to the Bibliography at the end of the paper.

Contributed by the Heat Transfer Division and presented at the Semi-Annual Meeting, Cincinnati, Ohio, June 15–19, 1952, of The American Society of Mechanical Engineers.

Note: Statements and opinions advanced in papers are to be understood as individual expressions of their authors and not those of the Society. Manuscript received at ASME Headquarters, February 18, 1952. Paper No. 52—SA-11.

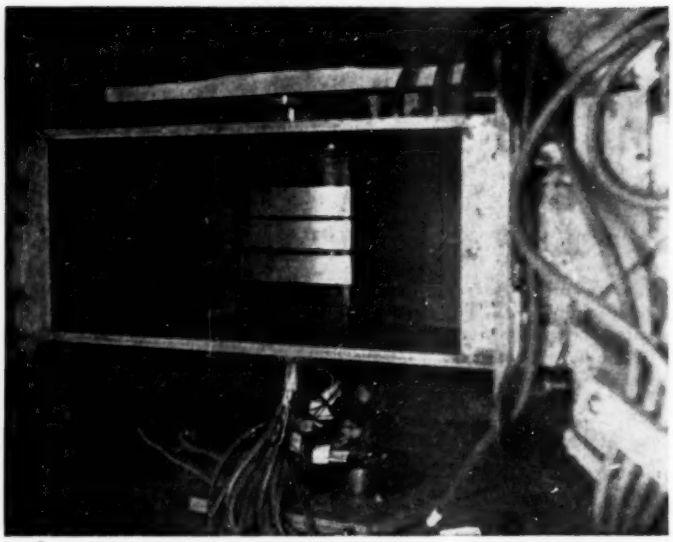

FIG. 1 ELLIPTICAL CYLINDER INSTALLED IN TUNNEL THROAT

tures under steady-state conditions with and without heating current. These measurements enabled the evaluation of the pressure coefficient, recovery factor, and heat-transfer coefficient at each of instrumented points on the cylinder surface.

The pressure coefficient was evaluated from the definition

$$C_p = \frac{p - p_a}{\frac{\rho_a U_a^2}{2}} \quad [1]$$

Subscript a refers to free-stream conditions taken at a point 3 in. upstream of the leading edge of the model. Because of tunnel-wall interference, which becomes more severe as the compressibility effects increase, the pressure coefficients given by the application of Equation [1] to the test data are not universal but apply only for the relative model thickness and tunnel height typical of the conditions of the test.

Recovery factors were evaluated from the data for unheated operation from the definition

$$r = 1 - \frac{T_s - T}{U_1^2/2gJc_p} \quad [2]$$

In this evaluation quantity $(T_s - T)$ was taken as the measured difference between stagnation and wall temperatures, and the local velocity U_1 was determined from the local static pressure and the assumption of reversible flow in the region external to the boundary layer.

Data for the heated runs enabled the evaluation of the local heat-transfer coefficient from the definition

$$h = \frac{q}{(T - T_s) + (1 - r)\frac{U_1^2}{2gJc_p}} \quad [3]$$

The local heat rate q, constant over the ribbon surface because of the electrical resistance heating, was evaluated from the observed current and separately determined ribbon resistance.

Heat transfer by radiation and by conduction along the ribbons and within the model affect the recovery factor and heat-transfer coefficient as defined by Equations [1] and [2]. Calculation of the rate of radiant heat transfer, based on a measured emissivity of the ribbon, revealed a negligible effect on both the recovery factor and heat-transfer coefficient. Conduction effects depend in relative magnitude on the variation in model temperature and should thus have been negligibly small in the unheated tests from which the recovery factors were determined. With heating, the temperature variation was significant and conduction effects may have been significant. Attempts to analyze the error so induced were largely unsuccessful but tended to indicate this error to be relatively small.

Data were taken at zero angle of attack with the ribbons covering the region $S/D < 0.80$, the "forward" position, and with the ribbons covering the region $S/D > 0.30$, the "reversed" position. Data taken in the reversed position yielded a check for the forward values for $0.30 < S/D < 0.80$ as well as values for the region $0.80 < S/D < 1.08$. The suitability of these reversed data for comparison with the forward data was affected by the unheated starting-length effect for heat-transfer observations in the region of $S/D = 0.3$, and the slight surface discontinuity at the point of juncture of the ribbons and the bar in the surface of the cylinder. The disturbance produced by even a slight discontinuity apparently did affect the boundary-layer transition point.

Data were obtained also at angles of attack of +5 deg and −5 deg. By means of a suitable combination of results for the upper and lower surfaces the results calculated from these data are presented for an effective angle of attack of +5 deg.

The position of the cylinder was established in terms of static pressure magnitudes. Thus the zero angle of attack was established by securing the same pressure distribution on top and bottom surfaces, while the 5-deg angle of attack was secured repetitively by duplicating a selected difference between a pair of pressure taps between the upper and lower surfaces.

Table 1 summarizes the range of variables covered by the experiments. All physical properties involved in the evaluation of these and other results and magnitudes were evaluated at the stagnation state unless otherwise indicated.

Analysis of the aggregate possible error in the heat-transfer coefficient produced by instrument errors as estimated on the

TABLE 1 VARIABLES COVERED BY EXPERIMENTS

Reynolds number	607000 to 1330000
Onstream velocity, fps	226 to 580
Stagnation pressure, psi	14.7
Stagnation temperature, deg F	75 to 80
Onstream Mach number	0.20 to 0.53
Temperature difference, surface to stagnation, deg F	15 to 25
Difference between stagnation and adiabatic wall temperature, deg F	0.5 to 10
Local Mach numbers	0.20 to 0.95

instrument least count indicates the maximum error of mensuration to be of the order of 4 per cent.

Results

The test results are given in terms of the pressure coefficient, the recovery factor, and the local heat-transfer coefficient, the latter being expressed in terms of the ratio of a Nusselt number to the square root of the onstream Reynolds number. These quantities are presented in terms of the peripheral distance from the forward end of the major axis of the cylinder, which distance corresponds to the peripheral distance from the stagnation point at zero angle of attack. The individual results obtained from all the instrumented points are so numerous as to be incompatible with a compact presentation of the data so that there are presented only mean curves for the various runs. Where shown as solid lines these curves represent all the results within about ±3 per cent, and the use of dashed lines indicates either that only one set of measurements formed the basis of the curve or that the consistency of the results was poorer.

Fig. 2 reveals the results for zero angle of attack, with the major axis of the cylinder parallel to the onstream flow. Erratic results were obtained consistently for the heat-transfer coefficient, and to some extent for the recovery factor, in the region of $S/D = 0.50$. The dashed lines on the plot of the heat-transfer coefficient reveal the limits of the results obtained in this region. An irregularity occurs also in the pressure coefficient in this region but the reason for the scatter of results is unknown. Except for the lowest Reynolds numbers, the heat-transfer coefficient is not represented for the entire cylinder surface because of the inferior consistency of some of the results for the reversed runs. At the higher velocity, reversed runs on one side of the ellipse produced data indicating completely turbulent flow, the rapid transition probably being due to some irregularity at the juncture of the ribbons and the copper bar in the cylinder surface. Higher recovery factors also gave evidence of the turbulent character of the boundary layer. These results were not employed for the final evaluation of the data leading to Fig. 2, and the one set of results remaining for the region $S/D > 0.80$ did not appear to justify continuation of the curves for the results in all the cases.

Fig. 3 contains the results for the under side of the cylinder at a 5-deg angle of attack, with the representation of the results being the same as that employed for the case of zero angle of attack. As previously noted, these results are composed from test data for the under side at a +5-deg angle of attack and the upper side at a —5-deg angle of attack, so that the curves shown are based

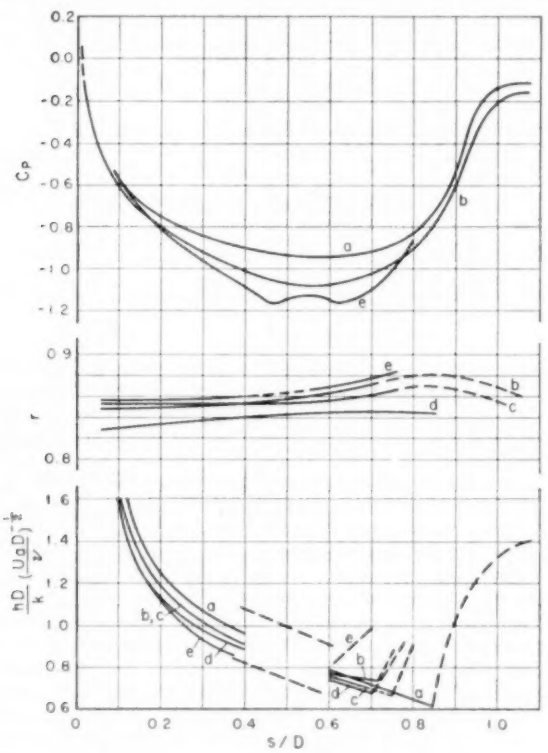

FIG. 2 RESULTS FOR CYLINDER AT ZERO ANGLE OF ATTACK

(Reynolds numbers: *a*, 607,000; *b*, 930,000; *c*, 714,000; *d*, 806,000; *e*, 1,330,000.)

Stagnation point $\frac{s}{D} = 0$ values of quantity $\frac{hD}{k}\left(\frac{UaD}{\nu}\right)^{-1/2}$

a, 2.50	*c*, 2.65	*e*, 2.77
b, 2.67	*d*, 2.71	

The Kármán-Tsien correction has been applied to the pressure coefficients shown for the run at a Reynolds number of 1,330,000.)

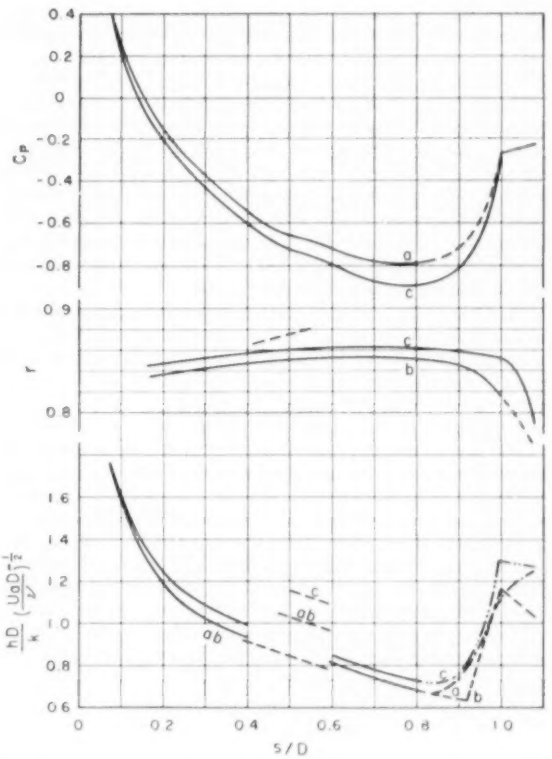

FIG. 3 RESULTS FOR UNDER SIDE OF CYLINDER AT +5 DEG ANGLE OF ATTACK

(Reynolds numbers: *a*, 720,000; *b*, 780,000; *c*, 915,000. Estimated location of stagnation point, $s/D = 0.037$.)

on at least two measurements at each instrumentation point. The general characteristics of the representation, in regard to erratic results near $S/D = 0.50$, and incomplete results in the rearward portion of the cylinder, are the same as for the case of zero angle of attack.

Fig. 4 reveals results for the under side of the cylinder at a 5-deg angle of attack, at a Reynolds number of 720,000. Individual experimental results are shown in this figure to illustrate the typical distribution of the results and reveal the basis upon which the mean-value curves appearing on the other figures were determined.

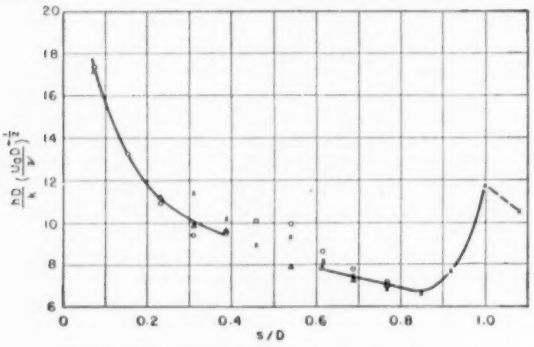

○ Operation, forward at −5 deg angle of attack
△ Operation, forward at +5 deg angle of attack
× Operation, reversed at +5 deg angle of attack

FIG. 4 HEAT-TRANSFER COEFFICIENTS FOR UNDER SIDE OF CYLINDER AT +5 DEG ANGLE OF ATTACK AT REYNOLDS NUMBER OF 720,000
(Estimated location of stagnation point, $s/D = 0.037$.)

Fig. 5 contains the results for the upper side of the cylinder at a 5-deg angle of attack, composed of results from the +5-deg and −5-deg operation as are the results in Fig. 4. This representation differs from the previous two in that the individual results are shown for the recovery factor for this case. This has been done because of the definite turbulent-flow regime which appears, and the good correlation between the transition from laminar flow and the departure of the recovery-factor magnitudes from values typical of laminar flow.

With the cylinder oriented at a 5-deg angle of attack, the stagnation point was not located at an instrumented point. The location of the stagnation point for these cases was determined from theoretical considerations.

DISCUSSION

The general characteristics of the local heat-transfer coefficient and the recovery factor are similar for the cylinder at zero angle of attack and for the under side of the cylinder at the 5-deg angle of attack. A region of laminar boundary-layer flow is revealed immediately downstream from the stagnation point, a short region of uncertainty exists near $S/D = 0.5$, and this is followed by an apparent continuation of the laminar boundary-layer flow. Either transition or separation then occurs.

The laminar boundary-layer flow is best confirmed by the correlation of the heat-transfer coefficient with the group

$$\frac{hD}{k}\left(\frac{U_0D}{\nu}\right)^{-1/2}$$

which correlation is indicated from analytical considerations for laminar boundary-layer flow (6). Despite the small discrepancy in the mean lines for the various Reynolds numbers the correlation achieved is quite satisfactory, since the ratio of maximum to minimum heat-transfer coefficient at any point was 1.4 in the range of velocities tested. Recovery-factor magnitudes also contribute to this conclusion, since they are near the value of the square root of the Prandtl number which approximates the recovery factor for laminar boundary-layer flow on a flat plate. The theoretical values of the recovery factor for flows with variable free-stream velocities are also near this value.

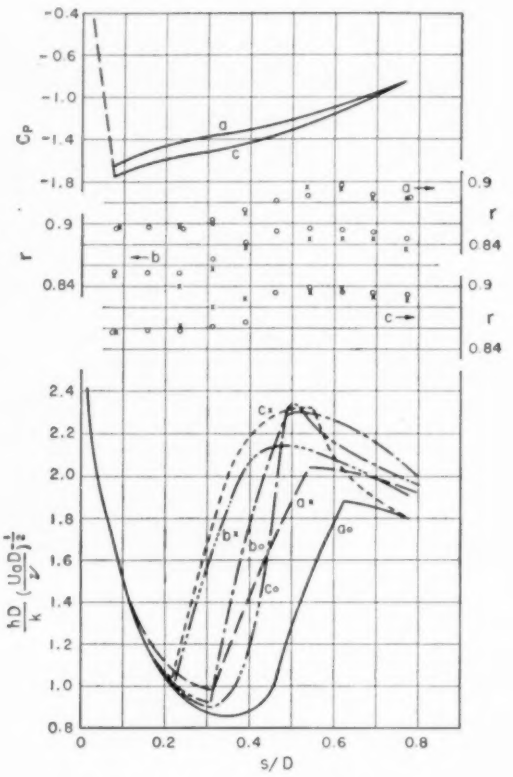

○ Operation at +5 deg angle of attack
× Operation at −5 deg angle of attack

FIG. 5 RESULTS FOR UPPER SIDE OF CYLINDER AT A +5 DEG ANGLE OF ATTACK
(Reynolds numbers: *a*, 720,000; *b*, 780,000; *c*, 915,000. Estimated location of stagnation point, $s/D = -0.037$.)

While the character of the variation of free-stream velocity should affect the local heat-transfer coefficient, the heat-transfer coefficient in the laminar-flow region has similar magnitudes of the same distance from the stagnation point in Figs. 2, 4, and 5. In this regard, the general character of the pressure coefficient is similar in all cases and the changes that did occur might not have been great enough to affect the heat-transfer coefficient significantly. In the case of the run at a Reynolds number of 1,330,000, a substantial change, due primarily to compressibility, did occur. In this case compressibility effects also may have contributed to the invariability of the heat-transfer coefficient with respect to the runs at lower Reynolds numbers.

In the region of $S/D = 0.5$, higher heat-transfer coefficients were usually obtained, as indicated in Figs. 2, 3, and 4. An irregularity also appears in the pressure coefficient for this point. This is of unknown cause. No reason existed for questioning the instrumentation at this point and there was insufficient instrumentation in the locality of the irregularity to provide the

detailed information needed for complete rationalization of the phenomenon. A local flow instability is a possible explanation, but no complete evidence is available for it. At values of $S/D > 0.60$, the heat-transfer coefficients again follow the original trend of the data. A beginning of transition is indicated, but the recovery factors, in general, do not indicate the development of a completely turbulent flow. The run at the lowest Reynolds number appears to indicate separation rather than transition, and the recovery factor is substantially reduced in the region downstream of the separation point.

The results for the upper side of the ellipse at a 5-deg angle of attack reveal somewhat different characteristics in the demonstration of laminar, transition, and turbulent boundary-layer flow. Because of the rapid acceleration at the stagnation point no details are available for this region; however, the first instrumentation point, at the end of the major axis, gives a heat-transfer coefficient as high as the maximum value obtained with zero angle of attack. The boundary layer remains laminar for a relatively short time, transition to turbulence occurring rather early, probably because of the greater instability of the decelerated flow. Excellent correspondence exists between the recovery-factor measurements and the heat-transfer coefficient measurements, with the recovery factor attaining a value of approximately the cube root of the Prandtl number as soon as the boundary layer appears to become turbulent. The differences in the transition point for the two sides of the ellipse tested may be due to some undetected difference in the surface condition of the model.

Acknowledgment

The results given herein were obtained in connection with Air Force Contract AF-33(038)-12941 and this support is gratefully acknowledged. L. J. Gee performed the experimental work and F. M. Sauer contributed substantially in the entire effort.

BIBLIOGRAPHY

1 "Distribution of Heat Flow About the Circumference of a Pipe in a Stream of Fluid," by T. B. Drew and W. P. Ryan, Publication No. 283 of the Massachusetts Institute of Technology, 1931.

2 "Heat Transfer Over the Circumference of a Heated Cylinder in Transverse Flow," by E. Schmidt and K. Wenner, NACA TM 1050, 1943.

3 "Investigation of the Variation of Point Unit Heat-Transfer Coefficient Around a Cylinder Normal to an Air Stream," by W. H. Giedt, Trans. ASME, vol. 71, 1949, pp. 375–381.

4 "Investigation of the Point Unit Heat-Transfer Coefficient for Laminar Flow Over an Inclined Flat Plate," by R. M. Drake, Jr., *Journal of Applied Mechanics*, Trans. ASME, vol. 71, 1949, pp. 1–8.

5 "On the Convection of Heat From the Surface of an Airfoil in a Wind Current," by T. Bryant, et al., Aeronautical Research Committee, Great Britain, Rand M 1163.

6 "Die Berechnung des Wärmübergangs in der laminaren Grenzschicht umströmter Körper," by E. Eckert, *VDI Forschungsheft* 416, September, 1942 (VDI Verlag-Berlin).

Discussion

E. R. G. Eckert.[4] The paper constitutes a contribution which will be welcomed by those interested in convective laminar and turbulent heat transfer in boundary-layer-type flow. The results should be useful in checking available calculation procedures especially in so far as the influence of a temperature variation along the surface and of frictional heating on heat transfer is concerned. For an investigation of the influence of a pressure variation along the surface the experiments are less suited since the large axis ratio of the ellipse used makes conditions over the major part of the surface quite similar to those on a flat plate. It will be interesting to check how well the surface temperatures, calculated with available heat-transfer coefficients obtained from low-velocity relationships, together with adiabatic wall temperatures obtained on the unheated cylinder with low heat conductivity, agree with measured surface temperatures.

Remarkable are the low values of the recovery factor measured on the rear part of the cylinder surface and presented in Fig. 3 of the paper. Such low values on surfaces in separated flow regions were first observed by Eckert and Weise on circular cylinders and have been investigated recently and extensively by L. F. Ryan.[5] Obviously, they are connected with vortex-type flow.

A. N. Tifford.[6] Because of wall interference, compounded by compressibility effects, the experimental data presented in the paper are not correct for the general case of an elliptical cylinder of 1:4 axis ratio. Rather, the data are valuable, as indicated in the Introduction, primarily for providing a check on theoretical methods of prediction of the distribution of the local heat-transfer rate. However, the paper itself makes no more than a qualitative comparison of theory and experiment. For this reason it is found to be incomplete. The fact that similar experimental data have been presented in the past without a detailed comparison with theory does not justify all future papers being in kind. After all, it has been only within the past few years that relatively precise theoretical methods of heat-transfer calculation (at least for the laminar boundary layer) have become available.

Essentially, two separate experimental studies have been reported: (*a*) The variation of the recovery factor on the surface of an unheated elliptic cylinder, and (*b*) the temperature distribution on the surface of an elliptic cylinder when the heating rate per unit surface area is held constant. On the basis of these data, the Nusselt-number variations along the surface have been given. In this presentation the heat-transfer coefficient has been based on the local temperature difference between the insulated cylinder surface and the heated cylinder surface. Contrary to the inference of the paper, however, there is nothing uniquely correct about this method of accounting for the effect of frictional heating. What does particularly recommend it is the lack of a significant pressure-gradient effect on the frictional heating factor. Computational studies—as well as the present data—have shown that Pohlhausen's square-root rule satisfactorily specifies the insulated-surface temperature in the laminar-flow region regardless of surface pressure-gradient conditions.

The relative invariability of the heat-transfer-coefficient distribution along the surface with changes in angle of attack and compressibility is primarily due to the constant surface-heating rate imposed. Any relative change in the operating conditions at a point on the surface tends to change the local heat-transfer coefficient and the local surface temperature in compensating directions. Thus a much smaller than expected change in local heat-transfer coefficient occurs. For example, if the relative local velocity at a particular point increases, the local heat-transfer coefficient thereby tends also to increase. Since the heating rate is held constant, the local surface temperature must decrease. This decrease in local surface temperature, as compared with the surface just ahead, introduces thermal gradients in the boundary layer which tend to decrease the local heat-transfer coefficient, and so on. (Of course, an equilibrium condition normally is rapidly established.)

[4] Professor, Department of Mechanical Engineering, University of Minnesota, Institute of Technology, Minneapolis, Minn. Mem. ASME.

[5] "Experiments on Aerodynamic Cooling," by L. F. Ryan, Mitteilung Institut Aerodynamik, Eidgen. Technische Hochschule, Zurich, Switzerland 1951, pp. 7–52.

[6] Aeronautical Engineering, The Ohio State University, Columbus, Ohio.

Two things are to be learned from the foregoing: (1) For the most precise check by means of the present data of general theoretical methods of calculation of heat transfer for nonisothermal surfaces, the surface-heating rate should be calculated on the basis of the measured surface temperature distribution and then compared with the actual heating rate; and (2) inherently less precise methods of heat-transfer calculation are satisfactory for surfaces subjected to a constant surface heating rate.

In summary, some very interesting experimental data have been presented but their analysis seems rather incomplete.

Authors' Closure

The utilization of the results for comparison with methods for predicting local heat-transfer coefficients has been noted in the paper and called for by one of the discussions. For the region in which the boundary layer is laminar, Eckert[7] has reviewed a number of methods and has presented a method simple enough to be of utility and applicable in the case of isothermal surfaces. Seban[8] has presented a similar method, modified to account for variable surface temperature, the modification being approximate and inducing some further uncertainty into the results. That method, when applied for the experimental velocity distribution over the elliptic cylinder and for the case of constant heat rate that obtained in the experiments, yielded the results shown in Fig. 6 of this closure for the laminar flow region in the three altitudes of the model presented in Figs. 2, 3, and 5 of the paper. As in those figures, the stagnation region is eliminated in favor of a larger ordinate scale.

The comparison between prediction and experiment is favorable, although the discrepancy is as much as 20 per cent in some regions. At the stagnation point, not shown in the figure, the heat-transfer coefficient predicted from the theoretical velocity distribution is always lower than that measured, the difference again not exceeding 20 per cent. Far from this region, at about $0.2 < S/D < 0.8$ for the results in Figs. 2 and 3, the free-stream velocity becomes almost uniform and Dr. Eckert has noted that the "flat-plate" equations might be applicable there. If used, they yield results about 10 per cent lower than the more elaborate prediction and this indicates their utility provided the pressure gradient is small. The comparison of the measured values and those predicted by accounting for and by ignoring the variation of pressure indicate that the theory does not account sufficiently for either the effect of pressure variation or for the surface-temperature variation.

The rapid decrease in the recovery factor in the rear region of the cylinder, evident in Fig. 3, does not appear consistently with equal Reynolds numbers, and was more evident in the runs shown in Fig. 3 than in those shown in Fig. 2. This has not been found

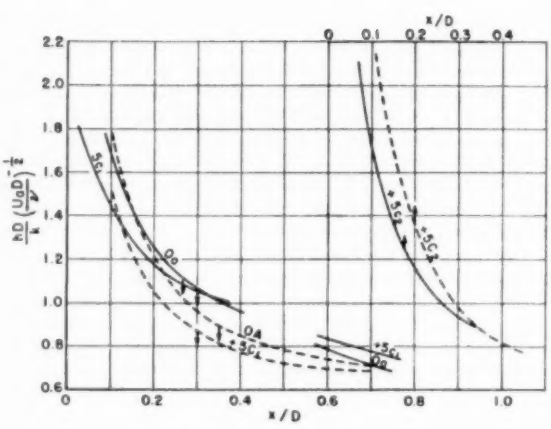

Zero angle of attack:

Oa experiment at $\frac{U_aD}{\nu} = 607{,}000$

OA prediction for $\frac{U_aD}{\nu} = 928{,}000$

5-Deg angle of attack, under side:

$5c_1$ experiment at $\frac{U_aD}{\nu} = 915{,}000$

$5C_1$ prediction for $\frac{U_aD}{\nu} = 917{,}000$

5-Deg angle of attack, upper side:

$5c_2$ experiment at $\frac{U_aD}{\nu} = 915{,}000$

$5C_2$ prediction for $\frac{U_aD}{\nu} = 917{,}000$

Fig. 6 Comparison of Experimental and Predicted Results

in experiments on a 1:3 elliptic cylinder, and may depend on attaining some appropriate type of flow in the wake region immediately adjacent to the cylinder.

It is recognized that different bases can be chosen for the temperature difference used in the evaluation of the heat-transfer coefficient, but the present method is consistent, as noted by Dr. Tifford, with the values of the recovery factor deduced by the adiabatic wall-temperature measurements. This is a sufficient argument for the elimination of other methods which yield heat-transfer coefficients which would refer to a different kind of surface-temperature distribution and yet not clearly specify a recovery factor.

There seem to be no grounds for considering the constant heat-rate surface condition to give a more invariable heat-transfer coefficient than would be the case with an isothermal wall. For the theoretical wedge flows, the variability of the heat-transfer coefficients with distance along the wall is the same for constant surface temperature and for constant heat rate. For the elliptic cylinder, since both cases coincide at the stagnation point, there is a slightly greater variation predicted for the isothermal case, but the relative difference between the constant heat-rate and constant wall-temperature cases is small.

[7] Refer to (6) of the authors' Bibliography.

[8] "Calculation Method for Two Dimensional Laminar Boundary Layers With Arbitrary Free Stream Velocity Variation and Arbitrary Wall Temperature Variation," by R. A. Seban, University of California, Institute of Engineering Research No. 12, Series 2, 1950

Torsional Vibration Notes With Solutions for an Untuned Viscous Damper and Flexible Coupling With Nonlinear Elasticity

By F. P. PORTER,[1] SCHENECTADY, N. Y.

Several special relations are derived that may be used to simplify the solution of certain phases of the torsional vibration problem. A solution is described for the vibration of a system with an untuned viscous damper. Numerical values are given for the nonlinear elasticity of the Falk-Bibby type couplings. These values are rearranged into a form suitable for calculating undamped resonance curves of an engine installation which includes one of these couplings. An approximate solution for the resulting vibration is described and illustrated by calculation.

Introduction

A DETAILED examination of the methods used in the computations for torsional vibration reveals several important characteristics that are useful in solving certain phases of the problem. For example, the undamped forced-vibration amplitude at the first mass of a concentrated-mass system may be obtained from the calculations of a standard Holzer table which is started at the end mass and carried through to the first mass. This amplitude, assuming that all the applied harmonic torques or impulses are equal, is the negative product of one impulse times the sum of the amplitudes at the impulses in the Holzer table divided by the residual torque of the table.

Another characteristic is that $I_{eq}\theta'\theta''$ is constant for any section of the system. In this relation I_{eq} is the equivalent inertia factor for the whole system at some section and θ' and θ'' are the amplitudes at this section for assigned values of the amplitudes at the first and last masses, respectively. A special case of this relation shows that the residual torque of a Holzer table which is started at the first mass and carried through to the end mass is equal to the residual torque of a Holzer table at the same frequency which is started at the end mass and carried through to the first mass.

Other important points are as follows: The undamped forced vibration of a system acted on by a number of harmonic impulses may be obtained at any section from the motion of an equivalent mass with inertia factor I_{eq} at that section acted on by an equivalent impulse. Furthermore, the effect at some section of the masses and impulses on one side of this section is the same as that of an equivalent mass acted on by an equivalent impulse.

These characteristics are derived in this paper and are applied to several examples to illustrate their usefulness. A solution is given for a system with an untuned viscous damper, which solution becomes relatively simple when using an equivalent mass for the whole system with this mass acted on by an equivalent impulse.

Finally, the vibration of a system with a flexible coupling having nonlinear elasticity is considered. The whole system is reduced to two equivalent masses, one at each hub of the coupling where one of the masses is acted on by an equivalent impulse. An approximate solution is made by using in place of the coupling torque its first harmonic for a harmonic variation of the amplitudes between the hubs.

Torque-Summation Method

The equivalent system consists of a number of concentrated masses with polar inertia factors $I_1, I_2, \ldots I_s$ lb-in. sec^2 connected along an axis of oscillation by a number of weightless shafts with stiffness factors $C_1, C_2, \ldots C_{s-1}$ lb-in. per radian. The whole system is assumed to vibrate torsionally at the same frequency with amplitudes $\theta_1, \theta_2, \ldots \theta_s$ radians and frequency constant $p = 2\pi n$ where n is in vibrations per second. The torque due to the simple harmonic motion of I_1 is $-I_1p^2\theta_1$. The torque in the first shaft is $C_1(\theta_2 - \theta_1)$. These two values of torque must be equal for equilibrium, so that

$$-I_1p^2\theta_1 = C_1(\theta_2 - \theta_1)$$

If θ_1 is assigned equal to unity and the corresponding values of θ for the other masses are indicated by θ'

$$\theta_2' = 1 - \frac{I_1}{C_1}p^2$$

The torque in the second shaft due to the first two masses when $\theta_1 = 1$ is $-I_2p^2\theta_2' - I_1p^2$ which is equal to $C_2(\theta_3' - \theta_2')$. Thus

$$\theta_3' = \theta_2' - \frac{I_2p^2\theta_2' + I_1p^2}{C_2}$$

Proceeding in this way to the rth shaft

$$\theta_{r+1}' = \theta_r' - \frac{\sum_1^r I_rp^2\theta_r'}{C_r}$$

The total inertia torque for all the masses at the end of the system is $-\sum_1^s I_rp^2\theta_r'$ which is zero for a natural frequency of the system.

This is the basis of the torque-summation method of calculation which may be carried out by the well-known Holzer table. The end value of the torque in the Holzer table is $\sum_1^s I_rp^2\theta_r'$ which is called the "residual torque" in this paper.

The calculation may be started at the end mass. In this case

$$-I_sp^2\theta_s = C_{s-1}(\theta_{s-1} - \theta_s)$$

If θ_s is assigned equal to unity and the corresponding values of the other masses are indicated by θ''

$$\theta_{s-1}'' = 1 - \frac{I_s}{C_{s-1}}p^2$$

[1] Engineering Department, American Locomotive Company.

Contributed by the Oil and Gas Power Division and presented at the Oil and Gas Power Conference, Buffalo, N. Y., June 23–27, 1952, of The American Society of Mechanical Engineers.

Note: Statements and opinions advanced in papers are to be understood as individual expressions of their authors and not those of the Society. Manuscript received at ASME Headquarters, April 29, 1952. Paper No. 52—OGP-7.

The torque in the next to the last shaft when $\theta_s = 1$ is $-I_{s-1}p^2\theta_{s-1}'' - I_sp^2$ which is equal to $C_{s-2}(\theta_{s-2}'' - \theta_{s-1}'')$. Thus

$$\theta_{s-2}'' = \theta_{s-1}'' - \frac{I_{s-1}p^2\theta_{s-1}'' + I_sp^2}{C_{s-2}}$$

Proceeding in this way to the rth shaft

$$\theta_r'' = \theta_{r+1}'' - \frac{\sum_{s}^{r+1} I_ip^2\theta_i''}{C_r}$$

The total inertia torque for the whole system at the first mass is $-\sum_{s}^{1} I_ip^2\theta_i''$ which is zero for a natural frequency of the system.

The residual torque of the Holzer table in this case is $\sum_{s}^{1} I_ip^2\theta_i''$.

The calculation may be made from each end up to the rth mass. The total inertia torque for the whole system at this mass for $\theta_r = 1$ is

$$-\frac{\sum_{1}^{r} I_ip^2\theta_i'}{\theta_r'} - \frac{\sum_{s}^{r+1} I_ip^2\theta_i''}{\theta_r''} \quad \text{or} \quad -\frac{\sum_{1}^{r-1} I_ip^2\theta_i'}{\theta_r'} - \frac{\sum_{s}^{r} I_ip^2\theta_i''}{\theta_r''}$$

which are zero for a natural frequency of the system.

Reduction Method

(*a*) *Concentrated-Mass System.* The same equivalent system as defined in the previous section will be considered first.

If a concentrated mass with inertia factor I_{11}' is assumed to be placed at the end of the first shaft to give the same torque at this section as that due to I_1

$$-I_{11}'p^2\theta_2' = C_1(\theta_2' - \theta_1') = -I_1p^2\theta_1'$$

Thus

$$\frac{I_{11}'}{I_1} = \frac{1}{1 - \frac{I_1p^2}{C_1}} = \frac{\theta_1'}{\theta_2'}$$

If I_{11}' is added to I_2 giving $I_{02}' = I_{11}' + I_2$ a new inertia factor I_{12}' may be placed at the end of the second shaft to give the same torque at this section as that due to I_{02}'. This may be repeated any number of times giving for end of the rth shaft

$$\frac{I_{1r}'}{I_{0r}'} = \frac{1}{1 - \frac{I_{0r}'p^2}{C_r}} = \frac{\theta_r'}{\theta_{r+1}'} \quad \text{and} \quad I_{0,r+1}' = I_{1r}' + I_{r+1}$$

The equivalent inertia factor for the whole system at the end is $I_{0s}' = I_{1,s-1}' + I_s$ which is zero for natural frequency of the system.

This is the basis of an inertia-summation method of calculation which the writer has called the reduction method.[3] The terms I_{1r}' or $I_{0,r+1}'$ are inertia factors for concentrated masses at the end of the rth shaft or beginning of the $r + 1$ shaft, respectively, which give the same value of inertia torque at these sections as result from the simple harmonic motion of all the masses from the beginning up to these sections. I_{1r}' and $I_{0,r+1}'$ are called inertia factors reduced from the beginning.

The same type of calculation may be started at the end mass and in this case the reduced inertia factors are indicated by a double prime mark. For example, if a concentrated mass $I_{0,s-1}''$ is assumed placed at the beginning of the last shaft to give the same torque at this section as that due to I_s

$$-I_{0,s-1}''p^2\theta_{s-1}'' = C_{s-1}(\theta_{s-1}'' - \theta_s'') = -I_sp^2\theta_s''$$

Thus

$$\frac{I_{0,s-1}''}{I_s} = \frac{1}{1 - \frac{I_sp^2}{C_{s-1}}} = \frac{\theta_s''}{\theta_{s-1}''}$$

If $I_{0,s-1}''$ is added to I_{s-1} giving $I_{1,s-2}'' = I_{0,s-1}'' + I_{s-1}$ a new inertia factor $I_{0,s-2}''$ may be placed at the beginning of the next to last shaft to give the same torque at this section as that due to $I_{1,s-2}''$. This may be repeated any number of times giving for the section at the beginning of the rth shaft

$$\frac{I_{0r}''}{I_{1r}''} = \frac{1}{1 - \frac{I_{1r}''p^2}{C_r}} = \frac{\theta_{r+1}''}{\theta_r''} \quad \text{and} \quad I_{1,r-1}'' = I_{0r}'' + I_r$$

The total equivalent inertia factor for the whole system reduced from the end to the beginning is $I_{10}'' = I_{01}'' + I_1$ which is zero for a natural frequency of the system.

The calculation may be made from each end up to the rth mass. The total inertia factor for the whole system at this mass is

$$I_{s0r} = I_{1,r-1}' + I_{1,r-1}'' = I_{0r}' + I_{0r}''$$

which is zero for a natural frequency of the system.

(*b*) *Including Distributed Mass in Equivalent System.* In the reduction method when one or more of the shafts or "steps" of the equivalent system is considered to have both uniformly distributed mass and elasticity, the inertia factors of all concentrated masses, which are assumed to occur only between the steps of the system, are given two subscripts. For example, the inertia factor between shafts r and $r + 1$ is indicated by $I_{r,r+1}$. An inertia factor with a single subscript such as I_r is the total inertia for the distributed mass of shaft r. Also, the amplitudes of the concentrated masses are indicated by double subscripts so that the amplitude of $I_{r,r+1}$ is $\theta_{r,r+1}$, θ_{1r}, or $\theta_{0,r+1}$.

Formulas for reduced inertia factor and amplitude at any point x from the beginning of the rth step with length l which has both mass and elasticity are as follows: No subscripts are needed on x and l since they refer to the same step as indicated by the subscript of ϕ.

$$I_r' = \frac{180}{\pi} I_r \frac{\tan\left(\phi_r n \frac{x}{l} + \gamma_r'\right)}{\phi_r n},$$

$$\tan \gamma_r' = \frac{\phi_r n I_{0r}'}{\frac{180}{\pi} I_r}, \quad \phi_r = 360\sqrt{\frac{I_r}{C_r}}$$

$$I_r'' = -\frac{180}{\pi} I_r \frac{\tan\left(\phi_r n \frac{x}{l} + \gamma_r''\right)}{\phi_r n},$$

$$\tan(\phi_r n + \gamma_r'') = -\frac{\phi_r n I_{1r}''}{\frac{180}{\pi} I_r}$$

$$\theta_r' = \alpha_r' \cos\left(\phi_r n \frac{x}{l} + \gamma_r'\right)$$

$$\theta_r'' = \alpha_r'' \cos\left(\phi_r n \frac{x}{l} + \gamma_r''\right)$$

[3] "Evaluation of Effects of Torsional Vibration," SAE, War Engineering Board, 1945, p. 157.

Relation Between Values From Holzer Table and Reduction Method

The values obtained in a Holzer table may be used to compute values of I' and I''. In the calculations starting at the beginning of the system

$$I_{l,r-1}'p^2\theta_r' = \sum_1^{r-1} I_i p^2 \theta_i'$$

$$I_{0r}'p^2\theta_r' = \sum_1^{r} I_i p^2 \theta_i'$$

so that

$$I_{l,r-1}' = \frac{\sum_1^{r-1} I_i p^2 \theta_i'}{p^2\theta_r'} \quad \text{and} \quad I_{0r}' = \frac{\sum_1^{r} I_i p^2 \theta_i'}{p^2\theta_r'}$$

Similarly, in the calculation starting at the end of the system

$$I_{0r}''p^2\theta_r'' = \sum_e^{r+1} I_i p^2 \theta_i''$$

$$I_{l,r-1}''p^2\theta_s'' = \sum_e^{r} I_i p^2 \theta_i''$$

so that

$$I_{0r}'' = \frac{\sum_e^{r+1} I_i p^2 \theta_i''}{p^2\,\theta_r''} \quad \text{and} \quad I_{l,r-1}'' = \frac{\sum_e^{r} I_i p^2 \theta_i''}{p^2\theta_r''}$$

The values of the amplitudes at the masses for a concentrated-mass equivalent system as obtained by the reduction method may be expressed as follows

$$\theta_{r+1}' = \theta_1' \frac{\theta_2'}{\theta_1'}\frac{\theta_3'}{\theta_2'}\cdots\frac{\theta_{r+1}'}{\theta_r'} = \theta_1'\left(1-\frac{I_1p^2}{C_1}\right)\left(1-\frac{I_{02}'p^2}{C_2}\right)\cdots\left(1-\frac{I_{0r}'p^2}{C_r}\right)$$

$$= \theta_1' \prod_1^r \left(1-\frac{I_{0i}'p^2}{C_i}\right)$$

$$\theta_r'' = \theta_e'' \frac{\theta_{e-1}''}{\theta_e''}\frac{\theta_{e-2}''}{\theta_{e-1}''}\cdots\frac{\theta_r''}{\theta_{r+1}''} = \theta_e''\left(1-\frac{I_ep^2}{C_{e-1}}\right)\left(1-\frac{I_{l,e-2}''p^2}{C_{e-2}}\right)\cdots\left(1-\frac{I_{lr}''p^2}{C_r}\right)$$

$$= \theta_e'' \prod_{e-1}^r \left(1-\frac{I_{li}''p^2}{C_i}\right)$$

Calculations in a Holzer table are illustrated in Table 1. Two Holzer tables are shown; the upper one gives the calculations when starting at the first mass, and the lower one gives the calculations when starting at the last mass. Columns 8, 9, and 10 are added to show the values of I' and I'' as obtained from the Holzer tables.

Calculations for the same system by the reduction method are given in Table 2. Two tables of calculations are shown, the upper one when starting at the first mass and the lower one when starting at the last mass. Columns 8, 9, and 10 are added to show the values of θ', θ'', $\Sigma Ip^2\theta'$ and $\Sigma Ip^2\theta''$ as obtained from the calculations by the reduction method. The results obtained from the calculations in the Holzer table or by the reduction method are seen to be the same.

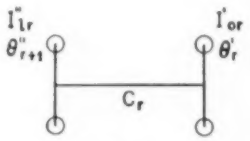

Fig. 1

Derivation of Relation $I_{eq}\theta'\theta'' = \text{Const}$

If the whole system at a given frequency is reduced to the two-mass system shown in Fig. 1

$$I_{eqr} = I_{0r}' + I_{0r}'' = I_{0r}' + \frac{I_{lr}''}{1-\dfrac{I_{lr}''p^2}{C_r}}$$

$$I_{eqr}\left(1-\frac{I_{lr}''p^2}{C_r}\right) = I_{0r}' + I_{lr}'' - \frac{I_{0r}'I_{lr}''p^2}{C_r}$$

Similarly

$$I_{eqr+1} = I_{lr}' + I_{lr}'' = \frac{I_{0r}'}{1-\dfrac{I_{0r}'p^2}{C_r}} + I_{lr}''$$

$$I_{eqr+1}\left(1-\frac{I_{0r}'p^2}{C_r}\right) = I_{0r}' + I_{lr}'' - \frac{I_{0r}'I_{lr}''p^2}{C_r}$$

Equating the two equals, gives

$$I_{eqr}\left(1-\frac{I_{lr}''p^2}{C_r}\right) = I_{eqr+1}\left(1-\frac{I_{0r}'p^2}{C_r}\right)$$

Since

$$1-\frac{I_{lr}''p^2}{C_r} = \frac{\theta_r''}{\theta_{r+1}''} \quad \text{and} \quad 1-\frac{I_{0r}'p^2}{C_r} = \frac{\theta_{r+1}'}{\theta_r'}$$

$$I_{eqr}\frac{\theta_r''}{\theta_{r+1}''} = I_{eqr+1}\frac{\theta_{r+1}'}{\theta_r'}$$

or

$$I_{eqr}\theta_r'\theta_r'' = I_{eqr+1}\,\theta_{r+1}'\,\theta_{r+1}''$$

Therefore, since r is any number from 1 to e

$$I_{eqr}\,\theta_r'\,\theta_r'' = \text{const}$$

at a given frequency for any value of r.

Table 3 shows the results of applying this constant relationship to the numerical values in Table 1 or Table 2.

If the foregoing constant is compared at the first and last masses

$$I_{eqe}\,\theta_e'\,\theta_e'' = I_{eq1}\,\theta_1'\theta_1''$$

Since $\theta_e'' = 1$ and $\theta_1' = 1$ in the Holzer tables

$$I_{eqe}\theta_e' = I_{eq1}\,\theta_1''$$

Also since

$$I_{eqe} = I_{0e}' = \frac{\sum_1^e I_i p^2\theta_i'}{p^2\theta_e'}$$

and

TABLE 1

HOLZER TABLE

$p^2 = 7700$ (CALCULATION STARTED AT FIRST MASS)

	1	2	3	4	5	6	7	8	9	10
n	I	$Ip^2 \times 10^{-6}$	θ'	$Ip^2\theta' \times 10^{-6}$	$\Sigma Ip^2\theta' \times 10^{-6}$	$C \times 10^{-6}$	$\frac{\Sigma Ip^2\theta'}{C}$	$p^2\theta'$	$\frac{I'_{l,n-1}}{(5)_{n-1}/(8)_n} \times 10^{-6}$	$\frac{I'_{0n}}{(5)_n/(8)_n} \times 10^{-6}$
1	708	5.4516	1	5.4516	5.4516	2070	.00263	7700		708.0
2	3920	30.184	.99737	30.105	35.557	730	.04871	7679.7	709.9	4630.0
3	3920	30.184	.94866	28.634	64.191	730	.08793	7304.7	4867.7	8787.6
4	3920	30.184	.86073	25.980	90.171	730	.12352	6627.6	9685.4	13605.4
5	3920	30.184	.73721	22.252	112.423	730	.15400	5676.5	15885.0	19805.0
6	3920	30.184	.58321	17.604	130.027	730	.17812	4490.7	25034.6	28954.7
7	3920	30.184	.40509	12.227	142.254	402	.35387	3119.2	41686.0	45605.9
8	139800	1076.46	.05122	55.136	197.390	1334	.14797	394.4	360685	500482
9	26400	203.28	-.09675	-19.667	177.723			-745.0	-264953	-238554

$p^2 = 7700$ (CALCULATION STARTED AT LAST MASS)

	1	2	3	4	5	6	7	8	9	10
n	I	$Ip^2 \times 10^{-6}$	θ''	$Ip^2\theta'' \times 10^{-6}$	$\Sigma Ip^2\theta'' \times 10^{-6}$	$C \times 10^{-6}$	$\frac{\Sigma Ip^2\theta''}{C}$	$p^2\theta''$	$\frac{I''_{0n}}{(5)_{n+1}/(8)_n} \times 10^{-6}$	$\frac{I''_{l,n-1}}{(5)_n/(8)_n} \times 10^{-6}$
9	26400	203.28	1	203.28	203.28	1334	.152384	7700		26400
8	139800	1076.46	.847616	912.425	1115.705	402	2.77539	6526.6	31146.4	170947
7	3920	30.184	-1.92777	-58.188	1057.517	730	1.44865	-14843.8	-75163.0	-71243.0
6	3920	30.184	-3.37642	-101.914	955.603	730	1.30905	-25998.4	-40676.2	-36756.2
5	3920	30.184	-4.68547	-141.426	814.177	730	1.11531	-36078.1	-26487.1	-22567.1
4	3920	30.184	-5.80078	-175.091	639.086	730	.87546	-44666.0	-18228.1	-14308.1
3	3920	30.184	-6.67624	-201.516	437.570	730	.59941	-51407.0	-12431.9	-8511.9
2	3920	30.184	-7.27565	-219.608	217.962	2070	.10530	-56022.5	-7810.6	-3890.6
1	708	5.4516	-7.38095	-40.238	177.724			-56833.3	-3835.1	-3127.1

$$I_{eq1} = I_{10}'' = \frac{\sum_{e}^{1} I_i p^2 \theta_i''}{p^2 \theta_1''}$$

it follows that

$$\sum_{1}^{e} I_i p^2 \theta_i' = \sum_{e}^{1} I_i p^2 \theta_i''$$

This shows that the last value of $\Sigma Ip^2\theta$ in the Holzer table or the residual torque is the same at a given frequency regardless of whether the calculation is started at the first mass or the last mass. This is illustrated in Table 1 where the residual torque when starting the calculation at the first mass is 177.723×10^6 and when starting the calculation at the last mass it is 177.724×10^6.

Undamped Forced Vibration and Equivalent Applied Torque

The amplitude of oscillation of a concentrated mass with inertia factor I acted on by a torque $m \cos pt$ is given by

$$-Ip^2\theta = m$$

Therefore, if the whole system is reduced to an equivalent inertia I_{eqi} at the ith mass, the forced vibration amplitude θ_i due to a torque $m_i \cos pt$ applied to this mass is

$$\theta_i = \frac{m_i}{-I_{eqi}p^2}$$

The amplitude of any other mass r is

TABLE 2

REDUCTION METHOD

$p^2 = 7700$ (CALCULATION STARTED AT FIRST MASS)

	1	2	3	4	5	6	7	8	9	10
r	I_r	$C_r \times 10^{-6}$	$\frac{p^2}{C} \times 10^6$	I'_{or} (1) + (7)	$\frac{I'p^2}{C}$ (3)×(4)×10^{-6}	$1 - \frac{I'p^2}{C}$ 1 − (5)	$I'_{\ell r-1}$ $\frac{(4)}{(6)}$ FOR $r-1$	θ' $\prod_{1}^{r-1}$ (6)	$p^2\theta'$	$\sum I p^2 \theta' \times 10^{-6}$ (4)×(9)×10^{-6}
1	708	2070	3.7198	708	.002634	.99737		1	7700	5.4516
2	3920	730	10.5479	4629.9	.04884	.95116	709.9	.99737	7679.7	35.556
3	3920	730	10.5479	8787.6	.09269	.90731	4867.6	.94866	7304.7	64.191
4	3920	730	10.5479	13605.3	.14351	.85649	9685.3	.86073	6627.6	90.170
5	3920	730	10.5479	19804.9	.20890	.79110	15884.9	.73721	5676.5	112.423
6	3920	730	10.5479	28954.6	.30541	.69459	25034.6	.58321	4490.7	130.026
7	3920	402	19.1542	45605.9	.873545	.126455	41685.9	.40509	3119.2	142.254
8	139800	1334	5.7721	500449	2.88864	−1.88864	360649	.051226	394.44	197.397
9	26400			−238579			−264979	−.096747	−744.95	177.729

$p^2 = 7700$ (CALCULATION STARTED AT LAST MASS)

	1	2	3	4	5	6	7	8	9	10
r	I_r	$C_{r-1} \times 10^{-6}$	$\frac{p^2}{C} \times 10^6$	$I''_{\ell r-1}$ (1) + (7)	$\frac{I''p^2}{C}$ (3)×(4)×10^{-6}	$1 - \frac{I''p^2}{C}$ 1 − (5)	I''_{or} $\frac{(4)}{(6)}$ FOR $r+1$	θ'' $\prod_{9}^{r+1}$ (6)	$p^2\theta''$	$\sum I p^2 \theta'' \times 10^{-6}$ (4)×(9)×10^{-6}
9	26400	1334	5.7721	26400	.152383	.847617		1	7700	203.28
8	139800	402	19.1542	170946	3.27433	−2.27433	31146.1	.847617	6526.65	1115.705
7	3920	730	10.5479	−71243.2	−.75147	1.75147	−75163.2	−1.92776	−14843.8	1057.520
6	3920	730	10.5479	−36756.2	−.38770	1.38770	−40676.2	−3.37641	−25998.4	955.602
5	3920	730	10.5479	−22567.1	−.23804	1.23804	−26487.1	−4.68544	−36077.9	814.174
4	3920	730	10.5479	−14308.1	−.15092	1.15092	−18228.1	−5.80076	−44665.9	639.084
3	3920	730	10.5479	−8511.9	−.08978	1.08978	−12431.9	−6.67621	−51406.8	437.570
2	3920	2070	3.7198	−3890.7	−.014473	1.01447	−7810.7	−7.27560	−56022.1	217.965
1	708			−3127.2			−3835.2	−7.38088	−56832.8	177.728

$$\theta_r = \theta_i \frac{\theta_r'}{\theta_i'} = \frac{m_i \theta_r'}{-I_{equ} p^2 \theta_i'} \qquad (r = 1, 2, \ldots i)$$

$$\theta_r = \theta_i \frac{\theta_r''}{\theta_i''} = \frac{m_i \theta_r''}{-I_{equ} p^2 \theta_i''} \qquad (r = i, i+1, \ldots e)$$

Since

$$I_{equ} \theta_i' \theta_i'' = I_{equ} \theta_r' \theta_r''$$

$$I_{equ} \frac{\theta_i'}{\theta_r'} = I_{equ} \frac{\theta_r''}{\theta_i''} \quad \text{or} \quad I_{equ} \frac{\theta_i''}{\theta_r''} = I_{equ} \frac{\theta_r'}{\theta_i'}$$

and the expressions for amplitude may be written

$$\theta_r = \frac{m_i \theta_i''}{-I_{equ} p^2 \theta_r''} \quad \text{or} \quad -I_{equ} p^2 \theta_r = \frac{m_i \theta_i''}{\theta_r''} \quad (r = 1, 2, \ldots i)$$

$$\theta_r = \frac{m_i \theta_i'}{-I_{equ} p^2 \theta_r'} \quad \text{or} \quad -I_{equ} p^2 \theta_r = \frac{m_i \theta_i'}{\theta_r'} \quad (r = i, i+1, \ldots e)$$

TABLE 3

r	I_{equ}	θ_r'	θ_r''	$I_{equ} \theta_r' \theta_r''$
1	−3127.2	1.0	−7.38095	23082
2	−3180.8	0.99737	−7.27565	23082
	−3644.3	0.94866	−6.67624	23081
	−4622.8	0.86073	−5.80078	23081
	−6682.2	0.73721	−4.68547	23081
	−11721.6	0.58321	−3.37642	23082
	−29557.3	0.40509	−1.92777	23082
	−531565	0.05122	0.847616	23079
	−238579	−0.09675	1.0	23083

This shows that the forced vibration amplitude of the rth mass in the system where the ith mass is acted on by an applied torque $m_i \cos pt$ is the amplitude of oscillation of the equivalent mass with inertia factor I_{equ} acted on by an equivalent applied torque $m_{equ} \cos pt$ where

$$m_{equ} = \frac{m_i \theta_i''}{\theta_r''} \text{ for } r = 1, 2, \ldots i$$

$$= \frac{m_i \theta_i'}{\theta_r'} \text{ for } r = i, i+1, \ldots e$$

Furthermore, the system from the last mass back to the rth mass where r is less than i may be considered reduced to an equivalent inertia factor I_r'' at this position acted on by an equivalent applied torque

$$m_{eqr} = \frac{m_i\theta_i''}{\theta_r''} \; (= m_{eqr}'')$$

Also, the system from the first mass up to the rth mass where r is greater than i may be considered reduced to an equivalent inertia factor I_r' at this position acted on by an equivalent applied torque

$$m_{eqr} = \frac{m_i\theta_i'}{\theta_r'} \; (= m_{eqr}')$$

The torque in the rth shaft may be written

$$\left.\begin{aligned} M_r &= C_r(\theta_{r+1} - \theta_r) \\ &= -I_{0r}'p^2\theta_r \qquad = -I_{1r}'p^2\theta_{r+1} \\ &= I_{0r}''p^2\theta_r + m_{eqr} \quad = I_{1r}''p^2\theta_{r+1} + m_{eqr+1}'' \end{aligned}\right\} \text{for } r = 1, 2, \ldots i-1$$

$$\left.\begin{aligned} &= I_{0r}''p^2\theta_r \qquad = I_{1r}''p^2\theta_{r+1} \\ &= -I_{0r}'p^2\theta_r - m_{eqr}' \quad = -I_{1r}'p^2\theta_{r+1} - m_{eqr+1}' \end{aligned}\right\} \text{for } r = i, i+1, \ldots e$$

If a number of torques with the same frequency given by $m_i \cos(pt - \psi_i)$ are applied at several masses with numbers indicated by i the equivalent applied torque at any mass between the first mass and the first applied torque is $m_{eqr}\cos(pt - \psi'')$ where

$$m_{eqr} = \frac{\Sigma m_i\theta_i''}{\theta_r''} \; (r \leq i)$$

$$\Sigma m_i\theta_i'' = \pm\sqrt{(A'')^2 + (B'')^2}$$

$$A'' = \Sigma m_i\theta_i'' \sin\psi_i$$

$$B'' = \Sigma m_i\theta_i'' \cos\psi_i$$

$$\tan\psi'' = \frac{A''}{B''}, \quad \sin\psi'' = \frac{A''}{\Sigma m_i\theta_i''}, \quad \cos\psi'' = \frac{B''}{\Sigma m_i\theta_i''}$$

The equivalent applied torque at any mass between the last applied torque and last mass is $m_{eqr}\cos(pt - \psi')$ where

$$m_{eqr} = \frac{\Sigma m_i\theta_i'}{\theta_r'} \; (r \geq i)$$

$$\Sigma m_i\theta_i' = \pm\sqrt{(A')^2 + (B')^2}$$

$$A' = \Sigma m_i\theta_i' \sin\psi_i$$

$$B' = \Sigma m_i\theta_i' \cos\psi_i$$

$$\tan\psi' = \frac{A'}{B'}, \quad \sin\psi' = \frac{A'}{\Sigma m_i\theta_i'}, \quad \cos\psi' = \frac{B'}{\Sigma m_i\theta_i'}$$

The equivalent applied torque at any mass ρ between the applied torques is $m_{eq\rho}\cos(pt - C\psi)$ and the torque in the ρth shaft is $M_\rho\cos(pt - S\psi)$ where

$$m_{eq\rho} = \pm\sqrt{(CA)^2 + (CB)^2}$$

$$CA = \frac{\sum^{\rho} m_i\theta_i' \sin\psi_i}{\theta_\rho'} + \frac{\sum_{\rho+1} m_i\theta_i'' \sin\psi_i}{\theta_\rho''}$$

$$CB = \frac{\sum^{\rho} m_i\theta_i' \cos\psi_i}{\theta_\rho'} + \frac{\sum_{\rho+1} m_i\theta_i'' \cos\psi_i}{\theta_\rho''}$$

$$\tan C\psi = \frac{CA}{CB}, \quad \sin C\psi = \frac{CA}{\pm\sqrt{(CA)^2 + (CB)^2}}$$

$$\cos C\psi = \frac{CB}{\pm\sqrt{(CA)^2 + (CB)^2}}$$

$$M_\rho = \pm\frac{1}{I_{eq\rho}}\sqrt{(SA)^2 + (SB)^2}$$

$$SA = -I_{0\rho}''\frac{\sum^{\rho} m_i\theta_i' \sin\psi_i}{\theta_\rho'} + I_{0\rho}'\frac{\sum_{\rho+1} m_i\theta_i'' \sin\psi_i}{\theta_\rho''}$$

$$SB = -I_{0\rho}''\frac{\sum^{\rho} m_i\theta_i' \cos\psi_i}{\theta_\rho'} + I_{0\rho}'\frac{\sum_{\rho+1} m_i\theta_i'' \cos\psi_i}{\theta_\rho''}$$

$$\tan S\psi = \frac{SA}{SB}, \quad \sin S\psi = \frac{SA}{\pm\sqrt{(SA)^2 + (SB)^2}}$$

$$\cos S\psi = \frac{SB}{\pm\sqrt{(SA)^2 + (SB)^2}}$$

Therefore the forced-vibration amplitude at any mass in the system is

$$\theta_r = \frac{m_{eqr}}{-I_{eqr}p^2}$$

The amplitude of any other mass s between the first mass and the first applied torque is

$$\theta_s = \theta_r\frac{\theta_s'}{\theta_r'} \; (r \text{ and } s \leq i)$$

The amplitude of any other mass s between the last mass and the last applied torque is

$$\theta_s = \theta_r\frac{\theta_s''}{\theta_r''} \; (r \text{ and } s \geq i)$$

Since

$$I_{eqr} = I_{1,r-1}' + I_{1,r-1}'' = I_{0r}' + I_{0r}''$$

$$= \frac{\sum_1^{r-1} I_i p^2\theta_i'}{p^2\theta_r'} + \frac{\sum_s^{r} I_i p^2\theta_i''}{p^2\theta_r''} = \frac{\sum_1^{r} I_i p^2\theta_i'}{p^2\theta_r'} + \frac{\sum_s^{r+1} I_i p^2\theta_i''}{p^2\theta_r''}$$

the expression for amplitude may be written

$$\theta_r(r \leq i) = -\frac{\Sigma m_i\theta_i''}{\frac{\theta_r''}{\theta_r'}\sum_1^{r-1} I_i p^2\theta_i' + \sum_e^{r} I_i p^2\theta_i''}$$

$$\theta_r(r \geq i) = -\frac{\Sigma m_i\theta_i'}{\sum_1^{r} I_i p^2\theta_i' + \frac{\theta_r'}{\theta_r''}\sum_s^{r+1} I_i p^2\theta_i''}$$

These expressions show that the amplitude for any mass between the first mass and first applied torque or the last applied torque and last mass may be obtained from the values computed in a standard Holzer table. The amplitude for any mass between the applied torques may be obtained by combining these expressions.

At the first and last mass since $\sum_1^0 I_i p^2\theta_i' = 0$ and $\sum_e^{e+1} I_i p^2\theta_i'' = 0$

$$\theta_1 = -\frac{\Sigma m_i\theta_i''}{\sum_e I_i p^2\theta_i''} \qquad \theta_s = -\frac{\Sigma m_i\theta_i'}{\sum_1^e I_i p^2\theta_i'}$$

This shows that the forced vibration amplitude of the first mass is $-\Sigma m_i\theta_i''$ divided by the residual torque where θ_i'' and residual torque are obtained from a Holzer table that starts from the last mass. Also, that the forced vibration amplitude of the last mass is $-\Sigma m_i\theta_i'$ divided by the residual torque where θ_i' and the residual torque are obtained from a Holzer table that starts from the first mass.

To illustrate these results numerically, the forced-vibration amplitude at the first and last mass of the system will be calculated from the values computed in Table 1 for the 6 order major vibration. The applied torques in this case are all equal to 34911 lb-in. and occur at masses 2 to 7, inclusive.

From Table 1, starting at the last mass, $\Sigma\theta''$ for the masses 2 to 7, inclusive = —29.74233. Therefore

$$\theta_1 = \frac{34911 \times 29.74233}{177.724 \times 10^6} = 0.0058424 \text{ radians} = 0.33475 \text{ deg}$$

Also from Table 1, starting at the first mass, $\Sigma\theta'$ for the masses 2 to 7, inclusive = 4.53227. Therefore

$$\theta_9 = \frac{-34911 \times 4.53227}{177.724 \times 10^6} = -0.0008903 \text{ radians} = -0.05101 \text{ deg}$$

These amplitudes are the same as those given in the previous reference,[3] where the calculations were considerably more lengthy since they were arranged to obtain the amplitudes of all the masses.

In a multicylinder engine with N equal cylinders firing at equal crank angles, the phase angles ψ_i in the expression $m \cos (pt - \psi_i)$ for a harmonic component of the torque at any cylinder relative to the harmonic $m \cos pt$ for the first cylinder are

$$0, \quad \frac{\mu\, 360}{N}, \quad \frac{2\mu\, 360}{N}, \ldots \frac{(N-1)\mu\, 360}{N}$$

for successively firing cylinders. The harmonic number μ indicates the number of complete waves of the harmonic per cycle of the engine. Order number is defined as the number of complete waves per revolution of the engine shaft and is μ for a 2-cycle engine and $\mu/2$ for a 4-cycle engine. The term "major" vibration refers to the vibrations that have μ/N an integer, so that the phase angles in this case are all integral multiples of 360. All of the other harmonics of the vibration are called "minor" vibrations.

To illustrate the calculation for a minor vibration, the amplitude at the first mass for the $6\frac{1}{2}$ order will be computed from the values in Table 1. The engine is a 6-cylinder, 4-cycle engine with a firing order of 142635. The cylinders are at masses 2 to 7, inclusive.

The $6\frac{1}{2}$ order applied torque at each cylinder is 26153 lb-in. The phase angles for successively firing cylinders are

$$0, \quad \frac{13 \times 360}{6}, \quad \frac{2 \times 13 \times 360}{6}, \quad \ldots \frac{5 \times 13 \times 360}{6}$$

which are equivalent to

$$0, 60, 120, 180, 240, 300$$

These are the phase angles of the $6\frac{1}{2}$ order applied torques at the cylinders taken in sequence of the firing order. This sequence when using the mass numbers is 253746 so that

$$\Sigma\, \theta_i'' \sin \psi_i = -4.68547 \sin 60 - 6.67624 \sin 120 - 1.92777 \sin 180 - 5.80078 \sin 240 - 3.37642 \sin 300 = -1.89185$$

$$\Sigma\, \theta_i'' \cos \psi_i = -7.27565 - 4.68547 \cos 60 - 6.67624 \cos 120 - 1.92777 \cos 180 - 5.80078 \cos 240 - 3.37642 \cos 300 = -3.14031$$

$$\Sigma\, \theta_i'' = -\sqrt{(1.89185)^2 + (3.14031)^2} = -3.66615$$

Therefore

$$\theta_1 = \frac{26153 \times 3.66615}{177.724 \times 10^6} = 0.0005395 \text{ radians} = 0.03091 \text{ deg}$$

This is the same as the value given previously.[3]

Untuned Viscous Damper

The following solution of the vibration of an undamped system with an untuned viscous damper[4] attached at some section illustrates the use of an equivalent inertia factor for the whole system with an equivalent applied harmonic torque acting on it. A diagram of the system with the damper attached is shown in Fig. 2.

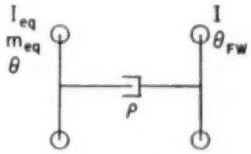

Fig. 2

The nomenclature is as follows:

I_{eq} = equivalent inertia factor for system at damper hub including damper hub but not damper flywheel

I or I_{FW} = inertia factor for damper flywheel

θ = amplitude of damper hub, radians

θ_{FW} = amplitude of damper flywheel, radians

ρ = damping factor or damping constant of damper, lb-in. sec./radian

$p = 2\pi n$ = frequency constant where n is frequency in VPS

$p_0 = 2\pi n_0$ = frequency parameter of damper such that $\rho = Ip_0 = 2\pi In_0$

m_{eq} = equivalent applied torque acting on I_{eq}

The differential equations of motion are

$$I\frac{d^2\bar{\theta}_{FW}}{dt^2} = \rho\left(\frac{d\bar{\theta}}{dt} - \frac{d\bar{\theta}_{FW}}{dt}\right)$$

$$I_{eq}\frac{d^2\bar{\theta}}{dt^2} = \bar{m}_{eq} - \rho\left(\frac{d\bar{\theta}}{dt} - \frac{d\bar{\theta}_{FW}}{dt}\right)$$

where the overbar indicates that the term is a function of t. If the harmonic expression for $\bar{m}_{eq}$ is

$$\bar{m}_{eq} = m_{eq}\cos(pt - \psi) = m_{eq}\sin\psi\sin pt + m_{eq}\cos\psi\cos pt$$

where ψ is chosen so that

$$\bar{\theta} = \theta\cos pt$$

[3] Reference 2, p. 231.

[4] A solution to this problem was given in "The Viscous Torsional Vibration Damper," by B. E. O'Connor, SAE Quarterly Transactions, vol. 1, 1947, pp. 87–97.

then

$$\theta = -\frac{m_{eq}}{\pm Ip^2\sqrt{\left[\frac{\frac{p}{p_0}}{\left(\frac{p}{p_0}\right)^2+1}\right]+\left[\frac{I_{eq}}{I}+\frac{1}{\left(\frac{p}{p_0}\right)^2+1}\right]^2}}$$

$$\tan\psi = \frac{\frac{p}{p_0}}{\left[\left(\frac{p}{p_0}\right)^2+1\right]\left[\frac{I_{eq}}{I}+\frac{1}{\left(\frac{p}{p_0}\right)^2+1}\right]}$$

$$m_{eq}\sin\psi = -\frac{\frac{p}{p_0}}{\left(\frac{p}{p_0}\right)^2+1}Ip^2\theta$$

$$m_{eq}\cos\psi = -\left[I_{eq}+\frac{I}{\left(\frac{p}{p_0}\right)^2+1}\right]p^2\theta$$

$$\theta_{FW} = \frac{\theta}{\sqrt{\left(\frac{p}{p_0}\right)^2+1}}\cos\left(pt-\tan^{-1}\frac{p}{p_0}\right)$$

This solution may be verified by direct substitution into the differential equations of motion.

If $I = \infty$, $p_0 = 0$, and $Ip_0 = \rho$, the foregoing solution applies to a system with damping proportional to velocity at one point, such as a marine installation when only the damping of the propeller is considered. In this case

$$\theta = -\frac{m_{eq}}{\pm p\sqrt{I_{eq}^2p^2+\rho^2}}$$

$$\tan\psi = \frac{\rho}{I_{eq}p}, \quad m_{eq}\sin\psi = -\rho p\theta, \quad m_{eq}\cos\psi = -I_{eq}p^2\theta$$

The vibration of all the masses of the system represented by I_{eq} is either in phase or 90 deg out of phase with the hub motion $\theta\cos pt$. The motion in phase is called the "normal phase" of the motion and is the same as the undamped forced vibration of the system with I_{eq} increased by

$$I_{FW}' = I\Big/\left[\left(\frac{p}{p_0}\right)^2+1\right]$$

stimulated by an applied torque equal to $m_{eq}\cos\psi\cos pt$.

The vibration 90 deg out of phase is called the "damping phase" of the motion and is the same as the undamped forced vibration of the system with an infinite mass at the damper hub stimulated by an applied torque equal to $m_{eq}\sin\psi\sin pt$.

The terms within the radical in the expression for θ may be arranged as follows

$$\left(\frac{I_{eq}}{I}\right)^2+2\frac{I_{eq}}{I}\frac{1}{\left(\frac{p}{p_0}\right)^2+1}+\frac{1}{\left[\left(\frac{p}{p_0}\right)^2+1\right]^2}+\frac{\left(\frac{p}{p_0}\right)^2}{\left[\left(\frac{p}{p_0}\right)^2+1\right]^2}$$

$$=\left(\frac{I_{eq}}{I}\right)^2+\left(2\frac{I_{eq}}{I}+1\right)\frac{1}{\left(\frac{p}{p_0}\right)^2+1}$$

Therefore, at frequencies that give $2\frac{I_{eq}}{I}+1=0$ or $I_{eq}=-\frac{I}{2}$, θ is independent of ρ and equal to

$$\theta = \pm\frac{m_{eq}}{\frac{I}{2}p^2}$$

These points on the resonance curves are called "fixed points" for the hub.

The general expression for θ may be written

$$\theta = -\frac{m_{eq}}{\pm Ip^2\sqrt{\left(\frac{I_{eq}}{I}\right)^2+\left(2\frac{I_{eq}}{I}+1\right)\frac{1}{\left(\frac{p}{p_0}\right)^2+1}}}$$

If

$$x = \frac{I_{eq}}{I}, \quad y = \frac{1}{\left(\frac{p}{p_0}\right)^2+1}$$

$$\theta = -\frac{m_{eq}}{\pm Ip^2\sqrt{x^2+(2x+1)y}}$$

The maximum value of $|\theta|$ for a particular damping factor or p_0 value occurs when $p^4[x^2+(2x+1)y]/m_{eq}^2$ is a minimum. Differentiating with respect to p and equating to zero gives

$$(2x+1)y^2+\left[2x+1+p\frac{dx}{dp}-(2x+1)\frac{p}{m_{eq}}\frac{dm_{eq}}{dp}\right]y+x\left(2x+p\frac{dx}{dp}-\frac{xp}{m_{eq}}\frac{dm_{eq}}{d_p}\right)=0$$

If y_1 is a root of this quadratic equation such that $0 < y_1 < 1$, the expression for ρ or p_0 as a function of the frequency at the maximum value of $|\theta|$ may be written as follows

$$\rho = Ip\sqrt{\frac{y_1}{1-y_1}} \quad \text{or} \quad p_0 = p\sqrt{\frac{y_1}{1-y_1}}$$

The minimum value of the curve for the maximum $|\theta|$ may be said to define optimum damping. This minimum will occur when $p^4[x^2+(2x+1)y_1]/m_{eq}^2$ is maximum. Differentiating with respect to p and equating to zero gives

$$\frac{p}{2}(2x+1)\frac{dy_1}{dp}+\left[2(2x+1)+p\frac{dx}{dp}-(2x+1)\frac{p}{m_{eq}}\frac{dm_{eq}}{dp}\right]y_1+x\left(2x+p\frac{dx}{dp}-\frac{xp}{m_{eq}}\frac{dm_{eq}}{dp}\right)=0$$

This is zero at the fixed-point frequency where $2x+1=0$ or $x=-1/2$, if the damping factor is given by

$$p\frac{dx}{dp}y_1-\frac{1}{2}\left(-1+p\frac{dx}{dp}+\frac{p}{2m_{eq}}\frac{dm_{eq}}{dp}\right)=0$$

or

$$y_1 = \frac{p\frac{dx}{dp}-1+\frac{p}{2m_{eq}}\frac{dm_{eq}}{dp}}{2p\frac{dx}{dp}}$$

Therefore the condition for optimum damping is

$$\rho = Ip\sqrt{\frac{p\frac{dx}{dp}-1+\frac{p}{2m_{eq}}\frac{dm_{eq}}{dp}}{p\frac{dx}{dp}+1-\frac{p}{2m_{eq}}\frac{dm_{eq}}{dp}}}$$

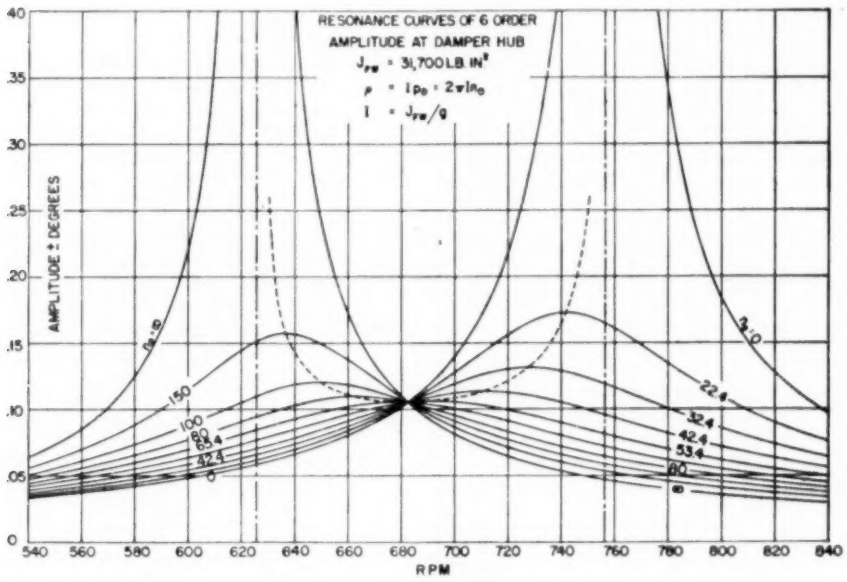

FIG. 3 RESONANCE CURVES OF 6 ORDER AMPLITUDE AT DAMPER HUB IN DEGREES, J_{FW} = 31,700 LB-IN² ($\rho = I p_0 = 2\pi I n_0$; $I = J_{FW}/g$.)

where p, x, and m_{eq} are the values at the fixed-point frequency of the hub. This condition shows that the minimum value of maximum $|\theta|$ is the value for the fixed point and occurs at the fixed-point frequency.

Since the damping factor is a function of the frequency at the maximum value of $|\theta|$, the damping factor of an untuned viscous damper may be determined from the test results of an installation equipped with the damper provided that:

1 The test obtains the frequencies of the maximum amplitudes for substantially constant applied harmonic torques.

2 Other damping effects in the system are not sufficient to change the frequency of the maximum amplitudes appreciably.

3 The mathematical equivalent system for the unit is sufficiently accurate to give accurate values for the natural frequencies of the unit with the damper flywheel removed or locked solid to the hub.

4 There is a measurable difference in the natural frequencies of the unit with the damper flywheel removed or locked solid to the hub.

The energy absorbed by the damper torque at any frequency is

$$K = \int_0^{pt=2\pi} \rho \left(\frac{d\bar{\theta}}{dt} - \frac{d\bar{\theta}_{FW}}{dt} \right) d\bar{\theta} \quad \text{or} \quad \int_0^{pt=2\pi} I \frac{d^2\bar{\theta}_{FW}}{dt^2}\, d\bar{\theta}$$

$$= \int_0^{pt=2\pi} \left[\frac{I p^2 \theta}{\left(\frac{p}{p_0}\right)^2 + 1} \cos pt + \frac{I p^2 \theta \frac{p}{p_0}}{\left(\frac{p}{p_0}\right)^2 + 1} \sin pt \right] \theta \sin pt\, dpt$$

$$= \pi \frac{I p^2 \theta^2 \frac{p}{p_0}}{\left(\frac{p}{p_0}\right)^2 + 1} = \pi \rho p \theta^2 \frac{\left(\frac{p}{p_0}\right)^2}{\left(\frac{p}{p_0}\right)^2 + 1}$$

If the angle θ in degrees is θ°, the energy absorbed by the damper torque may be written

$$K = 2 \left(\frac{\pi^2}{180} \right)^2 \rho n (\theta^\circ)^2 \frac{\left(\frac{p}{p_0}\right)^2}{\left(\frac{p}{p_0}\right)^2 + 1} = \frac{\rho n (\theta^\circ)^2}{166.3089} \frac{\left(\frac{p}{p_0}\right)^2}{\left(\frac{p}{p_0}\right)^2 + 1}$$

If these expressions for K are compared with the expressions for energy loss due to a marine propeller,[5] it will be noted that the expressions for the energy absorbed by the untuned viscous damper are the same as those for a marine propeller multiplied by the factor

$$\frac{\left(\frac{p}{p_0}\right)^2}{\left(\frac{p}{p_0}\right)^2 + 1}$$

Fig. 3 illustrates the type of resonance curves that are obtained for a system with an untuned viscous damper. The curves for the hub amplitude are for 10 different values of the damping factor from zero to infinity. The dotted line is the locus of the maximum amplitudes. The fixed point of the curves occurs at 682.3 rpm which gives an optimum damping factor of 31,600 lb-in. sec/radian and the maximum amplitude at optimum damping of 0.1049 deg.

These curves also illustrate that the damping factor can be considerably different than the optimum value without increasing the maximum amplitude very much. For example, as shown in Fig. 4, any damping factor between 21,000 and 48,000 will hold the maximum amplitude to less than 0.1154 deg which is only 10 per cent larger than the value at optimum damping.

Instead of computing complete resonance curves as was done for Fig. 3, the calculations may be made directly for the locus of the maximum amplitudes. For example, if curves of I_{eq} and m_{eq} are plotted from the results of calculations at several frequencies, values from these curves may be used to compute the maximum amplitudes and the corresponding damping factors.

[5] Reference 2, pp. 154 and 163.

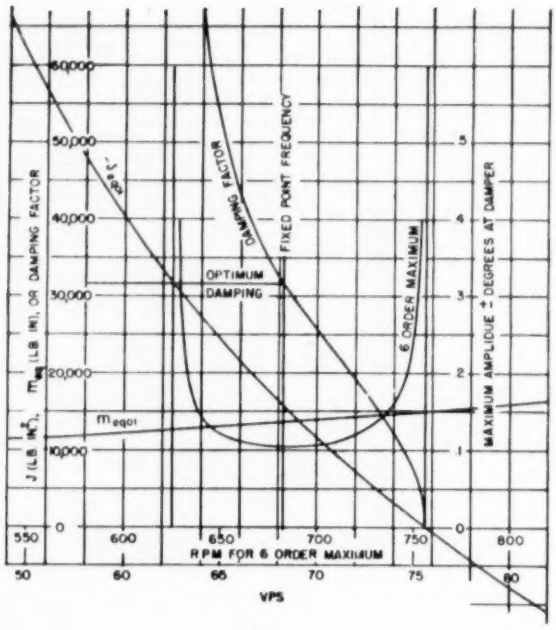

FIG. 4

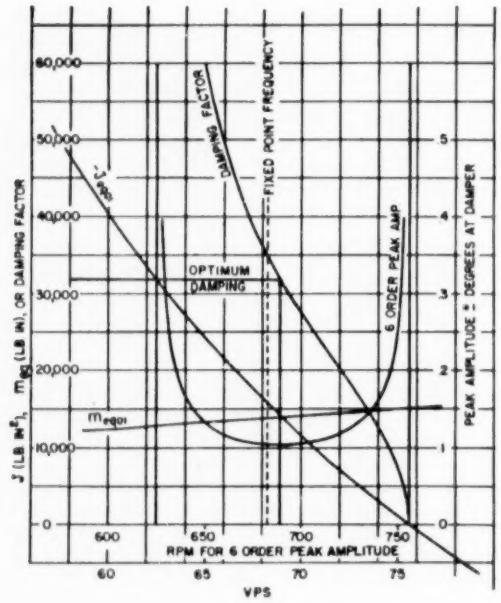

FIG. 5

The results of such calculations are shown in Fig. 4 where the symbol J indicates inertia factor in lb-in.^{2} which was used in the calculations instead of I. In this case $I = J/g$ where $g = 386.088$ in/sec^2 is the standard acceleration due to gravity.

Fig. 6 shows the results of similar calculations for different values of the damper flywheel-inertia factor. The effective action of the damper in reducing the amplitude of the hub for optimum damping is seen to be approximately inversely proportional to the damper flywheel-inertia factor.

Another way to evaluate the effect of the untuned viscous damper is as follows:

The general expression for θ in the form that it was first given shows that its maximum values occur near the frequencies that make the second term under the radical equal to zero, or

$$\frac{I_{eq}}{I} + \frac{1}{\left(\frac{p}{p_0}\right)^2 + 1} = 0$$

These near-maximum values are defined as peak amplitudes and will be denoted by Θ. If, as previously specified

$$I_{FW}' = \frac{I}{\left(\frac{p}{p_0}\right)^2 + 1} = \frac{I}{\left(\frac{n}{n_0}\right)^2 + 1} = \frac{I}{\left(\frac{Ip}{\rho}\right)^2 + 1}$$

then the natural frequencies of the system with I_{eq} increased by I_{FW}' are the frequencies of the peak amplitudes of the hub. The expression for Θ may be written

$$\Theta = \frac{m_{eq}}{\frac{p}{Ip^2 \frac{p_0}{\left(\frac{p}{p_0}\right)^2 + 1}}} = \frac{I^2p^2 + \rho^2}{I^2p^3\rho} m_{eq}$$

where ρ and p are connected by the relation

$$\rho = \frac{Ip}{\sqrt{\frac{I}{-I_{eq}} - 1}}$$

If this relation is used to eliminate ρ from the expression for Θ then

$$\Theta = \frac{m_{eq}}{-I_{eq}\, p^2 \sqrt{\frac{I}{-I_{eq}} - 1}}$$

It will be noted that Θ is the value of the hub amplitude that is obtained at the natural frequency of the system with I_{eq} increased by I_{FW}' when the energy input from the applied torques is equated to the energy absorbed by the damper.

The damping factor for the minimum Θ is a close approximation to its optimum value for the usual sizes of viscous dampers. Using $x = I_{eq}/I$ as was done before

$$\Theta = \frac{m_{eq}}{Ip^2\sqrt{-x(x+1)}}$$

The minimum of this occurs when $-p^4x(x+1)/m_{eq}^2$ is a maximum. Taking the derivative with respect to p and equating to zero gives the following equation

$$4x(x+1) + p\left[(2x+1)\frac{dx}{dp} - 2x(x+1)\frac{dm_{eq}}{m_{eq}dp}\right] = 0$$

If the resulting value of p is substituted into the relation connecting ρ and p, namely, $\rho = Ip\sqrt{\frac{-x}{x+1}}$, the value for the optimum damping factor as defined in this case is obtained.

The results shown in Fig. 5 were calculated as just described for the same vibrating system as that for Fig. 4. The optimum damping factor in either case was practically the same, namely, 31,900 for Fig. 5 and 31,600 for Fig. 4.

If the method to obtain the results in Fig. 5 is used to evalu-

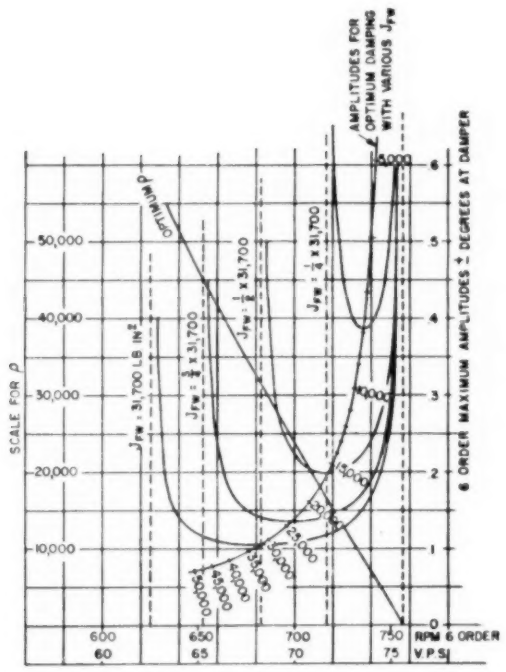

FIG. 6

ate the effect of the damper, it should be recognized that the peak amplitudes are near-maximum values that occur at frequencies slightly higher than those of the maximum amplitudes, and that the damping-factor curve is plotted on the frequencies of these near-maximum values. Therefore, when using such results as shown in Fig. 5, to evaluate the damping factor corresponding to test results from an actual installation, allowance should be made for the difference in the frequencies of the peak amplitudes and the maximum amplitudes of the resonance curves. This difference for the case of Fig. 5 is about 1.0 per cent of the frequency near the values for optimum damping.

Flexible Coupling With Nonlinear Elasticity

An approximate solution for the undamped vibration of a system which includes a flexible coupling having nonlinear elasticity will now be described.

The system may be reduced to two equivalent masses and an equivalent harmonic torque acting on one of the masses which are connected by the coupling as shown in Fig. 7.

If the coupling elasticity is designated as the kth step of the system, the inertia factors in Fig. 7 are

$$I_1 = I_{ek}', \quad I_2 = I_{lk}''$$

also

$$\theta_1 = \theta_k, \quad \theta_2 = \theta_{k+1}$$

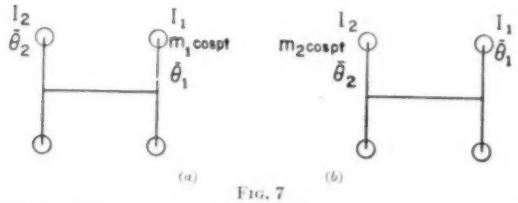

FIG. 7

and

$$m_1 = m_{eqk}', \quad m_2 = m_{eqk+1}''$$

Fig. 7(a) is the result of the reduction if the coupling is located at some section between the last applied torque and the end mass, and Fig. 7(b) is the result if the coupling is located between the first mass and the first applied torque.

If Q is the torque in the coupling due to $\bar{\theta}_2 - \bar{\theta}_1$, the two differential equations of motion for the case in Fig. 7(a) are

$$I_1 \frac{d^2\bar{\theta}_1}{dt^2} - Q = m_1 \cos pt$$

$$I_2 \frac{d^2\bar{\theta}_2}{dt^2} + Q = 0$$

An approximate solution may be made if Q is replaced by its first harmonic for an assumed simple harmonic variation of $\bar{\theta}_2 - \bar{\theta}_1$. Let this first harmonic of Q be $a \cos pt$ for

$$\bar{\theta}_1 = \theta_1 \cos pt$$

$$\bar{\theta}_2 = \theta_2 \cos pt$$

The sum of the two differential equations gives

$$-I_1 p^2 \theta_1 - I_2 p^2 \theta_2 = m_1$$

$$\theta_2 = -\frac{I_1}{I_2}\theta_1 - \frac{m_1}{I_2 p^2}$$

$$\theta_2 - \theta_1 = -\left(1 + \frac{I_1}{I_2}\right)\theta_1 - \frac{m_1}{I_2 p^2}$$

or

$$\theta_1 = -\frac{1}{1 + \dfrac{I_1}{I_2}}\left[\theta_2 - \theta_1 + \frac{m_1}{I_2 p^2}\right]$$

Replacing Q in the first differential equation by $a \cos pt$ gives

$$-I_1 p^2 \theta_1 - a = m_1$$

or

$$a = \frac{I_1 p^2}{1 + \dfrac{I_1}{I_2}}(\theta_2 - \theta_1) - \frac{m_1}{1 + \dfrac{I_1}{I_2}}$$

Similarly, the two differential equations of motion for the case of Fig. 7(b) are

$$I_1 \frac{d^2\bar{\theta}_1}{dt^2} - Q = 0$$

$$I_2 \frac{d^2\bar{\theta}_2}{dt^2} + Q = m_2 \cos pt$$

The sum after putting $\bar{\theta}_1 = \theta_1 \cos pt$ and $\bar{\theta}_2 = \theta_2 \cos pt$ gives

$$-I_1 p^2 \theta_1 - I_2 p^2 \theta_2 = m_2$$

$$\theta_1 = -\frac{I_2}{I_1}\theta_2 - \frac{m_2}{I_1 p^2}$$

$$\theta_2 - \theta_1 = \left(1 + \frac{I_2}{I_1}\right)\theta_2 + \frac{m_2}{I_1 p^2}$$

or

$$\theta_2 = \frac{1}{1 + \dfrac{I_2}{I_1}}\left[\theta_2 - \theta_1 - \frac{m_2}{I_1 p^2}\right]$$

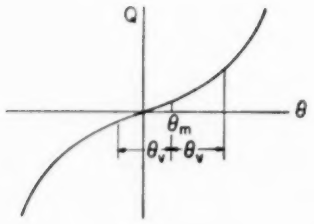

FIG. 8

Replacing Q in the second differential equation by $a \cos pt$ gives

$$-I_2 p^2 \theta_2 + a = m_2$$

or

$$a = \frac{I_2 p^2}{1 + \frac{I_2}{I_1}} (\theta_2 - \theta_1) + \frac{m_2}{1 + \frac{I_2}{I_1}}$$

A typical torque-deflection curve for the Falk-Bibby type coupling is shown in Fig. 8. The curve $Q = f(\theta)$ is an odd function such that $f(\theta) = -f(-\theta)$ and is assumed continuous at $\theta = 0$. If the variation of the deflection between the hubs is a simple harmonic

$$\theta = \theta_m + \theta_v \cos pt$$

where

θ_m = mean deflection between hubs, radians
θ_v = amplitude of harmonic variation of deflection between hubs, radians
$Q = f(\theta_m + \theta_v \cos pt) = \phi(pt)$

This curve has the characteristic that $\phi(pt) = \phi(2\pi - pt)$ so that it may be expanded into a cosine series.

The manufacturer of these couplings offers many sizes for engineering uses and each size has its own torque-deflection curve. However, by approximate curve fitting, the writer has found two formulas which give very close agreement with the manufacturer's published torque-deflection curves for all sizes of these couplings. Formula [1] applies to the coupling sizes 3 to 18, and Formula [2] applies to the coupling sizes 190 to 310 and 3310 to 3360. These formulas are dependent on two parameters, A and B, which have particular values for each coupling.

Formula [1] for Falk Steelflex Couplings—Sizes 3 to 18. Torque, deflection, and stiffness relations are as follows:

Q = torque, lb-in.

θ° = deflection between hubs, deg

$C = \frac{dQ}{d\theta}$ = stiffness factor, lb-in/radian for small variation of Q

A and B = parameters from Table 4.

$$A\theta^\circ = \frac{BQ}{118 + 0.61\,|BQ| + \frac{(BQ)^2}{1520}}$$

$$BQ = \frac{\theta^\circ}{|\theta^\circ|}\left[\left(\frac{760}{|A\theta^\circ|} - 463.6\right) - \sqrt{\left(\frac{760}{|A\theta^\circ|} - 463.6\right)^2 - 179360}\right]$$

$$C = \frac{180}{\pi}\frac{A}{B}\frac{\left[118 + 0.61|BQ| + \frac{(BQ)^2}{1520}\right]^2}{118 - \frac{(BQ)^2}{1520}}$$

FORMULA [1] TABULAR FORM FOR CALCULATING C

1	2	3	4	5	6	7	8
BQ	$\frac{(BQ)^2}{1520}$	118 + (2)	118 − (2)	0.61 BQ	(3) + (5)	$\frac{(6)^2}{(4)}$	$\frac{180}{\pi}\frac{A}{B}$ (7) $= C$

Formula [2] for Falk Steelflex Couplings—Sizes 190 to 310 and 3310 to 3360. Torque, deflection, and stiffness relations are as follows:

A and B = parameters from Table 5

$$A\theta^\circ = \frac{BQ}{74 + |BQ|}$$

$$BQ = \frac{74\,A\theta^\circ}{1 - |A\theta^\circ|}$$

$$C = \frac{180}{\pi}\frac{A}{B}\frac{(74 + |BQ|)^2}{74} = 0.7743\,\frac{A}{B}(74 + |BQ|)^2$$

FORMULA [2] TABULAR FORM FOR CALCULATING C

1	2	3	4
BQ	74 + BQ	(2)^2	$0.7743\frac{A}{B}$ (3) $= C$

If the mean torque Q varies as the square of the RPM as in the case of a marine propeller or centrifugal pump

$$Q = Q_f\left(\frac{\text{RPM}}{\text{RPM}_f}\right)^2, \quad Q_f = 63025\,\frac{\text{HP}_f}{\text{RPM}_f}$$

where the subscript f refers to full speed and power. Also, if σ is order number at engine speed of a vibration with frequency of n VPS, engine RPM $= \frac{60n}{\sigma}$. Thus, if the coupling turns at engine speed, the torque across the coupling is

$$Q = Q_f\,\frac{3600}{\sigma^2(\text{RPM}_f)^2}\,n^2 = \frac{35207\,Q_f}{\sigma^2(\text{RPM}_f)^2}\,\frac{p^2}{g}$$

If the coupling turns at any other speed, the torque across the coupling is the foregoing times the speed ratio of engine to coupling, where σ remains the order number at engine speed.

The mean value and first harmonic of the curve $BQ = f(A\theta^\circ)$ may be calculated for any assigned pair of values for $A\theta_m^\circ$ and $A\theta_v^\circ$ where

$A\theta^\circ = A\theta_m^\circ + A\theta_v^\circ \cos pt$
θ_m° = mean deflection between hubs, deg
θ_v° = amplitude of harmonic variation of deflection between hubs, deg

The results of such calculations for a number of pairs of values are summarized in Tables 6 and 7 for Formulas [1] and [2]. Curves of these values may be plotted and then replotted to obtain the sets of curves in Figs. 9 and 10, which are in a form that may be used in torsional vibration calculations.

For small values of $A\theta_v^\circ$ the first harmonic of BQ may be written

$$Ba = \frac{\pi}{180}\frac{BC}{A}A\theta_v^\circ \quad \text{or} \quad a = \frac{\pi}{180}C\theta_v^\circ = C\theta_v$$

where for Formula [1], if mean BQ is BQ_m

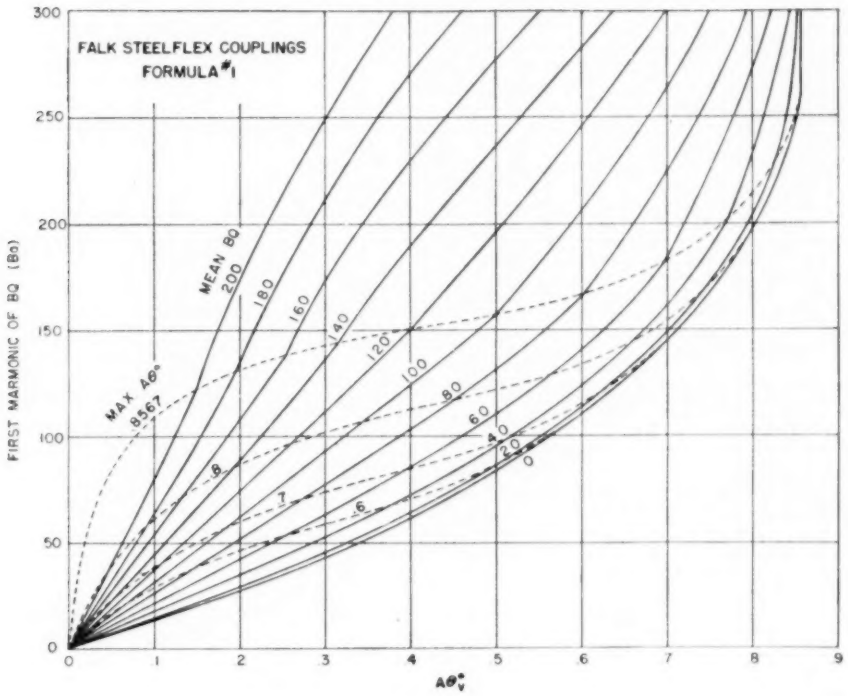
FALK STEELFLEX COUPLINGS
FORMULA #1
FIRST HARMONIC OF BQ (Bs)
MEAN BQ
200
180
160
140
120
100
80
60
40
20
0
MAX Aθ°
8567
8
7
6
Aθ°v

FIG. 9

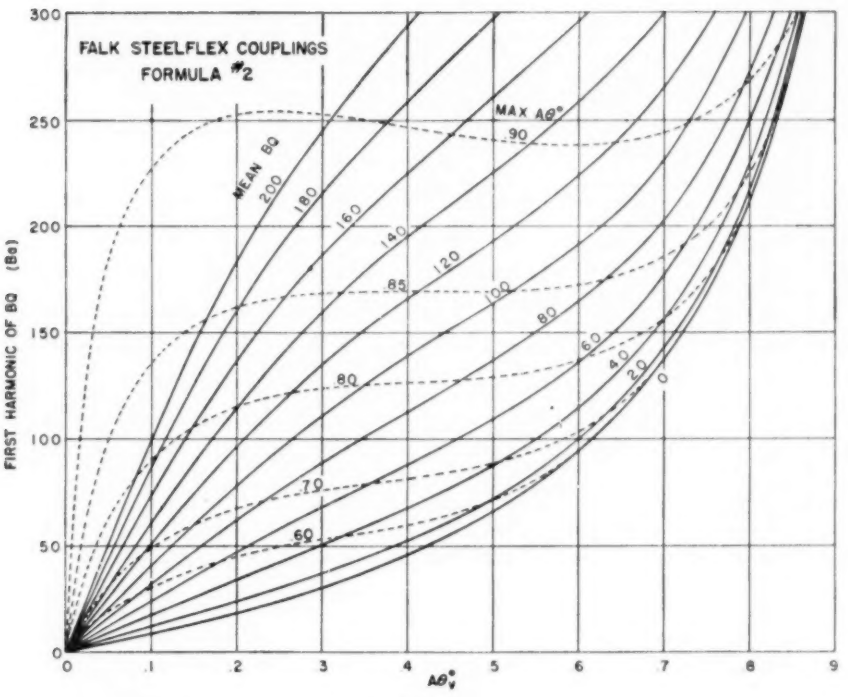
FALK STEELFLEX COUPLINGS
FORMULA #2
FIRST HARMONIC OF BQ (Bs)
MAX Aθ°
90
85
80
79
60
MEAN BQ
200
180
160
140
120
100
80
60
40
20
0
Aθ°v

FIG. 10

TABLE 4 FORMULA [1] FOR FALK STEELFLEX COUPLINGS 3 TO 18: FACTORS FOR TORQUE, DEFLECTION, AND STIFFNESS RELATIONS

COUPLING				MAX. TORQUE	MAX BORE	A	$\frac{I}{B}$	$\frac{A}{B}$	$\frac{180}{\pi}\frac{A}{B}$	MAX. RATING	
SIZE	OFFSET	RADIUS	GAP	LB. IN.	IN.					BQ	$A\theta^\circ$
3			1/8	252	1	.850	.87	.7395	42.37	289.7	.8279
4			"	567	1 1/4	.440	2.50	1.1	63.03	226.8	.7816
5			"	945	1 7/16	.500	4.40	2.2	126.05	214.8	.7688
6			"	1260	1 5/8	.575	6.15	3.53625	202.6	204.9	.7572
7			"	2433	1 7/8	.680	11.2	7.616	436.4	217.2	.7715
8			"	5040	2 3/8	.450	25.6	11.52	660.0	196.9	.7469
9			"	7560	2 5/8	.500	34.5	17.25	988.4	219.1	.7736
10	1/8*	16 1/2	3/16	10080	2 7/8	.575	44.4	25.53	1462.8	227.0	.7818
"	1/4	16 1/2	"	"	"	.430	44.4	19.092	1093.9	"	"
"	7/16	16 1/2	"	"	"	.342	44.4	15.1848	870.0	"	"
11	1/8*	16 1/2	"	14500	3 1/4	.620	64	39.68	2273.5	226.6	.7813
"	1/4	16 1/2	"	"	"	.465	64	29.76	1705.1	"	"
"	7/16	16 1/2	"	"	"	.370	64	23.68	1356.8	"	"
12	1/8	16 1/2	"	22050	3 1/2	.680	100	68	3896	220.5	.7751
"	1/4*	16 1/2	"	"	"	.510	100	51	2922	"	"
"	7/16	16 1/2	"	"	"	.405	100	40.5	2320	"	"
13	1/8	16 1/2	"	30240	4	.775	120	93	5329	252.0	.8038
"	3/4	33	"	"	"	.775	120	93	5329	"	"
"	7/8	33	"	"	"	.710	120	85.2	4882	"	"
"	1/4*	16 1/2	"	"	"	.656	120	78.72	4510	"	"
"	7/16	16 1/2	"	"	"	.522	120	62.64	3589	"	"
14	1/4	33	1/4	44100	4 3/8	.875	160	140	8021	275.6	.8200
"	5/8*	33	"	"	"	.625	160	100	5730	"	"
"	1	33	"	"	"	.484	160	77.44	4437	"	"
15	1/4	33	"	63000	4 5/8	.896	230	206.08	11808	273.9	.8190
"	5/8*	33	"	"	"	.640	230	147.2	8434	"	"
"	1	33	"	"	"	.496	230	114.08	6536	"	"
16	1/4	33	"	88200	5 1/2	1.050	325	341.25	19552	271.4	.8174
"	5/8*	33	"	"	"	.750	325	243.75	13966	"	"
"	1	33	"	"	"	.581	325	188.825	10819	"	"
17	1/4	33	"	113400	6	1.190	415	493.85	28300	273.3	.8186
"	5/8*	33	"	"	"	.850	415	352.75	20210	"	"
"	1	33	"	"	"	.659	415	273.485	15670	"	"
18	1/4	33	"	144900	7	1.358	520	706.16	40460	278.7	.8218
"	5/8*	33	"	"	"	.970	520	504.4	28900	"	"
"	1	33	"	"	"	.752	520	391.04	22400	"	"

* Standard.

TABLE 5 FORMULA [2] FOR FALK STEELFLEX COUPLINGS 190 TO 310 AND 3310 TO 3360; FACTORS FOR TORQUE, DEFLECTION, AND STIFFNESS RELATIONS

COUPLING				MAX. TORQUE LB. IN.	MAX. BORE IN.	A	$\frac{I}{B}$	$\frac{A}{B}$	$\frac{.7743\,A}{B}$	MAX. RATING	
SIZE	OFFSET	RADIUS	GAP							BQ	$A\theta^\circ$.
190	7/16	33	1/4	208,000	8	.88	690	607.2	470.2	301.4	.8029
200	5/8	33	"	315,000	8 3/4	1.00	1000	1000	774.3	315.0	.8098
"	1 13/16	70*	"	"	"	1.07	1000	1070	828.5	315.0	.8098
210	7/16	33	"	425,250	9 1/4	1.18	1340	1581.2	1224.3	317.4	.8109
220	5/8	33	"	551,250	10	1.20	1780	2136	1653.9	309.7	.8071
"	1 13/16	70*	"	"	"	1.28	1780	2278.4	1764.2	309.7	.8071
230	1 13/16	70	"	693,000	11	1.45	2220	3219	2492	312.2	.8084
240	1 1/2	70	1/2	945,000	12	.80	5250	4200	3252	180.00	.7087
250	1 1/2	70	"	1,386,000	13 1/2	.94	7500	7050	5459	184.80	.7141
260	1 1/2	70	"	2,142,000	14 3/4	1.05	11500	12075	9350	186.26	.7157
270	1 1/2	70	"	2,835,000	16	1.23	15500	19065	14762	182.90	.7120
280	1 1/2	70	"	3,780,000	17 1/2	1.32	21500	28380	21970	175.81	.7038
290	1 1/2	70	"	4,725,000	19	1.495	24200	36179	28014	195.25	.7252
300	5/8	70	"	5,670,000	20 1/2	2.56	30500	78080	60460	185.90	.7153
310	5/8	70	"	8,190,000		3.15	43000	135,450	104,880	190.47	.7202
3310				8,190,000		.60	494,000	296,400	229,500	16.579	.18303
3320				11,340,000		.80	500,000	400,000	309,700	22.680	.2346
3330				16,380,000		1.00	700,000	700,000	542,000	23.400	.2402
3340				22,650,000		1.00	1,200,000	1,200,000	929,200	18.875	.2032
3350				32,760,000		1.20	1,680,000	2,016,000	1,561,000	19.500	.2086
3360				45,360,000		1.60	1,960,000	3,136,000	2,428,000	23.143	.2382

* Standard.

$$\frac{\pi}{180}\frac{BC}{A} = \frac{\left[118 + 0.61\,BQ_m + \frac{(BQ_m)^2}{1520}\right]^2}{118 - \frac{(BQ_m)^2}{1520}}$$

and for Formula [2]

$$\frac{\pi}{180}\frac{BC}{A} = \frac{(74 + BQ_m)^2}{74}$$

FOR SYSTEM CORRESPONDING TO FIG. 7(*a*)

When the coupling occurs in the system beyond the last applied torque, the expression for a, the first harmonic of Q, from the solution of the differential equations of motion is

$$a = \frac{I_1 p^2}{1 + \frac{I_1}{I_2}}(\theta_2 - \theta_1) - \frac{m_1}{1 + \frac{I_1}{I_2}}$$

If $\theta_s^\circ = \theta_2^\circ - \theta_1^\circ$ in degrees, Ba may be written as

$$Ba = \frac{B}{A}\frac{\frac{\pi}{180}I_1 p^2}{1 + \frac{I_1}{I_2}}A\theta_s^\circ - \frac{Bm_1}{1 + \frac{I_1}{I_2}}$$

and

$$\theta_1^\circ = -\frac{1}{1 + \frac{I_1}{I_2}}\left[\theta_s^\circ + \frac{m_1}{\frac{\pi}{180}I_2 p^2}\right]$$

$$\theta_2^\circ = \theta_s^\circ + \theta_1^\circ$$

If this expression for Ba, which is a straight line, is plotted on the coupling curves, Fig. 9 or 10, roots for $A\theta_s$ are the intersections of this line and the curve for the required mean BQ due to the transmitted torque of the engine.

For small values of $A\theta_s^\circ$ the solution is linear and may be written in the following form

$$A\theta_s^\circ = \frac{Bm_1}{1 + \frac{I_1}{I_2}}\Bigg/\left[\frac{B}{A}\frac{\frac{\pi}{180}I_1 p^2}{1 + \frac{I_1}{I_2}} - \frac{\pi}{180}\frac{BC}{A}\right]$$

TABLE 6 FORMULA [1] FOR FALK STEELFLEX COUPLINGS 3 TO 18; SUMMARY OF MEAN *BQ* AND FIRST HARMONIC OF *BQ* FOR HARMONICALLY VARYING DEFLECTION BETWEEN HUBS

$A\theta_v°$	$A\theta_m°$	MEAN BQ	FIRST HARMONIC	$A\theta_v°$	$A\theta_m°$	MEAN BQ	FIRST HARMONIC	$A\theta_v°$	$A\theta_m°$	MEAN BQ	FIRST HARMONIC
.1	0	0	12.46	.3	0	0	42.29	.5	.35672	100.30	156.54
	.1	13.05	13.37		.1	15.72	44.02	.6	0	0	109.29
	.2	27.58	15.58		.2	32.52	49.36		.05	12.16	110.47
	.3	44.61	18.38		.3	51.81	58.88		.1	24.76	114.39
	.4	65.02	22.33		.4	75.96	73.88		.15	38.41	121.61
	.5	90.46	28.32		.5	110.58	102.25		.2	54.17	133.76
	.6	124.11	38.50		.55672	145.06	142.76		.25672	81.16	165.85
	.7	174.80	61.34	.4	0	0	60.66	.7	0	0	144.28
	.75672	230.75	109.08		.1	17.73	62.96		.025	7.75	144.86
.2	0	0	26.42		.2	36.49	69.63		.05	15.65	146.67
	.1	14.19	27.77		.3	59.31	84.44		.1	32.63	154.80
	.2	29.43	31.69		.4	89.73	111.67		.15672	59.88	182.01
	.3	47.14	37.63		.45672	120.30	150.44	.8	0	0	197.05
	.4	68.61	46.32	.5	0	0	82.44		.025	12.08	199.11
	.5	96.59	59.80		.1	20.54	85.73		.05	25.82	207.06
	.6	136.68	86.52		.2	43.20	96.59		.05672	31.38	213.17
	.65672	178.55	130.86		.3	72.21	120.76	.85672	0	0	260.26

Resonance curves for the torsional vibration of the system may be calculated as follows: Designating the coupling elasticity as the kth step of the system, compute the following values for several assumed values of frequency

$$J_{0k}' = J_1, \quad J_{1k}'' = J_2, \quad m_{eqk}' = m_1$$

where J is the inertia factors in lb-in.^{2} $\left(I = \frac{J}{g}\right)$

Then, for the same frequencies, compute the values indicated in the following tabular form:

(a)	(b)	(c)	(d)	(e)	(f)
$\frac{\pi}{180} J_{0k}' \frac{p^2}{g}$	$\frac{\pi}{180} J_{1k}'' \frac{p^2}{g}$	$1 + \frac{J_{0k}'}{J_{1k}''}$	$\frac{\frac{B}{A}(a)}{(c)}$	$\frac{Bm_{eqk}'}{(c)}$	$\frac{m_{eqk}'}{(b)}$

Plot the straight line $y = (d)\ A\theta_v° - (e)$ on the coupling curves for *Ba* (Fig. 9 or 10) and determine $A\theta_v°$ for the required mean *BQ*. Since the coupling torque may be either plus or minus and Fig. 9 or 10 is only plotted in the first quadrant, negative roots for $A\theta_v°$ may be obtained in the first quadrant also by plotting the straight line $y = (d)A\theta_v° + (e)$.

The remainder of the calculation for the amplitude of vibration at each hub of the coupling and the torque across the coupling may be carried out as follows:

(g)	(h)	(i)	(j)	(k)	(l)	(m)
$A\theta_v°$ roots from curves	$\frac{\theta_{1k}° - \theta_{0k}°}{(g)}$	$(h) + (f) - \frac{(i)}{(c)}$	$\theta_{0k}°$	$\theta_{1k}°$	a	C_k
	A		$(h) + (j)$	$(b)\,(k)$	$\frac{57.296\,(l)}{(h)}$	

These results are sufficient to determine the amplitude and torque at any section of the system.

FOR SYSTEM CORRESPONDING TO FIG. 7(*b*)

When the coupling occurs in the system ahead of the first applied torque, the expression for *Ba* from the requirements of the system may be written as

$$Ba = \frac{B}{A} \frac{\frac{\pi}{180} I_2 p^2}{1 + \frac{I_2}{I_1}} A\theta_v° + \frac{Bm_2}{1 + \frac{I_2}{I_1}}$$

and

$$\theta_2° = \frac{1}{1 + \frac{I_2}{I_1}} \left[\theta_v° - \frac{m_2}{\frac{\pi}{180} I_1 p^2} \right]$$

$$\theta_1° = \theta_2° - \theta_v°$$

If this expression for *Ba*, which is a straight line, is plotted on the coupling curves, Fig. 9 or 10, roots for $A\theta_v°$ are the intersections of this line and the curves for the required mean *BQ* due to the transmitted torque of the engine.

TABLE 7 FORMULA [2] FOR FALK STEELFLEX COUPLINGS 190 TO 310 AND 3310 TO 3360; SUMMARY OF MEAN *BQ* AND FIRST HARMONIC OF *BQ* FOR HARMONICALLY VARYING DEFLECTION BETWEEN HUBS

$A\theta_v^\circ$	$A\theta_m^\circ$	MEAN BQ	FIRST HARMONIC
.025	.475	67.11	6.72
	.575	100.42	10.27
	.625	123.77	13.20
	.675	154.37	17.59
	.725	196.21	24.62
	.775	256.94	36.88
	.825	353.24	61.35
	.850	426.33	83.98
	.875	530.21	122.08
.05	.35	40.18	8.80
	.45	61.10	12.31
	.55	91.47	18.44
	.6	112.46	23.40
	.65	139.62	30.67
	.7	176.17	41.99
	.75	228.10	61.04
	.8	308.13	97.08
	.825	367.25	128.76
	.85	449.26	179.55
.1	0	0	8.09
	.1	8.73	9.22
	.2	19.23	11.70
	.3	32.81	15.34
	.4	51.08	20.99
	.5	77.05	30.52
	.55	94.66	37.96
	.6	117.07	48.54
	.65	146.62	64.38
	.7	187.63	89.78
	.75	248.96	134.81
	.775	293.14	172.14
	.8	253.24	228.96
	.85	587.69	505.40
.2	0	0	17.86
	.1	10.07	19.46
	.2	20.95	24.27
.2	.3	36.31	32.19
	.4	56.82	44.89
	.45	70.43	54.38
	.5	87.48	67.41
	.55	109.57	86.07
	.6	139.62	114.48
	.65	183.62	161.70
	.675	214.84	198.78
	.7	256.85	252.70
	.75	419.33	493.33
.3	0	0	29.93
	.1	11.98	32.14
	.2	25.57	39.23
	.3	43.00	52.69
	.35	54.33	62.77
	.4	68.41	76.32
	.45	86.53	95.27
	.5	111.00	125.00
	.55	146.56	168.47
	.575	171.90	203.25
	.6	205.69	252.52
	.65	339.32	469.00
.4	0	0	45.25
	.1	14.72	48.49
	.2	31.75	59.20
	.25	42.13	68.35
	.3	54.64	81.21
	.35	70.39	99.55
	.4	91.42	126.35
	.45	121.87	168.86
	.475	143.99	201.77
	.5	172.67	246.67
	.55	288.80	444.07
.5	0	0	65.50
	.1	18.91	70.59
	.15	29.52	77.45
.5	.2	41.75	88.12
	.25	56.73	104.32
	.3	76.11	128.72
	.35	103.71	168.10
	.375	123.05	197.88
	.4	148.96	239.80
	.45	248.92	414.57
.6	0	0	93.76
	.05	12.53	95.90
	.1	25.94	102.65
	.15	41.31	115.18
	.2	60.42	136.09
	.25	86.69	171.32
	.275	104.77	198.41
	.3	128.77	236.82
	.35	220.48	398.53
.65	0	0	112.68
.7	0	0	135.60
	.05	18.75	140.90
	.1	39.78	155.18
	.15	66.63	184.25
	.175	84.39	208.02
	.2	107.50	242.56
	.25	193.83	390.25
.75	0	0	167.86
.8	0	0	211.13
	.025	16.12	213.55
	.05	33.84	223.18
	.075	53.52	240.30
	.1	77.90	268.07
	.15	162.71	400.01
.85	0	0	275.98
.875	0	0	322.99
.9	0	0	392.05
.95	0	0	647.00

For small values of $A\theta_v{}^\circ$ the solution is linear and may be written in the following form

$$A\theta_v{}^\circ = -\frac{Bm_2}{1+\frac{I_2}{I_1}} \Bigg/ \left[\frac{B}{A}\frac{\frac{\pi}{180}I_2p^2}{1+\frac{I_2}{I_1}} - \frac{\pi}{180}\frac{BC}{A} \right]$$

Resonance curves for the torsional vibration of the system may be calculated as follows: Designating the coupling elasticity as the kth step of the system, compute the following values for several assumed values of frequency

$$J_{1k}'' = J_2, \quad J_{0k}' = J_1, \quad m_{eqk+1}'' = m_2$$

where J is the inertia factors in lb-in.^{2}

Then, for the same frequencies, compute the values indicated in the following tabular form:

(a)	(b)	(c)	(d)	(e)	(f)
$\frac{\pi}{180}J_{1k}''\frac{p^2}{g}$	$\frac{\pi}{180}J_{0k}'\frac{p^2}{g}$	$1+\frac{J_{1k}''}{J_{0k}'}$	$\frac{\frac{B}{A}(a)}{(c)}$	$\frac{Bm_{eqk+1}''}{(c)}$	$\frac{m_{eqk+1}''}{(b)}$

Piston area $A = 122.718$ sq in.
Crank radius $R = 6.5$ in.

$AR = 797.7$ cu in.

Plot the straight line $y = (d)A\theta_v{}^\circ + (e)$ on the coupling curves for Ba (Fig. 9 or 10), and determine $A\theta_v{}^\circ$ for the required mean BQ. Since the coupling torque may be either plus or minus and Fig. 9 or 10 is only plotted in the first quadrant, negative roots for $A\theta_v{}^\circ$ may be obtained also by plotting the straight line $y = (d)A\theta_v{}^\circ - (e)$.

The remainder of the calculations for the amplitude of vibration at each hub of the coupling and the torque across the coupling may be carried out as follows:

(g)	(h)	(i)	(j)	(k)	(l)	(m)
$A\theta_v{}^\circ$ roots from curves	$\frac{\theta_{1k}{}^\circ - \theta_{0k}{}^\circ}{A}$	$(h)-(f)$	$\frac{(i)}{(c)}$	$(j)-(h)$	$-(b)(k)$	$\frac{57.296\,(l)}{(h)}$

These results are sufficient to determine the amplitude and torque at any section of the system.

Numerical Example of System With "Steelflex" Coupling

Fig. 11 shows two forms of the equivalent system of an installation which includes a 210 Steelflex coupling.

Engine data:

Diesel 6-cylinder $12\frac{1}{2} \times 13$, turbocharged, 4-cycle, 810 bhp at 600 rpm

Piston assembly weight = 148.9 lb

Connecting-rod assembly weight = 221.0 lb

Center of gravity at 0.25 × length from crankpin center line

Radius of gyration about center of gravity = 11.84 in.

Crank-to-connecting-rod ratio = 1/4.3077

Firing order 135642

Crankshaft without counterweights with rotating weight per crank = 175.1 lb at crank radius

One of the important phases of amplitude calculations is the selection of representative applied torques. The general expression[6] for the torque curve occurring at each crank of an engine may be written as follows:

Torque/AR at one crank for uniform rotation = torque/AR due to gas pressure

[6] "Harmonic Coefficients of Engine Torque Curves," by F. P. Porter, *Journal of Applied Mechanics*, Trans. ASME, vol. 65, 1943, p. A-33.

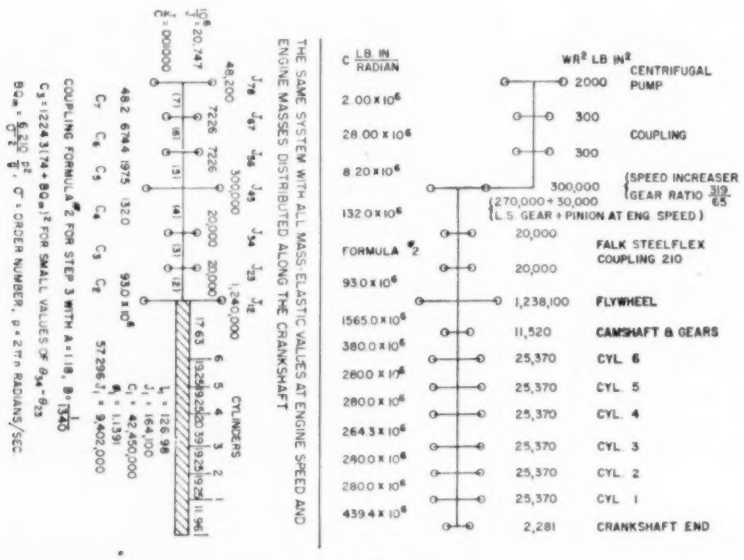
THE SAME SYSTEM WITH ALL MASS-ELASTIC VALUES AT ENGINE SPEED AND ENGINE MASSES DISTRIBUTED ALONG THE CRANKSHAFT
C LB. IN / RADIAN
WR² LB IN²
CENTRIFUGAL PUMP
COUPLING
SPEED INCREASER
GEAR RATIO 319/65
L.S. GEAR + PINION AT ENG. SPEED
FORMULA #2
FALK STEELFLEX COUPLING 210
FLYWHEEL
CAMSHAFT & GEARS
CYL. 6
CYL. 5
CYL. 4
CYL. 3
CYL. 2
CYL. 1
CRANKSHAFT END
CYLINDERS
COUPLING FORMULA #2 FOR STEP 3 WITH A = 1.18, B = 1/320
C₃ = 1224.3 (74 + BQ₃)² FOR SMALL VALUES OF θ₂₃ - θ₂₃
BQ₃ = C₃/74 p²/g, C = ORDER NUMBER, p = 2πn RADIANS/SEC

Fig. 11

$$+ \frac{W_r R}{\sigma^2 A} \frac{p^2}{g} F_a + \frac{W_d(h_1 h_2 - H^2)}{\sigma^2 AR} \frac{p^2}{g} F_c + \frac{W_r}{A} F_b \cos \psi + \frac{W_u U}{AR} \sin (\alpha + \alpha_u + \psi)$$

where

A = piston areas
R = crank radius
h_1 = center of mass of rod to center of crankpin
h_2 = center of mass of rod to center of piston pin
H = radius of gyration of rod about its center of mass
l = length of rod
k = crank-to-connecting-rod ratio
W_d = weight of connecting-rod assembly
W_r = reciprocating weight including $\frac{h_1}{l} W_d$
W_u = weight of unbalanced rotating parts at crank including $\frac{h_2}{l} W_d$ at crankpin center line
U = radius from shaft axis to center of mass of W_u
α = crank angle from piston position furthest from crankshaft
α_u = angle from crank arm to U in direction of rotation
ψ = inclination of cylinder center line from vertical in direction of rotation
σ = order of vibration
F_a, F_b, F_c = functions of k and α. Harmonic coefficients for these functions are given elsewhere.[6]

For practical purposes the harmonic coefficients of the torque due to the reciprocating and rotating masses for uniform rotation are insignificant above the 4 order, so that the harmonic components of the torque for all orders except 1, 2, 3, and 4 may be taken as the values due to gas pressure alone.

The harmonic torque/AR values for orders 1, 2, 3, 4 are obtained by adding the following quantities to the components due to gas pressure:

1 order

(Sine component) $$\frac{W_r R}{A} \frac{p^2}{g} F_a + \frac{W_r}{A} \cos \psi + \frac{W_u U}{AR} \cos (\alpha_u + \psi)$$

(Cosine component)

$$\frac{W_u U}{AR} \sin (\alpha_u + \psi)$$

2 order (sine component)

$$\frac{W_r R}{4A} \frac{p^2}{g} F_a + \frac{W_d(h_1 h_2 - H^2)}{4AR} \frac{p^2}{g} F_c + \frac{W_r}{A} F_b \cos \psi$$

3 order (sine component)

$$\frac{W_r R}{9A} \frac{p^2}{g} F_a$$

4 order (sine component)

$$\frac{W_r R}{16A} \frac{p^2}{g} F_a + \frac{W_d(h_1 h_2 - H^2)}{16AR} \frac{p^2}{g} F_c + \frac{W_r}{A} F_b \cos \psi$$

where the harmonic coefficients for the specified orders are used for the F-functions.

Calculations for the undamped resonance curves for the 3 order or first major vibration will be described. The torque/AR values due to gas pressure were taken from Set Q2 of the reference mentioned.[6] The sine and cosine harmonic coefficients for the 3 order of this set by approximate curve fitting may be written as

(Sine) $m_a = 0.105 \text{ MIP} + 17.15$
(Cosine) $m_b = -0.055 \text{ MIP} + 0.50$

The MIP at any power may be written

$$\text{MIP} = \text{MIP} - \text{MEP} + \text{MEP}$$

If it is assumed that MIP — MEP is constant for any power, and that the power required by the centrifugal pump is such that

$$\text{MEP} = \text{MEP}_f \left(\frac{\text{RPM}}{\text{RPM}_f}\right)^2$$

where the subscript f indicates full-speed values

$$\text{MIP} = \text{MIP}_f - \text{MEP}_f + \text{MEP}_f \left(\frac{\text{RPM}}{\text{RPM}_f}\right)^2$$

$$= \text{MIP}_f - \text{MEP}_f + \frac{35207 \text{ MEP}_f}{\sigma^2 (\text{RPM}_f)^2} \frac{p^2}{g}$$

If the mechanical efficiency of the engine is taken as 80 per cent, the expression for MIP at any frequency for the 3 order may be written

$$\text{MIP} = 27.925 + 1.2138 \frac{p^2}{g}$$

so that the 3 order torque/AR values due to pressure become

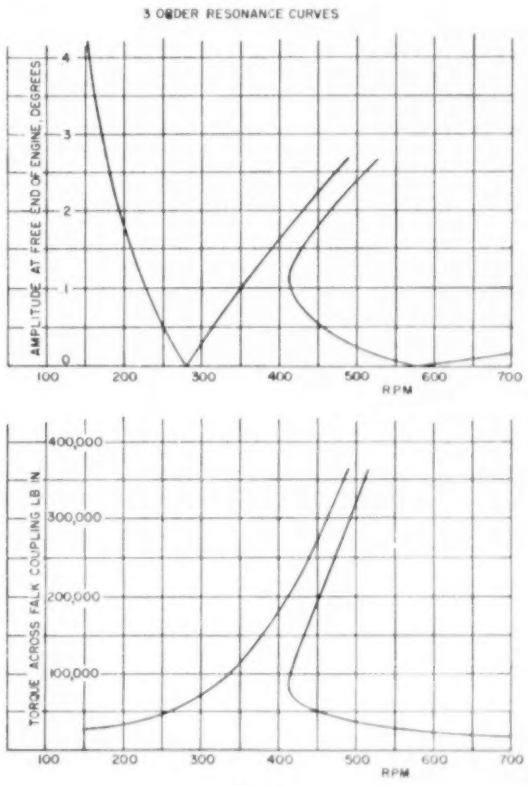

FIG. 12

TABLE 8 3 ORDER FORCED-VIBRATION CALCULATION—NONLINEAR C_1

1	2	3	4	5	6	7	8	9	10	11	12	13
n	$\frac{P^2}{\gamma}$ .102252 n^2	.001000 ×(2)	1-(3)	$J''_{07}\times10^{-6}$ .04820 / (4)	$J''_{26}\times10^{-6}$ (5)+ .007226	(6)(2) / 674.4	1-(7)	$J''_{06}\times10^{-6}$ (6) / (8)	$J''_{25}\times10^{-6}$ (8)+ .007226	(10)(2) / 197.5	1-(11)	$J''_{05}\times10^{-6}$ (10) / (12)
19	36.913	.03691	.96309	.050047	.057273	.00313	.99687	.057453	.064679	.01209	.98791	.065471
22	49.490	.04949	.95051	.050710	.057936	.00425	.99575	.058183	.065409	.01639	.98361	.066499
1	14	15	16	17	18	19	20	21	22	23	24	25
n	$J''_{24}\times10^{-6}$ (13)+ .30000	(14)(2) / 132.0	1-(15)	$J''_{04}\times10^{-6}$ (14) / (16)	$J''_{23}\times10^{-6}$ (17)+ .02000	$\phi_1 n$ 1.1391 n	T(19)	$J'_{21}\times10^{-6}$ (20)× .16410	$J'_{02}\times10^{-6}$ (21)+ 1.2400	(22)(2) / 93.0	1-(23)	$J'_{22}\times10^{-6}$ (22) / (24)
19	.36547	.10220	.89780	.40707	.42707	21.643	1.0504	.17237	1.41237	.56059	.43941	3.2142
22	.36650	.13741	.86259	.42488	.44488	25.060	1.0691	.17544	1.41544	.75323	.24677	5.7359
1	26	27	28	29	30	31	32	33	34	35	36	37
n	$J'_{03}\times10^{-6}$ (25)+ .02000	θ'_{21} cos(19)	θ'_{23} (27)(24)	← $\phi n \frac{\xi}{\ell}$ = n× FACTOR →						← cos $\phi n \frac{\xi}{\ell}$ = ϑ' →		
				.10729	.27998	.45266	.63557	.80826	.98095	cos(29)	cos(30)	cos(31)
19	3.2342	.92950	.40843	2.04	5.32	8.60	12.08	15.36	18.64	.99937	.99569	.98876
22	5.7559	.90586	.22354	2.36	6.16	9.96	13.98	17.78	21.58	.99915	.99423	.98493
1	38	39	40	41	42	43	44	45	46	47	48	49
n	← ϑ' →			$\Sigma\beta'$ 3 ORDER $\Sigma^{(40)}_{(35)}$	$\frac{\Sigma\beta'}{\theta'_{23}}$ (41)/(28)	.08610 ×(2)	.06676 ×(2)	m_a 20.082 -(43)	m_t -[1.036 + (44)]	m_1 $\sqrt{(45)^2+(46)^2}$	AR m_1 797.7(47)	$m'_{e_{23}}\times10^{-6}$ (42)(48)10^{-6}
	cos(32)	cos(33)	cos(34)									
19	.97786	.96428	.94755	5.87351	14.3807	3.178	2.464	16.904	-3.500	17.263	13771	.19804
22	.97038	.95224	.92990	5.83083	26.0841	4.261	3.304	15.821	-4.340	16.405	13086	.34134
1	50	51	52	53	54	55	56	57	58	59	60	
n	$\frac{\pi}{180}\frac{J'_{03}P^2}{\gamma}10^{-6}$ (26)(2) / 57.296	$\frac{\pi}{180}\frac{J''_{23}P^2}{\gamma}10^{-6}$ (18)(2) / 57.296	$1+\frac{J'_{03}}{J''_{23}}$ $1+\frac{(50)}{(51)}$	SLOPE 10^6(50) / 1581.2(52)	INTERCEPT 10^6(49) / 1340(52)	(49) / (51)	BQ$_m$ 3 ORDER .69(2)	← LINEAR SOLUTION 74+BQ$_m$	$\frac{(57)^2}{74}$	SMALL $A\theta^\circ_v$ → (53)-(58)	$A\theta^\circ_v$ (54)/(59)	
19	2.0836	.27514	8.573	153.71	17.24	.7198	25.47					
22	4.9717	.38427	13.938	225.59	18.28	.8883	34.15	108.15	158.06	67.53	.2707	
1	61	62	63	64	65	66	67	68	69	70	71	72
n	$A\theta^\circ_v$ ROOTS FROM CURVES	$\theta^\circ_{23}-\theta^\circ_{03}$ (61) / 1.18	(62)+(55)	θ°_{03} -(63) / (52)	θ°_{23} (62)+(64)	$M_3\times10^{-6}$ (51)(65)	$C_3\times10^{-6}$ 57.296(66) / (62)	(18)(2) / (67)	1-(68)	$J''_{03}\times10^{-6}$ (18) / (69)	$J''_{22}\times10^{-6}$ (70)+ .02000	(71)(2) / 93.0
19	-.630	-.5339	.1859	-.02168	-.5556	-.15287	16.405	.96095	.03905	10.936	10.956	4.3486
22	-.760	-.6441	.2442	-.01752	-.6616	-.25423	22.615	.97356	.02644	16.826	16.846	8.9646
"	.652	.5525	1.4408	-.10337	.4491	.17258	17.897	1.23021	-.23021	-1.9325	-1.9125	-1.01774
"	.263	.2229	1.1112	-.07972	.1432	.05503	14.145	1.55653	-.55653	-.7994	-.7794	-.41476

TABLE 8 (*Continued*)

1	73	74	75	76	77	78	79	80	81	82	83	84
n	1−(72)	$\frac{J''_{02}\times10^{-6}}{(71)/(73)}$	$\frac{J''_{21}\times10^{-6}}{(74)+1.2400}$	$\frac{-(19)(75)}{9.402}$	$\phi_1\eta+\gamma_1''$ TAN^{-1}(76)	γ_1'' (77)−(19)	$\phi_1\eta\frac{\xi}{\ell}+\gamma''$ (29)+(78)	(30)+(78)	(31)+(78)	(32)+(78)	(33)+(78)	(34)+(78)
19	−3.3486	−3.2718	−2.0318	4.6771	77.93	56.29	58.53	61.61	64.89	68.37	71.65	74.93
22	−7.9646	−2.1151	−.8751	2.3325	66.79	41.73	44.09	47.89	51.69	55.71	59.51	63.31
"	2.01774	−.9478	.2922	−.77883	142.09	117.03	119.39	123.19	126.99	131.01	134.81	138.61
"	1.41476	−.5509	.6891	−1.8367	118.57	93.51	95.87	99.67	103.47	107.49	111.29	115.09

1	85	86	87	88	89	90	91	92	93	94	95	96
n	$\cos(\phi_1\eta\frac{\xi}{\ell}+\gamma'')=\mathcal{S}''$ cos(79)	cos(80)	cos(81)	cos(82)	cos(83)	cos(84)	$\Sigma\beta''$ 3ORDER $\Sigma^{(90)}_{(85)}$	$\Sigma\beta''/\Sigma\beta'$ (91)/(41)	θ°_{12} (64)(73)	cos($\phi_1\eta+\gamma''$) cos(77)	α''_1 (93)/(94)	θ°_{01} (95)(92)
19	.52503	.47547	.42436	.36861	.31482	.26000	2.36829	.40322	.07260	.20911	.34719	.13999
22	.71825	.67056	.61992	.56338	.50739	.44916	3.52866	.60517	.13954	.39410	.35407	.21427
"	−.49075	−.54742	−.60168	−.65619	−.70476	−.75023	−3.75103	−.64331	−.20857	−.78898	.26435	−.17006
"	−.10227	−.16797	−.23294	−.30054	−.36309	−.42404	−1.59085	−.27283	−.11278	−.47823	.23583	−.06434

1	97	98	99	100	101	102
n	θ°_{45} (65)/(16)	PUMP RPM θ°_{45} (97) 319/65	θ°_{56} (98)/(12)	θ°_{67} (99)/(8)	θ°_{78} (100)/(4)	RPM 3ORDER
19	−.6188	−3.0369	−3.0741	−3.0838	−3.2020	380
22	−.7670	−3.7642	−3.8269	−3.8432	−4.0433	440
"	.5206	2.5549	2.5975	2.6086	2.7444	"
"	.1660	.8147	.8283	.8318	.8751	"

TABLE 9 SECOND FREQUENCY CALCULATION FOR C_1 = 23.147 × 10

1	2	3	4	5	6	7	8	9	10	11	12	13
n	$\frac{p^2}{g}$ .1022529n^2	.001000 ×(2)	1−(3)	$\frac{J''_{07}\times10^{-6}}{.04820/(4)}$	$\frac{J''_{76}\times10^{-6}}{(5)+.007226}$	$\frac{(6)(2)}{674.4}$	1−(7)	$\frac{J''_{06}\times10^{-6}}{(6)/(8)}$	$\frac{J''_{65}\times10^{-6}}{(9)+.007226}$	$\frac{(10)(2)}{197.5}$	1−(11)	$\frac{J''_{05}\times10^{-6}}{(10)/(12)}$
83	704.41	.70441	.29559	.163064	.170290	.17787	.82213	.20713	.21436	.76454	.23546	.91039
83.06	705.43	.70543	.29457	.163628	.170854	.17872	.82128	.20803	.21526	.76887	.23113	.93134

1	14	15	16	17	18	19	20	21	22	23	24	25
n	$\frac{J''_{14}\times10^{-6}}{(13)+.30000}$	$\frac{(14)(2)}{132.0}$	1−(15)	$\frac{J''_{04}\times10^{-6}}{(14)/(16)}$	$\frac{J''_{43}\times10^{-6}}{(17)+.02000}$	$\frac{(18)(2)}{23.147}$	1−(19)	$\frac{J''_{03}\times10^{-6}}{(18)/(20)}$	$\frac{J''_{32}\times10^{-6}}{(21)+.02000}$	$\frac{(22)(2)}{93.0}$	1−(23)	$\frac{J''_{02}\times10^{-6}}{(22)/(24)}$
83	1.21039	6.4592	−5.4592	−.22172	−.20172	−6.1387	7.1387	−.028257	−.008257	−.06254	1.06254	−.007771
83.06	1.23134	6.5805	−5.5805	−.22065	−.20065	−6.1150	7.1150	−.028201	−.008201	−.06221	1.06221	−.001721

1	26	27	28	29
n	$\frac{J''_{21}\times10^{-6}}{(25)+1.24000}$	$\frac{-J''_{21}/J_1}{-(26)/.16410}$	T^{-1}(27)	$\frac{n}{(28)/1.1391}$
83	1.23223	−7.509	94.61	83.06
83.06	1.23228	−7.509	94.61	83.06

TABLE 10 THIRD FREQUENCY CALCULATION FOR $C_3 = 23.147 \times 10^6$

1	2	3	4	5	6	7	8	9	10	11	12	13
n	$\frac{p^2}{g}$ .102252n^2	$\phi_3 n$ 1.1391n	$T(3)$	$J'_{21}\times10^{-6}$ (4)× .16410	$J'_{02}\times10^{-6}$ (5)+ 1.2400	(6)(2) / 93.0	1−(7)	$J'_{22}\times10^{-6}$ (6) / (8)	$J'_{03}\times10^{-6}$ (9)+ .02000	(10)(2) / 23.147	1−(11)	$J'_{23}\times10^{-6}$ (10) / (12)
94	903.50	107.08	−1.7415	−.28578	.95422	9.2703	−8.2703	−.115379	−.095379	−3.7229	4.7229	−.020195
92.5	874.89	105.37	−1.9782	−.32462	.91538	8.6114	−7.6114	−.120264	−.100264	−3.7897	4.7897	−.020933
92.80	880.58	105.71	−1.9269	−.31620	.92380	8.7471	−7.7471	−.119245	−.099245	−3.7756	4.7756	−.020782
1	14	15	16	17	18	19	20	21	22	23	24	25
n	$J'_{04}\times10^{-6}$ (13)+ .02000	(14)(2) / 132.0	1−(15)	$J'_{24}\times10^{-6}$ (14) / (16)	$J'_{05}\times10^{-6}$ (17)+ .30000	(18)(2) / 197.5	1−(19)	$J'_{25}\times10^{-6}$ (18) / (20)	$J'_{06}\times10^{-6}$ (21)+ .007226	(22)(2) / 674.4	1−(23)	$J'_{26}\times10^{-6}$ (22) / (24)
94	−.000195	−.00133	1.00133	−.000195	.299805	1.37151	−.37151	−.80699	−.79976	−1.07145	2.07145	−.38609
92.5	−.000933	−.00618	1.00618	−.000927	.299073	1.32484	−.32484	−.92068	−.91345	−1.18501	2.18501	−.41805
92.80	−.000782	−.00522	1.00522	−.000778	.299222	1.33412	−.33412	−.89555	−.88832	−1.15990	2.15990	−.41128
1	26	27	28	29	30							
n	$J'_{07}\times10^{-6}$ (25)+ .007226	$\frac{10^6}{J'_{07}}$ 1/(26)	$\frac{10^6}{J'_{07}}+\frac{10^6}{J_{78}}$ (27)+ 20.747	(28)× 48.20	$\frac{n}{\sqrt{(29)/.102252}}$							
94	−.37886	−2.6395	18.1075	872.78	92.39							
92.5	−.41082	−2.4342	18.3128	882.68	92.91							
92.80	−.40405	−2.4749	18.2721	880.72	92.81							

$$m_a = 20.082 + 0.12745 \frac{p^2}{g}$$

$$m_b = -1.0359 - 0.06676 \frac{p^2}{g}$$

The 3 order value due to the reciprocating weight is a sine component equal to

$$\frac{W_r R}{9A} \frac{p^2}{g} F_a = -0.21355 \frac{p^2}{g}$$

Therefore the 3 order applied torque at each crank is

$$m_a = 20.082 - 0.08610 \frac{p^2}{g}$$

$$m_b = -\left(1.036 + 0.06676 \frac{p^2}{g}\right)$$

The calculations for the 3 order forced-vibration amplitudes at two frequencies are shown in Table 8, which are carried out by the reduction method applied to the equivalent system with a distributed mass along the engine crankshaft. The original calculations were made at several other frequencies in similar tables with more horizontal lines below the column headings. The resulting resonance curves for the amplitude at the free end of the engine and the torque across the coupling are shown in Fig. 12. The calculations may be continued to obtain the vibration torque or stress in any section or the vibration torque across the gears.

The second natural frequency vibration occurs principally between the engine and flywheel. The calculations for this frequency with the coupling-stiffness factor for full power torque, $C_3 = 23.147 \times 10^6$, is given in Table 9. In this case the natural frequency is 83.06 VPS which shows that the 6 order of this natural vibration is above the full speed.

The third natural frequency vibration occurs principally between the centrifugal pump and the speed increaser gears. The calculation for this frequency using $C_3 = 23.147 \times 10^6$ is given in Table 10, which yields the result 92.80 VPS and indicates that the 9 order third-frequency vibration will occur at 619 rpm.

Discussion

E. L. Davis.[7] The author is to be congratulated for presenting a method of simplifying the problem of the "untuned viscous damper," by using an equivalent inertia factor for the whole vibrating system and an equivalent applied harmonic torque.

We also congratulate and thank him for his work and interest in deriving equations for the "torque versus stiffness factor" and "torque versus deflection" curves of our "Steelflex" coupling.

We like the convenient form of the equations for their use in solving values of the "undamped resonance curves" of an engine drive containing our nonlinear coupling.

The torque versus stiffness factor curves published to date are applicable directly for small vibratory amplitudes. The author's Formulas [1] and [2], based on these curves, cover the complete range of our standard couplings for small vibratory amplitudes as well as any larger magnitude of θ_v required for calculation.

An alternate graphical method for determining from the curves the stiffness factor of a coupling where appreciable vibratory torques θ_v across the coupling are encountered is explained by W. Ker Wilson.[8] Our company has used this method when extreme amplitudes of vibration were found in drives in the field that had not been calculated previously for torsional vibration.

[7] Analyst, The Falk Corporation, Milwaukee, Wis.

[8] "Practical Solution of Torsional Vibration Problems," by W. Ker Wilson, John Wiley & Sons, Inc., New York, N. Y., vol. 2, 1940–1941, p. 398.

We believe Mr. Wilson's method would coincide with the author's results, but the answers obtained would be somewhat less accurate and the work involved would be quite cumbersome; particularly for calculating undamped resonance curves, even though Table 8 of the paper were used in conjunction with Wilson's method. However, the latter has the advantage of being more easily interpreted and involves a simplified, if more tedious, form of mathematics.

B. E. O'Connor.[9] To the writer's knowledge the simple relationship between amplitude impulse and residual torque in an undamped system has not been published previously. Exact results are obtainable with this method with much less effort than is required using previously published methods including methods which lead to approximate solutions only.

The author's approach to the problem of a multimass system employing an untuned viscous damper with torque applied at several locations is quite novel.

To obtain exact solutions for the amplitudes, torques, and phase angles at any station in the system we use an extension of Holzer's method by which damping and applied torques are included in a single tabular solution for a given frequency.[10] Engine calculations are started at the flywheel end and the amplitude at the flywheel is not unity, but an unknown. Exciting torques are added to the torque-summation column at the proper stations. The proper phase relationship is taken into account by use of complex numbers when necessary. Damping is simply accounted for by an entry in the spring-constant column preceded by an imaginary operator.

The unknown amplitude at the flywheel end is obtained in the form of a complex number by equating the residual torque at the front end to zero. Since amplitudes and torques at each station are in terms of the amplitude at the flywheel and a unit impulse, all required information at each station is readily available.

For most practical cases the following solution is entirely satisfactory: The exact value of the common point frequency of the damper housing may be obtained by balancing a standard Holzer table with an inertia at the damper-housing location equal to the housing inertia plus one half the dampor-flywheel inertia. The exact housing common point amplitude may be calculated by equating the product of one impulse times the sum of the amplitudes at the impulses from the same table when the amplitude at the damper housing is unity to the expression for maximum energy dissipation by the damper. The values of torque obtained from the table are not exact but they are nearly exact. The common point amplitude will not be the greatest amplitude unless optimum damping is used. The product of the common point value of $2\pi N$ and the damper-flywheel inertia is a sufficiently close approximation to optimum damping for most purposes.

It would seem that the labor involved in obtaining correct values of I_{eq} and m_{eq} as proposed by the author would involve at least as much labor as does the completely rigorous method which is described in this discussion.

The writer would like to see a complete solution of a problem by the author to be sure that his procedure is understood.

J. D. Swannack.[11] The writer feels the amplitude and torque relations are very important. From experience with linear vibration, the Rayleigh-Maxwell reciprocal theorem is found to be useful. In the present case, suppose we have torsional masses $I_1, I_2 \ldots I_n$. If a Holzer table is worked through, beginning at I_n, we have resulting a set of influence numbers $\theta_1/Q_1, \theta_2/Q_1 \ldots \theta_n/Q_1$ where the θ are torsional amplitudes and Q_1 is the residual torque at mass I_1. Now we can write for the resultant angle at I_1

$$\bar{\theta}_1 = m_1 \frac{\theta_1}{Q_1} + m_2 \frac{\theta_1}{Q_2} \ldots\ldots\ldots\ldots\ldots m_n \frac{\theta_1}{Q_n}$$

where $\theta_1/Q_2, \ldots \theta_1/Q_n$ are unknown at the moment. From Rayleigh we have

$$\frac{\theta_1}{Q_2} = \frac{\theta_2}{Q_1}, \frac{\theta_1}{Q_2} = \frac{\theta_2}{Q_1}, \ldots\ldots\ldots\ldots \frac{\theta_1}{Q_n} = \frac{\theta_n}{Q_1}$$

so

$$\bar{\theta}_1 = m_1 \frac{\theta_1}{Q_1} + m_2 \frac{\theta_2}{Q_1} \ldots\ldots\ldots\ldots\ldots m_n \frac{\theta_n}{Q_1}$$

It is appreciated that the Falk coupling solution is approximate. Any so-called exact solution would, for any practical case, be a luxury few could afford. While the writer has considerable confidence in the method and data, does the author have torsiograph tests in any cases? If tests exist, do they show reasonable agreement on the lower branch (below resonance) of the amplitude curve up to the drop-off point?

Author's Closure

The author wishes to express his appreciation to the discussers for their comments.

Mr. O'Connor describes a "completely rigorous" method of solving the viscous-damper problem. The author does not object to the term completely rigorous since the method he has presented equals the rigor of that described by Mr. O'Connor.

Calculations for the system, shown in Fig. 13 of this closure, are described by Mr. O'Connor in the SAE *Quarterly Transactions*,

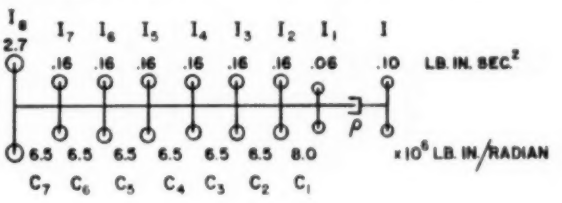

Fig. 13

January, 1947, and also in the reference mentioned in his discussion. The cylinders are at masses 2 to 7 inclusive, and the magnitude of the 6 order applied torque at each cylinder is $m = 66$ lb-in.

Calculations for this system will be described using the methods presented in the paper. Three Holzer tables are shown in Table 11, herewith. The first one applies to the fixed-point frequency of the damper hub corresponding to the natural frequency of the system with I_1 increased by $I/2$. The fixed-point amplitude of the hub for the 6 order may be calculated from the values in this table

$$\theta_1 = \frac{-13.97165m}{\pm .54042 \times 10^6} = \pm 25.8533m/10^6 \text{ radians}$$

The second and third Holzer tables in Table 11 were calculated

[9] Houdaille-Hershey Corporation, Buffalo Division, Buffalo, N. Y.

[10] "Viscous Dampers Tuned and Untuned," by B. E. O'Connor, Symposium on Torsional Vibration, sponsored by the Diesel Engine Manufacturers Association at Massachusetts Institute of Technology, June 13, 14, and 15, 1949.

[11] Chief Analyst, Fairbanks, Morse & Company, Beloit, Wis. Mem. ASME.

TABLE 11 HOLZER TABLES

$p^2 = 2.55940 \times 10^6$, $p = 1599.81$

	1	2	3	4	5	6	7
r	I	$Ip^2 \times 10^6$	θ''	$Ip^2\theta'' \times 10^{-6}$	$\Sigma Ip^2\theta'' \times 10^{-6}$	$C \times 10^{-6}$	$\frac{\Sigma Ip^2\theta''}{C}$
8	2.7	6.91038	1	6.91038	6.91038	6.5	1.06314
7	.16	.409504	-.06314	-.02586	6.88452	6.5	1.05916
6	.16	.409504	-1.12230	-.45959	6.42493	6.5	.98845
5	.16	.409504	-2.11075	-.86436	5.56057	6.5	.85547
4	.16	.409504	-2.96622	-1.21468	4.34589	6.5	.66860
3	.16	.409504	-3.63482	-1.48847	2.85742	6.5	.43960
2	.16	.409504	-4.07442	-1.66849	1.18893	8.0	.14862
1	.06	.153564	-4.22304	-.64851	.54042		

$\sum_7^2 \theta'' = -13.97165$

$p^2 = 2.53931 \times 10^6$, $p = 1593.52$

	1	2	3	4	5	6	7
r	I	$Ip^2 \times 10^{-6}$	θ''	$Ip^2\theta'' \times 10^{-6}$	$\Sigma Ip^2\theta'' \times 10^{-6}$	$C \times 10^{-6}$	$\frac{\Sigma Ip^2\theta''}{C}$
8	2.7	6.85614	1	6.85614	6.85614	6.5	1.05479
7	.16	.406290	-.05479	-.02226	6.83388	6.5	1.05137
6	.16	.406290	-1.10616	-.44942	6.38446	6.5	.98222
5	.16	.406290	-2.08838	-.84849	5.53597	6.5	.85169
4	.16	.406290	-2.94007	-1.19452	4.34145	6.5	.66792
3	.16	.406290	-3.60799	-1.46589	2.87556	6.5	.44239
2	.16	.406290	-4.05038	-1.64563	1.22993	8.0	.15374
1	.06	.152359	-4.20412	-.64054	.58939		

$\sum_7^2 \theta'' = -13.84777$

$p^2 = 2.57956 \times 10^6$, $p = 1606.10$

	1	2	3	4	5	6	7
r	I	$Ip^2 \times 10^{-6}$	θ''	$Ip^2\theta'' \times 10^{-6}$	$\Sigma Ip^2\theta'' \times 10^{-6}$	$C \times 10^{-6}$	$\frac{\Sigma Ip^2\theta''}{C}$
8	2.7	6.96481	1	6.96481	6.96481	6.5	1.07151
7	.16	.412730	-.07151	-.02951	6.93530	6.5	1.06697
6	.16	.412730	-1.13848	-.46988	6.46542	6.5	.99468
5	.16	.412730	-2.13316	-.88042	5.58500	6.5	.85923
4	.16	.412730	-2.99239	-1.23505	4.34995	6.5	.66922
3	.16	.412730	-3.66161	-1.51126	2.83869	6.5	.43672
2	.16	.412730	-4.09833	-1.69150	1.14719	8.0	.14340
1	.06	.154774	-4.24173	-.65651	.49068		

$\sum_7^2 \theta'' = -14.09548$

TABLE 12 AMPLITUDES AT FLYWHEEL AND TORQUES AT NODE OF MOTION OF NORMAL PHASE

$p^2 = 2.55940 \times 10^6$ NORMAL PHASE

	1	2	3	4	5	6	7
r	I	$Ip^2 \times 10^{-6}$	θ'	$Ip^2\theta' \times 10^{-6}$	$\Sigma Ip^2\theta' \times 10^{-6}$	$C \times 10^{-6}$	$\frac{\Sigma Ip^2\theta'}{C}$
1	.108335	.277273	1	.27727	.27727	8.0	.03466
2	.16	.409504	.96534	.39531	.67258	6.5	.10347
3	.16	.409504	.86187	.35294	1.02552	6.5	.15777
4	.16	.409504	.70410	.28833	1.31385	6.5	.20213
5	.16	.409504	.50197	.20556	1.51941	6.5	.23376
6	.16	.409504	.26821	.10983	1.62924	6.5	.25065
7	.16	.409504	.01756	.00719	1.63643	6.5	.25176
8	2.7	6.91038	-.23420	-1.61841	.01802		

$\sum_2^7 \theta' = 3.31905$

$$(\theta_8)_N = -\frac{3.31905m \times .033298}{.01802 \times 10^6} = -6.133\, m/10^6$$

$$(M_7)_N = 2.7 \times 2.55940 \times (-6.133m) = -42.38\, m$$

$p^2 = 2.55940 \times 10^6$ DAMPING PHASE

	1	2	3	4	5	6	7
r	I	$Ip^2 \times 10^{-6}$	θ'	$Ip^2\theta' \times 10^{-6}$	$\Sigma Ip^2\theta' \times 10^{-6}$	$C \times 10^{-6}$	$\frac{\Sigma Ip^2\theta'}{C}$
1	∞	∞	$\Delta\theta$	1 ASSUMED	1	8.0	.125
2	.16	.409504	-.125	-.05119	.94881	6.5	.14597
3	.16	.409504	-.27097	-.11096	.83785	6.5	.12890
4	.16	.409504	-.39987	-.16375	.67410	6.5	.10371
5	.16	.409504	-.50358	-.20622	.46788	6.5	.07198
6	.16	.409504	-.57556	-.23569	.23219	6.5	.03572
7	.16	.409504	-.61128	-.25032	-.01813	6.5	-.00279
8	2.7	6.91038	-.60849	-4.20490	-4.22303		

$\sum_2^7 \theta' = -2.48626$

$$(\theta_8)_d = -\frac{-2.48626\,\Delta\theta\, m\,(-.99945)}{-4.22303\,\Delta\theta \times 10^6} = .5884\, m/10^6$$

$$(M_7)_d = 2.7 \times 2.55940 \times .5884m = 4.066\, m$$

$$\theta_8 = \sqrt{(\theta_8)_N^2 + (\theta_8)_d^2} = 6.161\, m/10^6$$

$$M_7 = \sqrt{(M_7)_N^2 + (M_7)_d^2} = 42.57\, m$$

for frequencies slightly below and above the fixed-point frequency by the same value. For $p = 1593.52$

$$m_{eql} = \frac{-13.84777m}{-4.20412} = 3.29386m$$

$$I_{eql} = \frac{0.58939}{2.53931(-4.20412)} = -0.055209$$

For $p = 1606.10$

$$m_{eql} = \frac{-14.09548m}{-4.24173} = 3.32305m$$

$$I_{eql} = \frac{0.49068}{2.57956(-4.24173)} = -0.044845$$

Thus

$$\Delta p = 12.58,\ \Delta m_{eql} = 0.02919m,\ \Delta x = \frac{\Delta I_{eql}}{I} = 0.10364$$

$$p\frac{dx}{dp} = 1599.81\,\frac{0.10364}{12.58} = 13.180$$

$$1 - \frac{p}{2m_{eq}}\frac{dm_{eq}}{dp} = 1 - \frac{1599.81}{(3.29386 + 3.32305)} \times \frac{0.02919}{12.58} = 0.4390$$

Therefore the optimum damping factor is

$$\rho = 0.1 \times 1599.81\sqrt{\frac{13.180 - 0.4390}{13.180 + 0.4390}} = 154.74$$

$$p_0 = 1547.4$$

The value of the optimum damping factor given by Mr. O'Connor was 158.250747 which is not correct since it was obtained by equating amplitudes at the fixed-point frequency and a slightly smaller frequency. The author has extended these calculations to obtain a value by equating amplitudes at the fixed-point frequency and a slightly larger frequency where the difference of the two frequencies was the same as was used by Mr. O'Connor. The damping factor in this case was 151.29520. The optimum damping factor therefore is approximately the average of these two values or 154.77307. This agrees almost exactly with the value computed by the author, namely, 154.74.

The amplitude at any mass and the torque in any step may be obtained by computing the normal and damping phases of the motion as described in the paper. To illustrate this, the amplitude at the flywheel (mass 8) and the torque at the node of the motion of the normal phase (step 7) are computed in Table 12 at the fixed-point frequency. The same type of calculation may be made to obtain these results at any frequency. For the normal phase calculations, I_1 is increased by

$$I\Big/\left[\left(\frac{p}{p_0}\right)^2 + 1\right]$$

and the undamped forced vibration is computed for the system stimulated by the original set of applied torques with each multiplied by $\cos\psi$. For the damping-phase calculations, I_1 is put equal to infinity and the undamped forced vibration is computed for the system stimulated by the original set of applied torques with each multiplied by $\sin\psi$.

The values in the upper table of Table 11 give

$$I_{eql} = I_{1\infty}' = \frac{0.54042}{2.55940(-4.22304)} = -0.05000$$

$$m_{eql} = \frac{-13.97165m}{-4.22304} = 3.30843m$$

Also

$$\frac{p}{p_0} = 1.03387,\ \left(\frac{p}{p_0}\right)^2 = 1.06889$$

$$\frac{1}{\left(\frac{p}{p_0}\right)^2 + 1} = 0.483351$$

$$\tan\psi = \frac{1.03387}{2.06889(-0.016649)} = -30.015$$

$$\sin\psi = -0.99945,\ \cos\psi = 0.033298$$

The results obtained in Table 12 agree closely with results given by Mr. O'Connor. This example also shows that very little error is involved in neglecting the damping phase of the motion and only calculating the normal phase.

The advantages resulting from using a distributed mass for the masses along the engine crankshaft also are illustrated by this example. The equivalent system in Fig. 14, herewith,

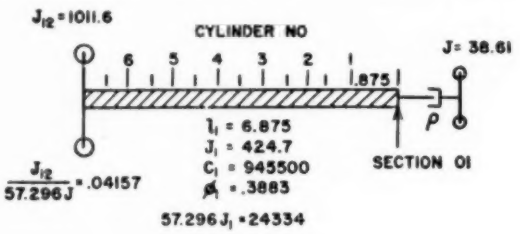

Fig. 14

represents the same system as is also represented in Fig. 13. The transformation of the one system into the other is obvious when it is recognized that the J-values in Fig. 14 are in lb-in.^{2} and the I-values in Fig. 13 are in lb-in. sec^2. Using inertia factors in lb-in^2 is a personal preference of the author and is not considered a necessity.

The fixed-point frequency for the section at the damper hub (section 01) is the natural frequency of the system with 38.61/2 added to the crankshaft at section 01. Adding this as a distributed mass gives $J_1 = 444.0$ and $\phi_1 = 0.40595$. Thus the fixed-point frequency is

$$n = T'^{-1}(-1011.6/444.0) \div 0.40595 = 255.3$$

or $p = 2\pi n = 1604.1$. The fact that this frequency is 0.268 per cent higher than the corresponding value for Fig. 13 is no reflection on either equivalent system.

The calculations for the optimum damping factor are given in Table 13 where the value of 155.16 is obtained. If this is reduced 0.268 per cent to compensate for the difference in the fixed-point frequencies, it becomes 154.74 which is identical to the previously calculated result for Fig. 13. The remainder of the calculations for the amplitude at the flywheel and the torque at the node of the motion of the normal phase are given in Table 14. (See page 268.)

An explicit expression for the optimum damping factor for the system in Fig. 15 was derived by Mr. O'Connor in the SAE Transactions, 1947. The author's solution for this problem is as follows, which is worthy of note because of its simplicity

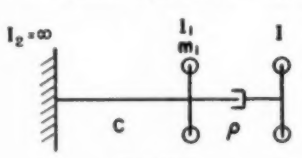

Fig. 15

TABLE 13 OPTIMUM DAMPING-FACTOR CALCULATIONS

1	2	3	4	5	6	7
n	$\phi_1 n$ $.3883n$	$-.04157$ $\times(2)$	$\phi_1 n+\gamma_1''$ $\tan^{-1}(3)$	γ_1'' $(4)-(2)$	TAN(5)	$I_{01}''=I_{eq01}$ $-24334\frac{(6)}{(2)}$
254.3	98.74	-4.1046	103.69	4.95	.08661	-21.345
256.3	99.52	-4.1370	103.59	4.07	.07115	-17.397
255.3	99.13	-4.1208	103.64	4.51	.07888	-19.363

		$n=254.3$			$n=256.3$		
CYL NO.	ℓ	$\phi_1 n\frac{x}{\ell}$	$\phi_1 n\frac{x}{\ell}+\gamma_1''$	$\cos\left(\phi_1 n\frac{x}{\ell}+\gamma_1''\right)$	$\phi_1 n\frac{x}{\ell}$	$\phi_1 n\frac{x}{\ell}+\gamma_1''$	$\cos\left(\phi_1 n\frac{x}{\ell}+\gamma_1''\right)$
1	.875	12.57	17.52	.95361	12.67	16.74	.95762
2	1.875	26.93	31.88	.84916	27.14	31.21	.85527
3	2.875	41.29	46.24	.69164	41.62	45.69	.69854
4	3.875	55.65	60.60	.49090	56.09	60.16	.49758
5	4.875	70.02	74.97	.25932	70.57	74.64	.26488
6	5.875	84.38	89.33	.01169	85.04	89.11	.01553
			SUM = 3.25632			SUM 3.28942	

$$m_{eq01}=\frac{3.25632m}{\cos 4.95}=3.2686m \qquad m_{eq01}=\frac{3.28942m}{\cos 4.07}=3.2977m$$

$$\Delta x=\frac{21.345-17.397}{38.61}=.10225$$

$$p\frac{dx}{dp}=n\frac{dx}{dn}=255.3\,\frac{.10225}{2}=13.052$$

$$1-\frac{p}{2m_{eq}}\frac{dm_{eq}}{dp}=1-\frac{255.3\times.0291}{6.5663\times2}=.4343$$

OPTIMUM ρ

$$=.10\times1604.1\sqrt{\frac{12.6177}{13.4863}}$$

$$=155.16\,,\quad p_0=1551.6$$

$$\theta_{01}=\frac{3.2832m}{19.305\times.102252(255.3)^2}=25.52\,m/10^6\,.$$

$$I_{01}''=\frac{I_2}{1-\frac{I_2p^2}{C}}=-\frac{C}{p^2}\,,\quad I_{eq1}=I_1-\frac{C}{p^2}$$

$$x=\frac{I_{eq1}}{I}=\frac{I_1}{I}-\frac{C}{Ip^2}\,,\quad \frac{dx}{dp}=\frac{2C}{Ip^3}$$

For the fixed point $x=-1/2$ so that

$$\frac{I_1}{I}-\frac{C}{Ip^2}=-\frac{1}{2}\,,\text{ or }\frac{2C}{Ip^2}=\frac{2I_1}{I}+1\,,\text{ or }p^2=\frac{2C}{2I_1+I}$$

Therefore the optimum damping factor, since $dm_1/dp=0$, is

$$\rho_{opt}=Ip\sqrt{\frac{p\frac{dx}{dp}-1}{p\frac{dx}{dp}+1}}=I\sqrt{\frac{2C\frac{2I_1}{I}}{\left(2I_1+I\right)\left(\frac{2I_1}{I}+2\right)}}$$

This may be reduced to the form of Equation [8] given by Mr. O'Connor, namely

$$\frac{\rho_{opt}}{2I\sqrt{\frac{C}{I_1}}}=\frac{1}{\sqrt{2\left(2+\frac{I}{I_1}\right)\left(1+\frac{I}{I_1}\right)}}$$

If the vector notation for simple harmonic motion is used, the author's methods may be extended to include outer damping at each mass and inner damping between each mass. If ρ is the outer damping factor proportional to the angular velocity of the mass, and if ρ' is the inner damping factor proportional to the difference of the angular velocities of two adjacent masses, the inertia factor of the mass may be taken as the complex number $I-j\rho/p$ and the stiffness factor of the shaft between the two adjacent masses may be taken as $C+j\rho' p$ where $j=\sqrt{-1}$. In this case the amplitudes and torques in the solution become complex numbers whose lengths and phases as vectors are the maximum values and phase angles of the simple harmonic expressions.

TABLE 14 CALCULATIONS FOR AMPLITUDE AT FLYWHEEL AND TORQUE AT NODE OF MOTION OF NORMAL PHASE

$n = 255.3$, $p = 1604.1$, $\frac{p}{p_o} = 1.03384$, $\left(\frac{p}{p_o}\right)^2 = 1.06882$, $\frac{1}{\left(\frac{p}{p_o}\right)^2+1} = .483367$

$\text{TAN}\,\psi = \frac{1.03384}{2.06882(-.018135)} = -27.556$, $\text{SIN}\,\psi = -.99934$, $\cos\psi = .036266$

$(\theta_{21})_N = -\frac{(meq_{21})_N \cos\psi}{(Ieq_{21})_N p^2}$

$(\theta_{21})_d = -\frac{(meq_{21})_d \text{SIN}\,\psi}{(Ieq_{21})_d p^2}$

$M_{21} = I_{12} p^2 \theta_{21}$

$M_x = \frac{\text{SIN}(\phi_1 n \frac{x}{l} + \gamma_1')}{\text{SIN}(\phi_1 n + \gamma_1')} M_{21}$

FOR X BETWEEN 5.875 & 6.875

NORMAL PHASE $J_{01} = 18.663$, $\frac{J_{01}}{57.296 J_1} = .0007670$

1	2	3	4	5	6	7	8
n	$\phi_1 n$ $.3883n$	$.0007670 \times (2)$	γ_1' $\text{TAN}^{-1}(3)$	$\phi_1 n + \gamma_1'$ $(4)+(2)$	TAN(5)	J_{21}' $24334\frac{(6)}{(2)}$	Jeq_{21} $(7)+1011.6$
255.3	99.13	.07603	4.35	103.48	-4.1717	-1024.05	-12.45

$\frac{p^2}{g} = .102252\,(255.3)^2 = 6664.6$

DAMPING PHASE

1	2	3	4	5	6
n	$\phi_1 n$ $.3883n$	$\phi_1 n + \gamma_1'$ $(\gamma_1' = 90)$	TAN(3)	J_{21}' $24334\frac{(4)}{(2)}$	Jeq_{21} $(7)+1011.6$
255.3	99.13	189.13	.16071	39.45	1051.0

$(\theta_{21})_N = -\frac{-14.0930m \times .036266}{-12.45 \times 6664.6} = -6.160\frac{m}{10^6}$

$(M_{21})_N = 1011.6 \times 6664.6\left(-6.160\frac{m}{10^6}\right) = -44.53m$

$(M_{x=5.979})_N = \frac{-41.53m}{\text{SIN}\,103.48} = -42.71m$

		NORMAL PHASE			DAMPING PHASE	
CYL NO.	l	$\phi_1 n \frac{x}{l}$	$\phi_1 n \frac{x}{l} + \gamma_1'$	COS $\phi_1 n \frac{x}{l} + \gamma_1'$	$\phi_1 n \frac{x}{l} + \gamma_1'$	COS $\phi_1 n \frac{x}{l} + \gamma_1'$
1	.875	12.62	16.97	.95646	102.62	-.21848
2	1.875	27.04	31.39	.85364	117.04	-.45461
3	2.875	41.45	45.80	.69717	131.45	-.66197
4	3.875	55.87	60.22	.49667	145.87	-.82777
5	4.875	70.29	74.64	.26488	160.29	-.94141
6	5.875	84.71	89.06	.01641	174.71	-.99574
			SUM = 3.28523		SUM = -4.09998	

$(\theta_{21})_d = -\frac{4.1526m(-.99934)}{1051.0 \times 6664.6} = .5925\frac{m}{10^6}$

$(M_{21})_d = 1011.6 \times 6664.6\left(.5925\frac{m}{10^6}\right) = 3.995m$

$(M_{x=5.979})_d = \frac{\text{SIN}\,176.21}{\text{SIN}\,189.13}\,3.995m = -1.664m$

$\theta_{21} = \sqrt{\theta_N^2 + \theta_d^2} = 6.188\,m/10^6$

$(M_{x=5.979})_N = \sqrt{M_N^2 + M_d^2} = 42.74m$

$(meq_{21})_N = \frac{3.28523m}{\cos 103.48} = -14.0930m$

$(meq_{21})_d = \frac{-4.09998m}{\cos 189.13} = 4.1526m$

On the Solution of the Reynolds Equation for Slider-Bearing Lubrication—II[1]

The Viscosity a Function of the Pressure

By A. CHARNES[2] AND E. SAIBEL,[3] PITTSBURGH, PA.

The solution of the Reynolds equation for slider-bearing lubrication is given for the finite bearing, side leakage included, when the viscosity is a known function of the pressure. The solution for the pressure distribution is obtained readily from the corresponding case of constant viscosity. The design factors—total load, center of pressure, friction force, and side leakage—also may be obtained, but, in general, the integrals involved must be worked out numerically. Qualitative properties of the pressure, total load, and center of pressure are obtained.

Introduction

THE effect of the pressure variation of viscosity on the lubrication of plane sliders has been shown to be important when the fluid pressures reach values high enough to affect the viscosity (1).[4] The increase in viscosity with an increase in pressure for normal lubricating fluids has been reported by many investigators, and relationships between these quantities both of an empirical and theoretical nature are available (2, 3).

Hitherto, exact solutions of the slider-bearing problem which take account of this variation have been confined to bearings of infinite width; that is, side leakage has been neglected.

It is the purpose of this paper to present an exact solution for the bearing of finite width when this variation of viscosity with pressure is taken into account. This exact solution for the pressure distribution is found to depend in a very simple way on the solution for the pressure distribution for the slider bearing when the viscosity is treated as constant. For this purpose, any of the existing solutions for the flat or exponential slider bearing with constant viscosity may be used (4).

In addition to the exact solution, qualitative results on the pressure distribution, total load, and center of pressure are obtained. These are believed to be new and are of interest in the design of slider bearings.

Theory

The starting point is the equation of Reynolds for the slider bearing, Fig. 1

$$\frac{\partial}{\partial x}\left(\frac{h^3}{\mu}\frac{\partial p}{\partial x}\right)+\frac{\partial}{\partial y}\left(\frac{h^3}{\mu}\frac{\partial p}{\partial y}\right)=6\,U\frac{\partial h}{\partial x} \qquad [1]$$

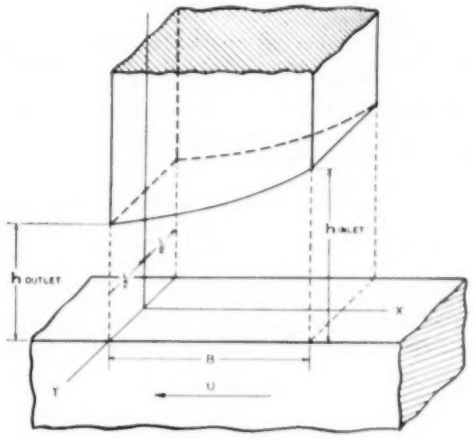

FIG. 1

where

p = pressure
h = thickness of oil film
U = velocity of slider (assumed to be in the x-direction)
x, y = co-ordinates in plane of slider
μ = coefficient of viscosity

It is assumed that μ is a function of p, that is, $\mu = \mu(p)$. The following transformation, used by Muskat and Evinger (1) simplifies Equation [1]:

Let

$$\mu^{-1}=\frac{1}{\mu_0}\frac{d\phi(p)}{dp} \qquad [2]$$

where ϕ is a function of the pressure which will be interpreted later. Then

$$\mu^{-1}\frac{\partial p}{\partial x}=\frac{1}{\mu_0}\frac{d\phi}{dp}\frac{\partial p}{\partial x}=\frac{1}{\mu_0}\frac{\partial \phi}{\partial x} \qquad [3]$$

Similarly

$$\mu^{-1}\frac{\partial p}{\partial y}=\frac{1}{\mu_0}\frac{d\phi}{dp}\frac{\partial p}{\partial y}=\frac{1}{\mu_0}\frac{\partial \phi}{\partial y} \qquad [4]$$

Substituting Equations [3] and [4] into Equation [1] there results

$$\frac{\partial}{\partial x}\left(\frac{h^3}{\mu_0}\frac{\partial \phi}{\partial x}\right)+\frac{\partial}{\partial y}\left(\frac{h^3}{\mu_0}\frac{\partial \phi}{\partial y}\right)=6U\frac{\partial h}{\partial x} \qquad [5]$$

which is precisely the Reynolds equation for the slider bearing when the viscosity is a constant μ_0, and ϕ may be interpreted as the pressure distribution for the case of constant viscosity. Since $\phi(p)$ is only determined by Equation [2] to within an arbitrary constant, we may specify it by taking $\phi(0) = 0$.

[1] The research underlying this paper was partially supported by funds from a U. S. Air Force contract with the Department of Mathematics of Carnegie Institute of Technology.

[2] Associate Professor, Department of Mathematics, Carnegie Institute of Technology.

[3] Professor of Mechanics, Department of Mathematics, Carnegie Institute of Technology. Mem. ASME.

[4] Numbers in parentheses refer to the Bibliography at the end of the paper.

Contributed by the Machine Design Division and the Research Committee on Lubrication and presented at the Semi-Annual Meeting, Cincinnati, Ohio, June 15–19, 1952, of THE AMERICAN SOCIETY OF MECHANICAL ENGINEERS.

NOTE: Statements and opinions advanced in papers are to be understood as individual expressions of their authors and not those of the Society. Manuscript received at ASME Headquarters, January 22, 1952. Paper No. 52—SA-2.

In what follows ϕ will be designated by the symbol $\hat{p}$ to emphasize the fact that it is the pressure distribution for constant viscosity μ_0.

Knowing the solution of Equation [5] for $\hat{p}$, the true pressure p may be found as follows:

Integrating Equation [3] leads to

$$\phi(p) = \mu_0 \int^p \mu^{-1}\, dp \quad [6]$$

However, the specification $\phi(0) = 0$, reduces this to

$$\hat{p} = \phi(p) = \mu_0 \int_0^p \mu^{-1}\, dp \quad [7]$$

Knowing the relationship between μ and p, Equation [7] may be integrated and p may be found in terms of $\hat{p}$, the solution of which is known.

Under the assumption of constant temperature, different relationships between viscosity and pressure have been assumed or derived from various assumptions regarding the nature of the mechanism of viscosity.

One such relationship which has had wide recognition and which originally was expressed as a purely empirical expression (5, 6) but has since been derived theoretically (3) is

$$\mu = \mu_0 e^{\alpha p} \quad [8]$$

This is the specific relationship which will be used subsequently.

Substituting μ from Equation [8] into Equation [7]

$$\hat{p} = \mu_0 \int_0^p \mu_0^{-1} e^{-\alpha p}\, dp$$

or

$$\hat{p} = \frac{1}{\alpha}(1 - e^{-\alpha p}) \quad [9]$$

Solving for p in Equation [9] we obtain

$$p = -\frac{1}{\alpha} \ln(1 - \alpha\hat{p}) \quad [10]$$

where ln denotes the natural logarithm. When $\hat{p}$ is known, it is seen that it is a simple matter to obtain p from Equation [10].

Note that as α approaches zero in Equation [10], p approaches $\hat{p}$ which is what should happen as the viscosity μ approaches the constant value μ_0.

Furthermore, if the series expansion for $\ln(1 - \alpha p)$ is used, Equation [10] becomes

$$p = \frac{1}{\alpha}\left[\alpha p + \frac{\alpha^2 \hat{p}^2}{2} + \ldots\right] \quad \text{for} \quad \alpha\hat{p} < 1 \quad [11]$$

Since α and $\hat{p}$ are both nonnegative quantities, it may be seen that at corresponding points

$$p \geq \hat{p} \quad [12]$$

Discussion

The relationship expressed by Equation [12] that the true pressure is never less than the pressure obtained under the assumption of constant viscosity is generally valid and does not depend on the particular form of the relation chosen to represent the variation of μ with p.

If the relation between μ and p is of the form shown in Fig. 2, then $(d\mu)/(dp) > 0$, or μ is an increasing function of p. Then it follows that

$$\frac{d^2p}{d\hat{p}^2} = \frac{1}{\mu_0}\frac{d\mu}{d\hat{p}} > 0$$

Consequently, p is a "convex" function of $\hat{p}$, see Fig. 3. From this it may be deduced that the pressure maximum for p must occur at the same point as the pressure maximum for $\hat{p}$ (7).

It is evident from the form of Equation [10] that the pressure becomes infinite when $\alpha\hat{p} = 1$. This is not due to the particular form (exponential) assumed for the variation of viscosity with pressure although the particular value of $\hat{p}$ at which the solution becomes singular depends upon the form chosen to represent μ as a function of p.

A schematic diagram of the relation between μ^{-1} and p is shown in Fig. 4. The area under this curve from $p = 0$ to an arbitrary value of p multiplied by μ_0 is equal to $\phi = \hat{p}$ from Equation [7]. As p goes to infinity, this area remains finite when the convergence is faster than p^{-1}. This finite value of the area corresponds to the value of $\hat{p}$ at which the true pressure becomes infinite. The remaining type of possibility, corresponding to a noninfinite true pressure for any value of $\hat{p}$, is exemplified by a relation of the type $\mu = A + Bp$, where A and B are constants. However, for lubricating oils in general, the increase in viscosity as the pressure increases, is greater than linear in the pressure. Consequently, some finite value of $\hat{p}$ will correspond to an infinite value of p.

This interesting result in its general form does not seem to have been noted in the literature. To the extent that temperature effects may be neglected and bearing surfaces considered rigid, a physical limitation is imposed on the system. This may be interpreted in a variety of ways. In particular, it may be thought of as a limitation on U/h_0^2 for given values of L, B, a, b, U_0, and α. The entire question is one which calls for further study.

Total Load

The total load on the slider is given by

$$W = \iint p\, dx\, dy \quad [13]$$

or

$$W = -\frac{1}{\alpha}\iint \ln(1 - \alpha\hat{p})\, dx\, dy \quad [14]$$

In general, it will be necessary to resort to numerical means to

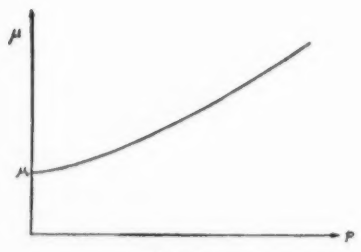

Fig. 2

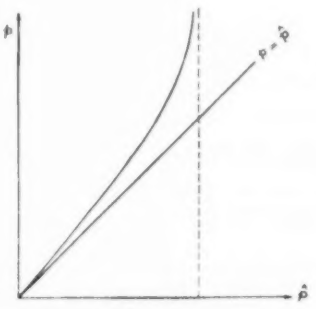

Fig. 3

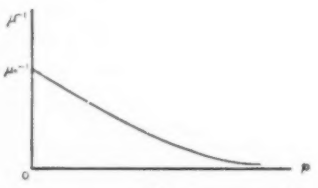

Fig. 4

effect the integration indicated in Equation [14]. However, a useful lower bound can be obtained from the following inequality, reference (7)

$$\frac{1}{A}\int_A \log(1-\alpha\hat{p})\,dA \leqslant \log\left[\frac{1}{A}\int(1-\alpha\hat{p})\,dA\right] \quad [15]$$

This may be written

$$\frac{1}{A}\int_A \log(1-\alpha\hat{p})\,dA \leqslant \log\left[\frac{1}{A}(A-\alpha\hat{W})\right] \quad [16]$$

where $\hat{W} = \int \hat{p}\,dA$ and corresponds to the total load for the case of constant viscosity. Thus

$$W \geqslant -\frac{A}{\alpha}\ln\left(1-\alpha\frac{\hat{W}}{A}\right) \quad [17]$$

The inequality of the type used in Equation [15] is true for the general class of convex functions rather than merely the logarithm function so that any slider-bearing problem having a convex function for $p(\hat{p})$ may be subjected to this treatment. As we have indicated, this is always the case for physically plausible variations of viscosity with pressure.

Other Design Factors

The other design factors such as center of pressure, coefficient of friction, and oil flow may be set up quite easily in terms of the true pressure. The evaluation of the integrals involved, however, is best done by any of the standard numerical methods.

Although the details will not be presented here, the procedure will be exemplified by the calculation for the center of pressure $\bar{x}$. This is given by

$$\bar{x} = \frac{\int\int xp\,dx\,dy}{W} \quad [18]$$

If one substitutes for p its value in terms of $\hat{p}$ in the numerator, it is easy to see how a numerical evaluation may be effected. The denominator which is the total load has been discussed already.

An interesting qualitative result may be obtained regarding the center of pressure. In Fig. 5, there is represented schematically

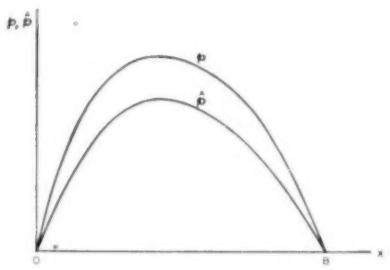

Fig. 5

a section of the slider bearing in the x, z-plane. The distributions of p and $\hat{p}$ are shown. In accordance with Equation [12] $p \geqslant \hat{p}$ and as pointed out herein, the maxima occur at the same value of x. It has been shown by the authors that the effect of increasing the ordinate of the $\hat{p}$-curve by a factor which increases with an increase of $\hat{p}$ is to displace the centroid of the curve toward the position of the maximum ordinate. The proof of this as well as other properties of these curves will appear elsewhere.

Numerical Example

The following example is given by Shaw and Macks (8) for a slider bearing:

B = 2 in.
L = 2 in.
Max film thickness = 0.00059 in.
h_0 = min film thickness = 0.0003 in.
U = 320 ips
$\mu_0 = 5 \times 10^{-6}$ reyn (SAE 20 oil)
Mean bearing temperature = 120 F

Considering viscosity and temperature constant, they find the pressure at the center to be about 8000 psi and a total load of 22,500 lb. This is based on the assumption of no side leakage, and constant viscosity. Considering the slider as finite and the viscosity constant, the Michell solution (4) gives 4730 psi for the center pressure and 9810 lb for the total load. The solution of Charnes and Saibel (4) gives 5050 psi for the pressure and 9650 lb for the total load. According to the work of Hersey and Shore (5) and Dow (9) a medium oil having a viscosity of 5 microreyns at 120 F has a value of α of about 15×10^{-6} in^2/lb. Using this value together with the foregoing data, the pressure at the center is calculated from Equation [10] using the value of $\hat{p}$ from reference (4)

$$p = \frac{1}{\alpha}\ln\frac{1}{1-0.142\dfrac{\alpha\mu_0 UB}{h_0^2}}$$

and is equal to 9450 psi when the variation of viscosity is taken into account.

The total load calculated from Equation [17] gives

$$W \geqslant 12{,}000 \text{ lb}$$

Bibliography

1 "Studies in Lubrication IX," by M. Muskat and H. H. Evinger, *Journal of Applied Physics*, vol. 11, 1940, pp. 739–748.

2 "Theory of Lubrication," by M. D. Hersey, John Wiley & Sons, Inc., New York, N. Y., 1938.

3 "The Theory of Rate Processes," by S. Glasstone, K. Laidler, and H. Eyring, McGraw-Hill Book Company, Inc., New York, N. Y., 1941.

4 "On the Solution of the Reynolds Equation for Slider-Bearing Lubrication," by A. Charnes and E. Saibel, ASME Preprint No. 51—A-43, presented at the Annual Meeting, Atlantic City, N. J., November 25–30, 1951, of The American Society of Mechanical Engineers.

5 "Viscosity of Lubricants Under Pressure," by M. D. Hersey and H. Shore, *Mechanical Engineering*, vol. 50, 1928, pp. 221–232.

6 "Influence of Pressure on Film Viscosity in Heavily Loaded Bearings," by S. J. Needs, Trans. ASME, vol. 60, 1938, p. 347.

7 "Inequalities," by G. H. Hardy, J. E. Littlewood, and G. Polya, Cambridge University Press, London, England, 1934.

8 "Analysis and Lubrication of Bearings," by M. C. Shaw and E. F. Macks, McGraw-Hill Book Company, Inc., New York, N. Y., 1949.

9 "The Effects of Pressure and Temperature on the Viscosity of Lubricating Oils," by R. B. Dow, *Journal of Applied Physics*, vol. 8, 1937, pp. 367–372.

Discussion

By H. Blok.[5] The present paper is thought to be very useful for obtaining a coherent view into the field concerned; this is particularly true if this paper is read in conjunction with the papers to be mentioned in the footnotes.[6,7,8,9]

[5] Professor of Mechanical Engineering, Technical University, Delft, Holland.

The basic transformation indicated by Equation [2] seems to date back to 1925, when it was used by Prof. W. Weibull.[6] It would appear, that, because it is in Swedish, this paper is less known than it deserves; this may explain why repeatedly the transformation has later been arrived at independently by others.

A short abstract of, and some extensions and physical limitations to, the paper of Weibull was recently given in a paper by the writer,[7] which was read before the 1951 Third World Petroleum Congress.

Finally, still more information can be obtained from a paper,[8] which was read by Prof. E. M'Ewen before the recent Gear Lubrication Symposium in London. In this paper the viscosity-pressure function is represented by the power relationship suggested in a paper by Hersey and Lowdenslager,[9] instead of by Weibull's and the authors' exponential relationship. In the discussion to this paper it was pointed out that the two sets of results deduced from the two relationships bear a close similarity to one another if they are expressed in the unifying manner indicated in that discussion.

H. J. Henry.[10] For the design of journal bearings, design factors such as $\mu n/p$, pU together with p are considered. Certain critical values of these design factors for a number of bearing materials have been compiled from values obtained from existing journal bearings that function properly. Bearings designed on the safe side of these design factors on occasion fail. The reason for this failure may be difficult to ascertain. There are perhaps dozens of other design factors which might have been considered, any one of which might have caused the failure.

In the case of slider bearings, we can hope for a more exact analysis to give us more reliable design factors. The usefulness of this analysis, if more reliable design factors are compiled, should be apparent.

The writer would like to ask the authors whether there has been, or is contemplated, any correlation of this work with values of load-carrying capacity obtained experimentally. Certainly the usefulness of this work would be extended.

One inconsistency in the paper is noted. In deriving the relationship for pressure, viscosity at a given temperature is taken as function of pressure. The viscosity certainly varies with temperature as well as pressure. Is it sufficiently accurate to consider the temperature of the oil film as being constant?

Authors' Closure

The authors wish to thank Professor Blok for his interesting and helpful discussion. The transformation used in Equation [1] to relate the problem to that of constant viscosity is a standard one which has been used from earliest times in works on differential equations. It was not the intent of the authors to attribute it to any one in particular in the lubrication field. It is interesting to know that it has been found useful by several authors in this field. As Professor Blok points out, the particular form of the viscosity-pressure relationship does not affect the general conclusions arrived at in the present paper.

In later papers the authors and F. Osterle consider viscosity as a function of both pressure and temperature. This constitutes an adiabatic treatment; the present one is isothermal.

Between the two lies the true situation. Thus in answer to the question of Dr. Henry, there is no inconsistency. The authors contemplate some experimental work in the future and indeed would like very much to see work of this sort carried on in other places too.

[6] "Glidlager-Teori med Variabel Viskositet" ("Theory of Slider Bearings With Variable Viscosity"), by W. Weibull, *Teknisk Tidskrift Mekanik*, vol. 55, 1925, pp. 164–167.

[7] "Viscosity—Temperature—Pressure Relationship," by H. Blok, Proceedings of the Third Works Petroleum Congress, E. J. Brill, Leyden, Holland, 1951, section vii, pp. 304–319.

[8] "Effect of Variation of Viscosity With Pressure on the Load-Carrying Capacity of the Oil Film Between Gear Teeth," by E. M'Ewen, Gear Lubrication Symposium, London, 1952; to be published in the Proceedings of the British Institute of Petroleum.

[9] "Film Thickness Between Gear Teeth—A Graphical Solution of Hallson's Problem," by M. E. Hersey and D. B. Lowdenslager, Trans. ASME, vol. 72, 1950, pp. 1035–1042.

[10] Director of Engineering, Chicago Pneumatic Tool Company, Franklin, Pa.

The Shear-Angle Relationship in Metal Cutting

By M. C. SHAW,[1] N. H. COOK,[2] AND I. FINNIE,[3] CAMBRIDGE, MASS.

The several analytical solutions that have been presented for the shear angle in metal cutting are described briefly and the underlying assumptions critically discussed. The friction process that obtains in cutting is considered in detail and it is shown that a variable restraint and accompanying variation in the effective hardness of the metal cut constitute a major difference between ordinary friction and that between chip and tool. This variation in relative restraint and effective hardness accounts for the wide variation of coefficient of friction with rake angle observed in metal cutting. Furthermore, this variable restraint constitutes a significant connecting link between shear and friction processes, and is responsible for the shear plane not being in the direction of maximum shear stress in the general case. These new concepts are incorporated with the best features of previous work, and an equation is presented, in which the angle between the shear plane and direction of maximum shear stress figures prominently. The new equation for shear angle is illustrated and discussed with the aid of experimental cutting data covering a wide range of operating conditions.

Introduction

ONE of the most important and persistent problems in metal cutting is that of deriving a relationship for the shear angle. When metal is cut a thin and well-defined shear zone is usually observed, which separates the chip from the main body of the workpiece, Fig. 1. The angle ϕ which this shear zone makes with the cutting-velocity vector V is called the shear angle. While the shear angle may be obtained from chip-length measurements or more directly from a photomicrograph, it is important that the relationship between this easily measured angle and other operating variables be known, if full use is to be made of the knowledge afforded by shear-angle measurements.

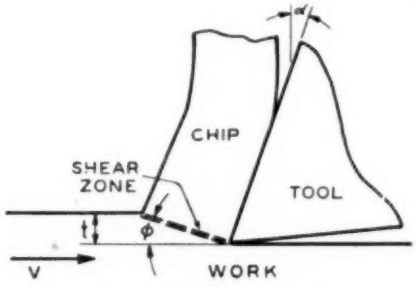

FIG. 1 THE SHEAR ANGLE

Dimensional Analysis

To begin, we might perform a dimensional analysis in an effort to determine the nature of the relationship that is to be expected for ϕ. In addition to ϕ, two quantities are needed to define completely the geometry of the two-dimensional process shown in Fig. 1, namely, the rake angle α and the depth of cut t. Two distinct operations are involved in the cutting process: a shearing action along the shear zone, and sliding with friction along the tool face. The coefficient of friction ($\mu = \tan \beta$) is usually sufficient to characterize a friction process and the shear stress τ will usually characterize the dynamic aspects of a shear process. The cutting velocity V, together with the geometry of the process, will fix the kinematics of the system. It would then appear that the several quantities that might figure in a determination of the angle ϕ are those listed in Table 1, where F, L, and T refer to the fundamental dimensions of force, length, and time. When a dimensional analysis is performed in the usual manner (1)[4] we obtain

$$\phi = \psi(\alpha, \beta) \quad [1]$$

which states that the shear angle ϕ is a function of α and β only.

Review of Past Work

There have been several notable attempts in the past few years to derive a complete physical equation corresponding to Equation [1]. The reasoning followed in these several analyses will next be briefly outlined followed by a discussion of this work.

In 1937 Piispanen (2) presented a graphical analysis for the shear angle, which was equivalent to the second analysis of Merchant given in the following. However, inasmuch as this early work did not lead to an analytical expression it will not be considered further.

In 1941 Ernst and Merchant (3) presented the analysis given in Table 1 for the shear angle.

TABLE 1 DIMENSIONAL ANALYSIS FOR SHEAR ANGLE

Quantity	Symbol	Dimensions
Shear angle	ϕ	...
Rake angle	α	...
Depth of cut	t	L
Friction angle	β	...
Shear stress	τ	FL^{-2}
Cutting velocity	V	LT^{-1}

In Fig. 2 the forces at the point of a tool are shown. Assuming the shear stress on the shear plane τ to be uniformly distributed, it is evident that

$$\tau = \frac{F_s}{A_s} = \frac{R' \cos(\phi + \beta - \alpha) \sin \phi}{A} \quad [2]$$

where A_s and A are the areas of the shear plane and that corre-

[1] Associate Professor of Mechanical Engineering, Massachusetts Institute of Technology. Mem. ASME.

[2] Instructor of Mechanical Engineering, Massachusetts Institute of Technology.

[3] Shell Fellow, Mechanical Engineering Department, Massachusetts Institute of Technology.

Contributed by the Production Engineering Division, Cutting Fluids Research Committee and the ASTM and presented at the Semi-Annual Meeting, Cincinnati, Ohio, June 15–19, 1952, of THE AMERICAN SOCIETY OF MECHANICAL ENGINEERS.

NOTE: Statements and opinions advanced in papers are to be understood as individual expressions of their authors and not those of the Society. Manuscript received at ASME Headquarters, April 28, 1952. Paper No. 52—SA-51.

[4] Numbers in parentheses refer to the Bibliography at the end of the paper.

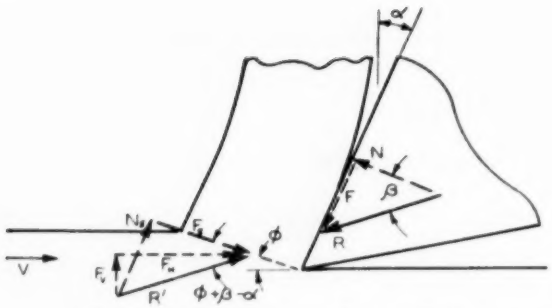

FIG. 2 FORCE RELATIONS AT POINT OF TOOL

sponding to the width b, times the depth of cut t, respectively. Ernst and Merchant reasoned that ϕ should be an angle such that τ would be a maximum, and a relationship for ϕ was obtained by differentiating Equation [2] with respect to ϕ and equating the resulting expression to zero. This led to the result

$$\phi = 45 - \frac{\beta}{2} + \frac{\alpha}{2} \quad [3]$$

However, it is to be noted that in differentiating, both R' and β were considered independent of ϕ.

In 1945 Merchant (4) presented a different derivation that led to Equation [3]. This time, an expression for the total power consumed in the cutting process was first written

$$P = F_s V = \tau A V \frac{\cos(\beta - \alpha)}{\sin\phi \cos(\phi + \beta - \alpha)} \quad [4]$$

It was then reasoned that ϕ would be such that the total power would be a minimum. An expression identical to Equation [3] was obtained when P was differentiated with respect to ϕ, this time considering τ and β to be independent of ϕ.

This is what Piispanen (2) had done previously in a graphical way. However, Piispanen immediately carried this line of reasoning one step further and assumed that the shear stress τ would be influenced directly by normal stress on the shear plane σ as follows

$$\tau = \tau_0 + K\sigma \quad [5]$$

Piispanen then incorporated this observation into his graphical solution for the shear angle.

Upon finding Equation [3] to be in poor agreement with experimental data, Merchant also assumed a relationship as given by Equation [5] and proceeded to work this into his second analysis as follows:

From Fig. 2 it may be seen that

$$\sigma = \tau \tan(\phi + \beta - \alpha) \quad [6]$$

or from Equation [5]

$$\tau = \tau_0 + K\tau \tan(\phi + \beta - \alpha) \quad [7]$$

hence

$$\tau = \frac{\tau_0}{1 - K \tan(\phi + \beta - \alpha)} \quad [8]$$

When this is substituted into Equation [4] we have

$$P = \frac{\tau_0 A V \cos(\beta - \alpha)}{[1 - K \tan(\phi + \beta - \alpha)] \sin\phi \cos(\phi + \beta - \alpha)} \quad [9]$$

Now when P is differentiated with respect to ϕ with τ_0 and β considered independent of ϕ we obtain

$$\phi = \frac{\cot^{-1}(K)}{2} - \frac{\beta}{2} + \frac{\alpha}{2} \quad [10]$$

Merchant called the quantity $\cot^{-1}K$ the "machining constant" C. In Fig. 3 the quantity C is seen to be the angle the assumed line relating τ and σ makes with the τ-axis.

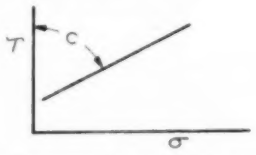

FIG. 3 RELATION BETWEEN FLOW STRESS AND NORMAL STRESS ASSUMED BY PIISPANEN AND MERCHANT

Stabler (5) has presented an analysis of three-dimensional cutting operations in which an expression for shear angle is also presented. When it was assumed that the maximum shear stress on the shear plane and the resultant shear strain were collinear, then it followed from purely geometrical considerations that

$$\phi = 45 - \beta + \frac{\alpha}{2} \quad [11]$$

Lee and Shaffer (6) have derived still other relationships for ϕ. These authors assumed (a) that the material cut behaves as an ideal plastic which does not strain-harden, (b) that the shear plane represents a direction of maximum shear stress in the material cut.

Upon applying the principles of ideal plastic flow, including boundary conditions based both upon the laws of statics and velocity continuity, the slip-line field A-B-C in Fig. 4(a), was obtained. It was found that region A-B-C must be plastically rigid and subject to a uniform state of stress. This means that the stress at any point in A-B-C may be represented by a single Mohr's stress circle diagram. The diagram in Fig. 4(b), in fact, satisfies

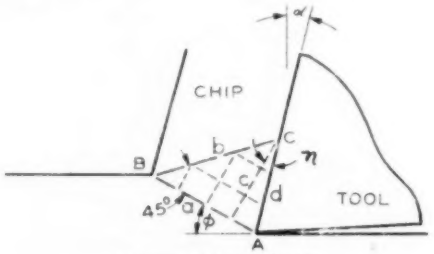

(a) Stress field at tool point

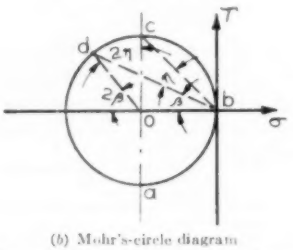

(b) Mohr's-circle diagram

FIG. 4 IDEAL PLASTIC SOLUTION FOR TOOL-POINT STRESS FIELD

all requirements of the ideal plastic solution. Here point a corresponds to the stress on face a in Fig. 4(a), i.e., on the shear plane. This is seen to follow the assumption that the shear plane is a direction of maximum shear stress. Line B-C in Fig. 4(a) is

a line along which the stress is zero. Due to the double-angle feature of Mohr's circle, the zero point of stress b in Fig. 4(b), which is 90 deg from point a, will be but 45 deg from point a in Fig. 4(a). Thus B-C makes an angle of 45 deg with A-B. In a similar way point c in Fig. 4(b) represents the stress on face c in Fig. 4(a), and the stress on the tool face is represented as point d in Fig. 4(b).

From Fig. 4(b) it is seen that angle $dbc = \eta$, since angle $doc = 2\eta$. Therefore

$$\eta = 45 - \beta \quad [12]$$

From Fig. 4(a)

$$\eta = \phi + \alpha \quad [13]$$

and hence from Equations [12] and [13]

$$\phi = 45 - \beta + \alpha \quad [14]$$

It is evident from Fig. 4 that the foregoing ideal plastic solution indicates that the shear stress on the shear plane τ, and the normal stress on the shear plane σ, should be equal. This, however, is generally not the case and hence Equation [14] cannot be regarded as a general solution. Upon finding Equation [14] to be in disagreement with experimental data, Lee and Shaffer (6) assumed that a small built-up edge was normally present and that this built-up edge was responsible for the lack of agreement. They then extended their analysis to include an idealized built-up edge bounded by straight lines and a circular arc as shown in Fig. 5(a). This time the slip-line field consisted of two parts, a rigid region A-B-C and a region of varying stress A-C-F having lines of maximum shear stress (slip lines) consisting of radial lines and circular arcs. The rigid region A-B-C is in a state of uniform stress and hence as before a single Mohr's-circle diagram is applicable for all points within this area. This diagram is given in Fig. 5(b) where τ_1 is the shear-stress axis.

From ideal plastic theory it is found that a slip-line field such as A-C-F has the same shear stress at all points in a given direction relative to the slip lines, but the normal stress varies in proportion to the angle θ turned through in going from point to point. Thus, if the maximum shear stress is taken to be τ_m (where τ_m is the radius of Mohr's circle), then the normal stress on line A-C would be τ_m but that along D-B would be $\tau_m + 2\tau_m\,\theta$ while that along slip line F-B would be $\tau_m + 2\tau_m \binom{2\theta}{3}$. The same Mohr's circle that was used for region A-B-C also can be used for region A-C-F provided the τ-axis is shifted in proportion to angle θ. Thus the stresses for points along line D-B are given by the circle in Fig. 5(b) if the τ-axis is at τ_4, the stresses for points along line F-B are given by the circle if the τ-axis is shifted to τ_3, while the stresses along line A-C (as well as all other points in region A-B-C) are given by the circle when the τ-axis is at τ_1.

From Fig. 5(a) it is evident that

$$\phi = \alpha + \eta + \theta \quad [15]$$

but from Fig. 5(b)

$$\eta = 45 - \beta \quad [16]$$

and hence

$$\phi = 45 + \theta - \beta + \alpha \quad [17]$$

This differs from Equation [14] only by the angle θ, which is a measure of the size of the built-up edge. When there is no built-up edge, θ is zero and Equations [14] and [17] give the same result. From Fig. 5(b) it is evident that

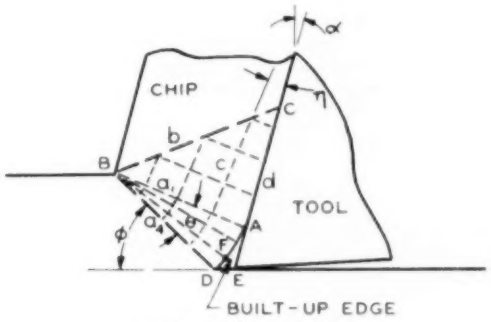

(a) Stress field at tool point

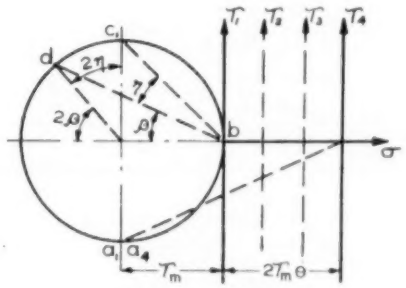

(b) Mohr's-circle diagram

FIG. 5 IDEAL PLASTIC SOLUTION WITH BUILT-UP EDGE PRESENT

$$\sigma = \tau_m(1 + 2\,\theta) \quad [18]$$

$$\tau = \tau_m \quad [19]$$

where σ and τ are the normal and shear stresses on the shear plane, respectively. Combining Equations [18] and [19]

$$\theta = \frac{\frac{\sigma}{\tau} - 1}{2} \quad [20]$$

From this it is evident that σ must no longer be equal to τ as required by the ideal plastic solution without built-up edge. However, it is evident from Equation [20] that the solution with built-up edge requires that σ be greater than τ, for otherwise, θ would be negative and this is physically impossible.

Hucks (7) recently presented a derivation which in many respects is similar to that of Lee and Shaffer, but was obviously arrived at without knowledge of the existence of their solution. Hucks reasoned that the stress between the chip and tool along the tool face could be considered uniform in accordance with the principle of Saint Venant inasmuch as the length of chip-tool contact would be small compared with the distance along the shear plane. Then as usual, he assumed the shear plane to be in the direction of maximum shear stress. Hucks further reasoned that the resistance to flow in the direction of chip motion would be relatively small and thus considered the stress on face b in Fig. 6(a), to be zero. The Mohr's-circle diagram corresponding to this set of assumptions is shown in Fig. 6(b).

Here it is evident that

$$\tan 2\omega = 2\mu \quad [21]$$

where μ is the coefficient of friction on the tool face.

From Fig. 6(a)

$$\phi = \eta + \alpha \quad [22]$$

and from Fig. 6(*b*)

$$\eta + \omega = 45 \text{ deg} \quad [23]$$

Combining Equations [21] to [23] we obtain

$$\phi = 45 - \omega + \alpha \quad [24]$$

where

$$\omega = {}^1/_2 \tan^{-1} 2\mu \quad [25]$$

It may be seen from Fig. 6(*b*) that $\beta > \omega$ and thus Equation [24] will yield values of ϕ that are larger than those obtained from Equation [14].

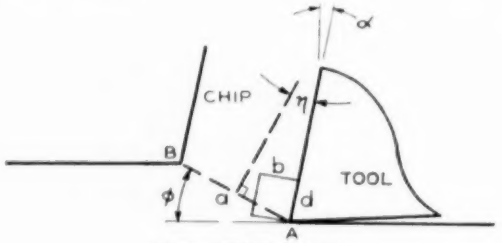

(*a*) Stress field at tool point

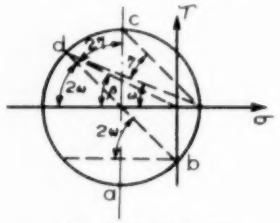

(*b*) Mohr's-circle diagram

FIG. 6 HUCK'S SOLUTION FOR TOOL-POINT STRESS FIELD

In order that the stress on face *b* in Fig. 6(*a*) be zero under all conditions, it is necessary that the τ-axis intersect the stress circle at some point *b*, as in Fig. 6(*b*). This requires that the shear stress on the shear plane τ always be greater than σ the normal stress on the shear plane. Inasmuch as σ is frequently observed to be greater than τ, Hucks' solution cannot be correct, in general.

Hucks (7) also extended the foregoing treatment to include the influence of normal stress on the shear plane. While the origin of the concept that shear strength is dependent upon normal stress is not clear, it was put forth and demonstrated as long ago as 1900 by O. Mohr (8). This idea may be expressed graphically with the aid of Mohr's stress circles as shown in Fig. 7. Here the shear strength is seen to correspond to point A_2 when the shear plane is subjected to a compressive stress but only to stress A_1 when the normal stress is tensile. The solid curve between points A_1 and A_2 is Mohr's strength criterion. It is to be noted that failure does not occur at the point of maximum shear stress, but at an angle ψ from this point on Mohr's stress circle, i.e., at points A_1 and A_2. While Mohr actually suggested that his strength criterion actually might hold for flow stress as well as breaking stress, he did not present any experimental data in support of this extension.

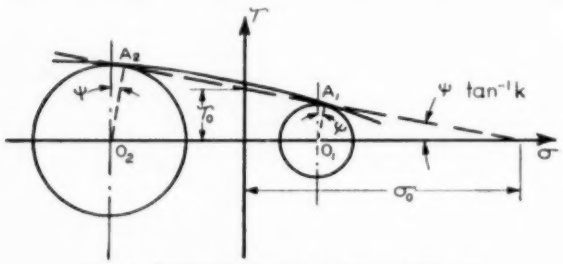

FIG. 7 MOHR'S CRITERION OF SHEAR STRENGTH

Piispanen (2), Merchant (4), and more recently Hucks (7) applied Mohr's strength criterion to the flow stress in metal cutting. If the curve between A_1 and A_2 is assumed to be linear as in Equation [5], (dash line in Fig. 7) then it is evident that

$$\psi = \tan^{-1} K \quad [26]$$

Since ψ is the Mohr's-circle angle between the actual point of failure and that corresponding to the point of maximum shear stress, it is evident that the effect of the assumed variation of flow stress with normal stress upon Fig. 6 would be to move points *a* and *c* counterclockwise through the angle ψ. This will cause 2η to be less by the amount ψ and hence (from Equation [22]) ϕ will be less by the amount $\psi/2$. Thus, when Equation [5] is incorporated into Hucks' solution, we obtain

$$\phi = 45 - \omega + \alpha - \frac{\tan^{-1} K}{2} \quad [27]$$

or

$$\phi = \frac{\cot^{-1} K}{2} - \omega + \alpha \quad [28]$$

where $\cot^{-1} K$ is what Merchant has called the machining constant. If the effect of normal stress also were to be incorporated into the Lee and Shaffer treatment, the effect would be to move *a*, in Fig. 4(*b*), counterclockwise through an angle ψ, away from the point of maximum shear stress, and Equation [14] would become

$$\phi = \frac{\cot^{-1} K}{2} - \beta + \alpha \quad [29]$$

In Table 2 the several equations that have been reviewed in the foregoing section are collected for convenience of reference.

TABLE 2 COLLECTION OF EQUATIONS FOR SHEAR ANGLE WITHOUT A BUILT-UP EDGE

Source	Equation	Equation
Dimensional analysis	[1]	$\phi = \psi(\alpha, \beta)$
Ernst and Merchant	[3]	$\phi = 45 - \beta/2 + \alpha/2$
Merchant	[10]	$\phi = \frac{\cot^{-1} K}{2} - \beta/2 + \alpha/2$
Stabler	[11]	$\phi = 45 - \beta + \alpha/2$
Lee and Shaffer	[14]	$\phi = 45 - \beta + \alpha$
Lee and Shaffer	[17]	$\phi = 45 + \theta - \beta + \alpha^*$
Hucks	[24]	$\phi = 45 - \frac{\tan^{-1} 2\mu}{2} + \alpha$
Hucks	[28]	$\phi = \frac{\cot^{-1} K}{2} - \frac{\tan^{-1} 2\mu}{2} + \alpha$

* With built-up edge of magnitude θ.

DISCUSSION OF PAST WORK

All of the equations in Table 2 are in agreement with the dimensional analysis with the exception of Equations [10] and [28]. These equations include the effect of normal stress on the shear plane, which was not included in the dimensional analysis. However, this does not mean that the dimensional analysis is necessarily incorrect.

When the various equations are tested against a wide range of experimental data, some are found to be in better agreement than others, but none is found to be really satisfactory. When the observed angle ϕ is plotted against $(-\beta + \alpha)$ for a wide

range of rake angles, the points are found to lie along a straight line whose slope indicates that

$$\phi = \text{const} - \beta + \alpha \quad [30]$$

However, the value of the "constant" is not always the same, nor does it correspond to the values given by the equations of Table 2. Before attempting to extend the work that already has been done on this problem it may be well to consider briefly the assumptions on which the several derivations have been based.

In Ernst and Merchant's analysis leading to Equation [3], the following assumptions were made:

1 That the shear stress is a maximum in the direction of the shear plane.

2 That the coefficient of friction is independent of the shear angle.

3 That the resultant force R is independent of the shear angle. All three of these are questionable. Items 1 and 2 will be discussed in the next section; item 3 is obviously incorrect since an examination of cutting data reveals a strong dependence of R on ϕ.

In the second derivation of Equation [3], a different set of assumptions were made as follows:

4 That the angle ϕ is such that the total power is a minimum.

5 That the coefficient of friction is independent of the shear angle.

6 That the shear stress on the shear plane is independent of the shear angle.

There is no clear physical reason why item 4 should be true. Many examples may be found in nature in which nonconservative processes, such as that of metal cutting, clearly occur in such a manner that the energy consumed is not an extreme. It is interesting to note that a minimum-energy principle similar to item 4 was proposed in the 1926 edition of Hütte (9) (but not in subsequent editions), and applied to metal-forming operations. It was apparently this source which led Piispanen to adopt the minimum-energy concept in his calculations. Speaking of the derivation of Equation [3], Hill stated in his recent book (10) on plasticity: "The comparative failure of this theory is almost certainly due to the inadequacy of the minimum-work hypothesis." As already mentioned, item 5 will be discussed later. Assumption 6 is only roughly approximate. The shear stress on the shear plane usually is observed to increase or decrease significantly as the shear angle is decreased.

In deriving Equation [10] assumption 7 which follows was introduced in addition to items 4, 5, and 6.

7 That the flow stress of the metal is increased by the presence of a normal compressive stress on the shear plane.

While it is well established that the rupture stress of both brittle and ductile materials is increased significantly by the presence of a compressive stress, as suggested by Mohr, there is no clear evidence that a similar relationship holds for flow stress as assumed in 7. Although several isolated test results are to be found in the literature which seem to indicate a dependence of flow stress on normal stress, these tests are generally so complex that one cannot be sure that they are being interpreted correctly. On the other hand, several fairly clear-cut experimental observations, such as the fact that the yield points of metals in tension and compression are equal (11), may be cited in support of the view that flow stress is virtually unaffected by normal stress. A thorough discussion of this question would require more space than is available here, and hence will be deferred to a later paper.

As already mentioned, Stabler's Equation [11] is based upon the assumption:

8 That the maximum shear stress and shear strain are collinear on the shear plane in three-dimensional cutting operations. Since it has been demonstrated experimentally in a recent paper (12) that assumption 8 is incorrect, Equation [11] will not be considered further.

In deriving Equation [14] it was assumed that:

9 The material cut is an ideal plastic.

10 The shear plane is along the direction of maximum shear stress. Now, nearly all metals that are machined do not behave as ideal plastics. The strain-hardening that occurs when metals are cut is very important. However, despite this fact, assumption 9 does not lead to a poor approximation for the reason that it is applied only to a region in which the material is essentially rigid, i.e., *A-B-C* in Fig. 4. All of the strain-hardening that takes place occurs as the metal crosses line *A-B*, and this is before the ideal plastic assumption is applied to the material within area *A-B-C*. Equation [14] could be derived directly without introducing the ideal plastic concept by making another assumption that is equivalent to 9, as follows:

11 That a uniform stress field exists in the vicinity of the tool point. This assumption together with 10 will yield the picture shown in Fig. 4, as well as Equation [14]. Assumption 10 will be discussed in detail in the next section.

Equation [17] differs from [14] only by the introduction of a built-up edge. In the treatment of the built-up edge the ideal plastic assumption must be considered as an approximation, since the material within zone *A-B-D* of Fig. 5 is actually highly deformed. However, if the built-up edge is small the degree of approximation associated with assumption 9 is probably slight since area *A-B-D* will then be small compared with *A-B-C*.

In deriving Equation [24] the following assumptions were made:

12 The stresses along the tool face and shear plane are uniformly distributed.

13 The shear plane is along the direction of maximum shear stress.

14 The normal stress on a plane perpendicular to the tool face is zero. Assumption 12 appears to be reasonable as a first approximation. Item 13 will be discussed in the next section. Assumption 14, however, appears to be a purely arbitrary one. While we should expect the normal stress on face (*b*) of Fig. 7 to be low there is no reason why it has to be zero. It would appear better to assume a uniformly stressed area as suggested by the ideal plastic solution (*A-B-C* in Fig. 4), one side of which has a direction such that both the normal and shear stresses are zero simultaneously. If assumption 14 is adopted there is no line corresponding to *B-C* in Fig. 4(*a*) beyond which the stress in the free chip is zero.

Equations [24] and [28] differ only by the introduction of the previously discussed concept of influence of normal stress on flow stress.

From the foregoing discussion of the assumptions on which the several equations for ϕ are based, it would appear that all but Equation [14] should be discarded on the basis of serious objections to the underlying assumptions. However, as noted at the beginning of this section, the constant in Equation [30] is not found to be 45 deg as given in Equation [14], nor, in fact, is it always the same. In the next section we will examine the assumption that the shear plane is in the direction of maximum shear stress to determine if this is responsible for the value of the constant in Equation [30] not always being 45 deg.

Friction and Shear Considerations

The sliding of one dry surface over another is governed by three

so-called laws of friction. These state that the coefficient of sliding friction is independent of the following:

1 Applied load.
2 Sliding velocity.
3 Area of contact.

These general rules hold quite well for dry clean metals sliding in air. However, if we examine dry-cutting data for a given tool-metal combination, obtained using a wide range of rake angles, we find a large variation in the coefficient of friction. It is not uncommon for the coefficient of friction to vary from about 0.5 for a rake angle of —10 deg to about 2.0 for a rake angle of 45 deg when steel is cut with an HSS tool. This represents an increase in the coefficient of friction of 300 per cent. Such a variation is unheard of with ordinary sliding contacts. Thus it would appear that there is a fundamental difference between the friction on a tool face and that between two ordinary sliding contacts.

There is considerable experimental evidence supporting the view that the friction of clean metallic contacts is due primarily to the welding of surface asperities (1, 13). When two clean surfaces are brought together under the action of a normal load, a real area of contact A_r is developed by plastic flow, that is just sufficient to support the load. If the hardness of the metal is τ_H, then the applied load will equal $(\tau_H A_r)$. The friction force will be equal to $(\tau_S \kappa A_r)$, where τ_S is the surface shear stress required to rupture the welds and (κA_r) is the fraction of the real area of contact over which welding has occurred. Then the coefficient of friction μ is

$$\mu = \frac{\tau_S \kappa A_r}{\tau_H A_r} = \frac{\kappa \tau_S}{\tau_H} \quad [31]$$

From this equation it is evident that the coefficient of friction for sliding contacts may be made small by use of the following:

1 A lubricant to decrease κ.[5]
2 Metals for which τ_S is small.
3 Metals that are hard.

[5] The action of a cutting fluid is to react chemically with the chip to form a low-shear-strength nonmetallic solid at the chip-tool interface and thus reduce the real area of metallic contact. Since the shear strength of the nonmetallic material will be small compared with that of the metal we may ignore its effect in computing the fracture force.

For heavily loaded sliding surfaces a solid lubricant may be used to reduce κ, such as that which is produced in situ when an effective extreme-pressure lubricant (cutting fluid) is employed. Inasmuch as the individual weld areas are very tiny, the value of τ_S should correspond to the theoretical strength of the softer and weaker of the sliding pair. This theoretical strength has been shown to be approximately equal to $G/2\pi$ in reference (14), where G is the shear modulus. The value of τ_H will normally be less than the theoretical strength since there is considerable flow in bulk associated with the development of the real area of contact. Therefore we may write Equation [31] as follows

$$\mu = \frac{\kappa G}{2\pi \tau_H} \quad [32]$$

It is evident from this equation that when a given metal is cut in dry air and under a wide variety of conditions, we should expect to obtain a constant coefficient of friction, provided the hardness of the metal remains constant. The fact that μ is not constant for all cutting conditions indicates that the effective hardness of the metal may not always be the same in cutting, even though the material be perfectly homogeneous. In making hardness tests of the Brinell type care must be taken that the specimen tested is sufficiently thick, or else a hardness reading that is too high will be obtained as a result of the restraint introduced by the anvil. Similarly a higher hardness would be indicated under the conditions shown in Fig. 8(*a*) than under the conditions of Fig. 8(*b*). In Fig. 9(*a* and *b*) stress fields of the Lee and Shaffer type are shown for negative and positive-rake tools. In Fig. 9(*c* and *d*) the stress fields are shown with the shear

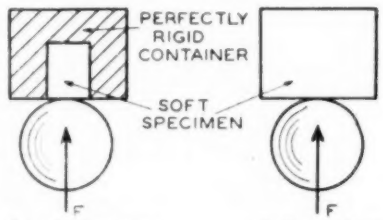

(*a*) Restrained specimen (*b*) Free specimen.

FIG. 8 HARDNESS INDENTATION WITH AND WITHOUT RESTRAINT

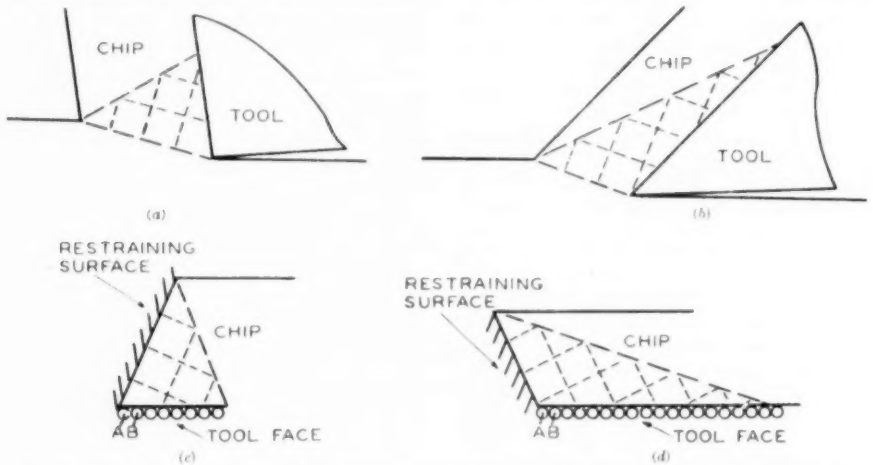

FIG. 9 COMPARISON OF DEGREES OF RESTRAINT TO HARDNESS INDENTATION ON THE TOOL FACE OF NEGATIVE AND POSITIVE RAKE TOOLS

[(*a*) Negative rake angle. (*b*) Positive rake angle. (*c*) Condition of restrain with negative-rake tool. (*d*) Condition of restraint with positive-rake tool.]

planes indicated as rigid restraining surfaces and the tool-face asperities as series of small spheres. The metal at the tool point obviously will resist penetration of sphere A to a greater extent in the case of Fig. 9(c) than 9(d), owing to the relative positions of the restraining surfaces (shear planes). The metal that flows before sphere A must move predominantly to the right in each case because of the asymmetry of the system. Metal flowing from in front of sphere A will move into the way of sphere B and hence the effect of the restraining surface will be transferred from sphere to sphere to the right. It is evident that the influence of the flow from one sphere to the next will be far greater in the case of Fig. 9(c) than 9(d). Therefore, according to Equation [32], the negative-rake tool should operate with a lower coefficient of friction than the positive-rake tool as a result of the difference in restraint.

Thus the coefficient of friction in cutting is influenced by the shape of the stressed zone and hence is a function of the shear angle. Furthermore, it is not permissible to apply coefficients of friction that are obtained in ordinary sliding tests to the cutting process because of the complex way in which the effective hardness which results from variable restraint varies with those cutting conditions that produce a change in the shear angle.

The stress field that exists between the tool face and the shear plane influences not only the coefficient of friction that obtains, but also the direction of the shear plane. If this connecting stress field were not present and the shear process occurred without influence from the friction process we should expect the shear plane

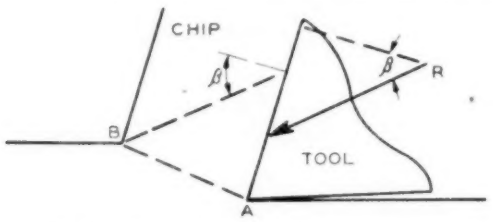

FIG. 10 RESULTANT FORCE AT POINT OF TOOL

to be in the direction of maximum shear stress. However, consider a tool operating with a fixed resultant force R as in Fig. 10, and hence a given coefficient of friction $\mu = \tan \beta$. In order to achieve this value of μ a given effective hardness and hence a given restraint are required. To get this restraint, shear plane A-B must have a particular position which need not correspond to the directions of maximum shear stress.

Thus we have considered the two remaining assumptions from the preceding section and have found that, in general:

1 The coefficient of friction is not independent of the shear angle.

2 The shear plane need not be in the direction of maximum shear stress.

These new concepts will now be incorporated into the theory of cutting.

EXTENSION OF THEORY

When a photomicrograph of a partially formed chip is examined it is found that essentially all of the plastic deformation is confined to a small zone along the "shear plane," and therefore the material between the shear plane and the tool face, across which the cutting force is transmitted, may be regarded as rigid. A good approximation is afforded by the assumption of a uniform state of stress in the region between shear plane and tool face. Furthermore, as in the ideal plastic solution, it seems reasonable to consider the stressed region to be bounded on its third side by a line on which the stress is zero. In view of the arguments presented in the preceding section the shear plane is not assumed to lie in the direction of maximum shear stress.

Because of the assumed uniform state of stress, a single Mohr's stress circle will suffice to give the stresses in all directions at any point in the stressed zone. In Fig. 11 (a, b) the stress field at the point of a tool having a 10-deg rake angle is shown, together with the corresponding Mohr's-circle diagram. Here point a represents the stress on the shear plane, and d the stress on the tool face. The angle between shear plane and direction of maximum shear stress η' has been taken equal to 10 deg, while the friction angle for the tool face β is 35 deg. The resultant forces R and R', the limit line of the stressed zone B-C, and the maximum principal stress are all in the same direction as shown in Fig. 11(a). From Fig. 11(a)

$$\phi = \eta + \alpha + \eta' \quad [33]$$

and

$$\eta = 45 - \beta \quad [34]$$

therefore

$$\phi = 45 + \eta' - \beta + \alpha \quad [35]$$

where η' is considered to be positive when point a is clockwise from the point of maximum stress in a Mohr's-circle diagram such as Fig. 11(b).

Let us next consider, for a given rake angle, the direction in which point a in Fig. 11(b) must move when the coefficient of friction is decreased, as by use of a superior cutting fluid. The first effect such a fluid would have would be to decrease the quantity κ in Equation [32]. This would produce a decrease in β and hence an increase in shear angle ϕ, provided η' is considered unchanged (see Equation [35]). This increase in ϕ would cause an increase in the degree of constraint at the tool point, and hence an increase in the effective hardness of the metal τ_H. The increased hardness would produce a further lowering of β, an increase in ϕ, and so on. Thus it is evident that a condition of instability would result, in which ϕ continued to increase until angle β went to zero, if angle η' were to remain unchanged when β decreased. In order that the increase in ϕ that accompanies a decrease in β be of reasonable amount, it is necessary that η' decrease if positive, or increase if negative when β is decreased. Furthermore, inasmuch as an increase in ϕ is always observed experimentally when β decreases, then from Equation [35] it is evident that the change in η' must be less than the change in β. It is thus seen that a counterclockwise motion of point d in Fig. 11(b) must always be accompanied by a counterclockwise movement of point a of lesser amount, regardless of whether η' is positive or negative.

The tool-point stress fields shown in Fig. 11(c, d) are for cases where the coefficient of friction on the tool face is, respectively, greater and less than that in Fig. 11(a). If the stress pattern in Fig. 11(a) were for a case where a plain mineral oil was used, let us first consider what might happen if no fluid other than air were to be used. The value of κ in Equation [32] would increase and this would result in an increase in the coefficient of friction of from, let us say, $\beta = 35$ to 45 deg as η changes from 10 to 0 deg. Now, this increase in β will cause a lesser increase in η' of, let us say, 5 deg (η' is then 15 deg) and hence from Equation [35]

$$\phi = 45 + 15 - 45 + 10 = 25 \text{ deg}$$

The points with subscript 1 in Fig. 11(b) correspond to the foregoing case of dry cutting, and the corresponding tool-point stress pattern is given in Fig. 11(c).

It should be noted that not all of the 10-deg change in β assumed in the example is due to an increase in κ. A substantial portion will be due to the afore-mentioned decrease in restraint and accompanying decrease in hardness that result from the initial

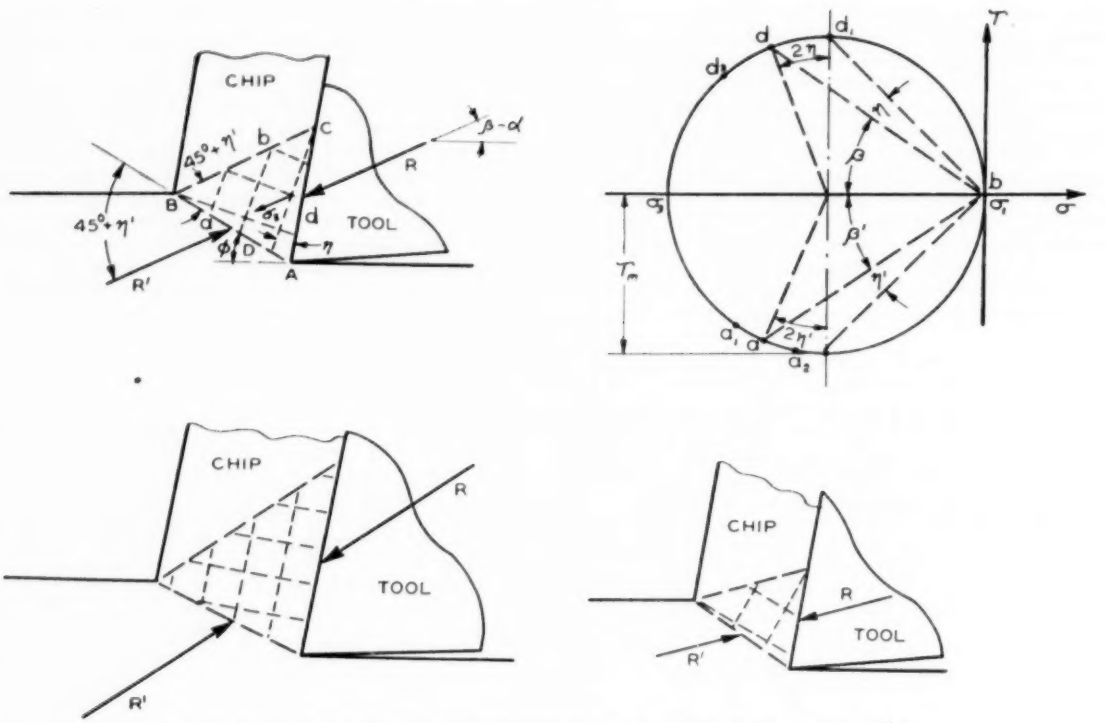

FIG. 11 STRESS FIELD AT TOOL POINT IN VIEW OF NEW CONCEPTS OF FRICTION AND SHEAR

(*a*, Stress field at tool point with medium friction: $\alpha = 10$ deg, $\beta = 35$ deg, $\eta = 10$ deg, $\eta' = 10$ deg. *b*, Mohr's circle diagram. *c*, Stress field at tool point with high friction: $\alpha = 10$ deg, $\beta = 45$ deg, $\eta = 0$ deg, $\eta' = 15$ deg. *d*, Stress field at tool point with low friction: $\alpha = 10$ deg, $\beta = 25$ deg, $\eta = 20$ deg, $\eta' = 5$ deg.)

increase in β due to κ. It is thus evident that in the cutting process small differences in lubrication efficiency are capable of much larger changes in the coefficient of friction than in the case of ordinary sliding contacts, by virtue of the changing condition of restraint.

If, in the example of Fig. 11(*a*), a better fluid had been used which resulted in a decrease in κ, the coefficient of friction could be reduced to 25 deg. As a result, η' should be expected to be less (let us say, 5 deg less, making $\eta' = 5$ deg) and hence from Equation [35]

$$\phi = 45 + 5 - 25 + 10 = 35 \text{ deg}$$

This example is represented by points in Fig. 11(*b*) having subscript 2, and the corresponding tool-point stress pattern is given in Fig. 11(*d*).

In the examples of Fig. 11 the shear stress τ_m (radius of Mohr's circle) was considered to remain constant as the coefficient of friction changed. In practice, τ_m may either increase or decrease when the coefficient of friction for a given tool is decreased (and hence the shear strain γ is decreased). The reason for this situation is to be found in the fact that there are two major items which control τ_m. These are as follows:

1 The degree of strain-hardening the metal undergoes and the shear strain which it obtains.

2 The thickness and character of the shear plane.

If a single stress-strain curve were involved when a given metal was cut, then τ_m would always increase with an increase in shear strain γ owing to strain-hardening. However, it has been shown recently (15, 16) that the thickness and shape of the "shear plane" changes with the coefficient of friction, and this in turn causes τ_m to vary because of a variation in the rate of strain and a size effect. Since it happens that item 2 causes a decrease in τ_m with increased (and hence increased ϕ), it then follows that τ_m may either increase or decrease when β is altered, depending upon the relative magnitudes of the opposite effects due to strain-hardening and change of shear-plane thickness and shape. In most practical cases τ_m is observed to increase with increased coefficient of friction which would indicate that in these cases the strain-hardening effect is predominant.

In Fig. 11 it is evident that the resultant force R becomes more nearly parallel to the cutting velocity vector V and also decreases in magnitude as the coefficient of friction is decreased. Therefore the force component on the tool tending to make it deflect and alter the intended depth of cut decreases with coefficient of friction for a double reason. The tool-force component normal to the velocity vector will become zero when β is just equal to α. Should β become less than α, then the force component normal to V is directed so as to pull the tool into the workpiece. Under certain conditions when $\beta < \alpha$, a condition of instability may be encountered and the tool may dive into the workpiece. For this reason, unless the tool support is very rigid it is advisable that the rake angle not be so large that β becomes less than α.

It is now clear why the result of the dimensional analysis is not in agreement with experimental data. In performing the dimensional analysis, the interrelationship between ϕ and β, which results from a variable restraint, was not recognized and ϕ and β were treated as independent. The angle η' (i.e., the angle between the shear plane and the plane of τ_m) is a measure of the degree of restraint that exists and this angle should have been in-

cluded in the dimensional analysis. When this is done we have

$$\phi = \psi'(\alpha, \beta, \eta') \quad [36]$$

which is obviously now in agreement with Equation [35].

Should a small built-up edge of size θ be present, then the incorporation of the Lee and Shaffer solution including the built-up edge (6) into the foregoing analysis would yield

$$\phi = 45 + \eta' - \beta + (\alpha + \theta) \quad [37]$$

The effect of a built-up edge may thus be thought of merely as an increase in the effective rake angle of θ degrees. However, we do not believe a built-up edge is present whenever the first Lee and Shaffer Equation [14] fails to hold. It will be shown in the next section that under some conditions a negative value of θ is indicated by experimental data when η' in Equation [37] is held to be zero. While a built-up edge corresponding to a negative θ is physically impossible, a negative value of η', on the other hand, is quite feasible.

Experimental Data

In order to illustrate the concepts of the preceding sections, tests were performed using a wide range of rake angles, and at low speed (V = 1 ipm) using four different fluids to provide a varying degree of lubrication. Chip-length measurements were made on annealed and straightened chips. The tools were all HSS two-dimensional planing tools which were lapped carefully after grinding to provide a keen cutting edge. The M.I.T. three-component broaching dynamometer was used to record the two tool forces F_H and F_V. The observed and computed results are given in Table 3 where the following notation is employed:

α = rake angle, deg
t = depth of cut, in.
r_L = chip-length ratio
ϕ = shear angle, deg
γ = shear strain
F_H = force component in V-direction, lb per in. width
F_V = force component normal to V-direction, lb per in. width
τ = mean shear stress on shear plane, psi
σ = mean normal stress on shear plane, psi
μ = coefficient of friction
β = friction angle = $\tan^{-1}\mu$, deg
η = angle between maximum shear direction and tool face
η = 45 — β, deg
η' = angle between maximum shear direction and shear plane
η' = ϕ — 45 + β — α, deg

Only those values are recorded which correspond to a continuous chip, and no built-up edge was evident in any of the tests.

TABLE 3 CUTTING DATA FOR ANNEALED SAE 1112 STEEL—DEPTH OF CUT 0.0030 IN.

Run no.	Fluid	α	r_L	F_H	F_V	ϕ	γ	$\tau \times 10^{-3}$	$\sigma \times 10^{-3}$	μ	β	η	η'
1	Benzene	45	0.602	600	84	36.5	1.20	85.6	84.0	1.33	53.0	—8.0	—0.5
2	Air		0.629	504	46	38.6	1.14	76.1	72.7	1.20	50.2	—5.2	—1.2
3	Ethanol		0.680	374	—6	42.7	1.04	63.1	56.5	0.97	44.1	0.9	—3.2
4	CCl_4		0.739	329	—41	47.4	0.96	62.1	52.5	0.78	37.9	7.1	—4.7
5	Benzene	30	0.380	912	251	22.2	2.31	94.4	72.7	1.01	45.4	—0.4	—7.4
6	Air		0.454	740	142	27.0	1.91	89.9	69.8	0.86	40.9	4.1	—7.1
7	Ethanol		0.521	541	40	31.4	1.66	76.4	54.8	0.68	34.2	10.8	—9.4
8	CCl_4		0.625	437	—30	38.2	1.41	74.9	50.7	0.49	26.1	18.9	—10.7
9	Air	16	0.301	1115	347	17.5	3.20	96.5	66.9	0.66	33.3	11.7	—10.2
10	Ethanol		0.362	850	168	21.1	2.68	87.9	55.6	0.51	27.2	17.8	—12.7
11	CCl_4		0.485	576	19	28.4	2.07	78.9	46.2	0.32	17.9	27.1	—14.7
12	CCl_4	0	0.340	816	108	18.8	3.28	79.2	39.2	0.13	7.6	37.6	—18.8

Discussion

All of the data of Table 3 are shown plotted on the Mohr's circles of Fig. 12. It is evident that when the points d (corresponding to stress on tool face) move counterclockwise, the corresponding points a (i.e., points corresponding to stress on shear plane) rotate through a lesser angle in the same directions. The reason for this has been given already. The values of η' in Fig. 12 all happen to be negative, and to explain these data in terms of the θ of Equation [17] rather than η' involves negative values of θ. As mentioned previously, negative values of θ have no physical meaning.

The lines through the points a (i.e., points corresponding to the stress on the shear plane) in Fig. 12, substantiate the straight lines obtained by Merchant (4) when shear stress was plotted against normal stress on the shear plane for a tool of given rake angle (or for tools of nearly the same rake angle). However, as seen in Fig. 12, a single curve cannot be drawn when τ is plotted against σ for a wide range of rake angles. It would thus appear that the normal stress on the shear plane σ is not responsible for the rise in τ that accompanies a rise in σ. Actually, all points would lie on the arc of a Mohr's circle when τ is plotted against σ, were it not for the fact that τ is not at all constant. The radius of Mohr's circle τ_m changes with several quantities including the rake angle and the degree of frictional resistance on the tool face. When τ is plotted against σ, for a given rake angle, τ_m decreases with a reduction of the coefficient of friction by an amount that is usually just sufficient to yield a curve that is approximately straight rather than the circular arc that would be obtained if τ_m remained constant.

When η' is essentially zero, the plot of τ versus σ for a given rake angle will be a line that is approximately parallel to the σ-

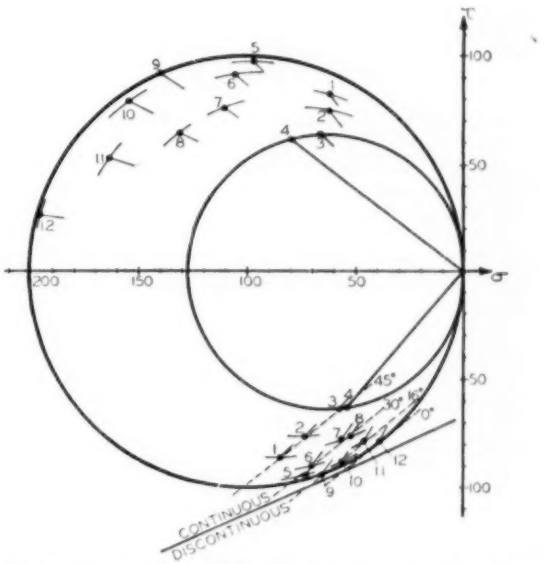

Fig. 12 Mohr's-Circle Diagrams for Data of Table 3

axis. This is illustrated by some data from the literature shown plotted in Fig. 13. Here, data for rake angles of —2 and +10 deg are shown. Point A represents the point of greatest coefficient of friction for the —2-deg-rake tool, and point B is the point

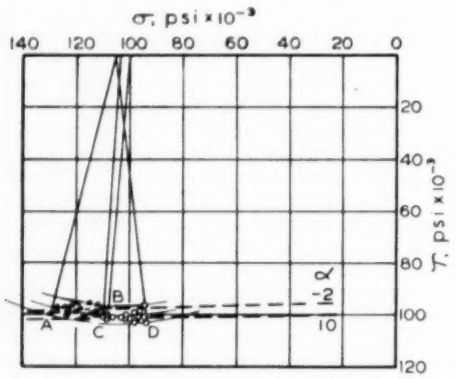

Fig. 13 Chao, Trigger, and Zylstra's Data, Reference 17, for SAE 52100 Steel Cut With Sintered-Carbide Tools of +10-Deg (Open Points) and —2-Deg (Solid Points) Rake-Angle Tools at Several Speeds and Depths of Cut

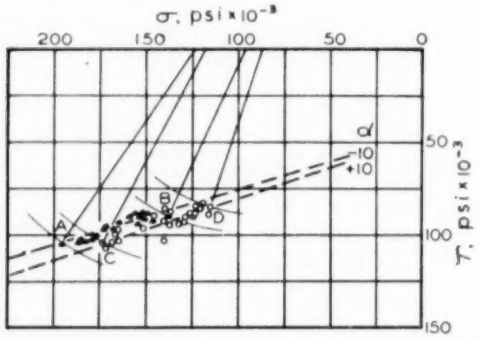

Fig. 14 Merchant's Data, Reference 4, for NE 9445 Steel Cut With Sintered-Carbide Tools of +10-Deg (Open Points) and —10-Deg-(Solid Points) Rake-Angle Tools at Several Speeds and Depths of Cut

of least friction for the same tool. Points C and D are the corresponding points for the 10-deg-rake tool. If the coefficient of friction could have been reduced greatly from the values obtaining in Fig. 13, then τ would have been found to decrease with decrease in σ as in Fig. 12, but not as a result of the decrease in σ.

Similar data from a paper by Merchant (4) are shown in Fig. 14. In this case the values of η' are strongly positive, and again the curve of τ against σ is roughly a straight line, for a given rake angle, for the same reason such a line was obtained in Fig. 12. Point A in Fig. 14 corresponds to the point of greatest coefficient of friction, and point B the point of lowest coefficient of friction for the —10-deg tool. It is to be noted that η' for point B is less than that for point A as it should be. In fact, the points in Figs. 12 to 14 are in agreement with the observation made in a previous section to the effect that η' must decrease if positive and increase if negative whenever the coefficient of friction for a given tool decreases.

In Fig. 15 stress fields at the tool point are shown to scale for the dry tests of Table 3 and those using carbon tetrachloride. It is evident here that F_V becomes negative for large values of rake angle, i.e., when $\beta < \alpha$. These stress fields show the manner in

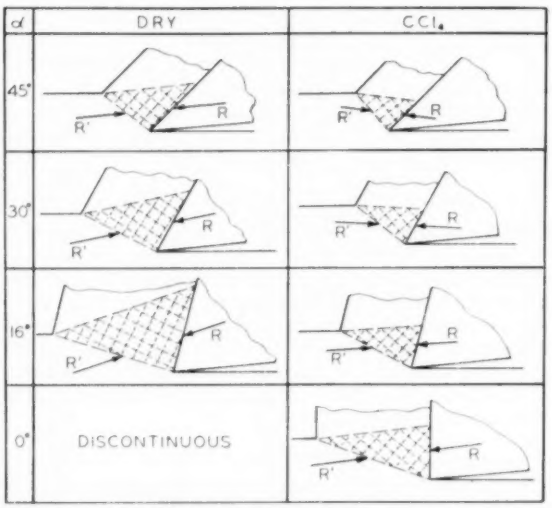

Fig. 15 Stress Fields at Tool Point for Several of the Cutting Conditions in Fig. 12

which the shape of the stressed zone and the magnitude of η' change with rake angle and coefficient of friction.

No stress field is shown for the dry zero-degree-rake tool, inasmuch as the chip produced was discontinuous. Chips were found to become discontinuous at lower values of τ when σ was low, and the solid line shown in Fig. 12 was drawn and indicates the limit of the continuous chip. Here it is seen that the shear strength of the chip along the shear plane increases with the normal stress on the shear plane. This influence of normal stress on shear strength is to be distinguished from the lack of an effect of normal stress on flow stress that has been discussed at several points throughout this paper.

Conclusions

1 Friction encountered in the cutting process is basically different from that for ordinary sliding contacts, owing to a variation of the effective indentation hardness of the metal at the point of the tool under different cutting conditions.

2 There is a significant interrelationship between the shear and friction processes in cutting brought about by the close proximity of the processes and the fact that they are connected by a common stress field.

3 The effective hardness of the chip metal increases as a result of the increased restraint associated with a decrease in the angle between shear plane and tool face.

4 The effective hardness of the chip thus increases with a decrease in rake angle, which in turn gives rise to a significant decrease in the coefficient of friction with decreased rake angle.

5 The interconnection between the shear and friction processes prevents the shear plane from being in the direction of maximum shear stress in the general case.

6 The assumption of a uniform state of stress in the vicinity of the tool point is a good first approximation.

7 Applying the concepts expressed in items 5 and 6, it is found that the shear angle is given by

$$\phi = 45 + \eta' - \beta + \alpha$$

where η' is the angle between the shear plane and the direction of maximum shear stress, and α and β are the rake and friction angles, respectively.

8 It is found experimentally that η' may be either positive or negative and hence the normal stress on the shear plane σ

may be either greater or less than the mean shear stress on the shear plane τ, inasmuch as

$$\frac{\sigma}{\tau} = \tan (45 + \eta')$$

9 It has been shown analytically and demonstrated experimentally that when the friction angle β decreases, η' must decrease if positive but increase if negative, the change in η' being less than the change in β.

10 Experimental data presented for a wide range of cutting conditions show that the mean stress on the shear plane is influenced an insignificant amount by the normal stress on the shear plane.

11 However, the normal stress on the shear plane does play a significant role in determining whether a given chip will be continuous or discontinuous.

Acknowledgments

The authors wish to express their sincere appreciation for a grant from the Shell Oil Company, which was used in connection with this project. They also wish to acknowledge the aid of Messrs. Erwin G. Loewen and Marsbad Hablanian of the Mechanical Engineering Department, Massachusetts Institute of Technology.

Bibliography

1 "Analysis and Lubrication of Bearings," by M. C. Shaw and E. F. Macks, McGraw-Hill Book Company, Inc., New York, N. Y., chapters 3 and 11, 1949.

2 "Lastunmuodostumisen Teoriaa," by Väinö Piispanen, Teknillinen Aikakauslehti, vol. 27, 1937, p. 315.

3 "Chip Formation, Friction and High Quality Machined Surfaces," by H. Ernst and M. E. Merchant, from "Surface Treatment of Metals," Trans. ASM, vol. 29, 1941, pp. 299–378.

4 "Mechanics of the Metal Cutting Process," by M. E. Merchant, *Journal of Applied Physics*, vol. 16, 1945, pp. 267, 318.

5 "The Fundamental Geometry of Cutting Tools," by G. V. Stabler, Proceedings of The Institution of Mechanical Engineers, London, England, vol. 165, 1951, p. 14.

6 "The Theory of Plasticity Applied to a Problem of Machining," by E. H. Lee and B. W. Shaffer, *Journal of Applied Mechanics*, Trans. ASME, vol. 73, 1951, pp. 405–413.

7 "Plastizitätsmechanische Grundlagen und Kenngrössen der Zerspannung," by H. Hucks, Dr. Ing dissertation, Technische Hochschule, Aachen, Germany, February, 1951.

8 "Welche Umstände Bedinger die Elastizitätsgrenze und den Bruch Eines Materiales," by O. Mohr, *Zeitschrift des Vereines deutscher Ingenieure*, vol. 44, 1900, pp. 1524, 1572.

9 "Des Ingenieurs Taschenbuch," edited by Hutte, part I, 1926, p. 349.

10 "The Mathematical Theory of Plasticity," by Rodney Hill, Oxford University Press, Oxford, England, 1950.

11 "The Yield of Mild Steel With Particular Reference to the Effect of Size of Specimen," by J. L. M. Morrison, Proceedings of The Institution of Mechanical Engineers, London, England, vol. 142, 1939, p. 193.

12 "The Mechanics of Three-Dimensional Cutting Operations," M. C. Shaw, N. H. Cook, and P. A. Smith, Trans. ASME, vol. 73, 1951, pp. 1055–1064.

13 "The Friction and Lubrication of Solids," by F. P. Bowden and D. Tabor, Oxford Press, London, England, 1950.

14 "The Size Effect in Metal Cutting," by W. R. Backer, E. R. Marshall, and M. C. Shaw, Trans. ASME, vol. 74, January, 1952, p. 61.

15 "The Rotary Cutting Tool," by M. C. Shaw, P. A. Smith, and N. H. Cook, Trans. ASME, vol. 73, 1951, pp. 1065–1076.

16 "Visual Metal-Cutting Study," by N. H. Cook and M. C. Shaw, *Mechanical Engineering*, vol. 73, 1951, p. 922.

17 "Thermophysical Aspects of Metal Cutting," by B. T. Chao, K. J. Trigger, and L. B. Zylstra, Trans. ASME, vol. 74, August, 1952, pp. 1039–1054.

Discussion

W. R. Backer.[6] In this paper the authors have made a notable contribution to basic metal-cutting research. The shear-angle relationships based on minimum energy or coincidence of the shear-zone inclination with the maximum shear-stress direction have long proved unsatisfactory for the general case. The new theory is a most welcome contribution to the literature.

It is noted that the authors failed to include the normal stress on the shear zone in the list of quantities for their dimensional analysis. Inclusion of this term is justified because it allows shear strains in the chip much larger than those predicted by conventional materials tests, and thus has some control on the strain process of chip formation. If this term is included, another parameter enters the dimensional equation, so that Equation [1] of the paper should read

$$\phi = \phi \left(\alpha, \beta, \frac{\sigma}{\tau} \right)$$

This new dimensional equation is in keeping with the authors' shear-angle theory because, as they point out

$$\frac{\sigma}{\tau} = \tan (45 + \eta')$$

Thus inclusion of the "restraint" indication, η', could have been dimensionally predicted; in fact, the ratio of normal stress to shear stress on the shear plane is itself a "restraint parameter." With the stress-ratio parameter included in the dimensional equation, Equations [10] and [28] of the paper are now in agreement with Equation [1] since the quantity K is a function of this ratio. Naturally, the other theories reviewed cannot be excluded for lack of this ratio, since the dimensional analysis only indicates possible functions, not essential ones.

The writer agrees, in general, with the authors' views on the past shear-angle relationship theories. Merchant's theory incorporating a machining constant, C, Fig. 3 of the paper, has received wide popularity in the past through such publications as the U. S. Air Force Machinability Research books, the Tool Engineers Handbook, and recent verification of the existence of such a constant by Trigger, Chao, and Zylstra.[7] Merchant claimed the existence of such a constant because of an effect found by Bridgman on drill rod. It is interesting to note that Bridgman, in the same report, found no effect on 1045 steel, but Merchant presents a machining constant for 1045 steel.[8] In light of the new theory, Merchant's constant takes on a new meaning. Combining Equations [10] and [35] of the paper, it can be shown that

$$45 + \eta' = C' - \phi$$

Since η' is a measure of restraint, and a function of ϕ as explained by the authors, the foregoing equation shows the nature of this relationship, with the machining constant acting as a limit on the restraint for any given material. The mentioned experimental proof of the existence of C' then makes Merchant's equation an empirical relationship for the η' and ϕ equation. However, the writer has found that C' is not a constant over a wide range of variables, an observation substantiated by the authors' data in Table 3.

The data provided in Table 3 illustrate but do not prove the new shear-angle theory unless other data were taken and not recorded. Proof requires an independent measure of η' which must then fit Equation [35] or [37]. If the points in Fig. 12 of the paper, for stress on the tool face are computed from dynamometer data plus contact-area measurement, then Fig. 12 is sufficient proof. However, it appears that these points for face stress were placed by drawing a circle through the points for the shear zone

[6] Research Engineer, Boeing Airplane Company, Seattle, Wash.

[7] Authors' reference (17).

[8] "Tool Engineers Handbook," McGraw-Hill Book Company, New York, N. Y., 1949, p. 314.

and the origin, then locating the points for the tool face on this circle, using the friction angle found from dynamometer data. It is hoped that the authors will provide verification for their theory; indirect tests of hardness versus restraint are one possibility, but the more direct method of chip contact-area measurement seems more promising.

Since no stress exists in the chip above point C in Fig. 11, it would appear that an accurate measure of distance A-C is possible by microscopic examination of a tool as done by Chao and Trigger.[9] The distance A-C is also obtainable by dynamometer data plus the chip-length ratio, employing Equation [35]. Values of ϕ and β are obtained in the usual way. This determines η and η'. By geometry, denoting the feed by t

$$AC = \frac{t \quad \sin (45 + \eta')}{\sin \phi \ \sin (45 + \eta)}$$

An equivalent check would be using the contact area to determine the stresses on the tool face as mentioned previously.

Orthogonal cutting data are available in the literature[9] for computing distance A-C. Unfortunately, the data do not cover a wide range of variables, but when A-C is computed as outlined, the discrepancy between the computed and measured values (the measured area of contact is divided by the chip width to give the contact length) is about 2 to 1. The added graph, Fig. 16 of this

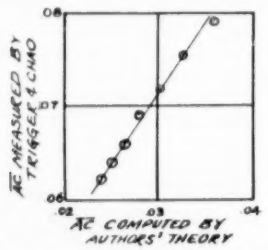

Fig. 16 Measured and Computed Values of Chip-Contact Length

discussion, shows the values obtained. It is interesting to note that a straight line is obtained, indicating a close correlation between these values. It does not appear likely that the chip would continue to rub the tool face hard enough to make an observable contact area in a region where the stress is essentially zero.

If the authors can revise their theory to include the true prediction of chip-contact area, the value of their shear-zone-angle equation will be enhanced greatly in that a basis for analytical evaluation of cutting temperatures will be available. This could lead the way to prediction of tool life from a few basic screening tests.

R. S. Hahn.[10] The authors have presented an excellent survey of the various metal-cutting theories and are to be encouraged in their fundamental studies of metal cutting.

There are several points, however, that warrant discussion.

The authors introduce the concept of restraint of the chip against the shear plane. This is then used, in effect, to explain the large observed increase in coefficient of friction on the tool face at high rake angles. There are several features about this theory that do not seem proper. Furthermore, as will be shown, a much simpler explanation of the rising tool-face friction at high rake angles can be given.

1 The restraint shown in Fig. 8 of the paper is valid; but if the specimen were hard and the container soft it would not be. The chip has been assumed to be rigid (and is highly work-hardened) and the restraining surface in Fig. 9 has not been cut yet and is relatively soft and consequently would not seem to be analogous to Fig. 8 and the degree of restraint questionable.

2 In the usual friction tests the real area of contact is very small compared to the apparent area of contact. As a result the coefficient of friction is practically independent of the apparent area. In metal cutting the real area of contact on the tool face is probably approaching closely the apparent area. Consequently, we should expect the friction force on the tool face to increase with the area of contact. Stated another way, we might expect the frictional stress on the tool face to remain constant as the area of contact varies. It will be found that the length of contact A-C, Fig. 11(a) of the paper, is given by

$$l = \frac{t \sin (\beta + \varphi - \alpha)}{\cos \beta \sin \varphi}$$

Using the authors' data in Table 3 and dividing the friction force by l to get the frictional stress (unit width assumed) gives the curves shown in Fig. 17, herewith. It will be seen that for air and ethanol, between 16 and 30-deg rake angle, the stress is practically constant.

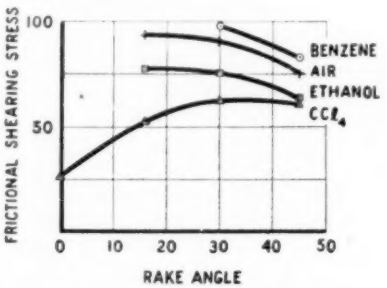

Fig. 17 Frictional Shearing Stress Versus Rake Angle

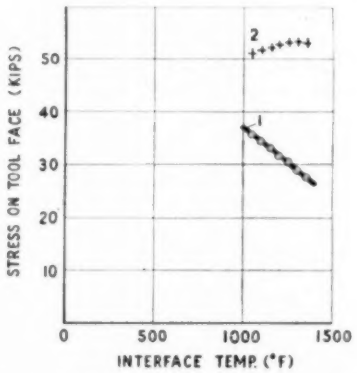

Fig. 18 Average Frictional Shearing Stress and Normal Stress at Tool-Chip Interface Versus Average Interface Temperature

(Curve 1, frictional shearing stress. Curve 2, normal stress.)

It may be interesting to recall the results of Chao and Trigger.[9] In the discussion of their paper by this writer, it was shown, using their data, that the frictional stress varied linearly with temperature as indicated in Fig. 18, herewith. Perhaps we should give

[9] "Cutting Temperatures and Metal-Cutting Phenomena," by B. T. Chao and K. J. Trigger, Trans. ASME, vol. 73, 1951, pp. 777–793.

[10] Consulting Engineer, The Heald Machine Company, Worcester, Mass. Mem. ASME.

more attention to the frictional stress and the tool-chip contact area and pay less attention to the coefficient of friction.

In view of the foregoing, the variation in coefficient of friction with rake angle can be explained in terms other than restraint, namely, frictional stress and tool-chip contact area.

Another feature of the authors' theory is that they have introduced an angle η' giving the direction of maximum shear stress relative to the shear plane. Since the direction of shear shifts from the direction of maximum stress in one sense in the tensile test and in the opposite in the compression test it would seem unnatural to have positive and negative values of η' occurring in metal cutting where the stress field is always compressive.

E. K. Henriksen.[11] This problem seems to become more and more complicated each time it is being attacked, and the authors have presented a new solution, which represents one further step ahead, although perhaps, it may not be the last word.

Another valuable feature of the paper is the clear tabulation and the detailed discussion of previous work in this field. The authors should be congratulated for the manner in which they have had the understanding to bring basic physical facts into the problem in order to explain and visualize the new solution.

E. H. Lee.[12] The authors are to be congratulated on presenting an interesting comparison of present theories of machining, and on providing new experimental results to check their validity. When these results are plotted using the co-ordinates suggested by Merchant ($\beta - \alpha$, ϕ) these new results lie well below previously published experimental results, and the values given by the earlier theories. In particular, they are far away from Merchant's[13] often quoted experimental results which have been confirmed by other workers. To the writer's knowledge in previously published work, positive η' has always been reported, which represents this discrepancy. Can the authors give any reason for this large difference in experimental results?

The discussion of the assumption of ideal plasticity seems somewhat restrictive. This assumption does not imply that work-hardening and strain-rate effects are neglected, but that they are averaged over the field, an appropriate yield stress being used (not necessarily that associated with cold static testing). This point is emphasized in work by Shaffer and the writer.[14,15] References[14] are given to dynamic test results which show close agreement with the ideally plastic assumption with an appropriately raised yield stress.

The criticism of a minimum-energy assumption seems too strong. If a complete theory leads to lack of uniqueness of solution, then minimum energy, or minimum force will commonly decide the correct solution. This is the usual problem of stability of a system. Hill's criticism arises since Merchant's analysis is not a complete theory, but neglects stress considerations. Minimum energy would be operative with these included, and, in fact, leads to the composite solution of Lee and Shaffer.[14]

Some of the comments in the paper concerning dimensional analysis seem to be open to misinterpretation. Equation [1] follows from such an analysis if α and β are the only nondimensional parameters occurring. If another nondimensional factor is introduced, for example κ, the hydrostatic pressure coefficient of Equation [5], this must also appear in the dimensional analysis and Equations [10] and [28] of the paper are in agreement with a correct dimensional analysis.[16] No difficulty arises as suggested by the authors. If η' is introduced instead of κ, Equation [36] arises, which contains three possible independent parameters and greater freedom than is expressed in Equation [1], not less freedom as indicated by a relation between ϕ and β as mentioned.

The discussion of friction and restraint appears to leave open a number of questions. The field shown in Fig. 9(*b*) of the paper is not in accordance with the theory by Shaffer and the writer.[14] This would imply a coefficient of friction greater than 1, and shear failure in the chip would be expected to determine a solution corresponding to unit coefficient of friction. Thus the difference in "restraint" will then be much less marked than that indicated in Figs. 9(*c* and *d*). The assumption that the shear plane behaves as a rigid restraining surface seems open to question since the material below it has not been strained appreciably and so may be softer and provide less restraint rather than more. This would reverse the discussion completely. Moreover, the use of the theoretical strength $G/2\pi$ in shear is believed to be at wide variance with physically measured stresses.

In spite of these queries the paper certainly introduces many important questions. The theory discussed by the writer[14] leads to Equation [30] with a constant other than 45 deg, but always with a nonnegative η', as indicated in Fig. 12 of the paper cited.[14] The integration of this with the new experimental results certainly poses an important problem.

B. W. Shaffer.[17] As usual, the authors have done a fine job of presenting their ideas on metal cutting. Nevertheless, the writer desires to add to their discussion of past work, and to comment on their experimental findings.

In the analysis of the machining process described by Lee and Shaffer,[14] it was shown that the solution to the problem is given by that configuration which would result in a minimum machining force, and a satisfactory stress distribution within the chip. The stresses induced in the chip are considered satisfactory whenever the yield point of the material being cut is not exceeded.

If we check the stress distribution associated with the Ernst and Merchant[18] analysis, given as Equation [3] in the paper, then we find that their solution can be applied to the simple shearing process whenever the friction angle is less than the rake angle. For then, the stress components do not exceed the yield condition. Their analysis, however, is not applicable for the more common case, where the friction angle is greater than the rake angle, because then the stress distribution associated with their solution is no longer satisfactory.

In view of this, Lee and Shaffer proceeded to find Equation [14] based on the maximum permissible stress distribution within the chip.

Even this new equation, it was found, did not hold over the entire remaining range of variables, because, for small or negative rake angles and high friction, the associated expressions for machining force and chip-thickness ratio would become infinitely large. This, we know, does not happen in practice. In fact, for such conditions, the development of a built-up nose usually is

[11] Professor-in-Charge, Materials Processing Department, Cornell University, Ithaca, N. Y.

[12] Professor of Applied Mathematics, Brown University, Providence, R. I. Mem. ASME.

[13] "Mechanics of the Metal Cutting Process. II. Plasticity Conditions in Orthogonal Cutting," by M. E. Merchant, *Journal of Applied Physics*, vol. 16, 1945, pp. 318–324.

[14] "The Theory of Plasticity Applied to a Problem of Machining," by E. H. Lee and B. W. Shaffer, *Journal of Applied Mechanics*, Trans. ASME, vol. 73, 1951, pp. 405–413.

[15] "The Theoretical Analysis of Metal-Forming Problems in Plane Strain," by E. H. Lee, *Journal of Applied Mechanics*, Trans. ASME, vol. 74, March, 1952, pp. 97–103.

[16] "A Dimensional Analysis of Metal Cutting," by D. C. Drucker and H. Ekstein, *Journal of Applied Physics*, vol. 21, 1950, pp. 104–107.

[17] Assistant Professor of Mechanical Engineering, New York University, New York, N. Y. Jun. ASME.

[18] Footnote 13, pp. 267–275, 318–324, and authors' reference (3).

observed. Certainly then, the next step was to seek a solution which would explain this phenomenon.

This solution was found, and is also described by Lee and Shaffer.[14] According to the analysis, the expression for machining force, within a prescribed range of variables, was less with a built-up nose than without one. Therefore, within this range, it is the solution of the machining problem.

The presence of the built-up nose, as we have just seen, was arrived at as a natural consequence of the analysis, and not as stated in the paper, that "upon finding Equation [14] to be in disagreement with experimental data, Lee and Shaffer assumed that a small built-up edge was normally present and that this built-up edge was responsible for the lack of agreement."

Let us now re-examine the limiting and nonlimiting stress solutions to the simple shearing process. The limiting stress solution refers to the case where the chip stress just satisfies the yield condition, while the nonlimiting solution refers to the case where the chip stresses are less than those associated with the yield condition.

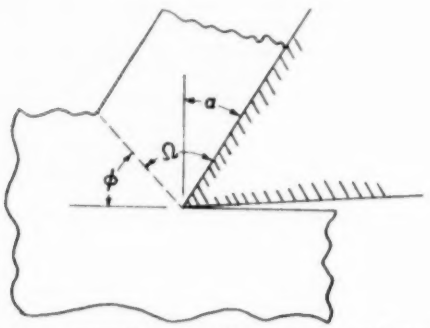

FIG. 19 RELATIONSHIP BETWEEN WEDGE ANGLE AND SHEAR ANGLE

From the geometry of Fig. 19 it can be seen that the wedge angle

$$\Omega = \frac{\pi}{2} + \alpha - \varphi \quad \ldots\ldots [38]$$

According to the limiting stress solution, given by Equation [14] of the text

$$\varphi = \frac{\pi}{4} - \beta + \alpha \quad \ldots\ldots [39]$$

and the corresponding wedge angle

$$\Omega_{\min} = \frac{\pi}{4} + \beta \quad \ldots\ldots [40]$$

is the minimum permissible for the simple shearing process.

If we are given another expression for the shear angle then it would be satisfactory, and represent an example of the nonlimiting stress solution, whenever the corresponding Ω is greater than that given by Equation [40]. The Ernst and Merchant solution satisfies this requirement whenever the friction angle is less than the rake angle.

For the shear-angle relationship

$$\varphi = \frac{\pi}{4} + \eta' - \beta + \alpha \quad \ldots\ldots [41]$$

given as Equation [35] in the paper, the corresponding wedge angle

$$\Omega = \frac{\pi}{4} + \beta - \eta' \quad \ldots\ldots [42]$$

Obviously, Equation [42] is greater than Equation [40], and therefore, a satisfactory nonlimiting stress solution, whenever η' is negative.

If we examine the experimental results shown in Table 3 of the paper, we find, for each case shown, η' was negative. However, these experimental results do not agree with the existing nonlimiting stress solution. Therefore the writer proposes that the correction suggested by the authors be thought of as a modification of the nonlimiting stress solution.

In the section of the paper entitled Discussion, the authors indicate that η' may be strongly positive, and refer to data published by Merchant. These same data were re-examined previously by Lee and Shaffer,[14] and it was found that all the data published in Merchant's paper fell within the built-up nose region. In fact the "average data" corresponded to the condition coefficient of friction equal to unity at the chip-tool interface, and under the built-up nose. When the deformation of an initially squared grid was studied for this case, shown as Fig. 13 in the Lee and Shaffer paper,[14] it was found that the size of the built-up nose was very small, and therefore easily could have been overlooked.

Referring to Fig. 9 of the paper, where η is shown to be negative (the angle η is defined in Fig. 4(a)), we can see by making use of the Mohr's circle diagram, Fig. 4(b), that negative values of η correspond to friction angles which are greater than 1. However, for the simple shearing process, shear failure rather than friction occurs at the tool-chip interface whenever the friction angle is greater than $\pi/4$. Therefore negative values of η should not have been shown.

Incidentally, the angle referred to as φ in Equation [17] does not have the same meaning as the shear angle φ referred to in the rest of the paper.

E. G. THOMSEN.[19] The authors are to be commended for their excellent analysis.

The arguments presented by the authors that the directions of maximum shear stress and shear plane are noncolinear are persuasive. In support of this hypothesis similar noncolinearity in metal cutting was reported as a probability by Ernst[20] in 1944. For deformation processes other than metal cutting, noncollinearity between maximum shear stress and shear directions may occur and has been observed with single crystals under various controlled applications of loading and with highly anisotropic polycrystalline metals. Polycrystalline metals with random orientation of grains, however, normally behave isotropically in the annealed state, but during severe deformation processes, such as rolling or torsion, for example, may develop anisotropy during the deformation process. Hence an initially isotropic metal may exhibit various kinds of anisotropy depending on the kind and extent of deformation.

In line with this thought the authors' data may be tested for anisotropy. Referring to Table 3 of the paper it is seen that η', which measures the angular departure of the shear plane from the maximum shear direction in their analysis is negative and hence unidirectional for all test conditions investigated. For the same tests the angle ϕ varies over the range from 17.5 to 47.4 deg. If it is assumed that the work-surface orientation was identical for all cutting tests, then the initial anisotropy should have caused some of the angles η' to be positive. Since no such values are observed, it may be concluded that the initial anisotropy is inactive in

[19] Associate Professor of Mechanical Engineering, University of California, Berkeley, Calif.

[20] "High Speed Milling With Negative Rake Angles," by Hans Ernst, *Mechanical Engineering*, vol. 66, 1944, pp. 295–299.

causing the angle of departure η' to be different from zero, or if present the effect is masked by another effect, possibly the anisotropy developed during plastic deformation itself. Inasmuch as the degree and kind of anisotropy developed are not known, a definite statement cannot be made in support of the authors' hypothesis nor can it be denied on the basis of anisotropy alone. It is questionable, however, that such a large angle $\eta' = -18.8$ deg as was obtained with $\alpha = 0$ and CCl_4 can be accounted for by this factor alone. In our search for support or rejection of the authors' theory we may ask next whether or not η' is a real angle subject to physical measurements, or only a figment of the imagination. It may be recalled that η' appears in essence as a correction factor applied in order that the angular relationship of Equation [35] of the paper is satisfied. Let us examine the validity of this assumption.

It appears to this writer that the assumptions of the Lee and Shaffer formulation and its extension most certainly represent an oversimplification of what is a complex mechanical process. The writer agrees that the constant-stress hypothesis is a reasonable first approximation. It describes the state of stress within the metal entrapped momentarily between the tool face and the shear plane, permitting the formulation of a simple theory. He feels, however, that such a simplifying assumption is undesirable if it requires in turn the explanation that the shearing process differs from those normally observed in deformation processes. It is, therefore, instructive to consider other factors which might possibly influence the angle relationship between ϕ, β, and α. In order to do this let us consider first the method by which these angles are measured. Such considerations will reveal at once that ϕ and α are measured from the cutting ratio and the rake angle, respectively, and their determination does not depend on the tool forces. The angle β, however, is the angle which is calculated from the measured tool forces. These forces, moreover, represent an over-all effect and it is not possible to say which portions of the forces are keeping the chip in static equilibrium and which the workpiece. An attempt of correcting measured dynamometer forces for workpiece deformation has been suggested by this discusser and others in the paper by E. G. Thomsen, J. T. Lapsley, Jr., and R. C. Grassi.[21]

The other factor which comes to mind, and which possibly may affect the angular relationship between the various angles, is the condition of the constancy of stress mentioned earlier. This hypothetical condition is not required for the force system to keep the chip in static equilibrium. It is easy to show that the resultant force, which is at an angle of $(\phi + \beta' - \alpha = 45 + \eta')$ to the shear plane does not require a constant stress in the metal on the shear plane nor in that located along the tool face. The condition for this angle to be 45 deg or 45 deg $+ \eta'$ is, therefore, arbitrary if we do not insist on the condition of constancy of stress.

The restraint which is imposed on the shearing process by the entrapped metal between shear plane and tool face certainly seems reasonable. This at once, however, raises the question of how the stress is distributed. Most certainly a high triaxiality of stress must exist at the tool point. At the free surfaces of the chip and workpiece, on the other hand, some of the normal stresses are zero; hence biaxial states of stress must exist. Because of this complexity and others it is not possible to say where the maximum shear stress resides and what its magnitude and direction locally may be. Thus detailed analysis of the shear process with average stresses calculated from nominal tool forces appears to the writer to be somewhat hazardous.

In connection with the restraint effect, it is interesting to note

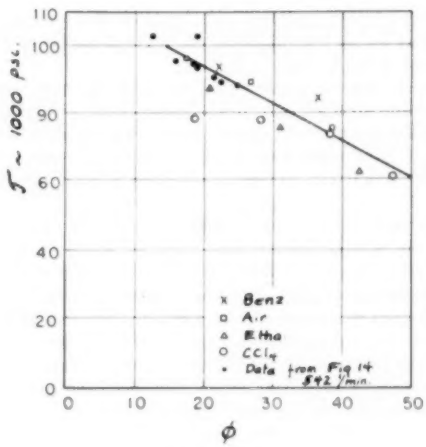

Fig. 20

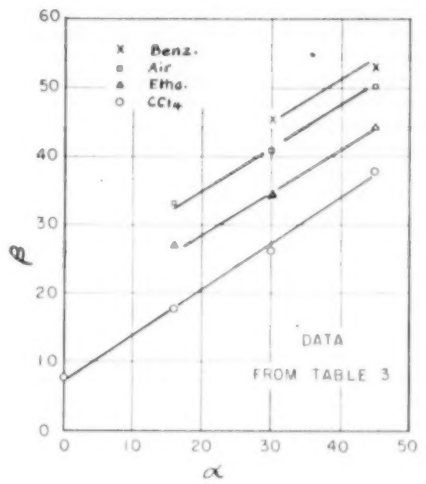

Fig. 21

that the nominal shear stress on the shear plane is, roughly speaking, a linear function of the shear angle ϕ. This relationship is shown in Fig. 20 of this discussion. It appears, therefore, that the restraint or state of stress depends on the combined effect of α and β. It is also interesting to note that the nominal friction angle is a linear function of α for each particular cutting condition given in Fig. 21. These relationships appear to be promising for exploration in order to find the phenomenological relationships between the various angles.

Authors' Closure

The authors sincerely thank the discussers for their time and effort, and hope that the following will tend to answer their questions.

As is pointed out by Backer, there is a simple geometrical relationship between η' and the ratio σ/τ. However, the authors feel that this particular ratio has no direct effect upon a continuous cutting operation, because there is considerable experimental evidence showing no effect of σ upon the subfracture flow stress τ. When the data in Table 3 of the paper were taken, the contact areas were measured. With either CCl_4 or ethanol, the

[21] "Deformation Work Absorbed by the Workpiece During Metal Cutting," by E. G. Thomsen, J. T. Lapsley, Jr., and R. C. Grassi, ASME Paper No. 52—F-24.

agreement between predicted and measured area was almost too good, while for air and benzene, the measured area was greater by a factor of 1.5 to 2.5.

The shear plane is considered to be a plane or thin zone which separates the strained chip from the unstrained workpiece. A rigid retaining surface is a surface across which there is no motion or strain. By definition there can be no strain across the shear plane and thus it can be considered to be a rigid retaining surface.

As yet there is no clear understanding of why the direction of shear shifts from the direction of maximum stress in tension and compression tests. Thus it is difficult to say whether or not it should shift one way or the other in metal cutting. However, it is important to note that even in the usual materials tests, the directions of maximum stress and strain are not coincident.

The apparent reason why the values of η' obtained by the authors were negative while most published values are positive is that the authors' data were obtained at extremely low cutting speeds. The speed of 1 ipm was used to minimize temperature effects. It should be noted that the friction conditions at the chip-tool interface can vary appreciably with speed.

In ideal plasticity the use of an appropriately raised yield stress is reasonable. However, the assumption of a homogeneous isotropic material leads to serious question in the case of metal cutting. As the result of a metal-cutting analysis is an angle ϕ, it would appear that the directional properties of the chip-workpiece combination should influence the result.

It is found that the principle of minimum energy holds in many cases; however, it does not hold in just as many cases. Indeed, sometimes stability of a system is reached at a point of maximum energy. It does not appear that there is any method to determine when such a principle can be applied.

There is no reason to believe that a coefficient of friction greater than 1 should lead to shear failure within the chip. Large coefficients of friction are frequently obtained in metal cutting with no BUE.

It is quite simple to demonstrate that with clean, smooth surfaces the coefficient of friction can be infinite. When such a case is approached it is evident that friction stress will have meaning while the coefficient of friction will not.

The authors contend that a coefficient of friction greater than unity does not mean that a built-up edge is present. For each data point in Table 3 the cut was stopped and a photomicrograph was made of the area under question. In no case was there a built-up edge. Perhaps it should be pointed out that just because a set of data does not agree with the ideal plastic theory, the data are not necessarily incorrect.

The theoretical shear stress $G/(2\pi)$ is approached in extremely small specimens. How closely it is approached in metal cutting depends of course upon the size of the contacting asperities at the chip-tool interface.

It is certainly agreed that all of the present analyses of metal cutting are undoubtedly oversimplifications of a very complex problem. However, until a more general solution is obtained, attempts to revamp existing theories undoubtedly will lead to a clearer understanding of the entire process.

Comparisons at Elevated Temperatures of Some Commercial Grades of Ferritic Cast Steels

By H. W. WYATT,[1] J. W. BOLTON,[2] AND M. L. STEINBUCH,[2] CINCINNATI, OHIO

This paper presents some direct elevated-temperature test comparisons of cast steel Grades WC4, WC5, WC6, and WC9 of ASTM Specification A217-49T. The materials studied are from commercial heats. Care has been taken to hold all variables in manufacture, treatment, and composition (aside from prescribed "alloy elements") as closely alike as possible. The tests show that at the temperatures under consideration the nominal 1 per cent molybdenum grades WC5 and WC9 are higher in "creep strength" than the nominal $^1/_2$ per cent molybdenum grades, WC4 and WC6. Grade WC5 has shown, in this direct comparison, higher "stress-rupture strength" than the other three grades.

Conditions of Tests

WIDELY variant results had been reported by various sources for some of the grades of cast steel, as tested at elevated temperatures. For example, creep strength values varying almost 500 per cent from minimum to maximum at a given temperature have been reported for Grade WC6.

It seems obvious that such large variations in reported properties for a given composition or grade must be brought about by differences in preparation and treatment. Since chemical composition is but one among those variables which affect creep and other characteristics, a comparison of compositions must hold variables of preparation and of treatment to a minimum. In the present case, it is desired to ascertain the effects of alloy elements (molybdenum, chromium, and nickel). Therefore compositions, aside from these alloy elements, also must be held within close limits.

If test values are to have practical engineering significance, conditions of preparation and treatment should correspond to those of commercial practice. Since the grades under consideration are those within an engineering-society specification, it is necessary that each grade comply with the prescribed compositions and other acceptance-test requirements of the current specification.

Review of data available in the literature and from other sources, shows that in some cases comparisons of alloy-element effects were made without full attention to other variables. The following are examples: Comparisons not at the same carbon levels, manganese beyond specification requirements, marked differences in unspecified elements, exception beyond specifications in alloy-elements content, the usage of laboratory melting media, treatments, and possibly of ladle additions, and fundamentally different treatments used in comparing one grade to others.

In the tests reported herein, all the grades were made under the same controlled commercial conditions. All are from commercial 6000-lb heats made in the same commercial furnace by the same operator. The same procedure log for charge, melt, boil to like precarbon, recarburization, and deoxidation was followed, corresponding to that for other regularly used commercial heats. Final carbons are alike.

All heat-treatments also were controlled alike. The method was determined by commercial practice. Because of the size of heat-treated lots of castings in commercial practice, limitations of the process determine air-quenching rates. In other words, a commercial heat-treatment-furnace charge cools slowly in normalizing because of its mass. To determine the range of commercial treatment cooling accurately, studies first were made of the cooling rates of different-size castings in heat-treated loads. Average or typical rates were ascertained. All test bars were heat-treated in laboratory precision-controlled furnaces that duplicated these commercial cooling rates.

In addition to the four commercial heats studied in some detail, (presented together at the top of Table 1) further partial comparisons are made on seven additional heats. These supplementary data suggest the range of values within normal and controlled manufacturing processes and serve to substantiate the data of the individual heat comparisons. Table 1 presents compositions and acceptance tensile tests of all heats tested.

The test specimens were taken from standard keel blocks regularly used in the industry. Comparison of the microstructures of these and of sections from various commercial castings of like grades shows each to be of same basic type of structure.

All heats reported herein comply with the requirements of ASTM Specification A217-49T for the respective grades.

In common with all those investigators who have studied creep, creep-rupture, and so on, the authors recognize that any one composition can be made to a wide range of values by using variables in processing. Creep and creep-rupture (stress-rupture) are not constants for a composition. Properties also are influenced by process, wrought or cast, induction furnace or arc, and quenched or annealed. It is confirmed by many published researches on various materials.

The compositions and acceptance tensile-test results of the various heats are shown in Table 1. For easy comparison, heat-treatment temperatures are those used commercially for subject grades. Studies of WC6 and WC9 showed that these and particularly WC6 are subject to grain coarsening when normalize top temperature of 1900 F is used. WC4 and WC5 are not affected.

Short-Time Elevated-Temperature Tensile Tests

Results of some short-time elevated-temperature tests, performed according to ASTM Recommended Practices for Short-Time Elevated-Temperature Tension Tests of Metallic Materials E21-43, are given in Table 2. (Controlled strain rate to yield

[1] Metallurgical Research Division, The Lunkenheimer Company. Jun. ASME.

[2] Metallurgical Research Division, The Lunkenheimer Company.

Contributed by the Steam Power Panel of the Joint ASTM-ASME Committee on Effect of Temperature on the Properties of Metals and presented at the Semi-Annual Meeting, Cincinnati, Ohio, June 15–19, 1952, of The American Society of Mechanical Engineers.

Note: Statements and opinions advanced in papers are to be understood as individual expressions of their authors and not those of the Society. Manuscript received at ASME Headquarters, April 9, 1952. Paper No. 52—SA-53.

TABLE 1 CHEMICAL COMPOSITION AND TENSILE TESTS

CHEMICAL COMPOSITION

Grade	Heat	Chemical composition, per cent C	Si	Mn	P	S	Ni	Cr	Mo
		Heats Used for Basic Comparisons							
WC4	28062	0.11	0.43	0.58	0.035	0.032	0.81	0.75	0.56
WC5	27845	0.12	0.28	0.40	0.039	0.039	0.81	0.57	1.08
WC6	28265	0.11	0.39	0.59	0.034	0.037	0.03	1.30	0.54
WC9	27113	0.12	0.41	0.51	0.031	0.033	0.11	2.70	0.94
		Additional Heats Tested							
WC4	28526	0.16	0.43	0.72	0.033	0.044	0.88	0.63	0.54
WC4	29260	0.13	0.37	0.51	0.035	0.037	0.77	0.53	0.51
WC5	28439	0.13	0.25	0.44	0.039	0.036	0.81	0.90	1.10
WC5	25296	0.17	0.36	0.40	0.035	0.031	0.88	0.79	1.00
WC6	29295	0.13	0.51	0.59	0.050	0.052	0.12	1.12	0.48
WC6	30011	0.14	0.37	0.59	0.028	0.032	0.12	1.33	0.49
WC9	29423	0.13	0.44	0.46	0.030	0.036	0.18	2.35	1.05

TENSILE TESTS

Grade	Heat	Tensile strength, psi	Yield strength, psi	Elong, per cent	RA, per cent	Bhn	Heat-treatment
WC4, WC5, WC6, WC9	Specification A217-49T minimum tensile properties	70000	40000	20.0 (18.0 for WC9)	35.0		
	Heats Used for Basic Comparison						
WC4	28062	79000	49100	29.1	56.3	166	1900 FC to 1650 AQ 1250 D
WC5	27845	81700	56900	31.0	62.8	163	1900 FC to 1650 AQ 1300 D
WC6	28265	70200	46800	32.3	54.9	140	1750 AQ 1250 D
WC9	27113	87800	60200	25.3	55.2	174	1750 AQ 1300 D
	Additional Heats Tested						
WC4	28526	81000	53900	27.0	48.6	149	1900 FC to 1650 AQ 1250 D
WC4	29260	76900	52200	32.1	55.2	149	1900 FC to 1650 AQ 1300 D
WC5	28439	75600	48700	28.9	59.4	146	1900 FC to 1650 AQ 1300 D
WC6	29295	82100	50100	26.3	48.0	149	1750 AQ 1250 D
WC6	30011	79000	46000	28.0	50.9	149	1750 AQ 1250 D
WC9	29423	81500	45100	27.2	55.2	159	1750 AQ 1300 D

TABLE 2 SHORT-TIME ELEVATED-TEMPERATURE TESTS

Grade	Test temperature, deg F	Tensile strength, psi	Yield strength psi, 0.2 per cent set	Elong, per cent	RA, per cent
WC4	950	55500	36000	34.9	69.0
	1000	50500	31200	38.1	75.0
	1050	46500	24500	40.9	76.5
WC5	1000	57000	37000	30.3	75.7
	1050	51500	34000	30.6	77.8
	1100	46000	30250	34.0	79.5
WC6	950	55000	27000	31.2	65.0
	1000	49500	26000	33.2	70.3
	1050	44750	24500	40.2	76.8
WC9	1000	54250	36200	36.9	70.0
	1050	50000	34500	40.9	74.5
	1100	41500	29300	45.1	79.0

TABLE 3 RESULTS OF V-NOTCH CHARPY IMPACT TESTS

Test temp, deg F	V-notch Charpy impact results, ft-lb 32	78	150	210	500	700	900	1000	1110
WC4 Heat 26958..	27½	48	66	66½	65	...	38	..	..
WC5 Heat 27845..	37	58	64	62	65½[a]	54	33½	24½	25
WC5 Heat 25296..	20	22	50	55	58[a]	46[b]	37	30	25
WC6 Heat 26935..	25	32	54	56	50	...	37½[b]	..	..

[a] At 400 F.
[b] At 800 F.

strength was 0.001 in. per in. per min using Baldwin "Strain Pacer." From there to fracture, head-travel rate of ¼ in. per min was used. Temperature control to yield point was ±½ deg F.

In general, the higher-molybdenum steels (WC5 and WC9) are appreciably higher in yield strength than the lower-molybdenum steels (WC4 and WC6) at 1000 F and 1050 F. The Grades WC5 and WC9 also are slightly higher in tensile strength.

CHARPY IMPACT TEST

Table 3 gives results of some V-notch Charpy impact tests of WC4, WC5, and WC6 at several temperatures. A large number of Charpy tests on many commercial heats indicates that room temperature is or may be close to a transition temperature for these grades. At modestly elevated temperatures, say, 210 F, all heats showing lower room-temperature test values showed marked improvement. Those of higher initial Charpy showed less increment. Such tests indicate that room-temperature Charpy is at best a questionable type of acceptance test for steels for elevated-temperature usage. It has been noted that as a rule the lower the carbon, the higher the Charpy (at room temperature), particularly so if the calculated hardenability also is lower.

CREEP CHARACTERISTICS

In the design of most parts for use at high temperatures, creep is an important property. The "creep rate," E22-43 as determined by ASTM Recommended Practice for Long-Time High-Temperature Tests of Metallic Materials, for 1 per cent in 100,000 hr is particularly significant for metal used for gate-valve body castings. Very slight distortion which might permit leakage is a limiting consideration. Creep tests that would predict 1 per cent in 100,000 hr creep strength were held at load 4000 to 7000 hr to attain constant or slowly decreasing rates.

Table 4 gives the creep strengths of the alloys at various temperatures.

WC4 and WC6 normally are recommended for temperatures not to exceed 1000 F. WC5 and WC9 are recommended and rated to 1100 F; 1050 F was selected as an intermediate tem-

TABLE 4 CREEP STRENGTH OF ALLOYS

	Creep strength, psi (1 per cent in 100,000 hr)		
Test temp, deg F	1000	1050	1100
Grade WC4	6300	4000 (approx[a])	
Grade WC5	..	6000	4800
Grade WC6	6300	4000 (approx[a])	
Grade WC9	..	5800	4600

[a] See the extension time (creep) curves for these grades in Fig. 1 and comparison of creep rates in Table 5. The immediate effect of initial loading is not included.

perature for direct creep comparisons. Unfortunately, the creep rates of several tests of WC4 and WC6 at the same loads as WC5 and WC9 were of rates of extensions such that it was not possible to determine accurate creep strengths of WC4 and WC6 at 1050 F. Other creep bars at lower stresses are in tests that will establish these creep strengths more precisely. A relationship can be shown by comparison of the creep rates of all alloys at 6000 and 7000 psi, 1050 F, Table 5 (also shown in Fig. 1).

TABLE 5 CREEP RATES, PER CENT IN 100,000 HR AT 1050 F

	6000 psi		7000 psi	
Grade	Creep rate	Total hours test	Creep rate	Total hours test
WC4	2.0	5190	2.5	3704
WC5	1.0	6885	1.6	5688
WC6	1.9	3935	2.3	4325
WC9	1.2	6802	2.1	5350

can be compared directly as to the effect of these alloy elements on properties. Check tests on the same heat and on other heats tend to substantiate the results and suggest a probable range of properties with normal commercial alloy variation within the specifications.

The creep results indicate, in general, that WC4 and WC6 have approximately the same creep strengths at 1000 F and 1050 F. The 1 per cent molybdenum grades, WC5 and WC9, are approximately equal in their creep strengths at 1050 F and 1100 F. The 1 per cent molybdenum steels are higher in creep strength than the ½ per cent molybdenum. In this range of temperatures the 1 per cent molybdenum grades have approximately a 50 deg F advantage over the ½ per cent molybdenum grades for the same creep-strength level.

The data from the creep tests of the four grades aligned to form straight and parallel curves on log-log plots of stress versus creep rate. Attention is called to the creep rate of WC4 check test No. 2 of the same heat, stress, and temperature as No. 1, and to test No. 4 at the same stress and temperature but from another heat, Table 6. Here, three creep tests on two different heats indicate practically the same creep rate. Attention also is called to tests Nos. 14, 15, 16, and 17 of WC5 at 1050 F. Here four tests at different loads gave a straight line of stress versus creep

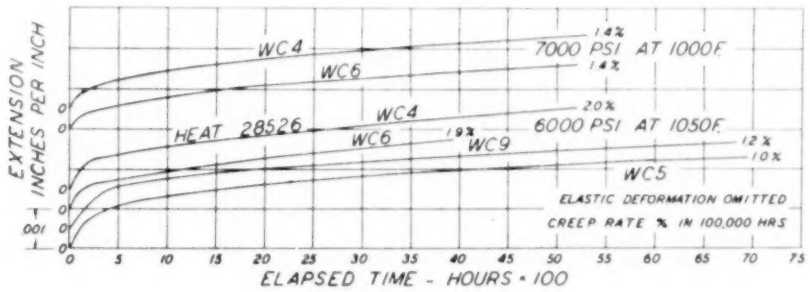

FIG. 1 EXTENSION-TIME CURVES

On a log-log plot of stress versus creep rate, it was thought that considering the slope of the curve as influenced by the two tests each of WC4 and WC6 and by the slope of other alloy data, 4000 psi creep strength at 1050 F is a fair approximation. The creep rates of WC4 and WC6 as compared to those of WC5 and WC9 for two different stresses in Table 5 indicate the higher creep strength of WC5 and WC9.

The International Nickel Company investigated the structural stability and creep strength of WC5, heat 25296 (Table 1). Creep strength was reported as 7000 psi at 1000 F and 6000 psi at 1050 F for a rate of creep of 1 per cent in 100,000 hr. These results at 1050 F confirm the creep tests obtained by the authors' company on material from the same heat.

It will be recalled that Grades WC6 and WC9 were introduced into ASTM Specification A217 and always have been furnished commercially at carbons below 0.20 per cent maximum according to that specification. Until revision of A217 in 1949, both WC4 and WC5 had been furnished to higher carbon levels. ASTM Specification change to lower carbons has improved the creep characteristics of WC4 and WC5 at the higher temperatures and had added to their room- and high-temperature ductility and impact characteristics.

A feature of the comparisons as presented here is that the materials tested are from commercial heats and heat-treated by commercial practices. Thus four grades of steel with the various amounts of alloy elements found in the different specifications

rate on log-log paper that indicates the general slope of data. Other heats of WC4, WC5, and WC6 are in test and at the time of writing (2000 hours) substantiate the creep strengths quoted.

Molybdenum evidently is the most important alloy element affecting creep. The higher the molybdenum content, the higher the creep strength within the range tested. This confirms what has been reported by others (1, 2).[2] Within the limits studied and under commercial manufacture, the ranges of nickel and of chromium do not have marked effects on creep. The creep strength of WC9 appears to be slightly lower than WC5 at 1050 F and 1100 F. This difference could be due to variation in 1 per cent molybdenum-base steel. However, it is well known that higher chromium, say, to 5 per cent, detracts from creep characteristics. Nickel may be responsible for the high creep-rupture strength of WC5, as shown in later data herein.

Various other data have been made public by other sources on WC6 and WC9. Details on composition, practices, and procedures are not fully available to us. The values given cover a wide range both well below and above the values given herein. Other data on WC4 and WC5 complying with present ASTM Specification A217-49T with full manufacturing data accompanying have not come to our attention. In so far as we are aware there

[2] Numbers in parentheses refer to the References at the end of the paper.

TABLE 6 RECORD OF CREEP TESTS

Test no.	Grade	Heat no.	Stress, psi	Temp, deg F	Creep rate, per cent in 100000 hr	Time of test, hr	After Creep Physical Tests: Tensile strength, psi	Yield strength, psi	Elong, per cent	RA, per cent	Bhn	Heat-treatment	
1	WC4	28062	7000	1000	1.4	5308	80200	50500	25.7	55.5	163		
2	WC4	28062	7000	1000	1.5	5820	77000	52500	30.1	58.9	149		
3	WC4	28062	8000	1000	2.6	3410	84400	55700	24.2	51.0	183	1900FC to 1650AQ 1250D	
4	WC4	28526	7000	1000	1.5	6018	81600	55000	27.1	53.7	159		
5	WC4	28526	6000	1050	2.0	5190	80800	53200	24.4	55.7	170		
6	WC4	28526	7000	1050	2.5	3704	82600	55100	24.5	52.6	166		
7	WC5	25296	4000	1000	0.3	2750							
8	WC5	25296	6000	1000	0.2	4600							
9	WC5	25296	7000	1000	0.9	4600							
10	WC5	25296	7000	1000	1.3	2500	Tests run by International Nickel Company						
11	WC5	25296	3500	1050	0.4	2750							
12	WC5	25296	5000	1050	0.4	4600							
13	WC5	25296	6000	1050	1.0	4600							
14	WC5	27845	6000	1050	1.0	6885	80900	51500	26.4	66.4	163		
15	WC5	27845	6500	1050	1.3	6388	80600	55000	25.2	61.8	159		
16	WC5	27845	7000	1050	1.6	5688	80700	52100	28.3	66.1	166	1900FC to 1650AQ	
17	WC5	27845	8000	1050	2.4	3850	82200	55900	25.7	64.0	166	1300D	
18	WC5	27845	5000	1100	1.2	6210					174		
19	WC5	27845	5500	1100	1.6	6162	75500	49400	25.2	62.8	170		
20	WC6	28265	7000	1000	1.4	5138	72200	40000	32.0	59.6	140	1750AQ	1300D
21	WC6	28265	8000	1000	2.2	6170	71600	42100	29.3	59.0	143	1750AQ	1250D
22	WC6	28265	6000	1050	1.9	3935	...	...	...	...	137	1750AQ	1250D
23	WC6	28265	7000	1050	2.3	4325	71000	42200	28.3	58.4	131	1750AQ	1250D
24	WC9	27113	6000	1050	1.2	6802	77200	46500	32.4	59.6	170	1750AQ	1300D
25	WC9	27113	7000	1050	2.1	5350	84300	52800	24.2	58.3	174	1750AQ	1300D
26	WC9	27113	8000	1050	2.8	3908	83000	49500	26.8	60.4	174	1750AQ	1300D
27	WC9	27113	5500	1100	1.7	5960	80500	48300	27.5	55.4	174	1750AQ	1300D

TABLE 7 RECORD OF CREEP-RUPTURE TESTS

Grade	Heat	Stress, psi	Temp, deg F	Time to fracture, hr	Elong, per cent	RA, per cent	Heat-Treatment		
WC4	29617	13000	1100	424	19.0	34.6	1900FC	1650AQ	1250D
WC5	27845	18000	1050	1752	21.8	63.5	1900FC	1650AQ	1300D
	27845	19000	1050	1274	30.9	81.5	1900FC	1650AQ	1300D
	27845	20000	1050	793	29.2	70.5	1900FC	1650AQ	1300D
	27845	23000	1050	310	23.1	74.0	1900FC	1650AQ	1300D
	27845	13090	1100	2829	14.3	46.9	1900FC	1650AQ	1300D
	27845	13000	1100	2891	11.6	39.1	1900FC	1650AQ	1300D
	27845	13000	1100	4423	18.0	53.6	1900FC	1650AQ	1300D
	27845	15000	1100	1297	26.3	61.0	1900FC	1650AQ	1300D
	27845	18000	1100	516	14.7	46.0	1900FC	1650AQ	1300D
	27845	20000	1100	282	47.7	84.0	1900FC	1650AQ	1300D
WC6	28265	15000	1050	1265	14.3	24.4	1750AQ	1650AQ	1250D
	28265	16000	1050	879	11.6	17.5	1750AQ	1650AQ	1250D
	28265	18000	1050	894	12.3	16.0	1750AQ		1250D
	28265	20000	1050	330	39.6	35.0	1750AQ		1250D
	28265	23000	1050	263	16.0	21.5	1750AQ		1300D
	29295	13000	1050	932	21.7	35.4	1750AQ		1250D
	29295	15000	1050	657	22.3	41.3	1750AQ		1250D
	29295	20000	1050	174	26.0	46.0	1750AQ		1250D
	30011	15000	1050	704	15.5	31.5	1750AQ		1250D
	30011	18000	1050	412	33.3	42.5	1750AQ		1250D
	30011	20000	1050	264	32.3	43.7	1750AQ		1250D
	28261	13000	1100	262	26.0	47.8	1750AQ		1250D
	28265	13000	1100	544	17.9	34.1	1750AQ		1250D
WC9	29423	15000	1050	1193	27.0	62.1	1750AQ		1300D
	29423	16000	1050	966	32.1	47.8	1750AQ		1300D
	29423	18000	1050	406	31.2	64.0	1750AQ		1300D
	27113	18000	1050	462	44.5	75.0	1750AQ		1300D
	29423	20000	1050	313	51.2	75.5	1750AQ		1300D
	29423	23000	1050	171	49.1	71.0	1750AQ		1300D
	29423	12000	1100	1734	31.3	55.2	1750AQ		1300D
	27113	13000	1100	1067	22.6	57.5	1750AQ		1300D
	27113	13000	1100	860	16.8	52.0	1900FC	1650AQ	1300D
	29423	15000	1100	336	30.0	60.5	1750AQ		1300D
	27113	18000	1100	160	42.5	77.5	1750AQ		1300D

are no restrictions (as by patent, or the like) on any manufacturer who desires to make any of the four grades.

Creep-Rupture Characteristics

Creep-rupture (or stress-rupture) tests have been commanding increasing attention. In this constant-load-type test, time to rupture and deformation at rupture are considered significant. Various investigators have extrapolated creep-rupture data to indicate the stress which should be sustained without fracture for periods to 100,000 hr. It has been noted that the decreasing ratio of stress to time may decrease even faster at certain test periods. If observed, this dip on the log-log curve has been noted in the range of 100 to 1000 hr. Test with no slope change within this period have been run to 20,000 hr without further increase in downward slope (3).

Basic test data on several heats of WC5, WC6, and WC9 are given in Table 7. It indicates as follows:

Grade	Heat	Creep-rupture strength, psi (extrap to 100000 hr) 1050 F	1100 F
WC5.....	27845	10000	6900[a]
WC6.....	28062	5900[b]	...
	29295	4800[b]	
	30011	5000[b]	
WC9.....	27113	6200	6000
	29423		

[a] 4423-hr test included.
[b] Or lower, note one long-time test below drawn curve.

The creep-rupture strengths are in all cases higher than the creep strengths. The creep-rupture strength of WC5 is higher than that of WC6 and WC9. The creep-rupture strengths of heats 29295 and 30011, WC6 and WC9 at 1050 F are only slightly higher than the creep strengths of these respective grades. The

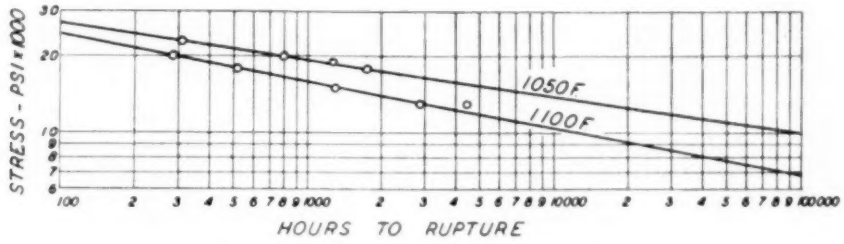

FIG. 2 WC5 CREEP RUPTURE, 1050 F AND 1100 F

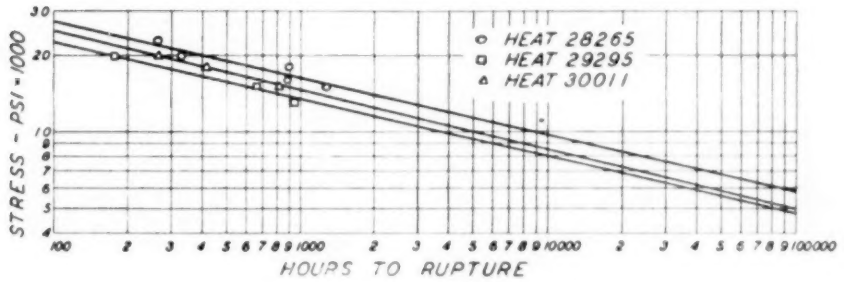

FIG. 3 WC6 CREEP RUPTURE, 1050 F

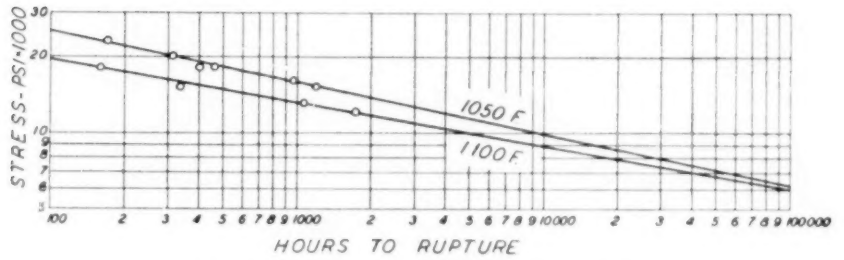

FIG. 4 WC9, CREEP RUPTURE, 1050 F AND 1100 F

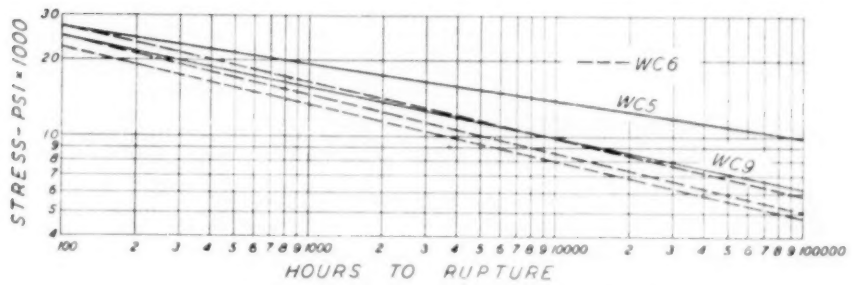

FIG. 5 WC5, WC6, AND WC9 CREEP RUPTURE, 1050 F

fact that WC9 has approximately the same creep-rupture strength as one heat of WC6 at 1050 F corresponds with what has been reported elsewhere in the literature (1). Log-log curves of stress versus time to rupture are shown in Figs. 2, 3, and 4. Fig. 5 shows all curves without actual test values taken from Figs. 2, 3, and 4.

Some difficulty was experienced in the case of WC6 and WC9 in drawing a straight line through the test points in Figs. 3 and 4. As many as six tests were needed at one temperature with WC9 at 1050 F. These many tests verified the proportionally low creep-rupture value of WC9 at 1050 F. In case of the curves drawn for the three heats of WC6, the longest time test point in

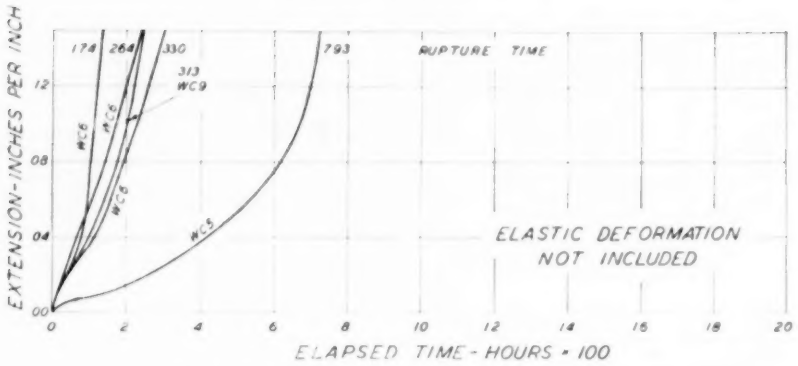

FIG. 6 EXTENSION-TIME CURVES 20,000 PSI AT 1050 F

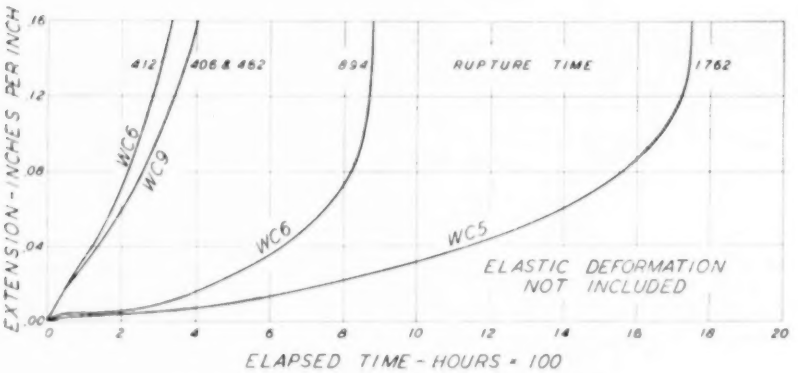

FIG. 7 EXTENSION-TIME CURVES 18,000 PSI AT 1050 F

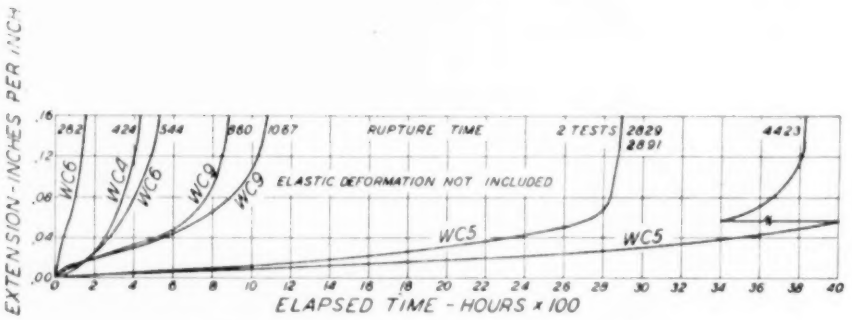

FIG. 8 EXTENSION-TIME CURVES 13,000 PSI AT 1100 F

each case is below the line. Long-time tests are being conducted to determine whether there is a tendency for WC6 to fall off in strength with length of test or whether this was an experimental variation. Figs. 6, 7, and 8 show the resistance to stress of the different alloys at one temperature and stress, and Table 7 lists actual length of test and the amount of ductility exhibited at the time of fracture.

The creep-rupture strengths of three WC6 heats are 5900, 4800, and 5000 psi, respectively. The recent recommended design stress of WC6 by the Unfired Pressure Vessel Code is 5500 psi. WC5 is rated at 5500 psi at 1050 F and its creep-rupture strength is far above this value. WC9 is rated at 5800 psi and its creep-rupture strength as indicated in these tests is 6200 psi.

TRANSFORMATION TEMPERATURES

To determine critical transformation temperatures, samples were heated and cooled in a dilatometer. The heating rate was 200 F per hr to lower critical and cooled at a rate of 920 F per hr through the upper criticals, slowing down to about 600 F per hr near room temperature for all grades.

It will be noted that WC6 and WC9 require a higher temperature on heating before AC_1. All four grades have a split trans-

TABLE 8 CRITICAL TRANSFORMATION TEMPERATURE

Grade	Heat	AC_1	AC_3	AR_3	AR_1	A^1R_3	A^1R_1
WC4.....	28062	1405	1620	1460	1330	915	680
WC5.....	27845	1395	1595	1495	1370	910	680
WC6.....	28265	1435	1635	1540	1425	905	610
WC9.....	27113	1500	1615	1525	1385	780	570

formation with the high-chromium WC6 and WC9 having the lowest temperature of secondary transformation.

Hardenability Characteristics

ASTM hardenability curves (Tentative Method of End Quench for Hardenability of Steel A255-48T) are presented for four heats of the different grades in Fig. 9. The ranges of hardnesses of WC4, WC5, and WC6 are approximately the same with WC9 having higher hardnesses. Quench temperature of 2100 F is used to indicate more nearly welding possibilities than ordinary foundry normalizing temperatures would.

Microstructure

In addition to the mechanical and related tests on the four grades herein reported, the relationships of properties to microstructure, and so on, were investigated. The findings can be summarized briefly as follows:

In actual castings of grades WC4, WC5, and WC6 heat-treated in commercial practice and in the test specimens, also, the structures are essentially ferrite—"semi-Widmanstätten." Substantial amounts of divorced ferrite are present. In the higher-chromium alloy, WC9, lesser amounts of free ferrite were found, with carbides being more of the acicular type. With these types of structures, it was noted that the final structures after creep, or other long-time exposure at temperature tests, were not basically changed from the initial or prior structures. Photomicrographs of representative after creep and typical commercial casting structures are shown in Figs. 10 and 11. There is but slight tendency for coalescence or spheroidization of the carbides. For these and other reasons, it appears that test results based on such relatively stable types of structures are of relative dependability.

Test data accumulated on less stable types of structures would be, in contrast, of lesser ultimate significance. Miller reference states: "The ferrite-Widmanstätten structure appeared to be the most satisfactory at 1000 F" (24). White and Crocker say substantially the same. They state their Widmanstätten structure is not a "true Widmanstätten." It is evident that the structures referred to by them are comparable to structures referred to herewith.

Weld Traverses

A number of weld-traverse and related studies also have been made. Summarizing a large volume of data briefly:

(*a*) Maxima in hardnesses, single bead, preheat but no stress relief are shown in Fig. 12. It is felt that with all these grades, and WC1, also, preheats should be used. This was indicated by early work in this laboratory by J. W. Bolton and A. J. Smith (30).

(*b*) Multiple beads are more effective in lowering hardnesses in WC4 compared to WC6. WC5 is lowered more in hardness than WC9. The apparent reason is that in the high-temperatures exposure of parts of weld-affected zones, the re-solution of chromium carbides is greater than is effected in usual normalizing heat-treatments. In other words, the higher potential hardenability of higher-chromium alloys makes itself more evident during welding operations.

(*c*) All grades are safely weldable with suitable procedures, and all requirements of ASME Code Sec. IX Welding Qualifications are met readily. However, WC4 may be regarded as the most "foolproof" or "safest" to weld, WC5 and WC6 are next, and WC9 should have more care.

(*d*) No cracking in weld-affected zones has been experienced in repair and construction welding in our shops, over many heats of WC4, WC5, and WC6. No evidence of cracking of these grades in the field has come to our attention.

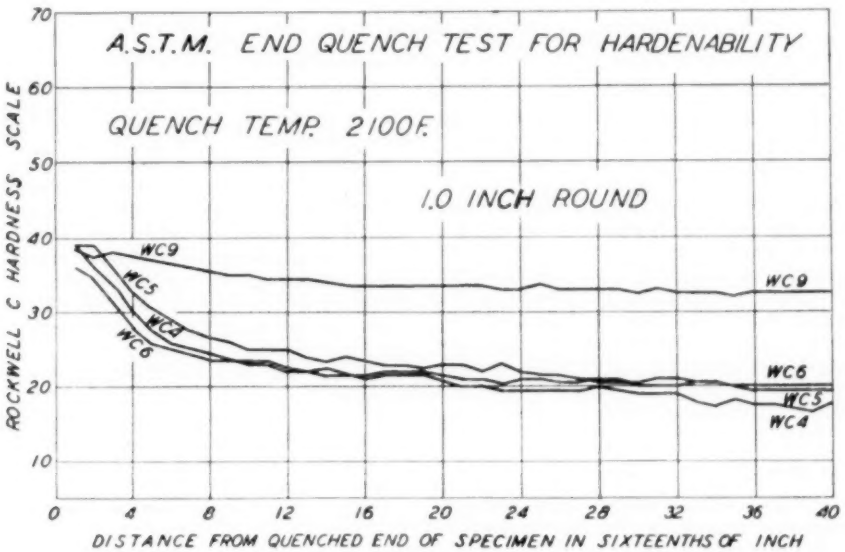

Type	Heat no.	Grain size	C	Mn	P	S	Si	Ni	Cr	Mo	Norm. Temp, F	Quench Temp, F
WC4	28062	...	0.11	0.58	0.035	0.032	0.43	0.81	0.75	0.56	1900	2100
WC6	28265	...	0.11	0.59	0.034	0.037	0.39	0.03	1.30	0.54	1750	2100
WC5	27845	...	0.12	0.40	0.038	0.039	0.28	0.81	0.57	1.08	1900	2100
WC9	27113	...	0.12	0.51	0.031	0.033	0.41	0.11	2.70	0.94	1750	2100

Fig. 9

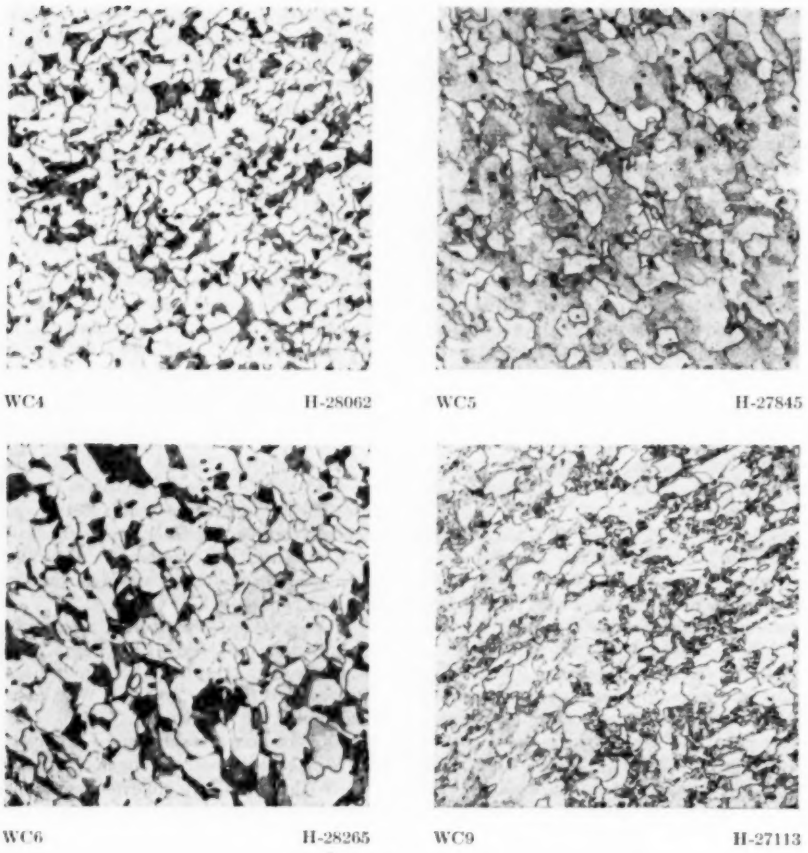

Nital-picral etch; × 100

FIG. 10 TYPICAL STRUCTURES FOUND IN CREEP-TEST BARS AFTER LONG-TIME EXPOSURE TO TEMPERATURE AND STRESS

In case of WC9, our experience is more limited, but to date has been satisfactory.

GRAPHITIZATION

Long-time exposure tests of many samples of all these grades in both welded and nonwelded condition have produced no evidence of graphitization. Freedom from graphitization in WC4 after 50,000 hr in field service was reported by T. N. Armstrong and R. J. Greene (8). This work, and that of groups such as Project 29—ASTM-ASME Joint Committee on Effects of Temperature on Properties of Metals indicates that steels containing the chromium contents of these grades (and the higher or 1 per cent molybdenum contents of Grades WC5 and WC9) will not graphitize under conditions of commercial manufacture, assembly, and service.

SUMMARY AND CONCLUSIONS

Comparable elevated-temperature test data are given on commercially made cast steels complying with ASTM Specification A217-49T Grades WC4, WC5, WC6, and WC9. Such data have direct significance for purposes of selection and rating:

1 The creep-strength characteristics of Grades WC5 and WC9 (within temperature ranges studied) are similar. Both these 1 per cent molybdenum grades are superior in creep strength to the $\frac{1}{2}$ per cent molybdenum grades WC4 and WC6 under these comparable conditions. The grades WC4 and WC6 are closely alike in creep strengths.

2 The creep-rupture (stress to rupture) strength of WC5 is superior to that of WC9. At 1050 F the creep-to-rupture strength of WC9 is only slightly above its creep strength. (Creep strength is a measure of deformation, without expected failure. Creep-rupture strength suggests breakage or failure at or within the extrapolated period, 100,000 hr or about 11 years.) The average creep rupture of three heats of WC6 at 1050 F is slightly lower than that of WC9 at the same temperature but is higher than the creep strength of WC6.

3 Graphitization is not an expectancy in any of the four grades studied.

Within the temperatures and time periods involved, over-all structures (with free ferrite) are of relatively stable type.

4 Some of the impact and hardenability characteristics of the grades are shown.

5 Short-time elevated tensile test data also are given.

ACKNOWLEDGMENT

Mr. Thomas Jacobs and Mr. Carl Neu co-operated with the authors in attainment of the test data. Appreciation is expressed to The Lunkenheimer Company and particularly to its president, Paul M. Arnall, for support of this work.

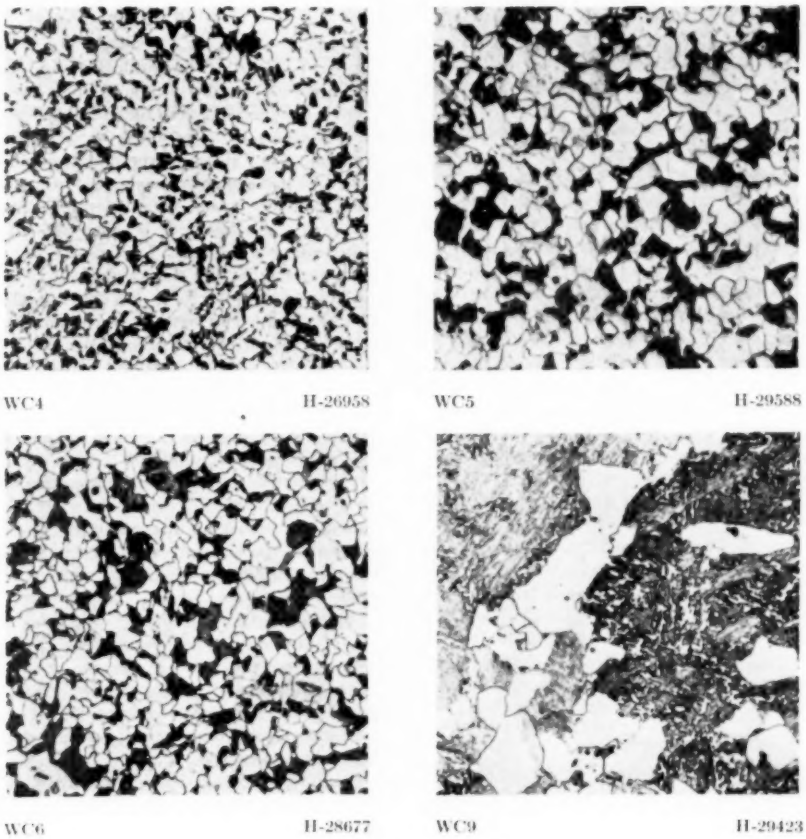

WC4 H-26958 WC5 H-29588

WC6 H-28677 WC9 H-29423

Nital-picral etch; × 100

FIG. 11 TYPICAL STRUCTURES FOUND IN COMMERCIALLY HEAT-TREATED CASTINGS

REFERENCES

1 "Long-Time Elevated Temperature Test of Cr-Mo Steels," by A. B. Wilder and J. O. Light, Trans. ASM, vol. 43, 1951, p. 341.

2 "The Creep Strength of 17 Low-Alloy Steels at 1000 F," by R. F. Miller, W. G. Benz, and W. E. Unverzagt, Proceedings of the American Society for Testing Materials, vol. 40, 1940, pp. 771–787.

3 "Safety Margins and Stress Levels in High-Temperature Equipment," by E. L. Robinson, Trans. ASME, vol. 73, 1951, pp. 89–99.

4 "Properties of Carbon and Alloy Seamless Steel Tubing for High-Temperature and High-Pressure Service," Technical Bulletin No. 6-E, The Babcock & Wilcox Tube Company, Beaver Falls, Pa. Sixth edition, 1948.

5 "Steels for Elevated Temperature Service," United States Steel Company.

6 "Digest of Steels for High Temperature Service," fifth edition, The Timken Roller Bearing Company, 1946.

7 "Pipe and Tubes for Elevated Temperature Service," Bulletin No. 26, National Tube Company.

8 "Nickel-Chromium-Molybdenum Steel Valve Casting After 50,000 Hours of Service at 900 F," by T. N. Armstrong and R. J. Greene, Trans. ASME, vol. 73, 1951, pp. 751–754.

9 "Fracture of Steels at Elevated Temperatures After Prolonged Loading," by R. H. Thielemann and E. R. Parker, Trans. AIME, vol. 135, 1939, pp. 559–582.

10 "Creep and Creep-Rupture Testing," by G. V. Smith, W. G. Benz, and R. F. Miller, Proceedings of the ASTM, vol. 47, 1947, pp. 615–638.

11 "Effect of Nickel on Physical Properties and Thermal Characteristics of Some Cast Chromium-Molybdenum Steels," by N. A. Ziegler and W. L. Meinhart, Trans. ASM, vol. 37, 1946, pp. 360–401.

12 "Characteristics and Properties of Some Cast Chromium-Molybdenum Steels," by N. A. Ziegler and W. L. Meinhart, Trans. ASM, vol. 34, 1945, pp. 589–629.

13 "Panel Session on Allowable Stresses Under the Auspices of The Boiler Code Committee of ASME, New York, N. Y., January 23, 1951.

14 "Report of ASME Subcommittee on Stress Allowances for Ferrous Materials," New York, N. Y., February 26, 1951.

15 "Creep Strength, Stability of Microstructure and Oxidation Resistance of Cr-Mo and 18 Cr-8 Ni Steels," by R. F. Miller, W. G. Benz, and M. J. Day, Trans. ASM, vol. 32, 1944, pp. 381–407.

16 "Influence of Heat Treatment on Creep of Carbon-Molybdenum and Chromium-Molybdenum-Silicon Steel," by R. F. Miller, R. F. Campbell, R. H. Aborn, and E. C. Wright, Trans. ASM, vol. 26, 1938, pp. 81–105.

17 "The Effect of Carbide Spheroidization Upon the Creep Strength of Carbon-Molybdenum Steel," by S. H. Weaver, Proceedings of the ASTM, vol. 41, 1941, pp. 608–628.

18 "The Metallurgy of Steel Castings," by C. W. Briggs, McGraw-Hill Book Company, Inc., New York, N. Y., 1946.

19 "The Rupture Strength of Steels at Elevated Temperatures," by A. E. White, C. L. Clarke, and R. L. Wilson, Trans. ASM, vol. 26, 1938, pp. 52–80.

20 "Structure and Creep Characteristics of Cast Carbon-Molybdenum Steel at 950 F," by H. E. Montgomery and John Urban, ASTM Bulletin, December, 1943, pp. 13–16.

21 "Effect of Manufacturing Practice on Creep and Creep-Rupture Strength of Low-Carbon Steel," by G. V. Smith and E. J. Dulis, Proceedings of the ASTM, vol. 49, 1949, pp. 584–601.

22 "Report on the Strength of Wrought Steels at Elevated Temperatures," by R. F. Miller and J. J. Heger, ASTM-ASME Joint Committee on Effect of Temperature on the Properties of Metals, Special Technical Publication No. 100, 1950.

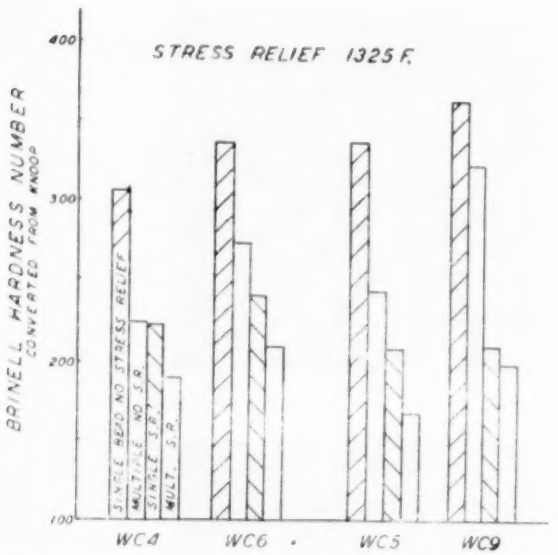

Alloy	Heat	C	Si	Mn	Ni	Cr	Mo
WC4	28047	0.14	0.37	0.60	0.83	0.72	0.57
WC6	28087	0.15	0.44	0.52	0.09	1.46	0.57
WC5	27845	0.12	0.28	0.40	0.81	0.57	1.08
WC9	27113	0.12	0.41	0.51	0.11	2.70	0.94

FIG. 12 MAXIMUM HARDNESS DEVELOPED IN BASE MATERIAL UPON WELDING WITH 500 F PREHEAT

23 "Some 1000 F Steam-Pipe Materials," by E. L. Robinson, Trans. ASME, vol. 70, 1948, pp. 855–865.

24 "Effect of Deoxidation Practice on Creep Strength of Carbon-Molybdenum Steel at 850 and 1000 F," by R. F. Miller, Trans. ASME, vol. 65, 1943, pp. 309–316.

25 "Effect of Grain Size and Structure on Carbon-Molybdenum Steel Pipe," by A. E. White and S. Crocker, Trans. ASME, vol. 63, 1941, pp. 749–764.

26 "Graphitization in Some Cast Steels," by A. J. Smith, J. B. Urban, and J. W. Bolton, Trans. ASME, vol. 68, 1946, pp. 609–624.

27 "Weldability of Cast Low-Alloy Steels," by V. T. Malcolm and S. Low, *The Welding Journal*, vol. 27, 1948, pp. 1029–1033.

28 "The Structural Stability of Several Cast Low-Alloy Steels at Elevated Temperatures," by V. T. Malcolm and S. Low, Trans. ASME, vol. 70, 1948, pp. 879–884.

29 "Welding Procedures for High-Pressure, High-Temperature Steam Piping," by N. L. Navarre, *The Welding Journal*, vol. 30, January, 1951, pp. 1-s–9-s.

30 "Welded Structures in Some Cast and Wrought Steels," by J. W. Bolton and A. J. Smith, *The Welding Journal*, vol. 18, November, 1939, pp. 398-s–417-s.

31 "Evaluating Carbon Plate Steels by the Keyhole Charpy Impact Test," by R. W. Vanderbeck, *The Welding Journal*, January, 1951, pp. 59-s–64-s.

32 "Effect of Alloying Elements on Notch Toughness of Pearlitic Steels," by J. A. Rinebolt and W. J. Harris, Jr., Trans. ASM, vol. 43, 1951, pp. 1175–1214.

33 "The Effect of Ferrite Grain Size on Notch Toughness," by J. M. Hodge, R. D. Manning, and H. M. Reichhold, *Journal of Metals*, vol. 1, 1949, pp. 233–241 (Transactions).

34 "Effect of Plastic Strain and Heat Treatment," by C. J. Osborn, A. F. Scotchbrook, R. D. Stout, and B. G. Johnston, *The Welding Journal*, vol. 28, August, 1949, pp. 337-s–353-s.

35 "Corrosion-Erosion of Boiler Feed Pumps and Regulating Valves at Marysville, Second Test Program," by J. M. Decker, H. A. Wagner, and J. C. Marsh, Trans. ASME, vol. 72, 1950, pp. 19–26.

36 "Influence of Microstructure on Creep Resistance," by Georges Delbart and Michael Ravery, *Metal Progress*, vol. 60, 1951, pp. 62–68.

37 "Characteristics and Properties of Cast Low Chromium-Molybdenum Steels," by N. A. Ziegler, W. L. Meinhart, and J. R. Goldsmith, Trans. ASM, vol. 42, 1950, pp. 175–205.

Discussion

J. K. Y. HUM.[4] The authors are to be complimented on their high-temperature study of some low-alloy ferritic steels. There is an increasing need for additional creep data to determine the limitations of these steels in order to meet the stringent requirements of steam-power design engineers. The time has arrived when a design engineer must utilize to the maximum, the usual low-alloy steels for moderate temperatures instead of specifying high-alloy steels because of the increasing shortage of critical alloying elements.

It is regrettable that the comprehensive work of Glen[5] was not available to the authors, since a slight modification in their testing technique would have provided more information, such as the effect by varying normalizing temperatures, or the effect by tempering these steels to obtain better creep strengths. There is a need to determine the optimum carbon content in these steels which will give the best high-temperature properties, since it appears that variations in carbon content materially affect the creep properties of these steels.

It seems that the good creep properties of WC4 and WC5 are due more to the high molybdenum content than from the nickel content. It would be interesting to determine whether or not nitrogen has the same effect as nickel in these steels. It is known that nitrogen can be substituted directly for nickel in the 18-8 stainless steels.

The use of the Charpy impact test as one of the evaluation tests is questionable, because in these steels with the usual slow cooling from normalizing temperature, the phenomenon of "temper brittleness" may occur even in the presence of molybdenum. After all, the steel is to be used at elevated temperatures, and tests at room temperature do not reflect what may occur at elevated temperatures.

The droop in log-log creep curves of WC6 may be eliminated by suitable tempering treatments. A similiar effect was observed by Glen.

D. L. NEWHOUSE.[6] The authors have presented an extensive set of creep and rupture test data for commercial grades of ferritic cast steels. Such test information is important to the proper application of high-temperature materials.

The authors conclude that molybdenum has the greatest effect in raising creep strength, nickel has no effect, and chromium may have lowered the creep strength in the case of WC9. These conclusions are in agreement with the data presented, and with generally accepted opinion on the effects of these elements.

The authors state that the higher rupture strength of WC5 as compared to WC9 may be due to the nickel addition. Although only one test was run on WC4, it falls within the scatter observed for WC6, indicating that for these two 0.5 per cent molybdenum steels, nickel confers no increase in rupture strength. Furthermore, rupture data available to the writer on commerial heats of 0.2 per cent C, 1 per cent Cr, 1 per cent Mo steel have shown consistently higher rupture-strength values than those reported for WC5.

Fig. 13 of this discussion shows the authors' data, together with the writer's plot of test data for a typical heat of 0.2 per cent C, 1 per cent Cr, 1 per cent Mo cast steel, plotted by means

[4] Job Engineer, Bechtel Corporation, San Francisco, Calif.

[5] "The Creep Properties of Molybdenum, Chromium-Molybdenum, and Molybdenum-Vanadium Steels," by J. Glen, *Journal of the Iron and Steel Institute*, vol. 158, 1948, pp. 37–80.

[6] Large Steam Turbine Engineering Department, General Electric Company, Schenectady, N. Y.

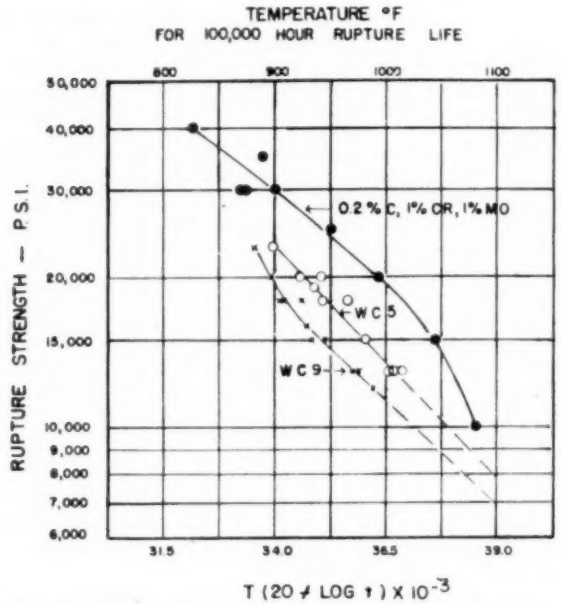

FIG. 13 RUPTURE STRENGTH VERSUS PARAMETER $T\ (20 + \text{LOG}\ t)\ 10^{-3}$ FOR WC 5, WC9, AND 0.2 PER CENT C, 1 PER CENT CR, 1 PER CENT MO CASTING ALLOYS

(T, temperature in deg R; t, time in hours.)

of the Larsen-Miller parameter, $T\ (20 + \log t)$.[7] The strengths predicted by this method for 100,000 hr at 1050 F and 1100 F fall in the order reported by the authors. The higher strength of the 1 Cr-1 Mo steel may be due to the high normalizing temperature (1050 C) or to the silicon-deoxidation practice used. It is assumed that the steels described in the paper were aluminum-killed.

The foregoing considerations are suggestive that, as the authors pointed out in the case of creep strength, the lower rupture strength of WC9 may be due to higher chromium, and not to the absence of nickel.

H. A. WAGNER.[8] As the authors point out, widely different results have been reported for the high-temperature properties for several of the alloys covered in the paper. For many materials in use today at elevated temperatures, far too few data are available to assess properly the high-temperature characteristics, and to set with assurance stress values which will guarantee satisfactory service for 300,000-hr service life. The authors are to be commended for making available their test results on these materials.

The writer wonders whether some of the variation in reported properties may not result from the fact that all of these alloys may not be made with equal facility by all manufacturers. In other words, possibly the optimum technique is not employed by every manufacturer for each of the alloys covered by this paper. If one manufacturer, by reason of a better heat-treatment or superior casting, or foundry technique consistently can produce a product with superior high-temperature properties, it would not seem reasonable to assign to that alloy the lowest stress possible corresponding to the poorest techniques.

[7] "A Time-Temperature Relationship for Rupture and Creep Stresses," by F. R. Larson and James Miller, Trans. ASME, July, 1952, vol. 74, p. 765.

[8] Assistant Chief Engineer, Engineering Department, The Detroit Edison Company, Detroit, Mich. Mem. ASME.

The authors state that "molybdenum evidently is the most important 'alloy' element affecting creep. The higher the molybdenum content, the higher the creep strength within the range tested." The creep strength of the WC4 and WC6 grades at about $^1/_2$ per cent moly are said to be essentially the same, likewise for the 1 per cent moly grades WC5 and WC9. The writer would be interested to know what is the specific effect of nickel on the properties of the WC4 and WC5 alloys as it apparently does not seem to influence the high-temperature strength significantly. Other characteristics for materials are, of course, important such as resistance to corrosion, stability after long-time exposure to high temperature, adequate ductility, and so on.

In examining the figures, the writer is again impressed with the dearth of data on which conclusions must be drawn. In Fig. 3, for instance, only one test has been carried beyond 1000 hr. It would seem that 200- to 300-hr tests are much too short to extrapolate to 300,000 hr, or even 100,000 hr, with any guarantee of assurance that the results are at all accurate.

From Fig. 2 of the paper it would seem that WC5 should be quite satisfactory at 1100 F. Do the authors recommend WC5 for 1100 F service?

In Fig. 4 it is interesting to speculate as to the effect of a slight shift in test results. If the 1750-hr point at 1100 F were to be raised 500 psi to 12,500 instead of 12,000 psi, one could argue readily that the 100,000-hr rupture value should be 7000 psi rather than 5900 psi. It would seem that further data must be obtained to establish more firmly just where such lines should be drawn.

Lest this be construed as a criticism for not having done enough work, the writer hastens to affirm that we are grateful for the additional data the authors have provided to supplement the all-too-meager information presently available.

AUTHORS' CLOSURE

The authors are appreciative of the excellent discussions of Messrs. Hum, Newhouse, and Wagner. It is interesting to note that each discusser affirms the need for truly comparative and additional data on high-temperature cast commercial steels and agrees with the main conclusions of the paper.

A desirable approach to a complete investigation is to segregate and determine the effect of each variable individually and in detail. In commercial practice there are certain limitations. Each alloy composition and heat-treatment is limited by specifications and manufacturing processes. The type of melting, the necessary deoxidation for proper pouring and sound steel, the composition prescribed by the specification, the cooling rate of castings in the normalizing process, the specification requirement for a tempering temperature of not less than 100 deg F above the service temperature and the amount of residual aluminum—all are limitations on commercial alloys. Recognizing that selection of materials is a compromise of many factors, the comparisons of various grades made under the same practice are both valid and of real engineering significance. These comparisons also indicate the actual strength of material in finished castings. May, then, the authors state again that the paper presents a direct comparison of four cast alloy steels made and treated according to carefully controlled, accepted commercial practices? Such data is necessary for sound relative stress ratings of such materials, as well as for engineering selection.

Mr. Hum refers to the extensive article by Glen.[5] This article presents data on the effect of different variables, such as type of melting, composition, heat-treatment and so on, for wrought materials. As stressed in the paper, a cast product often has different properties than a wrought product of somewhat similar alloy composition. Glen emphasizes this point by saying, "Comparatively minor differences in composition, degree of deoxida-

tion, or heat-treatment acquire an importance not hitherto fully appreciated." Many tests have been run by the authors' company and other manufacturers to determine the proper heat-treatment for the four grades.

It was noted in the paper that in the case of three heats of WC6 creep-rupture results, Fig. 3, the longest time test point in each case was below the drawn 100,000-hr extrapolated curve. This possibility of a "droop in log-log creep curves of WC6" was referred to by Messrs. Hum and Wagner. Long-time tests have been completed on heats 29295 and 30011, grade WC6, Table 9. These tests indicate that there is no tendency to depart from the original curve drawn, within the times to failure at the loadings chosen.

TABLE 9 RESULTS OF TESTS ON HEATS 29295 AND 30011

Heat no.	Stress, psi	Temp, deg F	Time to fracture, hr	Elong, per cent	RA, per cent	Heat-treatment
29295	11000	1050	3036	20 8	29 9	1750AQ 1250D
30011	13000	1050	1462	15 6	25 8	1750AQ 1250D

Mr. Newhouse mentions a comparison of creep-rupture strengths of WC4 and WC6 using the result of one WC4 test. As might be expected, a comparison using one test can be misleading. Results of recently completed creep-rupture tests on three heats of WC4 at 1050 F show on the average the strength of WC4 to be higher than that of WC6. Actually, the ranges of the two materials overlap slightly. The lowest creep-rupture strength of WC4 was approximately equal to the highest creep-rupture strength of WC6.

The information presented by Mr. Newhouse for a 0.2 per cent C, 1 per cent Cr, 1 per cent Mo steel is interesting. For long-time service applications, creep strength and its relation to creep rupture are important considerations. Since no mention is made of the creep strength, it is assumed that the creep strength is higher than comparable alloys and less than the creep-rupture strength at the indicated temperatures. If this steel had a small amount of vanadium, that could account for the higher strength. If the steel did contain any, perhaps inadvertent vanadium, then this composition might be subject to embrittlement as shown by several investigators. None of the grades tested for the authors' paper contained any vanadium.

The lower final hardnesses of WC4 and WC5, as compared to WC6 and WC9 upon welding, appear to be due at least in part to the presence of nickel. It is also possible that, as mentioned before, the higher rupture strengths of WC4 and WC5 were due in part to the addition of nickel. It has been noticed in the examination of the microstructures of WC4 and WC5 at high magnifications that there is a tendency for these alloys to have a finer, more even dispersion of carbides within the semipearlitic grains, even though WC4, WC5, and WC6 have the same basic type of structure. None of the alloys had a marked tendency to spheroidize. Armstrong and Greene's paper[9] showed WC4 had no tendency to spheroidize in 50,000 hr of commercial service at 900 F.

Referring to Mr. Wagner's question concerning the effect of nickel and the need of long-time tests on WC6, these points have been covered in part in the preceding discussion. Whether or not to recommend WC5 at 1100 F with swings to 1150 F should be determined by the effect on welded ends and high-temperature tests of the material well above 1100 F. WC5 has proved itself in commercial installation at 1050 F with swings to 1100 F. The results of the paper show that WC5 has a creep and creep-rupture strength at 1100 F higher than WC4 and WC6 at 1050 F.

A number of tests have been completed since the paper was submitted (among those tests are the WC4 results mentioned in the discussion) and more are planned. As tests are completed, the results will be made available.

A problem is to make available and/or recommend those compositions best adapted to consumer service requirements. Since the casting-production costs of the grades considered are not greatly different, economics is not necessarily a major factor in choice. Other than load-carrying capacity (creep and creep rupture), factors such as structural stability, good weldability, and so on, are involved. Certain data of the paper are useful in the evaluation of these features, plus the work here and elsewhere which indicates that all these grades are of high resistance to graphitization. Nickel (in these specific compositions) apparently provides some advantages in creep rupture and in hardness levels attained in welding procedures. In the presence of chromium, no adverse effects in respect to graphitization or otherwise have been found. The authors make no attempt to ascertain why.

[9] Bibliography (6).

AN ASME PAPER

Its Preparation, Submission and Publication, and Presentation

To a large degree the papers prepared and presented under the ASME sponsorship are evidence by which its professional standing and leadership are judged. It follows, therefore, that to qualify for ASME sponsorship, a paper must not only present suitable subject matter, but it must be well written and conform to recognized standards of good English and literary style.

The pamphlet on "AN ASME PAPER" is designed to aid authors in meeting these requirements and to acquaint them with rules of the Society relating to the preparation and submission of manuscripts and accompanying illustrations. It also includes suggestions for the presentation of papers before Society meetings.

CONTENTS

PREPARATION OF A PAPER—

General Information—Style, Preferred Spelling, Length Limitation, Approvals and Clearances.

Contents of the Paper—Title, Author's Name, Abstract, Body of Paper, Appendixes, Acknowledgments, Bibliographies, Tables, Captions, Photographs, Other Illustrations.

Writing the Paper—Outline Tabulations, Tables, Graphs, Charts for Computation, Drawings, Mathematics, Accuracy, Headings and Numbering, Lantern Slides, Motion Pictures, Typing, Number of Copies.

SUBMISSION AND PUBLICATION OF A PAPER—

Intention to Submit Paper Required in Advance, Meeting Dates, Due Dates for Manuscript, Discussers, Review and Acceptance, Proofs, Advance Copies and Reprints, Discussion and Closure, Publication by Others.

PRESENTATION OF A PAPER—

Time Limit, Addressing Your Audience, Public Address Systems, Use of Slides.

REFERENCES—

References on Writing and Speaking, Engineering Standards.

Price 40¢. No discount allowed. ***A remittance must accompany all orders for $5.00 or less. U. S. Postage Stamps are acceptable.***

THE AMERICAN SOCIETY OF MECHANICAL ENGINEERS

29 West 39th Street, New York 18, N. Y.